Microbial Bioprospecting of Auriferous Natural Samples from Mining and non-mining areas in Goa to detect Bacterioform Gold (BFG), source and screen Microbes potentially useful in Biomining of Gold and green synthesis of nanoparticles

A THESIS SUBMITTED TO GOA UNIVERSITY FOR THE DEGREE OF

DOCTOR OF PHILOSOPHY

in

BOTANY

SCHOOL OF BIOLOGICAL SCIENCES and BIOTECHNOLOGY

PROGRAMME BOTANY

GOA UNIVERSITY

By

Sujata Dabolkar

Under the guidance of

Dr. Nandkumar M. Kamat

September 2022

CERTIFICATE

This is to certify that **Sujata Dabolkar** has satisfactorily completed the thesis entitled "**Microbial Bioprospecting of Auriferous Natural Samples From Mining and non-mining areas in Goa to detect Bacterioform Gold (BFG), source and screen Microbes potentially useful in Biomining of Gold and green synthesis of nanoparticles**" submitted to Goa University for the award of the degree of **DOCTOR OF PHILOSOPHY** IN BOTANY is a record of original and independent work carried out from September 2015 through 2022 in the **DEPARTMENT OF BOTANY, at SCHOOL OF BIOLOGICAL SCIENCES AND BIOTECHNOLOGY**, GOA UNIVERSITY under my supervision and that it has not previously formed the basis for the award of any Degree, Diploma, Associateship or Fellowship or any other similar title to any candidate of this or any other university. I affirm that the thesis submitted by **SUJATA DABOLKAR** is independent research work she carried out under my supervision.

SIGNATURE OF THE GUIDE

DECLARATION

It is hereby declared that the thesis entitled "**Microbial Bioprospecting of Auriferous Natural Samples From Mining and non-mining areas in Goa to detect Bacterioform Gold (BFG), source and screen Microbes potentially useful in Biomining of Gold and green synthesis of nanoparticles**" submitted to Goa University for the award of the degree of **DOCTOR OF PHILOSOPHY IN BOTANY, at SCHOOL OF BIOLOGICAL SCIENCES AND BIOTECHNOLOGY** is a record of original and independent work carried out during the period of September 2015–2022 **at SCHOOL OF BIOLOGICAL SCIENCES AND BIOTECHNOLOGY** GOA UNIVERSITY under the supervision of **Dr. NANDKUMAR MUKUND KAMAT**, Asst. Professor, Department of Botany, Goa University and that it has not previously formed the basis for the award of any Degree, Diploma, Associateship or Fellowship or any other similar title to any candidate of this or any other university.

SIGNATURE OF STUDENT **SIGNATURE OF GUIDE**

ACKNOWLEDGEMENTS

I would avail myself of this opportunity to acknowledge all those who have helped me during the entire course of my research work. First, I express my deep sense of gratitude to my research guide Dr. Nandkumar M. Kamat for his tireless efforts, endless motivation and full cooperation during the entire period of my research work. I am highly indebted to him for his inspiring guidance with outstanding innovative ideas, helpful discussions and valuable suggestions from time to time without which the work would not have been completed. I am grateful to all former Heads of Department during the study and present Dr. Sellapan Krishnan, Head of Department of Botany, Goa University, for providing necessary research facilities. My sincere thanks to the cooperation faculty of the Department of Botany namely Dr. Bernard F. Rodrigues, Dr. Malapati K. Janarthanam, Dr. Prabhat K. Sharma, Dr. Sellapan Krishnan, Dr.Rupali Bhandari, Dr.Siddhi Jalmi for their support and co-operation. Special thanks to members of the Departmenatl research committee Dr. Sellapan Krishnan, vice-dean (research) for the School of Biological Sciences and Biotechnology, V.C.'s Nominee Vidhyadatta M. Shet Verenkar, Dean of School of Chemical Sciences for their valuable suggestions. I am grateful to Dr. Vishnu S. Nadkarni, former Dean of the School of Chemical Sciences, Goa University, for providing necessary research facilities in the Chemistry Department. We also thank the School of Earth Ocean and Atmospheric Sciences for identifying ore samples and technical guidance, especially Dr. Anthony Arthur A. Viegas, Vice-dean academic and Dr. A.G. Chachadi. It is a great pleasure to record my sincere thanks to Dr. Harilal B. Menon, former Head of the Department of Marine Science, Dr. Savita Kekar, Dr.Irene Futardo for mentoring their full co-operations, and helpful discussion, valuable suggestions and providing ideas on quality publications. I thank the entire non-teaching staff of Department of Botany Mr. Tari, Mrs. Nutan, Mr. Goankar, Mr. Dileep, Mr.Kushal and Mr. Shirodkar, Ms. Teja, Ms. Sneha, Mrs. Sahara Aga Special thanks to Mr. Vithal and Mr. Samrat for assisting me with all the chemicals and glassware. Work would not have been completed without centralised instrumental facilities provided by Sophisticated Analytical Instrument Facility BITS Pilani, Goa Campus for Zeta potential, Particle size distribution, Raman Spectrophotometry, Dynamic Light Scattering, **S**ophisticated Instrumentation **C**entre for **A**pplied Research and Testing **(**SICART) Gujarat for CHNS/O Elemental Analysis, Transmission Electron Microscopy (TEM), ICP-AES. I would like to thank Central Research Facility, Indian Institute of Technology Delhi (CRFIITD) for providing facilities for Atomic Mass Spectroscopy, Cryo-HR TEM. I would like to thank the Department of Botany and University Science Instrumentation Centre (USIC), Goa University, for providing the Scanning Electron Microscope facility and Mr. M. G. Lanjewar for helping me with the sputter coating facility. I wish to present my appreciation and gratitude to the operational in charge of AFM Mrs. Naminita Gogoi, Mr. Akshey Kaushal Senior Project Scientist (CRFIITD), Mr. Girish A Prabhu Principal, technical officer at CSIR-

National Institute Of Oceanography(NIO),Dr. Hiral Soni, Mr.Kartik Patel, technical assistant (SICART), Dr. Vikas Patel, Jr. Scientific Officer (SICART), Dr. Kenneth Rodrigues (Biotechnology Research Institute, Malaysia), Late Mr. Shailesh Mhatre, Proprietor of Cera Lab, Mumbai and Mr. Ganesh Shetgaonkar (Ex. Dy. General Manager at Excel Crop Care) for providing me helpful suggestions and instrumental facilities. I would also like to thank senior sales manager Anne Berger of MountainsMap7. I would like to thank ex-students of Master of Science Botany working in Mycological Laboratory for dissertation and contributing some valuable *Termitomyces* fruitbodies or cultures which were used during present research work by obtaining cultures from culture depository Goa University Culture Collection (GUFFC) and auriferous samples from mining and non-mining areas of Goa. I would like to thank all those who helped me during my international visit to Norway and Australia for attending the conference, especially I would like to thank Dr. Pradeep Sarmokadam, Mrs. Nilima Kamat Menezes, Mrs.Marisa and her family for all the help during my visit to World Gold Conference in Perth. I thank all the research scholars and project assistants past and present Department of Botany, Physics, Chemistry, microbiology and Biotechnology for all their support during my entire Ph.D. journey. A Special thanks to my friends Dr. Rosy Agnes de souza, Sheela Pal, Marina Albuquire, Dhillan Velip, Shravani Korgaonker, Ishan Mishal, and Prathamesh Naik for their encouragement, timely help and friendly support. I duly acknowledge the financial support provided by the NF-OBC Fellowship for carrying out this piece of valuable research work very smoothly. Heartfelt thanks for the inspiration, best wishes and blessings to my grandparents, parents, brother, husband, in-laws and other family members. Above all this, it was God's plan to complete my thesis that kept me strong spiritually, and in good health and answered all my prayers with unconditional love and blessings.

SUJATA DABOLKAR

DEDICATED

TO

Paternal Grandparents

Vishnu Shambhu Dabolkar

Daswanti Vishnu Dabolkar

My beloved parents

Mr. Satchit Dabolkar

Mrs. Shital Dabolkar

Research Guide

Dr. Nandkumar Mukund Kamat

Dedicated

to

Dr. Frank Reith

11 June 1972–14 October 2019

The man with the Gold bug

CONTENTS

TITLE	Pg. No.
CERTIFICATE	**I**
DECLARATION	**II**
ACKNOWLEDGEMENTS	**III-IV**
CONTENTS	**V-XIV**
LIST OF TABLES	**XV-XVII**
LIST OF FIGURES	**XVIII-XXI**
CHAPTER I	
INTRODUCTION	**1-3**
OBJECTIVES OF THE PRESENT STUDY	**3-4**
REVIEW OF LITERATURE	**5-77**

1.1. Microbial Bioprospecting of the major metallogenic ores

1.1.1. Metagenomics of major metallic ores

1.1.2. Specific isolation and culturing techniques

1.1.3. Winogradsky column technique to study chemolithotrophic Bacteria

1.2. Banded Iron Formation (BIF)

1.2.1. Occurrence of BIF

1.2.2. Distribution of Iron deposits

1.2.3. Formation of BIF

1.2.4. Distribution of Iron ore In India

1.3. Geological History of Goa

1.3.1. Gold occurrence

1.3.2. Biogeochemistry and Geomicrobiology of Gold

1.3.3. Microbially mediated formation of secondary Gold

1.3.4. Direct associations between secondary Gold and bacteria

1.4. Research work of Frank Reith and work on Bacterioform Gold

1.5. Gold nanoparticles

1.5.1. Mechanism of Gold nanoparticle synthesis using microbes

1.5.2. Gold nanoparticle synthesis using bacteria

1.5.3. Techniques used for characterization of GNPs

1.5.4. Nanoparticle synthesis using Actinobacteria

1.5.5. Gold nanoparticle synthesis using Yeasts

1.5.6. GNP synthesis using microfungi

1.5.7. Biosynthesis of Gold nanoparticles using different mushrooms

1.5.8. Application of Gold nanoparticles

1.6. Metal sulphide biooxidation

1.6.1. Microbes involved in Biooxidation

1.6.2. Gold sulphide bio-oxidation

1.6.3. Gold biomining -present status

1.6.4. Present techniques used for Gold mining

1.6.5. Cyanide in Gold mining and environmental problems

1.6.6. Problems faced by Gold mining industry in India

1.7. Indian Gold market

CHAPTER II MATERIALS AND METHODS 78-139

2.1. Literature survey and Bibliographic analysis

2.2. Use of VOSviewer for analysing bibliometric data

2.3. Study area

2.3.1. Preliminary survey for site selection

2.3.2. Collection of iron ore samples

2.3.3. Donated samples

2.3.4. Non-mining areas

2.3.4.1. Stream sediments

2.3.4.2. Vermicasts (Geophagous Earthworm deposits)

2.3.4.3. Termite mounds

2.3.4.4. laterites

2.3.4.5. Beach and placer sand samples

2.4. Photo documentation

2.5. Detection of Gold

2.5.1. Inductively Coupled Plasma Optical Emission Spectroscopy (ICP-OES)

2.5.1.1. Preparation of sample

2.5.2. SEM-EDX Study of bacterioform Gold particles

2.6. Morphological and typological classification of BFG particles

2.6.1. Optical microscopy

2.6.2. Sample preparation

2.6.3. Microscopic studies

2.7. Scanning Electron Microscopic (SEM) studies

2.7.1. Sample preparation

2.7.2. SEM studies of BFG particles

2.8. Metagenomic studies of BHQ and BMQ

2.9. Isolation of hyperacidophillic and chemolithotrophic bacteria

2.9.1. Selection of auriferous samples for Winogradsky technique

2.9.2. Preparation of Winogradsky column

2.9.3. Disruptive sampling of the wall deposit (Presumptive biofilm)

2.9.3.1. Preparation of coverslip size pieces from PET bottles

2.9.3.2. Slide preparation and microscopic observation

2.9.3.3. Formulation of specific medium for enrichment

2.9.3.1. Preparation of coverslip size pieces from PET bottles

2.9.3.2. Slide preparation and microscopic observation

2.9.3.3. Formulation of specific medium for enrichment

2.9.3.4. Suspension preparation and inoculation

2.9.3.5. Monitoring of the culture tubes

2.9.3.6. Confirmation by optical microscope with and without staining

2.9.3.7. Isolation of microbial pure cultures

2.9.3.8. Designation and maintenance of the colony

2.10. Isolation of actinobacteria

2.10.1. Selection of samples

2.10.2. Isolation of actinobacteria

2.11. Selection of promising Fungus cultures

2.11.1. Collection of mushroom fruitbodies

2.11.2. Pure culture isolation of *Termitomyces heimii* and *T. clypeatus*

2.12. GNP synthesis

2.12.1. GNP synthesis using actinobacterial cultures

2.12.2. Effect of thermal treatment of GNP assemblies

2.12.3. Use of *Termitomyces heimii* for GNP synthesis

2.12.4. Preparation of extracts

2.12.5. Stereomicroscopic visualization of test plates

2.12.6. Use of Digital Colorimeter

2.12.7. Digital color analysis and colorimetric data

2.12.8. Use of Venn diagrams

2.12.9. Preparation of crude extract of auriferous samples

2.13. Production of *T. heimii* Submerged condition for pellet production

2.14. Characterization of GNPs

2.14.1. UV Visible spectroscopy

2.14.2. Scanning Electron Microscopic (SEM) studies

2.14.3. Transmission electron microscopy (TEM)

2.14.4. Fourier Transmission Infra-Red spectroscopy (FTIR) Analysis

2.14.5. Particle size and its distribution

2.14.6. Zeta potential

2.14.7. X-ray Diffraction spectroscopy (XRD)

2.14.8. Raman Spectrophotometry

2.14.9. Atomic Force microscopy (AFM)

2.15. Biometrological analysis of SEM images

2.16. Multivariate Statistical Analysis

2.17. Detection of Gold sulphides in BHQ and low grade ore sample

2.17.1. Microscopic detection of Gold sulphide using powdered sample

2.17.2. Chemical test for detection of Gold sulphide

2.17.3. Separation and detection of Gold sulphides

2.18. Microfluidics assay for bio-oxidation of Gold sulphides

2.19. Molecular identification of most promising bacteria

2.20. Immobilized reaction system

2.20.1. Micro-organism (NOSOB)

2.20.2. Experimental design

2.20.3. Monitoring of the slides for formation of Gold

2.20.4. ICP-AES studies

CHAPTER III RESULTS 140-252

3.1. Literature based quantitative analysis

3.2. Use of VOSviewer for analysing bibliometric data

3.3. Preliminary site selections

3.4. Sample collection

3.5. Sieving of the samples

3.6. Detection of Gold

3.6.1. Inductively Coupled Plasma Optical Emission Spectroscopy

3.7. Morphological and typological classification of BFG particles

3.7.1. Optical microscopy

3.7.2. Scanning Electron Microscopy (SEM)

3.7.3. SEM typological analysis

3.8. Metagenomic studies of BHQ and BMQ sample

3.9. Isolation of hyperacidophillic and chemolithotrophic bacteria

3.9.1. Isolation of chemolithotrophs

3.9.2. Study of the biofilms

3.9.3. Enrichment technique

3.9.4. Microscopic studies of the bacterial cultures

3.10. Isolation of actinobacterial cultures

3.11. Sampling of wild *Termitomyces* mushrooms

3.12. Gold nanoparticle synthesis using Actinobacteria

3.12.1. Use of Actinobacterial cultures for synthesis of GNPs

3.12.2. GNP synthesis and Effect of thermal treatment of GNP assemblies

3.12.3. Testing of Aqua regia extracts

3.14. AuNPs synthesis using *Termitomyces* spp

3.14.1. GNP synthesis using extracts of *T. heimii* and *T.clypeatus*

3.15. Screening cultures for pelletisation

3.15.1. GNP synthesis using *Termitomyces heimii* pellets

3.15.2. Selection of suitable medium for pelletisation

3.15.3. Choice of strains and identification of promising strain for pelletization

3.16. Characterization of GNPs

3.16.1. UV Visible spectroscopy

3.16.2. Scanning Electron Microscopic (SEM) studies

3.16.3. SEM-EDX

3.16.4. Transmission Electron Microscopy (TEM)

3.16.5. FTIR studies of GNPs

3.16.6. Zeta Potential and Dynamic light scattering (DLS)

3.16.7. X-ray Diffraction spectroscopy (XRD)

3.16.8. Atomic force microscopy (AFM)

3.16.9. Raman Spectroscopy

3.17. Detection of Gold sulphides in BHQ and low grade ore (mining reject)

3.17.1. Separation and detection of Gold sulphide

3.17.2. Optical microscopic studies

3.17.3. Scanning Electron Microscopy (SEM-EDX)

3.17.4. CHNS/O Elemental Analysis

3.18. Micro test plate assay for Biooxidation of Gold sulphides

3.19. Immobilized reaction system

3.19.1. Monitoring of the slides and formation of Gold

CHAPTER IV DISCUSSION 253-323

4.1. Selection of this topic

4.2. Sample collection from mining and non-mining areas of Goa

4.3. Detection of secondary Gold forms in auriferous samples

4.4. Bacterioform Gold and Gold Geomicrobiology

4.5. Micromorphology and typological classification of BFG secondary forms

4.6. Use of Metagenomic technique to study the BHQ and BMQ samples

4.7. Use of Winogradsky Microcosm (WGMC)

4.8. Isolation of actinobacterial cultures from auriferous samples

4.9. AuNPs synthesis using Actinobacteria

4.10. AuNPs synthesis using *Termitomyces* by Bioinspired Microfluidics assay

4.11. Selection of *Termitomyces heimii* as promising bioreducing culture

4.12. Characterisation of GNPs based on spectroscopic techniques

4.13. Detection of Gold sulphides in BHQ and mining rejects

4.14. Detection of Gold sulphide and sea-floor massive sulphides

4.15. Micro test plate assay for Biooxidation of Gold sulphide

4.16. Molecular identification of the promising biooxidizing culture

4.17. Genome sequencing and problems

4.18. Immobilized reaction system for Gold sulphide biooxidation

4.19. Phylogenetic fingerprinting

4.20. Bioindicators for Gold exploration

4.21. Novel bioinspired microfluidics assay for rapid screening of Gold bioreduction

4.22. Novel bioinspired slide-based biosensor for rapid detection of Gold sulphides

4.23. Future perspectives / concerns

4.23. Potential of Biomining in India

4.24. Prospects of Biomining of Gallium

4.25. The eco-friendly and sustainable biomining of vermiform Gold

4.26. Phytomining

4.27. State of Goa could attain its potential in sustainable biomining

SUMMARY **324-325**

BIBLIOGRAPHY **326-390**

APPENDICES **391-401**

LIST OF TABLES

Chapter I

Table 1.1 | Use of Winogradsky column in studies of microbes

Table 1.2 | Occurrence of Banded Iron formation

Table 1.3 | The presence of Gold in the WDC and parts of Konkan region

Table 1.4 | Gold deposits In India

Table 1.5 | Gold reserves in India

Table 1.6 | Techniques used to study secondary Gold forms

Table 1.7 | Use of bacteria for Gold nanoparticle synthesis

Table 1.8 | Use of Actinobacteria for Gold nanoparticle synthesis

Table 1.9 | Use of Yeast for Gold nanoparticle synthesis

Table 1.10 | GNP Synthesis Using microfungi

Table 1.11 | Biosynthesis of Gold nanoparticles using different mushrooms

Table 1.12 | Microorganisms involved in Gold biomining

Table 1.13| Microorganisms potentially useful in Gold Biomining

Table 1.14| Biomining of Gold-Present status

Table 1.15 | Gold recovery plants located in world employing Biox and Bacox

Table 1.16 | Patents on biohydrometallurgical ore processing (1989-2022)

Table 1.17 | Price of Iron ore and Price of Gold

Chapter II

Table 2.1 | Samples from mining areas along with the designation and location

Table 2.2 | Geolocation of samples from non-mining areas

Table 2.3 | List of samples used in preparation of Winogradsky column

Table 2.4 | 9K medium used for isolation of *Acidithiobacillus*

Table 2.5| 9K medium used for the isolation of *Leptospirillum*

Table 2.6| 9K medium used for the isolation of *Sulfobacillus*

Table 2.7| Salt composition of 9K medium for enrichment of *Acidithiobacillus*

Table 2.8| Salt composition for 9K medium for enrichment of *Leptospirillum*

Table 2.9| Salt composition for each 9K medium for enrichment of *Sulfobacillus*

Table 2.10| Auriferous samples used for isolation of actinobacterial cultures

Table 2.11| AVA medium composition

Table 2.12| Molar composition of Czapek Dox medium

Table 2.13| Design of the Microtest plate wells

Chapter III

Table 3.1 | Relative expansion of webliographic knowledge using google.scholar database

Table 3.2 | Samples from mining areas

Table 3.3 | Samples from non-mining areas

Table 3.4 | Detection of Bacterioform secondary Gold in ore samples

Table 3.5 | Detection of Bacterioform secondary Gold in auriferous samples

Table 3.6 | Morphological characterisation of Gold particles from BHQ and BMQ

Table 3.7 | Morphological characterisation of Gold particles from low grade ore

Table 3.8 | Morphological characterisation of Gold particles from vermicast samples

Table 3.9 | Morphological characterisation of Gold particles from Termite mound

Table 3.10 | Morphological characterisation of Gold particles from stream sediments

Table 3.11 | Morphological characterisation of Gold particles from laterite samples

Table 3.12 | Morphological characterisation of Gold particles from beach sand samples

Table 3.13 | Differential colonization of biofilms of Iron and Sulphur bacteria

Table 3.14 | Actinobacterial cultures from auriferous samples

Table 3.15 | Tentative identification of Actinobacteria

Table 3.16 | Designation of pure *Termitomyces* cultures

Table 3.17| Bands of FTIR

Chapter IV

Table 4.1| Detection of Gold in mining and non-mining areas in Goa

Table 4.2| Detection of Gold in Goa, India and other regions of the world

Table 4.3| Morphology of the Gold particles showed in samples in other parts of the world

Table 4.4| Comparative FTIR spectroscopic characteristics of GNPs

Table 4.5| Classification of Gold nanoparticle morphology

Table 4.6| Global diversity of *Termitomyces* taxa which can be tested for GNPs

Table 4.7| List of Gold hyperaccumulating plants

Table 4.8| Recoverable Gold content

Table 4.9 | The rising Gold prices since 1950-2022 decade wise

Table 4.10| US Million per MT and Gold price of Gold in dollars

Table 4.11| Estimated recovery of Gold

LIST OF FIGURES

Chapter I

Figure 1.1 | Winogradsky column

Figure 1.2 | Distribution of BIF throughout the world

Figure 1.3 | Formation of BIF

Figure 1.4 | Generalised geological and tectonic map of the Indian shield showing the location of Dharwar craton

Figure 1.5 | Geological Map of Goa

Figure 1.6 | Southern India has Gold-favourable geology-Geological map of Dharwar Craton including the Kolar Greenstone Belt

Figure 1.7 | Schematic model showing the development and effect of Gold cycling biofilm on Gold grain surfaces

Figure 1.8 | Process of formation of Bacterioform Gold

Figure 1.9| Research by Australian Gold geomicrobiologist Frank Reith

Figure 1.10| Techniques used in the study of Bacterioform Gold

Figure 1.11| Biosynthesis of Gold nanoparticles

Figure 1.12| Application of Gold nanoparticles

Figure 1.13| Methods used in Mining of Gold

Chapter II

Figure 2.1 | Mining belt of Goa and some places of geological interest

Figure 2.2 | Distribution of key laterite-capped table-land (plateau) regions of Goa

Figure 2.3 | Various geomorphic features along the coastal zone of Goa

Figure 2.4 | Criteria for sample collection

Figure 2.5 | Potential auriferous sources of Gold inferred in Goa

Figure 2.6 | Locations of the sampling sites in mining areas

Figure 2.7| Sampling sites in North Goa and South Goa

Figure 2.8| Sampling sites from non-mining areas

Figure 2.9| Exploration of stream sediments

Figure 2.10| Exploration of vermicasts and Termites mounds

Figure 2.11| Exploration of laterites

Figure 2.12| Exploration of Beach sands

Figure 2.13| Scheme of detection of Gold and morphological studies

Figure 2.14| Winogradsky column

Figure 2.15| Sampling sites for *Termitomyces* mushrooms

Figure 2.16| Scheme for Gold nanoparticle synthesis and its characterization

Figure 2.17| Design of the microwell test plate for Microfluidic assay for bio-oxidation

Figure 2.18| Microfluidics Assay for Biooxidation of Gold sulphides

Chapter III

Figure 3.1 | VOSviewer for analysing bibliometric data

Figure 3.2 | Exploration of mining sites

Figure 3.3 | The sampling sites of samples from mining and non-mining areas of Goa

Figure 3.4 | Percentage of samples collected from mining sites

Figure 3.5 | Percentage of samples collected from non-mining sites

Figure 3.6 | Iron ore samples

Figure 3.7 | Samples from non-mining areas

Figure 3.8 | BHQ and BMQ samples with sieved fraction

Figure 3.9 | Vermicasts samples with sieved fraction

Figure 3.10 | Stream sediments with each sieved fraction

Figure 3.11 | Microscopic studies of the sieved fractions of BHQ and BMQ samples

Figure 3.12 | Microscopic studies of the sieved fractions of Vermicasts samples

Figure 3.13| Microscopic studies of the sieved fractions of stream sediments

Figure 3.14 | SEM-EDX spectra

Figure 3.15 | Morphological classification of BHQ and BMQ samples

Figure 3.16 | Morphological classification of BFG particles from Low grade ore

Figure 3.17 | Morphological classification of BFG particles from vermicasts samples

Figure 3.18 | Morphological classification of BFG particles from Termite mounds

Figure 3.19 | Morphological classification of BFG particles from Stream sediments

Figure 3.20 | Morphological classification of BFG particles from Laterite samples

Figure 3.21 | Morphological classification of BFG particles from Beach sand

Figure 3.22 | Scanning Electron microscopic images of the particles of Gold grain

Figure 3.23| Analysis of the BFG particles

Figure 3.24A | Percentage wise classification of microorganisms in case of BHQ

Figure 3.24B | Percentage wise classification of microorganisms in case of BMQ

Figure 3.25 | Phylogenetic tree representing the association of microorganisms with the BHQ sample

Figure 3.26 | Phylogenetic tree representing the association of microorganisms with the BMQ sample

Figure 3.27 | Winogradsky columns after several weeks after incubation and formation of Biofilms in different samples

Figure 3.28 | Differential colonization of biofilms of Iron and Sulphur bacteria

Figure 3.29 | Enrichment cultures on specific isolation medium

Figure 3.30 | Representative plate of *Acidithiobacillus* culture, colony characteristics and morphological studies

Figure 3.31 | Representative plate of *Leptospirillum* culture, colony characteristics and morphology

Figure 3.32 | Representative plate of *Sulfobacillus* culture, colony characteristics and morphological studies

Figure 3.33 | Microcosm set up for isolation of Actinobacteria

Figure 3.34 | *Streptomyces* colonies from auriferous samples

Figure 3.35 | Actinobacterial colonies on OMA

Figure 3.36 | The morphological characteristics of *Streptomyces* spp.

Figure 3.37 | Actinobacterial isolates from auriferous samples

Figure 3.38 | Colony morphology of *Termitomyces* culture

Figure 3.39 | Swarms of nanoparticles produced by Actinobacterial culture using chloroauric acid

Figure 3.40 | Swarms of nanoparticles produced by Actinobacterial culture using crude extracts

Figure 3.41 | Mushroom tissues used for GNP synthesis

Figure 3.42 | Positive bioreduction obtained with homogenized tissues of *Termitomyces heimii* and GNP swarm formations

Figure 3.43 | Positive bioreduction obtained with extracts of homogenized tissues of *Termitomyces heimii* and GNP swarm formations

Figure 3.44 | Microscopic characterization of GNP produced using extracts and chloroauric acid

Figure 3.45| Microscopic characterization of AuNPs formed using crude extracts and chloroauric acid

Figure 3.46| Venn diagram studies

Figure 3.47| Growth in submerged culture and studies on *Termitomyces* pelletisation

Figure 3.48| Pellets formed by *Termitomyces heimii*

Figure 3.49| UV visible spectra

Figure 3.50| SEM micrographs of AuNPs

Figure 3.51| EDX Spectra

Figure 3.52| TEM microphotographs of Gold nanoparticles of different shapes synthesized by *Termitomyces heimii* pellet and chloroauric acid

Figure 3.53| TEM microphotographs of Gold nanoparticles of different shapes synthesized by *Termitomyces heimii* pellet and crude chloroauric acid.

Figure 3.54| Analysis of TEM image of GNPs produced by chloroauric acid

Figure 3.55| Analysis of TEM image of GNPs produced by crude chloroauric acid

Figure 3.56A| The FTIR spectrum of *Termitomyces* pellet

Figure 3.56B| FTIR Spectra of GNP produced by chloroauric acid

Figure 3.56C| FTIR Spectra of GNP produced by crude chloroauric acid

Figure 3.57A| Dynamic Light Scattering spectra produced by chloroauric acid

Figure 3.57B| Dynamic Light Scattering spectra produced by crude chloroauric acid

Figure 3.58| Zeta size distribution of Gold nanoparticles

Figure 3.59| XRD pattern of Gold nanoparticles synthesized using pure chloroauric acid and crude extract.

Figure 3.60| AFM studies of the GNPs

Figure 3.61A| Raman spectra of GNPs produced using *Termitomyces* pelletes; results of chloroauric acid

Figure 3.61B| Raman spectra of GNPs produced using *Termitomyces* pellets, results of crude extract.

Figure 3.62| Microscopic studies of Gold sulphides

Figure 3.63| SEM based typological classification of Gold sulphide grains

Figure 3.64| Biooxidation of Gold sulphide and release of Gold

Figure 3.65| Fascinating fractal forms of pure Gold produced by bacterial culture

Figure 3.66| Set up of immobilized system for biooxidation of Gold sulphide

Figure 3.67| Film of Gold formed after dissolving in aquaregia indicating the formation of Gold

Chapter IV

Figure 4.1 | Geomicrobiology of Gold

Figure 4.2. | Overlap of the bacterial community in BHQ and BMQ

Figure 4.3 | National culture collection of chemolithotrophs using Winogradsky column

Figure 4.4 | Biosynthesis of GNPs using *Termitomyces Heimi*

Figure 4.5 | Biooxidation and release of Gold

Figure 4.6 | A robotic high throughput screening for selecting hyper Biooxidizer

Figure 4.7 | Phylogenetic tree of NOSOB

Figure 4.8| NOSOB culture and its possible role in biogeochemistry of Gold

Figure 4.9| Novel bioinspired microfluidics assay for rapid screening of Gold bioreduction systems in termitophilic mushrooms for designing Gold biosensor

Figure 4.10| Potential of Biomining in India

Figure 4.11| Conceptualization of a Gallium based supply chain

Figure 4.12 | Prospects of Bioming of Gallium

Figure 4.13| The eco-friendly and sustainable biomining of vermiform Gold from auriferous soils

Figure 4.14 | Potential of Gold Phytomining in India

The present thesis is organized into four chapters. Chapter I consists of brief introduction to the work presented, review of literature and objectives. Chapter II includes materials and methods involved, Chapter III consist of results obtained and final Chapter IV presents discussion with reference to important results concluding with prospects / scope for future work. At the end are placed associated sections such as summary, bibliography of literature cited, appendices regarding media, reagents, stains used, papers published / communicated in peer-reviewed journals, papers presented at national / international conferences, courses, workshops / other conference participation.

CHAPTER I

INTRODUCTION

OBJECTIVES

REVIEW

OF

LITERATURE

Introduction

Biomining is a natural, eco-friendly process of converting an insoluble metal, such as metal sulphides, into a soluble form using microbes employed at a commercial scale to extract metals (Schippers et al., 2014). Bioleaching employs microorganisms to facilitate the extraction of metals from sulphide or iron-containing ores or concentrates (Rawlings, 2002). There is a great knowledge available on the role of microorganisms in the formation of Banded Iron Formation (BIF) and other minerals in the earth system (Gagen et al., 2018; Dreher et al., 2021). Microbial thermophiles, cyanobacteria, Sulfate-Reducing Bacteria (SRB), and iron-reducing bacteria have been reported from the Gold mines in South Africa (Li et al., 2022). In India, iron formations are designated as "Banded Hematite Quartzite" (BHQ) and "Banded Magnetite Quartzite" (BMQ) (Prasad et al., 2012). Goa is situated in the north western part of the Western Dharwad Craton (WDC), which is Asia's major metallogenic province (Ugarkar et al., 2016) and is associated with greenstone and occurs as bands, reefs, and lenses of BHQ and BMQ (Desai, 2018). Non-mining materials mainly include beach placer deposits, alluvial river deposits, stream sediments, beach sands, laterite rocks, and vermicasts. There are reports on the presence of Si, Ti, Al, Fe, Mn, Mg, Ca, Na, K, P and trace elements such as Rb, Sr, Y, Ni Cu, Zn in laterite samples of Goa (Widdowson, 2009). There are reports on heavy minerals associated with the beach sands of Goa, such as magnetite, ilmenite, hornblende, garnet, rutile, zircon, and minor amounts of tourmaline (Sreenivasa et al., 2014). Soil and stream sediments based geochemical mapping of 502 stream sediment samples have been carried out and these samples were analyzed for Cu, Pb, Zn, Ni, and Co (Purushothaman et al., 2009). However, all these samples are not being explored for Gold contents, and thus, there was a need for the exploration and collection of samples from mining and non-mining areas of Goa. Mining in Goa began in 1945-46, which marks the beginning of modern-day mining and export of Iron ore. These exports of iron ore from Goa have steadily increased from 4,36,400 Metric Tonnes

(MT) (1951) to 35 Million Metric Ton (MMT) (2008-09) and reached 800 MMT of Iron ore exports cumulatively (1951-2011). Though Goa is restricted to Archean greenstone terranes of WDC, Gold mineralization of economic importance has been neglected by Iron ore centric mining and export strategy. There was a lack of knowledge of systematic geochemical evaluation of Goa's Iron ore, whereas other countries such as Australia and South Africa have their own international standards (Angerer et al., 2012; Pharoe et al., 2020). Although much work has been reported on the detection and mineralization of Gold in other parts of the WDC (Ganguly, 2016; Biswas, 2021; Mohakul et al., 2021), there were no studies reported on the presence of Gold in Goa. This work was primarily inspired by the extensive research done by Frank Reith in the field of Gold geomicrobiology. There are reports on studies of the biomineralization of Gold and on the formation of biofilm on Bacterioform Gold (BFG) in the Australian region (Reith & McPhail, 2006; Reith et al., 2013). Despite being endowed with chemically the most diverse and creative Archean rocks in WDC, Goa still lacks intensive studies on geomicrobiological associations with such samples, such as morphological and typological classification of BFG. Such studies were needed to be carried out in Goa. Actinobacteria and fungi isolated from different ecosystems have been recognized as the potential synthesizers of Gold nanoparticles (GNPs) (Karthik et al., 2014; Manivasagan, 2016). Specific and rational isolation of actinobacteria and fungi associated with such samples could be carried out, and promising cultures could be efficiently used in the green synthesis of GNPs (Manivasagan et al., 2016; Srivastava & Bhargava, 2021). Chemolithotrophic bacteria associated with such samples can be used in the bio-oxidation of Gold sulphides (Rana et al.,2020; Wang et al., 2021). BIF shows sulphide-facies promising for hosting Gold mineralization (Sawkar et al., 1995; Mandal et al., 2021) but there were no details on the Gold sulphide species available in Goa. No attempts were made earlier to separate Gold sulphides from the Iron ores of Goa. Various sulphide bio-oxidation experiments are being carried in

other countries (Gahan et al., 2012; Chingwaru et al., 2017). There was a need to carry out the bio-oxidation of Gold from the Iron ores of Goa and also need to set up the benchtop biomining experiment.

OBJECTIVES OF THE PRESENT STUDY

The central aim of the work was to test this hypothesis. The research work would be based on the following hypothesis-

"**Presence of metalliferous WDC in Goa affords sampling of auriferous materials from mining and non-mining area having hitherto unexplored interesting geo-microbiological dimensions such as detection of secondary bacterioform Gold and besides useful microbes associated with such material could be isolated and systematically screened for potential applications in biomining of Gold and green synthesis of Gold nanoparticles**"

The specific objectives of the work were:-

1.Exploration and collection of natural auriferous samples from mining and non-mining areas of Goa

2. Detection, morphological and typological classification of Bacterioform secondary Gold forms in auriferous samples

3. Specific and rational isolation of hyperacidophillic and chemolithotrophic bacteria, actinobacteria, and fungi from auriferous samples.

4. Systematic screening of the actinobacterial and fungal cultures for bioreduction of aqua regia extracts of promising auriferous materials (high- and low-grade ores, alluvial river sands etc) in order to select a few promising bioreducing strains and assessment of their efficacy for green synthesis of GNPs

5. Systematic screening of the chemolithotrophic cultures isolated under objective 3 above for biooxidation of pure Gold sulphides in order to select a few promising biooxidizing strains

6. Setting up of small Bench top biomining experiment for extracting Gold from local high- and low-grade Iron ore samples and mining rejects

Exploration and collection of samples from mining and non-mining areas of Goa would help in filling the gaps in knowledge regarding the systematic geochemical evaluation of the Iron ores of Goa. Objective two would fill the gap about knowledge of the presence of Gold in Goa. No studies were reported on BFG's morphological and typological classification in auriferous samples of Goa. Objective three would fill the gaps about interesting geo-microbiological dimensions, such as detecting BFG and hyperacidophillic and chemolithotrophic bacteria, actinobacteria, and fungi associated with such materials. Completing this objective would help in building the library of cultures. It would allow Indian researchers to make an indigenous collection of industrially applicable, diverse, and chemically creative strains of Iron and Sulphur bacteria. Objective four would help to select the most promising bioreducing strains that could be efficiently applied in the green synthesis of GNPs. Objective five will help to choose the promising biooxidizing strains, which will help to carry out the bio-oxidation of Gold sulphide. It will also fill in gaps about the lack of knowledge regarding Gold sulphide species of Goa and how to separate it from the ores of Goa. The sixth objective will help in setting up of small Bench top biomining experiment for extracting Gold from local high- and low-grade Iron ore samples and mining rejects, which will help Goa to develop sustainable, eco-friendly biomining and thus become self-sufficient in Biomining. Finally, this study would help Goa state in attaining its full economic potential as a metallogenic province in Asia.

The literature survey is presented in three parts, part **a** is the bioprospecting of the auriferous sample, part **b** and **c** is the application part where part **b** covers the Gold nanoparticle synthesis and part **c** covers the biomining of Gold.

Review of Literature

Part A

1.1. Microbial Bioprospecting of the major metallogenic ores

It is a systematic search for and development of new sources of chemical compounds, genes, microorganisms, and other valuable products from nature. It also entails the search for economically valuable genetic and biochemical resources from nature. Biomining is a natural, ecofriendly process of conversion of an insoluble metal such as metal sulphides into a soluble form using microbes. Bioleaching employs microorganisms to facilitate the extraction of metals from sulphide or iron- containing ores or concentrates (Rawlings, 2002). **S**amples which contains Gold are known as auriferous samples. Ambient temperature, abundance of water, organic carbon and bioavailable iron and other metal substrates provide a suitable environment for microbes to inhabit the minerals (Hao et al., 2010). *Acidithiobacillus ferrooxidans, Leptospirillum,* thermophilic bacteria and heterotrophs have been shown to be able to oxidize ferrous iron and to reduce sulphate (Hao et al., 2010). Despite a great knowledge on role of microorganisms in the formation of Banded Iron Formation (BIF) and other minerals, in earth system processes such as biological weathering of rocks metal tolerant species and recognition of new branches of mycology and geomicrobiology such as geomycology (Gadd, 2012, 2016). There are still interesting and intellectually exciting areas of research which call for specific attention. There is little knowledge available on the isolation of microorganisms from such minerals. More research can be carried out on such interesting and exciting areas of research.

1.1.1. Metagenomics of major metallic ores

Metagenomics is the analysis of DNA from a mixed population of organisms and initially involved the cloning of either total or enriched DNA directly from the environment (eDNA)

into a host that can be easily cultivated (Handelsman, 2004). Advances in next generation sequencing (NGS) technologies allow isolated eDNA to be sequenced and analyzed directly from environmental samples (Shokralla et al., 2012). Metagenomic studies of extreme temperature habitats such as subsurface microbial mat sample from Hishikari Gold mine (Japan) Sequence screening (Nunoura et al.,2005) as well as subsurface oil reservoir sample Norwegian Sea (Kotlar et al., 2011) has been reported. There are reports on microbial diversity from the continental shelf regions of the Eastern Arabian Sea using metagenomic approach (Sachithanandam et al., 2020; Yaman et al., 2020). There have been no record of metagenomic analysis of BIF associated microbes from Goa. This research fills the gap and obtains a better understanding of bacterial diversity associated with BIF from Goa.

1.1.2. Specific isolation and culturing techniques

The Gram-negative, acidophilic bacterium *Acidithiobacillus ferrooxidans* has attracted great interest because of its use in industrial mineral processing and its unusual physiology. *A. ferrooxidans* can oxidize ferrous iron, elemental sulfur and its reduced compounds, and sulfide minerals. This ability makes it suitable for use in biomining to recover metals such as copper, Gold and uranium (Brierley, 1978; Merroun et al., 2003). Identification and characterization of four strains of *Acidithiobacillus ferrooxidans* isolated from different sites in China has been reported (Chen et al.,2007) which are being isolated by 9K medium which was prepared according to a method described previously (Kai et al., 1989). *Bacillus cereus* has been found to be associated in soil and other regolith samples from Tomakin Park Gold Mine in south eastern New South Wales, Australia. This bacteria act as a biogeochemical indicator for concealed mineralization, including vein-type Gold deposits (Reith et al., 2005).

1.1.3. Winogradsky column technique to study chemolithotrophic Bacteria

The Winogradsky column was developed and named after Sergei Winogradsky (1856-1953), a Russian microbiologist. It is a miniature ecosystem that illustrate microbial succession of several groups of microbes. He studied the complex interactions between environmental conditions and microbial activities using soil enrichment to isolate pure bacterial cultures (Madigan et. al, 1997). As oxygen diffuses downward from the surface, fermentation products from the breakdown of cellulose and hydrogen sulfide diffuse upward from the reduced lower zone. With response to sulphate enrichment microbial metabolites migrate within the column and are used by sulfate-reducing organisms such as *Desulfovibrio* to produce hydrogen sulfide. The development of sulfate-reducing bacteria appears as blackened areas in the lower portion of the column and may even blacken zones throughout the sediment if sufficient aerobic bacteria are present to deplete the oxygen supply. The sulphides are then used by anaerobic photosynthetic populations such as green sulfur, *Chlorobium*, and purple sulfur, *Chromatium* bacteria. Evidence of this is seen as purple and green patches in areas throughout the column as these phototrophs respond to gradients of light and sulfide. In nature, purple and green sulfur bacteria may be found in any fresh or marine waters as long as there is a sufficient supply of hydrogen sulfide and the water is clear enough so that light penetrates to the anoxic (anaerobic) zone (Madigan et al., 1997). Ferric compounds may precipitate and appear as brown or greenish-gray deposits. The predominant iron-reducing bacteria within gleyed soils appear to be *Bacillus* and *Pseudomonas* (Atlas and Bartha, 1993) higher up in the column, in the microaerophilic zone, rust-colored patches will appear, generally from the photoheterotrophs, such as the purple non sulfur bacteria (*Rhodospirillum* and *Rhodopseudomonas*). These organisms trap light energy and use organic molecules as both electron and carbon sources. At the mud-water interface, where both hydrogen sulfide and oxygen are found, various aerobic,

sulfide-oxidizing organisms such as *Beggiatoa*, *Thiothrix* and *Thiobacillus* may colonize. Algae and cyanobacteria appear quickly in the upper portion of the water column, where sunlight is abundant. By producing oxygen, these organisms help to keep this zone aerobic. This watery top layer contains an interesting diversity of microbes-green algae, cyanobacteria, various aerobic bacteria, fungi and protozoa. **Fig 1.1** shows the Winogradsky column. The Use of Winogradsky column in studies of microbes is shown in the **Table 1.1.**

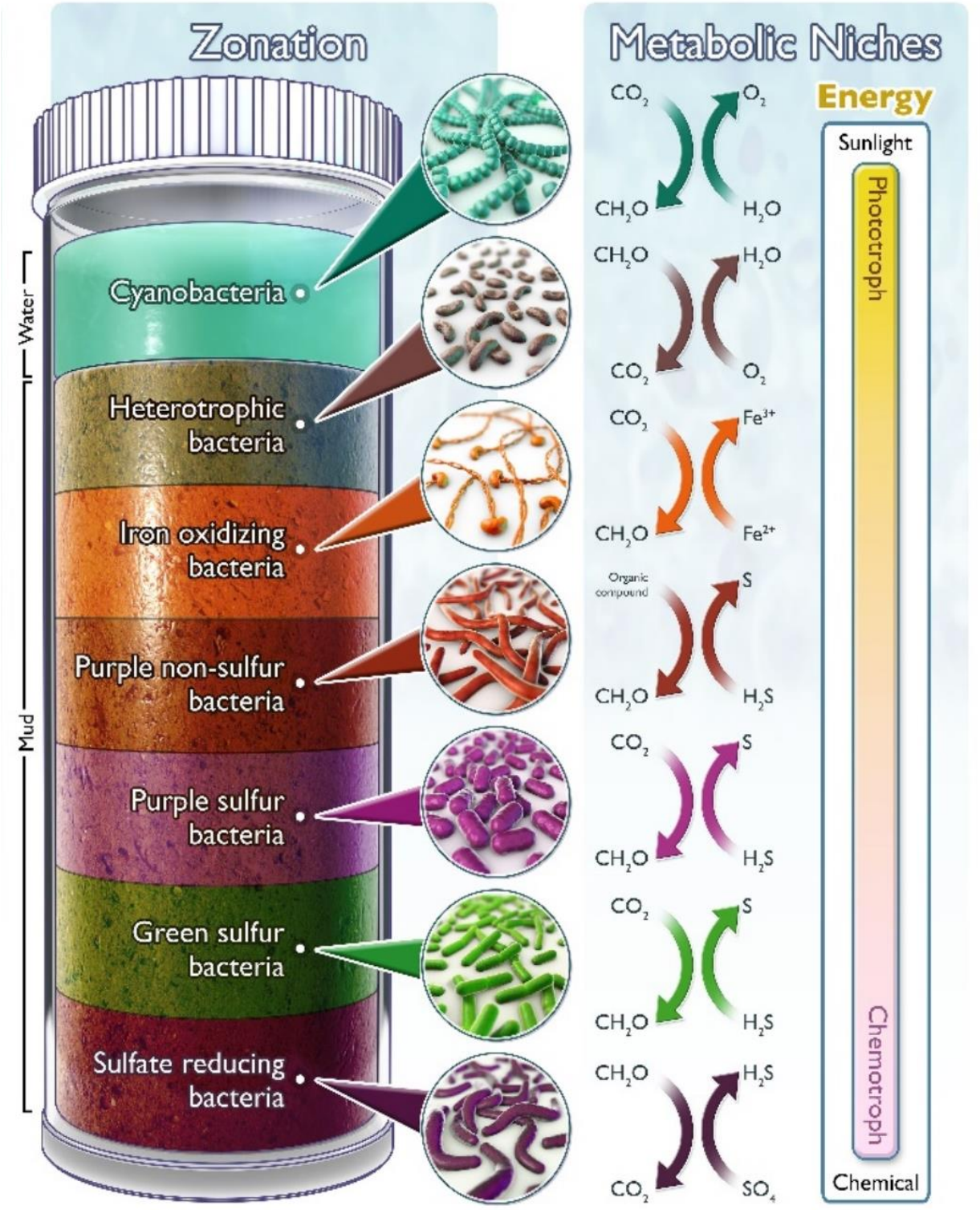

Figure 1.1: Winogradsky column (Biologyalive.com)

Table 1.1: Use of Winogradsky column in studies of microbes

Type of sample	Microbes	Country	Reference
Black mud in a lake or sea	chemoheterotrophs, chemolithotrophs, photoautotrophs and photoheterotrophs	Massachusetts, USA	Abbasian et al., 2015
Water and sediment	Chemolithotrophs	Gee Lake in Commerce, Texas	Kharashqah, 2002
Agriculture site and dump yard	Sulphur oxidizing bacteria	India	Sridharan et al, 2021
Mud	*Thiobacillus* species	Srilanka	Weerasingha & Gunawardane, 2015
Soil	*Thiobacillus* species	USA	Rogan et al., 2005
Soil or mud	Facultative chemo-organotrophs	USA	Hairston, 1999

1.2. Banded Iron formation (BIF)

Banded iron formations (BIFs) are chemical sediments that were precipitated throughout the Archaean and early Paleoproterozoic. The majority of BIFs consist of alternating silica-rich and iron rich bands that range from small-scale laminated microbands (few mm), through mesobands (≥10 mm) and up to metre-scale macrobands. BIF are iron-rich (ca 20 to 40% Fe) and siliceous (ca 40 to 50% SiO_2) sedimentary deposits that precipitated throughout much of the late Archean (27 to 25 Giga-annum (Ga)) and Paleoproterozoic (25 to 18 Ga). The mineral composition of BIF has been modified by diagenetic and metamorphic overprinting, and therefore the main mineral phases now found in BIF, such as hematite (Fe_2O_3), magnetite (Fe_3O_4), microcrystalline quartz (SiO_2), stilpnomelane ($K(Fe,Mg)_8(Si,Al)_{12}(O,OH)_{27}$), Fe-amphiboles, calcite and dolomite-ankerite are actually of secondary origin. Proposed primary minerals are ferric hydroxide $Fe(OH)_3$, siderite ($FeCO_3$), greenalite $(Fe)_3Si_2O_5(OH)_4$ and amorphous silica (Klein, 2005). The bulk of the iron in BIF originated as dissolved Fe (II) from submarine hydrothermal vents and was subsequently transformed to dissolve Fe (III) in the upper water column by either a biological or biological oxidation.

1.2.1. Occurrence of BIF

The banded rocks are scattered throughout the world and are actually ambassadors from the past because they offer clues to the environment of the early earth. The stripes in the BIF represent alternating layers of silica rich quartz silica (~40–50%) and iron (~20–40%) minerals like hematite and magnetite (Barton et al., 2010). The Superior type (S-type) first appears around 3 billion years ago (Ga) during the Archean and extends to around 1.7 Ga (in the Proterozoic). In India, iron-formations are designated as “Banded Hematite

Quartzite" (BHQ) and "Banded Magnetite Quartzite" (BMQ) (Prasad et al., 2012). Occurrence of Banded Iron formation is given in **Table 1.2.**

1.2.2. Distribution of Iron deposits

On the basis of the geological considerations, primarily the tectonic setting based on BIF size and lithological association has classified the major iron formations of the world into two types ie Algoma-type and superior type. The 'Superior' type BIFs, including those in the Hamersley Group, Western Australia, and the Transvaal Super group, South Africa, are hundreds of metres thick, over 105 km^2 in areal extent (Beukes, 1984; Trendall, 2002). These formations are characteristically laminated (James, 1954), with banding observed over a wide range of scales, from coarse macrobands (metres in thickness) to mesobands (centimetre thick units) to millimetre and sub-millimetre layers. Among the latter are the various varve-like repetitive laminae, known as microbands. Distribution of BIF throughout the world is shown in **Fig 1.2.**

Table 1.2: Occurrence of Banded Iron formation

Country/ Area	Formations	Composition	Reference
Western Australia	Brockman IF (~2.47 Ga) Hamersley Province	65 wt.% Fe (~0.05 wt.% P, 2.5 wt.% SiO_2, ~1.5wt.% Al_2O_3)	Evans et al.,2013
Western Australia	Yilgarn Craton-Greenstone	63 wt.% Fe (0.064 wt.% P, 3.3 wt.% SiO_2, 0.66wt.%Al_2O_3)	Angerer et al., 2013; 2015
South America	São Francisco Craton	Carbonate-quartz iron oxide, magnetite/hematite and specularite veins.	Rosière et al., 2018,2019
Republic of Guinea, West Africa	Simandou Iron Ore Deposit	High Grade 65%-Hematite-martite, Grano blastic hematite, micro plated hematite, goethite	Cope,2009
Egypt	Algoma-type BIF of Archean greenstone belts	Magnetite, hematite and microcrystalline quartz, in addition to ankerite in the carbonate-bearing bands	Basta et al., 2011
Greenland	Itilliarsuk banded iron formation	Alternating high iron (~68 wt.%) and high silica (~64 wt.%) bands with low total rare earths and yttrium, Al_2O_3, TiO_2	Haugaard et al., 2013

Southern Cameroon, West Africa	Greenstone belt	SiO_2 and Fe_2O_3 which constitute 95.6–99.5% of the bulk rock	Sylvestre et al., 2015
Argentina	Algoma Type	Plagioclase-biotite-muscovite-quartz (±rutile) paragneisses, quartz-bearing ortho amphibolites, amphibole + orthopyroxene-rich/spinel-bearing komatiitic metabasalts and minor meta chert lenses of the Nogolí Metamorphic Complex	González et al., 2009
Brazil	Archean carajás formation	SiO_2 and Fe_2O_3	Klein & Ladeira, 2002
China	Jingtieshan banded iron formation	oxide-, carbonate- and mixed carbonate–oxide facies, and consist of alternating iron-rich and silica-rich bands	Yang et al., 2015

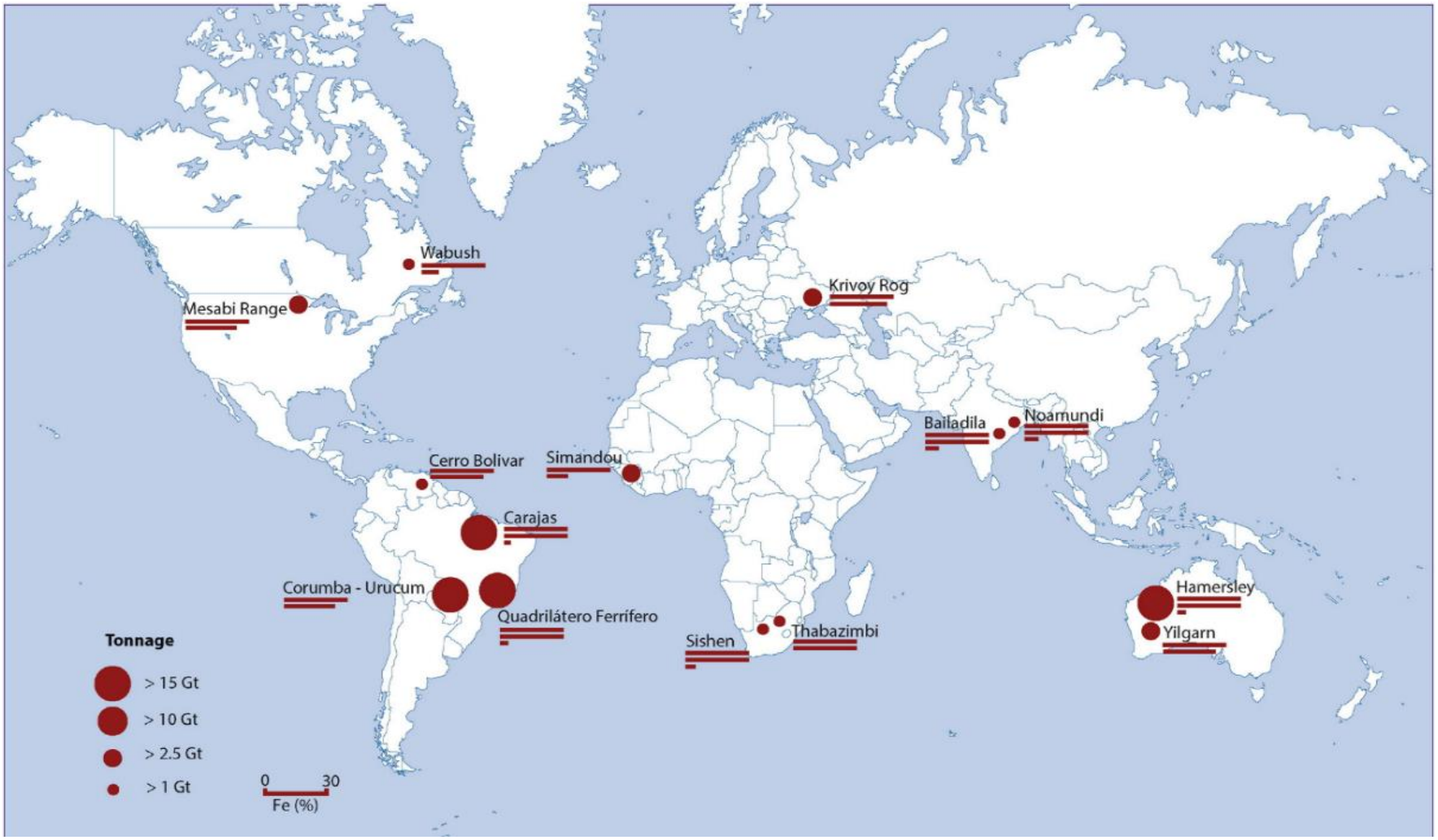

Figure 1.2: Distribution of BIF throughout the world (Hagemann et al., 2016)

1.2.3. Formation of BIF

Banded iron formations (BIFs) are Precambrian sedimentary deposits that generally consist of alternating layers of iron minerals and silica (Beukes and Klein, 1992). How these deposits formed at different periods in earth history has not been resolved, despite intensive investigation over the last century. One of the theories tells that primitive photosynthetic blue/green alga produced oxygen as the product of photosynthesis reacted with the iron ions and formed magnetite (Fe_3O_4) iron oxide (Konhauser, 1998). The preservation of bacteria in rocks is applicable to the search for the oldest evidence of life on earth found in Precambrian stromatolites and banded iron deposits (Cloud 1973; Lowe 1980; Schopf and Packer 1987). The formation of BIF theory is put in **Fig 1.3**.

In India Gold mineralization of economic importance is mainly restricted to Archean greenstone terranes of the Dharwar Craton (DC). DC is divided into Western Dharwad craton (WDC) and Eastern Dharwad craton and Goa forms the part of WDC (**Fig 1.4**). The geological map of Goa is shown in the **Fig 1.5.** Research findings show the presence of Gold in the WDC and parts of Konkan region (**Table 1.3**).

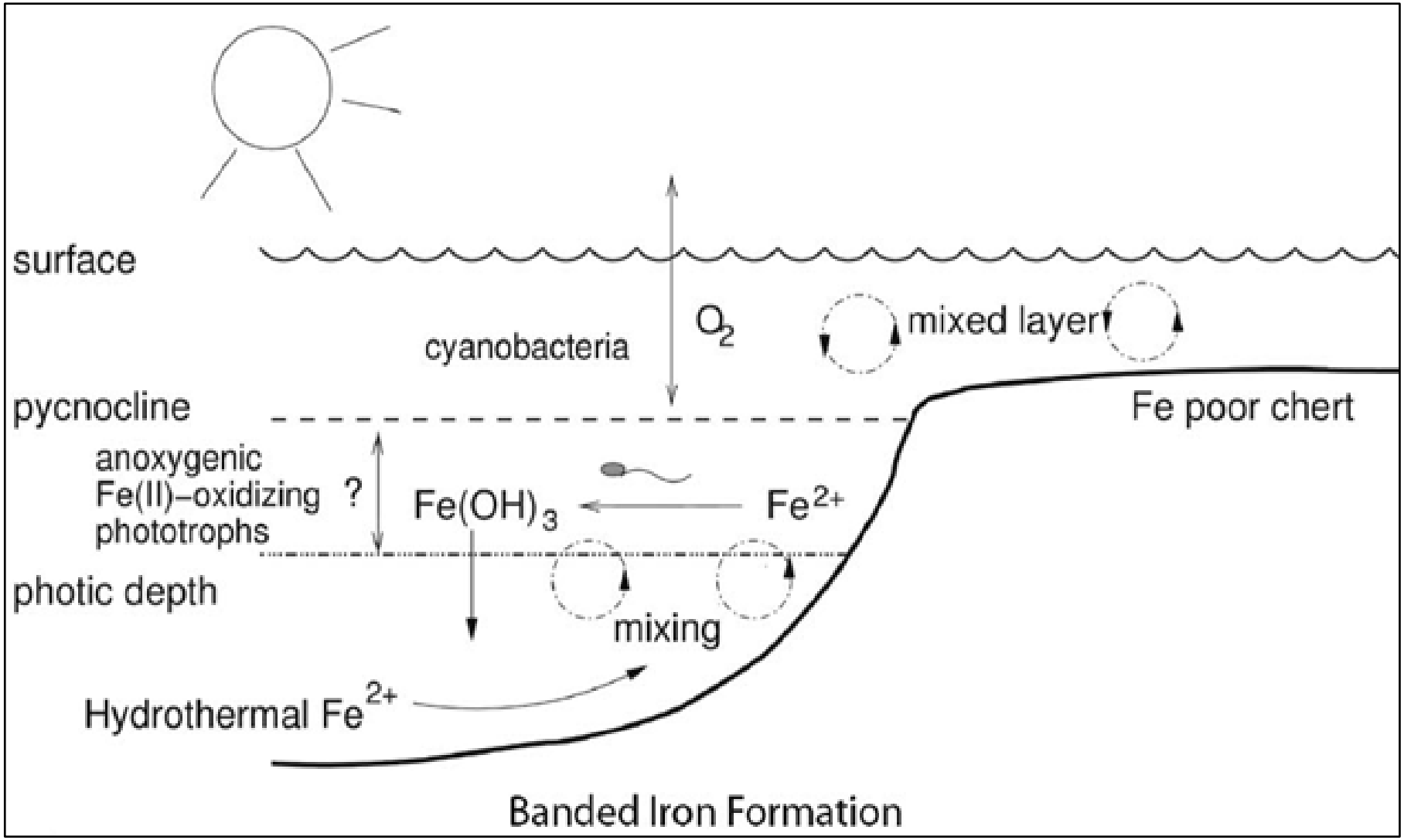

Figure 1.3: Formation of BIF (Konhauser, 1998)

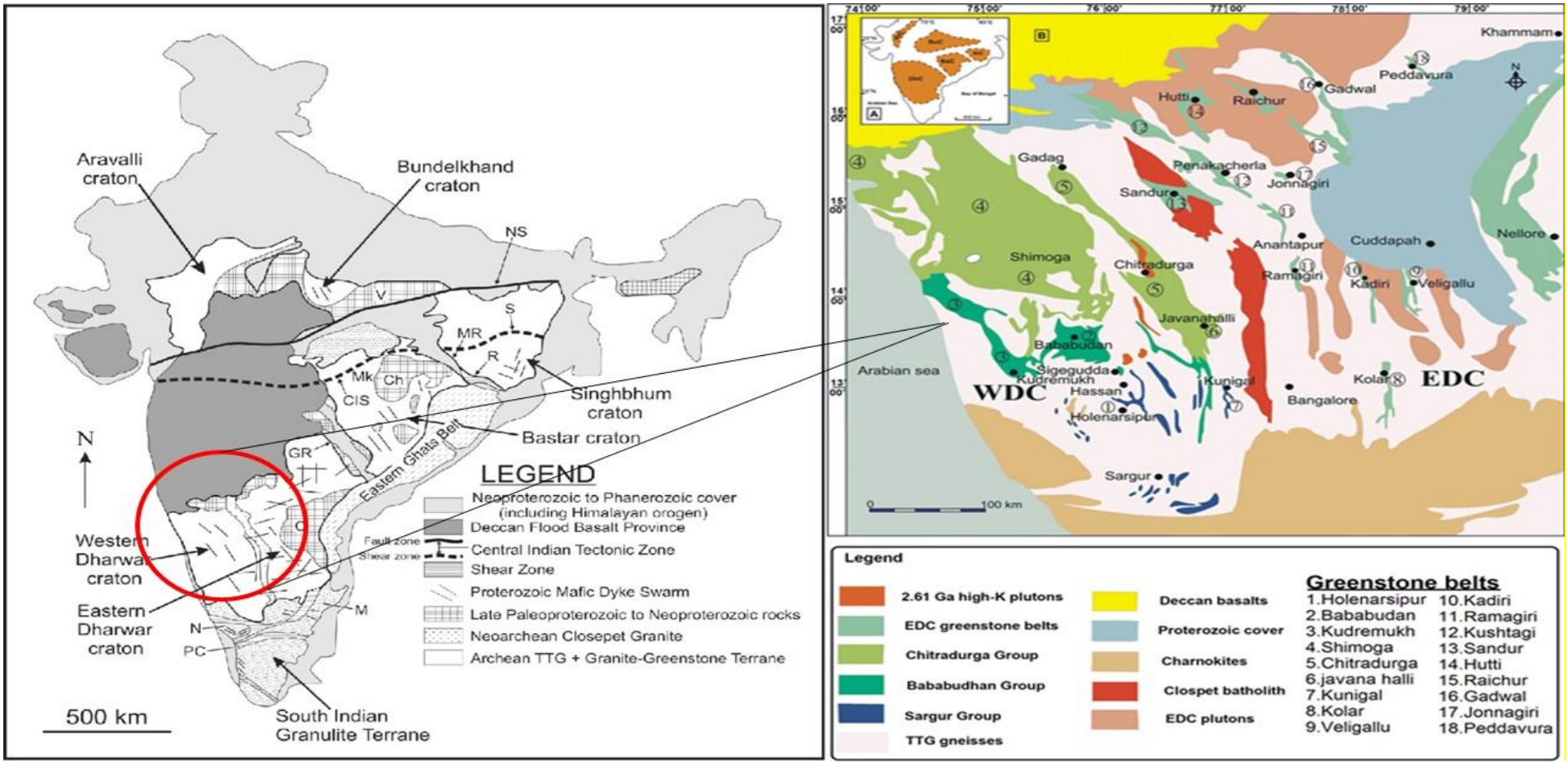

Figure 1.4: Generalised geological and tectonic map of the Indian shield showing the location of Dharwar craton (modified after French et al., 2008; Geological map of Dharwar Craton (Rajamanikam et al., 2014)

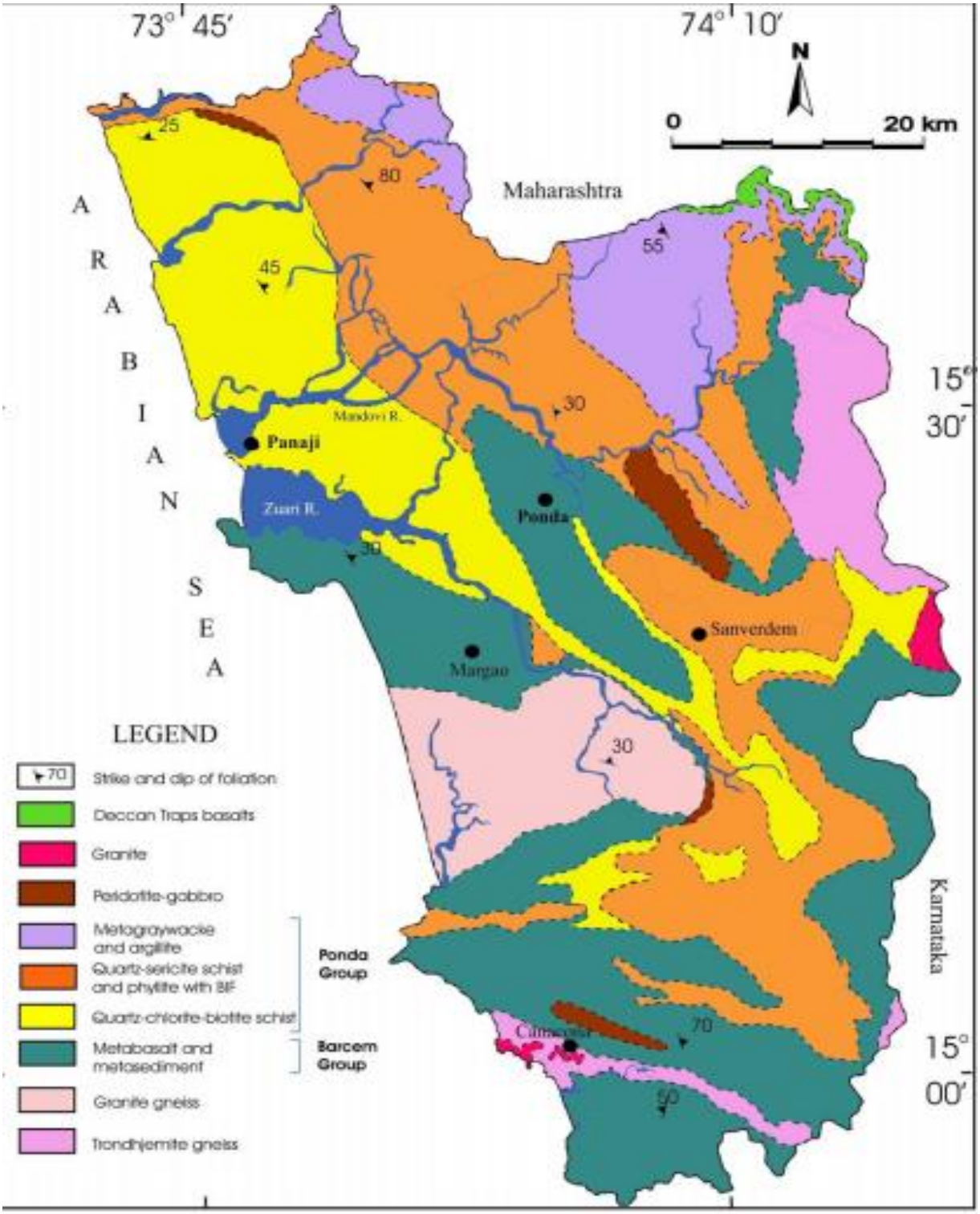

Figure 1.5: Geological Map of Goa (`GSI, 1996, by integrating arguments based on the field, petrological, geochemical and isotope data following the works of Dhoundial et al., 1987; Devaraju et al., 2007; 2010; Dessai et al., 2009).

Table 1.3: The presence of Gold in the WDC and parts of Konkan region

Work reported on presence of Gold in WDC and Konkan region	**References**
Association of Gold values from 0.06 to 0.16 ppm in laterite and powdery ore of Keri and Kalne village of Maharashtra	Umathay, 1993
Association of < 0.1 ppm Gold in laterite and iron ores in Sindhudurg district	Umathay, 1993
Occurrence of Gold in sulphidic BIFs ranging from 0.7 to 3.2 g/t	Sawkar et al., 1995
Huge studies on Gold bearing BIF in Karnataka region such as Shimoga belts, Chitradurga belt has been reported	Ganguly et al., 2015

1.2.4. Distribution of Iron ore In India

Total resources of iron ore in the country is around 28.52 Billion tonnes (National Mineral Inventory) as on 2010. Around 96% of hematite resources are confined in the States of Orissa (33.9%), Jharkhand (26.3%), Chhattisgarh (18.8%), Karnataka (12.3%), Goa (5.3%) and others such as Maharashtra, Uttar Pradesh, Rajasthan, Assam, etc. (3.4%) (IBM, 2011). Of the estimated 17.88 billion tonnes of hematite available, 8.09 billion tonnes (28%) are under 'reserve' category and 9.79 billion tonnes (in Goa only 713 Mt (5%)) under 'remaining resource' category. In India, around 70% of the hematite reserves, are located in the states of Orissa and Jharkhand only while, Chhattisgarh and Karnataka account for around 11% each of the hematite reserves (IBM, 2011). Whereas total resources of magnetite are estimated at 10.64 billion tonnes of which reserves are merely 0.02 billion tonnes (207 Mt) located mainly in Karnataka and Goa while 10.62 million tonnes (in Goa, 214 Mt, 2%) are remaining resources (IBM, 2011). Also, we need to look carefully at iron ore reserves in Goa quoted by Shah Commission or GSI which gives different figures in different reports. GSI, October 2006 report estimate the reserves of 730 Mt. Geological survey of India has reported 61 Gold and other metal mines in India. According to IBM (2012) total probable and proved iron ore (haemetite) in Goa is 469844 tonnes and 15675 tonnes of probable and proved iron ore (magnetite). Total remaining iron ore (haemetite) and iron ore (magnetite) resources in Goa is 457328 tonnes and 206998 tonnes.

1.3. Geological History of Goa

Goa has a rich and long geological record of the past. The oldest rock in India has been dated in the Anmod ghat to the east of the state at 3.4 billion (or 3400 million) years (Dhoundial, 1987) and this rock is a trondhjemite gneiss. Life had only just begun on the earth with some very primitive, simple microscopic organisms, that have left no definite clues of their existence. New rocks formed over 2500 million years ago (3000 to 2500 m.y.) on top and adjacent to the already exposed and eroding trondhjemite gneisses and today we call the remnants of these younger rocks (in and around Goa) 'The Dharwar Schists'. Continents and oceans have been reorienting and restructuring themselves, merging with one another and splitting apart throughout. A mega continent Pangaea had formed about 237 million years ago by accretion of older smaller continents into one single gigantic continental mass. Pangaea split into a northern continent called Laurasia which included North America, Europe and much of Asia and Gondwana land which included Antarctica, South America, Africa, India and Australia where Goa and India formed part of Gondwana land, the southern continent (Holmes, 1978). About 150 million years ago, India was slowly drawn away from Africa and Madagascar and Gondwana land began to split. About 80 million years ago, much before the advent of mankind, the Indian subcontinent split from Africa (Madagascar) and drifted North-Westwards. The Arabian Sea and the west coast of India were formed. The present-day topography and scenery have formed as a result of deposition, erosion, which varied according to the rock type and rock structure in the region. Preliminary investigations into the geological setting, petrography and geochemistry of BIF-hosted high-grade hematite iron ore deposits in South Africa, India, Western Australia and Brazil reveal distinct similarities, suggesting a very similar mode of

hydrothermal and supergene-modified hydrothermal origin for most BIF-hosted high grade hematite ore deposits (Beukes et al., 2003).

1.3.1. Gold occurrence

Gold occurs in India as lode Gold, in stratified sulphide deposits, in conglomerates, quartzites, in river placers, in laterite /weathering profile (Radhakrishna and Curtis 1991). The names such as suvarnarekha, Honnu hole, Suvarnavati, Ponnu Puzza which means Gold stream indicated that Indian rivers are great source of alluvial Gold. Occurrence of Gold as inclusion in amphiboles, in auriferous quartz in the beach sand of Chavakkad-Ponnani, Kerala Coast has been reported (Nayak 2011). The research has shown the appearance of both primary grains with jagged grain contours and secondary grains. The morphological, textural and chemical characteristics of Gold grains in stream gravels from the Siruvani River in Attappadi Valley, southern India has been reported (Nakagawa et al.,2005). In the Nilambur valley of Wynad Gold field in southern India, two types of Gold -bearing gravels have been found, the older one which are found at higher altitude and being richer in Gold and other types are the recent gravels (Santosh et al.,1992). Studies on the placer deposits of Attappadi valley in southern India has shown the presence of both primary and secondary Gold grains, and both these forms are differentiated by marked contrast in micro textures and chemical corrosive cavities (Nakagawa et al., 2005). Laterites have developed from Archean to lower Proterozoic Gold -rich formations under tropical climates on a transcontinental precambrium cratonic belt across the region of Africa, South America, India and Australia (Colin et al., 1997). Long term weathering of granites Gold rich quartz lenses, gneisses has led to the formation of laterites. Biofilm dominated by *C. metallidurans* were observed on the surface of Gold grain from moderate, sub-tropical and

wet-tropical zones in Australia (Reith et al., 2006, 2010). Gold grain formation model has been developed that integrates a primary origin with secondary mobilization and aggregation processes (Reith et al., 2010). There are reports on influence of biogeochemical processes on the transformation of Gold in arid environment (Fairbrother et al., 2012). In India, Wynad-Nilambur were the earliest Gold regions to be explored in state of Tamil Nadu and Kerala. In Nilambur region of south India scientist have reported the occurrence of supergene Gold associated with laterites weathering. The Gold grains associated with the laterite profile was found to be regular, rounded and also xenomorphic in nature. Gold is also recovered from the river terraces and residual laterites (Nair et al., 1987). During weathering the finest Gold particles are found migrating 70 cm into the saprolites as Gold has density 19.3 g/cm^3 being higher than other imported phases (Colin et al., 1997). Similar work has been reported in Australia on the occurrence of coarse, Ag-rich, primary, angular, secondary Gold in saprolite (Anand et al., 2019). Termites perform several activities that qualify them as soil engineers. Termites generally collect soil particles and minerals from the underlying rocks and thus transfer the geochemistry of the underlying rocks and mineralization to the termite mounds. Therefore, anomalies expressed by sampling termite mounds represent site-specific or in-situ mineralization (Arhin, 2010). The motivation of sampling termite mounds is based on the assumption that the mound building activity results in an upward transfer of clay, silt, sand and fine metal grain particles to the surface, a process opposite to leaching, which often results in significant mobilization and dispersion of trace elements (Arhin et al., 2015, 2018)**.** Termite mounds are surface mounds built from materials sourced from bedrocks at or near the water table below the lateritic cap and depositional material covers. Conventional geochemical exploration for Gold involves analysis of Gold and its pathfinder elements such as As, Sb, Bi, Hg, Cu, Pb and Zn and a

well-appointed laboratory is required for this, which is expensive in developing countries like Ethiopia. Hence, cost effective and simple methods of exploration are highly desirable. Termite mounds can be used in searching for economically important metals because it has been suggested that termite mounds might be used for geochemical prospecting in regions where thick regolith makes access to the bedrock difficult although the regolith in the study area is thin (Kebede, 2004). Stream sediment geochemistry and heavy mineral surveys are routinely used in the early stages of Gold (Au) exploration. The mobility and redistribution of elements in the secondary environment has been widely used as a tool for exploration especially in areas where weathering is intense and outcrops are rare. In state of Assam and Bihar, Gold associated with placer deposits has been reported in rivers such as Subarnarekha and Subansiri rivers (Radhakrishna and Curtis 1999; Radhakrishna 2002). Laterite is a rock found in tropical countries. Association of Gold with lateritic forms of rocks has been reported in Nilambur valley of Kerala and values from 0.06 to 0.16 ppm in laterite and powdery ore of Keri and Kalne, Sindhudurg district of Maharashtra (Umathay 1993). Laterite is a soil type rich in iron and aluminium, which forms mostly in tropical areas and is usually of rusty-red coloration as a result of high iron oxide content (Ingale & Savoikar, 2021). Earthworms are mentioned as one of the Uparasa in Indian Ayurvedic medicine due of their ability to take up heavy metals. In Rasagranthas, reference about Bhunaga satwa bhasma is explained as substitution to Tamra (Copper) bhasma (Patel et al., 2018), and different methods of Bhunag satwapatana are explained. Earthworms growing in copper mines are to be rubbed with guda, guggulu, laksha, una (wool), matsya, oil cakes (tilkhali) and tankan and made into a ball. This is to be dried to be heated, resulting in the discharge of a copper like essence. Ancient Indian alchemists knew about the properties of earthworms known in Sanskrit as Bhunaga as soil feeders and hyperaccumulators of heavy

metals. Probably they knew that the ash of the earthworms yield metals and metal oxides with some interesting and useful properties (Manojkumar, 2013). Physiographically diverse India with hundreds of soil subtypes sports a rich diversity of earthworms but there is comparatively very less work on soil feeding or geophagous earthworms and their unique behaviour. The earthworm fauna of India is well reported as compared to other Asian Countries. Presently, 451 valid species / subspecies of earthworms under 71 genera are known from the Indian territory, including the islands of Andaman, Nicobar and Lakshadweep (http://earthwormsofindia.com/). The ancient Greeks regarded the earthworms to play an important role in improving the quality of the soil. Earthworms participate in nutrient turnover by processing the organic matter and play a role in aeration and mixing of various soil horizons (Kiyasudeen et al.,2014). The drilosphere of geophagous earthworms involved in production of earthworms casts by dwelling inside soil and taking up of the organic and inorganic matters. The organic and mineral fraction bound to the organic matter are further subjected to hydrolytic decomposition by microbial and enzymatic actions inside the digestive track. The humification of organic matter occurs and ions are released which are available for plants whereas the mineralization occurs releasing the minerals which are further absorbed by tissue or further chelation and immobilization of metals. Earthworms in auriferous or heavy metal rich areas are likely to take in soil rich is secondary Gold which may pass through their gut and get deposited in the vermicasts and the whole cycle can get repeated several times. Previous studies have provided evidence for bioavailability of Gold nanoparticles from Soil and biodistribution within Earthworms (*Eisenia fetida*) and also trophic transfer of Gold nanoparticles from soil along a simulated terrestrial food chain (Urine et al., 2012). Potentiality of earthworms as bioremediating agent for nanoparticles has been reported earlier (Yadav, 2017). In India,

Gold mineralization of economic importance is mainly restricted to Archean greenstone terranes of the Dharwar Craton (DC). Studies on the geochemical characteristics of Gold bearing boninites and banded iron formations from Shimoga greenstone belt India has been reported (Ganguly et al., 2015). Shimoga greenstone terrane are linear volcanic and sedimentary centres surrounded by granite-gneissic basement rocks (Ganguly et al., 2016). Au grains occurs in quartz veins cutting across Kudrekonda meta volcanic rocks (Ganguly et al., 2016). Quartz and granite samples in Gadag greenstone belt (Dharwar craton) shows presence of pyrite and Gold in Ajjanahalli Gold deposit (Sarma et al.,2011). Arsenopyrite and pyrite with Gold attached to its rim associated with laminated quartz has been reported in Hutti-Maski greenstone belt (Kolb et al., 2005). Western, central and eastern auriferous zones of Gadag Gold field shows auriferous milky white vein quartz with rusty brown encrustations and bleb of native Gold in the vein quartz and native Gold inclusion within the arsenopyrite (Ugarkar et al., 2016). Wynad Gold Field shows auriferous quartz vein and Gold associated with in situ laterite (Krishnamurthi, 2012; Sahoo et al., 2016). The total reserves of Gold ore in India are shown in the **Table 1.5.** Geochronological data of Gold metallogeny revealed major periods of enrichment as Archaean and Proterozoic (Yang et al., 2003). Gold occurs in multiple geological environments settings such as greenstone belts, mantle derived intrusions, diaperic juvenile plutons and granulites. As per the Geological survey of India (GSI), prominent granite greenstone belts of Peninsular Sheild are located in Dharwar, Bastar, Singhbhum and Rajasthan cratons. The Dharwar craton, which is divided into eastern and western blocks hosts the maximum number of Gold occurrences. Primary Gold is progressively transformed by mechanical and (bio)geochemical processes, ultimately resulting in secondary grains and nuggets, which commonly occur in eluvial and alluvial deposits, so called placers and also in laterite, soil

and regolith. GSI has done a lot of work on Gold. Occurrence in variety of geological settings in India which is shown in **Table 1.4**. GSI has reported the presence of Gold in soil (0.035-4.25); termite mounds (0.025 to 0.07), pegmatite samples (0.035 to 0.25) and metabasalt 0.045 in ppm in Gadwal Schist Belt in Andra Pradesh (Murthy and Bhattacharjee, 1997). Previous work on Gold in Goa has been reported from different auriferous samples (Kamat, 2011a, b; 2012 a, b, c; 2015; 2018, 2019). In state of Assam and Bihar, Gold associated with placer deposits has been reported in rivers such as Subarnarekha and Subansiri rivers (Radhakrishna and Curtis 1999; Radhakrishna, 2002). There are reports on occurrence of Gold in the interstitial spaces of the sand grains as rounded, flattened and dendritic grains, ranging in size from 20 to 200 microns in archaean crystallines granites, gneisses, patches of greenstones and basic dykes, conglomerate, Bhima Basin, in state of Karnataka. Association of Gold with lateritic forms of rocks has been reported in Nilambur valley of Kerala and values from 0.06 to 0.16 ppm in laterite and powdery ore of Keri and Kalne, Sindhudurg district of Maharashtra (Umathay, 1993). Southern India has Gold favourable geology-Geological map of Dharwar Craton including the Kolar Greenstone Belt as **Fig 1.6**.

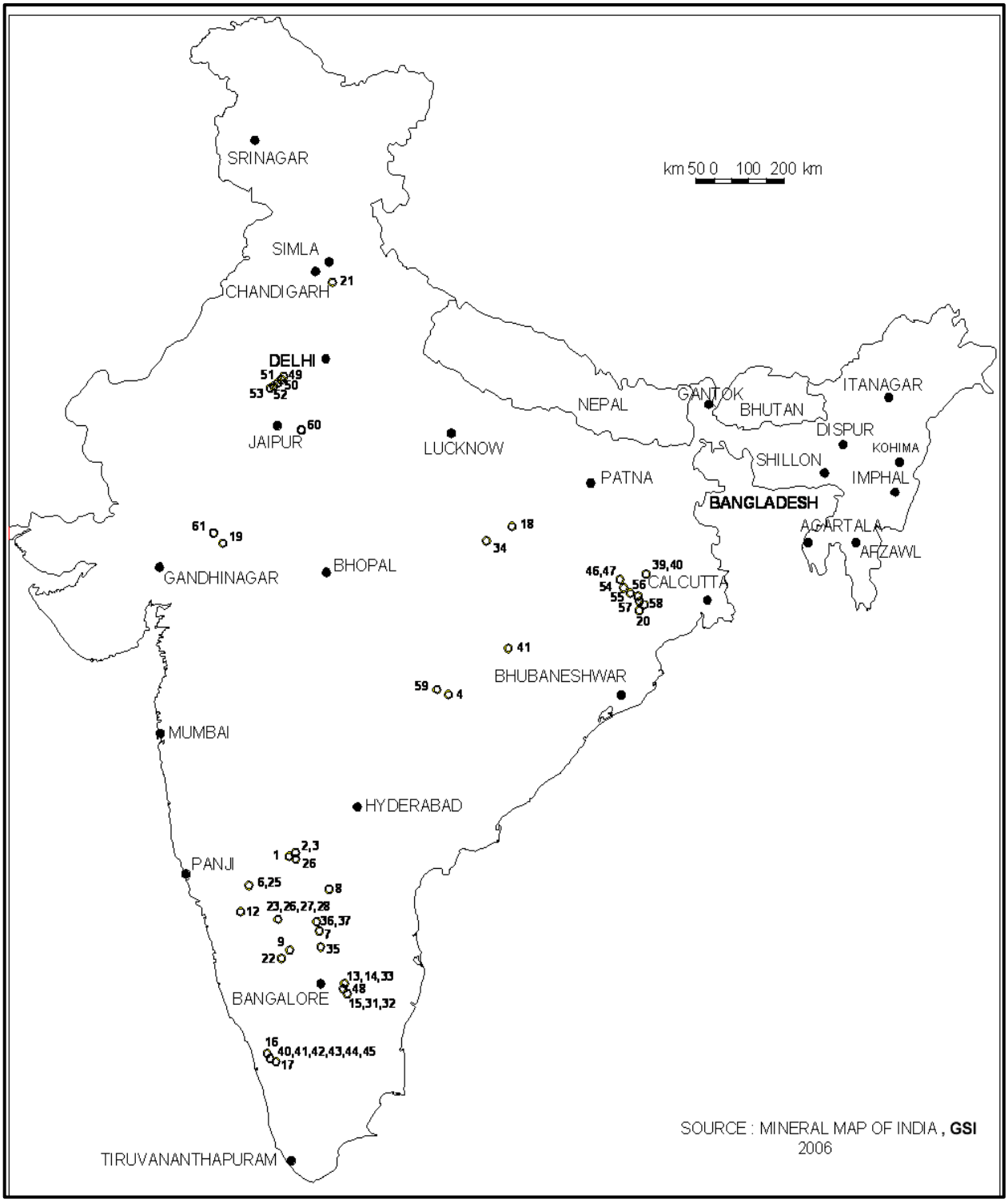

Figure 1.6: Gold in India -Southern India has Gold favourable geology-Geological map of Dharwar Craton including the Kolar Greenstone Belt (Source: http://www.portal.gsi.gov.in).

Table 1.4: Gold deposits In India

State	Area and Local Geology	Work on Gold	References
Uttaranchal	Sub greenschist to greenschist facies Metabasalt, Nainital District	Tiny Gold grains in disseminated fashion suggesting widespread hydrothermal activity	Shanker et al.,2002
Assam	Subarnarekha, Subansiri rivers	Placers deposits	Radhakrishna and Curtis, 1999
Bihar	1.Cu mines 2.Subarnarekha, Subansiri rivers	1. Association with copper, silver, cobalt 2. Placers deposits	Radhakrishna, 2002; Radhakrishna and Curtis, 1999
Rajasthan	1.Newania Carbonatite, Udaipur 2. Metalogenic rocks, dolomite-Sanjela-Manpur-Dugocha Belt, Salumber Area, Udaipur 3. Impure/amphibole-bearing marble and dolomite, Bhukia-Kundli	1. Evidence of Epithermal Activity and Gold Mineralization 2. Gold Mineralization in Paleoproterozoic Rocks, 3. Forms of fine specks and flakes (0.7 x 0.2 mm),	Golani and Pandit,1999; Nandan et al.,2003; Radhakrishna and Curtis, 1999

Madhya Pradesh	Malanjkhand	Disseminated Gold in intrusive sand volcanics	Radhakrishna and Curtis 1999
Gujarat	Cu mines	Studies on recovery as by-product during refining of copper	Radhakrishna, 2002
Orissa	Chromite ore	Occurrence in the form of grain in chromite ore	Rao et al., 2006
Andra Pradesh	Gadwal Schist Belt	Reported the occurrence in Soil (0.035-4.25); Termite mound (0.025 to 0.07), pegmatite samples (0.035 to 0.25) and metabasalt 0.045 in ppm	Murthy and Bhattacharjee 1997
Maharashtra	1.1aterite and powdery ore, Keri and Kalne 2. laterite and iron ores, Sindhudurg district	1. Association of Gold values from 0.06 to 0.16 ppm 2.< 0.1 ppm Gold	Umathay, 1993
Karnataka	1.Kolar 2.Archaean crystalline granites, gneisses, patches of greenstones and	1. Lode Gold associated with quartz-carbonate veins 2. Occurrence of Gold in the interstitial spaces of the sand grains as rounded, flattened and dendritic grains,	Radhakrishna and Curtis 1999; George 1995; Sawkar et al., 1995; Madusudan et al.,1994

	basic dykes, conglomerate, Bhima Basin 3. Conglomerates, graywacke, banded iron formation (BIFs) and laterite Chitradurga Schist Belt 4. Sericite-chlorite-phyllite/schist, argillites, greywackes and BIF. Hiriyur formation of Chitradurga Group	ranging in size from 20 to 200 microns 3. Occurrence in sulphidic BIFs ranging from 0.7 to 3. 2 g/t 4. Gold mineralization	
Kerala	1. Metamafic and metaultramafic rocks 2. Nilambur valley	1. Primary Gold mineralization is associated with quartz veins and veinlets intruding the amphibolites, talc- tremolite schists and iron-formations. 2. Association of Gold with lateritic forms of rocks	Nair 1993; Radhakrishna and Curtis1999

Table 1.5: Gold reserves in India

Mineral	**Reserves (MT)**	**Remaining resources (MT)**	**Total resources (MT)**
Ore (Primary)	24,124,537	469,570,375	493,694,912
Metal (Primary)	110.54	549.30	659.84
Ore (Placer)	-	26,121,000	26,121,000
Metal (Placer)	-	5.86	5.86

Source: Indian Bureau of mines (http://www.ibm.nic.in)

1.3.2. Biogeochemistry and Geomicrobiology of Gold

Gold is a chemical element with the symbol Au (from Latin: aurum) and atomic number 79, making it one of the higher atomic number elements that occur naturally. It is a bright, slightly orange-yellow, dense, soft, malleable, and ductile metal in a pure form. Chemically, Gold is a transition metal and a group 11 element. It is one of the least reactive chemical elements and is solid under standard conditions. Gold often occurs in free elemental (native) form, as nuggets or grains, in rocks, veins, and alluvial deposits. It occurs in a solid solution series with the native element silver (as electrum), naturally alloyed with other metals like copper and palladium, and mineral inclusions such as within pyrite. Less commonly, it occurs in minerals as Gold compounds, often with tellurium (Gold tellurides). Gold is resistant to most acids, though it does dissolve in aqua regia (a mixture of nitric acid and hydrochloric acid), forming a soluble tetra chloroaurate anion. Gold is insoluble in nitric acid, which dissolves silver and base metals, a property long used to refine Gold and confirm the presence of Gold in metallic substances, giving rise to the term acid test. Gold also dissolves in alkaline solutions of cyanide, which are used in mining and electroplating. Gold dissolves in mercury, forming amalgam alloys, and as the Gold acts simply as a solute, this is not a chemical reaction. Gold has the electronic configuration, Xe 4f145d106s1, and is unique in the group Ib elements (Cu, Ag, Au) in that it forms a number of high oxidation states. Its aqueous chemistry is in fact dominated by the Au (III) oxidation state and to a lesser extent by Gold (I). Organo Gold (lI) complexes have been studied in which the electron donors are sulphur-donor ligands or in which organic ligands coordinate Gold (II) in a complex having a dimeric Gold -Gold bond. The higher oxidation states are rather rarer. The only known Gold (IV) complex is the poorly characterized dinitrosyl Gold (IV) hexafluoride, (NO)zAuF6 (Sunder et at., 1979). Gold is the most malleable of all

metals. It can be drawn into a wire of single-atom width, and then stretched considerably before it breaks. Such nanowires distort via formation, reorientation and migration of dislocations and crystal twins without noticeable hardening. A single gram of Gold can be beaten into a sheet of 1 square metre (11 sq ft), and an avoirdupois ounce into 300 square feet (28 m^2). Gold leaf can be beaten thin enough to become semi-transparent. The transmitted light appears greenish blue, because Gold strongly reflects yellow and red. Such semi-transparent sheets also strongly reflect infrared light, making them useful as infrared (radiant heat) shields in visors of heat-resistant suits, and in sun-visors for spacesuits. Gold is a good conductor of heat and electricity. Gold has a density of 19.3 g/cm^3, almost identical to that of tungsten at 19.25 g/cm^3; as such, tungsten has been used in counterfeiting of Gold bars, such as by plating a tungsten bar with Gold, or taking an existing Gold bar, drilling holes, and replacing the removed Gold with tungsten rods. Common colored Gold alloys include the distinctive eighteen-karat rose Gold created by the addition of copper. Alloys containing palladium or nickel are also important in commercial jewellery as these produce white Gold alloys. Fourteen- and eighteen-karat Gold alloys with silver alone appear greenish-yellow and are referred to as green Gold . Blue Gold can be made by alloying with Iron, and purple Gold can be made by alloying with aluminium. Less commonly, addition of manganese, indium, and other elements can produce more unusual colors of Gold for various applications. Gold is a precious metal that is valued for its beauty as well as being conductive and malleable. These properties make Gold valued both in industry and in economics. Gold occurs in free elemental form as well as nuggets or grains in rocks, veins and in alluvial deposits. Gold is a noble metal with the average concentration in the earths crustal rocks and soils to be 5ng g-1 (Gold schmidt, 1954). Gold occurs in solid solution series with silver and naturally alloyed with copper and palladium. Gold

occurs naturally in the universe and thought to be produced in supernova nucleosynthesis and have to be present in the dust from which it is formed. On earth, Gold occurs in two forms primary and secondary forms. Primary form Gold occurs in the biosphere widely and in various rocks such as in case of igneous rocks (<50 mg.103 Kg^{-1}), sedimentary rocks (< 200 mg.103Kg-1), metamorphic rocks (Korubushkina et al., 1983). Under Earth surface conditions, primary Gold is progressively transformed by mechanical and (bio)geochemical processes, ultimately resulting in secondary grains and nuggets, which commonly occur in eluvial and alluvial deposits, so called placers (Southam et al.,2009; Reith et al.,2013). Secondary Gold is highly pure (>99 wt. % Au), finely crystalline (0.01–5μm), and occurs as nano-particulate, bacteriomorphic, sheet-like and wire Gold, as well as euhedral, hexagonal, octahedral and pseudo-trigonal micro-crystals, which can aggregate to form mm-sized grains (Reith et al., 2005; Falconer and Craw 2009; Southam et al.,2009). Microorganisms capable of actively solubilizing and precipitating Gold appear to play a larger role in the biogeochemical cycling of Gold than previously believed. Recent research suggests that bacteria and archaea are involved in every step of the biogeochemical cycle of Gold, from the formation of primary mineralization in hydrothermal and deep subsurface systems to its solubilization, dispersion and re-concentration as secondary Gold under surface conditions. Bacteria, archaea, fungi and algae play critical roles in driving the carbon-, nitrogen, sulfur-and phosphorus- cycles as well as many metal cycles (Ehrlich 1998). A variety of mineral oxidizing bacteria (iron oxidizing such as *Acidithiobacillus ferrooxidans, Leptospirillum ferrooxidans* and *Leptospirillum ferriphilum*, the sulfur-oxidizing *Acidithiobacillus thiooxidans* and *Acidithiobacillus caldus*) are known to break down Gold -hosting sulfide minerals in zones of primary mineralization and release the associated Gold. These microbes form biofilm on metal sulphides such as Gold bearing

pyrites and arsenopyrites and obtain metabolic energy through metabolic pathways such as Sulphur oxidase pathways (*Sox)* and reverse *Dsr* pathways (Friedrich et al. 2005). Morphological and media studies of Mogo mine soils has indicated the presence of microorganisms which may be actively mediating a Gold cycle, bacteria and fungi were found to be capable of precipitating Gold colloidal solutions (Reith, 2006). *Ralstonia eutropha* also known as *Cupriavidus metallidurans*, *Wautersia*, and *Alcaligens eutrophus* (Vandamme and Coenye 2004) is a facultative chemolithoautotrophic b-proteobacterium having high tolerance ability to heavy metals (Janssen et al., 2010). This unique property of bacteria makes it the organism of priority for biomineralization of heavy metals from the respective toxic forms from the environment. In moderate and wet tropical climatic zones of Australia, *C. metallidurans* was detected in biofilm formed on the surface of Gold grains which indicated that bioaccumulation may lead to Gold biomineralization by forming secondary "bacteriomorphic" Gold and increasing the duration of viable *C. metallidurans* cell exposure to Au(I)-complexes results in an increased amount of Gold uptake (Reith et al., 2006). *Chromobacterium violaceum* is a Gram-negative non-pathogenic bacterium (facultative anaerobe) found in tropical and subtropical areas of several continents (Kothari et al.,2017; Liu et al., 2016). *C. violaceum* produce cyanide as a secondary metabolite and this property serves to degrade cyanide and thus has been found to be the most effective for the bio-dissolution of Gold from different materials because of its cyanide-associated metabolic activities. Previous studies have shown that *C. violaceum* and *Bacillus megaterium* are known to synthesize the enzyme b-cyanoalanine synthase which converts cyanide into b-cyanoalanine during the late stationery and death phase. Therefore, this strain can potentially be used in ecological Gold recovery methods (Durans et al., 2010).

1.3.3. Microbially mediated formation of secondary Gold

The origin of coarse Gold grains and nuggets has long been the subject of discussion among geologists studying placer deposits. Three models have been established to explain their formation: detrital origin, chemical accretion and a combination of both (Southam et al., 2009). One major problem is that Gold grains in supergene environments are commonly coarser grained, that is, larger, than that observed in potential source rocks (Mossman et al.,1999; Falconer et al., 2009; Southam et al., 2009; Reith et al., 2007). A second problem is the wide range of morphologies associated with secondary Gold, which are not commonly observed in source ore deposits. These morphologies include wire, dendritic, octahedral, porous and sponge Gold (Reith et al., 2007; Fairbrother, 2013).

1.3.4. Direct associations between secondary Gold and bacteria

One of the study of untreated secondary Gold grains from two field sites has provided this important link; using SEM and CSLM combined with nucleic acid staining, bacterial pseudomorphs and active bacterial biofilms, respectively, were revealed on the surfaces of these grains (Reith et al., 2006). Molecular profiling showed that unique, site-specific bacterial communities are associated with Gold grains that differ from those dominating the surrounding soils. 16S rDNA clones belonging to the genus *Ralstonia* and bearing a 99% similarity to *C. metallidurans* were present on all DNA-positive Gold grains, but were not detected in the surrounding soils (Reith et al., 2006). The ability of *C. metallidurans* to actively accumulate Gold from solution was successfully tested suggesting that *C. metallidurans* may contribute to the formation of secondary Gold grains (Reith et al., 2006). Octahedral plate-like secondary Gold platelets are common in oxidized zones surrounding primary deposits (Reith et al., 2007; Fairbrother, 2013). Schematic model showing the

development and effect of Gold cycling biofilm on Gold grain surfaces (Rea et al., 2016) is shown in the **Fig 1.7.** The process of Bacterioform Gold formation is given in the **Fig 1.8.**

1.4. Research work of Frank Reith and work on Bacterioform Gold

Gold occurs widely in the biosphere and in minute amount in various rocks such as Igneous rocks which contains less than 50 mg.103 kg-1 (Zvyagintzev, 1941), Sedimentary rocks contains less than 200 mg.103 kg-1 of Gold (Zvyagintzev, 1941). Earth crust contains approximately 4.3 mg.103 kg-1 whereas waters of rivers, waters of auriferous deposits contain 0-3 mg.103 kg-1 (Zvyagintzev, 1935). Microbe-driven biogeochemical cycle for Gold has been proposed by Reith et al.,2006. In this biogeochemical cycle, the dissolution and precipitation of Gold in surface to near-surface environments are often directly linked to the transformation of iron and sulphur compounds (Southam and Saunders, 2005). Bacteria can actively oxidises metals by interacting with a metal stressed environment in which the metals are used in dissimilatory metabolic reactions (Shuster, 2005; Pandey & Natarajan, 2015; Natarajan, 2018). He described himself more simply as, “the man with the Gold bug”. Frank was awarded a prestigious Australian Research Council (ARC) Postdoctoral industrial fellowship for his research project, bacterial mechanisms of Gold mobilisation and precipitation with applications to mineral processing and exploration. Frank led an ARC Linkage Project that involved the collaboration between UA, Newmont, Barrick Gold, the South Australian Museum, and a network of interdisciplinary colleagues across the globe and this collaboration successfully developed a live cell biosensor that could detect Gold concentrations down to 1 ppb. The work done by Frank Reith is put in the **Fig 1.9.** There are various techniques used to study the Gold in the auriferous soil and microbes present on the surface of the Gold and it is given in the **Table 1.6** and in **Fig 1.10.**

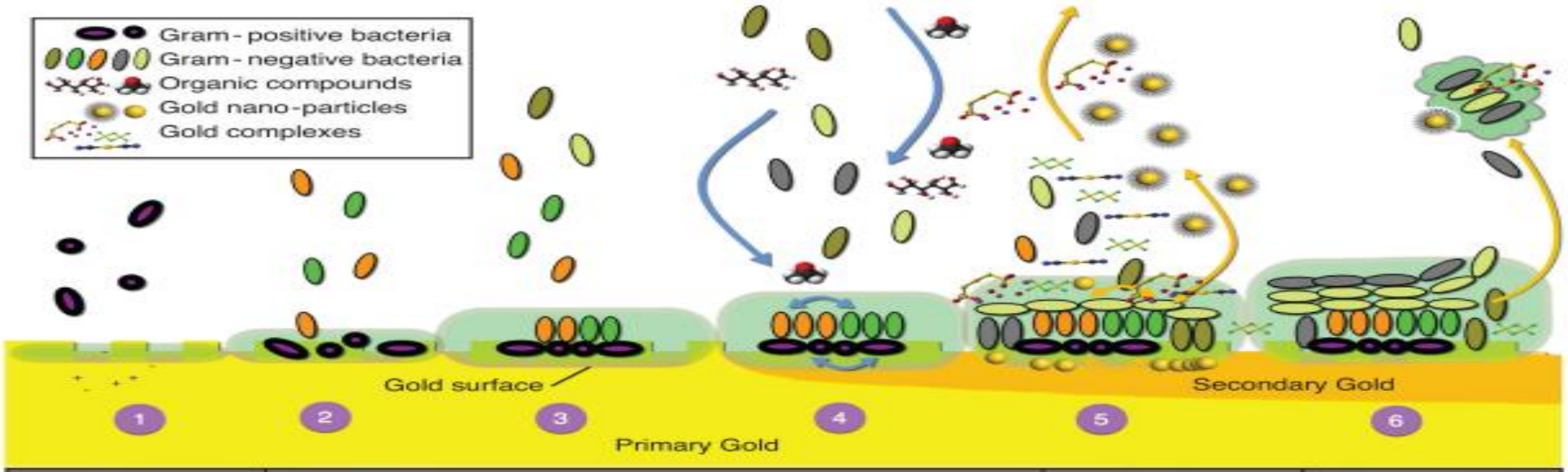

1. Surface Conditioning	Biofilm growth and recruitment			5. Gold mobility	6. Dispersal cells
	2. EPS production (E) Auto-aggregation (A)	3. Nutrient cycling C-fixation (C) N_2-fixation (N) Nitrification (NI) Denitrification (D)	4. Metabolic turnover of complex organics (O); xenobiotic (X), toxins (T)	Gold solubilisation (S) Gold detoxification (G) Metal resistance (M)	
Arthrobacter spp. *Corynebacterium* sp. *Deinococcus* sp. *Kocuria* sp. *Microbacterium* spp. *Micrococcus* spp. *Propionibacterium* spp. *Staphylococcus* spp.	*Pseudomonas* spp. (E) *Burkholderia* spp. (E) *Methylobacterium* sp. (E) *Acinetobacter* spp. (E) *Sediminibacterium* spp. (A) *Rhodobacter* sp. (A)	*Rhodobacter* sp. (C) *Beijerinckia* sp. (N) *Rhizobium* spp. (N) *Herbaspirillum* sp. (N) *Pelomonas* sp. (N) *Nitrobacter* sp. (NI) *Diaphorobacter* sp. (NI,D) *Acidovorax* sp. (D) *Achromobacter* sp. (D) *C. metallidurans* (D) *S. maltophilia* (D) *Pseudomonas* spp. (D)	*Acinetobacter* spp. (O) *Burkholderia* spp. (O) *Pelomonas* sp. (O) *Pseudomonas* spp. (O) *Sphingobium* sp. (O) *Sphingomonas* spp. (O) *Arthrobacter* sp. (X) *Diaphorobacter* sp. (X) *Phenylobacterium* sp. (X) *Xanthomonas* sp. (X) *Methylobacterium* sp. (T)	*Diaphorobacter* sp. (S) *Sphingomonas* spp. (S,M) *Methylobacterium* sp. (S) *C. metallidurans* (G) *D. acidovorans* (G) *S. maltophilia* (G) *Achromobacter* spp. (M) *Halomonas* sp. (M) *Herbaspirillum* sp. (M) *Burkholderia* spp. (M) *Shewanella* sp. (M) *Acinetobacter* spp. (M) *Pseudomonas* spp. (M) *Ideonella* sp. (M)	*Acinetobacter* spp. *Lysobacter* sp. *Duganella* sp.

Figure 1.7: Schematic model showing the development and effect of Gold cycling biofilm on Gold grain surfaces (Rea et al., 2016)

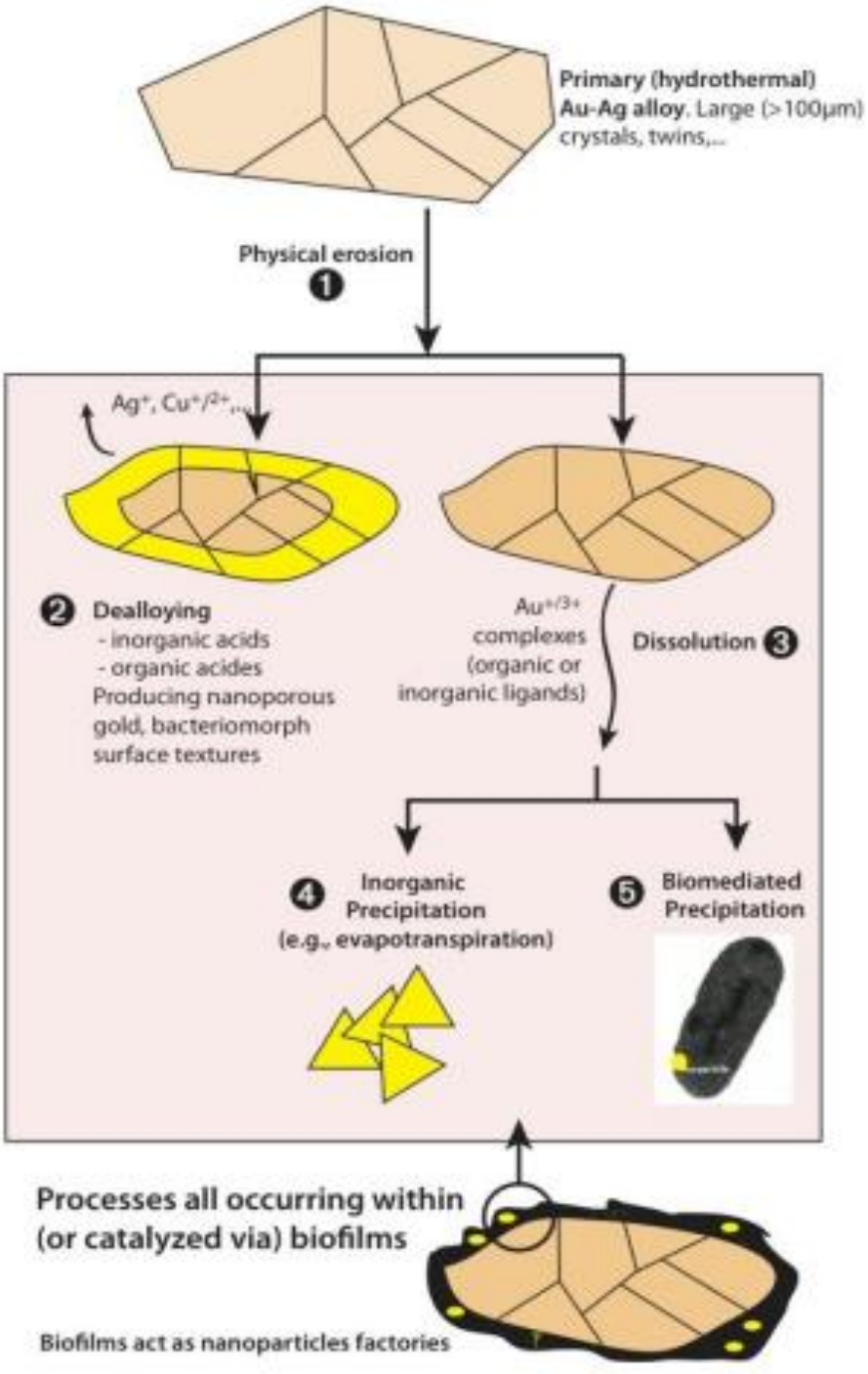

Figure 1.8: Process of formation of Bacterioform Gold (Reith et al., 2013)

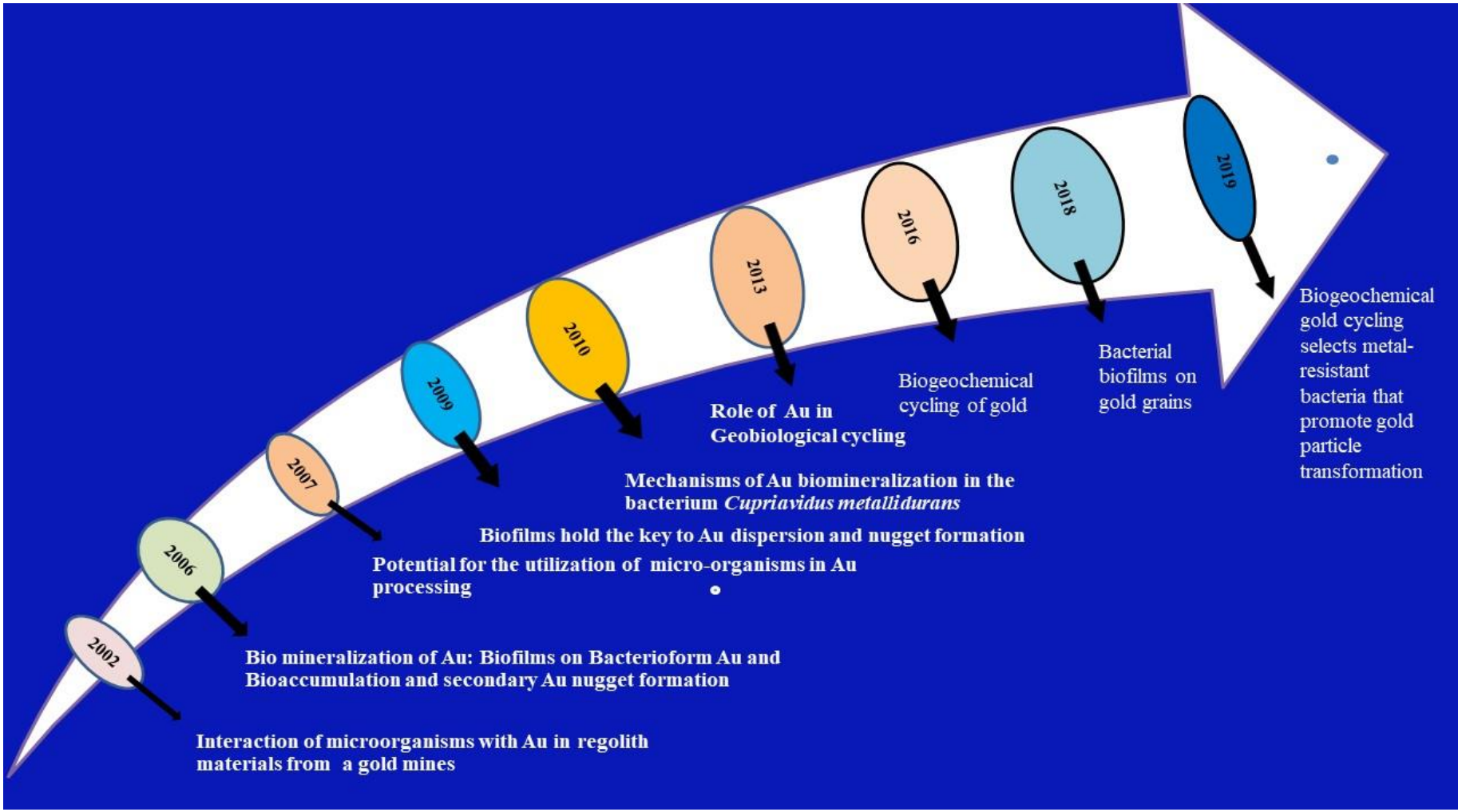

Figure 1.9: Research by Australian Gold geomicrobiologist Frank Reith

Table 1.6: Techniques used to study secondary Gold forms

Technique used	Types of samples	Country	Reference
1.Scanning electron microscope (SEM) 2.SEM-EDX 3. PCR 4.DGGE 5. UV confocal stereo laser microscope (CSLM)	Gold grains and auriferous soils	Tomakin Park Gold Mine in New South Wales and Hit and Miss Mine in the Palmer River Gold fields in northern Queensland-Australia	Reith et al., 2006
16S rRNA gene next generation sequencing	Gold grains and auriferous soils	Australia	Reith, 2007
LA-ICP-MS	Gold grains and auriferous soils	Australia	Reith, 2007
HPLC-ICP-MS	Gold grains and auriferous soils	Australia	Reith, 2007

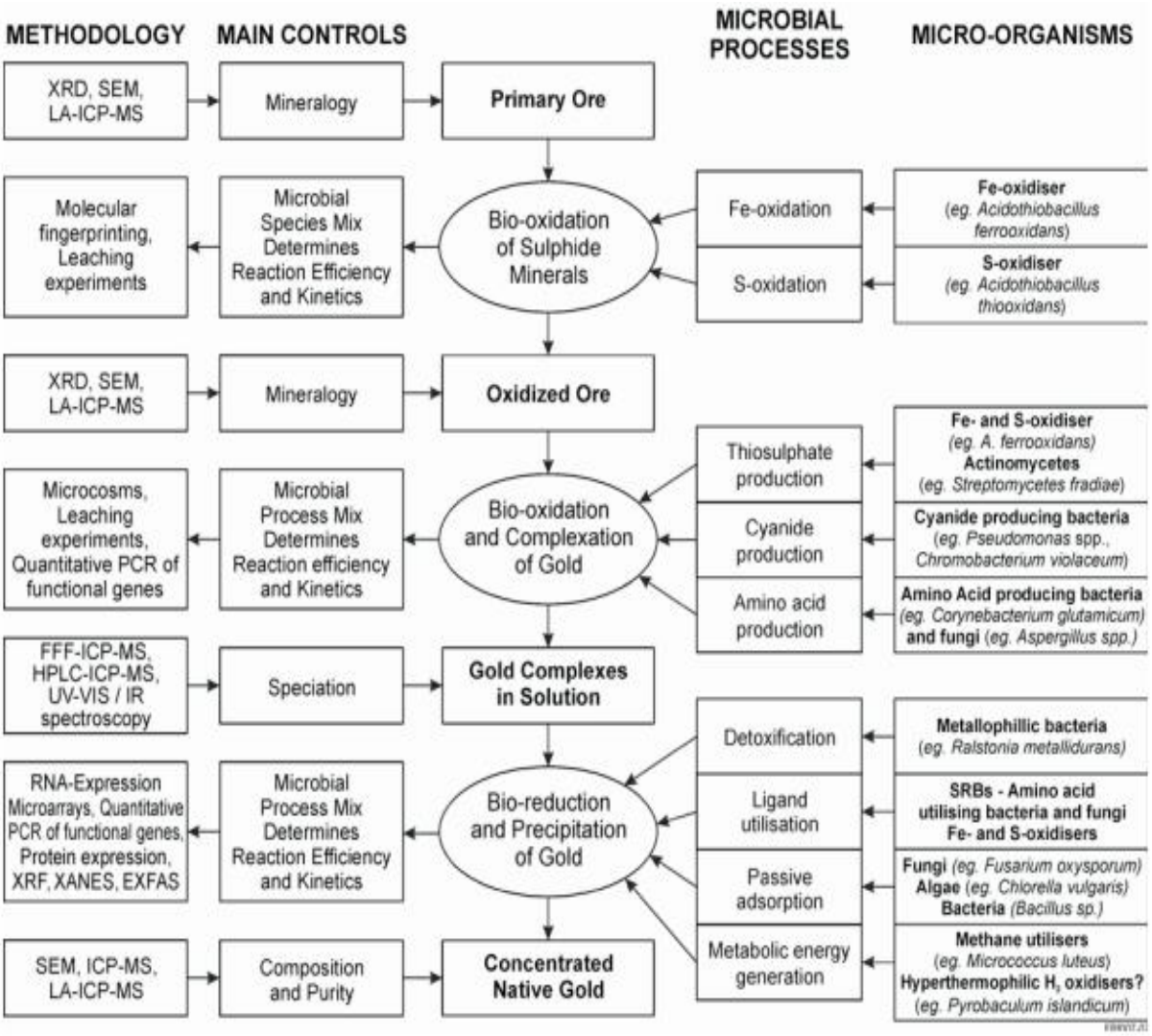

Figure 1.10: Techniques used in the study of Bacterioform Gold (Reith, 2006)

Part B. Gold nanoparticles synthesis

1.5.1. Gold nanoparticles

Nanotechnology research is one of the major emerging areas of research with its application in science and technology for the purpose of manufacturing new materials at the nanoscale level (Albrecht et al., 2006). Nanotechnology deals with the production and stabilization of various types of nanoparticles. Nanoparticles are usually 0.1–1000 nm in each spatial dimension and are commonly synthesized using two strategies: top–down and bottom–up (Manivasagan et al., 2016). In the top– down approach, the bulk materials are gradually broken down to nanosized materials whereas in the bottom-up approach, atoms or molecules are assembled to molecular structures in nanometer range. Bottom–up approach is commonly used for chemical and biological synthesis of nanoparticles. At present, there exists a need to develop eco-friendly processes for the synthesis of nanoparticles. Therefore, the attention of the researchers is shifted from physical and chemical processes towards 'green' chemistry and bioprocesses. These methods employ plants or microorganisms which are inexpensive, easily available, simple to grow, and safe to handle. Nanoparticles are smaller than 1 mm in diameter (typically 5–500 nm), the larger microbeads are 0.5–500 mm in diameter. Noble metal nanoparticles (Gold, silver, ruthenium, platinum, copper, and palladium) in particular, are versatile agents with a variety of biomedical applications including their use in highly sensitive diagnostic assays, thermal ablation, and radiotherapy enhancement, as well as drug and gene delivery.

1.5.1. Mechanism of Gold nanoparticle synthesis using microbes

Many review articles have been published to describe different ways of biosynthesizing nanoparticles, especially microorganisms. Research demonstrates how diverse group of metal nanoparticles as well as their alloys are biologically blended by bacteria, fungi, actinomycetes,

and yeasts. Preparation of nanoparticles using green chemistry approach is advantageous over physical and chemical methods owing to its environmental significance. In the biological methods, it is found that the extracts of living organisms act both as reducing and capping agents in the synthesizing process of the nanoparticles. The reduction of metal ions in combination with biomolecules found in the extracts of enzymes/proteins, amino acids, polysaccharides, and vitamins is environmentally benign, it is difficult to understand the mechanism of the biochemical reaction. In this regard rapid and green synthetic methods using biological extracts have gained more importance in nanoparticle synthesis. **Fig 1.11** shows the mechanism of synthesis of GNPs. Nanoparticles are generally characterized by their size, shape, surface area, and dispersity (Jiang et al., 2009). A homogeneity of these properties is important in many applications. The common techniques of characterizing nanoparticles are UV–visible (UV–VIS) spectrophotometry, dynamic light scattering (DLS), field emission scanning electron microscopy (FE-SEM), energy dispersive X-ray (EDX) analysis, transmission electron microscopy (TEM), Fourier transform infrared spectroscopy (FTIR), and powder X-ray diffraction (XRD) (Kim et al., 2008). UV–VIS spectroscopy is a commonly used technique (Pal et al., 2007). Light wavelengths in the range of 200– 800 nm are generally used for characterizing various metal nanoparticles in the size range of 2–100 nm (Manivasagan et al., 2016). DLS is used to characterize the surface charge and the size distribution of the particles suspended in a liquid (Jiang et al., 2009). Electron microscopy is another commonly used method of characterization (Cao, 2004). Scanning electron microscopy and TEM are used for morphological characterization at the nanometer to micrometer scale (Eppler et al., 2000; Schaffer et al., 2009). Elemental composition of metal nanoparticles is commonly established using energy dispersive spectroscopy (EDS) (Strasser et al., 2010). XRD is used for the phase identification and characterization of the crystal structure of the nanoparticles (Sun et al.,

2000). X-rays penetrate into the nanomaterial and the resulting diffraction pattern is compared with the standards to obtain the structural information. FTIR spectroscopy is useful for characterizing the surface chemistry (Chithrani et al., 2006).

1.5.2. Gold nanoparticle synthesis using bacteria

Micro-organisms can be used for biosynthesis of Gold nanoparticles either extracellularly or intracellularly. Extracellular method is most popular as it eliminates various processing steps required for recovery of Gold nanoparticles. In extracellular biosynthesis, after the subculture of micro-organisms for 1–2 days, the culture is centrifuge to remove the biomass. The Gold nanoparticles can be synthesized by adding supernatant to auric salt solution. The Gold nanoparticles synthesis can be monitored by change in colour of culture media from ruby red to deep purple colour. After bio reduction, the Gold nanoparticles can be collected by similar methodologies as in plant extract mediated synthesis. Synthesis of Gold nanoparticles using biogenic agents (plants and micro-organisms) is an eco-friendly method and this method requires only a short period for the conversion of metal ions into nanoparticles.

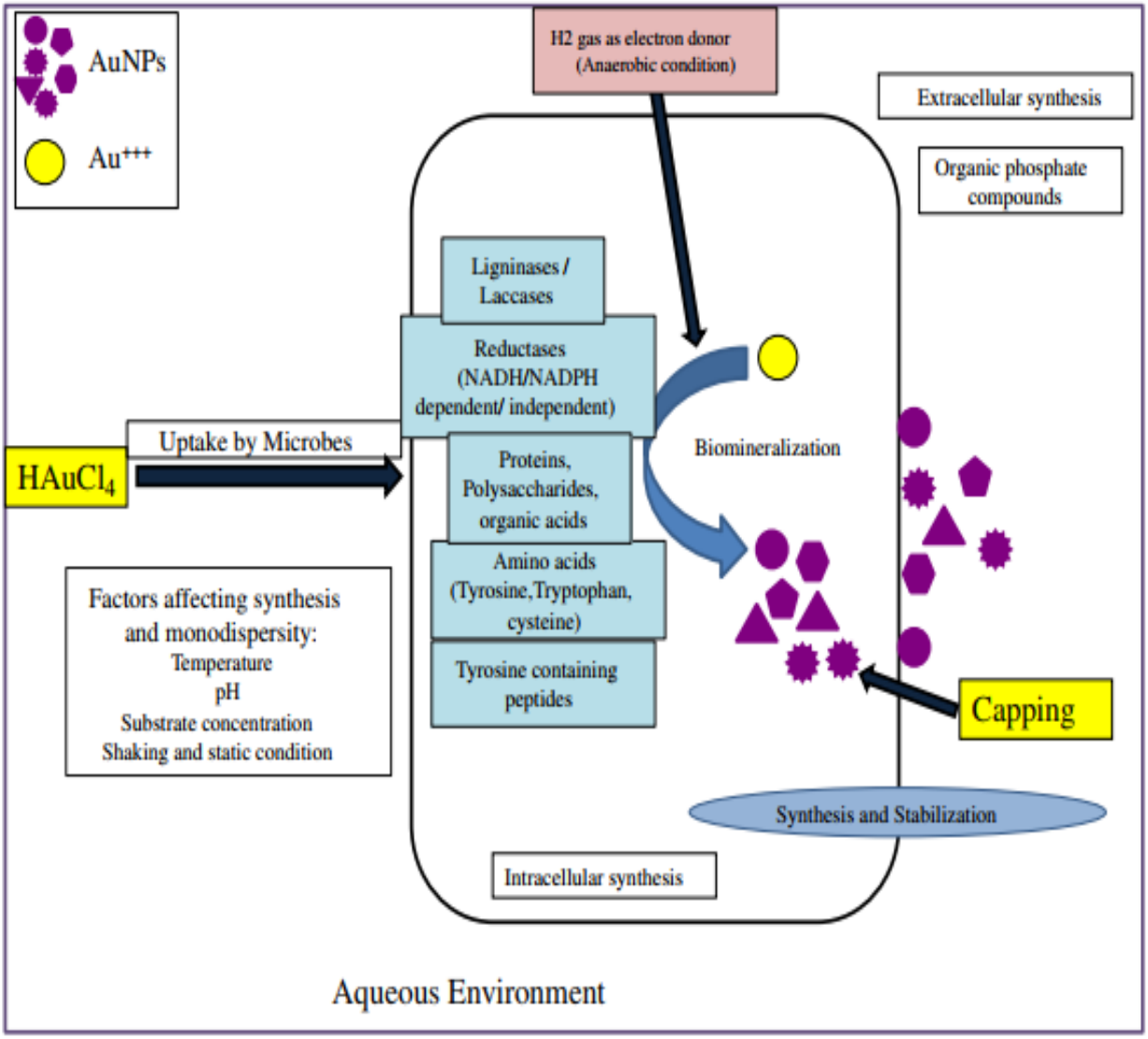

Figure 1.11: Biosynthesis of Gold nanoparticles (Panda et al., 2011)

1.5.3. Techniques used for characterization of GNPs

Two broad approaches are used for the synthesis of nanoparticle top-down approach and bottom-up approach. In top-down approach, there occurs the material size reduction of particles via the physical and chemical process to produce nanoparticles. The shape, size, overall physiochemical properties and surface structure are processed throughout the process (Meyers et al., 2006; Qiu et al., 2022). Bottom-up approach deals with engineering at atomic, molecular level (Andreo et al., 2022). Nanoparticles of different size, shape, surface area are characterized by various techniques like UV-visible spectroscopy (UV-VIS). UV spectra wavelengths range between 300 and 800 nm depicts the presence of various metallic nanoparticles of size range 2 nm to 100 nm. Generally, Gold nanoparticles are detected by peak range between 500 and 580 nm (Mishra et al., 2012). Powder X-ray diffraction (XRD), Fourier transform infrared spectroscopy (FT-IR), Gas chromatography mass spectrometry (GC-MS), High performance liquid chromatography (HPLC), energy dispersive spectroscopy (EDS). Dynamic light scattering (DLS) estimates the size distribution and quantifies the surface charges of nanoparticles. Element composition is the determination by EDAX analysis. Zeta potential, scanning electron microscopy (SEM), transmission electron microscopy (TEM), atomic force microscopy (AFM) (Reshawn et al, 2022). XRD identifies the crystallite size. FTIR Spectroscopy identifies the surface residues and functional groups like flavonoid, phenol, hydroxyls which attach to the surface of nanoparticles during the course of their synthesis for their efficient reduction and stabilization.

1.5.3. Nanoparticle synthesis using Actinobacteria

Actinobacteriology is one of the important emerging areas of research in tropics. Actinobacteria are aerobic, non-motile, Gram-positive, often filamentous, bacteria known for their unsurpassed capacity for the production of secondary metabolites with various biological activities (Zotchev, 2012). Many representatives of the order Actinomycetales are prolific producers of thousands of biologically active secondary metabolites (Manivasagan et al.,2013b). Recently, actinobacteria isolated from different ecosystems have been recognized as the potential synthesizers of metal nanoparticles and biosynthesis of nanoparticles has been reported in *Thermomonospora* sp. (Manivasagan, 2016), *Streptomyces hygroscopicus* (Sadhasivam et al., 2012), *Rhodococcus* sp. (Ahmad et al., 2003), *Streptomyces viridogens* (HM10) (Balagurunathan et al., 2011), *Nocardia farcinica* (Oza et al.,2012), *Streptomyces naganishii* (MA7) (Shanmugasundaram et al., 2013), *Streptomyces* sp. (Karthik et al., 2014), *Nocardiopsis* sp. MBRC-1 (Manivasagan et al., 2013a), and *Streptomyces avidinii* (Park et al.,2006). Use of bacteria for Gold nanoparticle synthesis is given in **Table 1.7.** Whereas use of Actinobacteria for Gold nanoparticle synthesis is given in **Table 1.8.**

1.5.5. Gold nanoparticle synthesis using Yeasts

Fungi and yeast are very effective secretors of extracellular enzymes and number of species grow fast and therefore culturing and keeping them in the laboratory are very simple. They are able to produce metal nanoparticles and nanostructure via reducing enzyme intracellularly or extracellularly. Due to the mass production of NPs as the easiness of controlling yeasts in laboratory circumstances, the synthesis of numerous enzymes and rapid growth with the use of simple nutrients, the yeast strains possess more benefits over bacteria. To synthesize silver and Gold NPs, yeast strains have been utilized and the list of the same is given in **Table 1.9**.

Table 1.7: Use of bacteria for Gold nanoparticle synthesis

Bacterial strain	Family	Size (nm)	Shape	Reference
P. aeruginosa (ATCC 90,271)	Pseudomonadaceae	50–30	-	Jayaseelan et al.,2013
Pseudomonas denitrificans	Pseudomonadaceae	25-30	Spherical	Bennur et al., 2016
Pseudomonas fluorescens 417	Pseudomonadaceae	5-50	Spherical	Husseiny et al., 2007
Pseudomonas veronii AS41G	Pseudomonadaceae	5-25	-	Mewada et al., 2012
Rhodopseudomonas capsulata	Rhodospirillaceae	10-20	Spherical	Syed et al., 2016
Shewanella algae (ATCC 51181)	Shewanellaceae	9.6	Spherical	Mishra et al., 2011
Bacillus	Bacillaceae	20-50	Spherical	Zhang et al., 2016
Escherichia coli *Proteus mirabilis*	Enterobacteriaceae	11.8-130 321	Spherical	Cai et al., 2011
Escherichia coli DH5a	Enterobacteriaceae	20	Spherical	Fayaz et al., 2011
Escherichia coli	Enterobacteriaceae	5-20	Spherical	Arshi et al., 2011
Klebsiella pneumonia	Enterobacteriaceae	5-65	Spherical	Malarkodi et al., 2013
Bacillus stearothermophilus	Bacillaceae	5-30	Triangular	Fayaz et al., 2011
Spirulina platensis	Phormidiaceae	5	Spherical	Kalabegishvili, 2012

Stenotrophomonas maltophilia	Xanthomonadaceae	5-65	Spherical	Nangia, 2009
Geobacillus stearothermophilus	Bacillaceae	5-30	Spherical	Manikprabhu, 2017
Magnetospirillum gryphiswaldense MSR-1	Rhodospirillaceae	10-40	Spherical	Cai et al., 2011
Shewanellao neidensis	Shewanellaceae	2-50	Spherical	Menon et al., 2017
Sporosarcina koreensis DC4	Planococcaceae	30-50	Spherical	Singh et al., 2016
Staphylococcus epidermidis	Planococcaceae	20-25	Spherical	Srinath et al., 2015

Table 1.8: Use of Actinobacteria for Gold nanoparticle synthesis

Actinomycete strains	Family	Size (nm)	Shape	Reference
Thermomonospora	Thermomonosporaceae	8	Spherical	Ahmad et al., 2003
Streptomyces hygroscopicus	Streptomycetaceae	20	Spherical	Sadhasivam et al., 2012
Gordoniaamarae	Gordoniaceae	15–40	Spherical	Bennur et al., 2016
Streptomyces fulvissimus	Streptomycetaceae	20-50	Spherical	Soltani et al., 2015
Streptomyces viridogens (HM10)	Acidothermaceae	18-20	Spherical and rod	Balagurunathan, et al., 2011
Rhodococcus sp.	Nocardiaceae	5–15	Spherical	Ahmad et al., 2003b
Streptomyces viridogens	Streptomycetaceae	18–20	Spherical	Balagurunathan et al., 2011
Thermomonospora sp.	Thermomonosporaceae	8	Spherical	Ahmad et al., 2003b
Streptomyces hygroscopicus	Streptomycetaceae	10-20	Spherical	Sadhasivam et al., 2012
Streptomycec griseus	Streptomycetaceae	50	Spherical	Khadivi Derakhshan et al., 2012

Table 1.9: Use of Yeast for Gold nanoparticle synthesis

Yeast	Size (nm)	Shape	Reference
Extremophilic yeasts	30 - 100	Spherical	Mourato et al., 2011
Saccharomyces cerevisiae, AP22 and *CCFY*-100	15–20	Spherical	Sen et al., 2011
Magnusiomyces ingens	16 -420	Mixture of sphere, plates (triangle, hexagon, pentagon), and irregular shaped nanoparticles	Zhang, 2016
Magnusiomyces ingens LH-F1	80.1 ± 9.8	sphere, triangle and hexagon	Zhang, 2016
Candida guilliermondii	50–70	Spherical	Mishra et al., *2010*
Yarrowia lipolytica	15–20	Nanoparticles and nanoplates	Pimprikar *et al.*,2009

1.5.6. GNP synthesis using microfungi

Conventional methods of synthesis of Gold nanoparticles has resulted in environmental contamination due to release of hazardous by products and thus, 'green synthesis' of the nanoparticles has paid much more attention in the rapidly growing area of nanoscience and nanotechnology (Sarkar et al., 2011). Currently, an exhaustive study on biological synthesis of nanoparticles has been carried out using a wide array of microorganisms such as algae, bacteria, actinomycetes, fungi, yeasts, and viruses among which fungi are the most advantageous microorganisms (Sakthivel, 2010; Thakkar et al., 2010). They are fastidious to grow, easy to handle and synthesize nanoparticles (Thakkar et al., 2010). The extracellular synthesis of Gold nanoparticles has been reported recently by the bacteria *Pseudomonas aeruginosa (*Husseiny et al., 2007). The actinomycetes *Thermomonospora sp.* has also shown capacity to synthesis of Gold nanoparticles extracellular (Ahmad et al., 2003). Fungi are simpler to grow both in the laboratory and at an industrial scale, fungi also secrete large amount of proteins thus appear to be more promising for large scale production of NPs (Das et al., 2010). Different fungal species, e.g., *Fusarium oxysporum*, *Verticillium* sp, *Penicillium sp., Aspergillus fumigatus, Fusarium solani* have been reported to synthesize NPs either intra or extracellularly (Mukherjee et al., 2001; Mandal et al., 2006 D'souza et al., 2006). More recently, (Mishra et al., 2014) have reported that Gold nanoparticles derived from *Trichoderma* sp. showed their potential as a new generation antimicrobial agent. The same is given in the **Table 1.10.**

1.5.7. Biosynthesis of Gold nanoparticles using different mushrooms

Only few studies were achieved to reduce Gold ions using isolated fungal compounds from mushrooms like glucan (polysaccharide) from *Pleurotus florida* (Sen et al.,2013), laccase (protein) from *Pleurotus ostreatus* (El-Batal et al.,2015) and *Schizophyllan* from *Schizophyllum commune* (Bae et al., 2007). But most of publications in this field used crude extracts of mushrooms both mycelia and fruiting bodies to synthesize AuNPs (Owaid and Ibraheem, 2017), such as *Volvariella volvacea* (Philip, 2009), *Pleurotus florida* (Bhat et al., 2013), *Pleurotus sapidus* (Sarkar et al., 2013), *Grifola frondosa* (Vetchinkina et al., 2013), *Hericium erinaceus* (Raman et al., 2015), *Pleurotus cornucopiae var. citrinopileatus* (Owaid et al., 2017), *Flammulina velutipes* (Narayanan et al., 2015; Rabeea et al.,2020), *Agaricus bisporus* (Eskandari-Nojedehi et al., 2018; Eskandari-Nojehdehi et al., 2016), and *Lentinula edodes* (Owaid et al., 2019). The **Table 1.11** gives the list of mushrooms used in GNP synthesis along with their size and shape.

Table 1.10: GNP Synthesis Using microfungi

Species	Shape	Size nm	Reference
Alternaria alternata	Spherical, triangular, hexagonal	12±5	Sarkar et al., 2012
Aspergillus clavatus	Triangular, spherical and hexagonal	24.4	Verma et al., 2011
Aspergillus niger	Spherical, elliptical	12.8	Bhambure et al.,2009
Aspergillus oryzae var. viridis	Spherical	10-60	Binupriya et al., 2010a
Aspergillus sydowii	Spherical	8.7-15.6	Vala, 2014
Candida albicans	Spherical	20-40	Chauhan et al.,2011
Colletotrichum sp	Large aggregate Spherical	60-80	Shankar et al.,2003
Cylindrocladium floridanum	Spherical	8-40	Narayanan and Sakthivel, 2011b
Epicoccum nigrum	Spherical, triangular	undefined	Sheikhloo et al.,2011
Fusarium oxysporum	Spherical	5-35	Mukherjee et al.,2002
Fusarium semitectum	Spherical	5-50	Sawle et al., 2008
Helminthosporum solani	Spheres, rods, triangles, pentagons, pyramids, stars	8-40	Kumar et al.,2008
Hormoconis resinae	Spherical	10-80	Mishra et al.,2010
Neurospora crassa	Spherical	2-70	Castro-Longoria et al., 2011

Penicillium brevicompactum	Spherical, triangular and hexagonal	3-20	Mishra et al., 2011
Penicillium rugulosum	Spherical, triangular, hexagonal	32	Mishra et al., 2012b
Penicillium	Spherical	10-60	Du et al., 2011
Rhizopus orzyae	Spherical	20-80	Das et al.,2012a
Saccharomyces cerevisiae	Spherical	20-40	Sen et al.,2011
Sclerotium rolfsii	Spherical	30-50	Narayanan and Sakthivel, 2011a
Verticillium	Spherical	40-60	Mukherjee et al.,2001
Volvariella volvacea	Spherical	16-25	Philip, 2009
Yarrowia lipolytica	Triangular, spherical, hexagonal	15-20	Pimprikar et al.,2009

Table 1.11: Biosynthesis of Gold nanoparticles using different mushrooms

Fungi	Size (nm)	Shape	Reference
Volvariella volvacea	20–150	Triangular nano prisms, spherical, hexagonal	Philip, 2009
Pleurotus florida	5-15	Triangular nano Prisms, spherical, hexagonal	Sen et al., 2013
Pleurotus cornucopiae var. citrinopileatu	16–100	Spherical	Owaid et al, 2017
Agaricus bisporus	25	Spherical	Eskandari-Nojedehi et al.,2018
Lentinula edodes	72	Triangular, hexagonal, spherical, irregular shapes	Owaid et al.,2019
Agaricus bisporus	53	Oval, spherical, drum-like, hexagonal, triangular	Dheyab et al.,2020
Flammulina velutipes	74.32	Triangular, spherical, irregular	Rabeea et al., 2020
Inonotus obliquus	23	Spherical, triangle, hexagonal, rod shaped	Lee et al., 2015
Coprinus comatus	<100	Spherical	Naeem et al., 2020
Cordyceps militaris	15- 20	Face-center-cubic structure	Ji et al., 2019
Lignosus rhinocerotis	50-83	Spherical	Katas et al., 2019
Ganoderma applanatum	18.70	Face-centered cubic	Abdul-Hadi et al., 2020
Morchella esculenta	20- 150	Spherical and hexagonal	Acay, 2021
Volvariella volvacea	20–150	Triangular nanoprisms, spherical and hexagonal	Philip, 2009
Pleurotus ostreatus, Lentinus edodes, Ganoderma lucidum, Grifola frondosa	2 -20	Spherical	Vetchinkina et al., 2017

1.5.8. Application of Gold nanoparticles

Nanoparticles possess particular intrinsic reactivity as a result of increased surface area, so an appropriate choice of materials for the manufacture of nanoparticle-based therapeutics would be made. The surface functionalities and depending on the particle size, shape and state of aggregation, the interaction will occur between nanomaterials and biological systems in various ways depending on the cell type, employing different uptake routes or targeting different organelle. Gold nanoparticles (AuNPs) are used in immunochemical studies for identification of protein interactions (Tvrdonova et al., 2019; Zhao et al.,2022). They are used as lab tracer in DNA fingerprinting to detect presence of DNA in a sample. Gold nanorods are being used to detect cancer stem cells, beneficial for cancer diagnosis and for identification of different classes of bacteria. Gold nanoparticles-based colorimetric sensors (Ag/Au-NPs-CSns) allow potential prospects for the development of efficient sensors owing to their unique shape- and size-dependent optical properties (Ali et al., 2021). Colorimetric sensing of biological molecules using Gold nanoparticles-based probes has been reported (Negi, 2022). Gold nanoparticles have unique electric and magnetic properties due to their shape and size so they have been received great attention in research areas especially in the field of biological tagging, chemical and biological sensing, optoelectronics, photo thermal therapy, biomedical imaging, DNA labelling, microscopy and photoacoustic imaging, surface-enhanced Raman spectroscopy, tracking and drug delivery, catalysis and cancer therapy.There are many nanomedical applications for dendrimers including nanoscale catalysts and reaction vessels, micelle mimics, imaging agents and chemical sensors, and agents for delivering drugs or genes into the cells. Carbon nanotubes are allotropes of carbon with a cylindrical nanostructure. The various biological effects and potential applications of green synthesized metal nanoparticles (Rónavár et al., 2021) is shown in **Fig 1.12.**

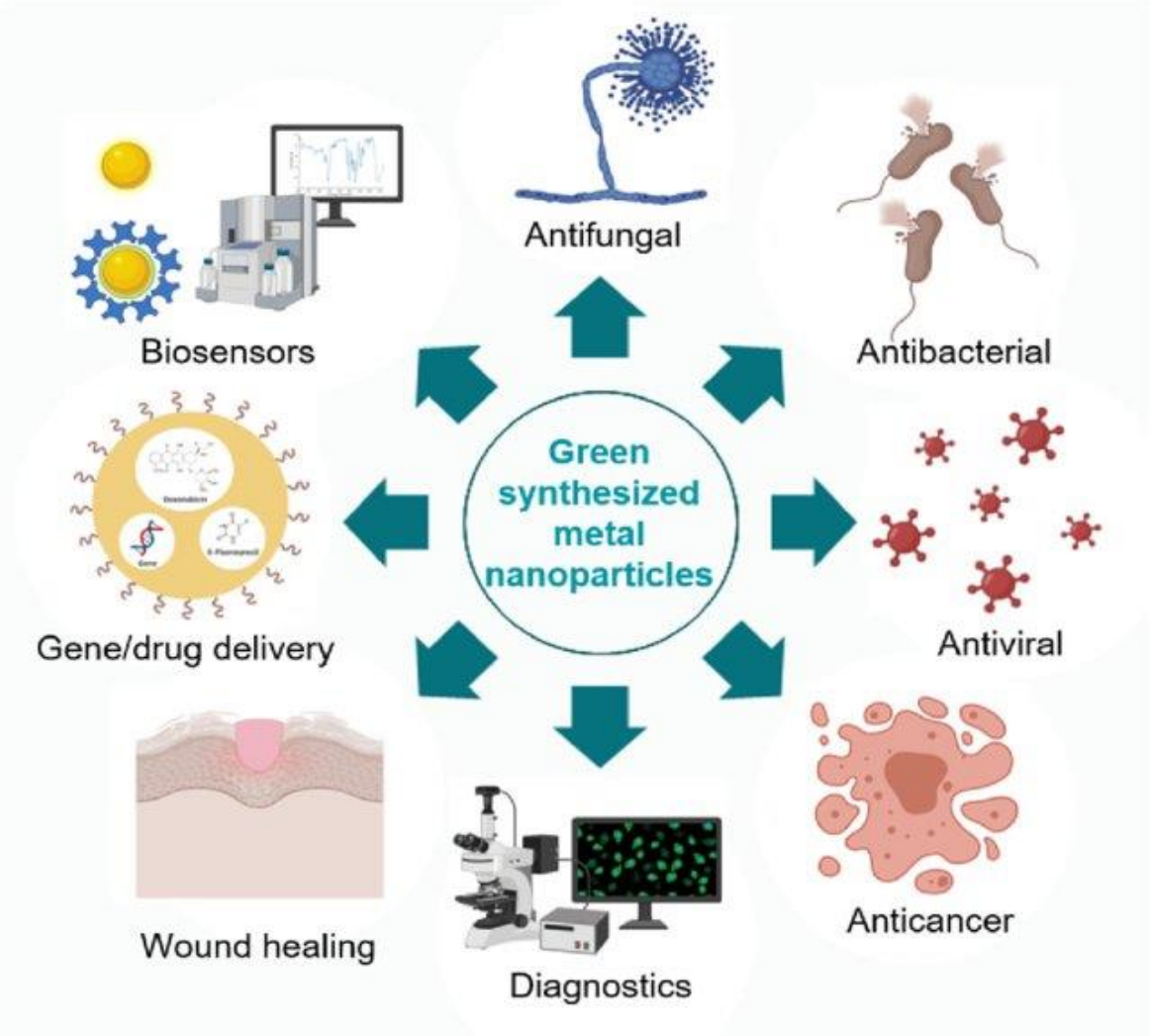

Figure 1.12: The various biological effects and potential applications of green synthesized metal nanoparticles (Rónavár et al., 2021).

Part C: Biomining

1.6. Metal sulphide biooxidation

Biooxidation refers to a pre-treatment process that uses bacteria as to catalyse the degradation of mineral sulphides, usually pyrite or arsenopyrite, which host Gold, Silver or both. Several studies have shown that Gold solubilization occurs when microorganisms such as *C. violaceum* which directly attach to the surface of Gold, forming biofilms and cyanide (Campbell et al.,2001). Strains of *Bacillus megaterium, Bacillus mesentericus, Pseudomonas liquefaciens,* and *Bacterium nitrificans,* isolated from Gold bearing deposits were found to dissolve up to 35 mg L-1 of Gold using 30 days of incubation (Korobushkina, 1974). *Acidithiobacillus ferrooooxidans* has been used in the oxidation of elemental sulphur to the reduction of ferric iron in the goethite fraction of a limonitic nickel ore at 30°C, metals such as nickel, Co, Cr and Mn were effectively solubilized (Johnson et al.,2013). Studies on auriferous soils from Australian mine sites have shown that the resident microbiota are capable of solubilizing up to 80 wt.% of the Gold contained in these soils (Reith et al.,2006). Reith and McPhail, 2006 demonstrated that microorganisms play a vital role in the solubilization of Gold and that microorganisms native to soils maybe useful for the in situ leaching of Gold.

1.6.1. Microbes involved in Biooxidation

Metal sulphides are oxidized by certain bacteria, forming soluble metal sulfates and sulfuric acid. Pyrite and arsenopyrite are prominent minerals in refractory sulfidic Gold deposits and are readily bio-oxidized. The most commonly studied pyrite oxidizing bacteria are mesophilic *Thiobacillus ferrooxidans,* that oxidizes ferrous iron or reduced sulfur compounds, and *Leptospirillum ferrooxidans* that oxidizes ferrous iron but not sulfur. These organisms are prominent components of microbial communities which develop in environments where metal

sulphides are exposed to air and water, often as a result of mining. Participation of these iron- and sulfur-oxidizing bacteria in commercial-scale copper and uranium extraction is well known. During the past ten years, laboratory and pilot plant scale studies of bio-oxidation of sulfidic Gold ores have been conducted with pure cultures of pyrite-oxidizing bacteria, mixtures of laboratory cultures, and consortia of microorganisms cultured from environments where pyrite is undergoing oxidization. In most cases, little characterization of the cultures has been done. However, since ore samples often contain indigenous iron- and sulfur-oxidizing bacteria, it is likely that consortia of microorganisms best suited to the particular conditions of ore oxidation will develop. Furthermore, cultures pre-grown on the test ore are generally used in order to eliminate or minimize lag times in bio-oxidation studies. Moderately thermophilic (45-55°C) pyrite oxidizing bacteria are also found in mine spoils containing pyritic materials that are undergoing weathering. These organisms oxidize Gold ores in bench scale continuous stirred tank reactors. An unidentified proprietary culture of moderately thermophilic bacteria oxidizes Gold ores containing pyrite and arsenopyrite and is adaptable to the high dissolved salt levels that are sometimes encountered in mine waters. Laboratory studies have shown these organisms can oxidize pyrite more rapidly than *T. ferrooxidans*, and at elevated temperatures, abiotic reactions between pyrite and water, oxygen, and ferric ions are also significantly faster. A strain of *Sulfolobus* successfully oxidized an arsenopyrite-pyrite flotation concentrate in bench scale batch and semicontinuous oxidation experiments. The leaching rate of the concentrate was reduced above a pulp density of 1.5% w/v. This decrease was attributed to elevated soluble arsenic levels. However, at the higher pulp densities the organism may have been subjected to abrasive damage. The list of microbes involved and potentially used in Gold biomining is given in **Table 1.12** and **Table 1.13.**

Table 1.12: Microorganisms involved in Gold biomining (Source: Compiled from Brombacher et al.,1997; Rea et al., 2016; Reith et al., 2007).

Micro-organisms	Microbial processes
Acidothiobacillus ferroxidans	Fe oxidation
Acidothiobacillus thiooxidans	S-oxidation
Fe- and S-oxidizer (*A. ferroxidans, Actinomycetes Streptomycetes fradiae)*	Thiosulphate production
Cyanide producing bacteria *(Pseudomonas, Chromobacterium violaceum*)	Cyanide production
Bacteria such as *Corynebacterium glutamicum*, Fungi such as *Penicillium* spp	Amino acid production
Fungi such as *Fusarium oxisporum*, Bacteria such as *Bacillus* sp	Bio-reduction of Gold passive absorption

Table 1.13: Microorganisms potentially useful in Gold Biomining (Source: Compiled from Brombacher et al.,1997; Rea et al., 2016; Reith et al., 2007).

Microorganisms	Role in biosphere
Arthrobacter spp., *Corynebacterium* sp., *Deinococcus* sp., *Kocuria* sp., *Microbacterium* sp., *Micrococcus* spp., *Propionibacterium* spp.	1. Mediate initial colonization on the grains 2. Produce EPS 3. Conditions the grain surfaces
Pseudomonas spp., *Burkholderia* spp., *Methylobacterium* sp. *Acinetobacter* sp. *Pseudomonas* spp.	Production of EPS to further stabilize the biofilm
S-oxidizing or cyanide producing bacteria, e.g., *Diaphorobacter* sp., *Sphingomonas* spp. and *Methylobacterium* sp., *Sphingomonas* spp.	Gold solubilization
C.metallidurans, D.acidovorans, Stenotrophomonas sp., *Achromobacter* spp., *Halomonas* sp. and *Herbaspirillum* sp.	Metal-resistant bacteria with the ability to detoxify Gold complexes.

1.6.2. Gold sulphide biooxidation

A biooxidation process has been used to mobilize Gold from spent materials. There are two possible ways of applying bio-oxidation of Gold from spent materials namely heap or dump leaching and stirred tank leaching. The static bio-oxidation techniques are based on the principle of circulating water and air through heaps of spent materials to activate the growth of microorganisms that amplify the oxidation (Morin et al.,2006). Cyanogenic *Chromobacterium violaceum, Pseudomonas fluorescens,* and *Pseudomonas plecoglossicida* were able to mobilize Gold, when grown in the presence of various metal-containing solids such as Gold -containing electronic scrap. Gold was bacterially solubilized from shredded printed circuit boards. Maximum dicyanoaurate concentration corresponded to 68.5% dissolution of the total Gold added (Helmut et al., 2008). Different cyanogenic bacterial strains (*C. violaceum*, *P. fluorescens*, *Bacillus megaterium*) were cultivated under cyanide-forming conditions in the presence of metal-containing solids such as electronic scrap. All microorganisms were able to form water-soluble metal cyanides, however, with different efficiencies.

1.6.3. Gold biomining -present status

Biomining is a desired approach to mine minerals from ore by using microorganisms which demands very low capital, low operational cost, and also environmentally friendly. The first recognized application of biomining was by the Kennecott Copper Corporation in the 1960s. Traditional methods of mining using extreme heat and chemicals are hazardous to environments and thus use of microorganisms to leach minerals from ore is promising up-and-coming technology. Biomining is commercially applied using three different engineered methods which includes dump, heap and Stirred tank bioleaching/ bio-oxidation. Chemolithotrophic bacterium such as *Thiobacillus thiooxidans*, *Thiobacillus acidophilus,*

Thiobacillus organoparus, *Leptospirillum ferrooxidans*, and *Sulfolobus acidocaldarius* obtains energy necessary for growth from the oxidation of ferrous iron and reduced-valence inorganic sulfur compounds (Ehrlich, 2002; 2022). The bioleaching cyanidation method is successfully applied in several countries for the recovery of Gold from refractory sulphide ores and concentrates (Aswegen et al., 2007). Biohydrometallurgy as part of mineral or mining biotechnology incorporates several microbially mediated processes, such as Bioleaching. Bioleaching involves the solubilization of an insoluble metal sulfide to a soluble metal, which can be recovered from the leachate. Biohydrometallurgy is an interdisciplinary field consisting of the areas of research such as geomicrobiology, microbial ecology, hydrometallurgy and microbial biogeochemistry (Jain and Sharma, 2004) which includes the solubilization of metals compounds from ores. Leaching technology is divided into three main types and can be carried out at three different levels first is at the laboratory scale, the pilot scales and the commercial scale. Laboratory scale leaching can be obtained by various means such as by stationary or shake flask or air lift percolators (Brombacher et al., 1997). Whereas in case of pilot scale the procedure is carried out in columns or in agitated tanks or reactors. **Table 1.15** gives the Gold plants located in world employing Biox and Bacox. The microbial mineral processing and microbial hydrometallurgy of metal sulphides is currently a well-established technology (Gahan et al., 2012; Anjum et al., 2012; Ghorbani et al., 2016). Over past years, there has been a huge amount of developments with regards to the understanding of its both engineering perspective as well as fundamental approach with regards to the microorganisms. The present research work and patents available on biomining techniques of Gold are listed in the **Table 1.14** and **Table 1.16.**

1.6.4. Present techniques used for Gold mining

First step in Gold mining is crushing and grinding, followed by gravity separation, amalgamation, flotation, leaching. Once the floatation process is done auriferous quartz, sulphides are separated and again regrinding, roasting, bio-oxidation, pressure oxidation is carried out which is followed by leaching process which includes heap leaching, agitation etc and the extraction process is followed either by absorption or precipitation. The method is summarized in the **Fig 1.13**.

1.6.5. Cyanide in Gold mining and environmental problems

Free cyanide (HCN plus CN^{-1}), which is a primary toxic agent has been heavily used in the major mining areas for the extraction of Gold by the major Gold mining companies. There have been major environmental problems. In October 2004, there was a spill of cyanide from the Bogosu Gold 's new tailings dam, which drained into the Ajoo stream, the only stream left in the community. The deadly chemical killed fish, crabs and lobsters and polluted the stream, which is the main source of drinking water for the Dumasi community and its environments. Thus, cyanide spillage as result of mining has been a major environmental problem. The potential impact of cyanide on groundwater has not been measured. It has been known from groundwater monitoring data from a number of mining operations throughout the world that, generally, there is little or no impact of cyanide on groundwater quality due to the natural degradation process of cyanide. The use of cyanide in Gold mining is becoming an increasingly sensitive issue (Logsdon et al., 1999; Stenson, 2006). Potential health effects of cyanide use in artisanal and small-scale Gold mining in Burkina Faso has been reported (Knoblauch et al., 2020).

Table 1.14: Biomining of Gold -Present status

Projects	References
Microbial oxidation of Gold ores and Gold bioleaching	Olson, 1994
Biogenic production of cyanide and its application in Gold recovery	Campbell et al, 2001
Bio recovery of Gold	Eisler, 2003
Potential for the utilisation of microorganisms in Gold processing	Reith et al., 2007
Useful approach of biomining towards metal extraction, microorganisms useful in biomining, and mining mechanisms	Siddiqui et al.,2009
Use of biotechnology in Gold exploration and processing	Zammit et al., 2012
The potential use microorganisms in the biooxidation of Gold ore from a mine in Bulawayo	Matsvayi, 2016
Improving Gold recovery from refractory Gold ores through biooxidation	Mubarok et al., 2017
Studies on potential for biotechnology for extraction of metals in Zimbabwe	Chingwaru et al., 2017

Table 1.15: Gold recovery plants located in world employing Biox and Bacox (Brierley & Brierley, 2001; Brombacher et al., 1997).

Plant and location	MT/day
Suzdal, Kazakhstan,Asia	196
Kokpatas, Uzbekistan,Asia	1,069
Laizhou, China, Asia	100
Jinfeng, China,Asia	790
Sansu, Ghana, Africa	960
Fairview, South Africa	40
Wiluna, Australia	158
Beaconsfield, Australia	70
Harbour Lights, Western Australia	40
Fosterville, Victoria, Australia	211
Sao Bento, Brazil, South America	150

Table 1.16: Patents on biohydrometallurgical ore processing (1989-2022)

Inventor/Publication date assignee	Patents	Treated material	Microorganisms	References
Louisiana State University, Baton Rouge, USA	US 5.021.088	Carbon Containing Gold ore	Heterotrophic fungal and bacterial strains- *Thiobacilli*	Portier, 1991
Geobiotics Inc., San Francisco, USA	EP 0.432.935	Gold ore	*Chromobacterium violaceum*, *Chlorella vulgaris*	Kleid et al.,1991
Bac Tech (Australia) Pty. Ltd., Nedlands, Australia	WO 92/16667	Sulfidic material	Autotrophic, acidophilic, Thermotolerant bacteria	Spencer et al.,1992
Newmont Mining Corp., Denver, USA	EP 0.522.978	Sulfidic ore	*Thiobacillus*, *Leptospirillum ferrooxidans*	Hill and Brierley, 1993
Geobiotics Inc., Hayward (Calif.), USA	WO 95/15403	Sulfidic ore	*Thiobacillus ferrooxidans*	Kohr, 1995
Yellowstone Environ. Sci. Inc., Bozeman, USA	WO 96/00308	Sulfidic ore	Sulfate- and hydrogen-reducing bacteria	Hunter et al.,1996
Geobiotics Inc., Hayward (Calif.), USA	WO 96/12826	Sulfidic ore	*Thiobacillus*, *Sulfolobus* and *Sulfobacillus* strains	Kohr et al.,1996

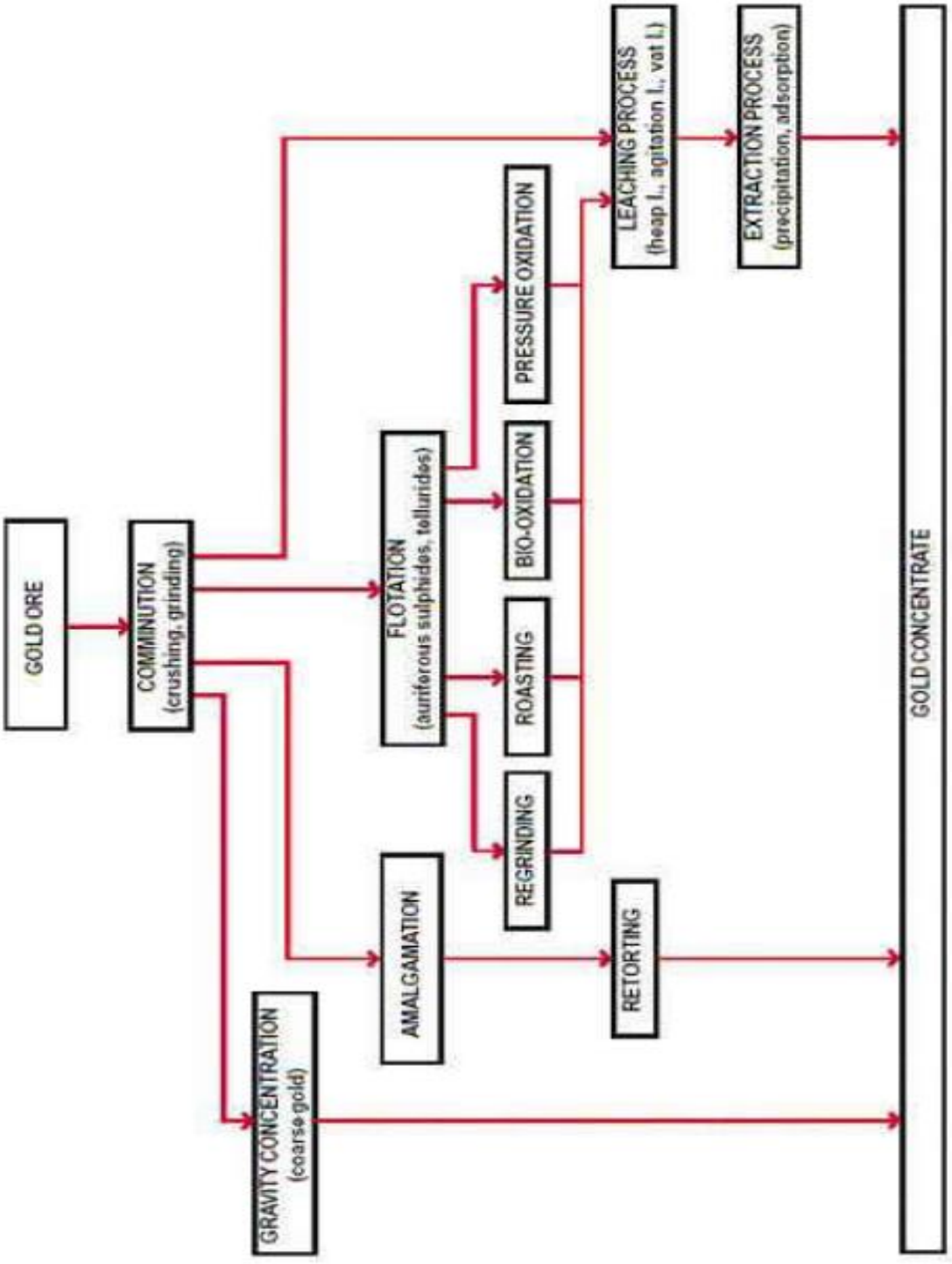

Figure 1.13: Methods used in Mining of Gold (Eugene and Mujumdar, 2009)

1.6.6. Problems faced by Gold mining industry in India

Due to the rapid increase in the demand for metals worldwide, reserves of high-grade ores are diminishing at an alarming rate and there is need to excavate new sources of metals. But there are many problems in metal extraction. The problems which comes on the way includes massive investment in exploration and upgrading of technology, mitigation of environment degradation due to mining, adoption of environment friendly technologies. Due to high energy and capital inputs, the recovery of metals from low and lean grade ores using conventional techniques is also very expensive. In the case of low-grade ore bodies, it is very important to remove as much of the desired ore from the mined material as possible so that mining operation remains economically feasible. Miners must not only monitor the incoming material to maximize the extraction process, but the waste material must be monitored just as closely to ensure that none of the valuable minerals are lost. Another major problem in mining industry is environmental costs due to the high level of pollution from these technologies. Mining processes produce large volumes of waste, some of it highly toxic. This waste can result in acid mine drainage and groundwater contamination. Mining companies mainly use cyanide and mercury to extract Gold from crushed ore. Very low-grade ore, with minimal residues of Gold, is crushed and piled on the ground, then sprayed with a cyanide solution. Use of mercury has led to major public-health problems for miners and communities around mining districts. Despite having some of the best potential ground for Gold mineralization, India's annual primary Gold mine output has reduced significantly to below 5 tonnes.

1.7. Indian Gold market

India's Gold market is driven primarily by the consumption and fabrication of Gold and both these factors have a significant impact in terms of economic value add, contribution to foreign exchange earnings, employment, and the trade balance. Gold made a direct contribution of more than $30 billion to the Indian economy in 2012 as per the recent report (2013) commissioned by the World Gold Council from Price water house Coopers. India is one of the largest Gold jewellery exporters in the world. Indian Gold jewellery shipments came to US$8.6bn during the financial year 2015–2016, with around half delivered to UAE, India's largest jewellery export destination. India's Gold stocks are around 23,000- 24,000 MT. In India, highest market share for Gold demand of 40% is in Southern India, western India at 25% and northern and eastern India have 20% and 15% of the market share respectively (World Gold Council). Indian Gold refining capacity jumped in recent years from a mere three or four refineries in 2013 to 30 in 2015, taking the total capacity above 1,450MT. Gold market also makes a sizeable contribution to employment. According to a report by consultants, AT Kearney, commissioned by the federation of Indian Chambers of Commerce and Industry (2013), the gems and jewellery industry employs over 2.5 million people having the potential of adding a further 0.7–1.5 million by 2020. The prices of the iron ore and Gold is shown in the **Table 1.17.**

Table 1.17: Price of Iron ore and Price of Gold (www.indexmundi.com)

Year	Price of Gold (Rs.)	Iron ore price in dollars
1987	2570.00	10.94
1988	3130.00	10.51
1989	3140.00	12.03
1990	3200.00	14.05
1991	3466.00	15.03
1992	4334.00	14.31
1993	4140.00	12.58
1994	4598.00	11.45
1995	4680.00	12.27
1996	5160.00	12.97
1997	4725.00	13.04
1998	4045.00	13.41
1999	4234.00	11.93
2001	4300.00	12.99
2002	4990.00	12.68
2003	5600.00	13.82
2004	5850.00	16.39
2005	7000.00	28.11
2006	8400.00	33.45
2007	10800.00	36.63
2008	12500.00	60.80

2009	14500.00	72.51
2010	18500.00	97.67
2011	26400.00	169.36
2012	29000.00	128.87
2013	33000.00	97.00
2014	30000.00	97.00
2015	26,343.50	55.90
2016	28,623.50	58.40
2017	29,667.50	71.80
2018	31,438.00	69.80
2019	35,220.00	93.80
2020	48,651.00	162.00

CHAPTER II

MATERIALS AND METHODS

2.1. Literature survey and Bibliometric analysis

Precise scientific literature survey was carried out using various online strategies of querying and using search term associated with the work in different databases such as general search engines, academic/institutional databases, specific journal search, patent websites, culture collections, biological and chemical databases. Growth rate of online sources related to specific search terms present in the google scholar (https://scholar.google.co.in/) was also estimated for 20th (1900–1999) and 21 st (2000–2022 August) century. Standard literature surveys included printed books, search engines and web based ejournal based literature reviews. Reports from different websites related to the research areas were studied such as World Gold council, Geological Survey of India (GSI), Indian Bureau of Mines (IBM), Directorate of mines and Geology-Goa, Ministry of mines. Use of specialist journals in the field on Gold, geomicrobiology and biomining were also referred. Visits to the museum of rock at School of Earth, Ocean and Atmospheric Sciences (Earth science department) of Goa University. Bibliometric analysis of the trends and key terms in relevant literature using standard bibliometric visualizers was carried out (De Souza and Kamat, 2018).

$$\text{Relative expansion of online sources } (\%) = \frac{\text{Number of documents}}{\text{Total number of years in the specified period}} \times 100$$

2.2. Use of VOSviewer for analysing bibliometric data

VOSviewer is a software tool for creating maps based on network data and for visualizing and exploring these maps. VOSviewer can be used to construct networks of scientific publications, scientific journals, researchers, research organizations, countries, keywords, or terms. Items in these networks can be connected by co-authorship, co-occurrence, citation, bibliographic coupling, or co-citation links. To construct a network, bibliographic database files (i.e., Web of Science, Scopus, Dimensions, Lens, and PubMed files) and reference manager files (i.e., RIS, EndNote, and RefWorks files) can be provided as input to VOSviewer. Alternatively, VOSviewer can download data through an API (i.e., Crossref API, OpenAlex API, Europe PMC API, and several others). Literature survey was done using key terms of the objectives and for identification of trends in research specialized bibliometric software was used leading to identification of different research clusters focused on research on bioethical and other aspects of Gold. The articles reviewed were obtained with a search of the pubmed and were submitted to a bibliometric analysis using VOSviewer software (version 1.6.17) (https://www.vosviewer.com/).

2.3. Study area

Goa is the smallest state of India with an area of 3702 sq. km. It covers a length of 105 km and a width of 60 km. The Dharwar Craton is divided into Eastern and Western Cratons wherein Goa is situated in the north western part of the Dharwar craton known as Western Dharwar Craton (WDC). WDC includes Sanvordem, Bicholim, and Vagheri Formations (Dessai, 2011). **Fig 2.1** gives the map of Goa showing the mining belt and some places of geological interest. **Fig 2.2** shows the map of distribution of key laterite-capped table-land (plateaux) regions of Goa. **Fig 2.3** gives the map depicting various geomorphic features along the coastal zone of Goa. The most conspicuous, and a really extensive examples of

laterite are those seen along the north Goa coastal tract from 15°10' N to 15°45'. Laterite in Goa is mainly distributed in Harmal in Keri and Mandre in Morjim plateau in Pernem taluka, Mapusa, Assagao, Saligao, Porvorim, Verem, and Aguada Plateau in Bardez taluka. Dona Paula, Taleigao, Bambolim, Kadamba and Merces plateau in Tiswadi taluka. Ponda area plateaux in Ponda taluka. Vasco de Gama headland, Dabolim and Murmugaon plateau in Marmagao taluka. Quepem area plateaux in Quepem taluka and finally Cabo de Rama and Canacona areas Plateau in Canacona taluka (Widdowson, 2009).

2.3.1. Preliminary survey for site selection

During exploration field visits were carried out at sampling sites in mining and non-mining belt of Goa. The mining areas were visited during September till end of month of May. The mining areas were studied for types of rocks, soil characteristics, types of ores, types of low-grade ore (mining reject). The streams were visited during monsoon when water flow was very less. Streams were studied for their source of water and types of rocks. Stream sediments are characterized more by their variability in composition, grain size, sorting and colour than by uniformity in any of these features. Entire coastline of Goa was covered from Keri in the north to Pollem in south. The types of sand and its characteristics such as color, moisture, grain size, presence of seashells was studied. Physico-chemical properties of the soil plays an important role in maintenance of earthworm biodiversity. Termite mounds were explored from wild life sanctuaries. These mounds are generally restricted to the well-drained soils of hill crests. The laterites were collected from the weathered profile which comprises an important subset of the wider range of ferruginous and related aluminous weathering. The criteria for sample selection are given in **Fig 2.4.** Potential auriferous sources of Gold inferred in Goa is shown in **Fig 2.5.**

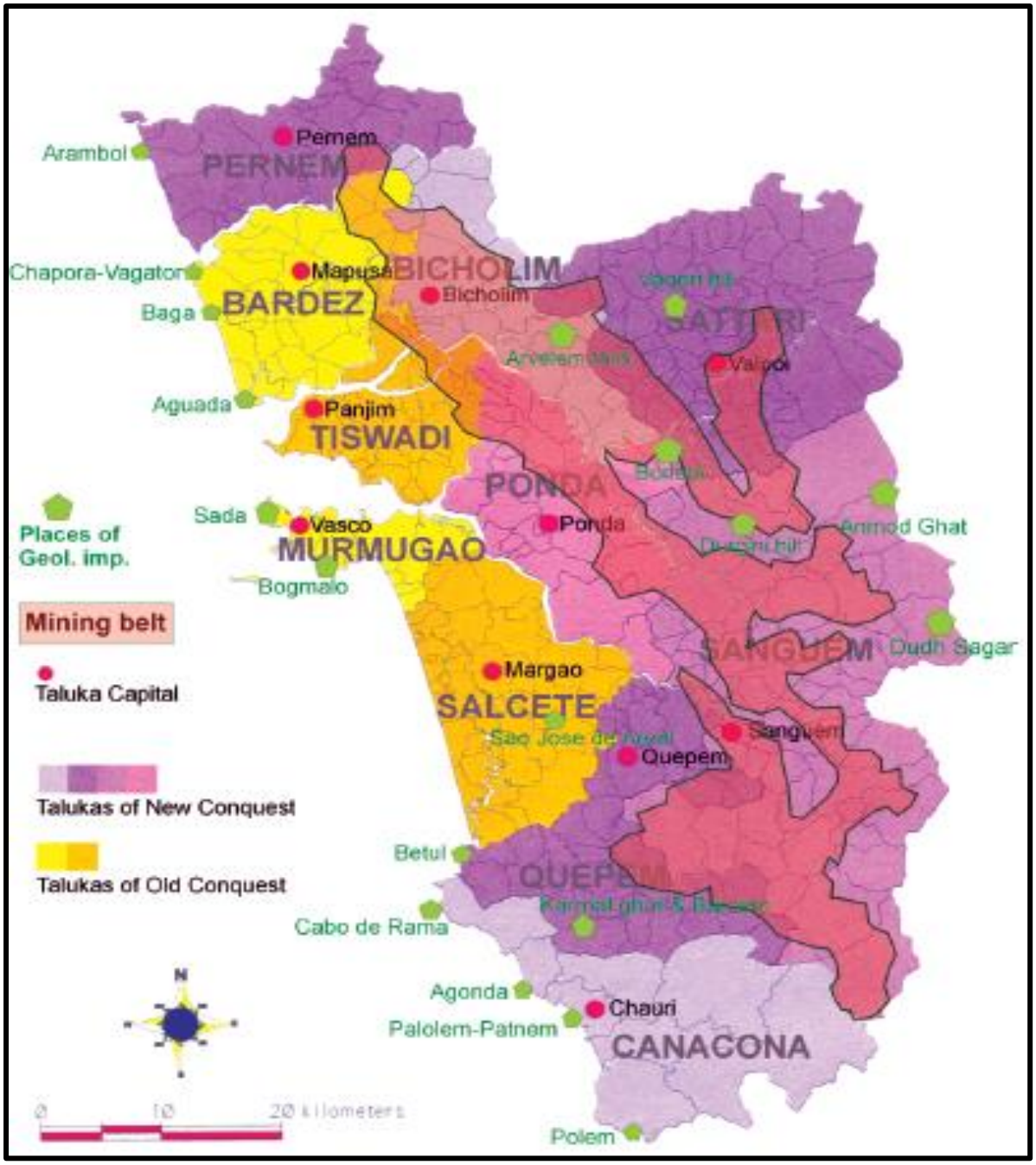

Figure 2.1: Mining belt of Goa and some places of geological interest (prepared by O.A. Fernandes)

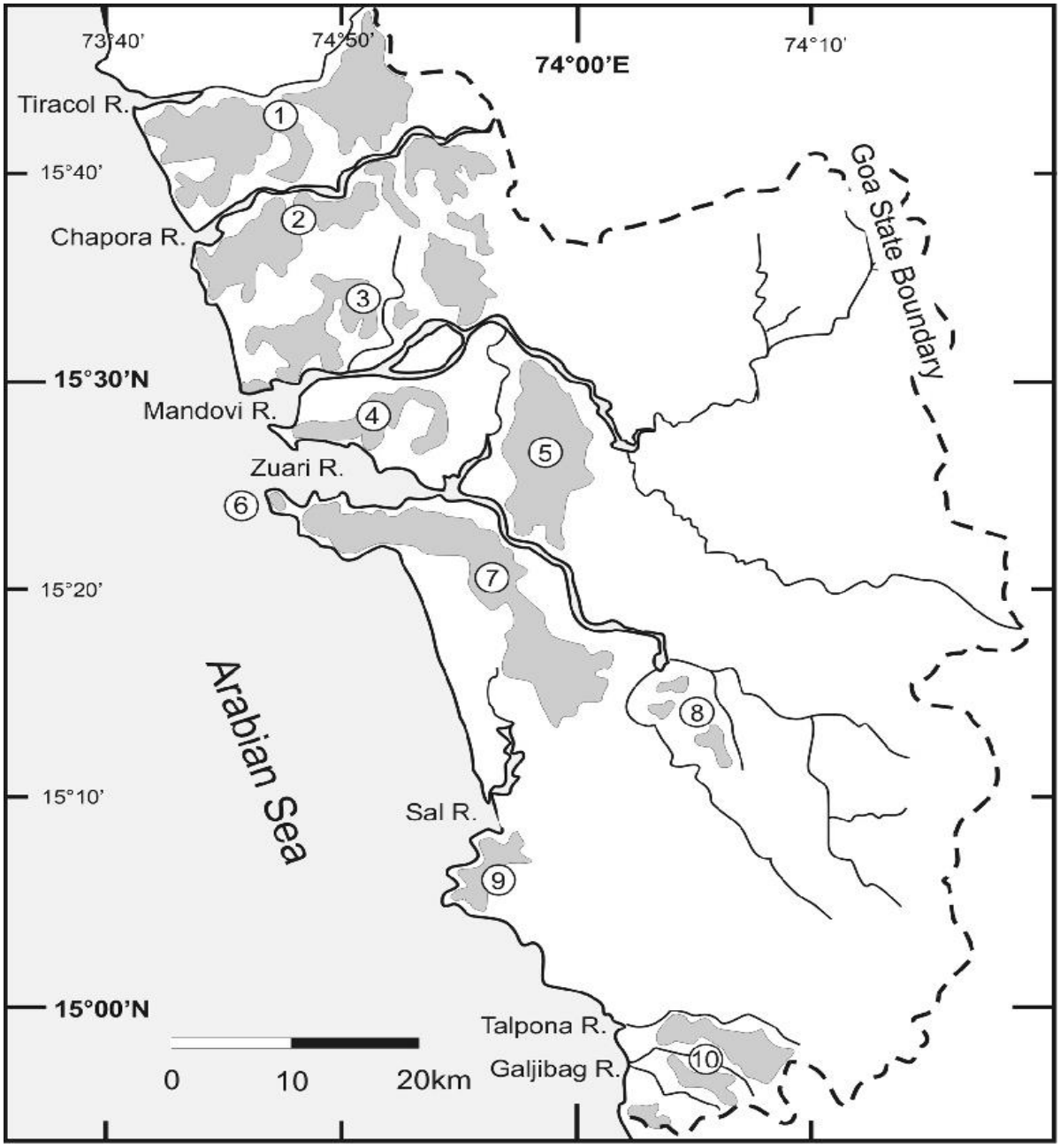

Figure 2.2: Distribution of key laterite-capped table-land (plateaux) regions of Goa. 1, Pernem Plateaux; 2, Mapusa Plateaux; 3, Porvorim Plateaux; 4, Panjim Plateaux; 5, Ponda Plateaux; 6, Vasco de Gama Plateau; 7, Dabolim – Madgaon Plateaux; 8, Quepem Plateaux; 9, Cabo de Rama Plateaux; 10, Canacona Plateaux. (Source: Geological Society of Goa)

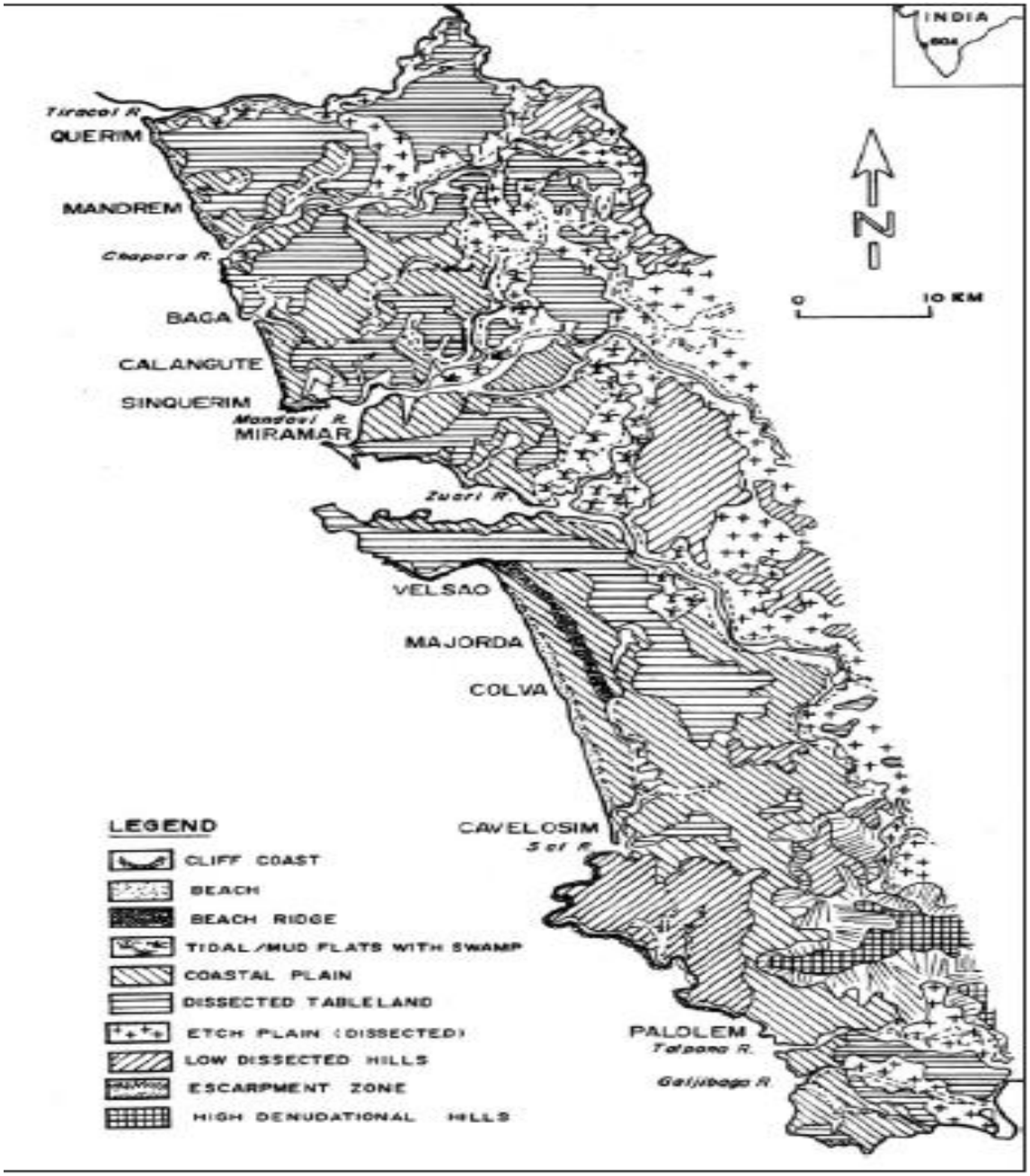

Figure 2.3: Various geomorphic features along the coastal zone of Goa (Adapted from Rao et al., 1985)

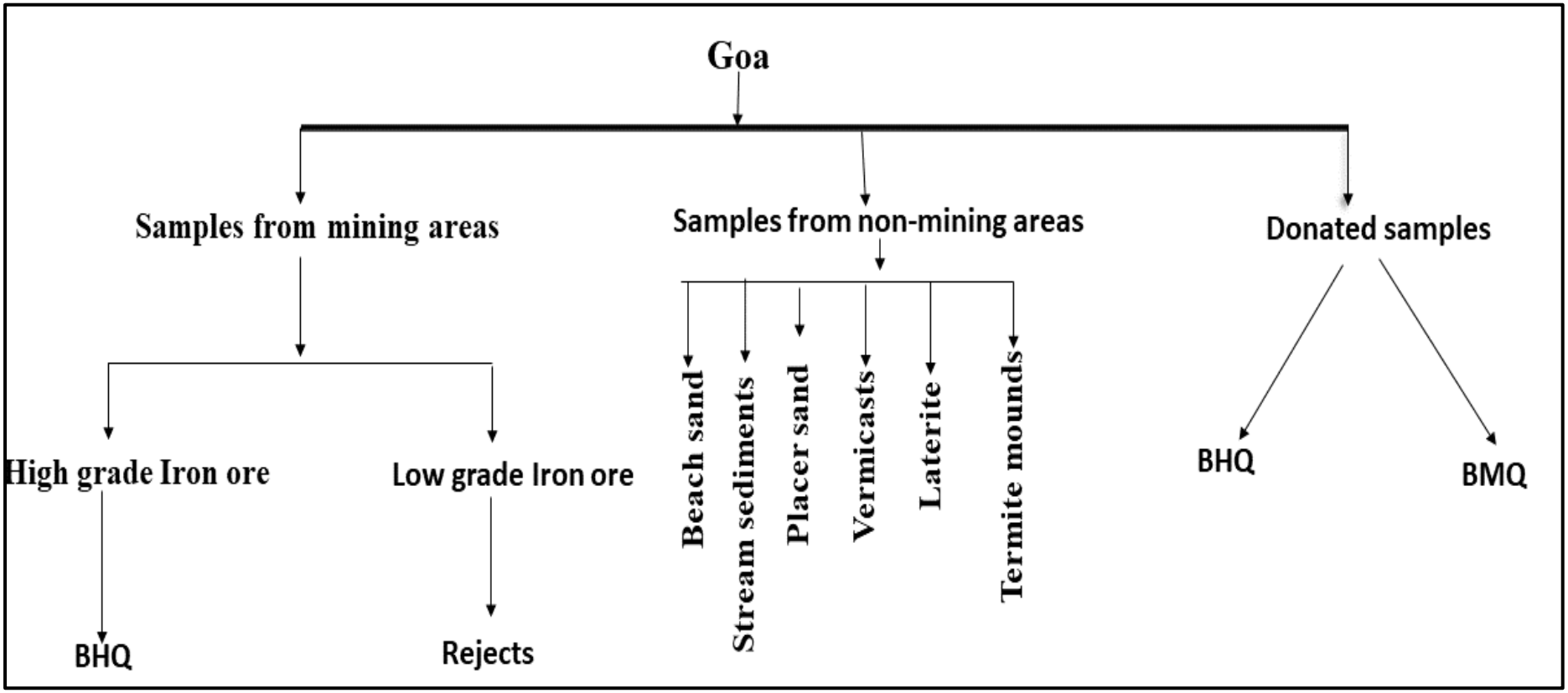

Figure 2.4: Criteria for sample collection

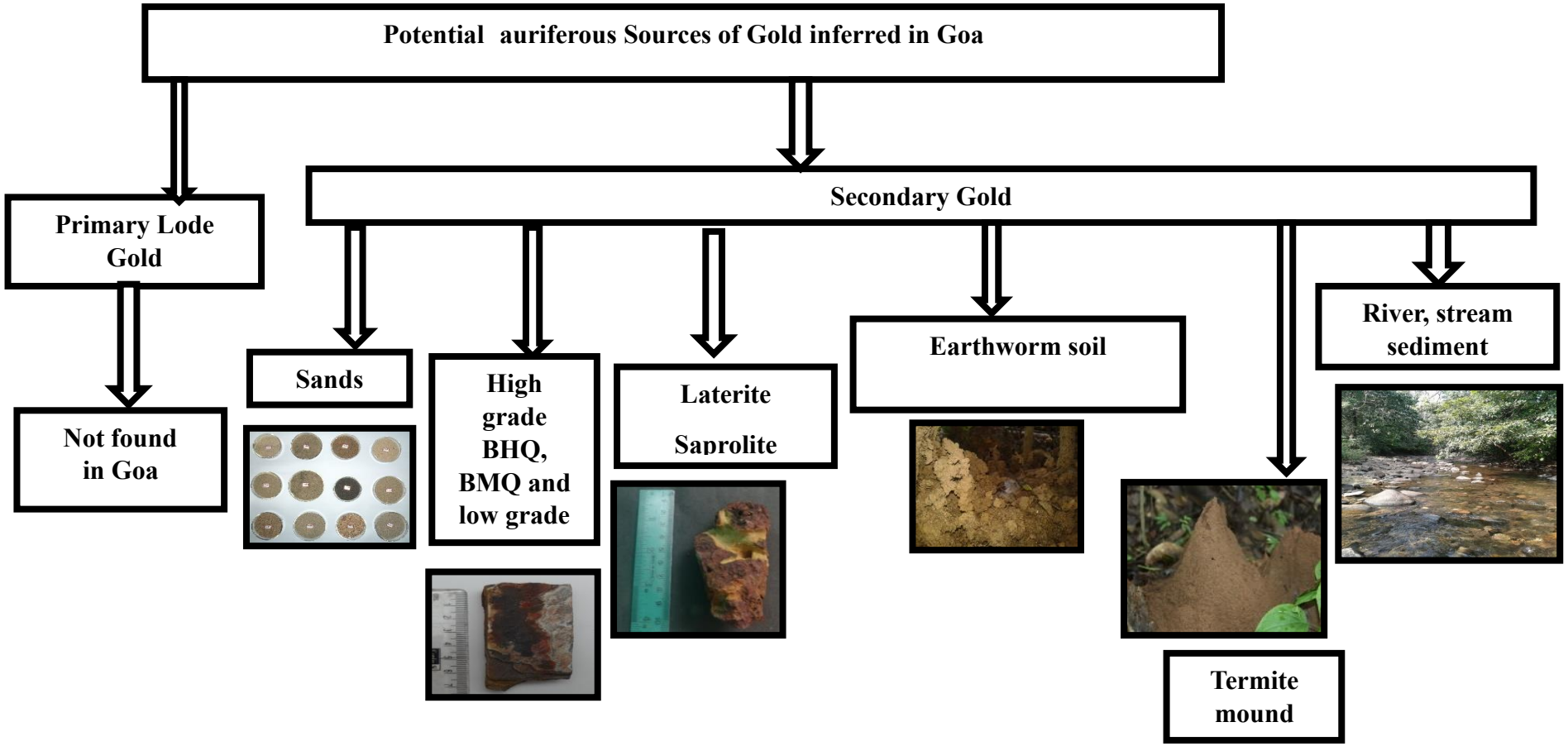

Figure 2.5: Potential auriferous sources of Gold inferred in Goa

2.3.2. Collection of iron ore samples

Samples from the mining areas where mining activities are active were considered as presumptive auriferous mining samples. Iron ore samples were collected from mining areas of Goa during the period from September 2015-September 2019. The samples were collected from the North Goa and South Goa mining belt. The sampling sites includes Shirgao, Bicholim, Pissurlem, Surla, Velguem, Codli, Maina. The samples collected from mining areas include low grade ore (mining reject), iron ore which were identified with the help of School of Earth, Ocean and Atmospheric Sciences (Earth science department) of Goa University. Samples were designated as MR for low grade (mining reject) ore, IO for BHQ, BM for BMQ. The designation and description of the sample is given the **Table 2.1** and the location is shown in **Fig 2.6**. The sampling sites are shown in the **Fig 2.7.**

2.3.3. Donated samples

BHQ and BMQ samples were also obtained from the School of Earth, Ocean and Atmospheric Sciences (Earth science department), Goa University. The BHQ sample was from Velguem North Goa whereas the BMQ sample was from Sacorda South Goa.

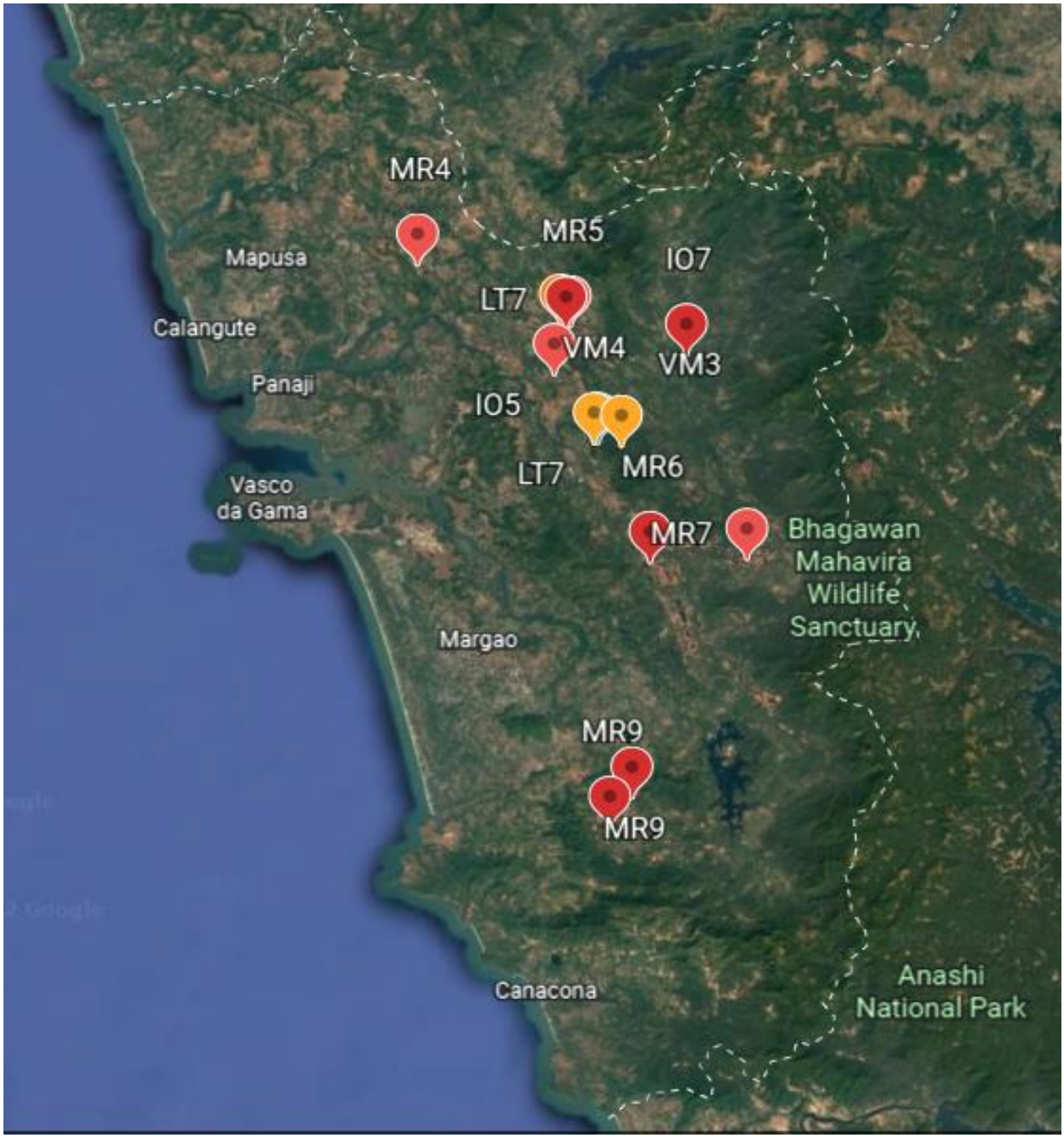

Figure 2.6: Locations of the sampling sites from mining areas superimposed on Google earth image

Table 2.1: Samples from mining areas along with the designation and locations (https://www.google.com/earth/versions/)

Sample designation	location	
	Latitude	**Longitude**
MR-01	15’36’38.30” N	73’54’48.51” E
MR-02	15’36’38.30” N	73’54’48.51” E
MR-03	15’12’42.30” N	74’14’11.09” E
MR-04	15’36’19.54” N	73’53’39.45” E
MR-05	15’29’17.55” N	74’04’17.28” E
MR-06	15’29’26.64” N	74’05’50.37” E
MR-06	15’29’28.64” N	74’02’52.37” E
IO-01	15’36’00.52” N	73’56’08.83” E
IO-02	15’12’42.30” N	74’14’11.09” E
IO-03	15’06’50.89” N	74’09’14.72” E
BM-1	15’06’50.89” N	74’09’14.72” E
BM-2	15’06’60.89” N	74’12’14.72” E

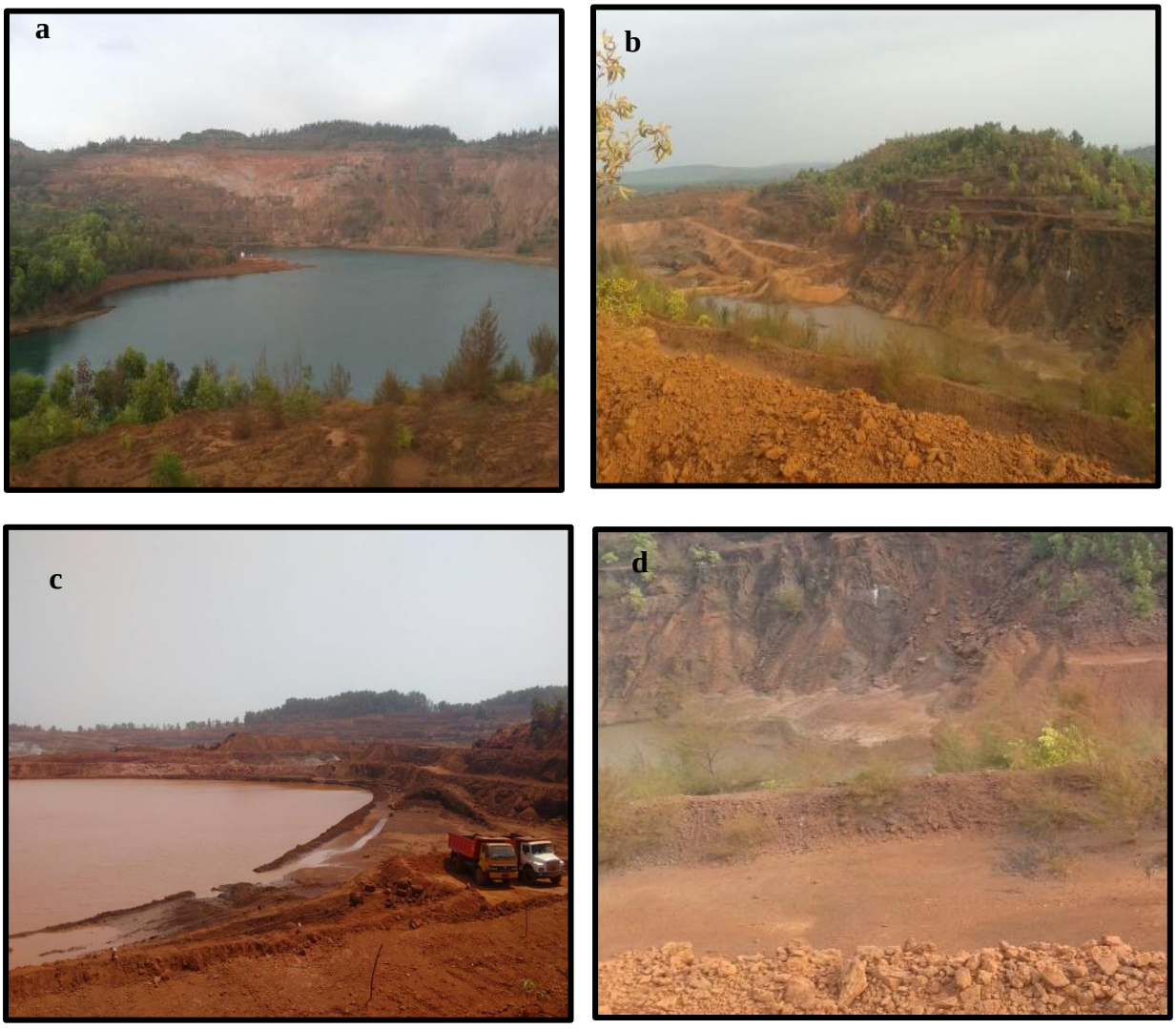

Figure 2.7 (a-b): Sampling sites in North Goa and South Goa. a- Shirgao, b-Bicholim, c-Velgeum, d-Sacorda

2.3.4. Non-mining areas

The aim of this study was the detection of secondary Gold and to isolate useful microbes associated with such material. The samples away from the mining activities were considered as presumptive auriferous non-mining samples. Samples were collected from non-mining areas of Goa during the period from September 2015-September 2019. Samples collected from non-mining areas includes stream sediments, termite mounds, vermicast, laterite, and beach placer deposits. The sampling area is shown in the **Fig 2.8.** The sample location is given in the **Table 2.2.**

2.3.4.1. Stream sediments

The sediments were collected from the Mhadei wildlife sanctuary, Bondla wildlife sanctuary, and Mahavir wildlife sanctuary. Several kgs of sediment was collected from the stream bed, firstly placing the top 10-20 cm back into the stream. Particularly large pieces of rock were similarly removed, and then the rest was fed through a series of increasingly finely-meshed sieves until the desired size of sediment particles was isolated for bagging, to be sent for lab chemical analysis. The stream sediment samples were collected randomly from the bottom of active stream channels using a spade onto a stainless steel, flat-bottom conical pan (Mimba et al., 2014). During repeated shaking cycles, the lighter particles were washed away whereas the heavier ones settled down the pan. This process was repeated until a residue of heavy minerals was obtained (Grema et al., 2021). The samples were designated as SS-03 to SS-07. The sampling sites are shown in the **Fig 2.9**.

2.3.4.2. Vermicasts (Geophagous Earthworm deposits)

Several well-structured vermicasts were handpicked from different locations in Goa as shown in **Fig 2.10 (a-c)**. Around 1000-2000 single samples were handpicked from different locations (Dabolkar and Kamat, 2019). The samples were designated as VM-01 to VM-06.

2.3.4.3. Termite mounds

In and around forest, 20 termite mounds were explored. Composite samples of soils from each termite mound and its adjoining soil samples were collected in a tray and plastic bags as shown in **Fig 2.10 (d-f)** (Gleeson & Poulin, 1989). The samples were designated as TM-01 to TM-07.

2.3.4.4. Laterites

Laterite is a product of intense sub aerial weathering; it hosts numerous valuable economic deposits like Nickel, Manganese, Iron, Alumina, Gold etc. Laterites were collected from different occurrence of lateritic areas in Goa in trays and plastic bags and transferred to the laboratory (Santosh et al.,1992). The sampling sites and samples are shown in the **Fig 2.11.** The samples were designated as LT-01 to LT-09.

2.3.4.5. Beach and placer sand samples

The sand samples were collected from the North Goa and South Goa beaches. The sampling sites of sand includes beaches like Keri, Arambol, Ashvem, Morjim, Chapora, Vagator, Anjuna, Baga, Miramar, Colvale, Velsao, Arrosim, Majorda, Colva, Varca, Fatrade, Cavellosim, Mobor, Patnem, Agonda, Palolem, Pollem, Galjibag. The sand samples were collected using the pool sampling method. Metal rod (10 cm deep) was used to dig out the sand (Atherton et al., 2001). The samples were collected in the bottles and plastic bags and

brought to the laboratory. The samples were designated as BS-01 to BS-19. The sampling site is shown in the **Fig 2.12 (a-f).**

2.4. Photo documentation

All photos were taken in the field using Canon EOS 300D DSLR camera and iPhone 8plus with 12 MP f/1.8,28 mm(wide), 2X optical zoom with Quad -LED dual-tone flash, HDR.

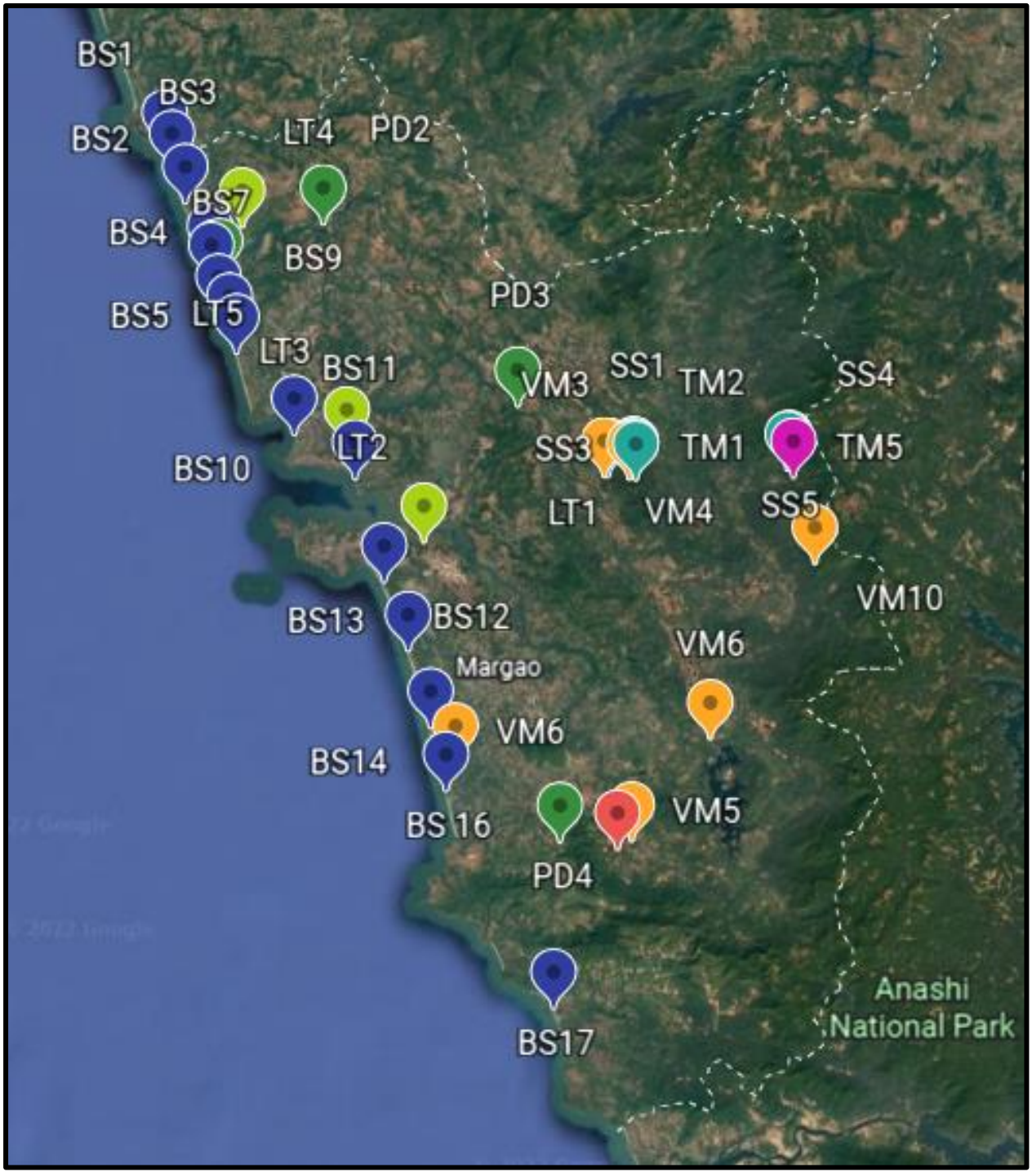

Figure 2.8: Sampling sites from non-mining areas superimposed on google earth terrain view

Table 2.2: Geolocation of samples from non-mining areas (Source: https://www.google.com/earth/versions/)

Sample designation	Longitude and longitude	
SS-03	15’11’13.33” N	74’01’06.15” E
SS-04	15’25’57.79” N	74’15’36.59” E
SS-05	15’26’24.91” N	74’06’26.81” E
SS-06	15’11’13.33” N	74’01’06.15” E
SS-07	15’11’13.33” N	74’01’06.15” E
PD-01	15’25’57.79” N	74’15’36.59” E
PD-02	15’26’24.95” N	74’06’26.91” E
VM-01	15’10’37.05” N	74’11’14.39” E
VM-02	15’10’37.05” N	74’11’14.39” E
VM-03	15’11’13.33” N	74’01’06.15” E
VM-04	15’11’13.33” N	74’01’06.15” E
VM-05	15’25’57.79” N	74’15’36.59” E
VM-06	15’26’24.91” N	74’06’26.81” E
LT-01	15’27’59.13” N	74’02’19.77” E
LT-02	15’10’37.05” N	74’11’14.39” E
LT-03	15’27’59.13” N	74’02’19.77” E
LT-04	15’10’37.05” N	74’11’14.39” E
LT-05	15’27’59.13” N	74’02’19.77” E
LT-06	15’10’37.05” N	74’11’14.39” E
LT-07	15’27’59.13” N	74’02’19.77” E
LT-08	15’10’37.05” N	74’11’14.39” E
LT-09	15’27’59.13” N	74’02’19.77” E

Fig 2.9 (a-f): Exploration of stream sediments a-c: Bhagwan Mahavir wildlife sanctuary, d-f: Stream sediment at Tambdi surla

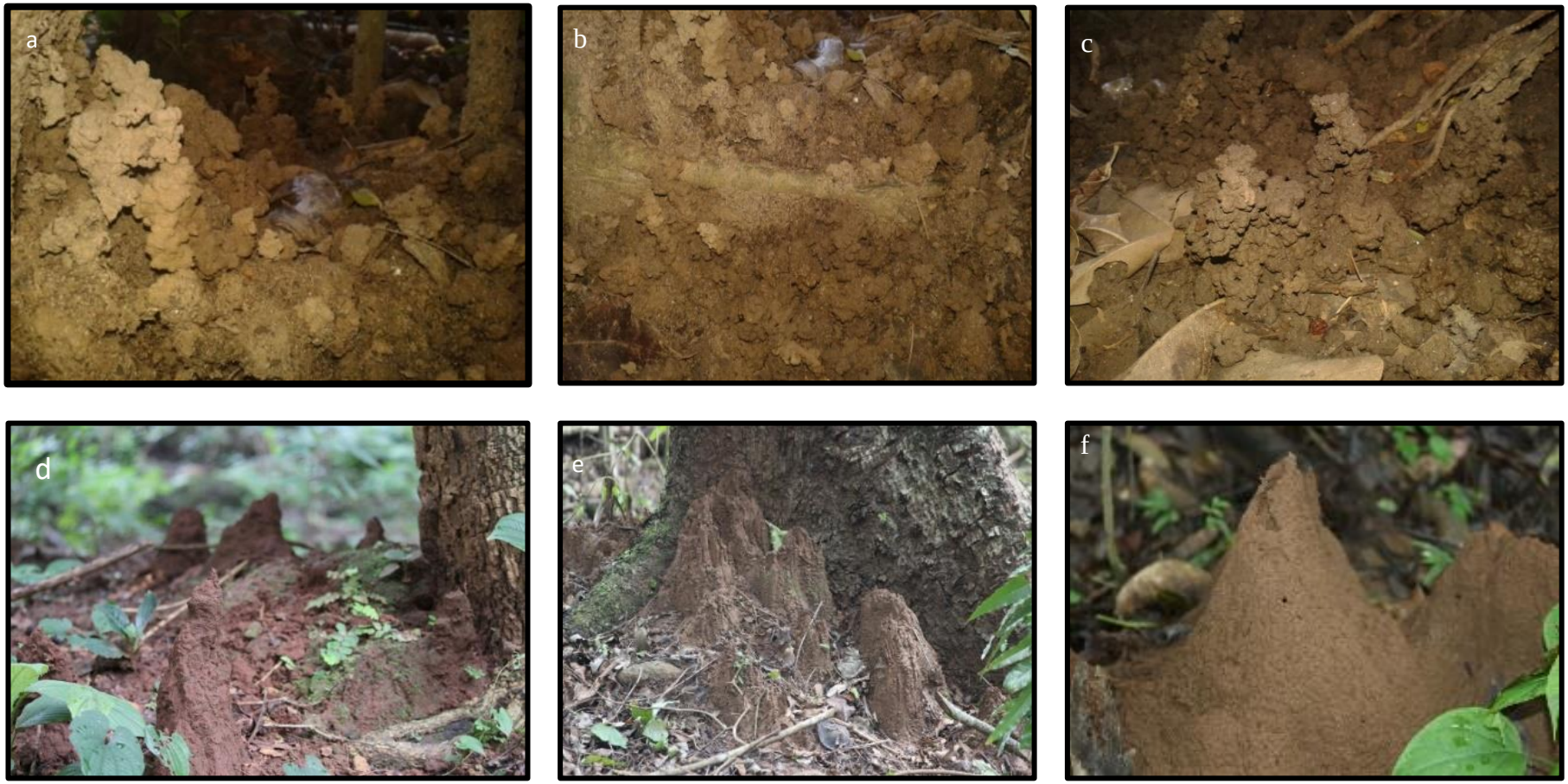

Figure 2.10 (a-f): Exploration of vermicasts and Termites mounds a-Vermicasts at Taleigao, b-Vermicasts at Shiolim, c-Vermicasts at Goa University under *Phycus Bengalensis;* d, e-Termite mound at Bondla; f- Termite mound at Tambdi Surla.

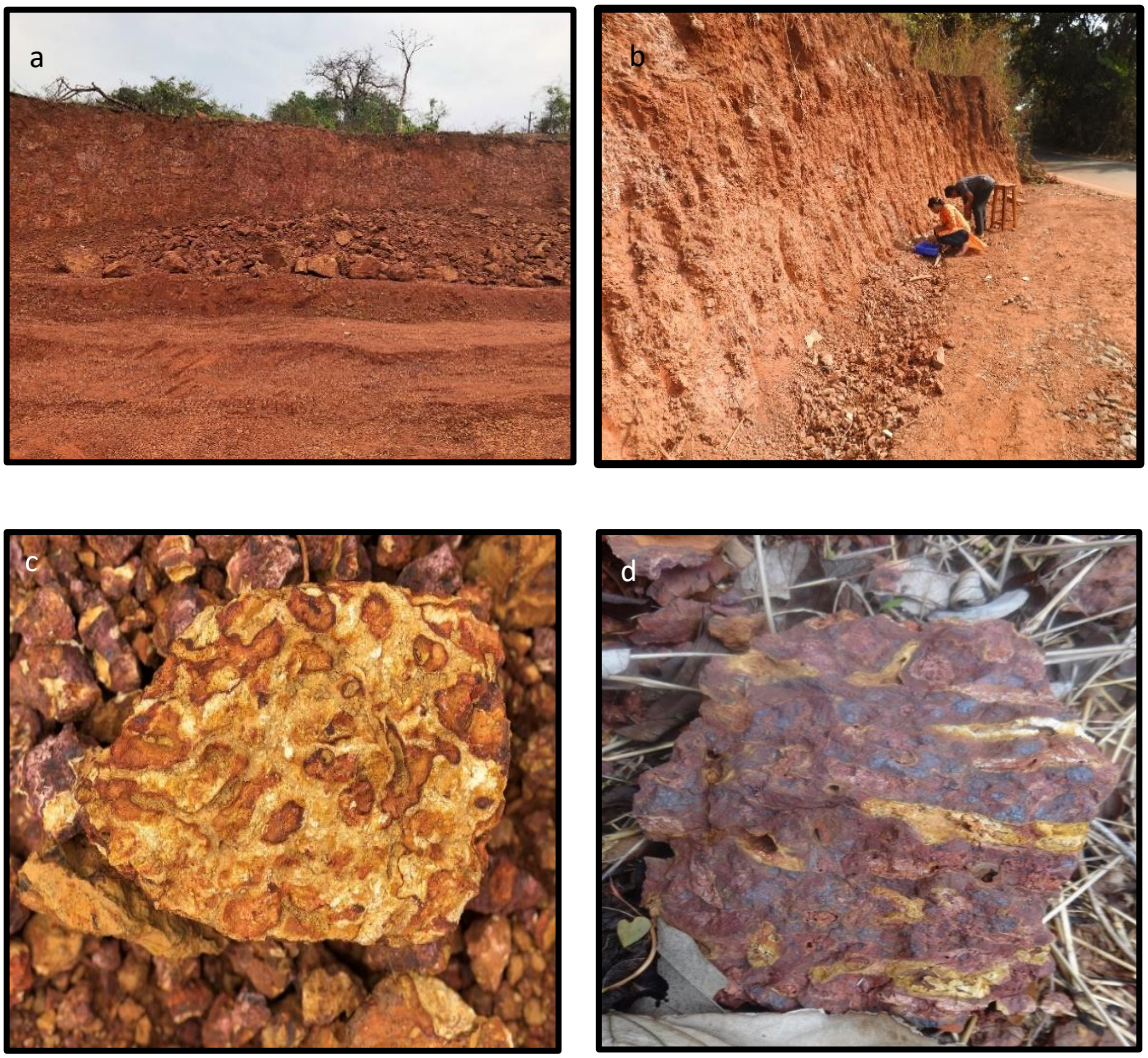

Fig 2.11 (a-d): a-Laterites at Bambolim, b-Laterite at Sancaole, c-Porvorim, d-Bondla

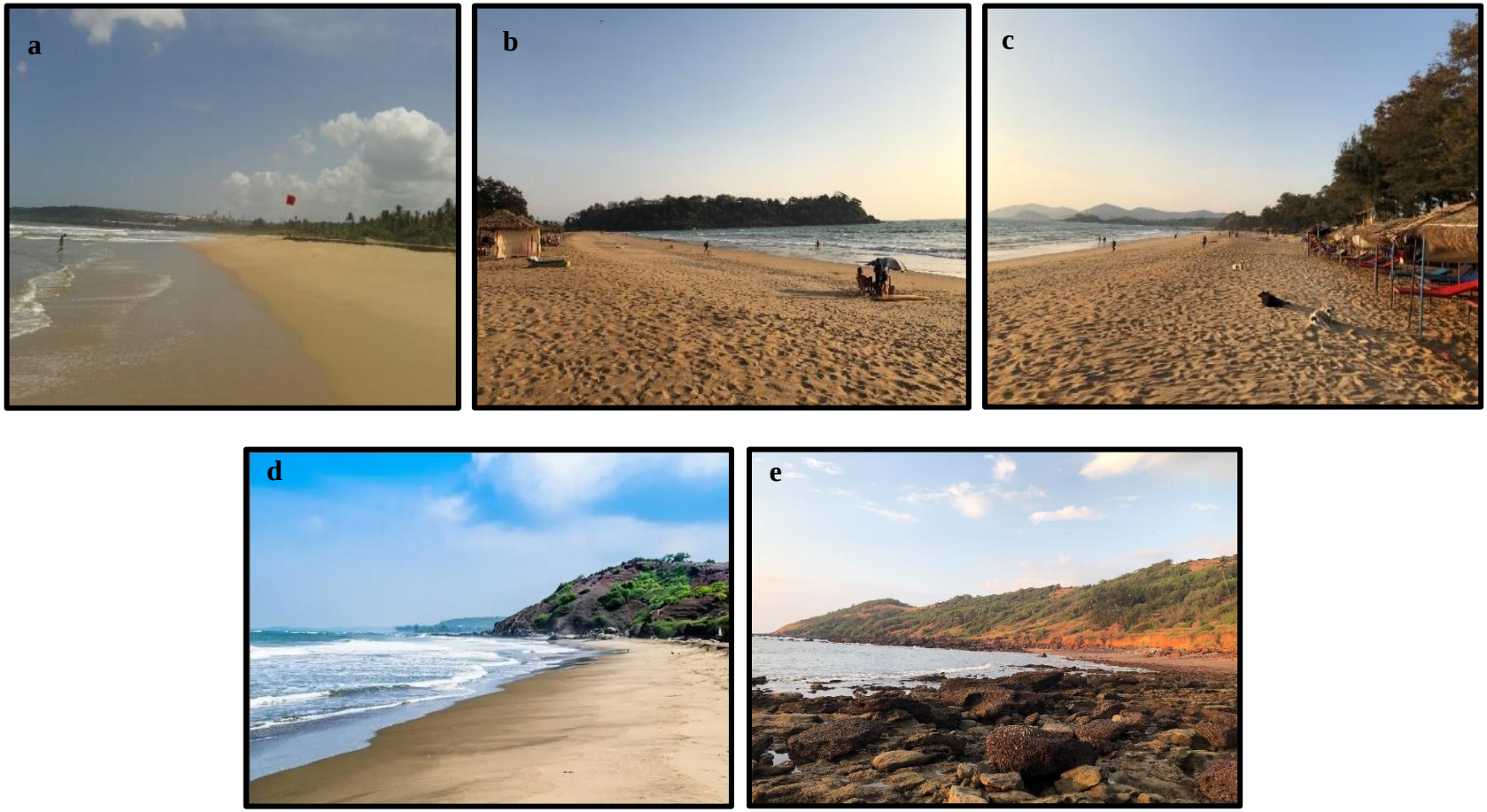

Figure 2.12 (a-f): a-Velsao beach; b-Patnem beach, c-Agonda beach, d-Vagator beach, e-Anjuna beach

2.5. Detection of Gold

2.5.1. Inductively Coupled Plasma Optical Emission Spectroscopy (ICP-OES)

Inductively Coupled Plasma Optical Emission Spectroscopy (ICP-OES) is used to detect less than a nanogram of AuNPs from complex un purified biological samples. ICP-OES is a non-optical analytical technique which is unaffected by optically active molecules, opaque solutions, and organic or inorganic contaminants. Quantification of Gold was carried out using Agilent 5110 ICP-OES (Cera Laboratories Mumbai). To carry out these following steps were followed:

2.5.1.1. Preparation of sample

1 kg of each sample was dried, powdered using mortar and pestle (Panda et al., 2011). The recovered sample was concentrated by panning method (Southam et al., 2009) and subjected to magnetic separation using 2 Tesla neodymium magnet (deOliveira and Larizzatti, 2006) and sieved into different fractions with the sieve size of 250, 150, 106, 53 μm. 10 grams of each sample was dried completely at 105°C (Panda et al., 2011). 106-micron size sieved fraction of each sample was packed in a sterilized screw capped tubes and sent for the analysis. ICP-OES is an analytical technique used for the detection of chemical elements (Pyrzyńska, 2005; Tang, 2020). Quantification of Gold was carried out using Agilent 5110 ICP-OES (Cera Laboratories Mumbai).

2.5.2. SEM-EDX Study of bacterioform Gold particles

SEM provides detailed high-resolution images of the sample by rastering a focussed electron beam across the surface and detecting secondary or backscattered electron signal. Samples showing presence of Gold were analyzed using Carl-Zeiss Scanning Electron Microscope (SEM-EDX) (USIC, Goa University) (Falconer and Craw, 2006).

2.5.2.1. Sample preparation

50 grams of each sample was used to carry out the studies. Samples were dried, powdered using mortar and pestle (Panda et al, 2011). The recovered sample was concentrated by panning method (Southam et al., 2009) and subjected to magnetic separation using 2 Tesla neodymium magnet (deOliveira and Larizzatti, 2006) and sieved into different fractions with the sieve size of 250, 150, 106, 53 μm. 1 gram of each sample was dried completely at 105°C (Panda et al., 2011). 106 micron size sieved fraction of each sample was packed in a sterilized screw capped tube and sent for SEM-EDX analysis. This instrument is equipped with an energy dispersive spectrometer (EDX). Analysis was conducted using acceleration voltages between 15 and 20 keV (Falconer and Craw, 2006).

2.6. Morphological and typological classification of BFG particles

2.6.1. Optical microscopy

The samples previously analyzed for Gold content using ICP-OES were studied for their morphological characteristics such as shape, size, color, surface texture and typological characteristics. Samples showing the high ppm values were used for this study.

2.6.2. Sample preparation

1 kg of each sample was used to carry out the study. Samples were dried and powdered using mortar and pestle (Panda et al., 2011). The recovered sample was concentrated by panning method (Southam et al., 2009) and subjected to magnetic separation using 2 Tesla neodymium magnet (deOliveira and Larizzatti, 2006) and sieved into different fractions with the sieve size of 250, 150, 106, 53 μm. 10 grams of each sample was dried completely at 105°C (Panda et al., 2011). Each sieved fraction was dried completely and mounted with the DPX mountant. Each slide was labelled and preserved for the future study. The

morphological parameters documented during the present study include the general shape of the BFG particles, size, colour, and surface texture.

2.6.3. Microscopic studies

Slides were studied using light microscopy (Nikon Eclipse E200 MVR, Tokyo) and phase contrast microscopy (Olympus BX41). Each slide was studied under different fields. Each slide was labeled and stored for future studies.

2.7. Scanning Electron Microscopic (SEM) studies

2.7.1. Sample preparation

50 grams of each sample was used to carry out the studies. Samples were dried, powdered using mortar and pestle (Panda et al, 2011). The recovered sample was concentrated by panning method (Southam et al., 2009) and subjected to magnetic separation using 2 Tesla neodymium magnet (deOliveira and Larizzatti, 2006) and sieved into different fractions with the sieve size of 250, 150, 106, 53 μm. One gram of each sample was dried completely at 105°C (Panda et al., 2011). 106-micron size sieved fraction of each sample was packed in a sterilized screw capped tube and analyzed for SEM.

2.7.2. SEM studies of BFG particles

BFG particles were analyzed using Scanning Electron Microscope (SEM) using VEGAS3 TESCAN instrument. Gold is electron dense and do not require sputter coating and thus samples were analyzed uncoated. The images were obtained with operational conditions 15 to 35 kV (Falconer et al., 2006). The samples were C-coated prior to analysis (Falconer and Craw, 2006). Several SEM based commercial software packages such as ® Mountains Map SEM software (Digital Surf), 3D Surface Modelling (3DSM) (Carl Zeiss Microscopy), MeX (Alicona), Scandium Height (Olympus Soft Imaging Solutions), 3D SEM Three-

Dimensional Image Software (JEOL) could be used to study three-dimensional (3D) SEM typological studies. In present study SEM images were processed using ® Mountains Map software version 6.2.7200 released on 18 September 2014. 7.3 version SEM software (Digital Surf, Besancon, France) surface imaging and metrology software for 3D SEM biometrologic image analysis and colourization of SEM images were done using SEM Color 7.4 version (http://www.digitalsurf.com/) (de Souza and Kamat, 2018).

The summary of the same is given in the **Fig 2.13.**

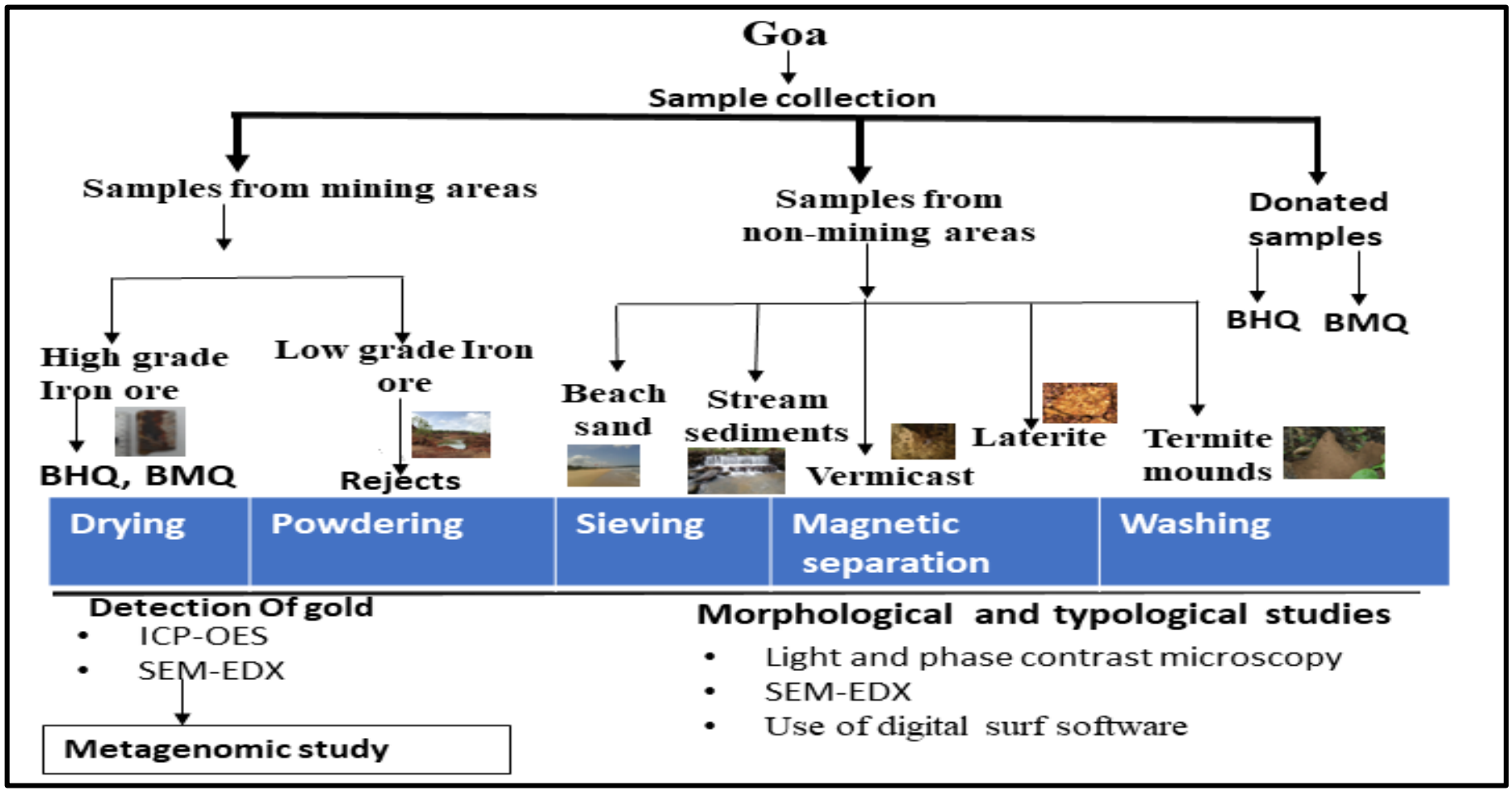

Figure 2.13: Scheme of detection of Gold and morphological studies

2.8. Metagenomic studies of BHQ and BMQ

The samples were surface sterilized and scraped using 70% ethanol treatment on the exolithic surface of the samples and flame sterilized near the spirit lamp (Hirsch et al., 1995) and sent for metagenomic analysis in a sterilized screw capped tube. Surface sterilized samples were scraped using sterile scrapper till the sufficient amount is obtained and collected on a sterile aluminum foil and transferred into the sterile tube. The samples were labelled as A1 and A2 ie A1-Banded Hematite Quartzite (BHQ), A2-Banded Magnetite Quartzite (BMQ). Metagenomic studies were carried out using Oxford nanopore sequencing at Triyat Genomics (A division of Triyat Scientific Co.) Nagpur, Maharashtra, India. The methodology followed includes DNA isolation metagenomics, 16s primer amplification, library preparation and Bioinformatics (Dabolkar and Kamat, 2022).

2.9. Isolation of hyperacidophillic and chemolithotrophic bacteria from the auriferous samples

2.9.1. Selection of auriferous samples for Winogradsky technique

Total six samples showing the presence of Gold were used in this study**.** The samples used from mining areas included BHQ-Banded Hematite Quartzite, BMQ-Banded magnetite Quartzite and low-grade ore (mining reject). The samples from non-mining areas includes vermicasts, laterites, stream sediments and beach sands. The list of the sample used in the study is given in **Table 2.3** with its designation.

2.9.2. Preparation of Winogradsky column

Sterile plastic bottles were filled with 5-7 cms with charging mixture which included 10 gm slurry of shredded filtre paper (sterilized), 10 gm of each calcium sulphate, calcium carbonate and 1 gram of unsterilized soil sample. Column was filled carefully with the

sterile D/W to about ½ inches from the top and kept the bottle in dark for 1-2 weeks away from the light. After two weeks, the columns were kept in light and incubated for several weeks (Hairston, 1999). The preparation of Winogradsky column is shown in **Fig 2.14.**

2.9.3. Disruptive sampling of the wall deposit (Presumptive biofilm)

The sampling of the biofilm was carried out under sterile condition. The biofilms were carefully sampled by using alcohol sterilized plastic tube which were used to stiffened out the liquid by applying suction and was transferred to another bottle without disturbing the biofilm.

2.9.3.1. Preparation of coverslip size pieces from PET bottles

The preparation of the coverslip size pieces was carried out under laminar air flow after selecting the biofilm areas. Alcohol sterilized scissor was used to cut the bottle to make two semi cylindrical parts. The area of interest from the biofilm deposited on the bottle was further cut into coverslip size (2X 2 cm or 400 mm^2) pieces. The coverslip size pieces with biofilm attached were further used for microscopic studies (Dabolkar and Kamat, 2022).

2.9.3.2. Slide preparation and microscopic observation

The coverslip size pieces were mounted on a microscopic slide (Borosil, 9100D01 - double frosted, 76 x 26 x 1 mm) and sealed with DPX mountant and allowed to dry. The slides were observed stereoscopically (Olympus SZ51) for the presence of biofilms.

2.9.3.3. Formulation of specific medium for enrichment

The media used for the enrichment was specific 9K broth medium (Starkey, 1935) without agar. The specific medium composition for all three microorganisms ie. *Acidithiobacillus, Leptospirillum* and *Sulfobacillus* is given in the **Table 2.3, Table 2.4 and Table 2.5.**

Column was filled carefully with the sterile D/W to about 1-2cms from the top

10gm slurry of shredded filter paper (sterilized), 10 gram of each calcium sulphate, calcium carbonate and 1 gram of unsterilized soil sample

Figure 2.14: Winogradsky column

Table 2.3: List of samples used in preparation of Winogradsky column along with its designation.

Sample	Sample designation
Banded Haematite Quartzite (BHQ)	BHQ-WC
Banded magnetite Quartzite (BMQ)	BMQ-WC
Low grade Iron ore (Reject)	LGIO-WC
Laterite	L-WC
Vermicasts	V-WC
Stream sediments	SS-WC

Table 2.4: 9K medium used for isolation of *Acidithiobacillus* (Starkey, 1935)

Medium composition	Metal salts g/100ml distilled water
$FeSO_4.7H_2O$	4.42 g
$(NH_4)_2SO_4$	0.30 g
KCl	0.010 g
$K_2HPO_4.3H_2O$	0.050 g
$MgSO_4.7H_20$	0.050 g
$Ca(NO_3)_2.4H_2O$	0.0010 g
pH	1.8-2.0
Temperature	25-30˚C

Table 2.5: 9K medium used for the isolation of *Leptospirillum* culture (Starkey, 1935)

Medium composition	Metal salts g/100ml distilled water
$FeSO_4.7H_2O$	1.4
$(NH_4)_2SO_4$	0.02 g
$K_2HPO_4.3H_2O$	0.010 g
$MgSO_4.7H_20$	0.04 g
pH	1.9-4
Temperature	25-30˚C

Table 2.6: 9K medium used for the isolation of *Sulfobacillus* (Starkey, 1935)

Medium composition	Metal salts g/100ml distilled water
$FeSO_4.7H_2O$	2.210 g
$(NH_4)_2SO_4$	0.050 g
KCl	0.010 g
$K_2HPO_4.3H_2O$	0.02 g
$MgSO_4.7H_20$	0.030 g
$Ca(NO_3)_2.4H_2O$	0.0070 g
$Na_2S_2O_3$	0.0248 g
Yeast extract	0.002 g
pH	1.9
Temperature	25-30˚C

2.9.3.4. Suspension preparation and inoculation

First, the enrichment was done in a selective enrichment broth (in order to promote their growth, increase their numbers, causing extinction by reducing other micro-organisms present in the sample). The scrapped biofilm from each bottle of each sample were suspended into sterile 10 ml tubes glass tube (Thomas scientific) of 9K broth medium without sulfur in a triplicate. The composition of the same medium is given in the **Table 2.7, 2.8 and 2.9.** It was carried out at 150 rpm in sterile tube with approximate throw up 1.5 cm for three weeks. And temperature (30-35^{o}C) in dark on a orbital shaker.

2.9.3.5. Monitoring of the culture tubes

Each tube was studied after every week under the stereomicroscope (Olympus SZ2, Tokyo, Japan) for biofilm formation and turbidity. The slide preparation of tube from each sample was carried out.

2.9.3.6. Confirmation by optical microscope with and without staining

A drop of culture was mounted directly on a slide and covered with coverslip and observed under light microscope examined using Nikon Eclipse E200 microscope with Nikon DS-fi2 camera and NIS element microscope imaging software. Crystal violet staining was carried out and observed under the same microscope. The culture tubes showing the positive results where further subjected for enrichment.

2.9.3.7. Isolation of microbial pure cultures

Pure cultures of iron and sulphur bacteria were successfully obtained on specific hyperacidic media (9K medium) after two weeks. The tubes showing most positive results were used for the isolation of the culture. Monitoring of the plates was carried out after every seven days. The plates were observed under stereomicroscope for the formation of

any growth. The pure cultures were studied by monochrome staining and microscopically observation of slides was carried out under light microscope examined using Nikon Eclipse E200 microscope with Nikon DS-fi2 camera and NIS element microscope imaging software. The pure cultures were analyzed using Carl-Zeiss Scanning Electron Microscope (SEM-EDX) (USIC, Goa University) (Dec et al., 2018).

2.9.3.8. Designation and maintenance of the colonies

Cultures were designated as GUTHIOBHQ-1, GUTHIOBHQ-2, GUTHIOBHQ-3, GUTHIOBHQ-4, GUTHIOBHQ-5, GUTHIOBHQ-6, GUTHIOBHQ-7, GUTHIOBMQ-8, GUTHIOBMQ-9, GUTHIOBMQ-10, GUTHIOBMQ-11, GUTHIOMR-12, GUTHIOMR-13, GUTHIOMR-14, GUTHIOMR-15, GUTHIOLT-16, GUTHIOLT-17, GUTHIOLT-18, GUTHIOVM-19,GUTHIOSS-20,GULEPTOMR-21,GULEPTOBHQ-22, GULEPTOBHQ-23,GULEPTOBMQ-24,GULEPTOMR-25,GULEPTOVM-26, GUSULPHOBHQ-27, GUSULPHOBMQ-28, GUSULFHOMR-29, GUSULFOMR-30. Long term cultures were stored in 10% (v/v) sterile glycerol (4 ml) in gamma sterilized cryovials (Tarsons Products Pvt. Ltd., Kolkata, India) and kept at 30^{o}C and were checked at 3–4 months interval for viability. All chemicals used for media preparation were obtained from HiMedia Laboratories, Mumbai, India. Tentative identification of the culture was based on colony characteristic, biochemical test, microscopic characteristics.

Table 2.7: Salt composition of 9K medium for enrichment of *Acidithiobacillus* (Starkey, 1935)

Medium composition	Metal salts g/100ml distilled water
$FeCl_3$	4.42 g
NH_4Cl	0.30 g
KCl	0.010 g
$K_2HPO_4.3H_20$	0.050 g
$MgCl_2$	0.050 g
$Ca(NO_3)_2.4H_2O$	0.0010 g
pH	1.8-2.0
Temperature	25-30 ˚C

Table 2.8: Salt composition for 9K medium for enrichment of *Leptospirillum* cultures (Starkey, 1935)

Medium composition	Metal salts g/100ml distilled water
$FeCl_3$	1.4 g
NH_4Cl	0.02 g
$K_2HPO_4.3H_2O$	0.010 g
$MgCl_2$	0.04 g
pH	1.9-4
Temperature	25-30 ˚C

Table 2.9: Salt composition for each 9K medium for enrichment of *Sulfobacillus* cultures (Starkey, 1935).

Medium composition	Metal salts g/100ml distilled water
$FeCl_3$	2.210 g
NH_4Cl	0.050 g
KCl	0.010 g
K_2HPO_4. $3H_2O$	0.02 g
$MgCl_2$	0.030 g
Ca $(NO_3)_2$. $4H_2O$	0.0070 g
Yeast extract	0.002 g
pH	1.9
Temperature	25-30 ˚C

2.10. Isolation of actinobacteria

2.10.1. Selection of samples

Samples which were showing positive results for Gold were used in this study. Total six samples were used from mining areas such as BHQ-Banded Haematite Quartzite, BMQ-Banded magnetite Quartzite and non-mining areas such as vermicasts and laterite. The list of the sample used is given in **Table 2.10** with its designation.

Table 2.10: Auriferous samples used for isolation of actinobacterial cultures

Sample	Sample designation
Banded Haematite Quartzite (BHQ)	BHQ-WC
Banded magnetite Quartzite (BMQ)	BMQ-WC
Low grade Iron ore (Reject)	LGIO-WC
Laterite	L-WC
Vermicasts	V-WC
Stream sediments	SS-WC

2.10.2. Isolation of actinobacteria

2.10.2.1. Isolation medium

It was prepared by modifying the components to selectively capture actinobacteria diversity by pour plate and soil imprint technique (Kamat & Velho-Pereira, 2012). The composition of modified AVA medium is given in **Table 2.11**. The basal medium and the stock trace element solution were sterilized by autoclaving at 121^{o}C for 20 min and pH of the medium was adjusted to 6.8 by using 0.1N NaOH/HCl. The stock vitamin and antibiotic solution was membrane sterilized and added later to the presterilized basal medium.

Table 2.11: AVA medium composition (Velho-Pereira and Kamat, 2011)

Basal medium	
Glycerol	0.08 ml
Glucose	0.1 g
K_2HPO_4. $3H_2O$	0.03 g
L-arginine	0.03 g
NaOH	0.03 g
$MgSO_4.7H_2O$	0.02 g
Agar	1.8 g
Distilled water	100 ml
Stock trace element solution (Add 0.1 ml to the basal medium)	
$Fe_2 (SO_4)_3$	50 mg
$CuSO_4.5H_2O$	50 mg
$MnSO_4.4H_2O$	50 mg
$ZnSO_4.7H_2O$	50 mg
Distilled water	50 ml
Stock vitamin solution (Add 0.1 ml to the basal medium)	
Thiamine	100 mg
Calcium panthothenate	25 mg
Meso-inositol	25 mg
Nicotinic acid	25 mg
P-aminobenzoic acid	25 mg
Pyridoxine	25 mg
Riboflavin	25 mg

Biotin	12.5 mg
Distilled water	50 ml
Antibacterials	
Nalidixic acid	0.0176 mg/ml
Neomycin and polymyxin b sulphate	0.01 mg/ml
Antifungals	
Nystatin	0.004 mg/ml
Actidione	0.00192 mg/ml

2.10.2.2. Samples

For testing the technique, the same samples as mentioned in **Table 2.10** Goa, India were selected as sampling site.

2.10.2.3. Sieving of the soil fractions and determination of the percent dry weight

50 grams of each of the air-dried soil samples was passed through surface sterilized brass sieves (Kumar Test sieves, Bombay) having mesh of sizes 1000, 250, 150, 105 & 53 µm. The sieved fraction was collected carefully to avoid minimum retention of soil particles on the respected sieves. These sieved fractions were subsequently labelled and weighed to obtain the percent dry weight (Velho-Pereira and Kamat, 2011)

2.10.2.4. Preparation of the coated slides (Velho-Pereira and Kamat, 2011)

AVA medium as mentioned in **Table 2.11** was used as 'Slide Coating Medium' (SCM). Two treatments were used in first the slides coated with AVA homogeneously mixed with antibacterials and antifungals and the second without. Standard plain microscope glass slides (HiMedia, Mumbai, India) 75 x 25 mm and 1.0 mm thick were used as inert coating

surface. To permit routine direct stereomicroscopic observations in a marked pre-defined area, a quadrat of the size of a standard cover slip, app. 324 mm^2 (Corning Glass, USA, Type n No.1, 18 x 18 mm, thickness 0.16 mm) was chosen at the centre of the reverse side of the area to be coated and was marked carefully. The slides were then sterilized by autoclaving at 121^oC for 20 min. The slides were transferred in an 11 cm diameter sterile petri plate (Himedia, Mumbai, India) for coating of the medium to the marked central area. Two sets of slides in triplicates one with the coating medium incorporated with antibacterial and antifungals and other without were prepared. Sterile homogenous molten AVA medium cooled to 40^oC was carefully poured in a single thin stream from a 500 ml Erlenmeyer flask on each slide to get a uniform coating. The coated slides were then transferred back to the petri plate for solidifying and excess medium crossing the edges of the marked area was removed. The solidified coated slides were designated as per a present scheme and used within 15- 30 min. All the operations were performed on a laminar air flow bench (Velho-Pereira and Kamat, 2011).

2.10.2.5. Removal and screening of slides

A pair of slides was sequentially extricated from respective SIS on 4, 7, 12, 15, 22, 26 and 28 days. After removing loose extraneous soil particles, these were observed under Olympus BX41TF microscope (Tokyo, Japan) with digital photomicrographic attachment.

2.10.2.6. Actinobacteria isolation from colonized surface

For sampling, AM colony forming units (CFUs) from colonized surface, jets of 2 ml of sterile distilled water were directed (for each pair of extricated slides) using a sterile accipient model T1000 (Tarsons Products Pvt. Ltd., Kolkata, India). Washings were collected in a sterile glass beaker and an aliquot (0.1 ml) was then plated on AVA medium with antibiotics (as described previously) and incubated at 28-30^oC for upto 30 days.

2.10.2.7. Assessment of Actinobacteria diversity

Plates were observed daily under Olympus SZ2-ILST stereomicroscope (Tokyo, Japan) and morphologically dissimilar colonies were identified by recording growth, aerial spores-mass colour, texture, elevation; substrate mycelium colour, margin, pigment production and presence or absence of exudates (Velho-Pereira and Kamat,2012). Isolates representing dissimilar morphotypes were then identified, selected and purified on AVA plates. Pure colonies were transferred to AVA slants. Isolated pure strains were designated and maintained at the ambient temperature of 26-34^{o}C. One set of pure cultures/strains were transferred in cryovials containing sterile 20% glycerol and kept at 4^{o}C for ensuring long term preservation.

2.10.2.8 Taxonomic characterization of isolates

For recording micromorphological details, air dried smears were stained in 1 % (w/v) crystal violet and the spore bearing hyphae were identified with entire spore chain along with other microstructures (Locci, 1989). Using the keys described by (Locci, 1989) the isolates were classified as Genus *Streptomyces* (spore chain with coiling, spiral and looped), Genus *Nocardia* (Fragmented mycelium both in substrate and aerial) and others were unidentified and maintained on same media on slants.

2.11. Selection of promising fungus cultures *Termitomyces heimii and T. clypeatus*

Termite mounds is an important bioindicator for Gold and helped in extraction of Gold from the mines of different parts of the world such as India, Africa and Australia. They have been used in biogeochemical exploration of heavy metals (Prasad, 1987). *Termitomyces* mushrooms only grow in association with termites and their nests and are dependent on the organic matter brought by the insects from their feeding on trees.

2.11.1. Collection of fruitbodies of *Termitomyces heimii and T. clypeatus* for culture

Fresh fruitbodies were collected from various termite hill habitat in year 2017−2019 were identified and which were previously studied and identified from same location. The sampling sites are shown in **Fig 2.15**. *Termitomyces heimii* being the most dominant species and state mushroom of Goa was used for the present investigations (De Souza and Kamat, 2018). Mushrooms were divided into two lots one was used for obtaining cultures for GNPs and entire mushrooms was used for GNPs.

2.11.2. Pure culture isolation of *Termitomyces heimii* and *T.clypeatus*

Pure cultures were obtained from context tissues of fruitbodies Cultures obtained from a fresh healthy living mushroom fruitbody were cultured by tissue culture method previously described by Stamets and Chilton (1983). Tissue explants of 0.5 cm^2 were taken from sterile exposed context tissue and were inoculated in 2% MEA medium with 0.01 mg/ml conc. of Nalidixic acid and Neomycin, incubated in dark at 28 °C, subcultured on fresh medium and incubated for 2−12 weeks. Colony characters were recorded. Long term cultures were stored in 10% (v/v) sterile glycerol (4 ml) in gamma sterilized cryovials (Tarsons Products Pvt. Ltd., Kolkata, India) and kept at 25^oC and were checked at 3-4 months interval for viability. All chemicals used for media preparation were obtained from HiMedia Laboratories, Mumbai, India. All this work was tried earlier was found to be having good results as done in dissertation and PhD work by earlier students (Sharma and Kamat, 2017, Petkar and Kamat, 2017, D'Souza and Kamat, 2018).

Figure 2.15 (a-c): a,b-The sampling sites of the *Termitomyces heimii* and *T.clypeatus*, c-collection of the *T.heimii*

2.12. GNP synthesis

2.12.1. GNP synthesis using actinobacterial cultures

For testing the GNPs formation, live suspension of culture was treated with $HAuCl_4$ on a clean slide (ratio 1:2) to form thick smear onto the slide and observations were carried out after interval of time at RT.

2.12.2. Effect of thermal treatment of GNP assemblies

For testing the GNPs formation, live suspension of culture was treated with $HAuCl_4$ on a clean slide in the ratio 1:2 to form thick smear onto the slide. The slides were allowed to dry and subjected to various thermal condition and different interval of time. The slide preparation was subjected to heat treatment of 5 secs, 15 secs, 30 secs, 60 secs, 120 secs, 300secs and 600 secs. The slides were made to cool and observed under light microscope for GNPs assemblies.

2.12.3. Use of *Termitomyces heimii* for GNP synthesis

The collected mushroom specimens were cleaned with 95% ethanol (v/v) for 30 seconds and subsequently photographed. Specific processing of each part of the fruitbody, ie umbonal tissue, pileus context, lamellae, stipe context, stipe, epicutis, pseudorrhiza context, pseudorrhiza epicutis was carried out. Using a sterile forceps small pieces of the tissues were transferred into a micro test plate (Tarson, Mumbai) with 96 wells having volumetric capacity of 420 µl under a Laminar air flow bench. Due care was taken to use identical appropriate fragments of tissue size equivalent to 200 µm. Tissues were tested with 200 µl chloroauric acid (one mM) and at an interval of 5, 10, 15, 30, 45, 60, 120 minutes and 12, 24 and 48 hours. Nine replicates of each tissue were taken for experimentation.

2.12.4. Preparation of extracts

Sterile water-soluble extracts (SWSE) were prepared by grinding the material in sterile mortar and pestle, which was then centrifuged and membrane filtered (0.22 µm pore size, 30 mm diameter-HIMedia laboratories). The SWSE were stored at refrigerated temperature in sterile test tubes. The extracts (210 µl) and chloroauric acid (210 µl) were mixed in a equal proportion in a well of microwell test plate and checked after interval of 5, 10, 15, 25, 30, 45, 60, 120 minutes and after 12, 24, 48 hours (Dabolkar and Kamat, 2020).

2.12.5. Stereomicroscopic visualization of test plates

The microtest plate with the GNP swarms was visualized under stereomicroscope (Olympus SZ51, model SZ2-ILST, olympus corporation, Tokyo, Japan). Due care was taken to bring the swarm view under uniform illumination in bright light.

2.12.6. Use of Digital Colorimeter

Scanning of the swarms was done using 12 MP plus dual rear (F 1.5/ F 2.4) camera on Samsung Galaxy Note 9 with colorimeter software (http://researchlabtools.blogspot.com/) (Ravindranath et al., 2018) version 3.5.2, (developed by Research Lab Tools, São Paulo, Brazil; purchased from Google Play) which was installed on an android smartphone. There is built in colorimetric software sensor between 350 to 700 nm. Optical sensor is present in the smart phone. This is used for colorimetric operation by this software. Size was determined by standard relationship between the absorbance based on surface plasmon resonance and size of nanoparticles (https://www.sigmaaldrich.com).

2.12.7. Digital color analysis and colorimetric data

The color terminology used is according to color data based on the App which allows online and offline analysis of the samples. Mobile based digital colorimeter was used for the

analysis and obtain spectra in the visible band. Such synthetic nanomaterials are of considerable interest as they are reported to have implications for the future in nanomachinery, nanomedicine, and chemical sensing (Hougaard et al., 2011). Colorimeter software was used to record values such as CIE LAB, Chroma, Hue^{o}, RGB, color names, real time visible spectra (400 nm to 700 nm). Among these Chroma and Hue^{o} have no units of measurements (http://www.huevaluechroma.com). The available digital tools are quite helpful in recording values such as CIE LAB, Chroma, Hue^{o}, RGB, color names, real time visible spectra (400nm to 700nm), etc. The CIE LAB color space (also known as CIE L*a*b* or sometimes abbreviated as simply "Lab" color space) refers to the color space defined by International Commission on Illumination (CIE) in 1976 which expresses color in three values where L* stands for the lightness from black to white, a* from green to red, and b* from blue to yellow. Chroma (Saturation) refers to the strength or dominance of the hue, the quality of a color's purity, intensity or saturation (Solomon and Breckon, 2011). Hue is a common distinction between colors positioned around a color wheel. On the outer edge of the hue wheel are the intensely saturated hues whereas towards the center of the color wheel no hue dominates and becomes less and less saturated. The RGB color model is an additive color model in which red, green and blue light are added in various ways to reproduce an array of colors (Meruga et al., 2014).

2.12.8. Use of Venn diagrams

Venn diagrams are commonly used to display list comparison. However, when the number of input lists exceeds four, the diagram becomes difficult to read. Alternative layouts and dynamic display features can improve its use and its readability. The jvenn library accepts three different input formats “Lists”, “Intersection counts” and “Count lists”. For “Intersection counts”, the lists are given a label (“A” or “B”) which is used to make the correspondence between the list and its count. Finally, “Count lists” provide a count

number for each element of a list. Hence, with “Count lists” the figures presented in the diagram correspond to the sums of counts of all elements shared between lists for “Lists” and “Count lists”, jvenn computes the intersection counts and displays the chart (http://bioinformatics.psb.ugent.be/). Vein diagrams were plotted using tissues and lambda max values.

2.12.9. Preparation of crude aqua regia extract of auriferous samples

Dried Auriferous soils samples were sieved and weighed.10grams of weighed sample was taken in 25ml beaker with glass funnel on top and transferred to fume hood. To this soil samples 25ml of Aqua regia was added very carefully and warmed while stirring every 10mints for 30min (Wakelin et al., 2012). Aqua regia was obtained from Mr. Vijaydatta Lotlikar, local Gold craftman from Parra, Bardez, Goa. Cool it at room temperature and decant muddy extract with crude chloroauric acid into another beaker and centrifuge it, filtere and used for screening of nanoparticles. Prepared CFE and crude $HAuCl_4$ with different concentration were mixed in equal proportion (50:50 v/v) on a slide. Slides were heated for 15 sec, 30 sec, and 45 sec on lamp (Spirit and methanol) and observed for nanoparticle synthesis.

2.13. Production of *T.heimii* Submerged condition for pellet production

2.13.1. Formulation of growth medium

Morphological stable *Termitomyces heimii* cultures were grown on Czapek Dox Agar (CDA) containing 5% sucrose (Carbon source), 0.2% sodium nitrate (Nitrogen Source), 0.1% dipotassium phosphate, 0.05% magnesium sulfate heptahydrate, 0.05% potassium chloride, 0.001% ferrous sulfate heptahydrate, pH 5.5, incubation Temp. 28^{o}C in dark for six days (D'Souza & Kamat, 2017). **Table 2.12** gives the media composition.

2.13.2. Pellet production for nanoparticle synthesis

Pellet is 3-dimentional colony, since more biomass was required, we carried out the palletization (D'souza and Kamat, 2018). Ten cultural plugs (5 mm diam.) from the peripheral growth zone of 6 days old culture were inoculated for cultivation under submerged condition in 100 ml Czapek Dox solution with 5 gm/L Sucrose as carbon source, in 250 ml flasks and were kept on optical shaker at 150 rpm at 28^{o}C, dark for six days. Mycelial suspensions were prepared as per Kalisz et al.,1986 by centrifuging liquid cultures on a research centrifuge (5000 rpm, 20 min) in sterile centrifuge tubes (D'souza and Kamat, 2017).

Table 2.12: Molar composition of Czapek Dox medium

Components	Formula	Mol. Wt. (g)	g/L	Molarity (M)
Sucrose	$C_{12}H_{22}O_{11}$	342.3	5	0.01460
Di-potassium hydrogen phosphate	K_2HPO_4	174.18	1	0.00574
Potassium chloride	KCl	74.56	0.5	0.01341
Sodium nitrate	$NaNO_3$	84.99	2	0.02353
Magnesium sulphate, heptahydrate	$MgSO_4.7H_2O$	246.47	0.5	0.00202
Ferrous sulphate, heptahydrate	$FeSO_4.7H_2O$	278.02	0.01	0.000036

2.13.4. Harvesting pellets

After 20 days of incubation final pH of each flask was determined (Elico, Water Quality Analyzer, PE138, Hyderabad, India) and then the pellets were transferred aseptically to sterile Petri plates in laminar air flow using sterile stainless-steel mesh with pore size 100 µm. Pellets were repeatedly washed three times with sterile distilled water to remove any debris or traces of culture filtrate.

2.13.5. Testing of the pellets for GNP production using pelletised fungal biomass

Five grams of fungal pellets wet biomass were exposed to 50 ml of a sterilized aqueous solution of 200 µL (one mM) $HAuCl_4$ concentrations in 250 ml Erlenmeyer flasks and the flasks placed on a shaker at 200 rpm and incubated at 35°C for 4 days. Same way five gram of fungal pellets were exposed to 50 ml of crude chloroauric acid prepared according to 2.10.9.

2.14. Characterization of GNPs

2.14.1. UV Visible spectroscopy

The formation of GNPs was confirmed by UV visible spectrometer. The change in colour from pale yellow to a pinkish appearance was indicative of the formation of Gold nanoparticles. U.V visible spectroscopy biosynthesis of metal ions was monitored by taking 2 ml aliquots of reaction mixture at different time intervals and centrifuging them at 5000 rpm for 10 min. The centrifuged biomass was washed twice with double distilled water and biofilms were prepared. The biofilms were dried in an oven at 45°C for 1 h and examined by spectroscopic analysis using Shimadzu UV spectrophotometer (UV-1800) (300 to 800 nm) at Goa University. The biomass samples showing the desired color change were used for further studies (Ahmad et al., 2003).

2.14.2. Scanning Electron Microscopic (SEM) studies

The meta treated biomass was centrifuged at 1500 rpm for 20 min and washed twice with double distilled water. The pelletized biomass was washed with sterile distilled water and dried in an oven maintained at 75^{o}C for 48 h and were mounted onto carbon-coated copper grid. Micrographs were obtained using Carl-Zeiss scanning Electron Microscope (SEM-EDX) (USIC, Goa University) analysis were conducted using acceleration voltages between 15 and 20 keV (Falconer and Craw, 2006)

2.14.3. Transmission Electron Microscopy (TEM)

Transmission electron microscopy (TEM) was used to evaluate of the synthesized AuNPs morphology. 3 mg of sample was dispersed in 3ml of ethanol, sonicated for 10 mints. One drop of suspension was placed onto a grid of carbon coated copper grid (6 microlitre) and kept for 20s seconds, and grid was allowed to dry. The analysis was carried out using TECNAI G2 TWIN FEG (Thermo fisher) at 200 KV was carried out at central Research facilities IIT Delhi.

2.14.4. Fourier Transmission Infra-Red spectroscopy (FTIR) Analysis

The pelletized biomass was washed with sterile distilled water and dried in an oven maintained at 75^{o}C for 48 h. Dried composite of whole pelletized biomass was macerated using mortar and pestle. Samples of 1 mg were mixed with 100 mg of spectroscopic grade KBr, HiMedia. The FTIR spectra were determined between 4000 and 400 cm^{-1} using a Shimadzu IR Spirit following parameter: Spectral resolution 4 cm^{-1}, 40 scans min^{-1}, encoding interval 1 cm^{-1}, Happ-Genzel apodization and scanning speed 2.8 mm s^{-1}.

2.14.5. Particle size and its distribution

A dynamic light scattering (DLS) particle size analyzer (Nanotrac Wave, Microtrac, USA) was used to assess the mean particle size, the particle size distribution (PSD). DLS technique scatters a laser light beam at the surface of dispersed NPs, which results in the detection of the backscattered light. PDI is a dimensionless value that shows the uniformity of the synthesized NPs. 2 ml of aliquot was tested for DLS at central sophisticated instrumentation facilities (CSIF) BITS Pilani, Goa Campus.

2.14.6. Zeta potential

The zeta potential (surface charge) measurement is an approximation value related to the NPs surface electric charge, which is an indirect description of the physical stability of the synthesized NPs in the mixture solution. 2 ml of aliquot was tested for DLS at central sophisticated instrumentation facilities (CSIF) BITS Pilani, Goa Campus. The zeta potential of green synthesized AuNPs was determined at 25°C using DLS (Nanotrac Wave, Microtrac, USA). Water was used as dispersant, and measurements were conducted in triplicates

2.14.7. X-ray Diffraction spectroscopy (XRD)

The nanoparticles emulsion was oven dried at 40^{o}C for one day. The dried sample was collected and examined for the structure and composition using powder X-ray diffraction spectroscopy. The data was recorded using Ultimate IV powder Diffractometer, Rigaku Corporation-Japan at 45 kV and 20 mA. The dried sample was scanned in the range of 2 teta =10-80^{o} with 2/min.

2.14.8. Raman Spectrophotometry

Raman Spectroscopy is a non-destructive chemical analysis technique that provides detailed information (Banerjee & Ravishankar Rai, 2018) about chemical structure, phase and polymorphy, crystallinity, and molecular interactions. It is based upon the interaction of light with the chemical bonds within a material. Raman is a light scattering technique, whereby a molecule scatters incident light from a high-intensity laser light source. Most of the scattered light is at the same wavelength (or color) as the laser source and does not provide useful information this is called Rayleigh Scatter. The Raman spectroscopy was carried out using LAB RAM HR Horiba France at CSIF, BITS, Pilani Goa Campus. Spectral Ranged from 200-2100 nm and microscope with three objectives; 5x, 10x, and 100x. Available lasers were 532 nm, Nd-YAG laser, 100 mW, 633 nm HeNe, laser 17 mW and 785 nm diode and laser 100 mW.

2.14.9. Atomic Force Microscopy (AFM)

The atomic force microscope (AFM) is one kind of scanning probe microscopes (SPM). SPMs are designed to measure local properties, such as height, friction, magnetism, with a probe. To acquire an image, the SPM raster-scans the probe over a small area of the sample, measuring the local property simultaneously. The AFM studies were carried out at CRF IIT Delhi using Asylum Research MFP3D-BIO which is a very versatile atomic force microscope, suitable for use with a wide range of samples and features a vast array of modes. It has a z-range of 40 um (extended head model) and an x and y movement of up to 90 μm in a closed loop scan. The MFP-3D is able to image conductive, semiconductive and insulating samples in both air and liquid environments. Analysis was carried out by placing the drop of the sample on a mica slide. Sample preparation for AFM imaging involved a deposition of nanoparticle solution on freshly cleaved mica surface during the nanoparticle

synthesis. Freshly cleaved quadratic mica sheets (Structure Probe Inc./SPI Supplies, West Chester, PA, USA) with sizes 10x10 mm glued to the metal pads were used for the deposition of nanoparticle solution.

2.15. Biometrological analysis of SEM images

Biometrology is defined as a study of measurements for quantitative characterization of biological samples. Several SEM based commercial software packages such as ® MountainsMap SEM software (Digital Surf), 3D Surface Modelling (3DSM) (Carl Zeiss Microscopy), MeX (Alicona), Scandium Height (Olympus Soft Imaging Solutions), 3D SEM Three-Dimensional Image Software (JEOL) could be used to study three-dimensional (3D) SEM typological studies. In present study, SEM images were processed using ® MountainsMap 7.3 version SEM software (Digital Surf, Besancon, France) surface imaging and metrology software for 3D SEM biometrologic image analysis and colourization of SEM images were done using SEM Color 7.4 version (http://www.digitalsurf.com/). SEM images at 3000 x were used for measuring furrow density, isotropy, number of motifs and fractal dimensions (de Souza and Kamat 2018). For each species three SEM images of pellets were used to calculate each parameter and statistical significance was determined.

Summary of the Gold nanoparticle synthesis and its characterization is given in the **Fig. 2.16.**

2.16. Multivariate Statistical Analysis

These spectra were analyzed for signal processing procedure by smoothing on spectral second derivatives using Savitzky-Golay method with 9 points of window using Origin version 8 (OriginLab Corporation) graphing and analysis software (Savitzky et al., 1964).

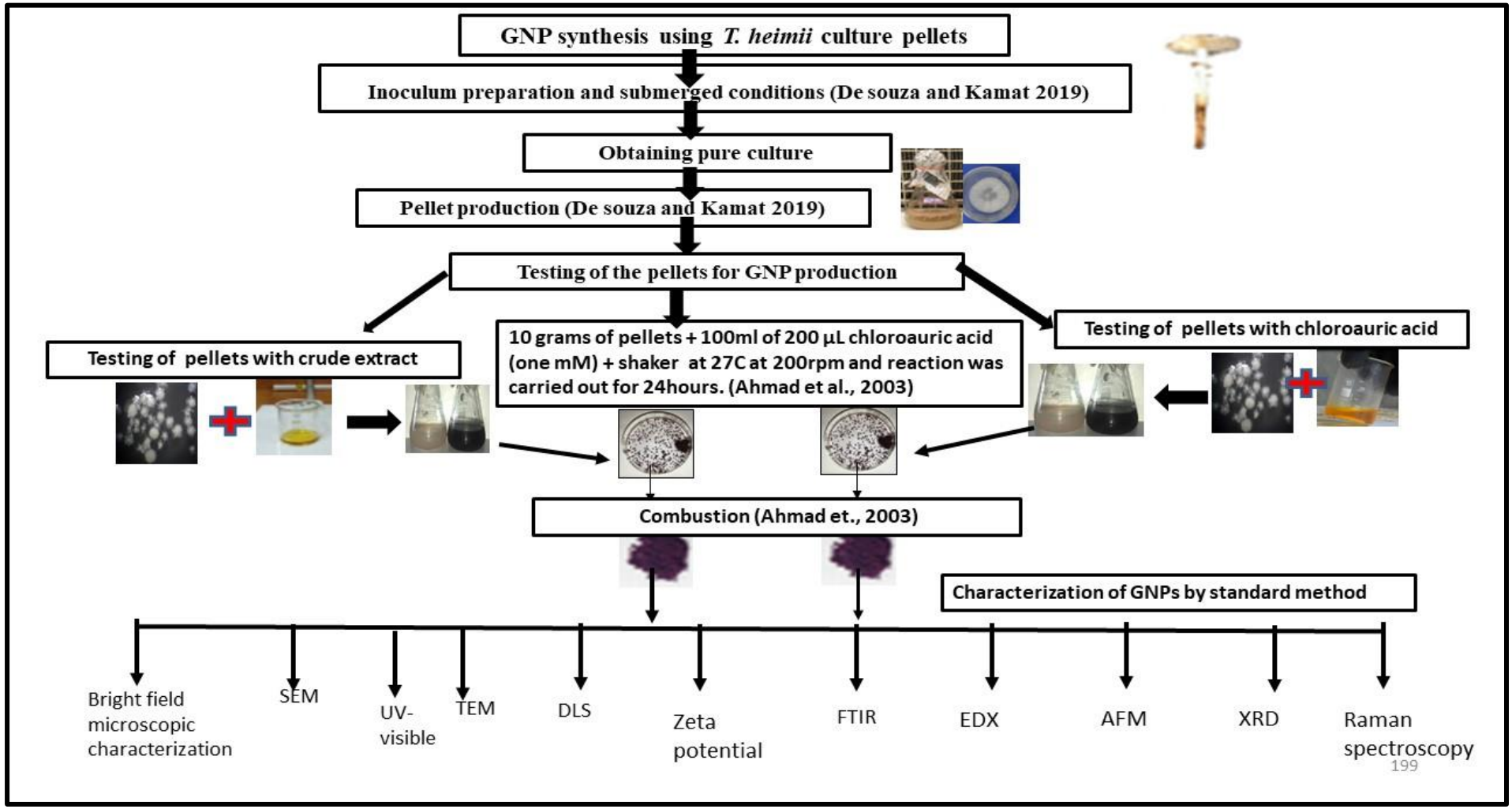

Figure 2.16: Scheme of the Gold nanoparticle synthesis and its characterization

2.17. Detection of Gold sulphides in BHQ and low grade ore samples

It was necessary to identify raw material for Gold biomining, based on the literature survey it was decided to use Gold sulphide. The bacteria gradually breakdown the sulphides and release Gold (Shahverdi et al., 2001). Thus, first step was to detect the Gold sulphide in BHQ and low-grade ores.

2.17.1. Microscopic detection of Gold sulphides using powdered sample

2.17.1.1. Sample preparation

BHQ and low-grade ore which was tested using ICP-OES and showed presence of Gold was used for this study. One Kg of BHQ, BMQ and low-grade ore (mining reject) were dried, powdered using mortar and pestle (Panda et al., 2011). The recovered sample was concentrated by panning method (Southam et al., 2009) and subjected to magnetic separation using neodymium magnet (Oliveira and Larizzatti, 2006). Sieved into different fractions with the sieve size of 150 µm. Each fraction was studies under stereomicroscope for the presence of Gold sulphide (Dabolkar and Kamat, 2022). The recovered sample was concentrated by panning method and subjected to magnetic separation using 2 Tesla Neodymium magnet and sieved into different fractions with the sieve size of 250, 150, 106, 53 µm.

2.17.2. Chemical test for detection of Gold sulphide

2.17.2.1. The sodium fusion test or Lassaigne's test

This test is used to carry out elemental analysis for the qualitative determination of the presence of foreign elements, namely halogens, nitrogen, and sulphur, in an organic compound. Nitrogen, sulphur, and halogens present in organic compounds are detected by Lassaigne’s test. Here, a small piece of Na metal is heated in a fusion tube with the organic

compound where Na converts all the elements present into ionic form. The extract is treated with sodium nitroprusside. The appearance of violet colour indicates the presence of sulphur.

2.17.2.2. Lead acetate

The sulfur-containing amino acid such as cysteine and methionine (sulfhydryl/thiol group) react with lead acetate under alkaline conditions to form a brown precipitate. These sulfur-containing amino acids are degraded in strongly alkaline media to release sulfide ion (S^{2-}) in the form of H_2S (hydrogen sulfide). The sulphide ions can react with lead (II) acetate to form a brownish-black precipitate.

2.17.3. Separation and detection of Gold sulphides

BHQ samples with known Gold concentration were used for sulfide detection. Ten grams of dry BHQ sample was powdered and sieved through 106 µm sieve. The 106 µm fraction was subjected to magnetic separation using 2 Tesla Neodymium magnet. The coarse ferromagnetic materials were removed by multiple washing using tap water by removing the lighter and soluble fraction and heavier insoluble fraction (I) was subjected to magnetic separation to remove fine ferromagnetic particles, which had escaped previous treatment. The heavier fraction (II) was then dried and tested for detection of sulfur by Lassaigne's and lead acetate tests. Samples were prepared for optical and phase contrast microscopic studies and used for detection of Gold sulfide by SEM-EDS and for detection of total sulfur content by elemental analysis (Dabolkar and Kamat, 2022).

2.17.3.1. Optical microscopic studies of the Gold sulphides

The 106 µm sieve size dried heavy fraction was used to prepare slides by mounting the material directly in DPX mountant. Slides were studied to detect components of heavy

fraction such as Gold particles, auriferous quartz and presumptive black Gold sulfidic material using optical microscopy (Nikon Eclipse E200 MVR, Tokyo) and phase contrast microscopy (Olympus BX41).

2.17.3.2. Scanning Electron microscopic (SEM-EDS) study of the Gold sulphide

A small sample of heavy fraction with presumptive Gold sulphide was mounted on a carbon tape and was analyzed using SEM-EDS technique by Carl-Zeiss Scanning Electron Microscope (SEM) (USIC, Goa University) and images were obtained with operational conditions 15 to 35 kV.

2.17.3.3. CHNS/O Elemental Analysis

Total elemental Sulphur analysis was carried out on one gram of heavy fraction using CHNS/O Elemental Analyzer Perkin Elmer PE 2400 series II, which works on frontal chromatography technique for separation and estimation of elements such as C, H, N, S and O in a sample. It was carried out at the Sophisticated Instrumentation Centre for Applied Research and Testing (SICART), Gujarat.

2.18. Microfluidics assay for bio-oxidation

A micro test plate (MWP) is a small, plastic plate which has a number of holding wells containing a microfluidics element as shown in the **Fig. 2.17.** MWPs are frequently used for heterotrophic microbial growth. In essence, Micro test plate research tool can obtain the same results of multiple shake flask experiments without tedious experimental procedures using multiple individual shake flasks. Furthermore, the broad range of complexities in bioleaching requires the investigation for the use of mixed cultures of different microbial species and strains, or their individual component species, and potentially different ranges of operating and growth conditions. MWPs have the potential to investigate many such variables in one experiment concurrently. Micro test plates (Tarsons) used in the studies

are made from high-quality polystyrene. The plates therefore provide consistent optical quality. In order to facilitate quick coordination when filling the wells, the hollows are also labelled alphanumerically (Meissner et al., 2014). The combination of the mixture of media and presumptive cultures added to the sterile micro test plate is given in the **Table 2.18**. Total 200 µL of each was added using micropipette.

2.18.1. Stereomicroscopic examination

The Microwell test plates were observed after every seven days under the stereomicroscope under the Laminar air flow. The wells were studied from A1 to A12 for the formation of Gold which was followed by the remaining wells.

2.19. Molecular identification of most promising bacteria

Freshly grown 2 ml culture was sent for molecular identification at Muppandal genomics and immunological pvt Ltd by using 16S rRNA sequencing (Salvà-Serra et al., 2018).

Table 2.13: The design of the Micro test plate wells

Sr. No.	Type of culture (210 µL)	Modified 9K medium (without sulfur) 210 μL	Pure/Crude Gold sulphide
A_1-A_{12}	Presumptive *Acidithiobacillus*	9K medium for *Acidithiobacillus*	Pure
B_1 -B_{12}	Presumptive *Thiobacillus*	9K medium for *Acidithiobacillus*	Crude
C_1-C_{12}	Presumptive *Leptospirillum*	9K medium for *Leptospirillum*	Pure
D_1-D_{12}	Presumptive *Leptospirillum*	9K medium for *Leptospirillum*	Crude
E_1-E_{12}	Presumptive *Sulfobacillus*	9K medium for *Sulfobacillus*	Pure
F_1-F_{12}	Presumptive *Sulfobacillus*	9K medium for *Sulfobacillus*	Crude

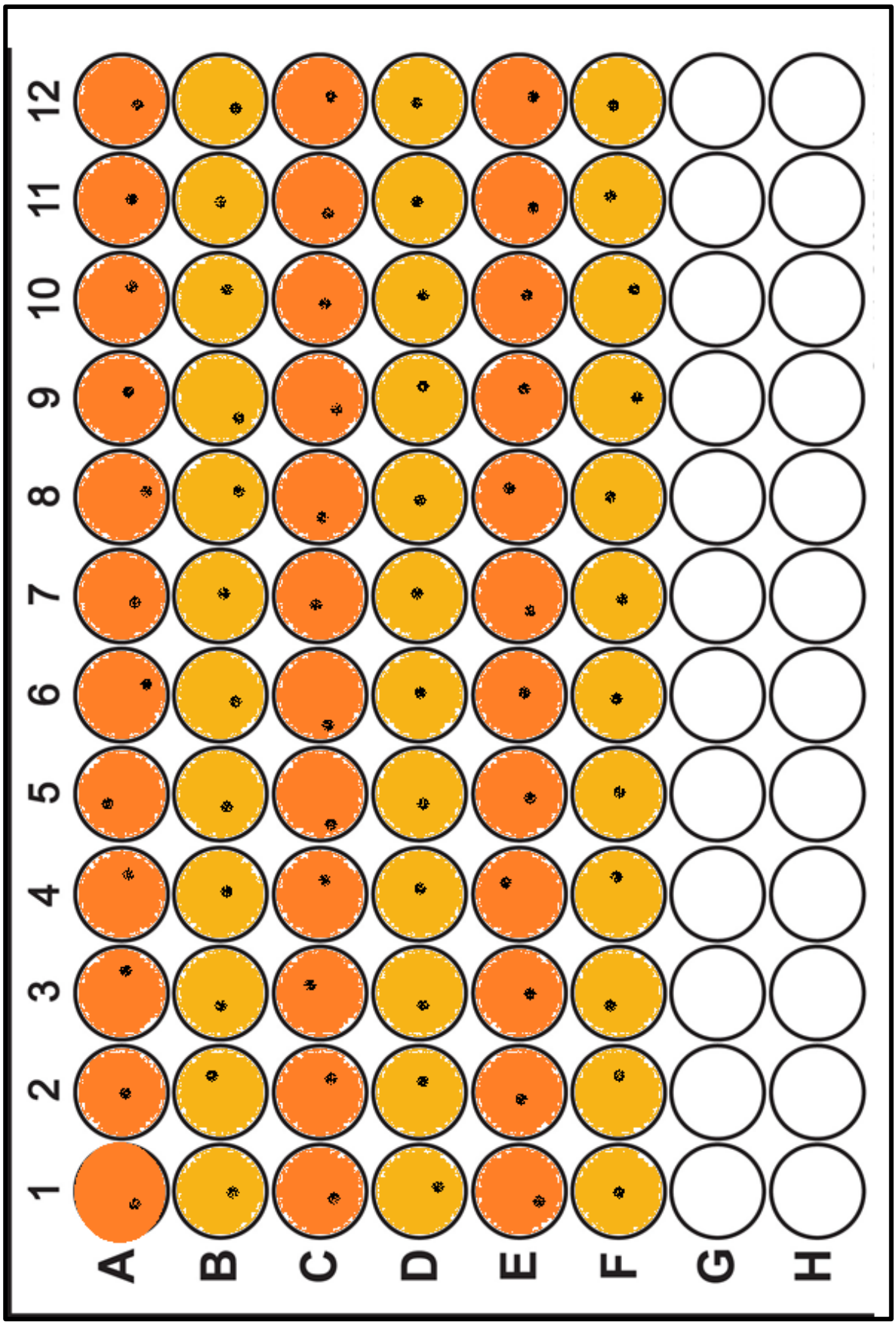

Figure 2.17: Design of the micro test plate for Microfluidic assay for bio-oxidation

2.20. Immobilized reaction system

2.20.1. Micro-organism (NOSOB)

NOSOB was cultivated aerobically at 28–30°C and 150 rpm in an Erlenmeyer flask with 50 mL of a specific media (9K) without sulphur source (Garcia, 1991). The pH was adjusted at 2 with concentrated H_2SO_4. For the bench top experiment, inoculums of ca. 108 cells/mL were transferred to flasks with 100 mL of culture media, pH 2 without a source of sulphur (García-Meza et al., 2012).

2.20.2. Experimental design

The biooxidation experiment was carried out in a 1000 ml Borosil beaker (BRL_1000D29). The sterilized thermocol was placed at the base of the beaker. The slides (75 mm x 25 mm CAT No.7101) were coated in a coverslip size area with 1.5 ml of 9K medium and culture. The volume of 9K medium used to immobilize culture (X) was 40 ml and that of culture (Y) was 10 ml. The Gold sulphide used in this experiment was obtained by previously described technique **2.15**. 4 grams of Gold sulphide was immobilized at the centre of the cover slip shape agar and distributed evenly on all 21 slides (0.19 grams). Total slides placed in a in a thermocol inside each beaker without each other touching were 10. The beaker was filled with 600 ml of dilute HCl with pH 2 so that coated area of the slide is completely dipped in the acid. Oxygen was supplied using external aerator. The entire beaker was completely covered with the aluminium foil and kept at 32°C. The summary of the same is given in the **Fig. 2.18.**

2.20.3. Monitoring of the slides for formation of Gold

After every 3 days each slide was studied under microscope. The edges of the slides showing positive results were cut. Incineration of the agar pieces on a slide by charring till evaporates, then scrapping of the small material, resuspended in a drop of water and washed to remove light impurities. Heavy Gold particles were retained. This fraction was mounted on a slide with DPX after drying and checked for Gold. Slides were prepared with few drops of the Aqua regia to check formation of metallic film.

2.20.4. ICP-OES studies

1 g of the sample was collected from the slide and dissolved in 5ml of aqua regia and boiled to digest and dilute with water and send for ICP-OES (Model: Perkin Elmer, U.S.A.; Make: Avio 200) analysis at Sophisticated Instrumentation Centre for Applied Research and Testing (SICART) supported by Department of Science & Technology (Govt. of India) managed by Charutar Vidya Mandal (Liang-Cheng et al., 2018).

The results obtained specific to the objectives of the work are presented in chapter III.

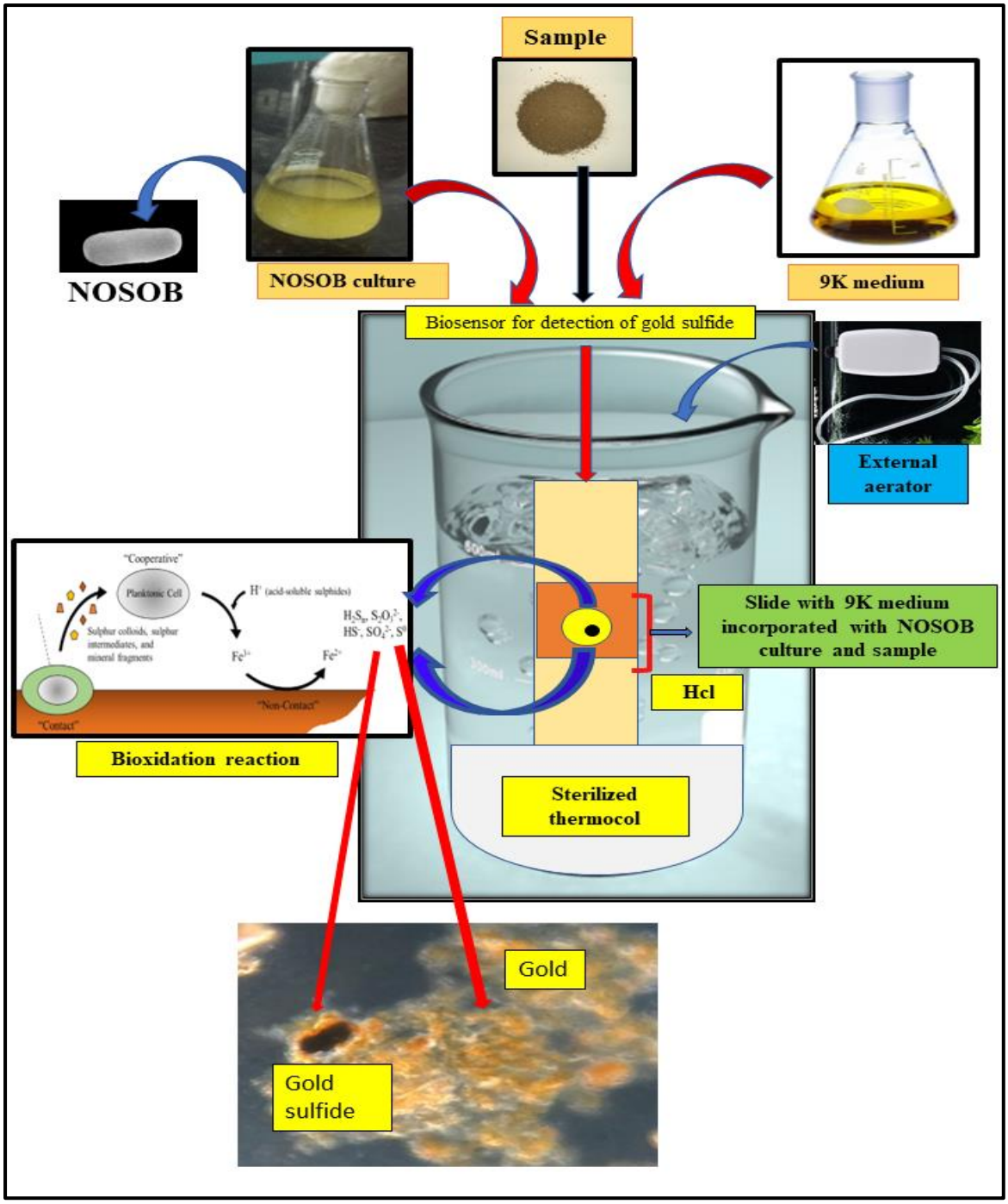

Figure 2.18: Microfluidics Assay for Biooxidation of Gold sulphides

CHAPTER III

RESULTS

RESULTS

This chapter presents the findings of present study on microbial bioprospecting of auriferous natural samples from mining and non-mining areas in Goa to detect Bacterioform Gold (BFG), source and screen microbes potentially useful in biomining of Gold and green synthesis of Gold nanoparticles. The chapter begins with quantitative analysis of available data on the samples followed by results of field sampling, identification of samples, detection of the Gold, cultural work and finally details of biosynthesis of nanoparticles and biomining of Gold.

3.1. Literature survey and bibliometric analysis

The information technology has made it possible to mine data related to Gold and bioprospecting of auriferous samples from mining and non-mining areas of Goa to detect bacterioform Gold and screen microbes potential useful in biomining and Gold nanoparticle synthesis. It is acknowledged that some of the knowledge may be available only in print form. Relative expansion of knowledge using google scholar (https://scholar.google.co.in/) database indicated in **Table 3.1 (As on 15 June 2022).**

3.2. Use of VOSviewer for analysing bibliometric data

In VOSviewer three visualizations are available in the main panel, the network visualization, the overlay visualization, and the density visualization**. Fig 3.1a** is a network visualisation, here items are represented by their label, default and also by a circle. The size of the label and the circle of an item is determined by the weight of the item. The higher the weight of an item, the larger the label and the circle of the item. For some items, the label may not be displayed. This is done in order to avoid overlapping labels. The color of an item is determined by the cluster to which the item belongs. Lines between items represent links. By default, at most 1000 lines are displayed, representing the 1000 strongest links between items. On the density visualization

map of VOSviewer as seen in **Fig 3.1b**, each point will be filled with color according to the density of elements around the point, the higher the density, the darker the displayed keyword color. The distance between two journals in the visualization approximately indicates the relatedness of the journals in terms of co-citation links. In general, the closer two journals are located to each other, the stronger their relatedness. The strongest co-citation links between journals are also represented by lines. In the item density visualization, items are represented by their label in a similar way as in the network visualization and the overlay visualization. Each point in the item density visualization has a color that indicates the density of items at that point. By default, colors range from blue to green to yellow. The larger the number of items in the neighborhood of a point and the higher the weights of the neighboring items, the closer the color of the point is to yellow. The other way around, the smaller the number of items in the neighborhood of a point and the lower the weights of the neighboring items, the closer the color of the point is to blue.

Table 3.1: Relative expansion of webliographic knowledge using google scholar database

Search terms	Number of publications (Including patents and citations)		Relative expansion of online sources (%)	
	20th century (1900 – 1999)	21st century (2000 – 2022)	20th century	21st century
Auriferous samples	1,570	8,170	1585	7204
Geology of Goa	1,590	12,200	1606	7300
Western Dharwad Craton (WDC) + Gold	2	19	2	9
Mining areas in Goa	1,590	17,000	1606	7300
Non-mining areas in Goa	11	113	11	50
Banded Iron Formation (BIF)	1,160	10,400	1171	5272
Gold in Banded Iron formation	17,000	19,500	17171	77,272
Banded Haematite Quarzite (BHQ)	13	307	13	59
Banded Magnetite Quarzite (BMQ)	10	191	10	45
Gold	17,10,000	15,90,000	17,27,272	785,1236
Occurrence of Gold	1,74,000	17,60,000	175,757	798,895
Gold in India	74,700	16,10,000	75,454	342,972
Gold associated with BHQ	49	3,250	49	222
Gold associated with BMQ	53	982	53	240
Bacterioform Gold	8	233	8	36
Laterite + Gold	1,570	11,700	1585	7204
Stream sediments +Gold	1,13,000	18,700	114,141	51,881
Vermicast + Gold	1	327	1	4
Termite mound + Gold	964	8,180	973	4422
Beach sand + Gold	15,600	59,400	15,757	71622
Placer sand + Gold	2,350	11,800	2373	10786
Detection of Gold	7,61,000	19,30,000	768,686	3494027
Bacterioform secondary Gold forms	7	157	7	31
Chemolithotrophic bacteria	4,470	16,400	4515	20522
Hyperacidophillic bacteria	928	3,810	937	4259
Rational isolation of actinobacteria	19	7,330	100	454
Winogradskys column	904	2,800	913	4150
Biosynthesis of GNPS	8	3,820	8	36
***Termitomyces* + GNP synthesis**	-	8	-	-
Characterization of GNPs	296	4,050	298	1354

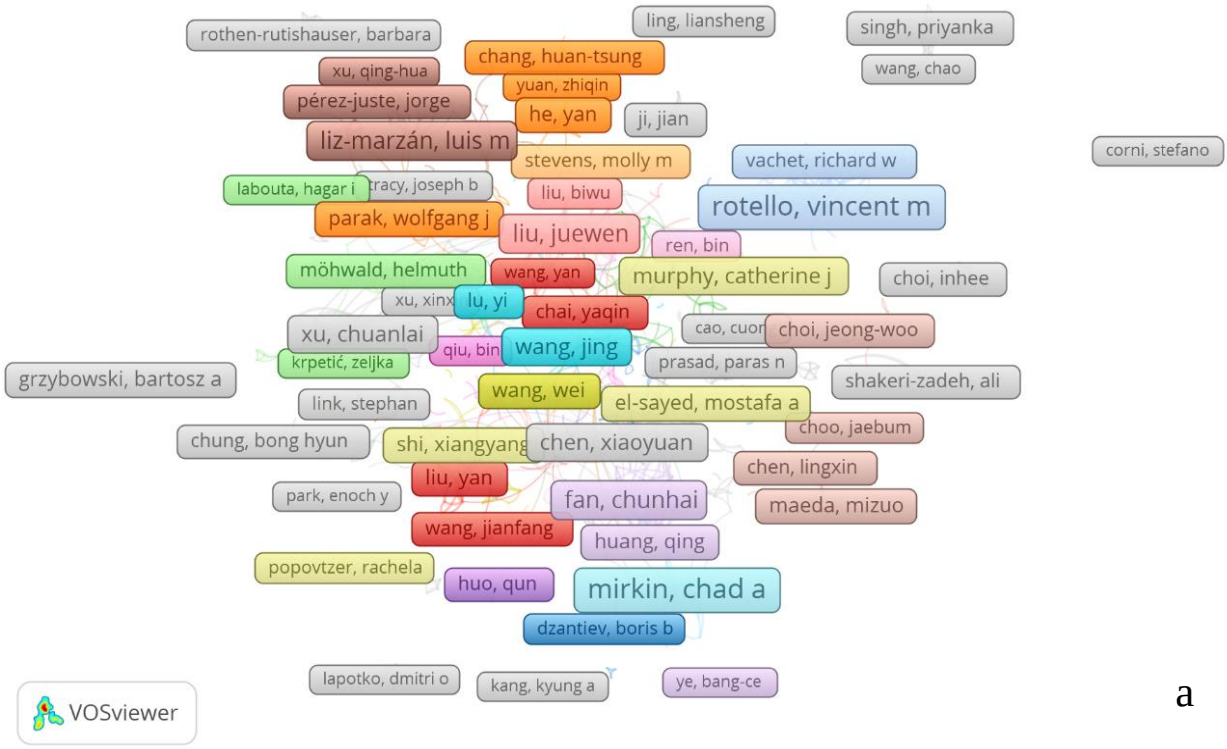

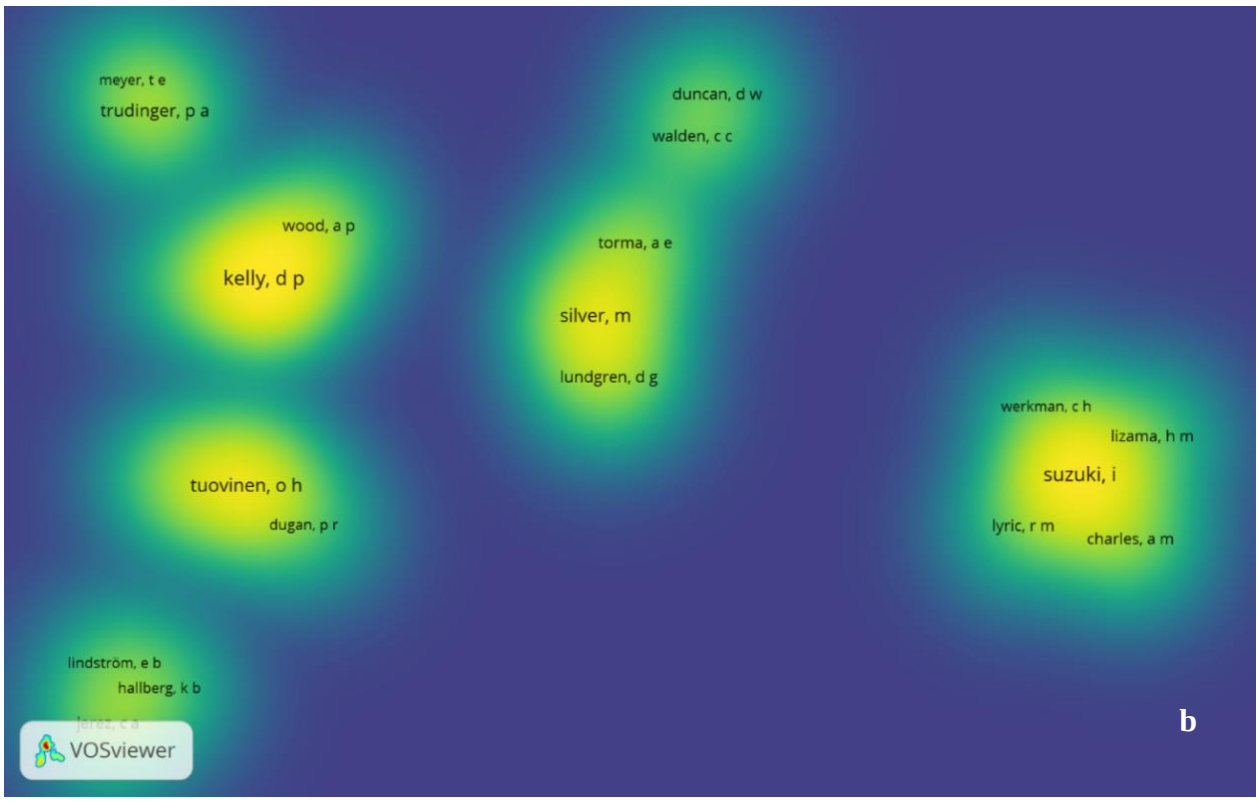

Figure 3.1 (a-b): a-Network Visualization, b- Density visualization

3.3. Preliminary site selections

The mining belt of Goa covers an area of approximately 700 sq. Kms, concentrated in 4 talukas namely Bicholim, Sattari, Sanguem and Quepem. Goa has open-pit mining and this method is particularly advantageous in the Goan context as it lowers cost and enables the economically effective exploitation of lower-grade ores. The drilosphere of geophagous earthworms are involved in production of earthworm casts by dwelling inside soil and taking up of the organic and inorganic matters. The organic and mineral fraction bound to the organic matter are further subjected to hydrolytic decomposition by microbial and enzymatic actions inside the digestive track. Vermicasts were found to be mostly present under the tress and organically rich soils. The size, color of the vermicast varied depending on the size of earthworms and also on types of soil. Termite mounds were mostly found to be present in forested areas. The architectures of the termite mounds have some relationships to termite species constructing the mounds. The sites of the termite mounds are shown in **section 2.3.4**. Three known types of termite mounds exist in the study area: cathedral, conical, and mushroom. Stream sediment geochemistry and heavy mineral surveys are routinely used in the early stages of Gold (Au) exploration. Stream sediments were mainly explored from Mhadei wild life sanctuary, Netravali wild life sanctuary, Bhagwan Mahaveer wildlife sanctuary and Mollem National Park. The forest is immense, luxuriant with a continuous canopy of leaves that shade the underneath from sunlight. Sporadic rainfall is experienced during the period from July to August. Entire coastline of Goa was covered from Keri in the North to Polem in the South, and it was found that the texture, color and composition of the sands varied from north to south. North Goa beaches were showing more of calcareous nature. A beach is a geological land form along the shoreline of an ocean usually consists of loose particle often composed of rock such as sand, gravel, pebbles, cobblestones among them are economically important heavy mineral placers. The exploration sites are shown in the **section 2.3.4.** Laterites are soil types rich in iron and aluminium, formed

in hot and wet tropical areas. Nearly all laterites are rusty-red because of iron oxides. They develop by intensive and long-lasting weathering of the underlying parent rocks.

3.4. Sample collection

Samples from the mining areas were collected from north Goa mines such as Shirgao mines as well as south Goa mines were covered. The samples collected from mining areas included iron ore and low-grade ore (mining rejects). The exploration of samples from non-mining areas was carried out which included samples such as stream sediments, laterites, termite mounds, beach sands, placer sands, and vermicasts. About 350-450 km^2 of mining region and 450-500 Km^2 of the non-mining region were covered. Total samples collected from mining areas were 45 and those collected from non-mining areas were 100. The sampling sites from mining and non-mining area is shown in **Fig 2.6** and **Fig 2.8** section **2.3**. Samples collected from mining areas of Goa included Shirgao, Bicholim, Sanquelim, Velgeum, Surla and are shown in **Table 3.2**. **Fig 3.4** shows that 67% of the samples collected from mining areas were BHQ, 18% of BMQ and 15% were low grade ore (Mining reject). The list of samples collected from non-mining area is given in **Table 3.3.** The sampling sites are shown in the **Fig 3.3.** The representative samples of Banded Hematite Quartzite (BHQ) and Banded Magnetite Quartzite (BMQ) are shown in **Fig 3.6.** Vermicasts from Goa University campus and beach placer deposits and beach sands from the non-mining areas are shown in **Fig 3.7**. The percentage of sample collection from non-mining sites is shown in **Fig 3.5**. It was found that 44% were beach sand, 17% were laterite, 15% were vermicasts, 12 % were stream sediments,10 % were Termite mounds, and 4% were beach placer sands.

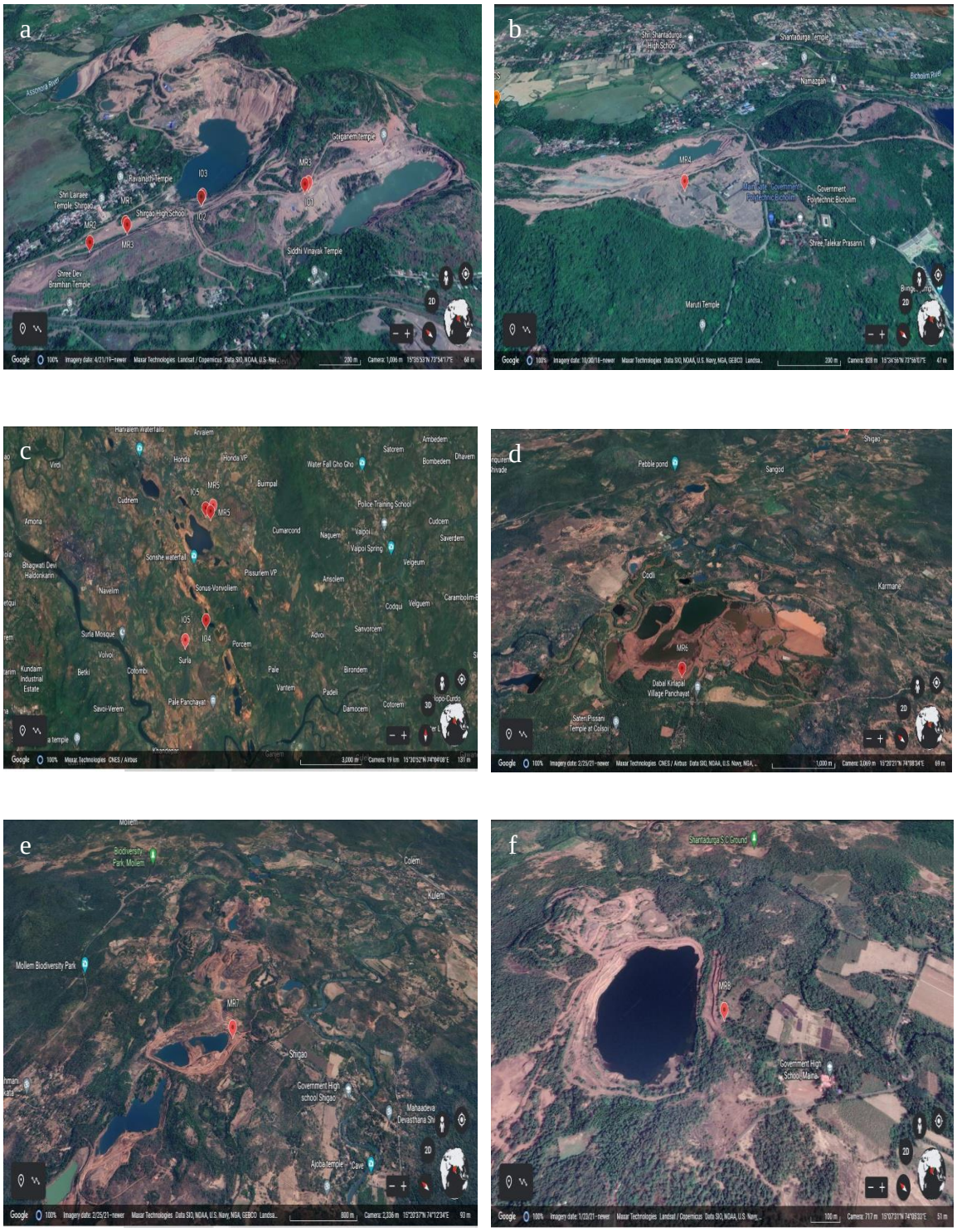

Figure 3.2 (a-f): Exploration of mining sites: a-Mining site Shirgao, North Goa, b-Bicholim, Velgeum, Pissurlem and Surla; c-Codli; d-Sampling sites in Shigao; e-Sampling sites in Maina.

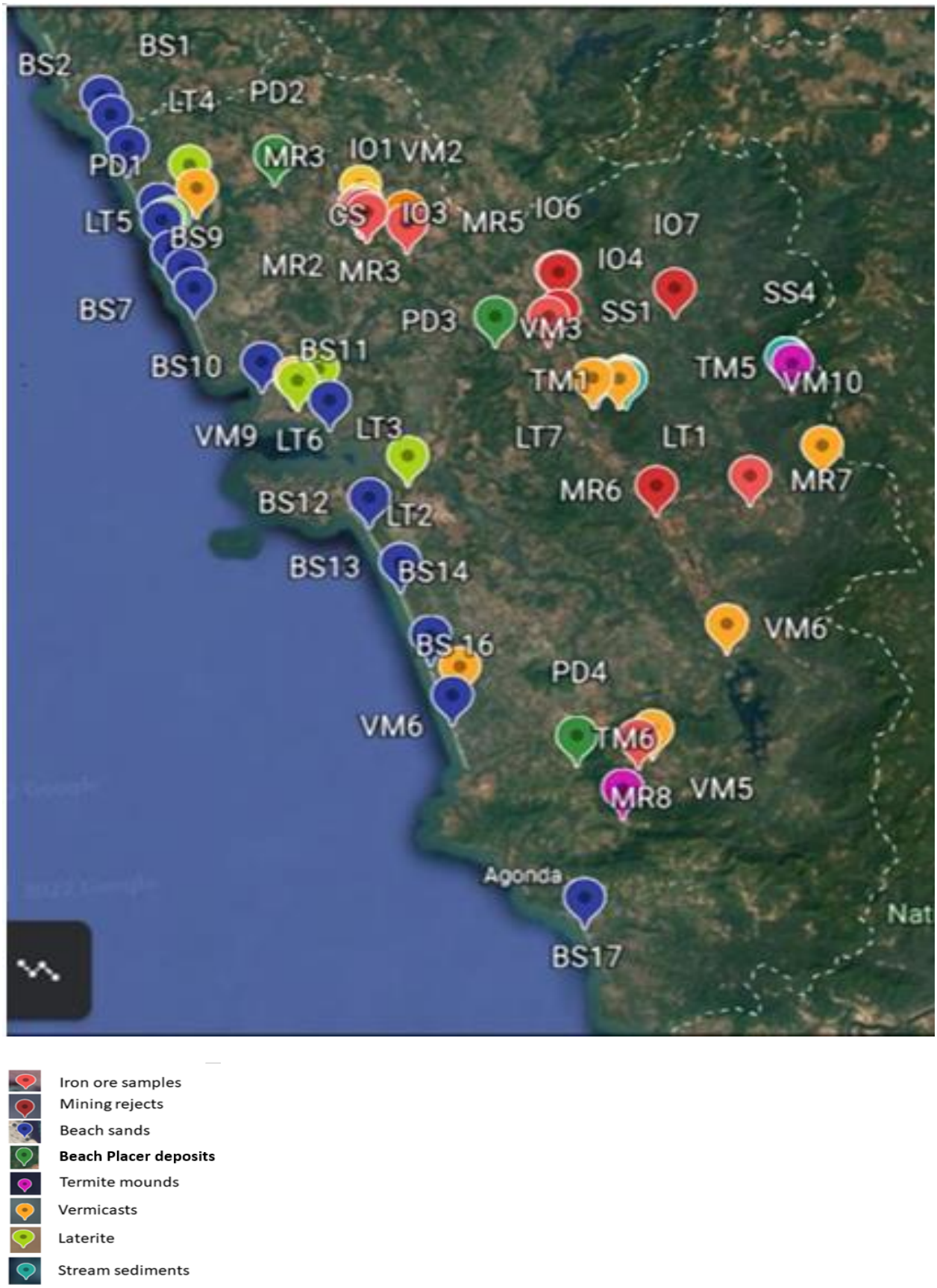

Figure 3.3: The sampling sites of samples from mining and non-mining areas of Goa

Table 3.2: Samples from mining areas

Sample designation	Location		No of samples
MR-01	15’36’38.30” N	73’54’48.51” E	6
MR-02	15’36’38.30” N	73’54’48.51” E	6
MR-03	15’12’42.30” N	74’14’11.09” E	4
MR-04	15’36’19.54” N	73’53’39.45” E	4
MR-05	15’29’17.55” N	74’04’17.28” E	4
MR-06	15’29’26.64” N	74’05’50.37” E	2
MR-06	15’29’28.64” N	74’02’52.37” E	4
IO-01	15’36’00.52” N	73’56’08.83” E	4
IO-02	15’12’42.30” N	74’14’11.09” E	2
IO-03	15’06’50.89” N	74’09’14.72” E	2
BM-1	15’06’50.89” N	74’09’14.72” E	3
BM-2	15’06’60.89” N	74’12’14.72” E	4

Table 3.3: Samples from non-mining areas

Sample designation	Latitude	Longitude	No of samples
BS-01	15’25’57.79” N	74’15’36.59” E	5
BS-02	15’26’24.91” N	74’06’26.81” E	5
BS-03	15’25’57.79” N	74’15’36.59” E	5
BS-04	15’26’24.91” N	74’06’26.81” E	6
BS-05	15°42'42.63" N	73°41'28.40" E	2
BS-06	15°41'1461" N	73°42'18.62" E	3
BS-07	15°39'27.58" N	73°43'0169" E	2
BS-08	15°36'59.82" N	73°44'0320" E	1
BS-09	15°36'19.89" N	73°44'2954" E	2
BS-10	15°41'03.36" N	73°53'1114" E	3
BS-11	15°36'18.75" N	73°45'0634" E	1
BS-12	15°34'37.25" N	73°42'5.82" E	2
BS-13	15°33'45.15" N	73°44'57.56" E	3
BS-14	15°28'57.81" N	73°48'30.79" E	2

BS-15	15°37'04.09" N	73°44'39.66" E	2
BS-16	15°42'42.63" N	73°41'28.40" E	2
BS-17	15°41'14.61" N	73°42'18.62" E	2
BS-18	15°41'14.68" N	73°43'0169" E	3
BS-19	15°42'42.63" N	73°44'0320"E	3
BS-20	15°42'42.60" N	73°44'2954"E	2
SS-01	15’25’57.79” N	74’15’36.59” E	6
SS-02	15’26’24.91” N	74’06’26.81” E	6
SS-03	15’11’13.33” N	74’01’06.15” E	6
SS-04	15’25’57.79” N	74’15’36.59” E	6
SS-05	15’26’24.91” N	74’06’26.81” E	6
SS-06	15’11’13.33” N	74’01’06.15” E	4
ss-07	15’11’13.33” N	74’01’06.15” E	2
PD-01	15’25’57.79” N	74’15’36.59” E	2
PD-02	15’26’24.95” N	74’06’26.91” E	4
VM-01	15’10’37.05” N	74’11’14.39” E	9
VM-02	15’10’37.05” N	74’11’14.39” E	2
VM-03	15’11’13.33” N	74’01’06.15” E	4
VM-04	15’11’13.33” N	74’01’06.15” E	2
VM-05	15’25’57.79” N	74’15’36.59” E	2
VM-06	15’26’24.91” N	74’06’26.81” E	1
LT-01	15’27’59.13” N	74’02’19.77” E	2
LT-02	15’10’37.05” N	74’11’14.39” E	5
LT-03	15’27’59.13” N	74’02’19.77” E	1
LT-04	15’10’37.05” N	74’11’14.39” E	2
LT-05	15’27’59.13” N	74’02’19.77” E	2
LT-06	15’10’37.05” N	74’11’14.39” E	3
LT-07	15’27’59.13” N	74’02’19.77” E	1
LT-08	15’10’37.05” N	74’11’14.39” E	2
LT-09	15’27’59.13” N	74’02’19.77” E	2

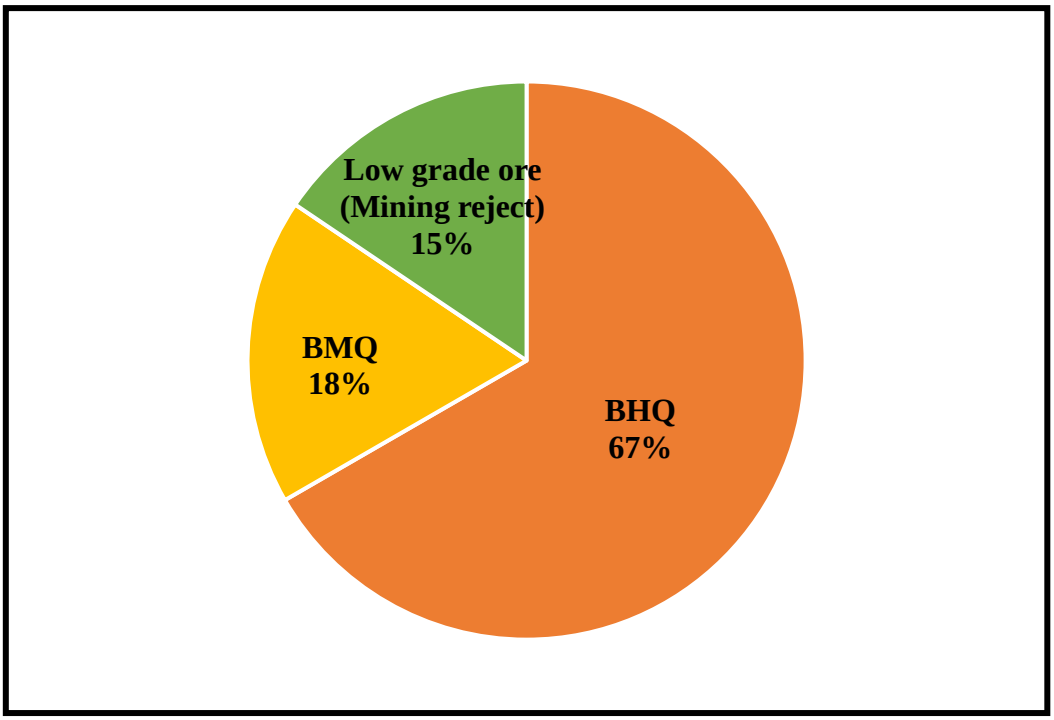

Figure 3.4: Percentage of samples collected from mining sites

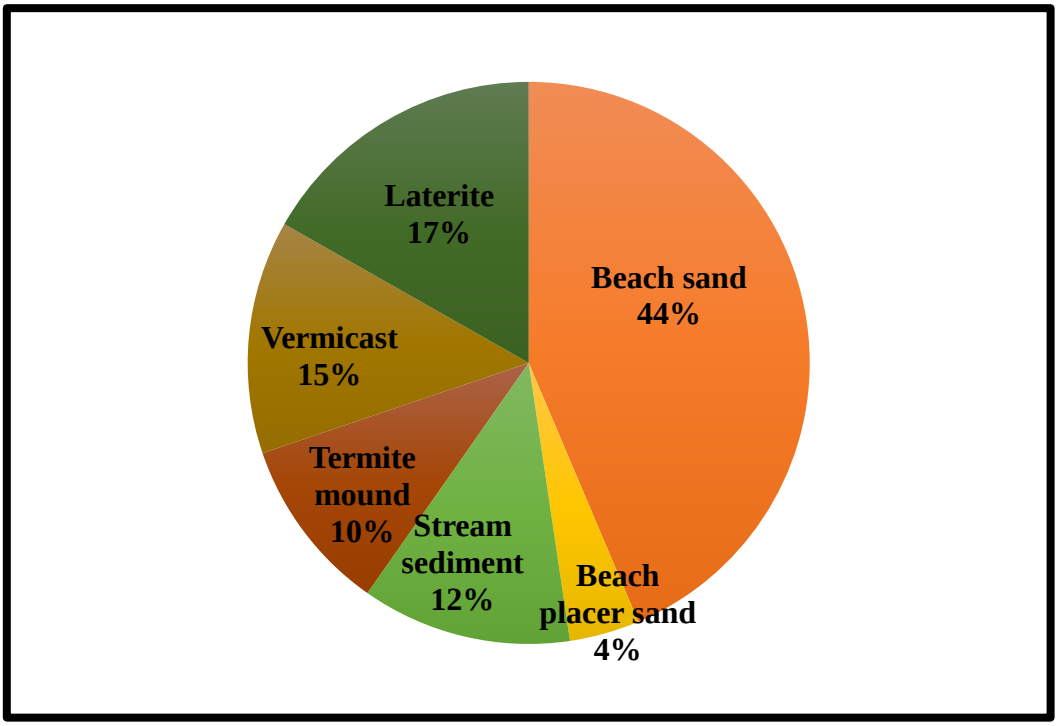

Figure 3.5: Percentage of samples collected from non-mining sites.

Figure 3.6 (a-d): **The representative samples of Banded Hematite Quartzite (BHQ) and Banded Magnetite Quartzite (BMQ); a-BHQ sample from Velguem; b-BMQ from Sacorda, South Goa; c, d-BHQ from Shirgao.**

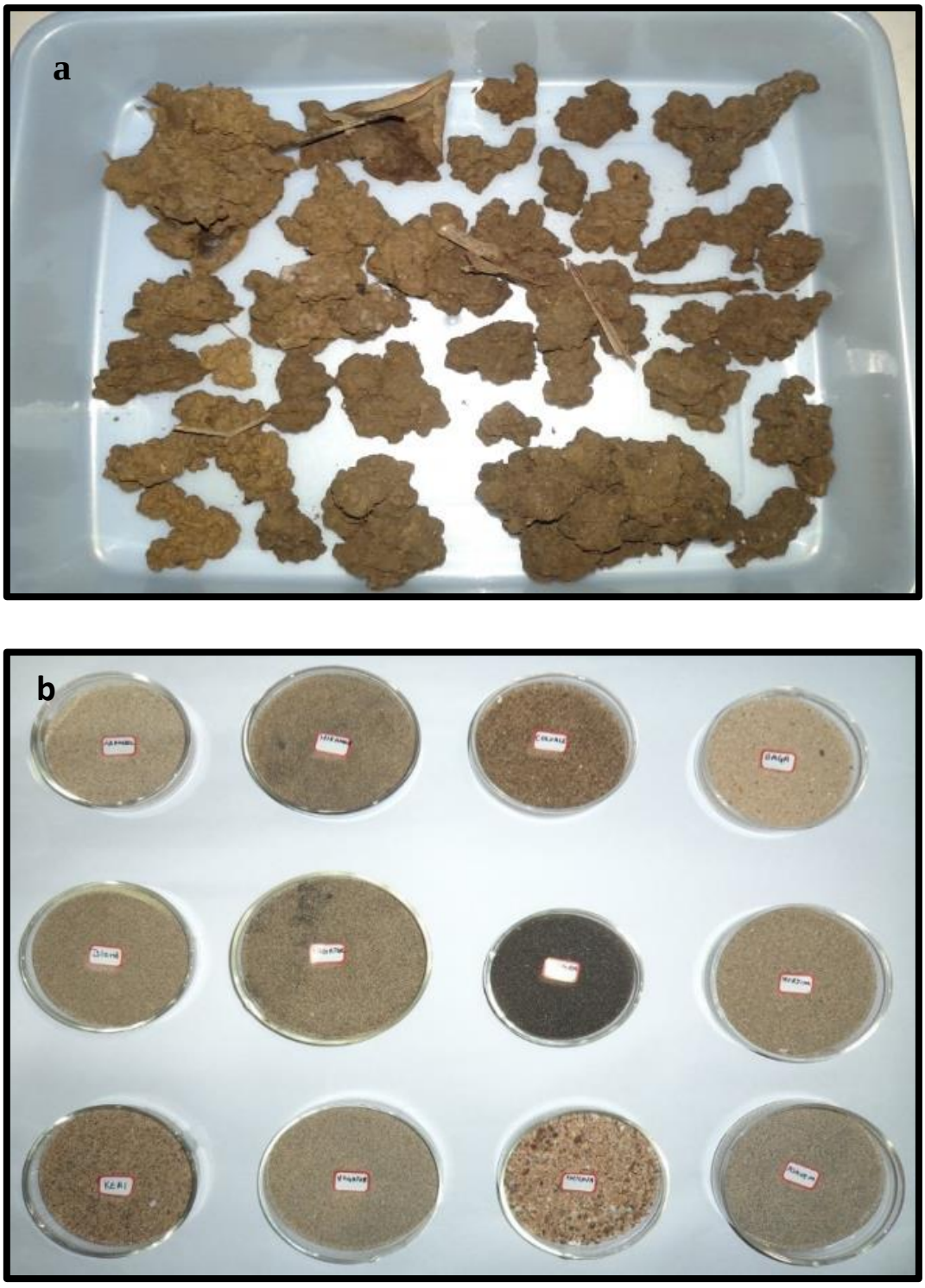

Figure 3.7(a-b): a-Vermicasts from Goa University campus; b-Beach placer deposits and beach sands from the non-mining areas

3.5. Sieving of the samples

Sieving helped in enrichment of the samples. In practice, each fraction contains particles between definite limits, these being the openings of standard test sieves. Each sample was sieved into different sieved sizes. I was successful in obtaining the powdered, dried sieved fractions of the samples as shown in **Fig 3.8** to **Fig 3.10**. The fractions 150, 106, 53 µm and below 53 µm showed high concentration of Gold and same fraction were thus used for the further studies. The most promising sieve fraction was found to be 106 µm**.** Slide prepared from each fraction showed the presence of Gold. The samples which showed the most promising results were send for ICP-OES analysis of Gold and also for SEM EDX studies. The BHQ, BMQ and mining reject samples showed the presence of presumptively identified as quartz, auriferous quartz, presumptive Gold, Gold sulphides, and presence of pyrite in all fraction and these were presumptively identified as can be seen in **Fig 3.11, Fig 3.12** and **Fig 3.13.** Vermicast samples showed the presence of quartz, auriferous quartz, presumptive circular Gold, presence of zircons and organic matter. Each fraction showed presence of Gold ranging from macro to nano size and is shown in the image by the red arrow.

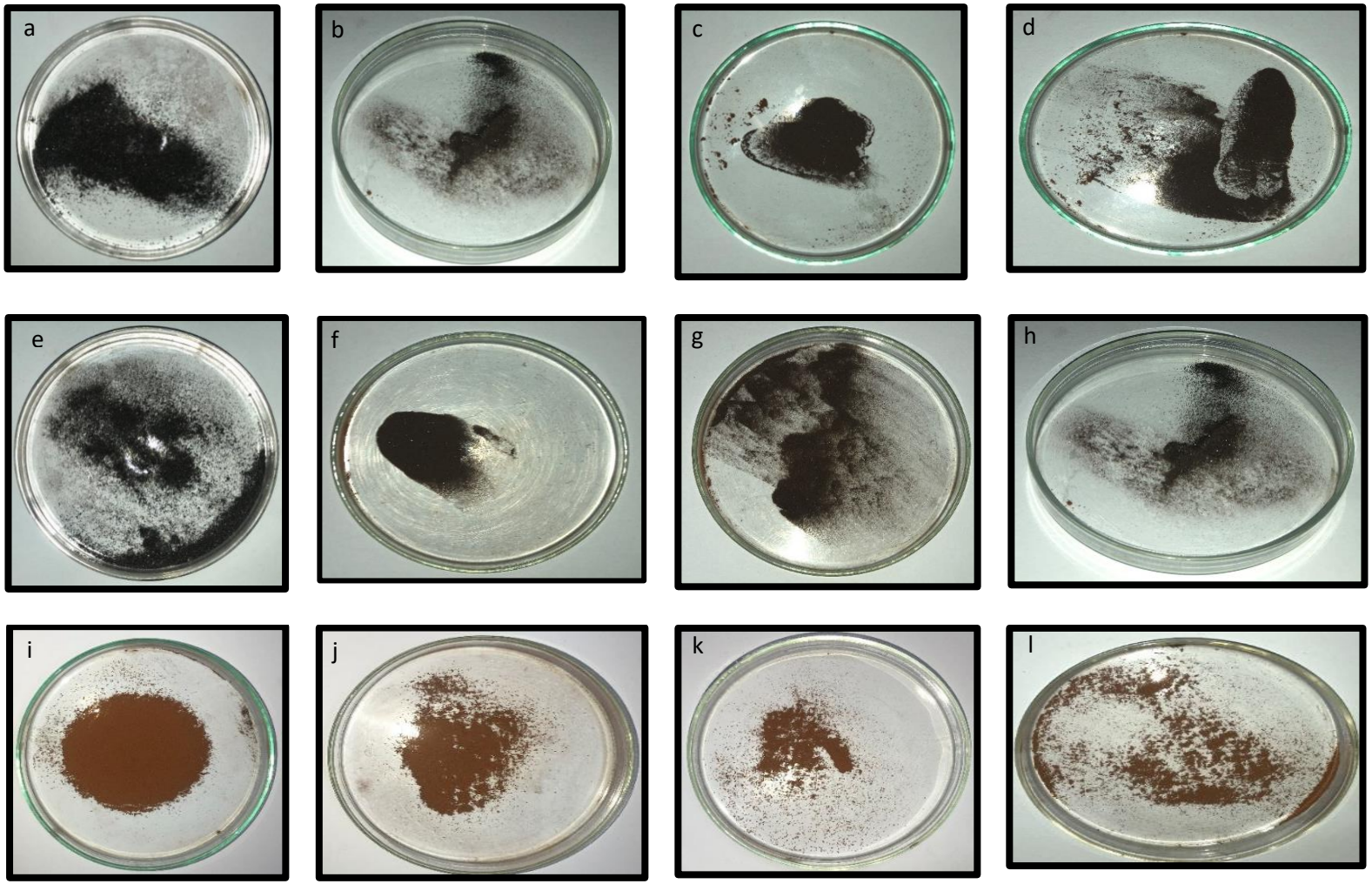

Figure 3.8 (a-l): a-d: BHQ sample with fraction size 150 µm, 106 µm, 53 µm, below 53 µm; e-h: BMQ sample with fraction size 150 µm, 106 µm,53 µm, below 53 µm; i-l: low grade iron ore (mining reject) sample with fraction size 150 µm, 106 µm, 53 µm, below 53 µm.

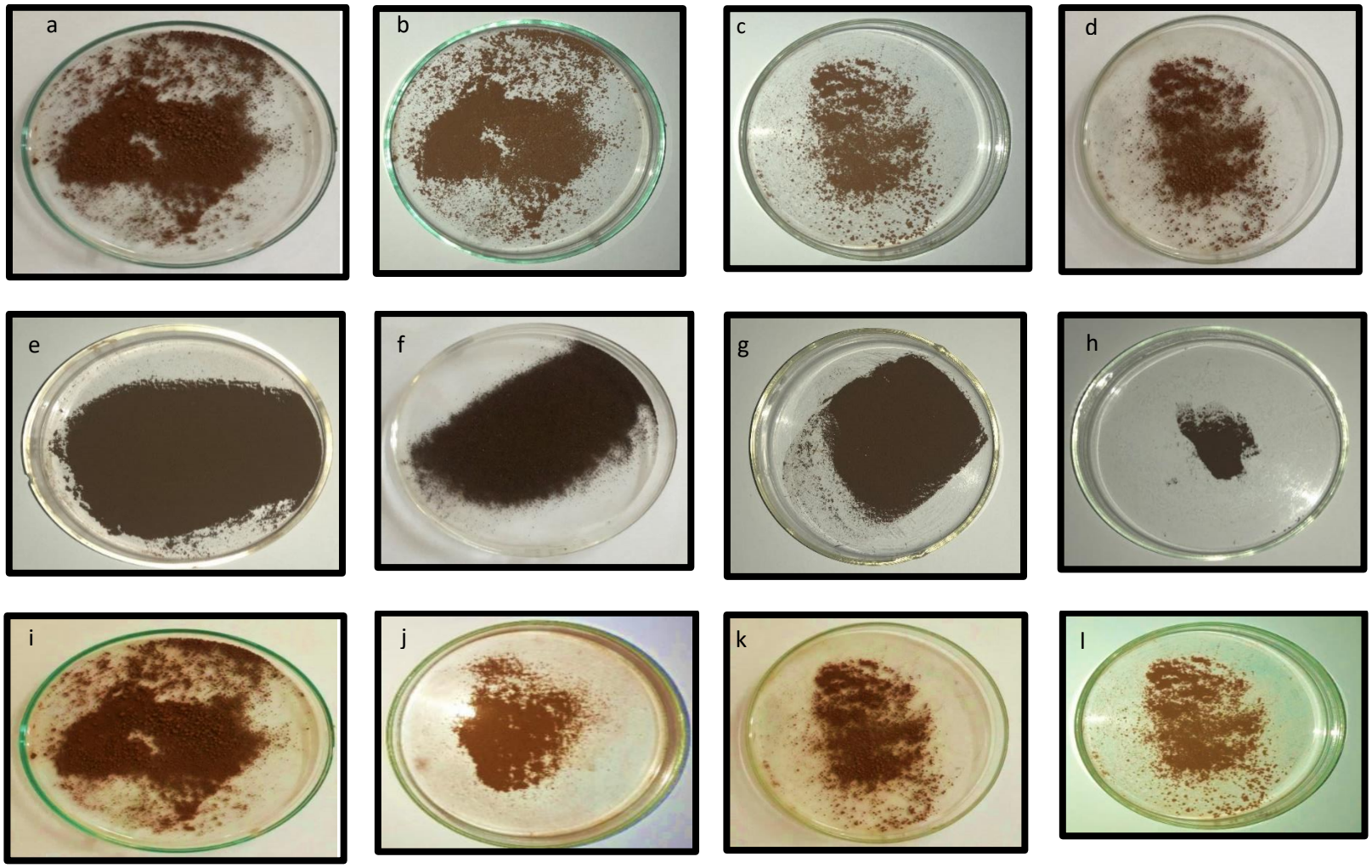

Figure 3.9 (a-l): a-d: Vermicast sample with fraction size 150 µm, 106 µm, 53 µm, below 53 µm; e-h: Termite mound ample with fraction size 150 µm, 106 µm,53 µm, below 53 µm; i-l: Laterite sample with fraction size 150 µm, 106 µm, 53 µm, below 53 µm

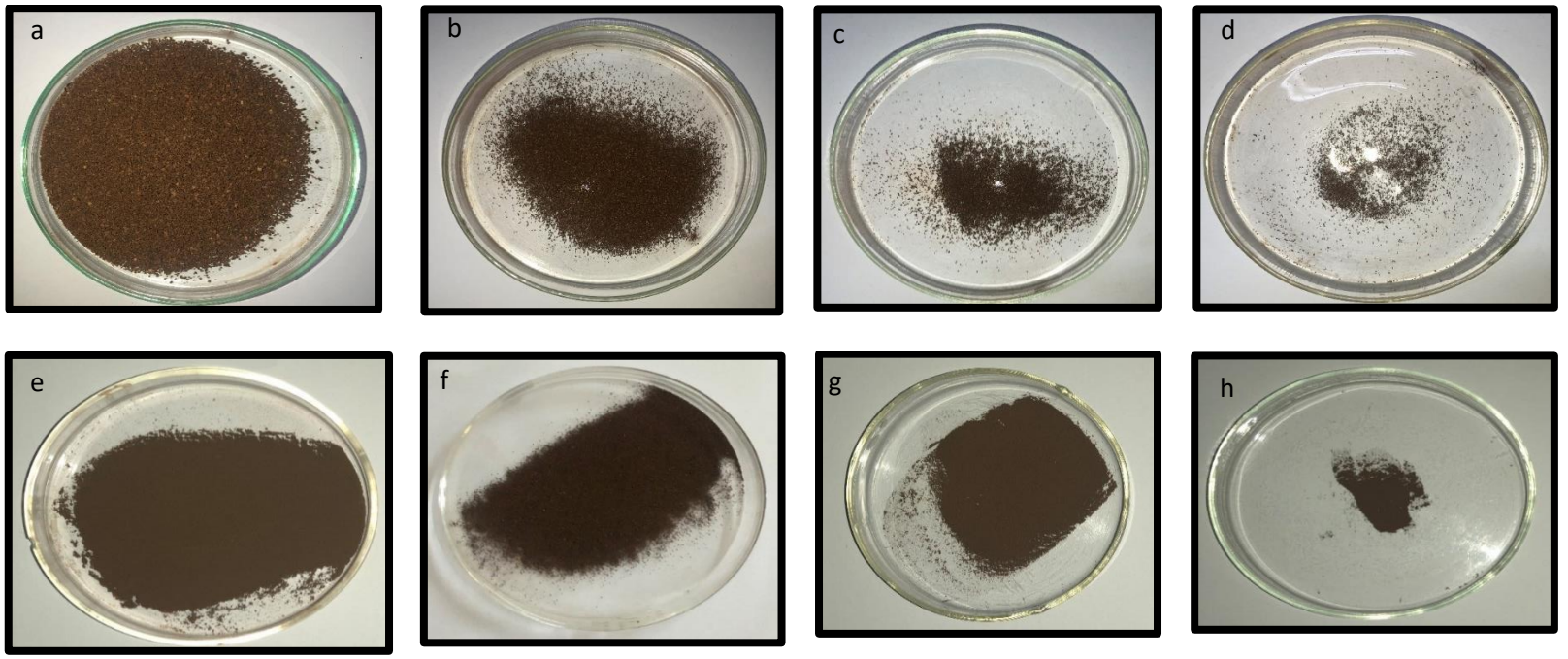

Figure 3.10 (a-l): a-d: Stream sediment samples with fraction size 150 µm, 106 µm,53 µm, below 53 µm; e-h: Beach sand sample with fraction size 150 µm, 106 µm, 53 µm, below 53 µm.

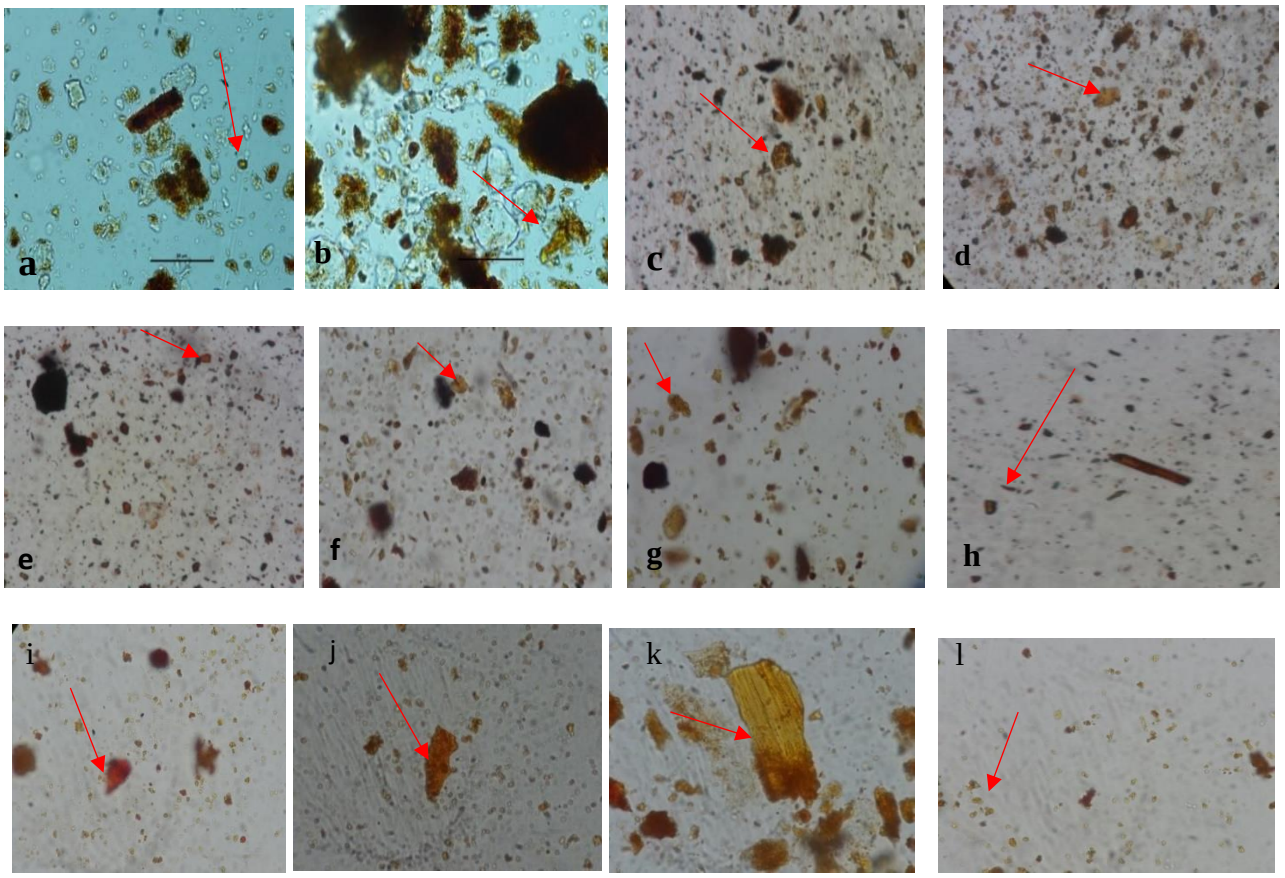

Figure 3.11 (a-l): a-d: Microscopic studies of the BHQ sample with fraction size 150 µm, 106 µm, 53 µm, below 53 µm; e-h: BMQ sample with fraction size 150 µm, 106 µm, 53 µm, below 53 µm; i-l: low grade iron ore (mining reject) sample with fraction size 150 µm, 106 µm, 53 µm, below 53 µm (scale: 1000x).

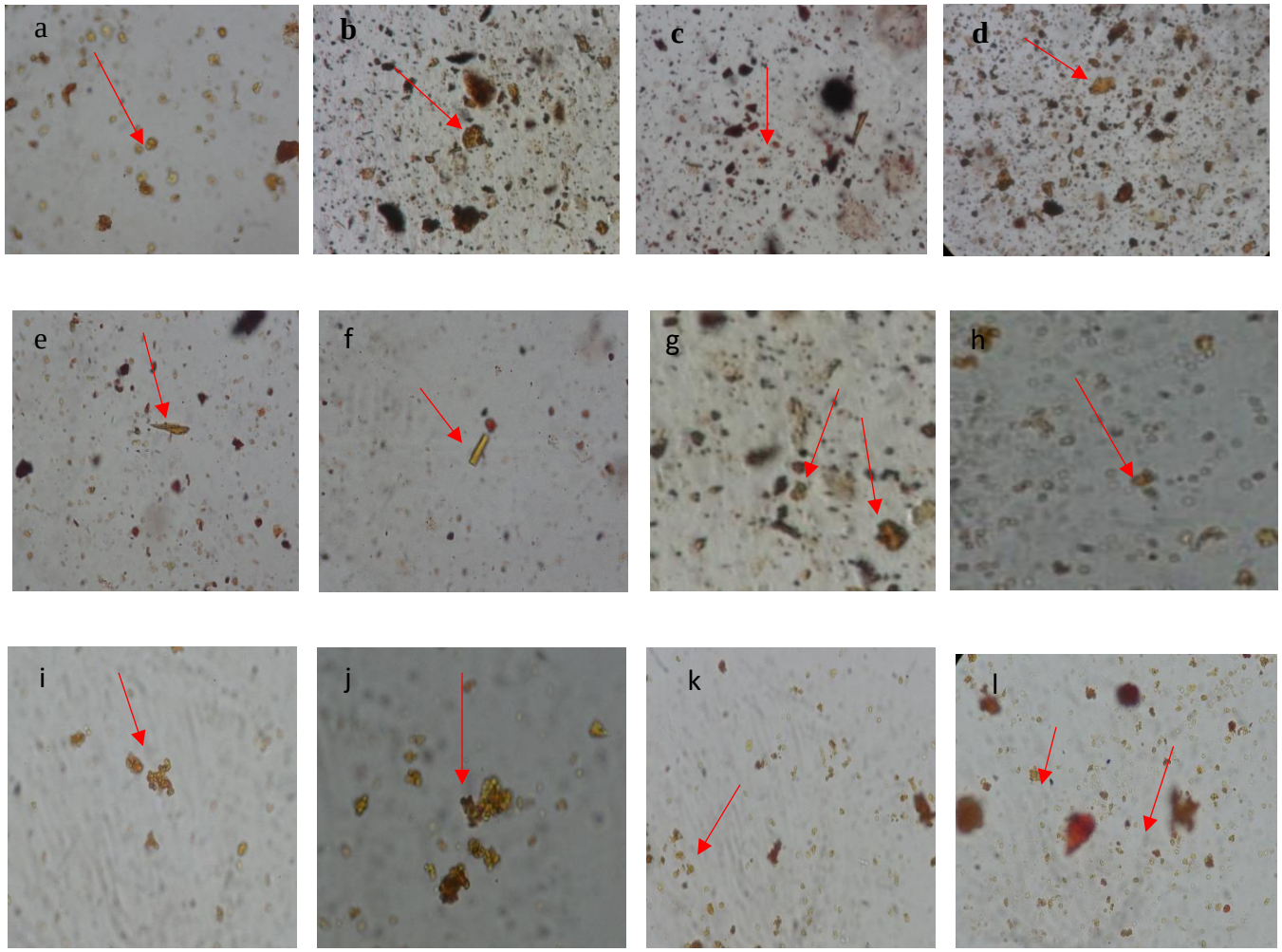

Figure 3.12 (a-l): a-d: Vermicast samples with fraction size 150 µm, 106 µm, 53 µm, below 53 µm; e-h: Termite mound sample with fraction size 150 µm, 106 µm, 53 µm, below 53 µm; i-l: Laterite sample with fraction size 150 µm, 106 µm, 53 µm, below 53 µm (Scale 1000x).

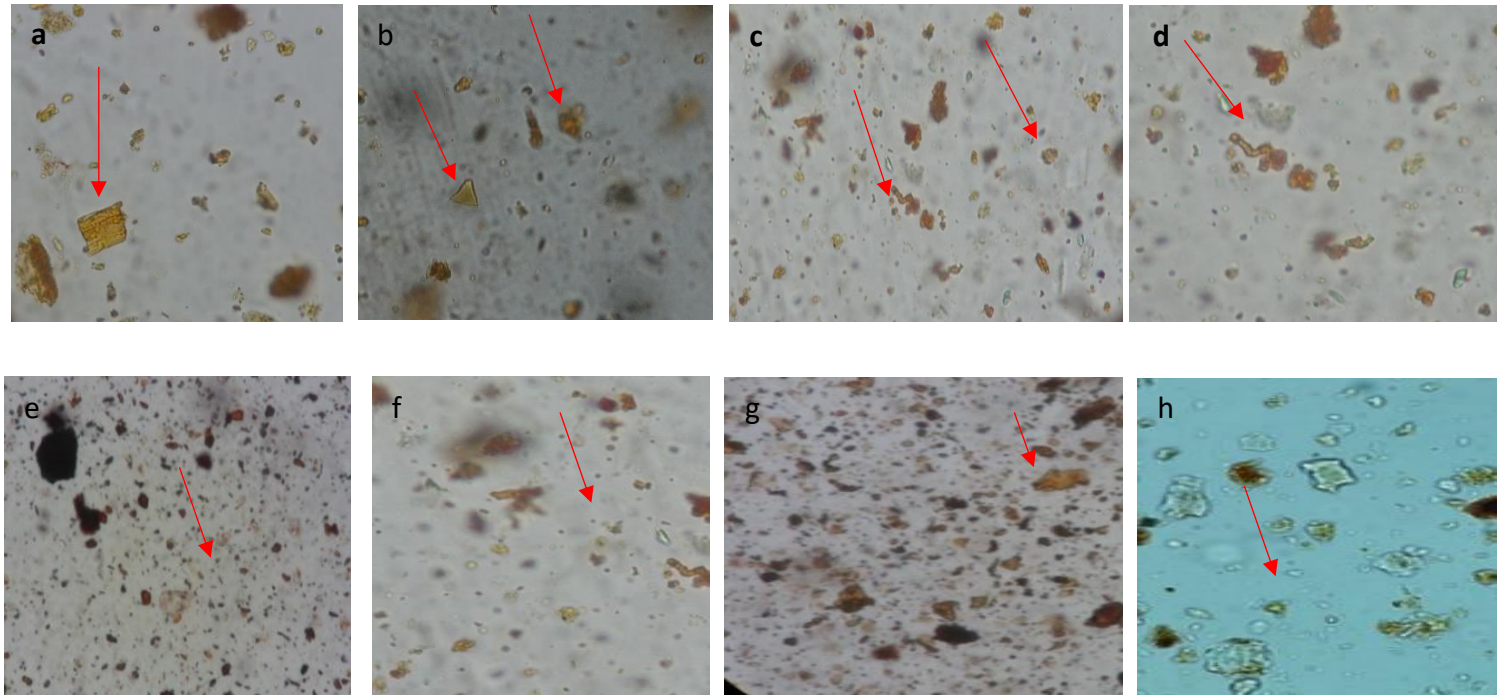

Figure 3.13 (a-h): Stream sediment sample with fraction size 150 µm, 106 µm, 53 µm, below 53 µm; e-h: Beach sand sample with fraction size 150 µm, 106 µm, 53 µm, below 53 µm. (Scale 1000X)

3.6. Detection of Gold

3.6.1. Inductively Coupled Plasma Optical Emission Spectroscopy (ICP-OES)

We were successful in obtaining the powdered, dried sieved fractions of the samples. The fractions 150, 106, 53 µm showed concentration of Gold and 106 µm was showing high concentration and thus same fraction were used for the further studies. The iron ore from BIF of Goa has not been subjected to multi-elemental analysis (such as Au, Ag, Pt including REE). However, our studies have established that BHQ contains 12-13 ppm and BMQ 8.4 ppm whereas the Iron ore reject dumps contain 7.71 ppm as seen in **Table 3.4**. The samples from non-mining areas also showed presence of Gold. The stream sediments showed between range from 12.96-15.03 ppm. Sand sample showed very negligible between 0.02-0.29 ppm, river sand ranged from 0.88-6.28 ppm, termite mounds sample ranged from 1-1.29 ppm, vermicast samples ranged from 0.66 -6.85 ppm and laterite and other rock samples ranged from 0.87-3.78 ppm. **Table 3.4** and **Table 3.5** gives the details of the same. The presence of the elemental Gold can be seen in the EDX spectra presented in **Fig 3.14 (a-f).**

Table 3.4: Detection of Bacterioform secondary Gold forms in ore samples

Sample designation	Type	Gold in ppm
MR-01	**Soil**	**7.71**
IO-01	**Soil**	**10.35**
BH-01	**Soil**	**12.93**
BM-01	**Soil**	**8.4**

Table 3.5: Detection of Bacterioform secondary Gold forms in auriferous samples

Designation	Samples	Gold in ppm	Location
BS-01	Beach Sand	0.29	Keri
BS-02	Beach Sand	0.12	Mandrem
BS-03	Beach Sand	0.13	Morjim
BS-04	Beach Sand	0.02	Anjuna
BS-05	Beach Sand	0.1	Vagator
BS-06	Beach Sand	0.02	Miramar
BS-07	Beach Sand	0.28	Varca
BS-08	Beach Sand	0.03	Arossim
BS-09	Beach Sand	0.19	Cavellosim
BS-10	Beach Sand	0.17	Patnem
BS-11	Beach Sand	0.94	Pollem
PD-01	River Sand	0.88	Betki
PD-02	River Sand	6.28*	Colvale
PD-03	Monozitic Black Sand	1.12	Chapora

TM-01	Termite Mound	1.13	Bondla
TM-02	Termite Mound	1.29	Tamdi Surla
SS-01	Stream Sediment	**12.96***	Bondla
SS-02	Stream Sediment	**15.03***	Tambdi Surla
VM-01	Vermicast	0.76	Taleigao
VM-02	Vermicast	0.87	Taleigao
VM-03	Vermicast	1.77	Shirgoa
VM-04	Vermicast	1.03	Usgoa
VM-05	Vermicast	0.76	Assnora
VM-06	Vermicast	0.66	Shiolim
LT-01	Laterite	**6.85***	Shirgoa
LT-02	Laterite	3.78	Bambolim
RK-01	Laterite	2.83	Bondla

* **High concentration**

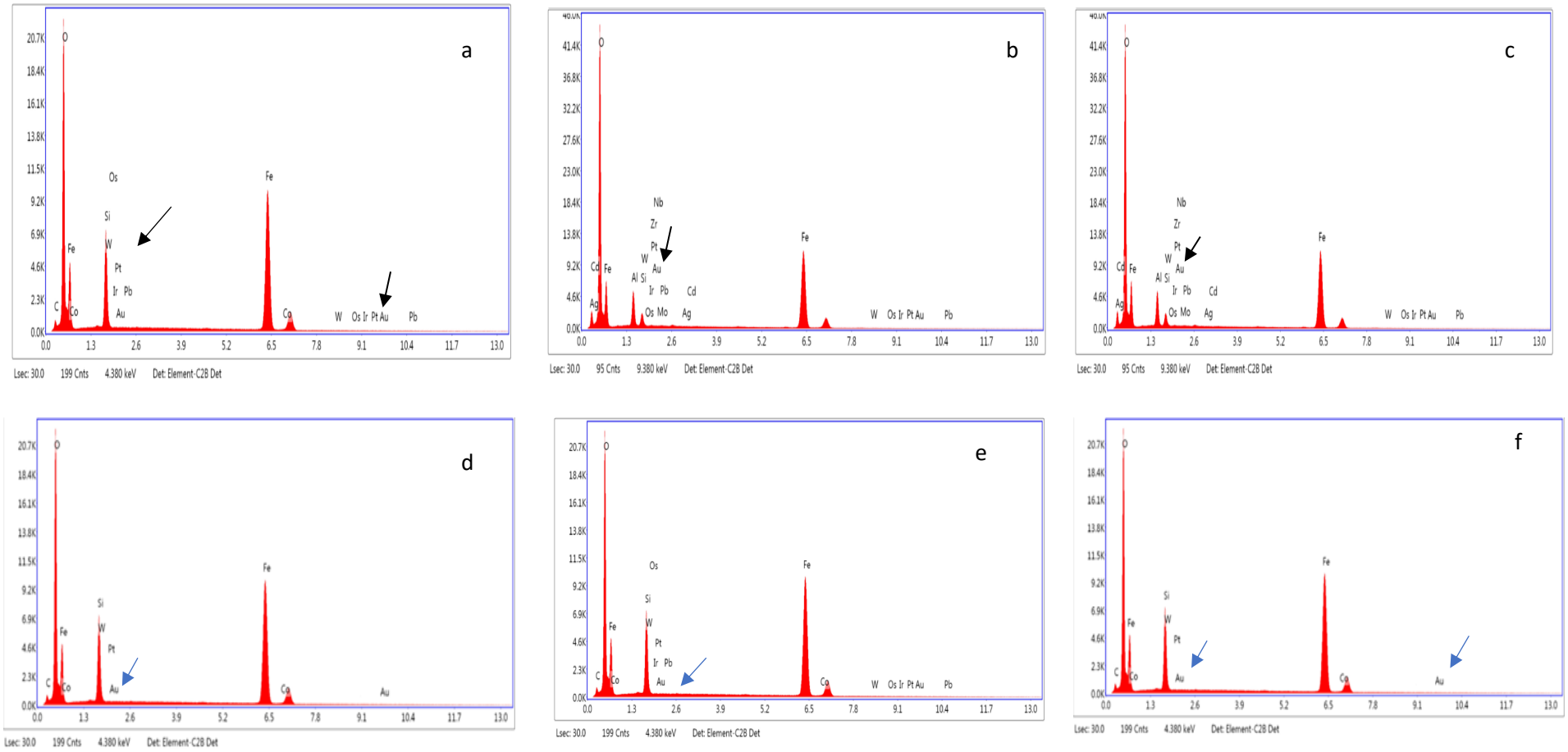

Figure 3.14 (a-f): The presence of the elemental Gold can be seen in the spectra presented by the EDX analysis

3.7. Morphological and typological classification of BFG particles

3.7.1. Optical microscopy

3.7.1.1.BHQ and BMQ samples

The morphological studies of BFG particles showed that the size varied ranging from 10 μm to 100 μm. BFG particles studied in each fraction per slide were between 100-400. The color of the BFG particles ranged from yellow, lemon yellow, canary yellow, Golden yellow, and orange to red. The BHQ and BMQ samples showed lot of shapes such as Bird shape, tortoise shape, kite shape, rod shape, star shape. The size of the particles varied from 10 μm to 50 μm. All particles were showing surface plasmon resonance. The texture of the particles varied from smooth to rough. The BFG particles are shown in the **Fig 3.15 (a-t)**. The **Table 3.6** gives the morphological classification of the particles.

3.7.1.2. The low-grade ore (Mining reject) sample

The low-grade ore (Mining reject) sample showed varying shapes such as rod shape, harpoon, star shape, irregular shape. The size of the particles varied from 10 μm to 50 μm. All particles were showing surface plasmon resonance. The texture of the particles varied from smooth to rough. The BFG particles are shown in the **Fig 3.16 (a-p).** The **Table 3.7** gives the morphological classification of the particles.

3.7.1.3. Vermicasts

Vermicast sample showed varying shapes such as rod shape, harpoon, star shape, irregular shape. The size of the particles varied from 10 μm to 50 μm. All particles were showing surface plasmon resonance. The texture of the particles varied from smooth to rough. The BFG particles are shown in the **Fig 3.17(a-l).** The **Table 3.8** gives the morphological classification of the particles.

3.7.1.4. Termite mounds

Termite mound sample showed varying shapes such as rod shape, harpoon, star shape, irregular shape. The size of the particles varied from 10 μm to 50 μm. All particles were showing surface plasmon resonance. The texture of the particles varied from smooth to rough. The BFG particles are shown in the **Fig 3.18 (a-h).** The **Table 3.9** gives the morphological classification of the particles.

3.7.1.5. Stream sediments

Samples showed varying shapes such as rod shape, harpoon, star shape, irregular shape. The size of the particles varied from 10 μm to 50 μm. All particles were showing surface plasmon resonance. The texture of the particles varied from smooth to rough. The BFG particles are shown in the **Fig 3.19 (a-p).** The **Table 3.10** gives the morphological classification of the particles.

3.7.1.6. Laterites samples

Laterites samples showed varying shapes such as rod shape, harpoon, star shape, irregular shape. The size of the particles varied from 10 μm to 50 μm. All particles were showing surface plasmon resonance. The texture of the particles varied from smooth to rough. The BFG particles are shown in the **Fig 3.20 (a-p).** The **Table 3.11** gives the morphological classification of the particles.

3.7.1.7. Beach sand samples

Sample showed varying shapes such as rod shape, harpoon, star shape, irregular shape. The size of the particles varied from 10 μm to 50 μm with SPR. The texture of the particles varied from smooth to rough. The BFG particles are shown in the **Fig 3.21 (a-f). Table 3.12** gives the morphological classification of the particles.

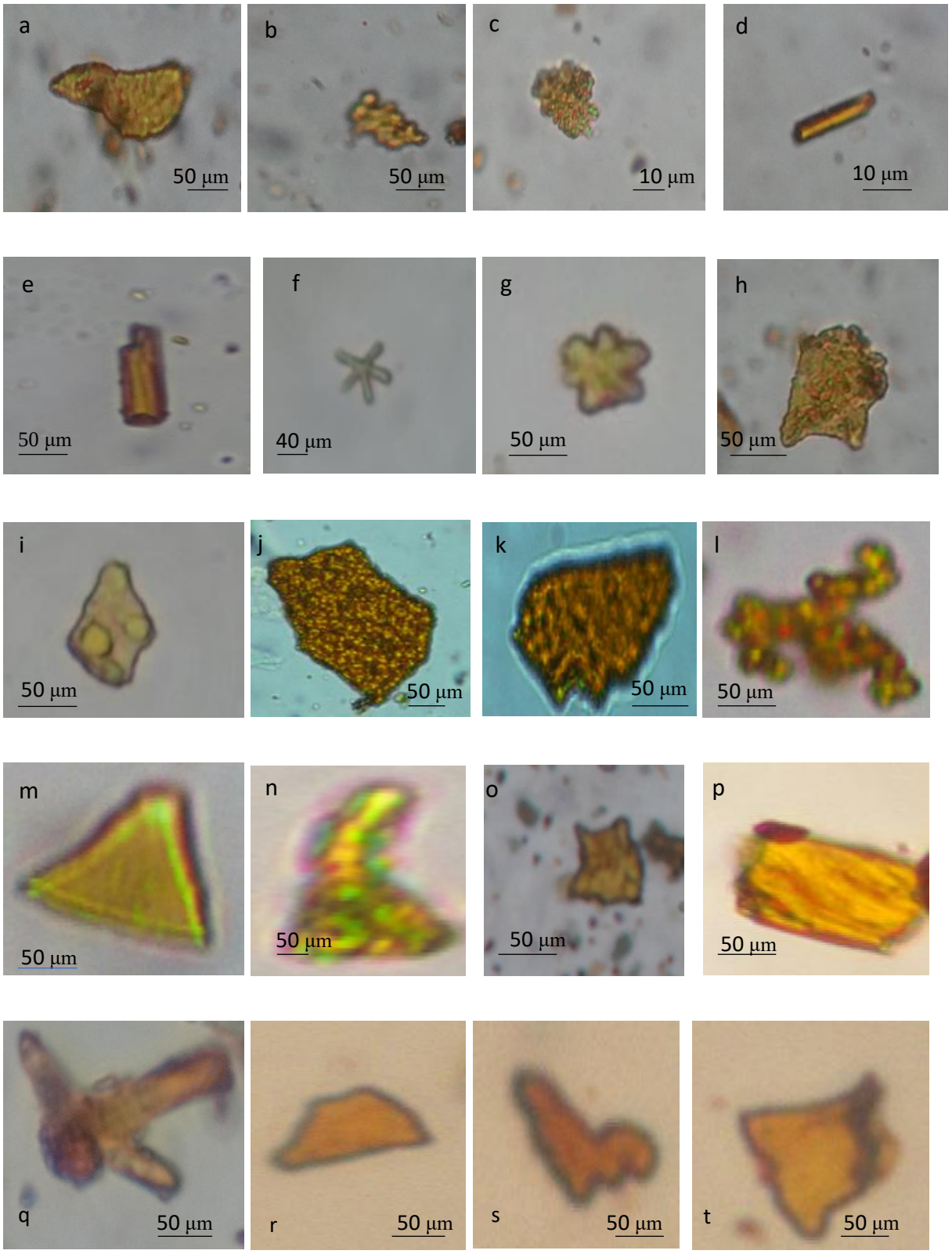

Figure 3.15 (a-t): Morphological classification of BHQ and BMQ samples of BFG; a-h: morphological classification of BHQ ; (i-t)-morphological classification of BMQ sample

Table 3.6: Morphological characterisation of BFG particles from BHQ and BMQ samples

Sr. No.	Fraction size In µm	Morphology			
		Shape	Mean Size	Texture	Colour
A	150-53	Bird shape	50 µm	Smooth	Yellow
B	150-53	Tortoise shape	50 µm	Rough	Dark yellow
C	53-below 53	Irregular	10 µm	Rough	Greenish yellow
D	53-below 53	Rod	10 µm	Smooth	Lemon yellow
E	53	Rod	50 µm	Rough	Yellow
F	53-below53	Star shape	40 µm	Smooth	Lemon yellow
G	53	Star shape	50 µm	Smooth	Lemon yellow
H	150-53	Stingray	50 µm	Rough	Lemon yellow
I	150-53	Kite shape	50µm	Rough	Lemon yellow
J	53-below 53	Irregular	50 µm	Rough	Dark yellow
K	53-below 53	Irregular	50 µm	Rough	Dark yellow
L	53	Dragon shape	50 µm	Rough	Greenish yellow
M	53-below 53	Prism	50 µm	Smooth	Greenish yellow
N	150-53	Irregular	50 µm	Rough	Greenish yellow
O	150-53	Kite shape	50 µm	Rough	Yellow
P	53-below 53	Irregular	50 µm	Smooth	Yellow
Q	53-below 53	Axe	50 µm	Rough	Yellow
R	53	Irregular	50 µm	Smooth	Yellow
S	53-below 53	Gun shape	50 µm	Smooth	Yellow
T	150-53	Trapezoid	50 µm	Smooth	Yellow

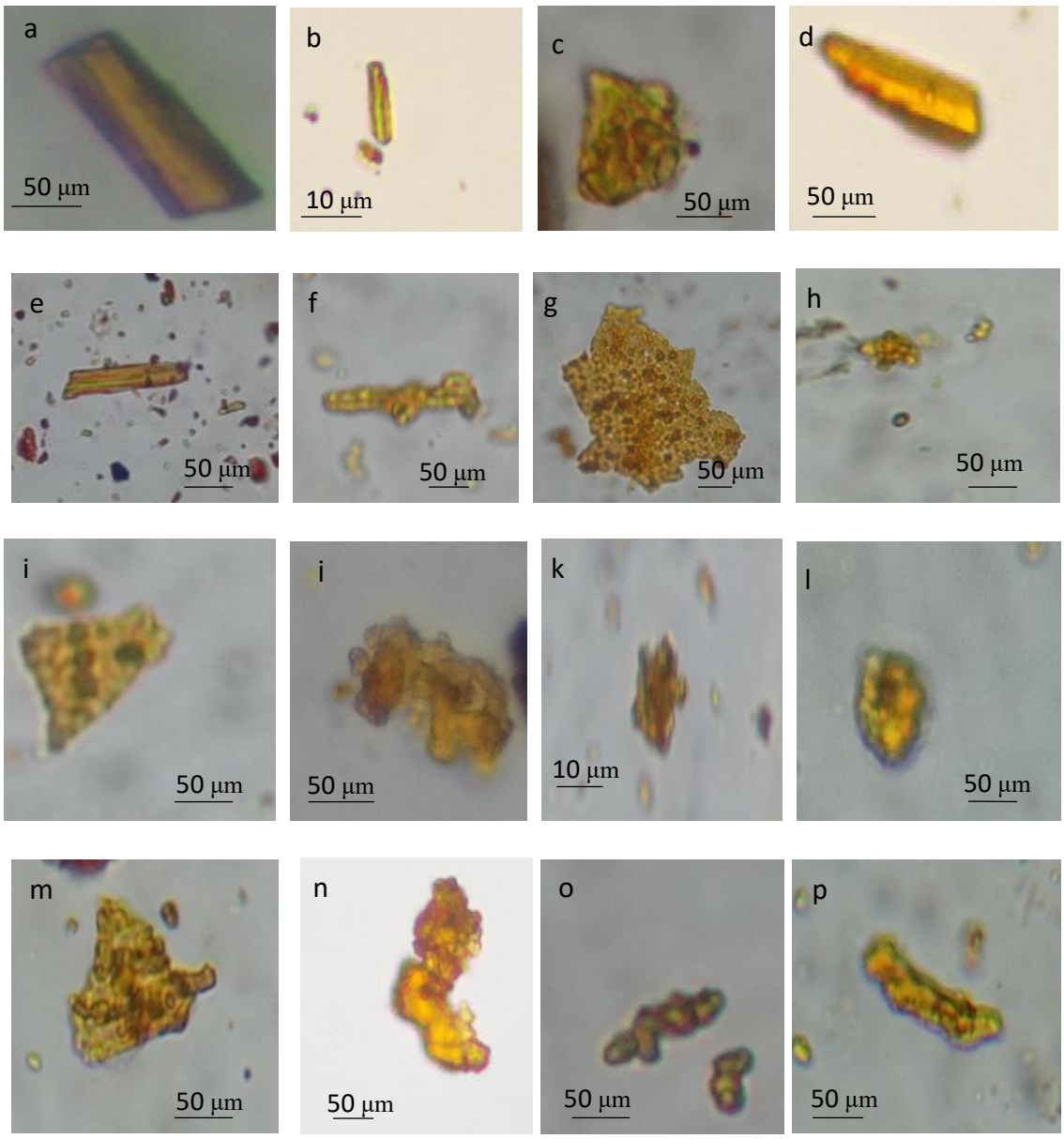

Figure 3.16 (a-p): Morphological classification of BFG particles from Low grade ore (Mining reject)

Table 3.7: Morphological characterisation of BFG particles from low grade ore (mining reject samples)

Type of sample	Fraction size In µm	Morphology			
		Shape	Mean size	Texture	Colour
A	150-53	Rod	50 µm	Smooth	Yellow
B	150-53	Rod	10 µm	Smooth	Dark Yellow
C	53-below 53	Star	50 µm	Smooth	Greenish Yellow
D	53-below 53	Harpoon Shape	50 µm	Smooth	Lemon Yellow
E	53	Rod	50 µm	Rough	Yellow
F	53-below 53	Harpoon Shape	50 µm	Rough	Yellow
G	53	Irregular	50 µm	Rough	Lemon Yellow
H	150-53	Irregular	50 µm	Rough	Lemon
I	150-53	Irregular	50 µm	Rough	Yellow
J	53-below 53	Irregular	50 µm	Rough	Lemon
K	53-below 53	Irregular	10 µm	Rough	Yellow
L	53	Irregular	50 µm	Rough	Lemon
M	53-below 53	Irregular	50 µm	Rough	Yellow
N	53	Irregular	50 µm	Rough	Lemon
O	150-53	Irregular	50 µm	Rough	Yellow
P	150-53	Irregular	50 µm	Rough	Lemon

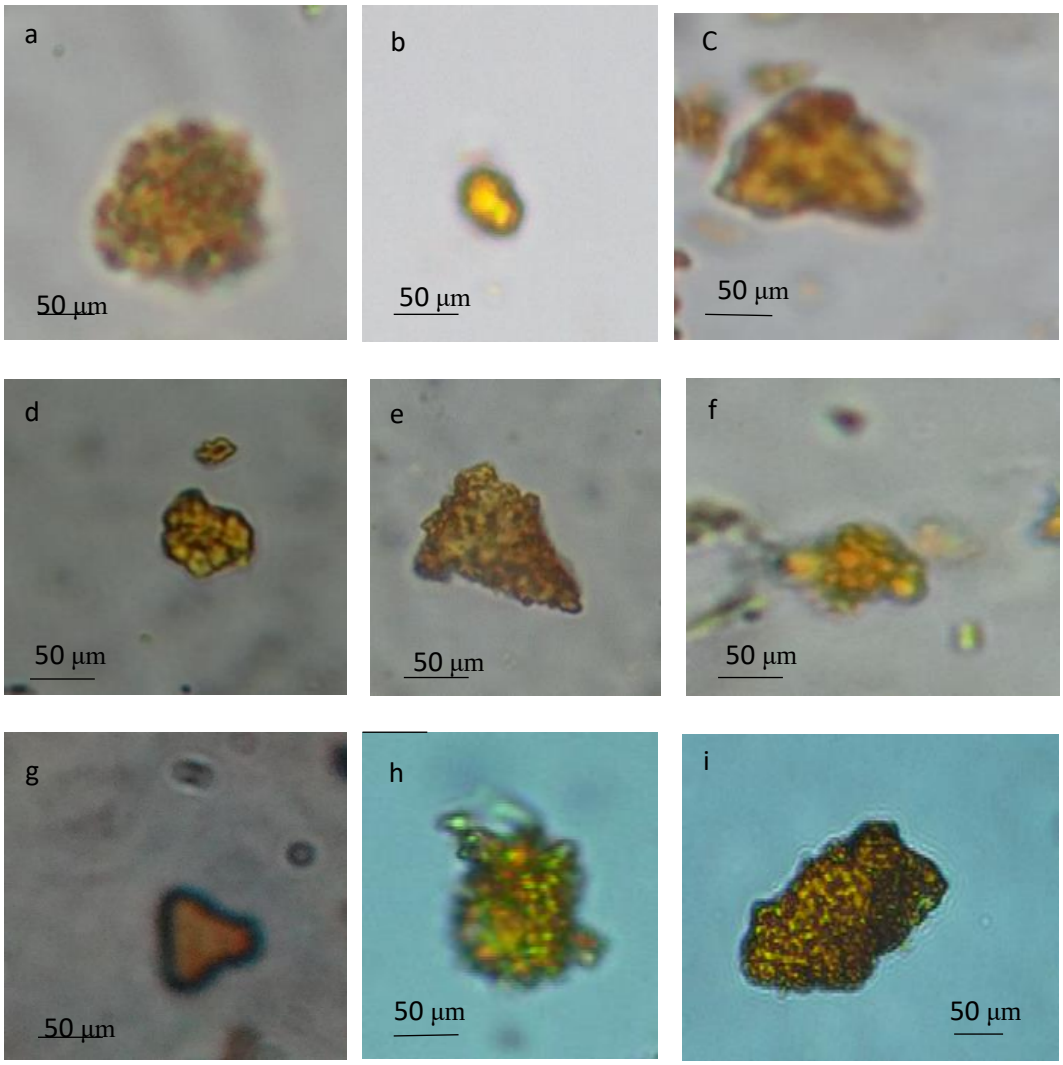

Figure 3.17 (a-l): Morphological classification of BFG particles from vermicasts samples

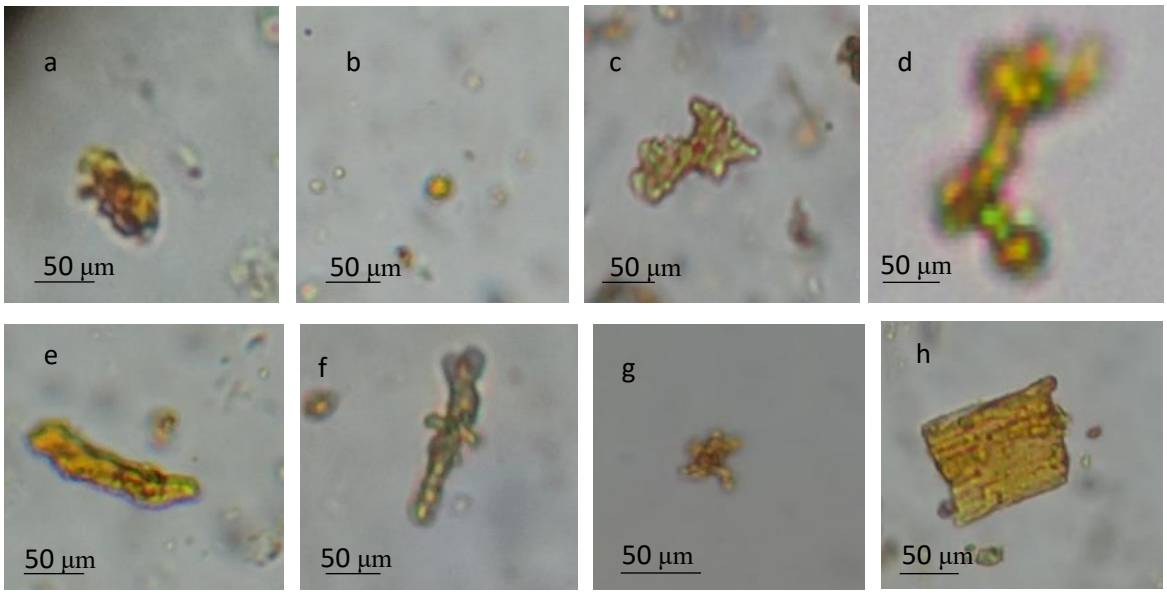

Figure 3.18 (a-l): Morphological classification of BFG particles from Termite mounds

Table 3.8: Morphological characterisation of BFG particles from vermicast samples

Type of sample	Fraction size In µm	Morphology			
		Shape	Mean size	Texture	Colour
A	150-53	Circular	50 µm	Rough	Yellow
B	150-53	Circular	50 µm	Rough	Dark yellow
C	53-below 53	Irregular	10 µm	Rough	Lemon yellow
D	53	Irregular	50 µm	Rough	Yellow
E	53-below 53	Irregular	40 µm	Rough	Yellow
F	150-53	Irregular	50 µm	Rough	Yellow
G	150-53	Prism	50 µm	Rough	Yellow
H	53-below 53	Irregular	10 µm	Rough	Yellow
I	53-below 53	Irregular	10 µm	Smooth	Yellow

Table 3.9: Morphological characterisation of BFG particles from Termite mound samples

Type of sample	Fraction size In µm	Morphology			
		Shape	Mean size	Texture	Colour
A	150-53	Irregular	50 µm	Rough	Yellow
B	150-53	circular	50 µm	Rough	Dark yellow
C	53-below 53	Irregular	50 µm	Smooth	Greenish yellow
D	53-below 53	Sea horse	10 µm	Rough	Lemon yellow
E	53	Irregular	50 µm	Rough	Yellow
F	53-below 53	Irregular	40 µm	Rough	Yellow
G	53	Irregular	50 µm	Rough	Lemon yellow
H	150-53	Irregular	50 µm	Rough	Yellow

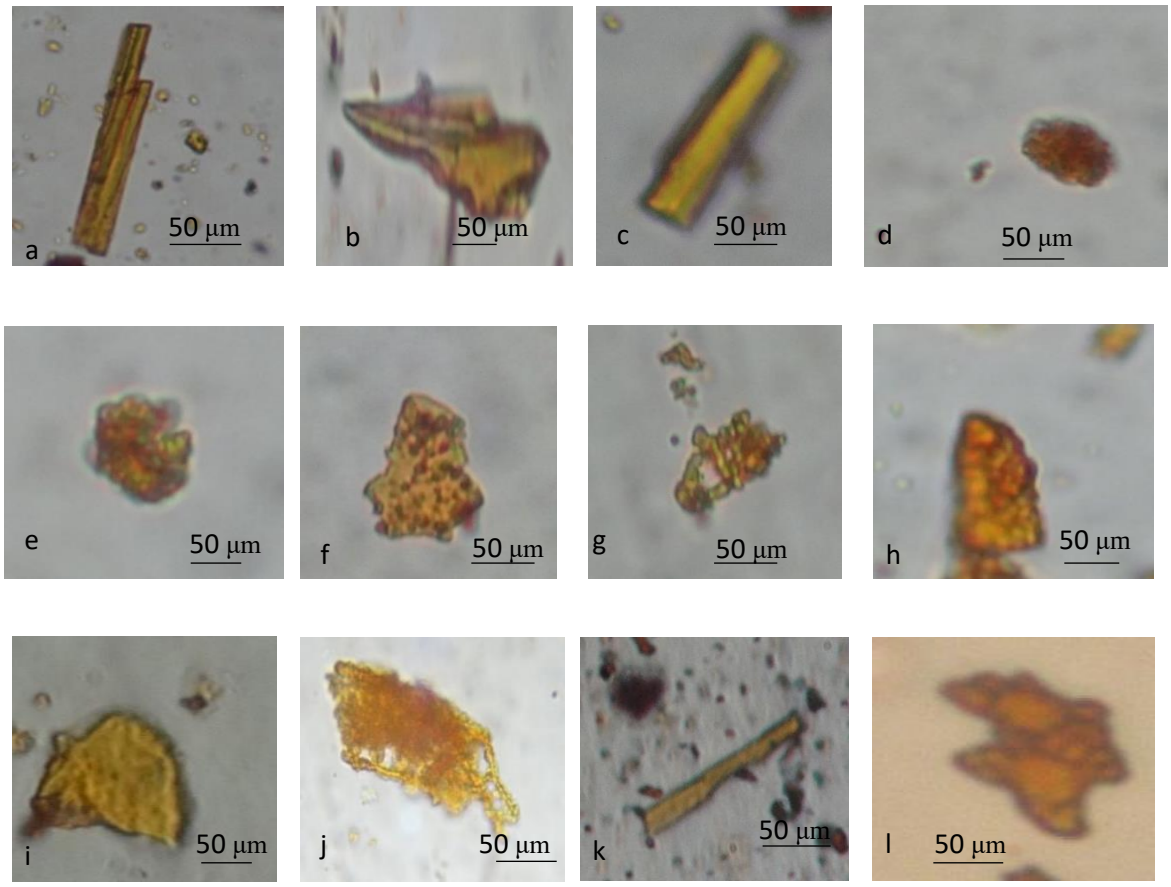

Figure 3.19 (a-p): Morphological classification of BFG particles from Stream sediment samples

Table 3.10: Morphological characterisation of BFG particles from stream sediments

Type of sample	Fraction size In µm	Morphology			
		Shape	Mean size	Texture	Colour
A	150-53	Rod	50 µm	Rough	Yellow
B	150-53	Harpoon	50 µm	Rough	Dark yellow
C	53-below 53	cylinder	50 µm	Smooth	Greenish yellow
D	53-below 53	circular	10 µm	Rough	Lemon yellow
E	53	Irregular	50 µm	Rough	Yellow
F	53-below 53	Irregular	40 µm	Rough	Yellow
G	53	Irregular	50 µm	Rough	Lemon yellow
H	150-53	Irregular	50 µm	Rough	Yellow
I	150-53	Irregular	50 µm	Rough	Yellow
J	150-53	Irregular	50 µm	Rough	Yellow
K	53-below 53	Rod	50 µm	Smooth	Yellow
L	53-below 53	Irregular	10 µm	Rough	Yellow

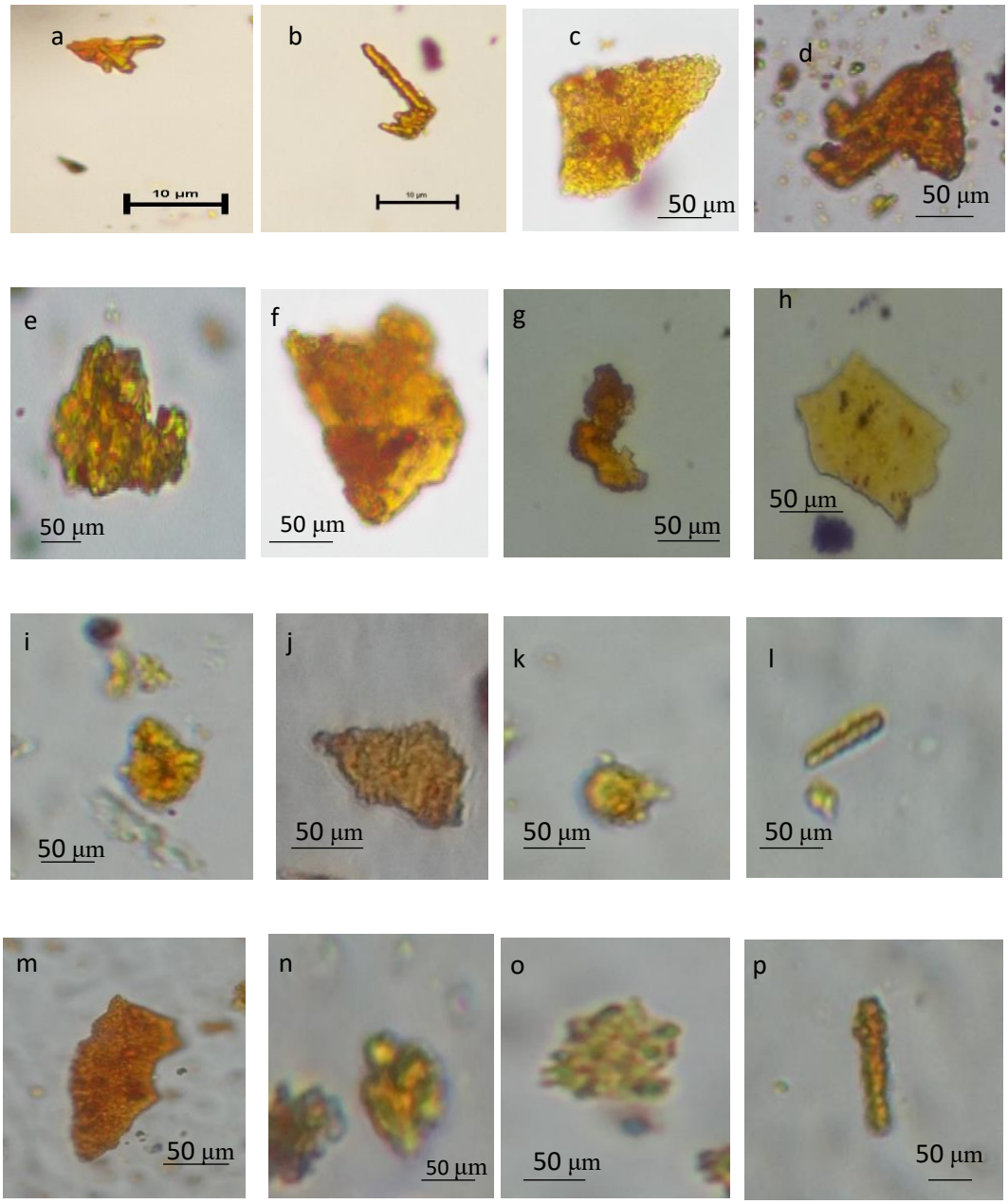

Figure 3.20 (a-p): Morphological classification of BFG particles from Laterite samples

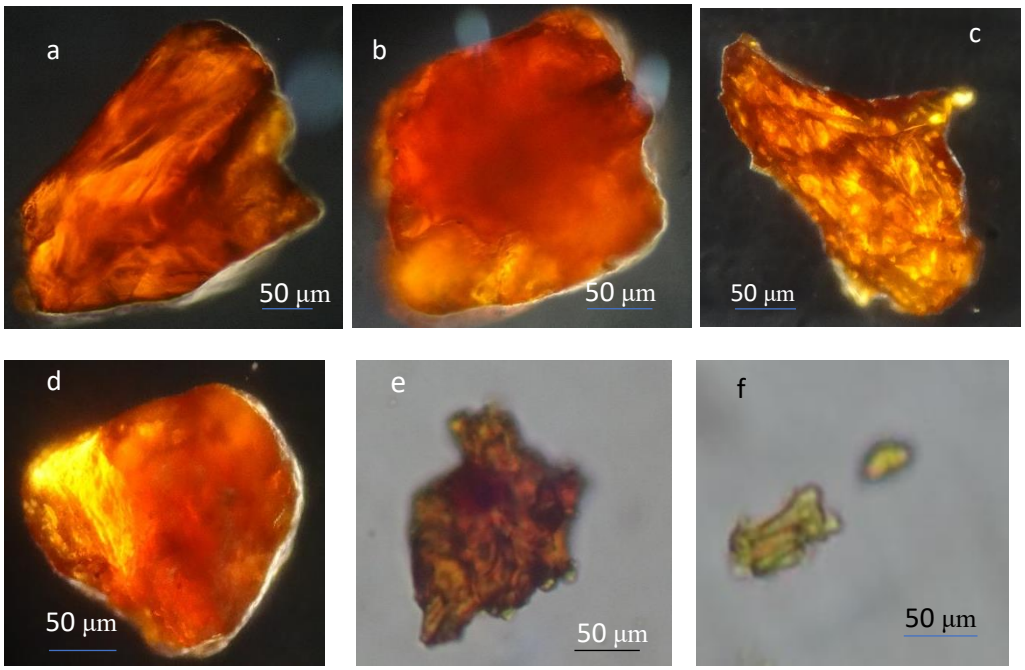

Figure 3.21: (a-f): Morphological classification of BFG particles from Beach sand samples

Table 3.11: Morphological characterisation of BFG particles from laterite samples

Type of sample	Fraction size In µm	Morphology			
		Shape	Mean size	Texture	Colour
A	150-53	A shape	50 µm	Rough	Yellow
B	150-53	Crown	50 µm	Rough	Dark yellow
C	53-below 53	Irregular	50 µm	Smooth	Greenish yellow
D	53-below 53	Irregular	10 µm	Rough	Lemon yellow
E	53	Irregular	50 µm	Rough	Yellow
F	53-below53	Irregular	40 µm	Rough	Yellow
G	53	Irregular	50 µm	Rough	Lemon yellow
H	150-53	Irregular	50 µm	Rough	Yellow
I	150-53	Rod	50µm	Rough	Yellow
J	53-below 53	Irregular	10 µm	Rough	Yellow
K	53-below 53	Irregular	10 µm	smooth	Yellow
L	53	Rod	50 µm	Rough	Yellow

Table 3.12: Morphological characterisation of BFG particles from beach sand samples

Fraction size In µm	Morphology			
	Shape	Mean Size	Texture	Colour
150-53	Irregular	50 µm	Smooth	Dark Yellow
150-53	Irregular	50 µm	Smooth	Dark yellow
53-below 53	Irregular	10 µm	Rough	yellow
53-below 53	Irregular	10 µm	Smooth	yellow
53	Irregular	50 µm	Rough	Dark Yellow
53-below 53	Irregular	40 µm	Rough	Lemon Yellow

3.7.2. Scanning Electron Microscopy (SEM)

Scanning electron microscopy (SEM) helped to reveal the size, shape and topography of the Gold particles. The shapes include rods, triangles, cubes, spherical, irregular shapes. Mostly irregular shapes were noticed on the surface of the BFG particles. The presence of bacterial fossils or Gold nanoparticles on BFG's and other Gold particles were observed on some of the samples. Triangular plate form Gold was found to be appearing on the surface of Gold. cylindrical rod shape BFG particle with a rough surface was found showing the influence of weathering. The auriferous fractions also showed the presence of xenomorphic single Gold grain with irregular and rough surface**.** Typological classification of microbioform secondary Gold is shown in **Fig 3.22 (a-f).**

3.7.3. SEM typological analysis

The analyses helped to reveal the microfeatures, topographical details of the BFG particles, the 3-D structure. **Fig 3.23 a, e** shows the rough irregular BFG particle with a layers like forms on the surface. **Fig 3.23 b, c, f** showed the pseudo image of the BFG particle, **Fig 3.23 d** shows the 3-D structure of the BFG particles whereas the length of the rod shape BFG particle is shown in **Fig 3.23 g**. **Fig 3.23 h** shows the rod shape BFG particle with sharp, smooth striated Gold surface and edges of the same were also found to be smooth.

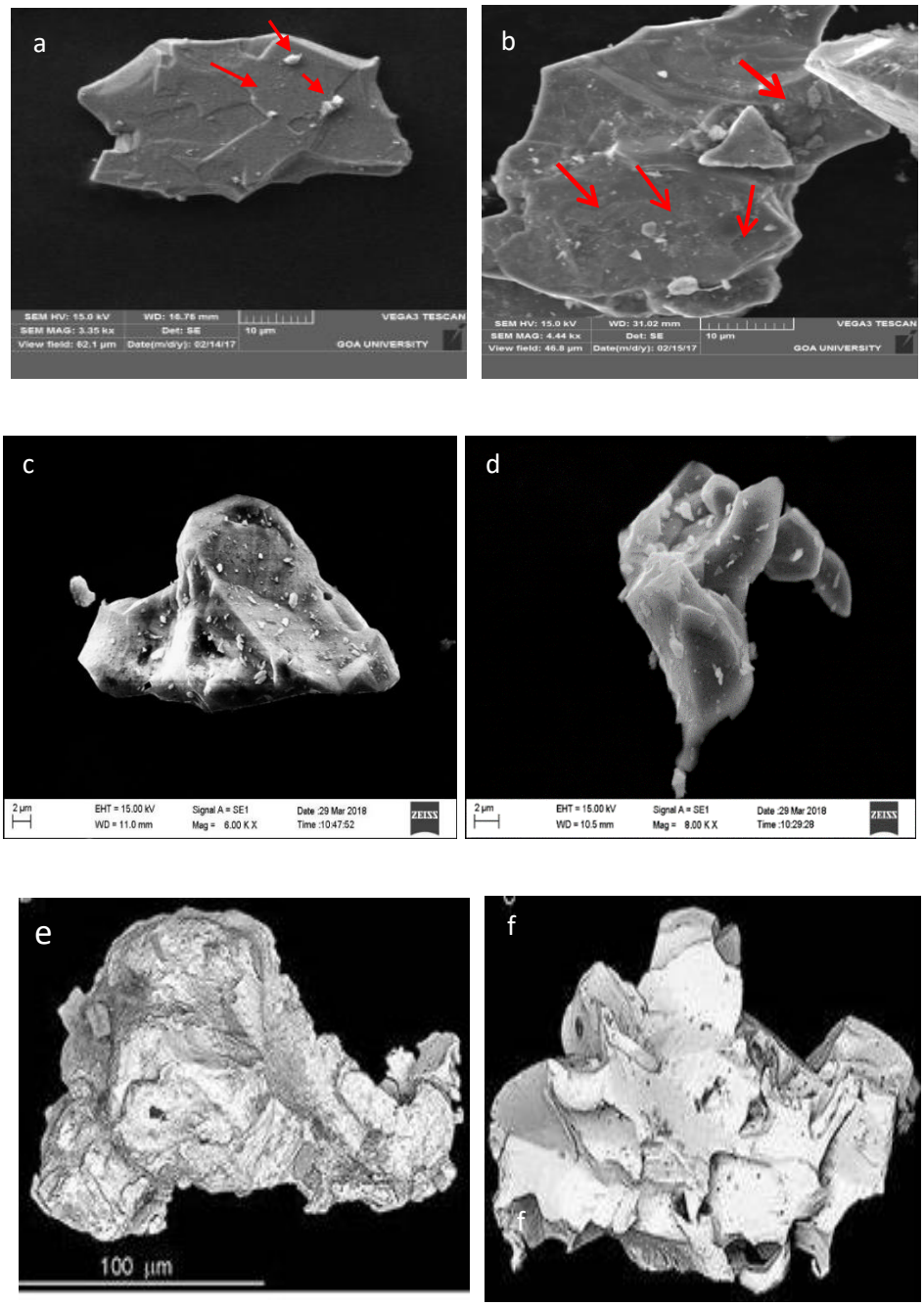

Figure 3.22 (a-f): Scanning Electron microscopic images of the particles of Gold with irregular and rough surface. a, b, d, f- shows the smooth surface with irregular shapes; c, d, e- Shows the irregular BFG particles with rough surface

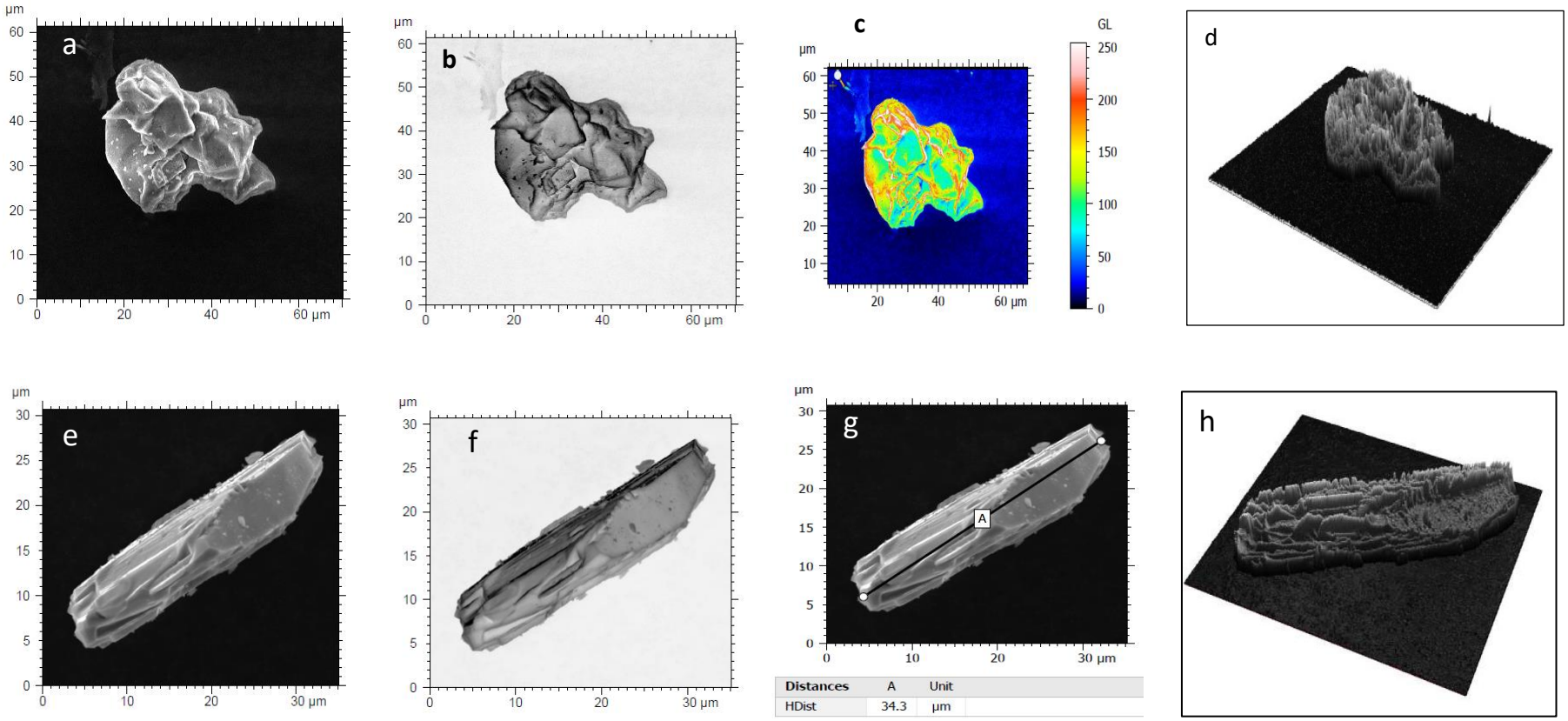

Figure 3.23 (a-e): Analysis of the BFG particles. a- Rough irregular BFG particle with a layers like forms on the surface; (b, c, f)- Pseudo image of the BFG particle, d-h: 3-D structure of the BFG particles; e- Rod shape BFG particle with sharp, smooth striated Gold surface

3.8. Metagenomic studies of BHQ and BMQ sample

It was found that both the samples were showing association of microorganisms. Sterile samples were successfully obtained in a sufficient amount. The number of sequences reads from the BHQ were 37,618. In case of BHQ, reads analyzed were 18,809, reads classified were 669 whereas the remaining reads were unclassified and were 18,140 in number. BHQ sample showed presence of 71% Bacteria, 27% Eukaryota and 1% archaea as seen in **Fig 3.24 a**. Diversity of Microorganisms found associated with the BHQ has been represented in the form of phylogenic tree and seen in **Fig 3.25.** In case of BMQ sample the total number of sequence reads were 72,758. In case of BMQ, reads analyzed were 36,379, reads classified were 1,016 and reads unclassified were 35,363. Sample showed presence of 69% of Bacteria, 30% of Eukaryota, <1% of archaea and <1% viruses as seen in **Fig 3.24 b.** Diversity of Microorganisms found associated with the BMQ has been represented in the form of phylogenic tree and seen in **Fig 3.26.** Metagenomic analysis serves as a useful technique to study the microbes associated with the BIF samples of Goa. This is the first study on the metagenomic analysis of BIF of Goa. In both the samples the bacterial association was high as compared to Eukaryotes, archaea.

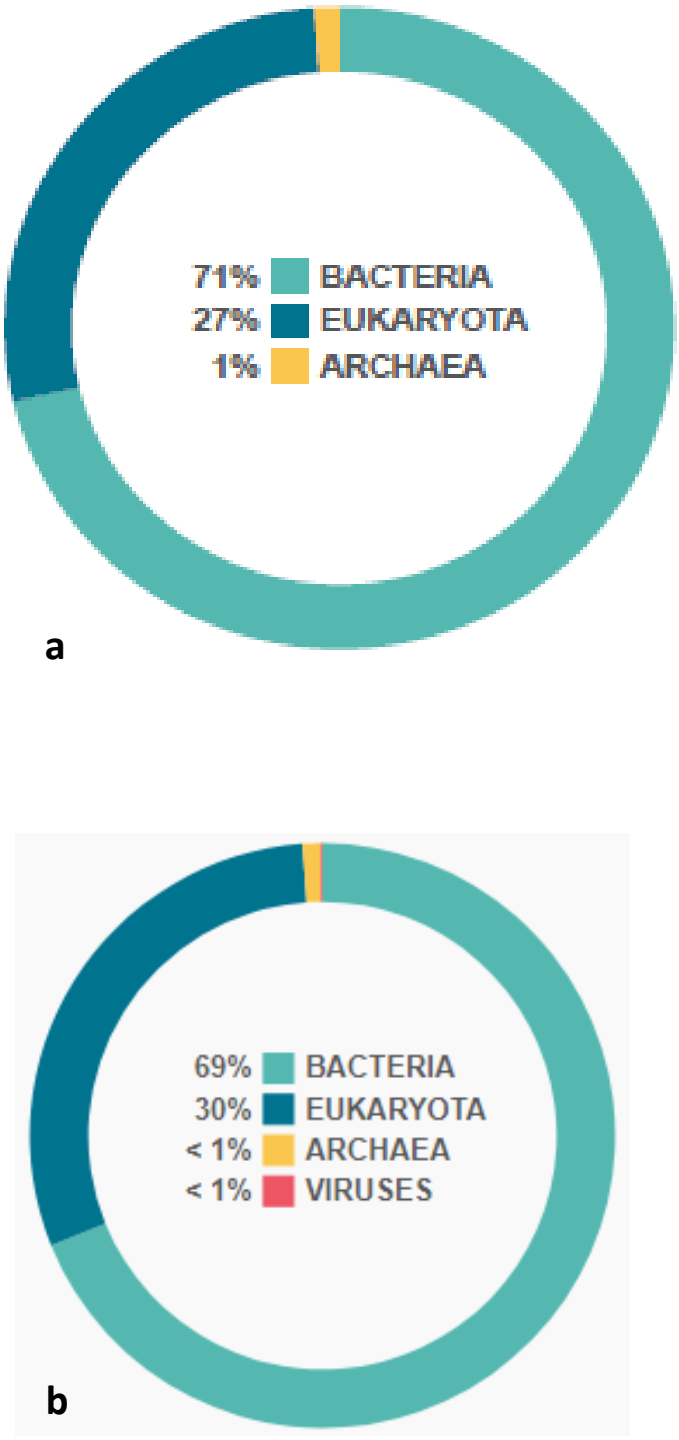

Figure 3.24 (a-b): Percentage wise classification of microorganisms at different levels in case of BHQ and BMQ

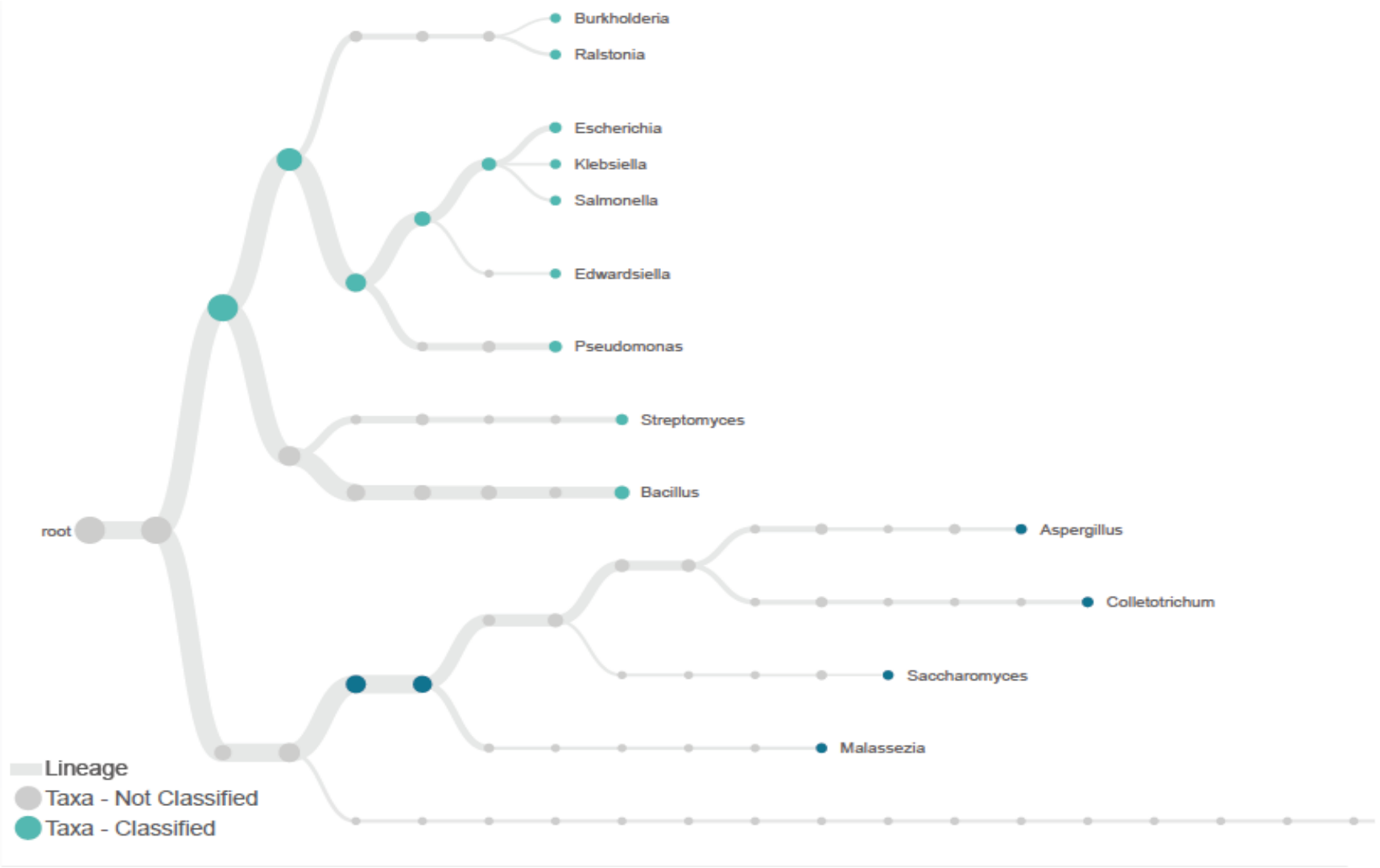

Figure 3.25: Phylogenetic tree representing the association of microorganisms with the BHQ sample

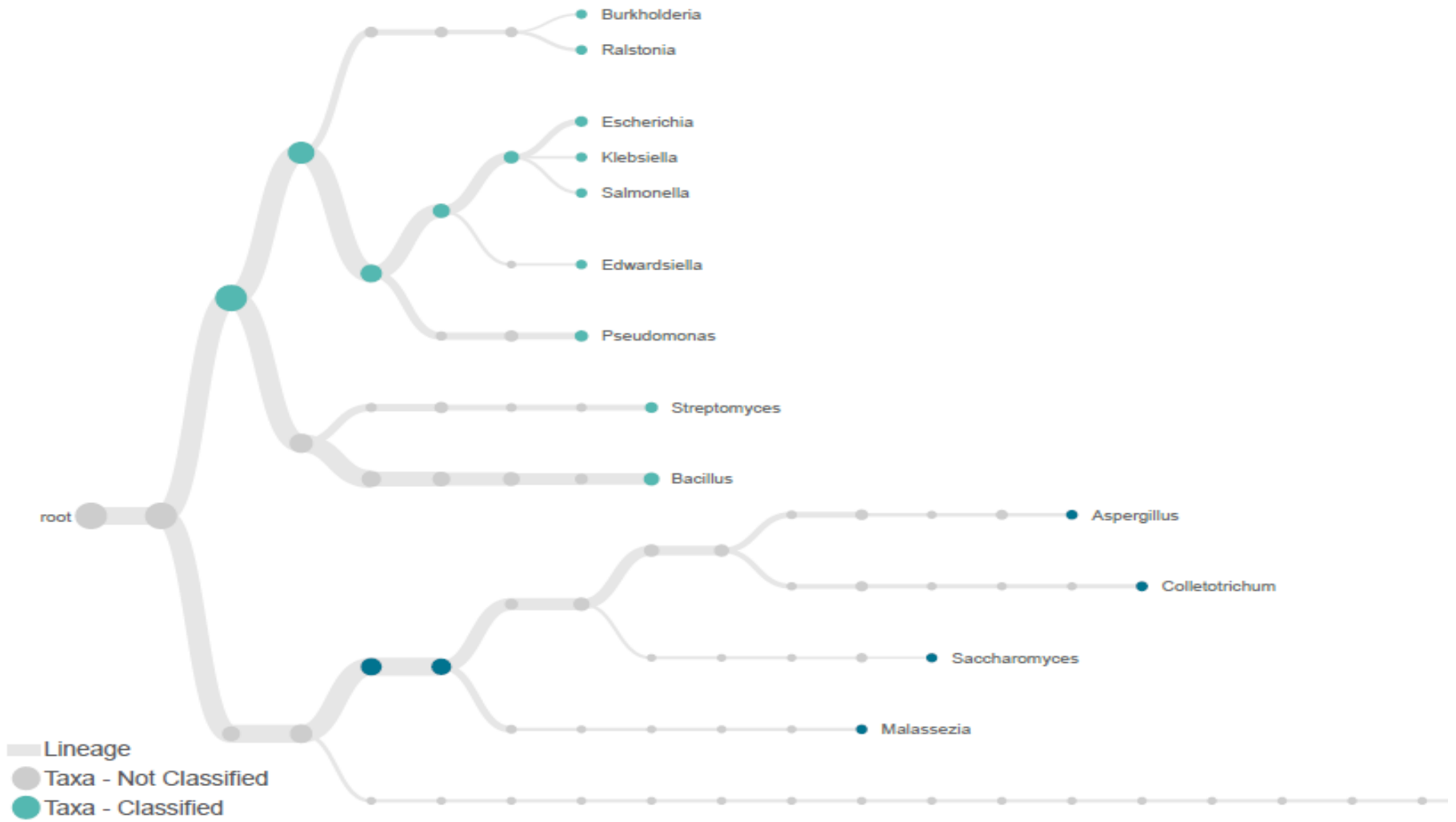

Figure 3.26: Phylogenic tree representing the association of microorganisms with the BMQ sample

3.9. Isolation of hyperacidophillic and chemolithotrophic bacteria by Winogradsky technique

3.9.1. Isolation of chemolithotrophs

Total 6 samples were used for the study from mining and non-mining areas in Goa as given in **Table 3.13**. We were successful in use of Winogradsky Microcosm (WGMC) by modification using simple, low-cost PET bottles. After prolonged incubation in dark followed by exposure to light, interesting coloured zones were identified in 24 columns from six samples indicating differential colonization of biofilms of Iron and Sulphur bacteria as seen in **Fig 3.27 (a-f)**. The Winogradsky column is a miniature ecosystem in which microorganisms and nutrients interact over time.

3.9.2. Study of the biofilm from coverslip size pieces from bottles and its microscopic observation

After prolonged incubation in dark followed by exposure to light, interesting coloured zones were identified in 24 columns from six samples indicating differential colonization of biofilms of Iron and Sulphur bacteria **Fig 3.28 (a-b).** The development of biofilms is initiated by microorganisms forming a monolayer attachment on the surface.

3.9.3. Enrichment technique

Over time, this film becomes more complex with layers of organisms of different types colonizing the surface and enriched tube as seen in **Fig 2.29 (a-d).** Depending on the energy sources available, photosynthetic microbes, facultative chemo-organotrophs, or sulfate-reducing microorganisms may be present (Prescott et al.,1996). Enrichment technique helped to promote their growth, increasing their number, causing extinction by reducing other micro-organisms present in the sample.

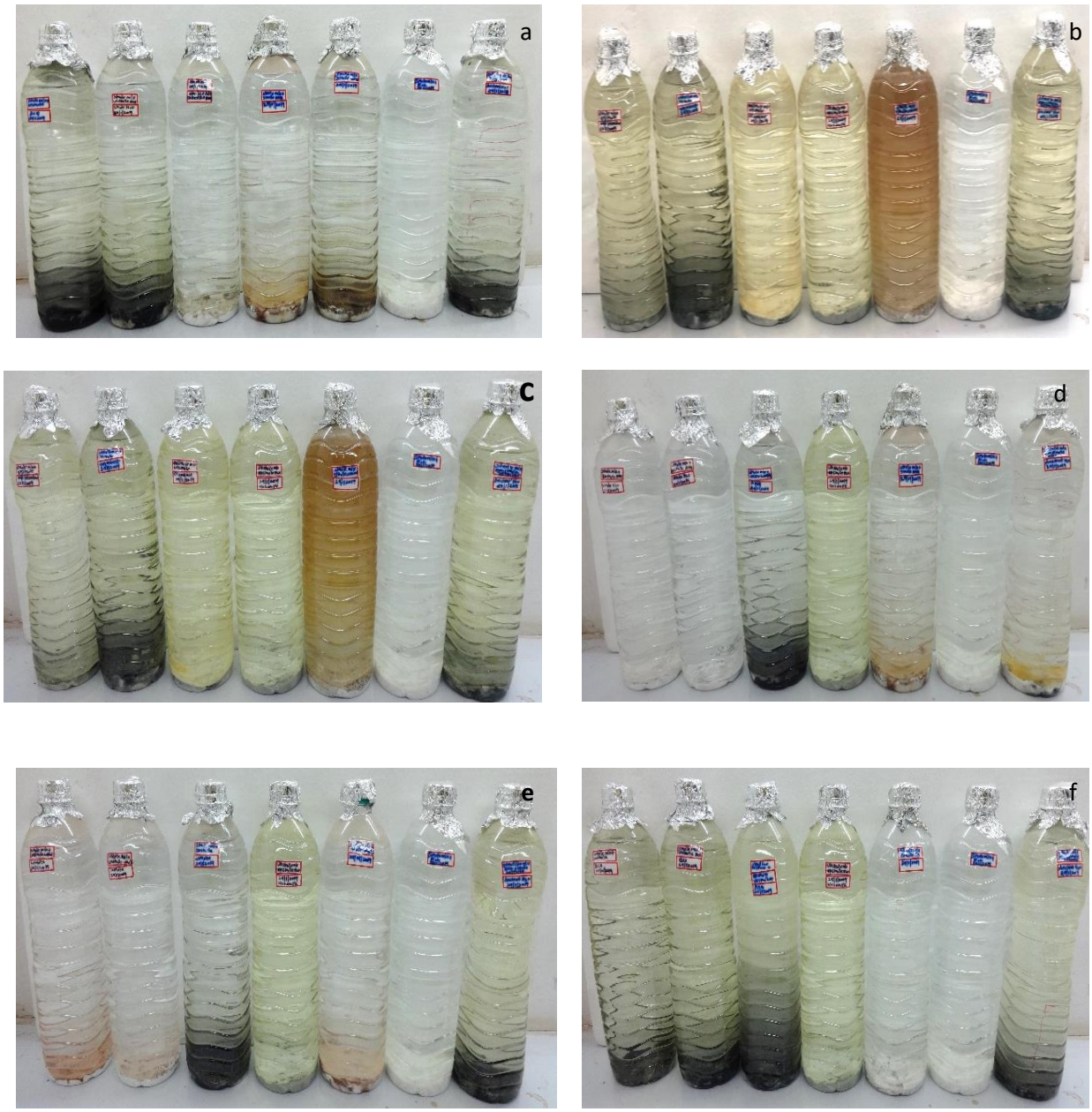

Figure 3.27 (a-f): Winogradsky column after several weeks after incubation and formation of Biofilms in different samples

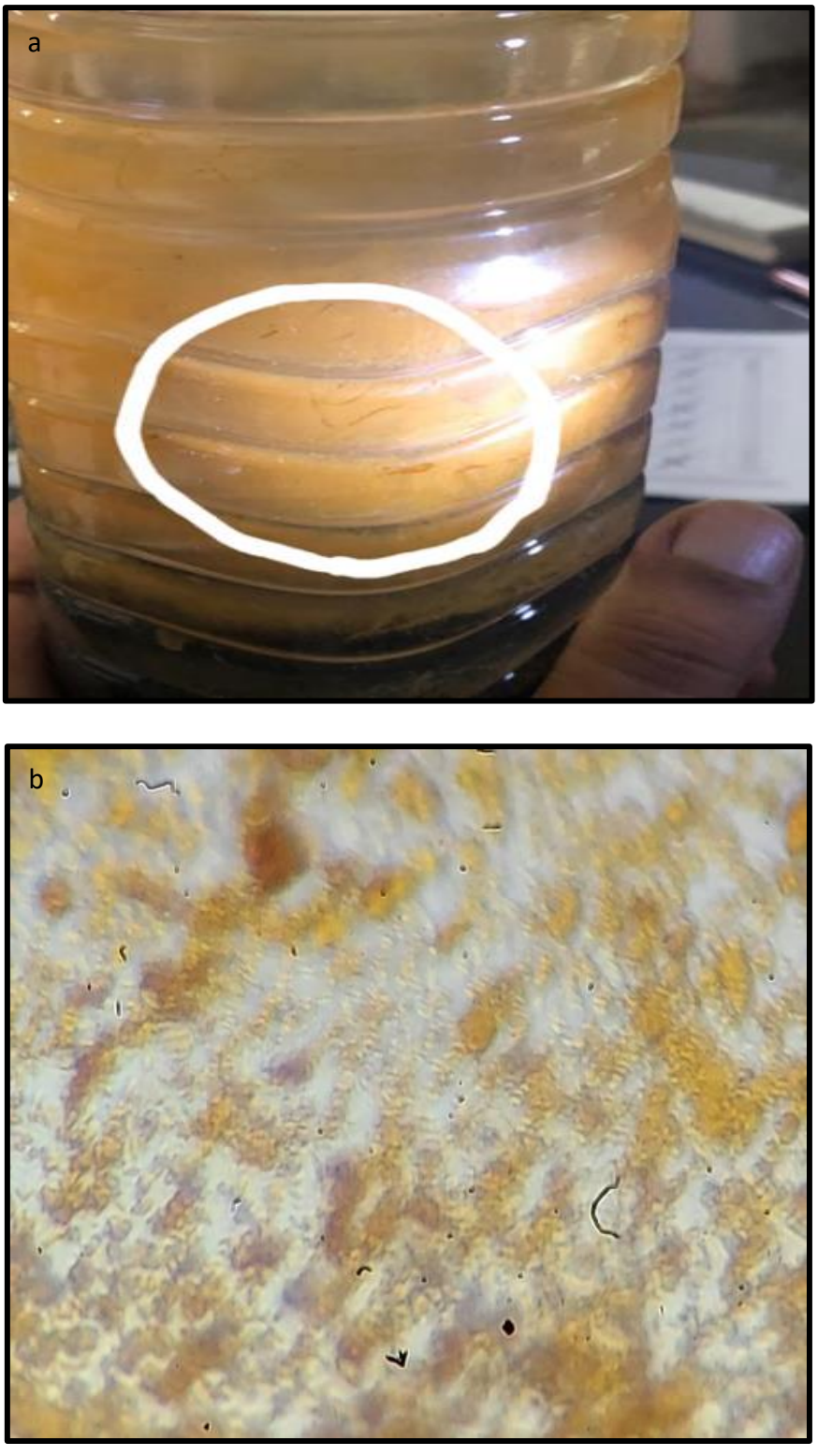

Figure 3.28 (a-b): a-Differential colonization of biofilms of Iron and Sulphur bacteria; Micromorphology of the marked zone

Table 3.13: Differential colonization of biofilms of Iron and Sulphur bacteria

Sample designation	Sterile mixture	Sterile mixture + sterile sample	Sterile mixture + Non-sterile sample	Non-sterile mixture + Sterile water
BHQ-WC	-	-	+ +	++
BMQ-WC	-	-	++	++
LGIO-WC	-	-	+++	+++
L-WC	-	-	+++	+++
V-WC	-	-	+++	+++
SS-WC	-	-	++	++

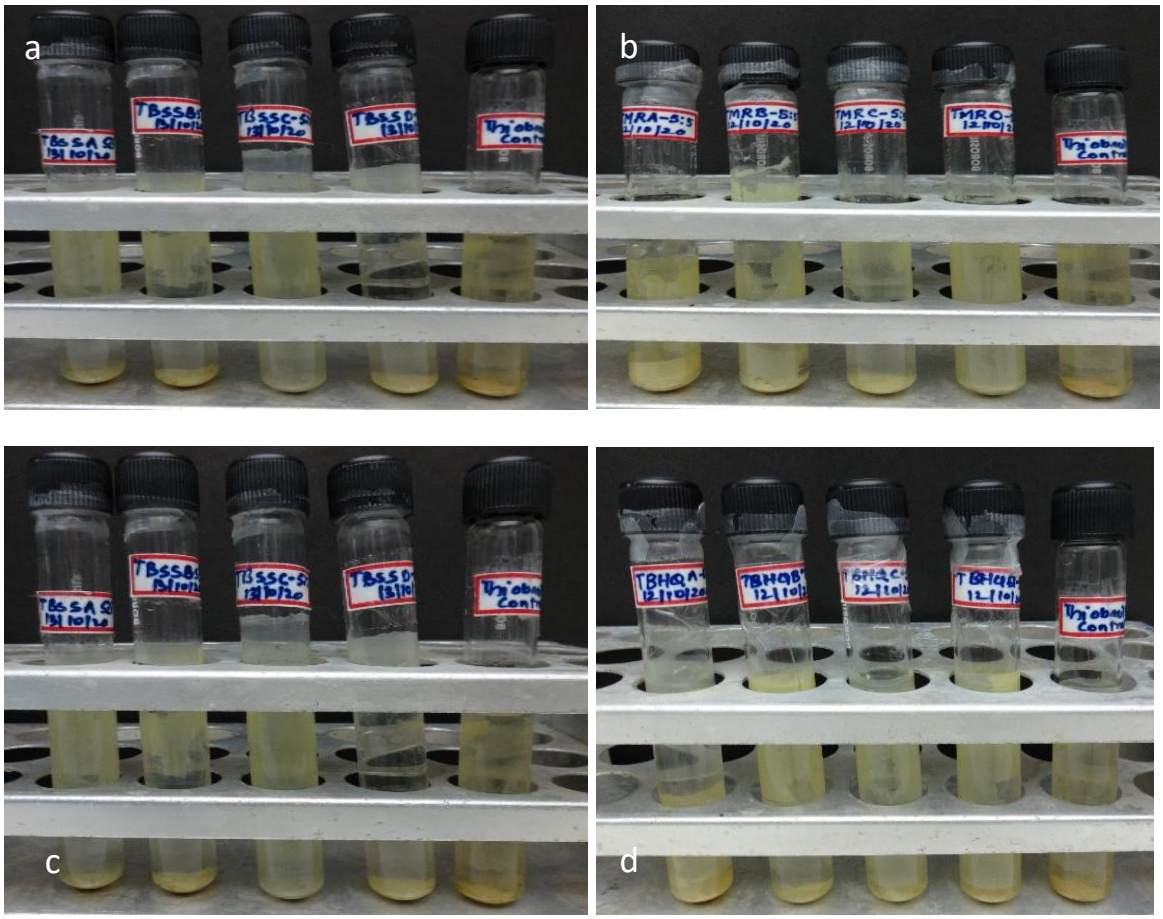

Figure 3.29 (a-d): Enrichment cultures on specific isolation media

3.9.4. Microscopic studies of the bacteria cultures

We were successful in obtaining pure cultures tentatively identified as *Acidithiobacillus ferrooxidans, Leptospirillum* and *Sulfobacillus.*

3.9.4.1. *Acidithiobacillus ferrooxidans*

Acidithiobacillus obtain their energy through the oxidation of ferrous to ferric iron or through the reduction of inorganic sulphur compound to sulfate. It was found that this culture was able to show biofilm formation as seen in **Fig 2.30 (a-d).** The Gram negative, rod shape bacteria can be seen in **Fig 2.30 (i-l).** Culture was found to be showing characteristic polymorphic colony margin showing fractal characteristic.

3.9.4.2. *Leptospirillum*

Leptospirillum cells were found to be Gram-negative and spiral-shaped. Metabolically they are strictly chemolithoautotrophic, fixing carbon using ferrous iron as their electron donor and oxygen as the electron acceptor. Cultures was found to be showing ccharacteristics polymorphic colony margin showing fractal characteristic of motile cells. Because of this, they are some of the most metabolically-restricted organisms known. Spiral cells of *Leptospirillum* were observed as seen in **Fig 3.31 (i-l) and Fig 3.31 (m-p).**

3.9.4.3. *Sulfobacillus*

This culture was found to be gram positive showing cream color colonies on a 9K medium **(Fig 3.32).**

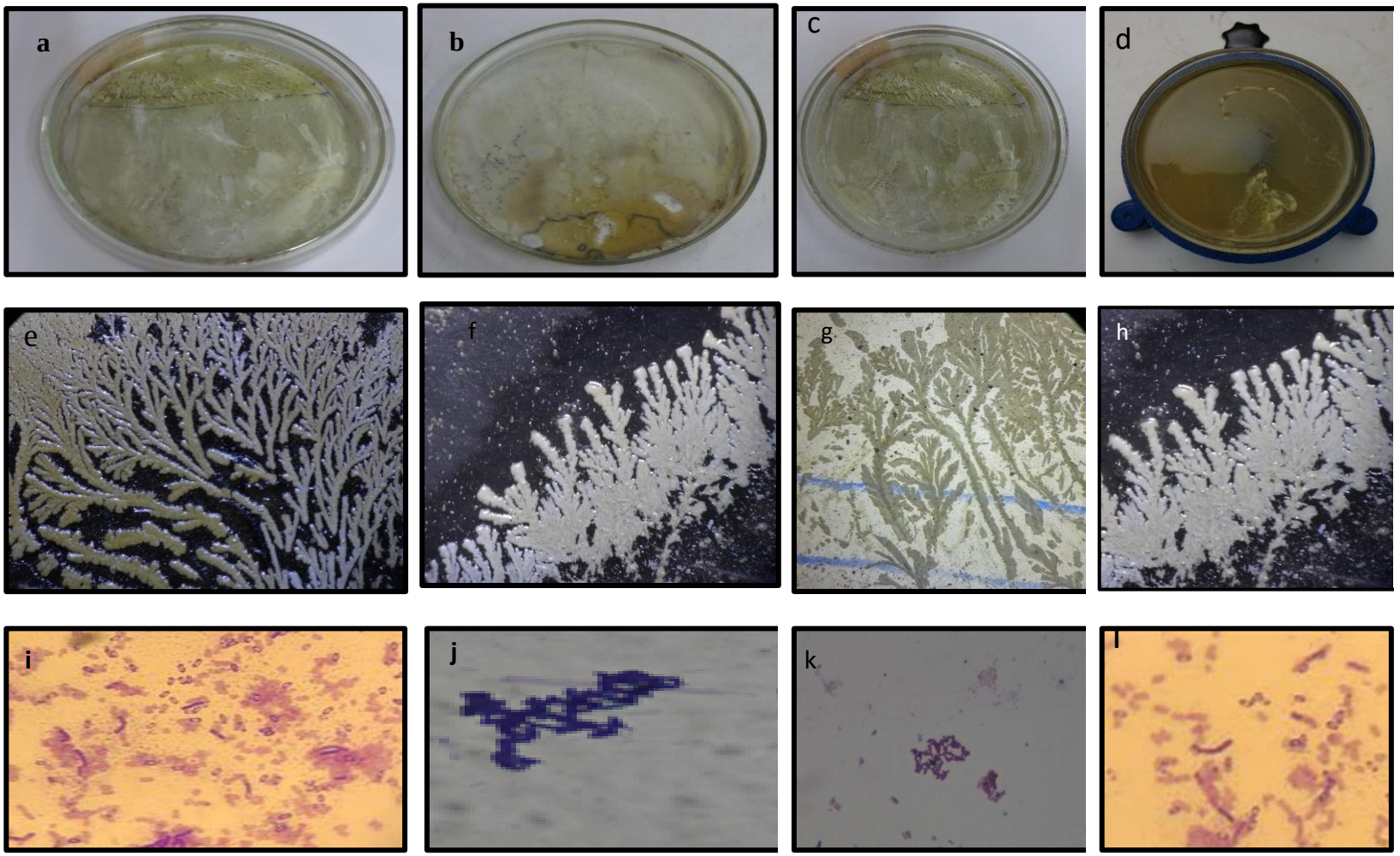

Figure 3.30 (a-l): a-d: Representative plate of *Acidithiobacillus* culture, e-h: Characteristic polymorphic colony margin showing fractal characteristic of motile cells of *Acidithiobacillus* spp. Culture (16 x magnification) e-h: Rod shaped cells of *Acidithiobacillus* (1000x); i-l: Rod shaped morphology of the culture

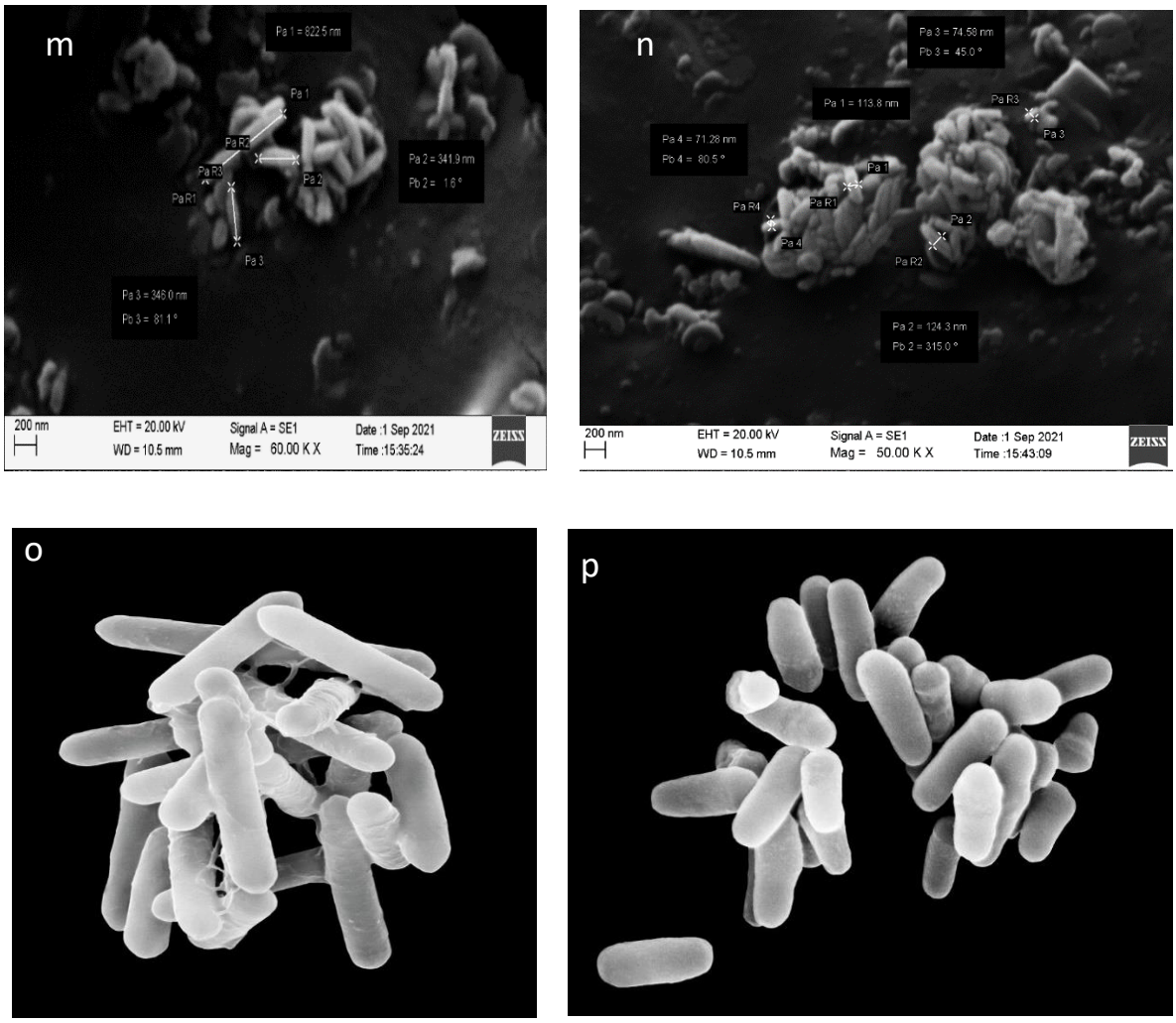

Figure 3.30 (m-p): m-n: Rod shaped cells of *Acidithiobacillus* (50,000x); O-p: Rod shaped morphology of the culture (4X of m and n)

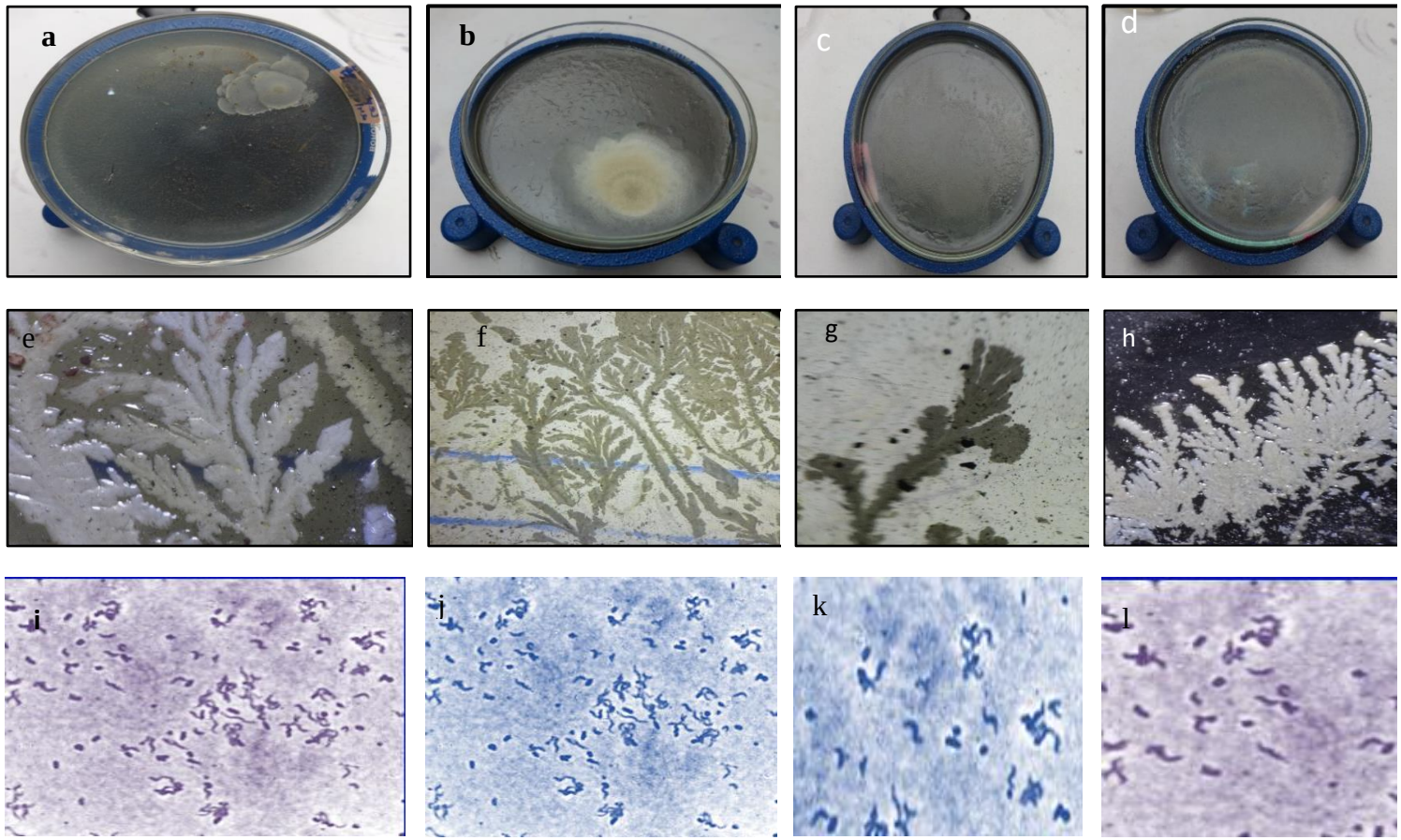

Figure 3.31 (a-l): a-d: Representative plate of *Leptospirillum* culture, e-h: Characteristic polymorphic colony margin showing fractal characteristic of motile cells of *Leptospirillum* Culture (16 x magnification) e-h: Rod shaped cells of *Leptospirillum* (1000x); i-l: Spiral cell shaped morphology of the culture

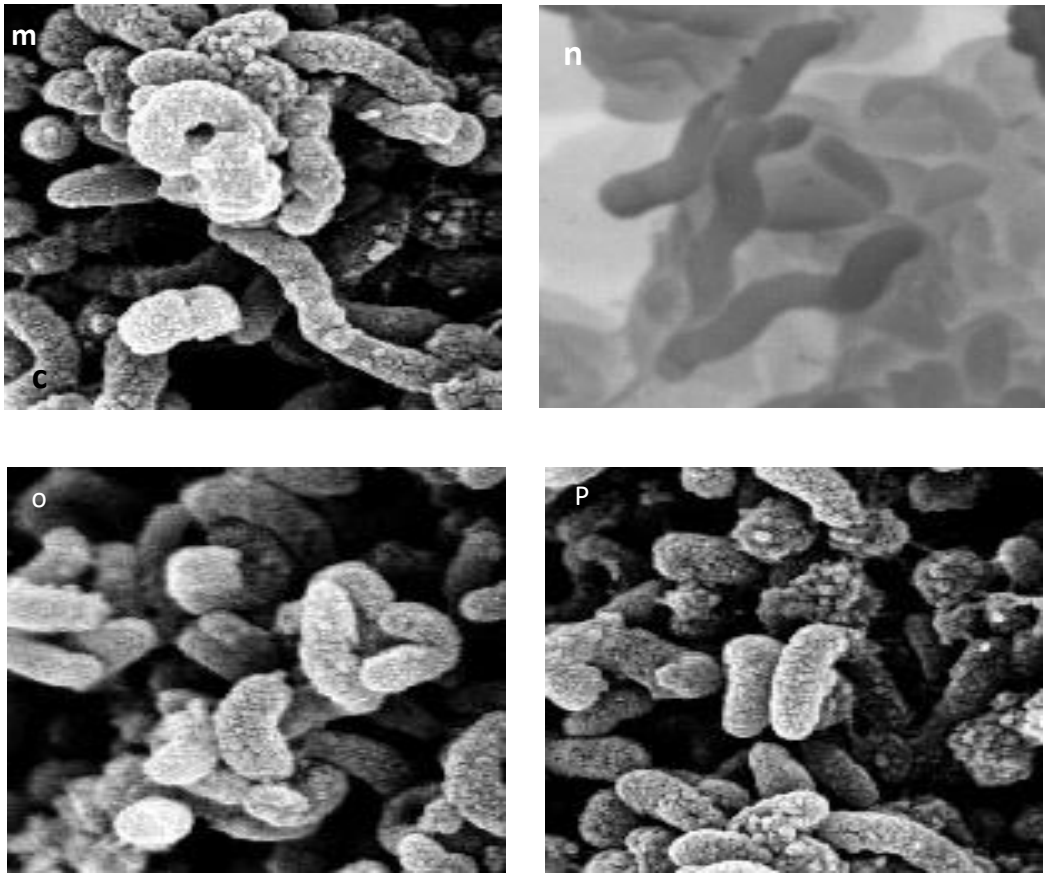

Figure 3.31 (m-p): Spiral shaped cells of *Leptospirillum* (50,000x)

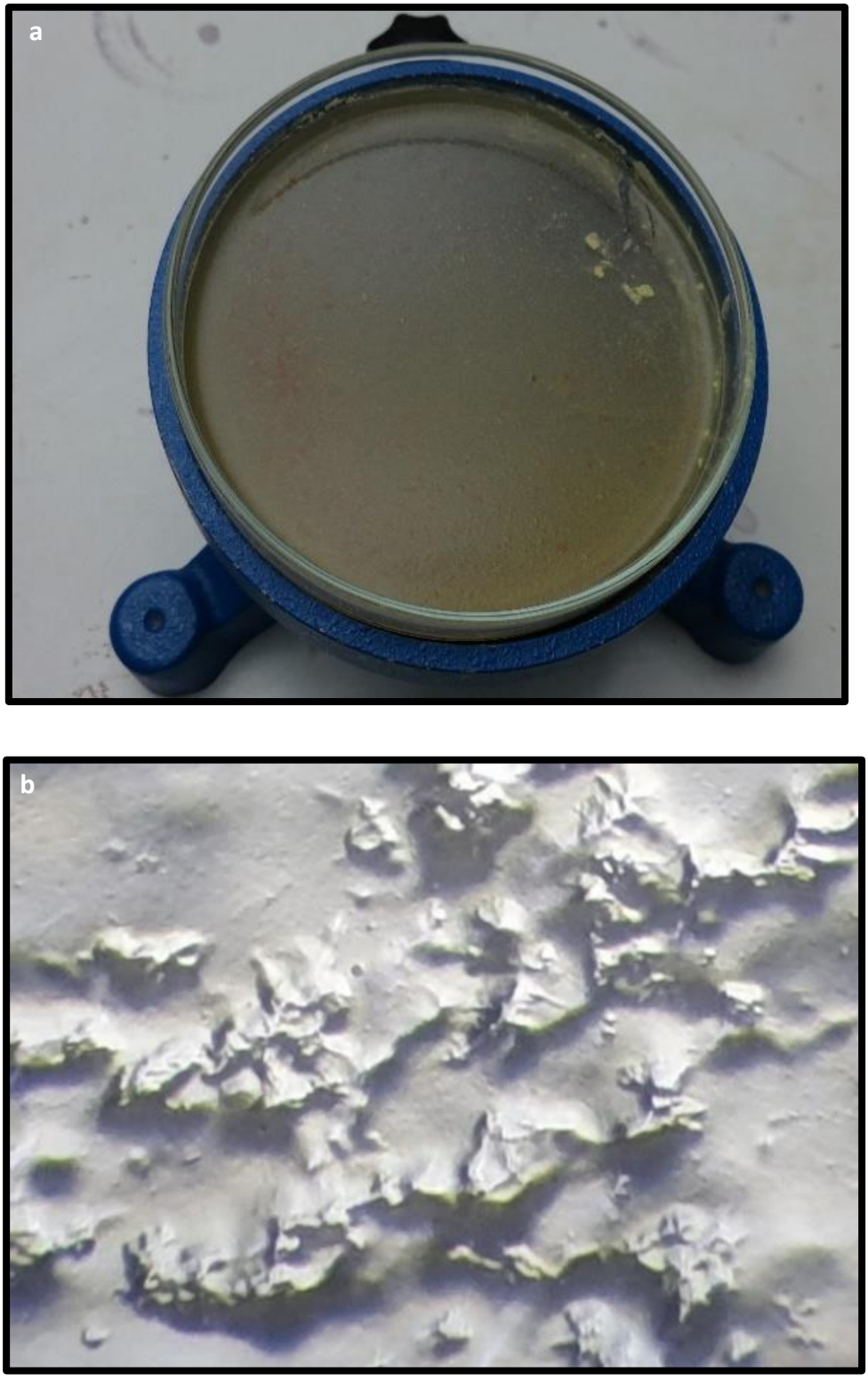

Figure 3.32 (a-b): a-*Sulfobacillus* culture growing on acidophilic medium; b-Colony of *Sulfobacillus*

3.10. Isolation of actinobacterial cultures

3.10.1. Colonization

The microbial colonization microcosm set up is shown in **Fig 3.33.** Successful colonization of actinobacterial species was observed as shown in the **Fig 3.34 (a-f).** The microorganisms yielded colonized slides showing excellent colonization by actinobacteria after 2 days. It showed successful increase in colonization on 4th day. On 7th day after incubation heavy colonization by *Streptomyces* species was noticed. very scanty competition from other members of microbial community such as eubacteria and fungi were seen. In all 7 distinct morpho types were identified.

3.10.2. Isolation

Isolation of actinobacterial was carried out and total 30 isolates were obtained. The isolated strains were classified into various genera based on the spore morphology and mycelium. The list of Actinobacterial cultures isolated from auriferous samples is given in the **Table 3.14**.

3.10.3. Macroscopic colony characters

The colonies grown on oat meal agar showed a flat and hard texture. The aeriel mycelial showed abundant growth after 10 days of incubation which were cream in colour. The isolates obatined on the Oat meal agar is shown in the **Fig 3.35 (a-h).** The microscopic character showed the presence of vegetative hyphae and spore chains are spiral. The morphological characters are shown in the **Fig 3.36 (a-h).** BSSA-01 Family: *Streptomycetes*, Genus: *Streptomyces* spp. Out of the 30 actinobacterial isolates, 12 isolates were tentatively identified as genus *Streptomyces* (spore chain with coiling, spiral and looped), 10 isolates as *Nocardia* and 10 were unidentified actinobacterial strains as shown in **Table 3.15**.

Among the genera recorded in the present study, *Streptomyces* was the most predominant as compared to others in all the samples as shown in the **Fig 3.37**. The dominance of *Streptomyces* among the actinobacteria especially in soils has also been reported earlier (Velho-Pereira and Kamat, 2011). Such fertile samples can be thus used for the isolation of micro-organisms, which can be further used in nanoparticle synthesis and biotechnology.

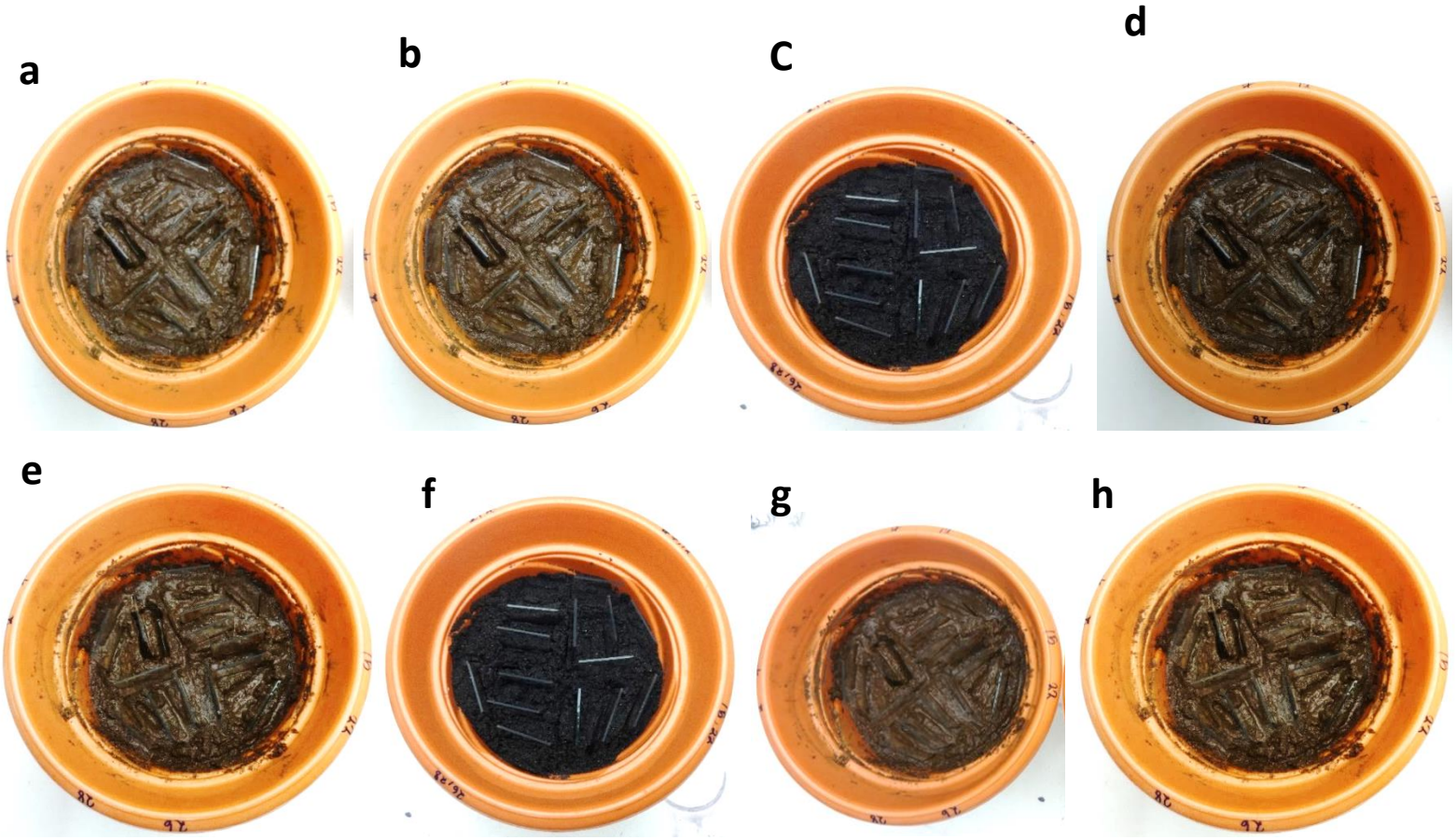

Figure 3.33(a-h): Microcosm set up for isolation of Actinobacteria

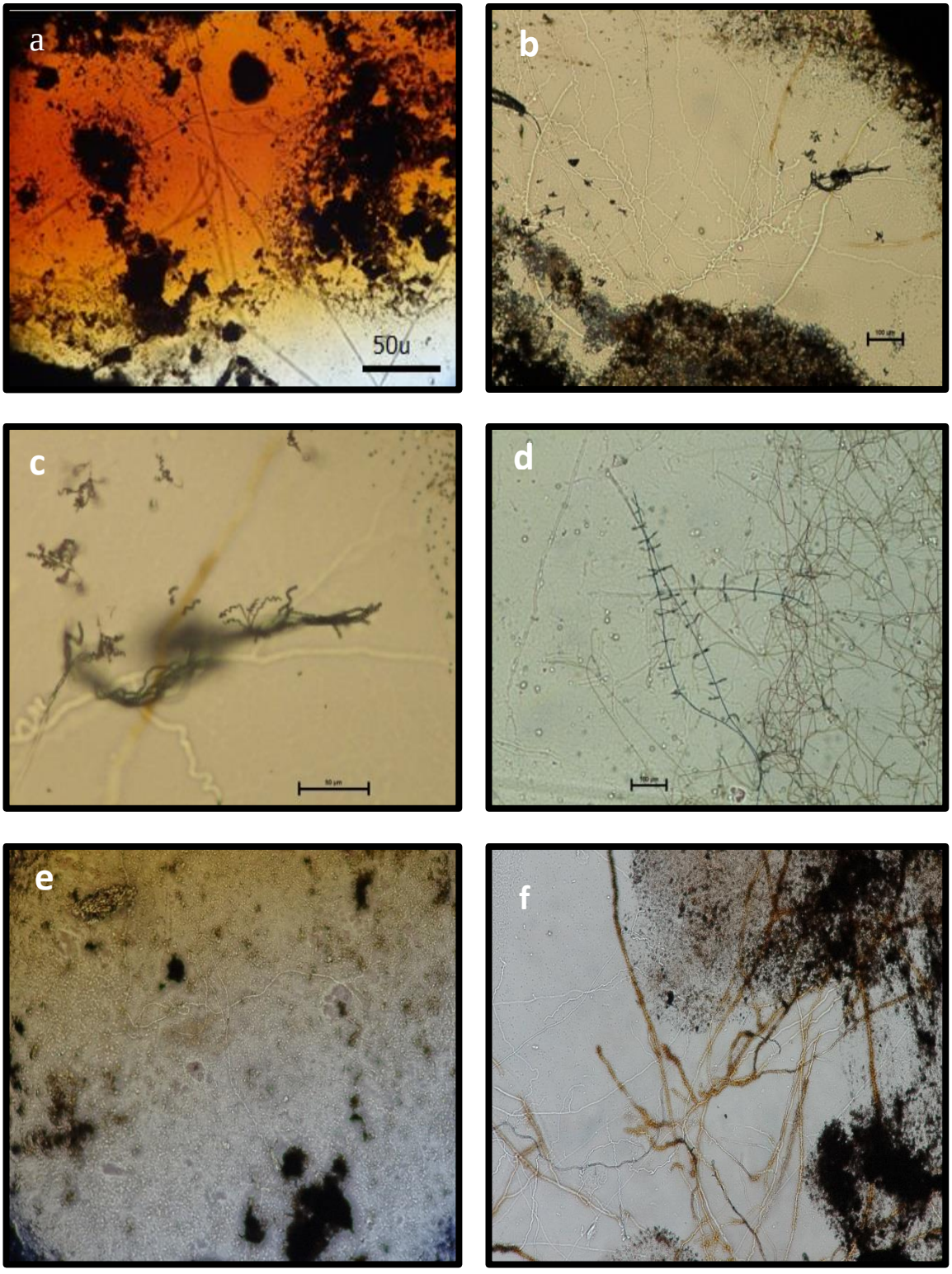

Figure 3.34 (a-f): *Streptomyces* colonies from auriferous samples (scale: 50µm)

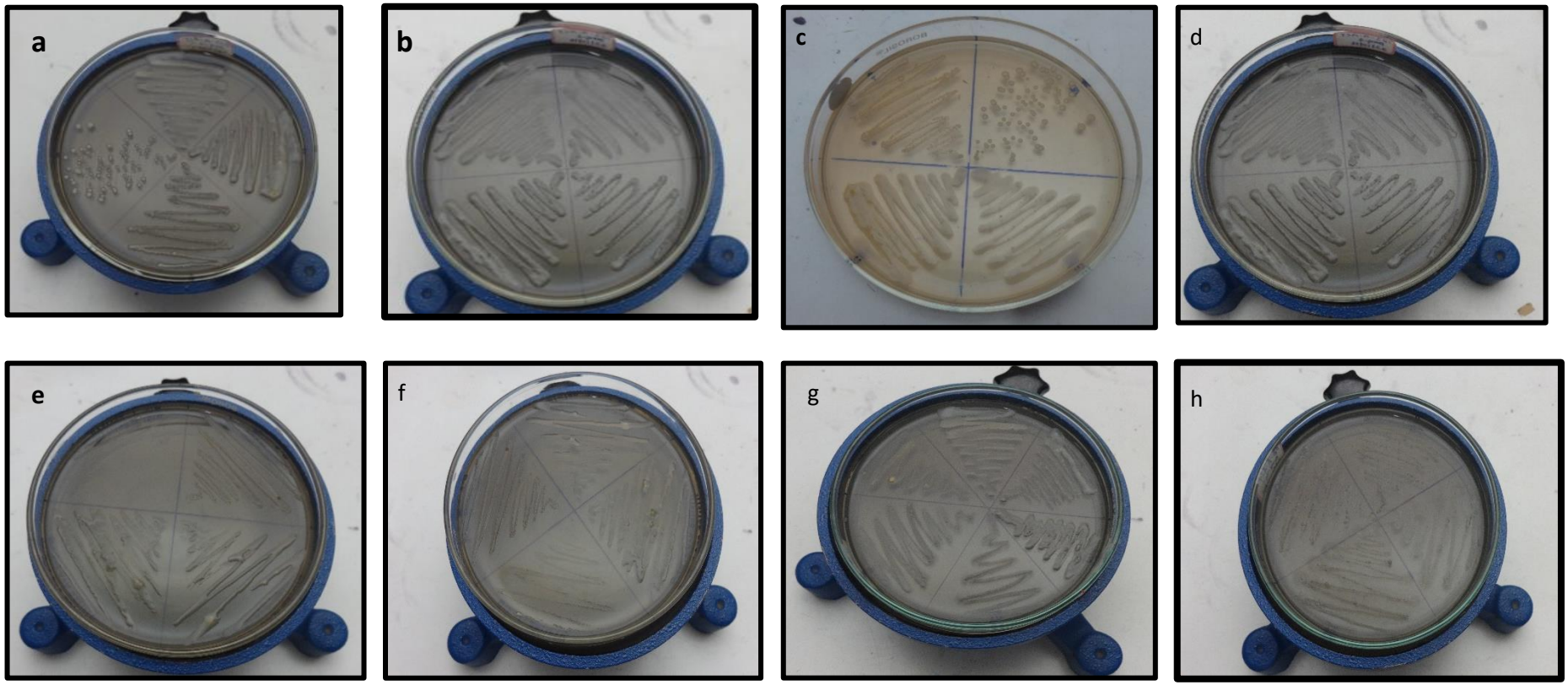

Figure 3.35 (a-h): Actinobacterial colonies on OMA

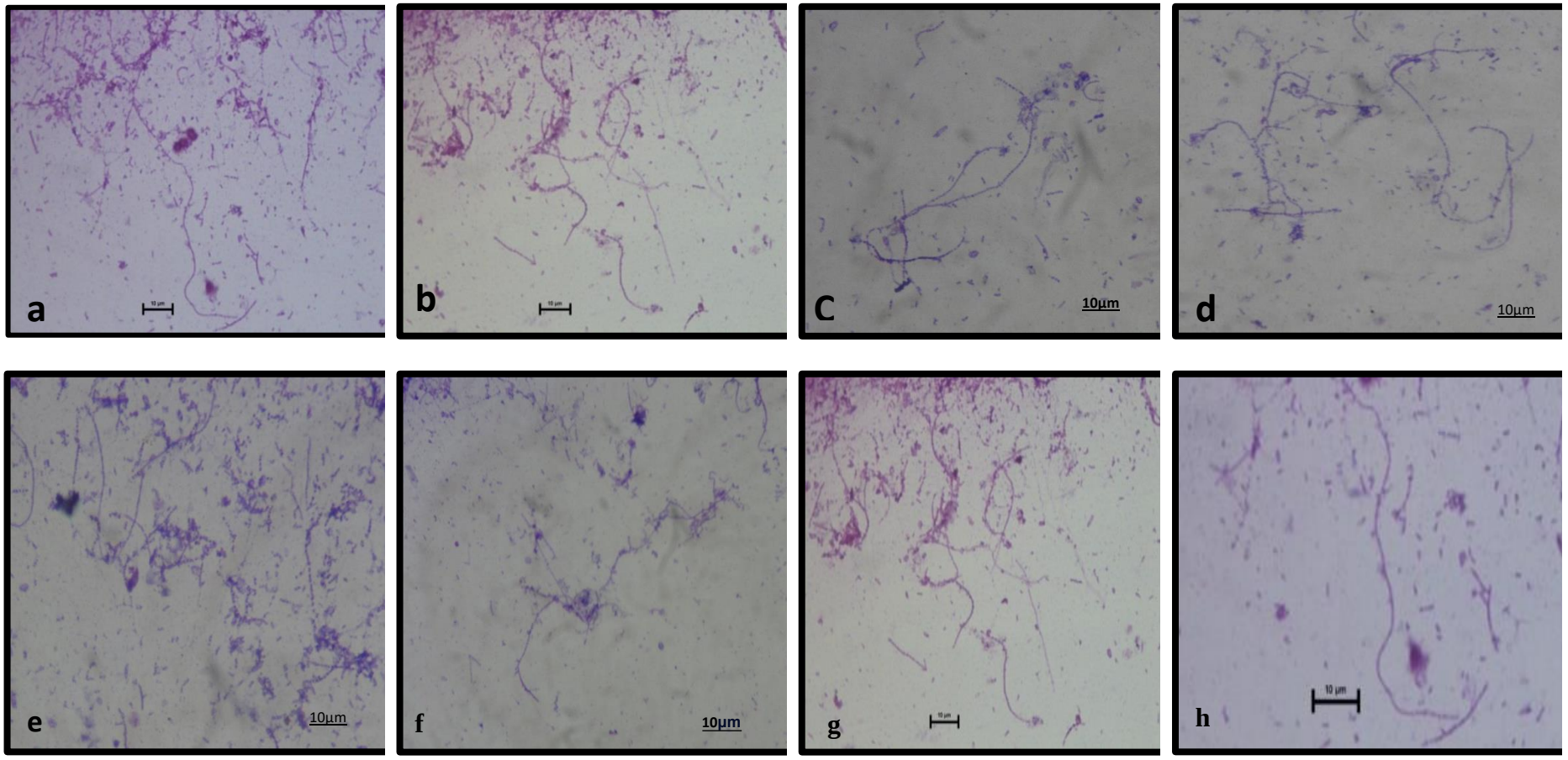

Figure 3.36 (a-h): The micromorphological characteristics of *Streptomyces* spp. (Scale 10µm)

Table 3.14: Actinobacterial cultures from auriferous samples

Source	Sample Designation	No of actinobacterial Isolates
Stream Sediments	**BSSA**	**9**
Stream sediments	**TSSA**	**10**
Sediment	**PDA**	**6**
Placer deposits	**MRA**	**5**

Table 3.15: Tentative identification of Actinobacteria

Total no of actinobacterial isolates	Tentative identification of Actinobacteria		
	Streptomyces	***Nocardia***	**Unidentified**
9	**6**	**2**	**3**
10	**2**	**5**	**3**
6	**3**	**1**	**2**
5	**1**	**2**	**2**

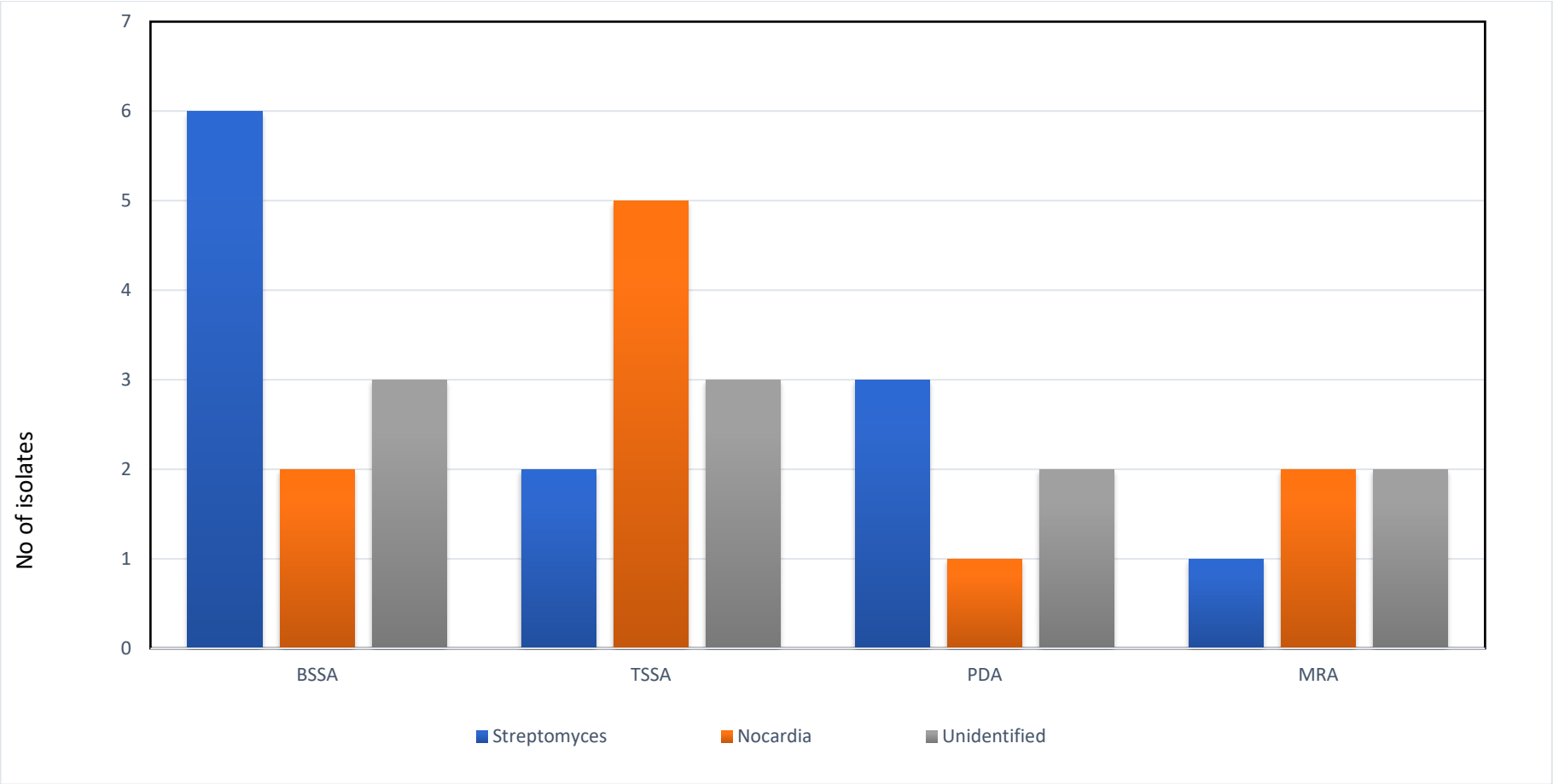

Figure 3.37: Actinobacterial isolates from auriferous samples

3.11. Sampling of wild *Termitomyces* mushrooms

3.11.1. Diversity and taxonomy

In all approx. 400-500 specimens were collected. These comprised approx. 300 from field sampling locations and approx. 200 from five market.

3.11.2. Pure cultures of *Termitomyces heimii* and *Termitomyces clypeatus*

In all from 10 explants about 1−2 explants per species yielded healthy colonies leading to isolation of 10 cultures (**Table 3.16**). From these 5 cultures were found to be growing rapidly and 5 showed slow growth. *Termitomyces* cultures exhibited strictly filamentous colonies indicating typical hyphal morphology and branching patterns. A few strains showed partially mycelial but largely farinaceous or powdery colonies indicating mitosporic structures. However, for present study only rapidly growing cultures with filamentous growth morphology, without forming any sporodochial masses / mitosporic structures were selected for further bioprocess and bioproduct studies. All isolates grew at temperature of 25− 30° C with satisfactory growth at 28^{o}C. All isolates showed purity when microscopically checked for presence of any contamination**.** All the isolates indicated excellent viability over a period of five years despite repeated subcultures.

3.11.2.2. Colony characteristic

On basis of consistently stable, strictly filamentous colony morphology only strains having rapid growth rate (4 mm / day or more) were only selected for screening. Total 2 *Termitomyces* species (*T. clypeatus, T. heimii*) and 5 corresponding cultures were studied for their macro and micromorphological colony characters as depicted in **Fig. 3.38.**

Table 3.16: Designation of pure *Termitomyces* cultures

Species	Cultural designation	Number of morphotypes (isolates)
T. clypeatus R. Heim	TCL1	**2**
T. heimii Natarajan	THE2	**3**

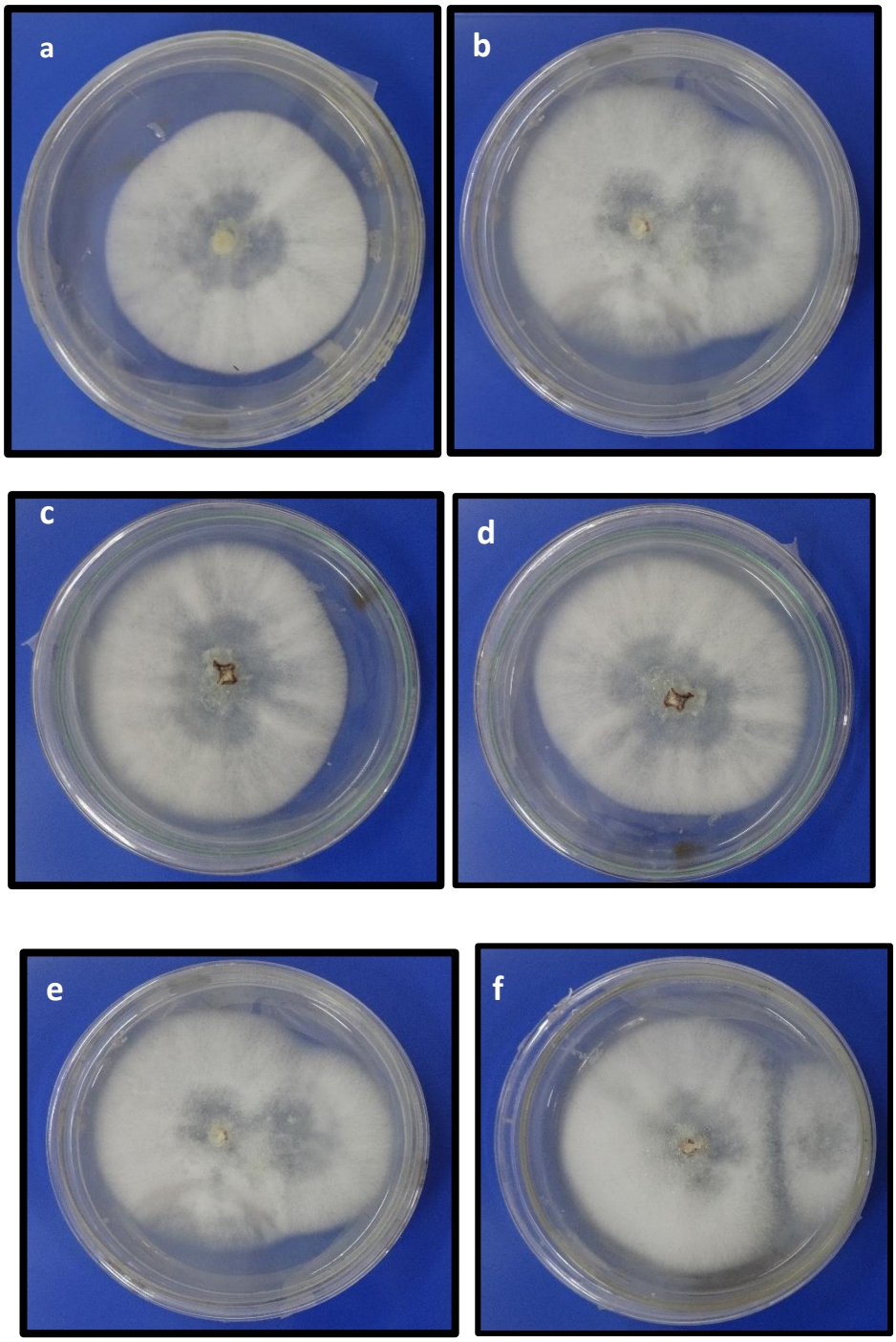

Figure 3.38 (a-f): Colony Morphology of *Termitomyces* cultures

3.12. Gold nanoparticle synthesis using Actinobacteria

3.12.1. Use of Actinobacterial cultures for synthesis of GNPs

In the present study the actinobacterial cultures were treated with $AuHcl_4$ which produced GNps at RT. As the time interval and thermal treatment increased the production of the AuNPs increased and thermal treatment led to the production of a complexed assemblages of GNPs. Both monodispersed and polydispered type of nanoparticles were produced.

3.12.2.GNP synthesis and Effect of thermal treatment of GNP assemblies

45 sec thermal treatment showed most promising results. Cell Free Extract (CFE) showed good results compared to cell cultures. The results shows that a simple, glass slide based technique can be successfully used for rapid production, microscopic visualization, morphological analysis, study of swarming behavior and monitoring of effect of heat on Au NPs and Au MPs forms and assemblages using cell free microbial system. The results of the same are shown in **Fig 3.39.**

3.12.3. Testing of Aqua regia extracts (crude chloroauric acid) of promising auriferous materials to produce Putative GNPs

Crude extracts of $HAuCl_4$ prepared successfully as shown in **Fig 3.40 (a-b).** 5 sec thermal treatment showed most promising results. Isodimentric, monodispered as well as oceans of swarms particles of different sizes were produced **Fig 3.40 (c-f).**

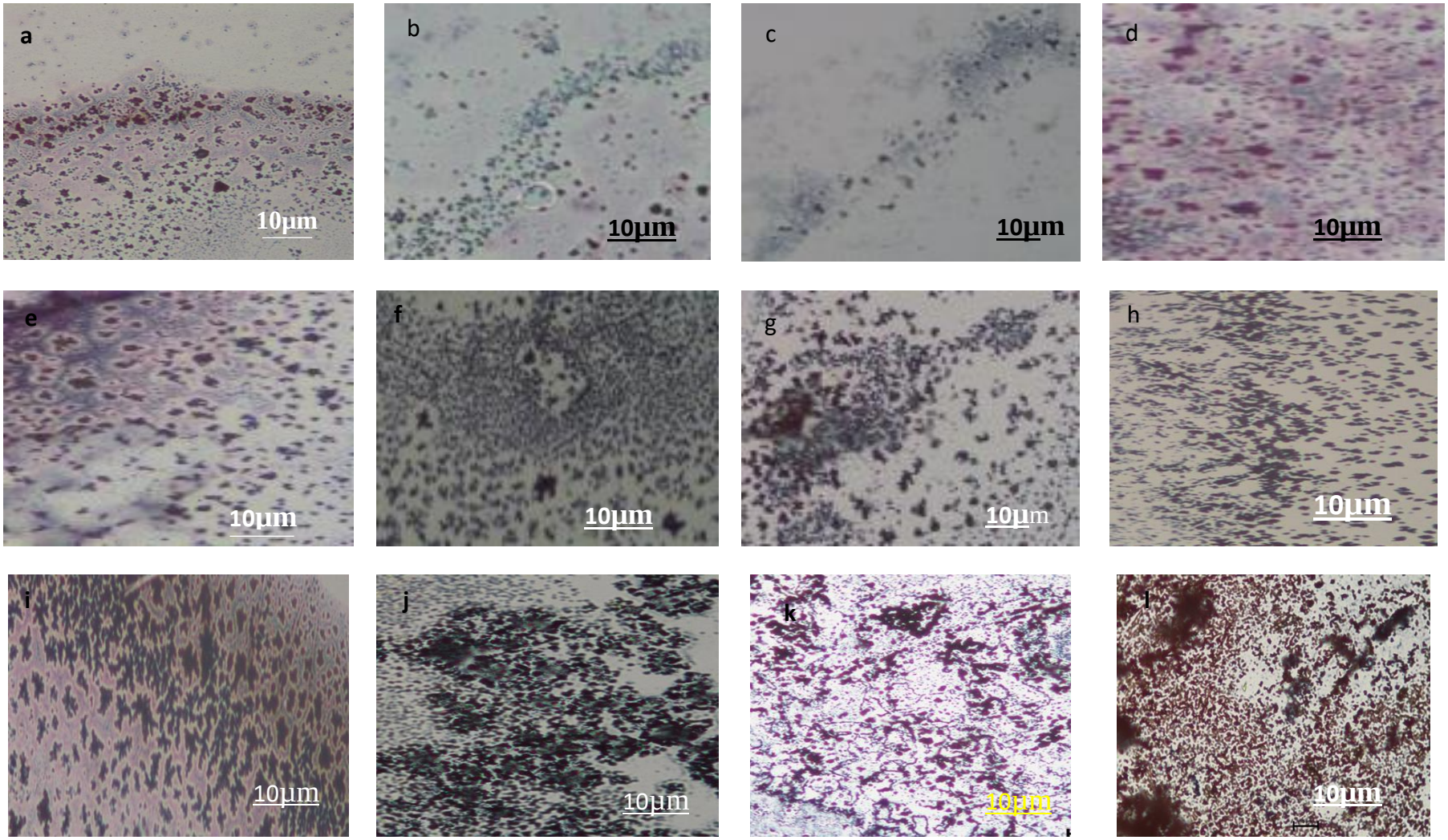

Figure 3.39 (a-l): Swarms of nanoparticles produced by Actinobacterial culture; Microscopic image Scale:10 µm

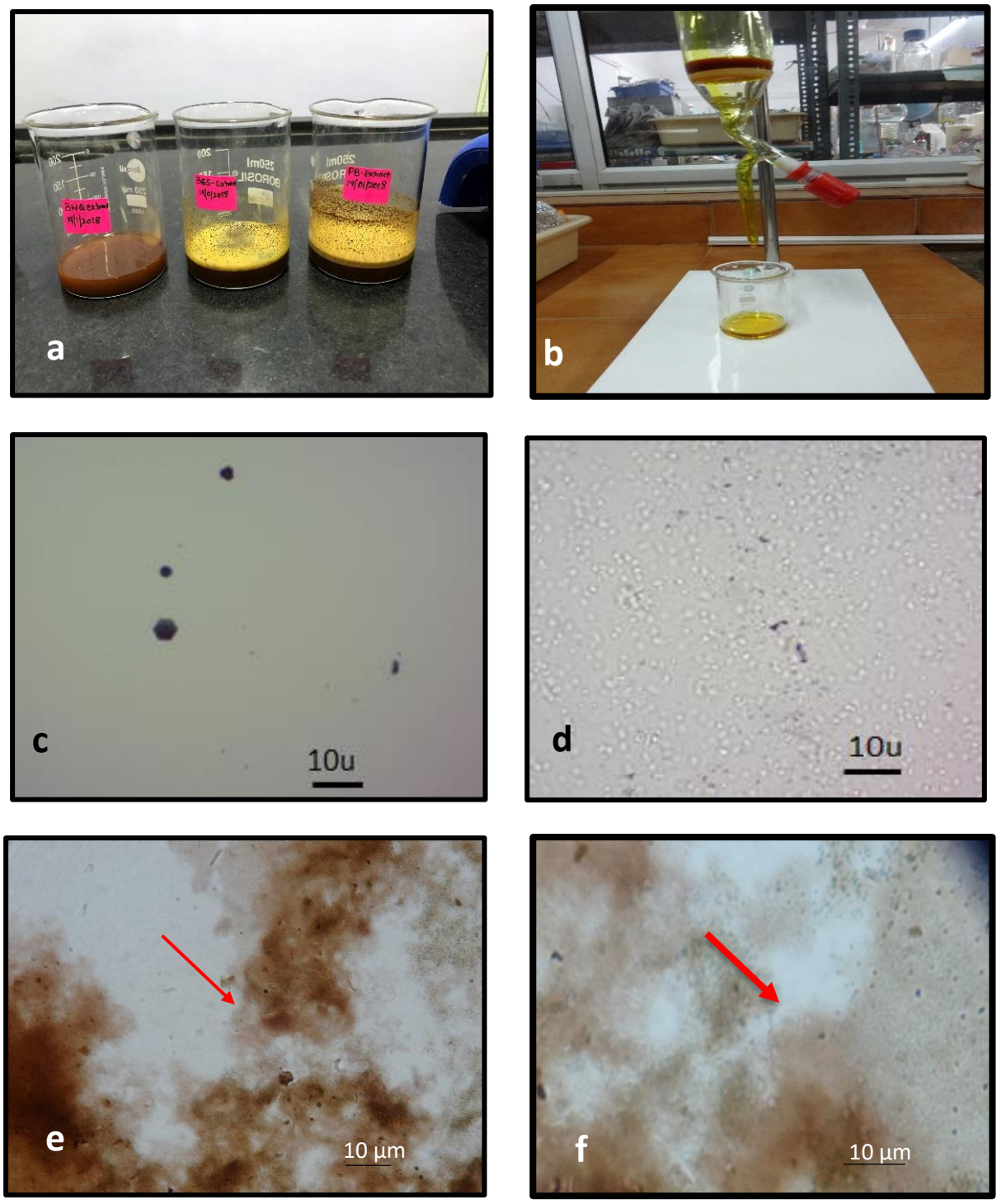

Figure 3.40 (a-f): a- Extracts of crude $HAuCl_4$; b-Clear extract; c-Monodispered AuNps; d- Particle swarms; e-Monodispersed AuNPs, f-Polydispersed AuNPs

3.14. AuNPs synthesis using *Termitomyces* spp

Synthesis of nanoparticles using edible and medicinal mushrooms has emerged as an interesting field of research as these macrofungi act as eco-friendly biofactories, they secrete enzymes essential for reduction of metal ions into their zerovalent or nano-form. Apart from being an environmentally friendly, the nanoparticles synthesized using mushrooms exhibit higher stability, longer shelf life and enhanced biological activities.

3.14.1.GNP synthesis using extracts of *Termitomyces heimii* and *Termitomyces clypeatus*

Micro test well plate was used to produce nanoparticles using fungal tissues as shown in **Fig 3.42** and **Fig 3.43.** It was found that all body parts of the mushrooms were producing GNPs. Swarms were produced. Umbonal tissue produced autonomous swarms, self-recognition, identical, monodispersed GNPs. They were found to be producing islands and were rotating to get stable state. Other body parts of the mushrooms also successfully produced GNPs. *Termitomyces clypeatus* paste prepared by using mortar and pestle in order to prepare extracts. Extracts and chloroauric acid in equal concentration produced nanoparticles. The purple colour change indicates the production of nanoparticles as seen in **Fig 3.43** and **Fig 3.43.** It was found that stipe was showing most promising results in case of both tissue and SWSE. CIE chromaticity values ranged from L (16-75), a (3-33) and b (1-46) thus indicating the lightness from black to white, green to red and blue to yellow. Choma values ranged from 4 to 47 and hue values from 40 to 199 indicating the strength or dominance of the hue, the quality of a color's purity, intensity or saturation (http://www.huevaluechroma.com/018.php). Same is presented in the **Fig 3.46.**

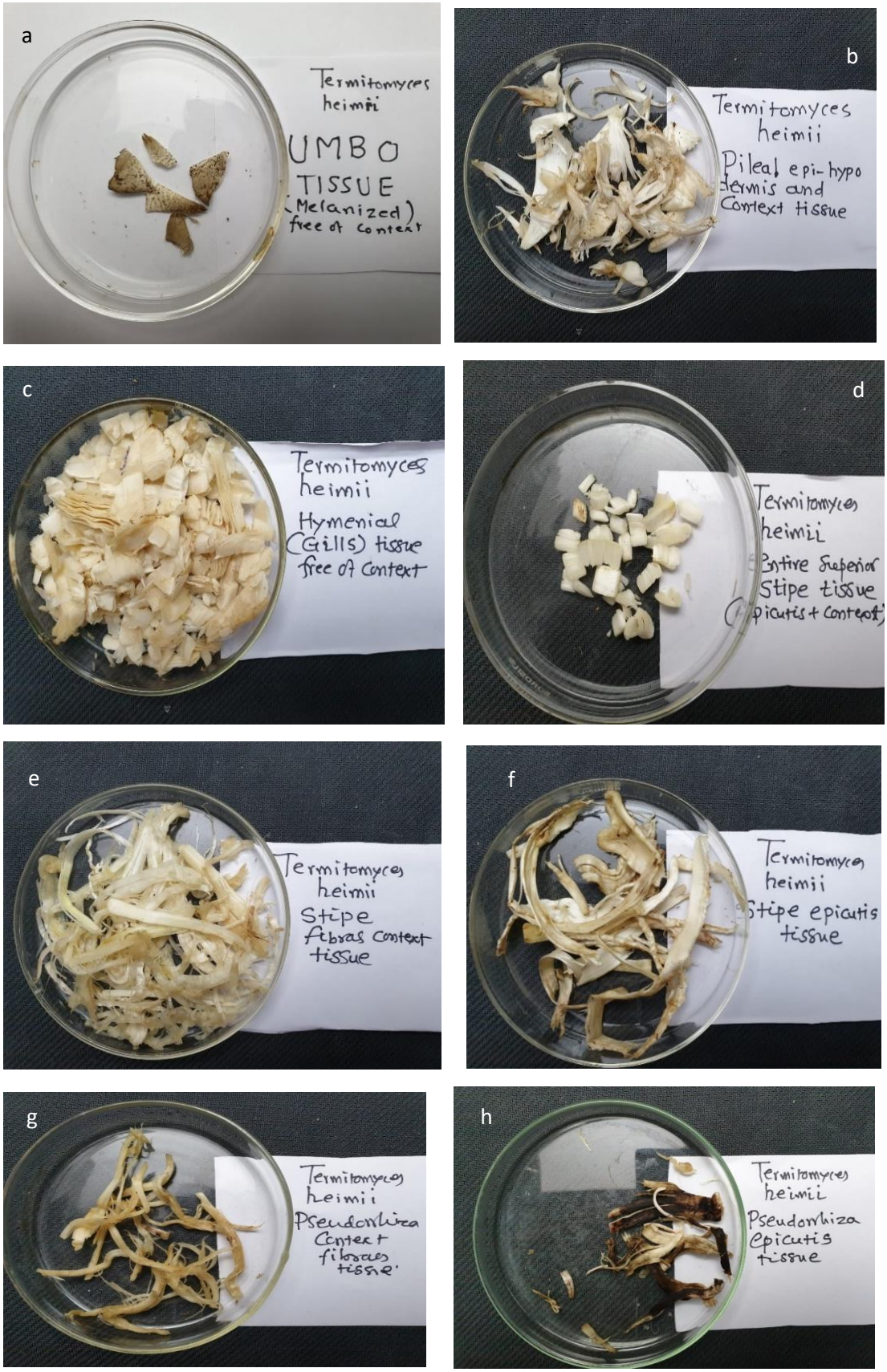

Figure 3.41 (a-h): Mushroom tissues used for GNP synthesis

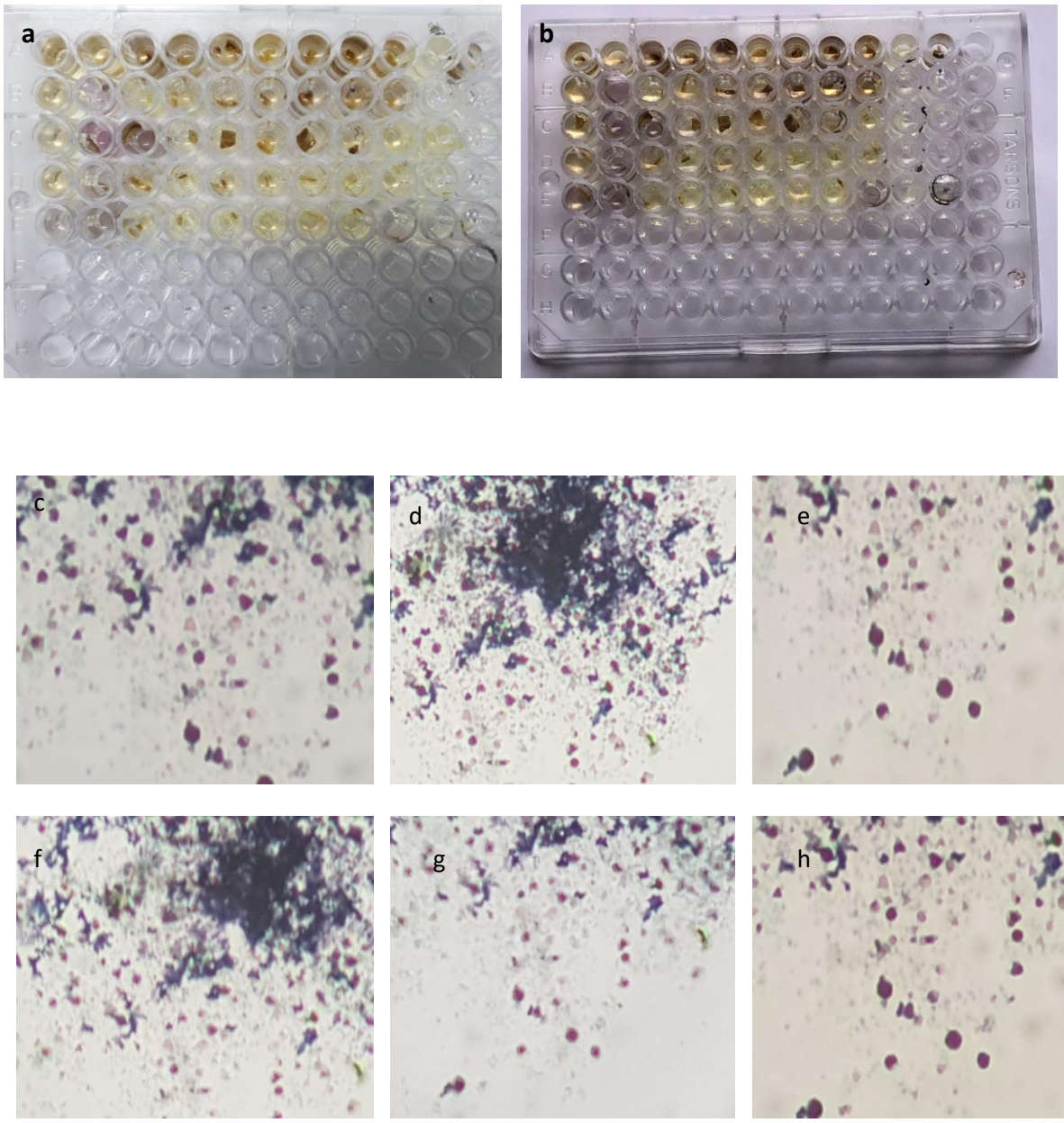

Figure 3.42 (a-h): a-Positive bioreduction obtained with homogenized tissues of *Termitomyces heimii* as indicated by color changes; b-Positive bioreduction using crude extract of chloroauric acid, yellow is control; c-h: GNPs swarms (X 6000)

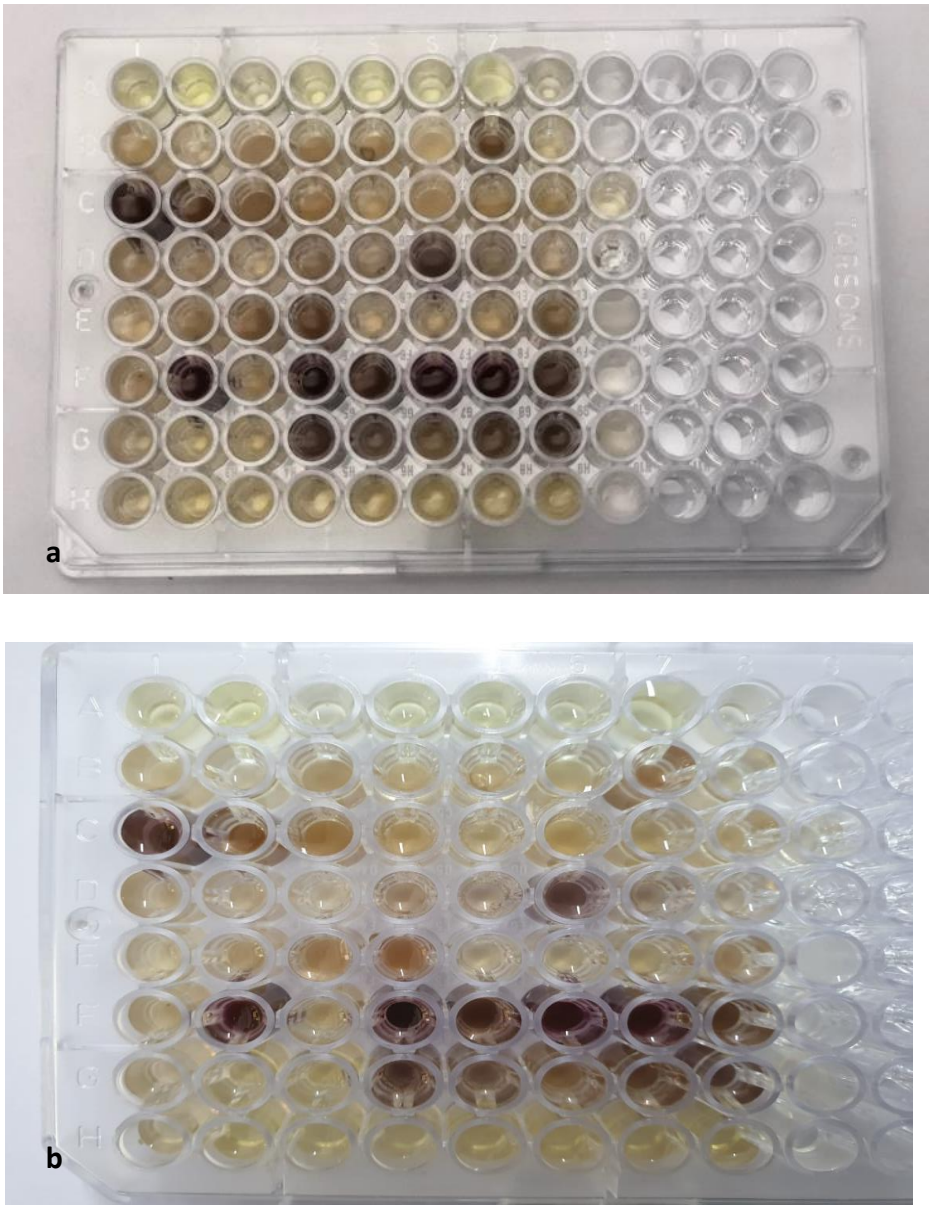

Figure 3.43 (a-b): a, b-Positive bioreduction with cell free membrane filtered SWSE and crude extracts of chloroauric acid

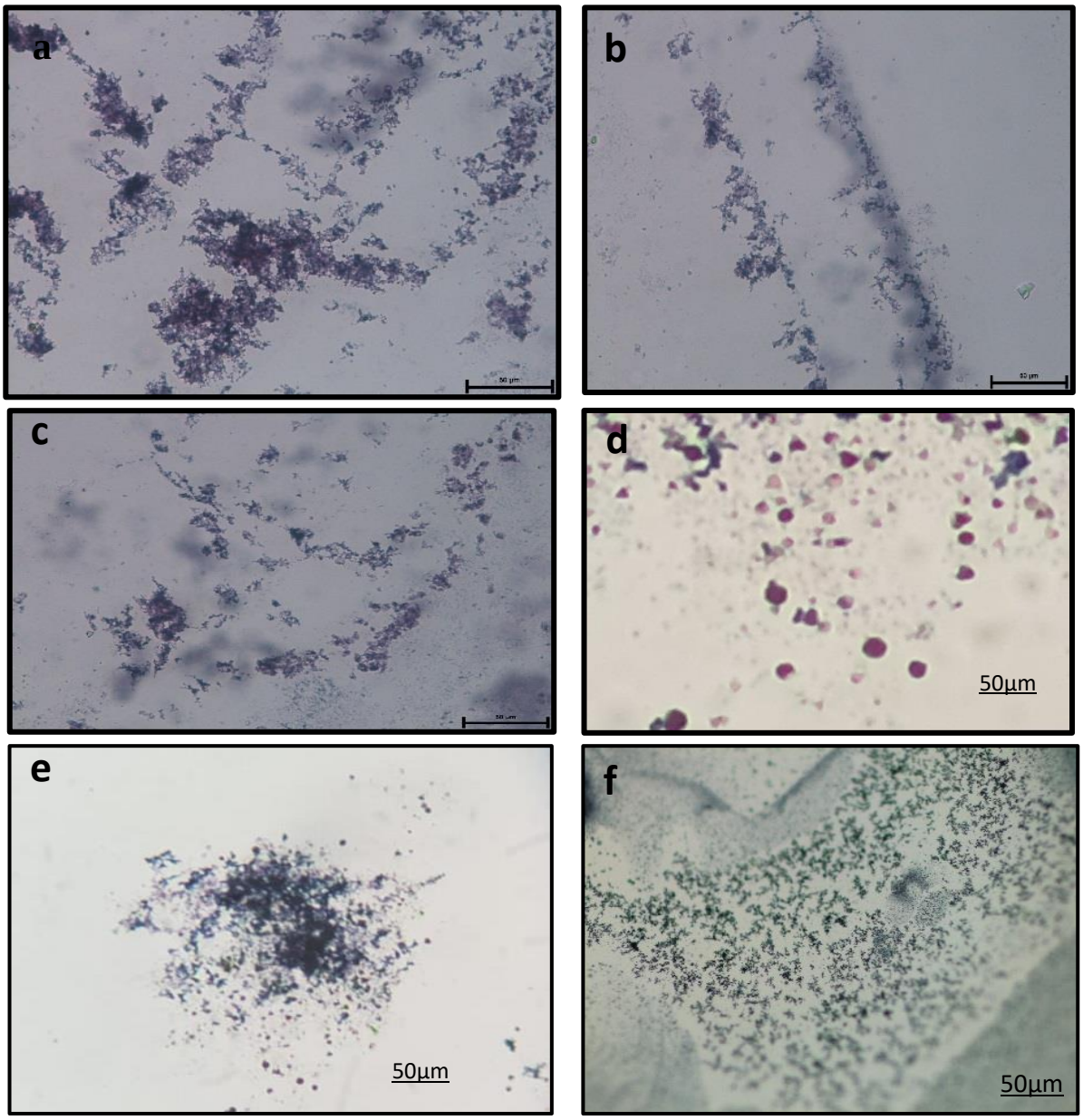

Figure 3.44: (a-f): Microscopic characterization of GNP swarms produced using extracts and chloroauric acid (X 6000)

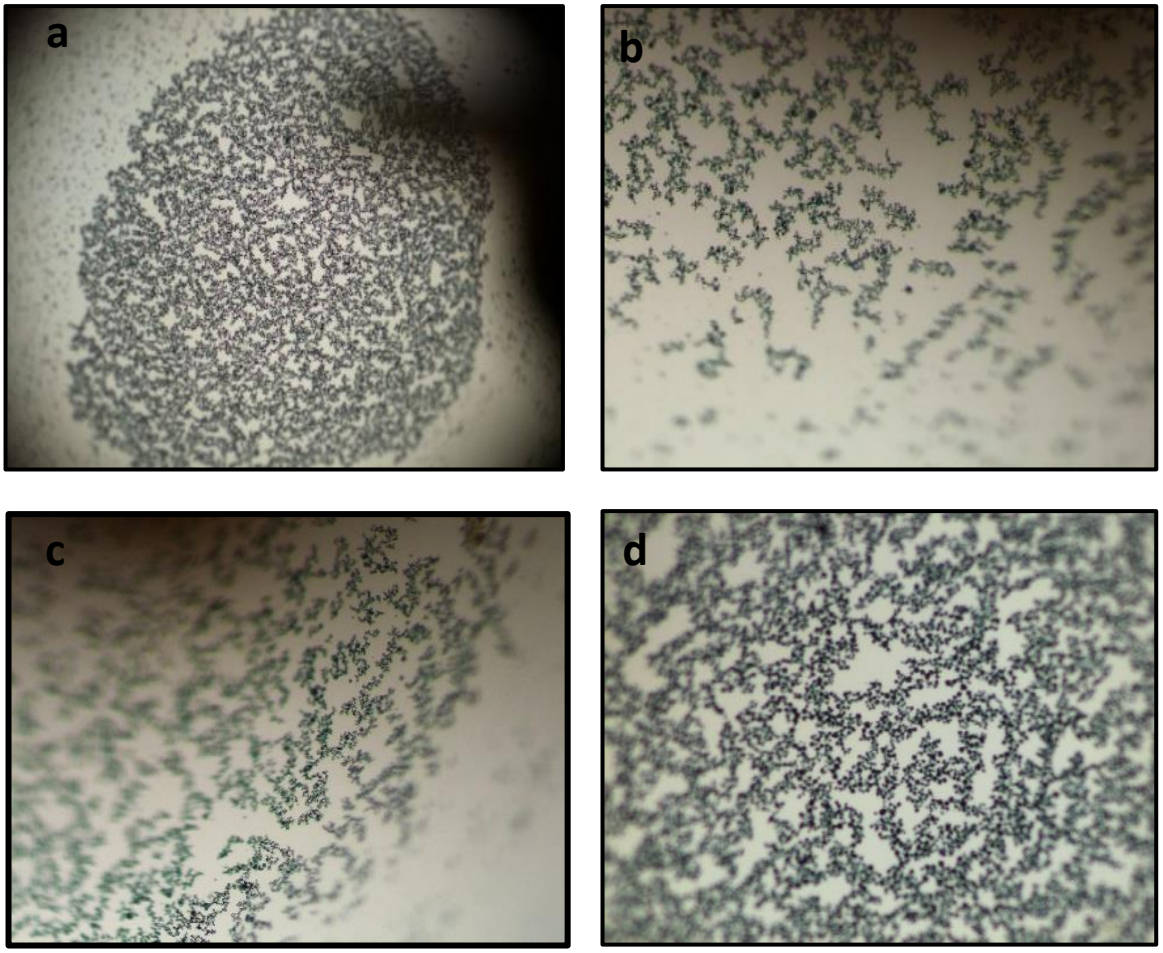

Figure 3.45 (a-d): Microscopic characterization of AuNPs formed in Micro test well plates (scale-50um) using extracts and crude extracts of chloroauric acid (Scale: 2X)

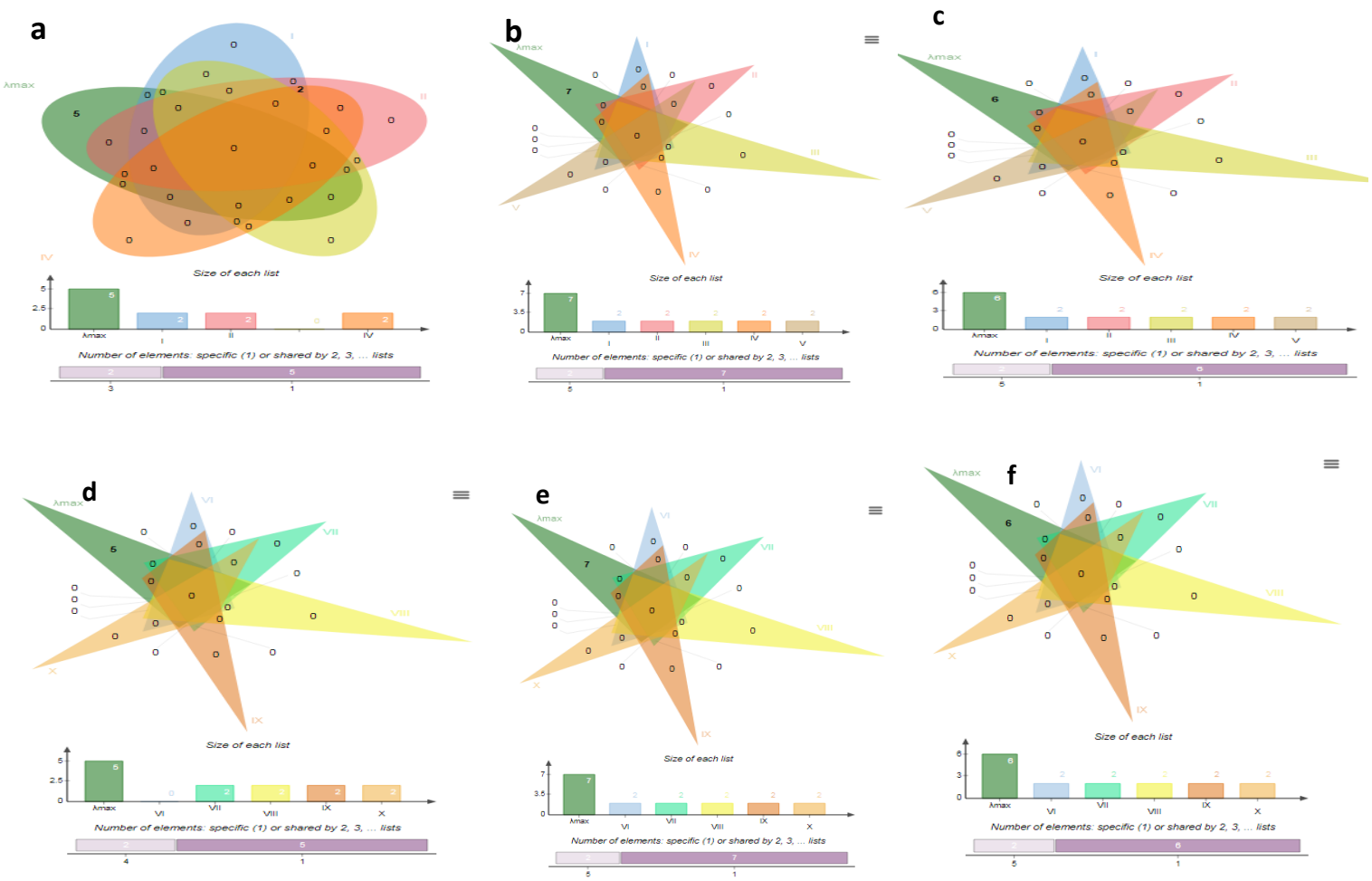

Figure 3.46 (a-f): Venn diagram studies. a-c: The shape corresponding to the lists involved in the intersection are highlighted in case of tissue, (a-455-463 λ max, b-510-540, c-632-644). d-f: The shape corresponding to the lists involved in the intersection are highlighted in case of extracts, (a-455-463 λ max, b-510-540, c-632-644)

3.15. Screening cultures for palletisation

3.15.1.GNP synthesis using *Termitomyces heimii* pellets

Pelletized growth reflects under submerged aeration condition the tendency of filamentous fungi to produce typical three-dimensional colonies (Papagianni, 2004). Fungal strains may produce well defined pellets or mycelial aggregates depending on number of factors. In present work successful palletisation was obtained.

3.15.2. Selection of suitable medium for palletisation

Throughout this work CDS proved to be appropriate well defined basal medium for pelletization. All subsequent results were obtained by using this medium.

3.15.3. Choice of strains and identification of promising strain for pelletization

The choice of the promising strain was governed by identification of a pelletized form with a relatively stable morphology and satisfactory biomass yield (dry biomass 0.72 g/L) under normal growth conditions. All 5 cultures were used to identify the promising strain and all produced pellets as seen in **Fig 3.47 (a-d)**. The morphology of aggregate mycelium varied from compact rafts to loose entangled mass (**Fig. 3.48 a-h**). Pellets forming cultures are again divided into isomorphic / homomorphic (uniform / single type) pellet and polymorphic (mixed type) pellet. Fungal cultures grew slowly initially and growth increased vigorously after two days in shaken conditions. Pellet sizes increased during long term submerged fermentation and after 15 – 20 days the pellet colour changes and shows staling in pellet growth. Pellet morphology varied from spiky, fluffy, compact, smooth and flakes. Pellet number varied drastically. More pellet number was observed at high pH and vice versa in acidic. Pellet dimensions ranged from 1 – 12 mm whereas for aggregates size varied upto 3 – 80 mm.

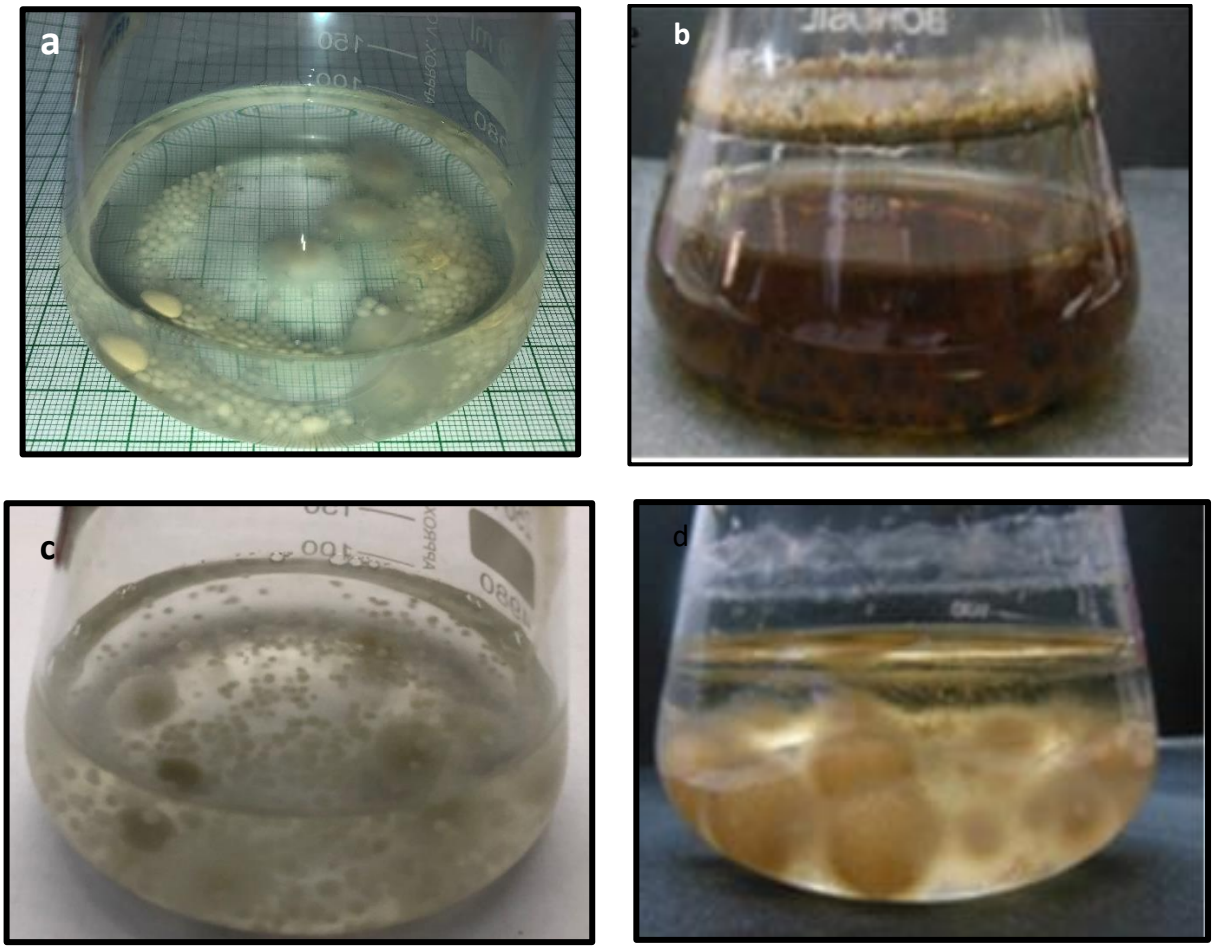

Figure 3.47 (a-d): Growth in submerged culture and studies on *Termitomyces* palletisation

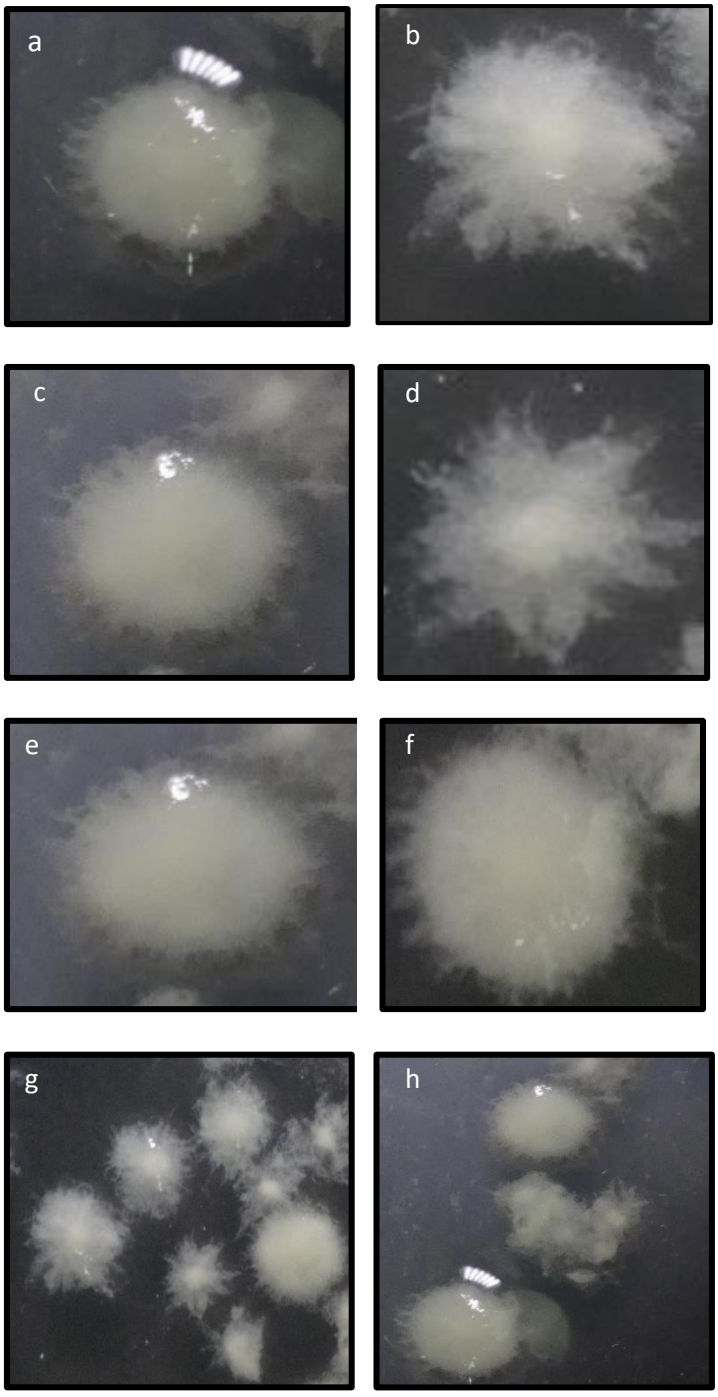

Figure 3.48 (a-h): Pellets formed by *Termitomyces heimii* (Scale: 2X)

3.16. Characterization of GNPs

The confirmation of nanoparticle formation by analysis is important for them to be able to be used in various applications. In this study, the characterization of the biologically synthesized AuNPs was carried out with UV-VIS spectrophotometry, X-ray crystallography (XRD), scanning electron microscopy (SEM), Fourier transforms infrared spectroscopy (FT-IR) energy dispersive X-ray spectrum (EDAX), Transmission Electron Microscopy (TEM). The most reliable way to monitor particle formation in a formulated solution is to visually observe the color change that occurs.

3.16.1. UV Visible spectroscopy

UV-VIS spectroscopy involves the absorption of light by molecules in the UV-VIS region and can be used to determine the color changes and concentration of the formed NPs solution based on the absorbance as seen in **Fig 3.49 (a-b)**. Generally, AuNPs absorb in the visible region of the electromagnetic spectrum at 510–570 nm because of Surface Plasma Resonance (SPR) transition. Metal NPs have free electrons, which cause an SPR absorption band because of their combined vibration in resonance with the light wave.

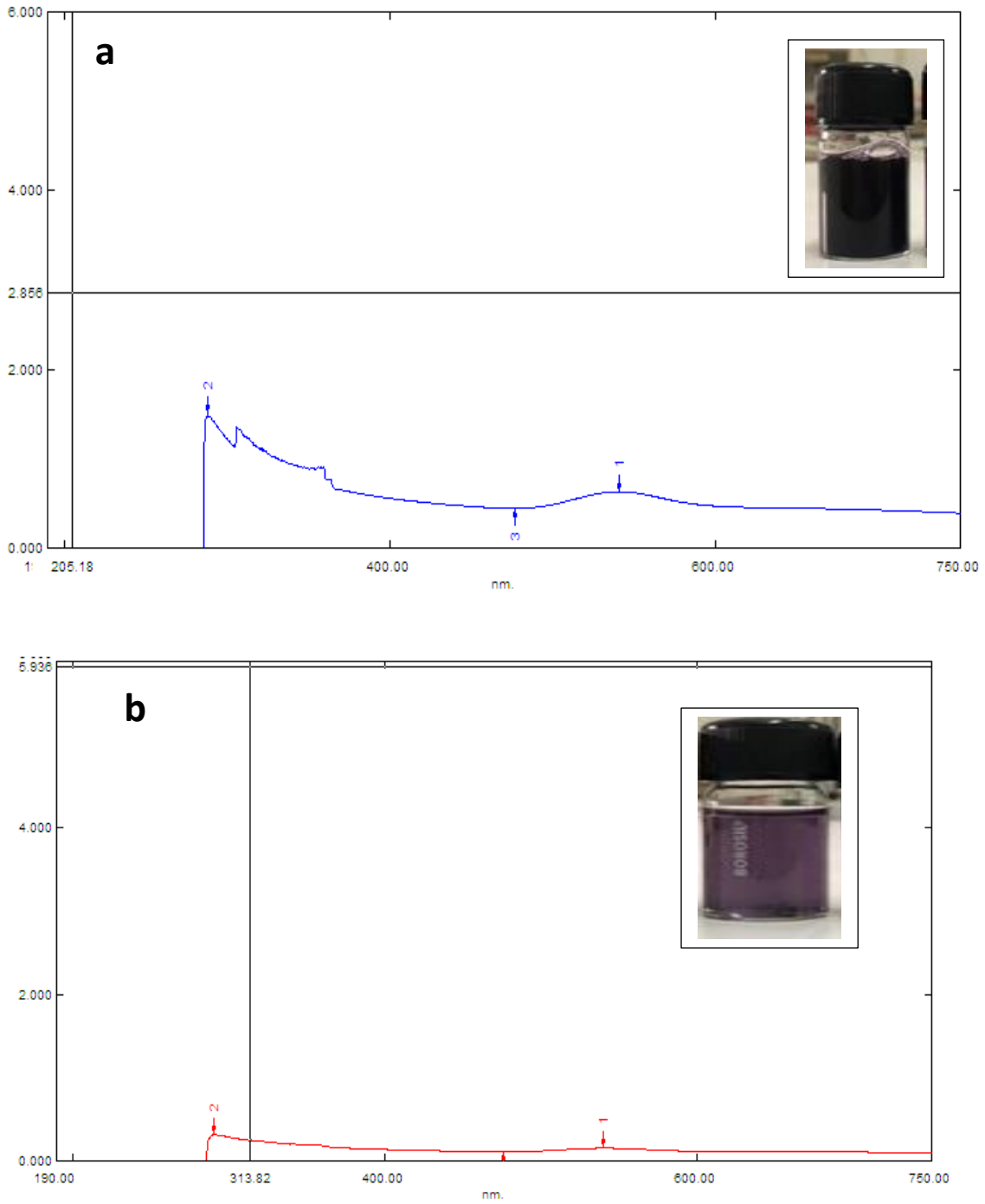

Figure 3.49 (a-b): UV-visible spectra. a-Visual confirmation of formation of GNPs and change in the color indicating the formation of GNPs; an SPR spectrum for AuNPs was obtained at 552 nm in case of pure chloroauric acid, b-An SPR spectrum for AuNPs was obtained at 552 nm in case of crude extract

3.16.2. Scanning Electron Microscopic (SEM) studies

SEM micrographs of AuNPs in the form of different shapes such as spheres, hexagons, triangles, rhomboids and rectangular are formed which are shown in the **Fig 3.50 (a-d)**. Nanoparticles with varied morphologies have been reported in previous study. SEM demonstrated a polymorphic distribution in size and shapes of AuNPs. Maximum nanoparticles were in the range of 20–50 nm. Few nanoparticles were in the range of 50–150 and 150–500 nm.

3.16.3. SEM-EDX

Energy-dispersive X-ray spectroscopy (EDX) is an analytical technique used for the elemental analysis or chemical characterization. The energy dispersive spectroscopic analysis is done to get an indication of the amount of Gold nanoparticles present in the biomass. EDS analysis of thin film of fungal biomass shows strong signals for Gold atoms along with weak signals from oxygen and potassium. These weak signals could have arisen from macromolecules like proteins/enzymes and salts of fungal biomass. **Fig 3.51(a-b)** shows presence of Gold which is the Gold nanoparticles by SEM-EDX.

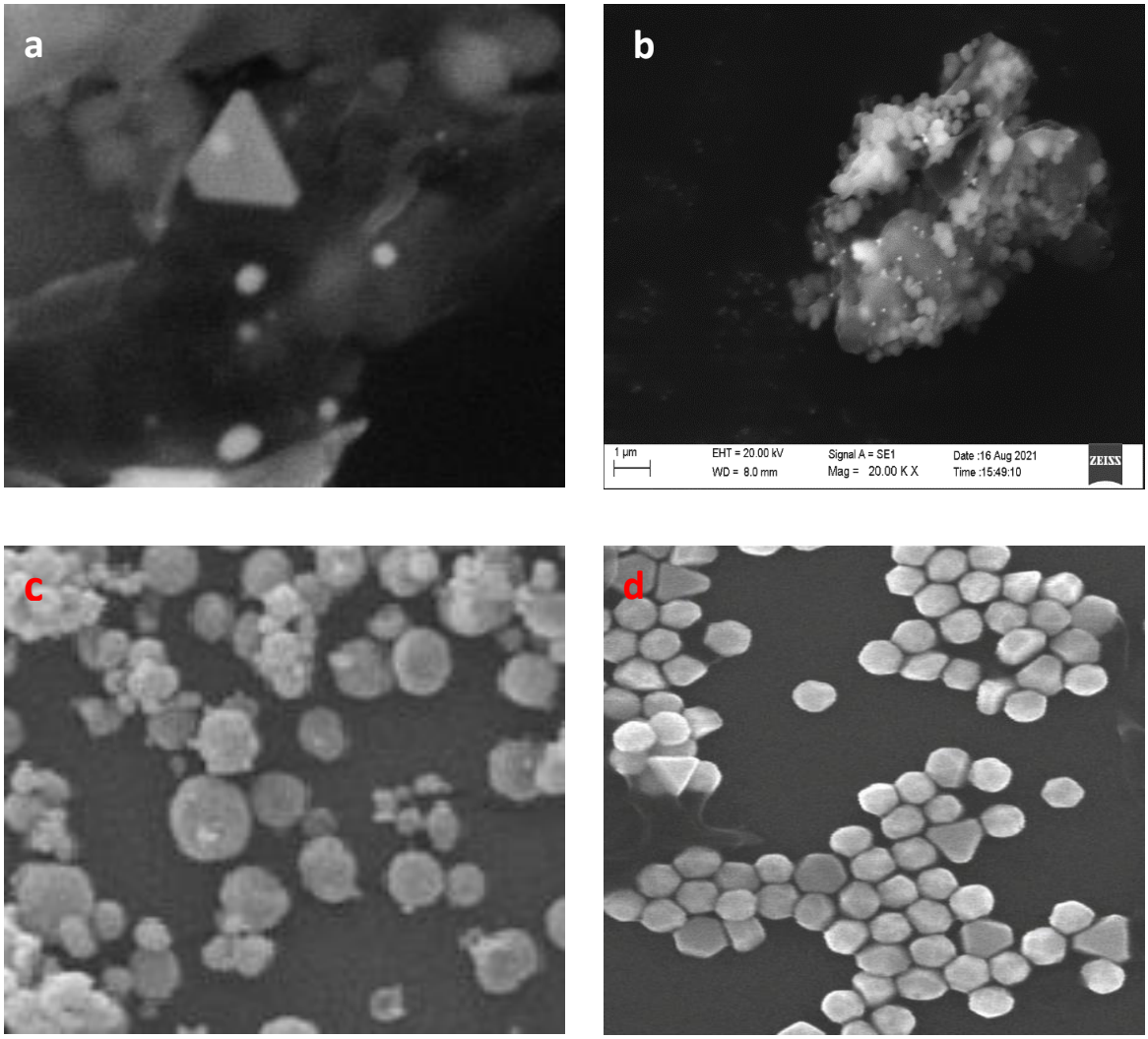

Figure 3.50 (a-d): a-b: SEM micrographs of AuNPs in the form of different shapes such as spheres, hexagons, triangles, rhomboids and rectangular formed by pure chloroauric acid; c-d: SEM micrographs of AuNPs in the form of different shapes such as spheres, hexagons, triangles, rhomboids and rectangular formed by crude extract

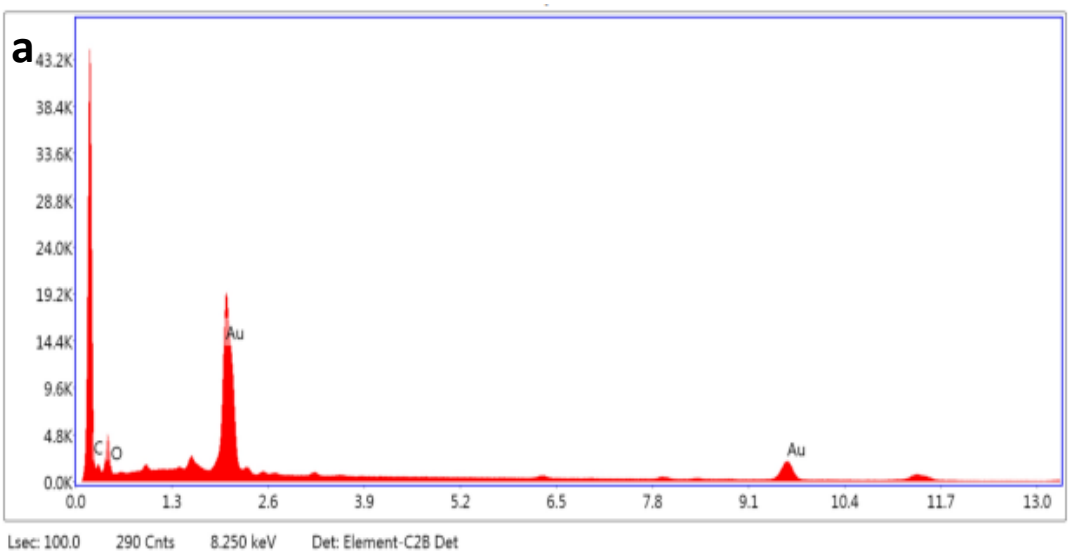

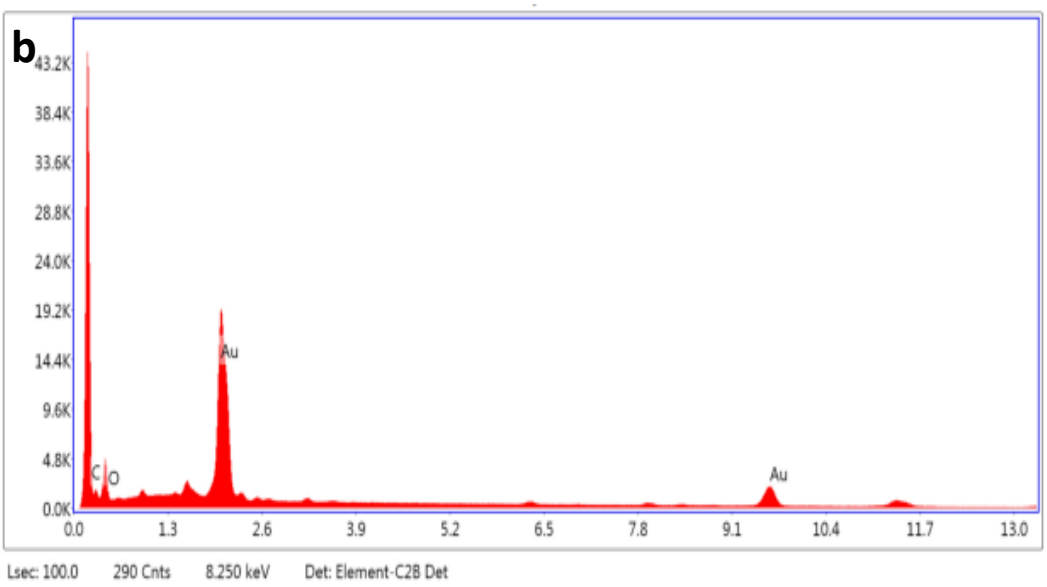

Figure 3.51 (a-b): The presence of the elemental Gold can be seen in the spectra presented by the EDX analysis.

3.16.4. Transmission electron microscopy (TEM)

TEM analysis was conducted to evaluate the shape and microstructure of the synthesized AuNPs. A typical TEM image of the synthesized AuNPs is shown in **Fig 3.52 (a-b).** As clearly observed, the synthesized NPs were well dispersed with spherical structures. In fact, spherical NPs were more abundant than NPs of other shapes. This spherical shape indicated that the synthesized NPs had minimum surface energy and high thermodynamic stability, which confirmed the high value of the zeta potential of the synthesized AuNPs. The obtained results were in agreement with the finding of Bhat et al.,2013. They indicated that the edible mushroom *Termitomyces* pellets can be used to biosynthesize spherical AuNPs with the particle size ranging from 10 to 50 nm. The TEM images showed a successful synthesis of triangular nano prisms to nearly spherical and hexagonal with different sizes between 20 and 150 nm. The produced NPs were 23.2 nm in size and were mostly spherical in shape. Similar results were shown by the GNPs produced by the crude chloroauric acid as seen in the **Fig 3.53 (a-d)** and **Fig 3.54 (a-d).** The results of analysis of the TEM images revealed the 3D images, Pseudo image as well as the isotropy as seen in the **Fig 3.55 (a-f)** and **Fig 3.56 (a-f).**

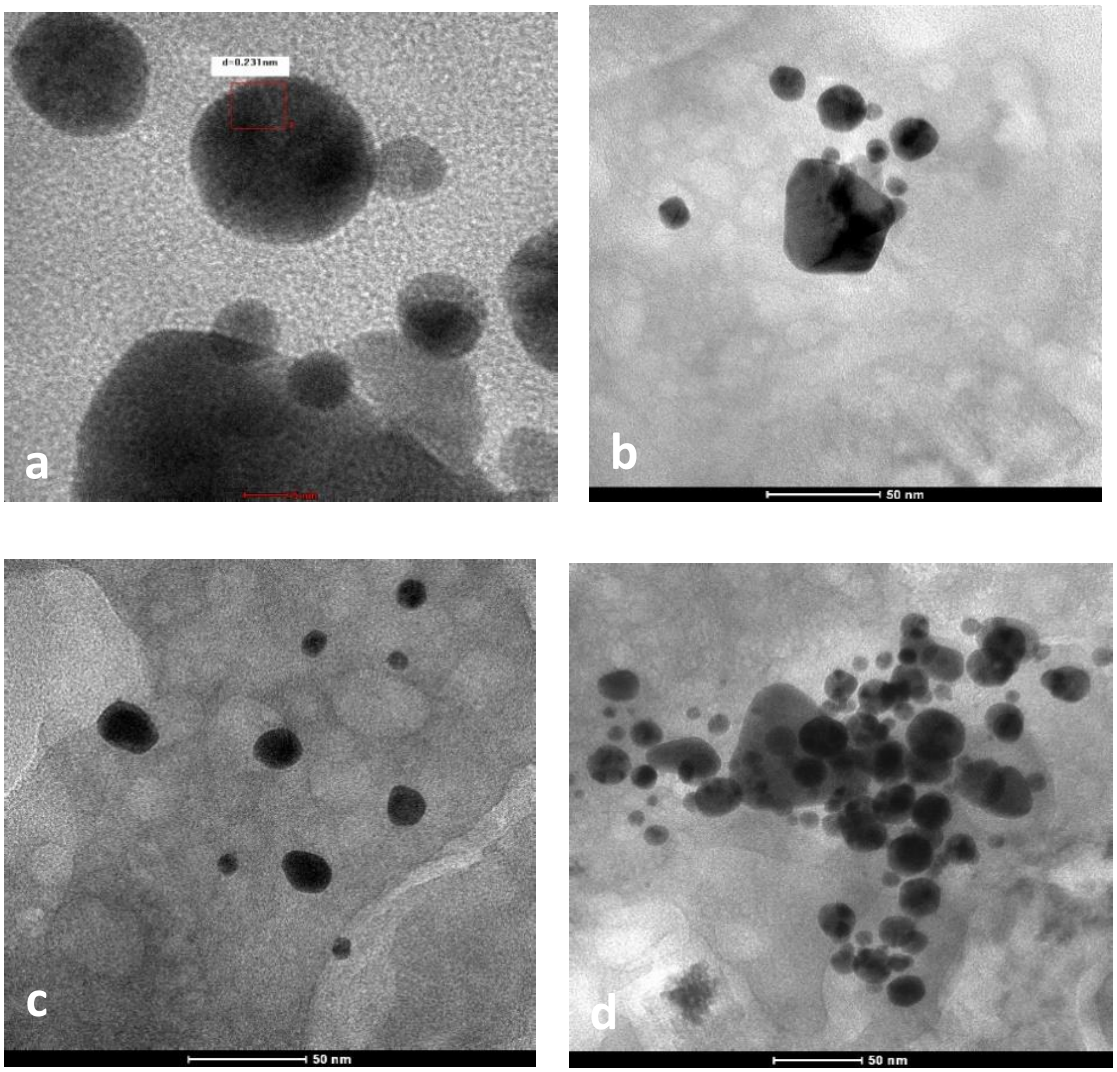

Figure 3.52 (a-d): TEM microphotographs of Gold nanoparticles of different shapes synthesized by *Termitomyces heimii* pellets using pure chloroauric acid

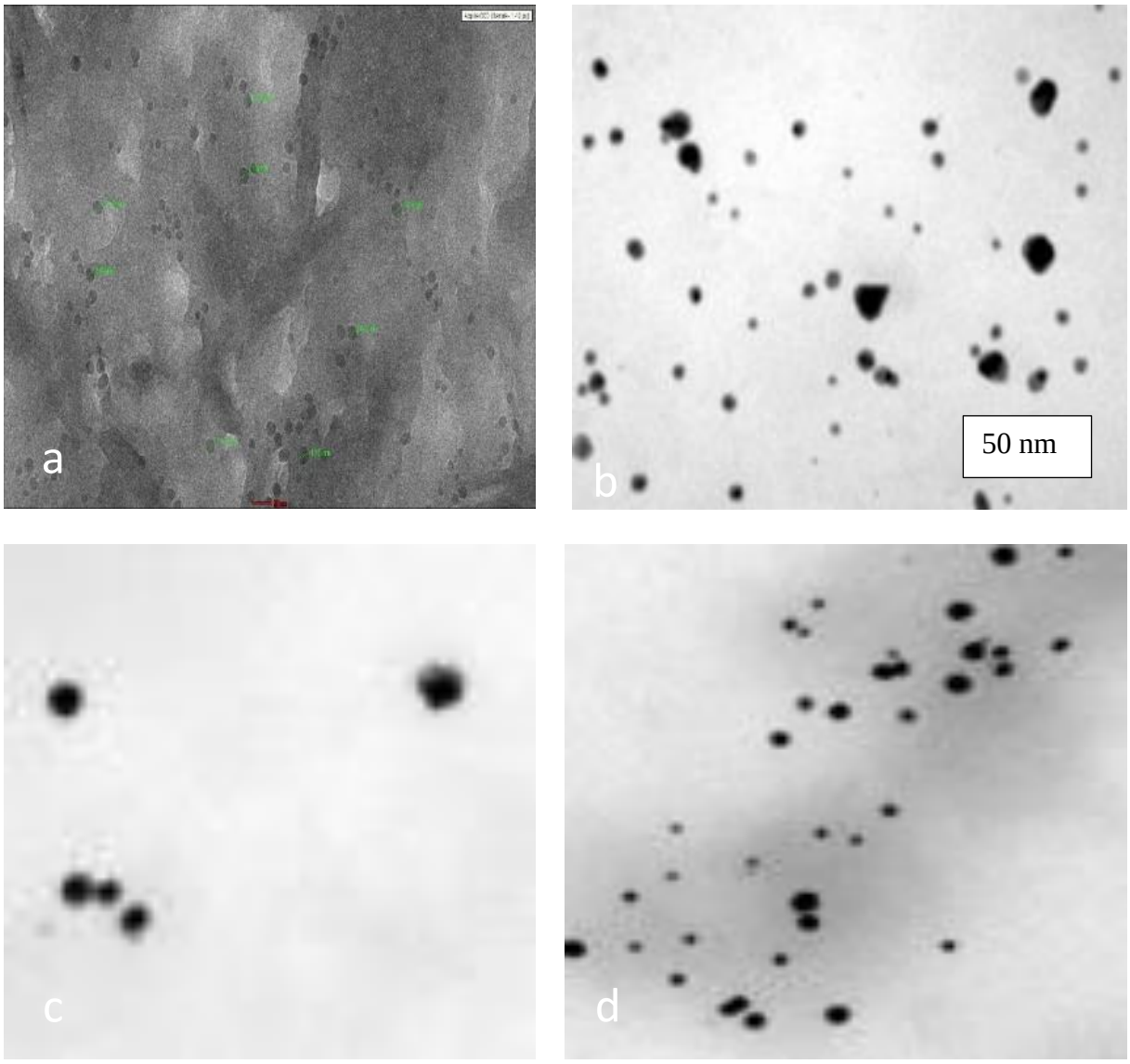

Figure 3.53 (a-d): TEM microphotographs of Gold nanoparticles of different shapes synthesized by *Termitomyces heimii* pellets using crude chloroauric acid

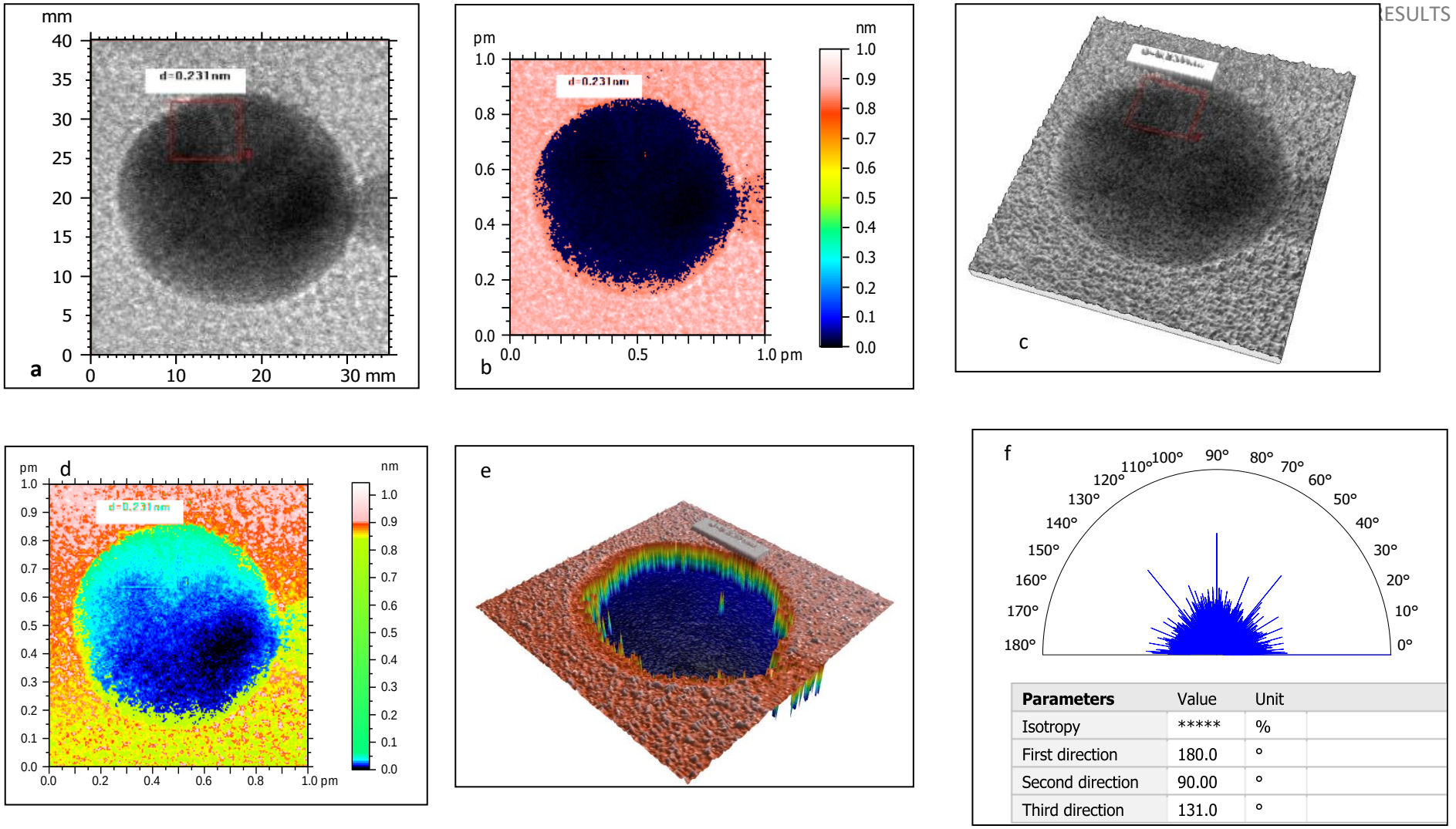

Figure 3.54 (a-f): TEM image analysis; a- TEM image of the GNPs; b, d-Pseudo image of the GNP particle; c, e-3D image; f-Isotropy

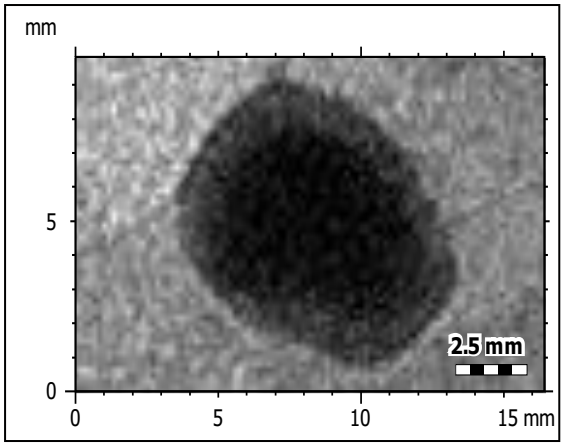

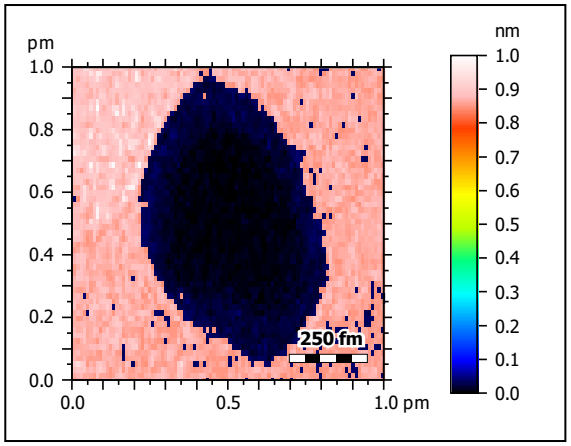

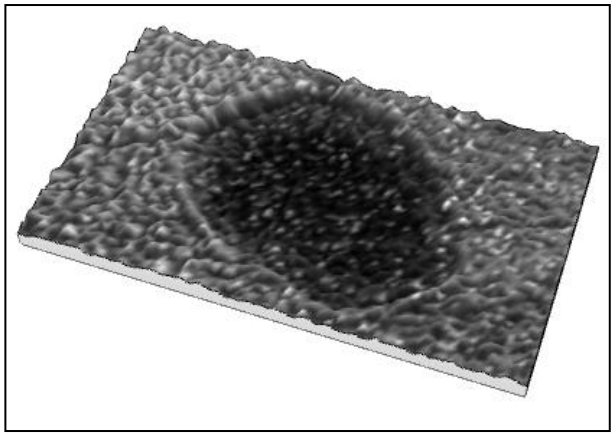

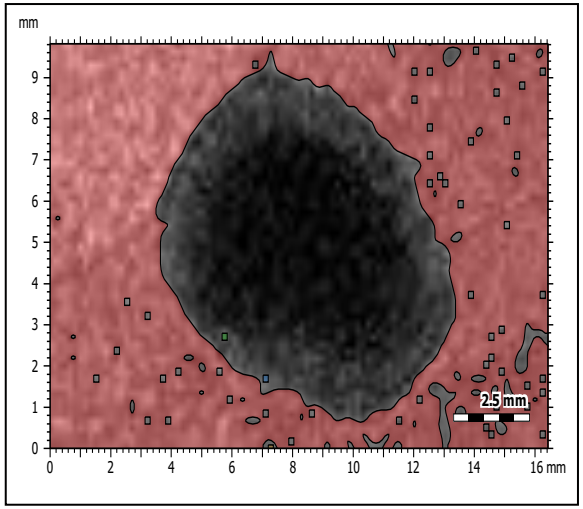

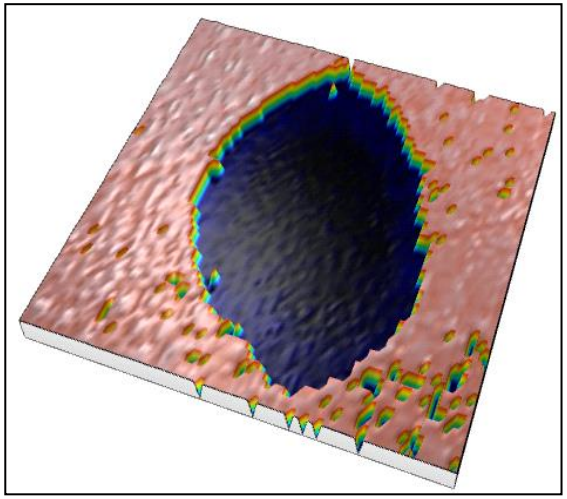

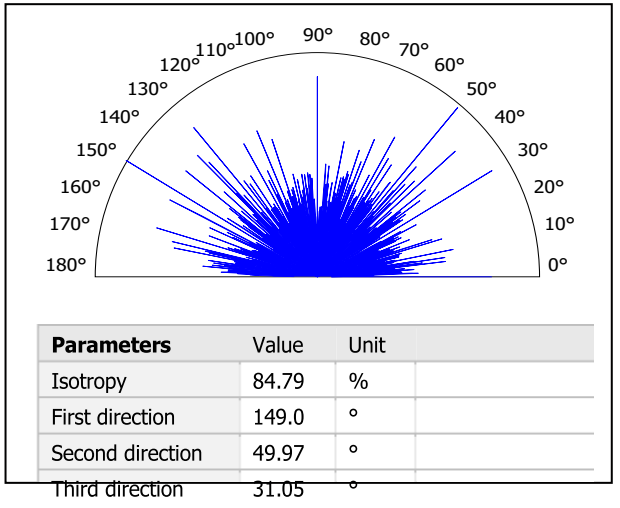

Parameters	Value	Unit
Isotropy	84.79	%
First direction	149.0	°
Second direction	49.97	°
Third direction	31.05	°

Figure 3.55 (a-f): TEM image analysis; a- TEM image of the GNPs; b, d-Pseudo image of the GNP particle; c, e-3D image; f-Isotropy

3.16.5. FTIR studies of GNPs

The FTIR spectrum of *Termitomyces* pellet is shown in figure **Fig 3.56a.** Chemically significant regions of FTIR called spectral windows were identified which included fatty acid region dominated by C–H (3450 –2850 cm-1); amide region dominated by C=O amide I and N–H amide II bands of proteins and peptides (1800–1500 cm-1); Mixed region (1500–1200 cm-1); polysaccharides region (1200–900 cm-1); true finger printing region (900 to 700 cm-1). As clearly observed in the spectrum, several absorption peaks were cantered at 607, 1073, 1299, 1392, 1547, 1632, 2925, 3271 cm−1. The AuNPs synthesized by pellets of *Termitomyces* mushroom and chloroauric acid were subjected to FTIR analysis to identify the biomolecules involved in stabilizing the nanoparticles in solution. As seen in the **Fig 3.56b** the absorption peak centered at 1070 cm−1 referred to the C-O stretch vibration, which could be related to the Ester linkages, β (1→3) glucan, cell wall polysaccharide. Wave number 1315 cm−1 was corresponded to the O-H bending polysaccharide, Amide III. The wave number of 1424 cm−1 was corresponded to the O-H bending polysaccharide. The intense peak at 1547 cm−1 was related to N-H bending -Amide II, chitosan. The peak at 1652 cm−1 was related to amide I, which was created because of the vibrations of carbonyl stretch bonded to the protein. It seems that the proteins have binding ability with Au ions, which in turn creates a surrounded layer on the AuNPs and acts as a capping agent to decrease AuNP agglomeration and increases their stability in the medium. The AuNPs synthesized 2916 cm−1 represents CH_3, CH_2 stretching and peak at 3271 cm−1 represents O-H stretching vibration of hydroxyl groups, Amine N-H stretching. Additionally, the bands at 3400 cm−1 can be assigned to the O-H stretching vibration of hydroxyl groups, and Amine N-H stretching. These bands correspond to the amide I, II, and III bands of polypeptides/proteins, and are consistent with previous reports.

The AuNPs synthesized by pellets of *Termitomyces* mushroom and crude extract were subjected to FTIR analysis to identify the biomolecules involved in stabilizing the nanoparticles in solution. As seen in **Fig 3.56 c** the absorption peak centered at 1070 cm−1 referred to the C-O stretch vibration, which could be related to the Ester linkages, β (1→3) glucan, cell wall polysaccharide. Wave number 1388 cm−1 was corresponded to the O-H bending polysaccharide, Amide III. The wave number of 1425 cm−1 was corresponded to the O-H bending polysaccharide. The intense peak at 1547 cm−1 was related to N-H bending -Amide II, chitosan. The peak at 1650 cm−1 was related to amide I, which was created because of the vibrations of carbonyl stretch bonded to the protein. It seems that the proteins have binding ability with Au ions, which in turn creates a surrounded layer on the AuNPs and acts as a capping agent to decrease AuNP agglomeration and increases their stability in the medium. The AuNPs synthesized 2916 cm−1 represents CH_3, CH_2 stretching and peak at 3271 cm−1 represents O-H stretching vibration of hydroxyl groups, Amine N-H stretching. Additionally, the bands at 3400 cm−1 can be assigned to the O-H stretching vibration of hydroxyl groups, and Amine N-H stretching. These bands correspond to the amide I, II, and III bands of polypeptides/proteins, and are consistent with previous reports. **Table 3.17** gives the bands of FTIR.

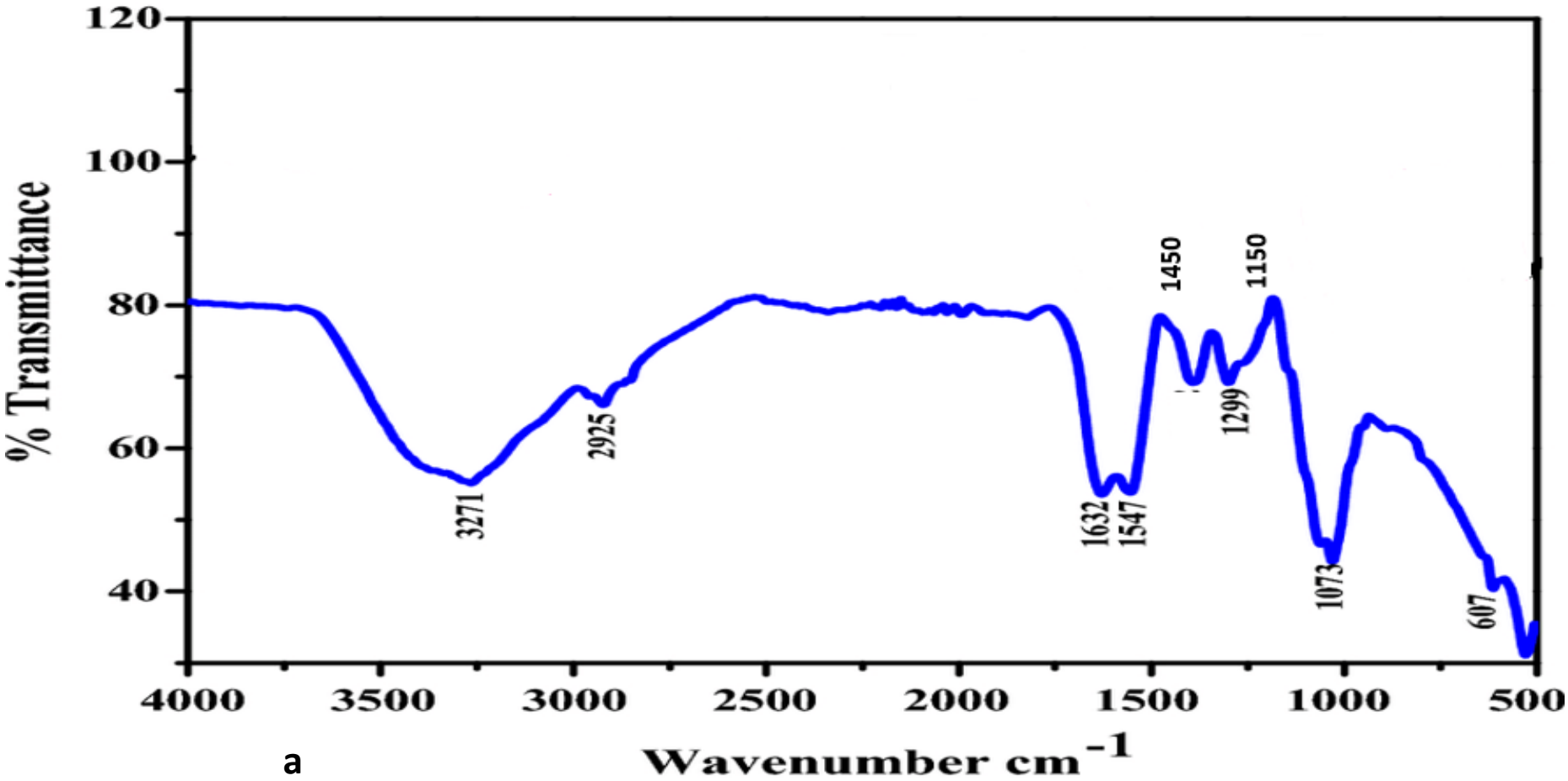

Figure 3.56 a: The FTIR spectrum of *Termitomyces* pellets

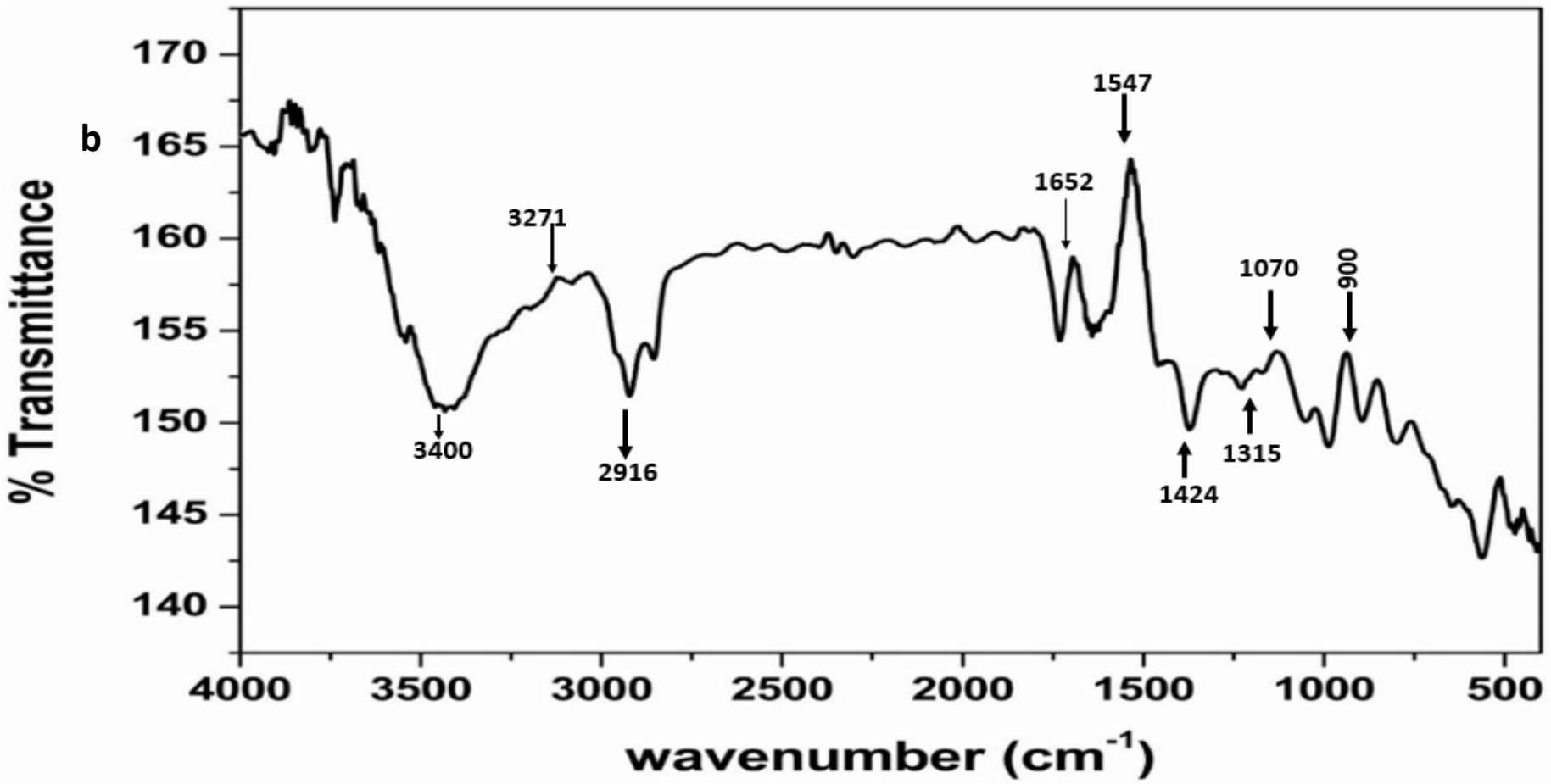

Figure 3.56 b: Spectra of GNP produced by chloroauric acid

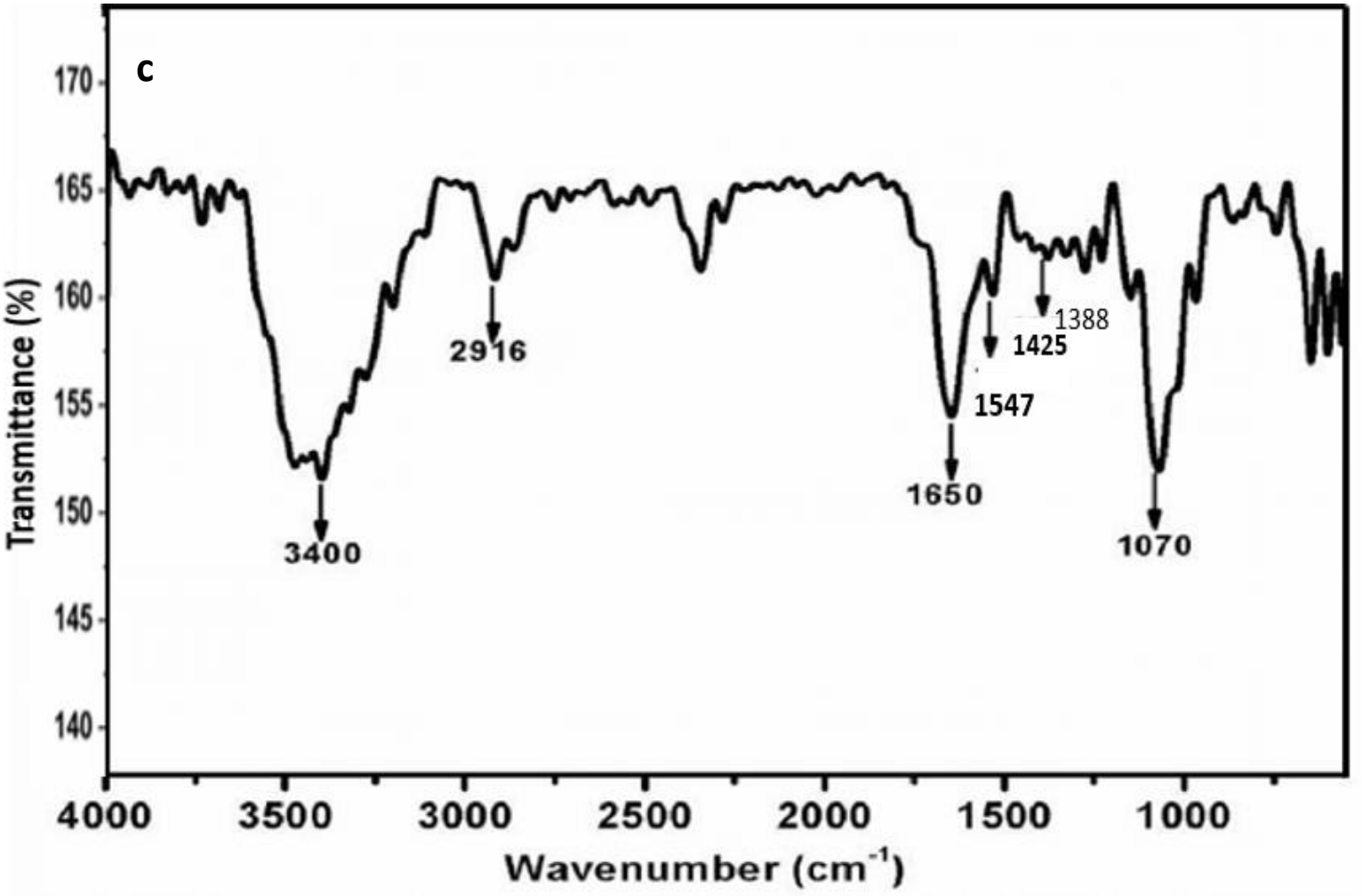

Figure 3.56 c: Spectra of GNPs produced using crude extracts

Table 3.17: Bands of FTIR

Frequency (cm^{-1})	Band Assignment
3400 – 3200	O-H stretching vibration of hydroxyl groups, Amine N-H stretching
2900 – 2850	CH3, CH2 stretching
2350 – 2215	C=C alkyne stretching
1750 C=O	C=O carbonyl stretching of esters
1658 – 1625	Amide I
1582, 1550, 1547	N-H bending -Amide II
1450 – 1425	O-H bending
1375 – 1315	O-H bending, Amide III
1250 – 1025	C-O bond, β (1,3) glucan

3.16.6. Zeta Potential and Dynamic light scattering (DLS)

The stability of Au-NPs was performed using zeta potential. A zeta value of ±30 mV is needed for a suspension to be physically stable while ±20 mV is necessary for a combined electrostatic and steric condition. The reading of Au-NPs formed reduced to −21.07 mV. Same can be seen in **Fig 3.58 (a-b).** Thus, Au-NPs formed show an acceptable stability with reading not less than the required stable expression. Dynamic light scattering (DLS) is an analytical tool used routinely for measuring the hydrodynamic size of nanoparticles and colloids in a liquid environment. 10% of the GNPs produced by chloroauric acid were found to be with a average mean size of 85nm as seen in **Fig 3.57.**

3.16.7.X-ray Diffraction spectroscopy

The crystalline nature of prepared AuNPs was confirmed using XRD. The presence of intense peaks corresponding to the (111), (200), (220) and (311) Bragg reflections of Gold agree with those reported for Gold nanocrystals. An estimate of the mean size of the Gold nanoparticles formed in the cells was made by using the Debye–Scherrer equation by determining the width of the (111) Bragg reflection (Ahmad et al., 2003). Diffraction peaks, which appeared at 31.6°C and 45.4°C corresponded to the (111) and (200) planes, respectively. No extra peak was observed in the diffraction peaks, which indicates that the as-prepared AuNPs were highly purified without any contamination. Gupta and Bector, observed four different intense peaks at 2θ angle: 38.22, 44.42, 64.71, and 77.62 with Bragg reflections corresponding to (111), (200), (220), and (311) in biomass-associated AuNPs. Alternatively, only a single prominent peak was observed at 2θ angle: 38.22 with a Bragg reflection corresponding to (111) in extracellular AuNPs. The results of the same are shown in the **Fig 3.59 (a-b).**

a

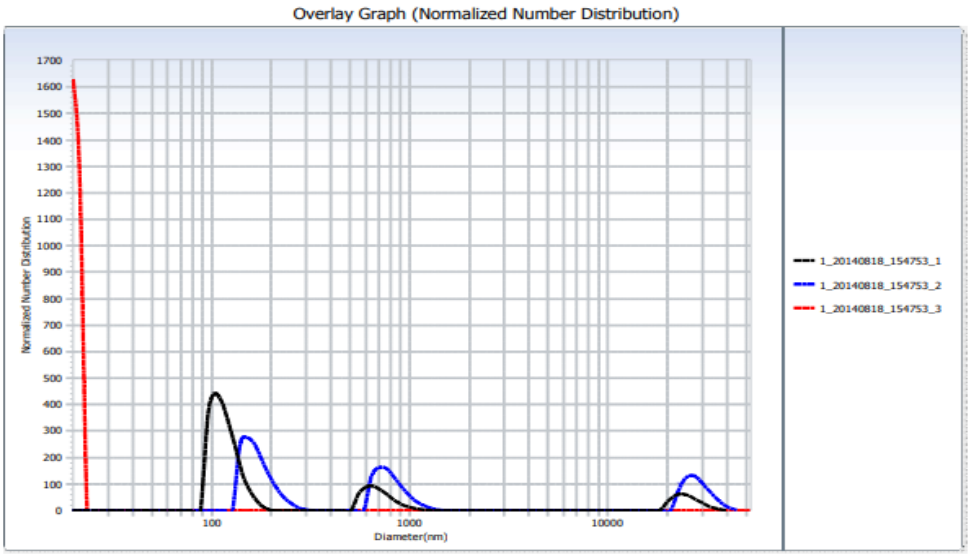

No	Data	Repet. No	pH	Ave.Diameter(nm)	PD	Mean.(nm)	D (10%) (nm)	D (50%) (nm)	D (90%) (nm)
1	1_20140818_154753_1	1	NA	1338.9	0.654	2895.0	93.5	117.8	19320.7
2	1_20140818_154753_2	2	NA	1455.3	0.724	6815.1	139.8	619.3	27185.1
3	1_20140818_154753_3	3	NA	1624.0	0.794	26.1	21.7	21.7	21.7
Average :				1472.7	0.724	3245.4	85.0	252.9	15509.2

b

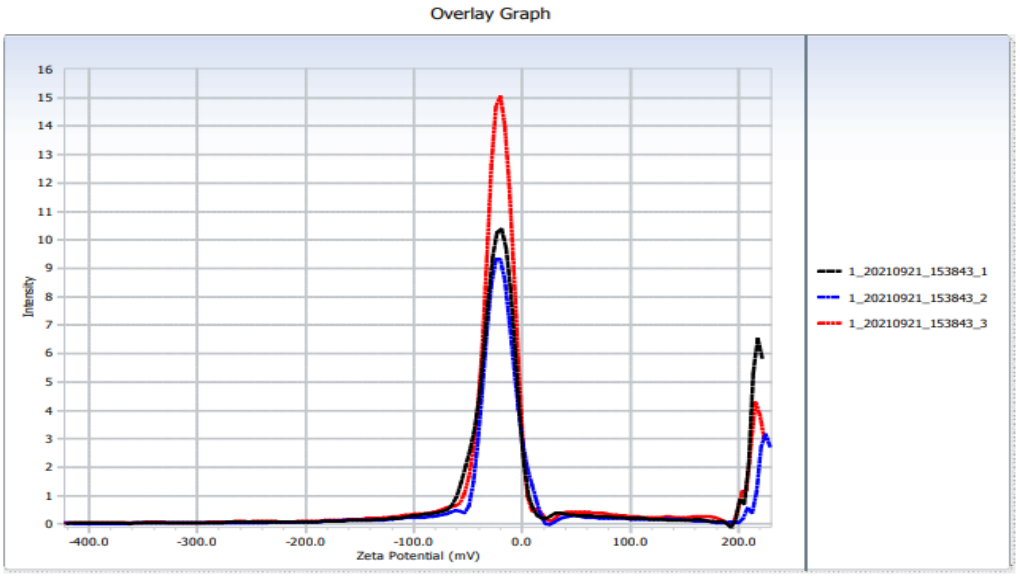

No	File Name	Repet. No	MeasTime	pH	Zeta Potential (mV)	Surface Zeta Potential(mV)	Mobility (cm²/Vs)	E. Field (V/cm)
1	1_20210921_153843	1	15:38:43	NA	-21.03	NA	-1.640e-004	-15.74
2	1_20210921_153843	2	15:38:43	NA	-20.96	NA	-1.635e-004	-15.74
3	1_20210921_153843	3	15:38:43	NA	-21.22	NA	-1.655e-004	-15.74
Average					-21.07		-1.643e-004	-15.74

Figure 3.57 (a-b): a-Dynamic Light Scattering spectra produced by chloroauric acid and b-Crude chloroauric acid

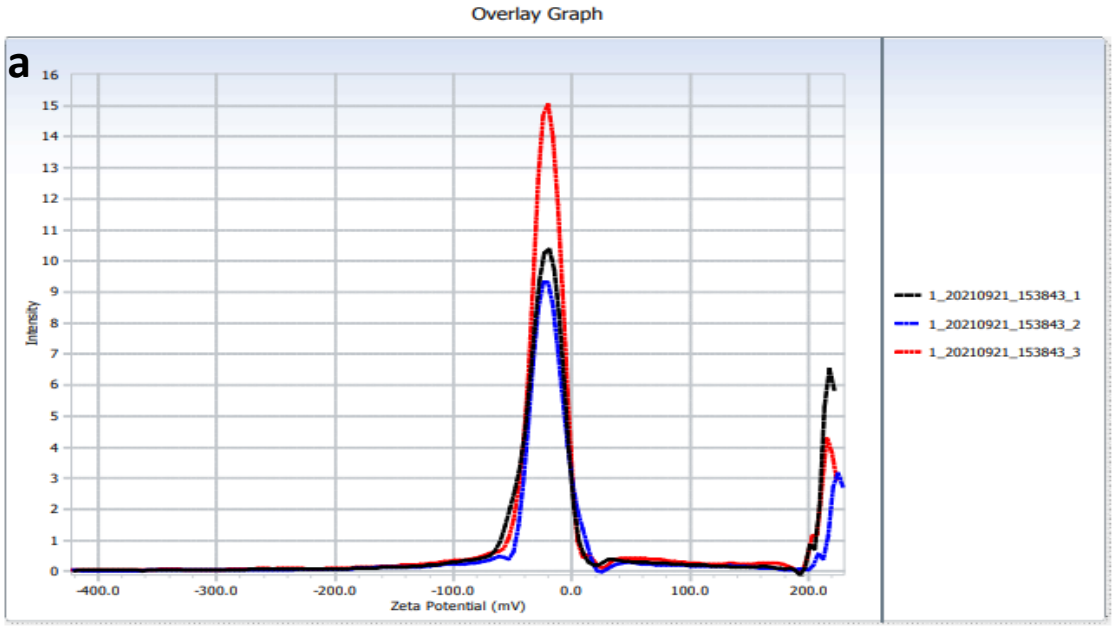

No	File Name	Repet. No	MeasTime	pH	Zeta Potential (mV)	Surface Zeta Potential(mV)	Mobility (cm²/Vs)	E. Field (V/cm)
1	1_20210921_153843	1	15:38:43	NA	-21.03	NA	-1.640e-004	-15.74
2	1_20210921_153843	2	15:38:43	NA	-20.96	NA	-1.635e-004	-15.74
3	1_20210921_153843	3	15:38:43	NA	-21.22	NA	-1.655e-004	-15.74
Average					-21.07		-1.643e-004	-15.74

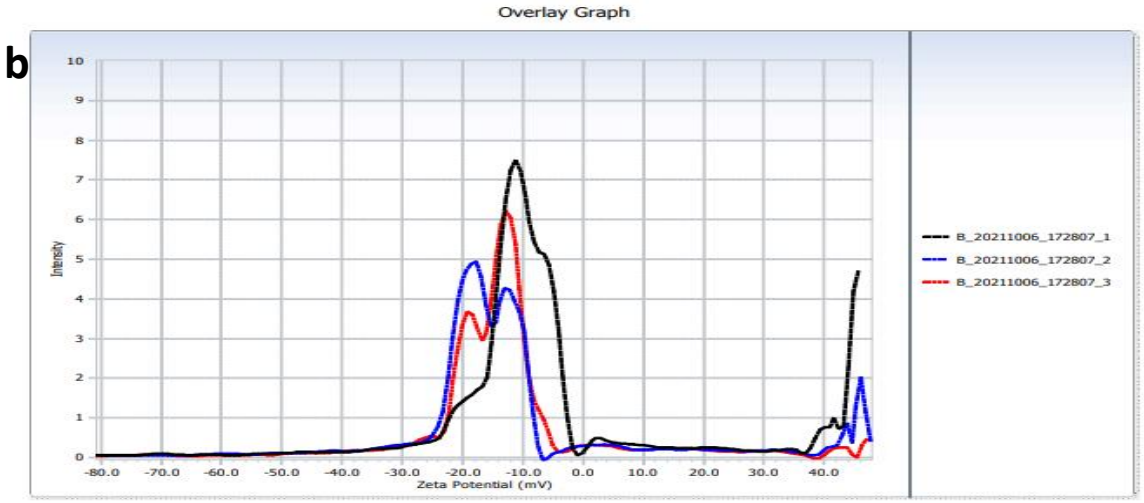

No	File Name	Repet. No	MeasTime	pH	Zeta Potential (mV)	Surface Zeta Potential(mV)	Mobility (cm²/Vs)	E. Field (V/cm)
1	B_20211006_172807	1	17:28:07	NA	-10.43	NA	-8.123e-005	-82.79
2	B_20211006_172807	2	17:28:07	NA	-16.47	NA	-1.284e-004	-82.79
3	B_20211006_172807	3	17:28:07	NA	-13.53	NA	-1.055e-004	-82.80
Average					-13.48		-1.051e-004	-82.80

Figure 3.58 (a-b): Zeta size distribution of Gold nanoparticles

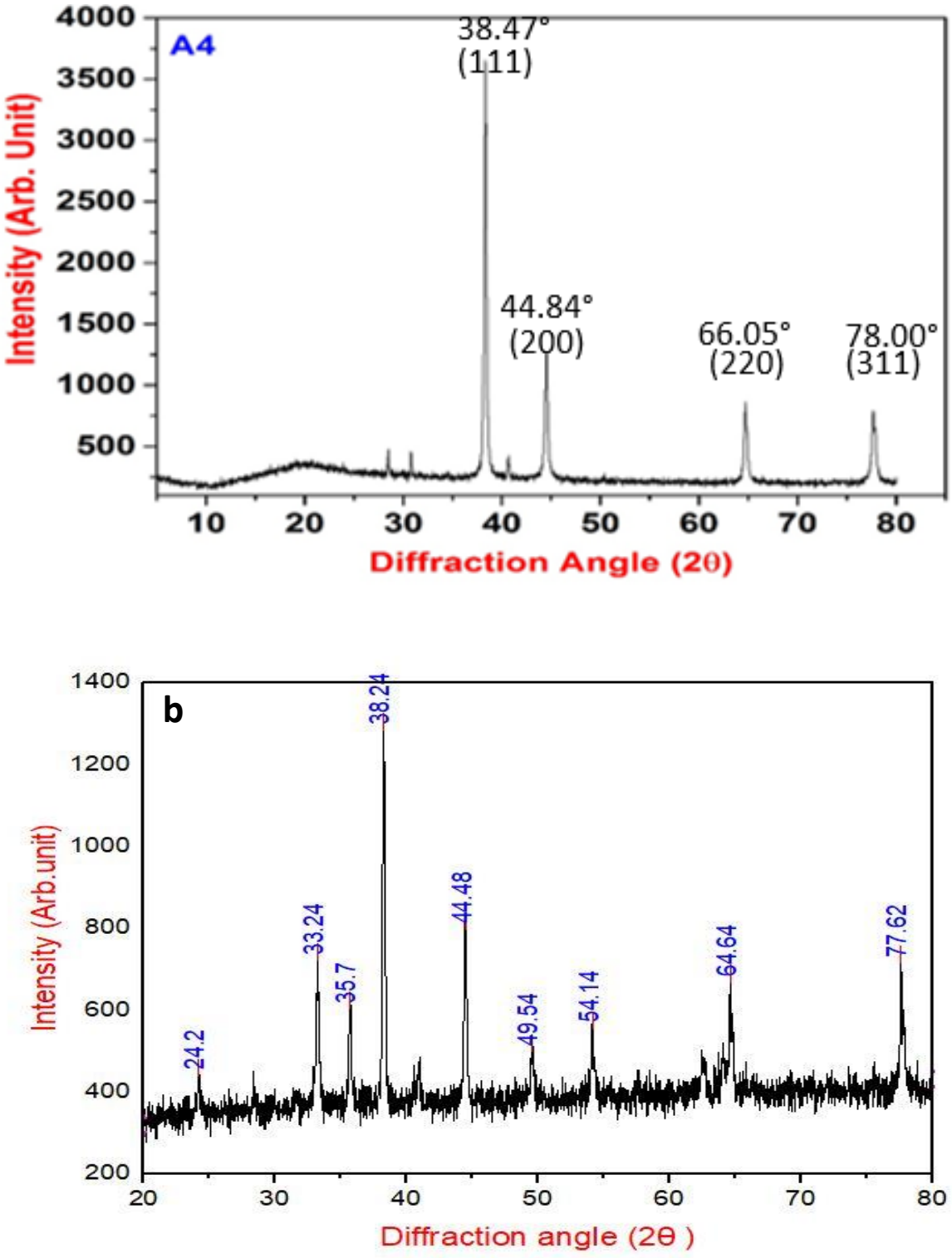

Figure 3.59 (a-b): XRD pattern of Gold nanoparticles synthesized using pure chloroauric acid and crude extract.

3.16.8. Atomic force microscopy (AFM)

A typical example at **Fig 3.60**, are presented AFM images in 2D- and 3D- format respectively, together with section analysis performed across one of the imaged Gold nanoparticles. The small nanoclusters were easily distinguishable. **Fig 3.60 (e-f)** presents a 3D- image of Gold nanoclusters at the mica surface. In the next three images the process of nanoparticle growing is easily detectable. The performed section analysis of the individual particles within the time interval of the synthesis (1 ÷ 80 min) showed that the particles sizes span in the range from 1.5 nm to 20 nm (some data are not shown). The histograms of the normalized number of Gold nanoparticles obtained from the analysis of about 200 nanoparticles of each of the samples taken is shown in **Fig 3.60 (g-h).**

3.16.9. Raman Spectroscopy

SERS effect occurs because of the very strong electromagnetic fields and field gradients available in the so-called “hot spots” of the colloidal cluster. Therefore, the molecules involved in the SERS effect are pre-dominantly those adsorbed on aggregates that have favourable surface plasmon resonances. They showed that the longer wavelength, inter particle plasmon resonances of nanoparticle aggregates provide an even better excitation frequency for SERS. 1326.23, 1338.99, 1356, and 1363.52 cm−1 which are due to δCH2(wag), δCH2(twist) and νC single bond N modes, respectively. 1556.16 are due to υ(C-(NO2)) whereas 1577.87 cm−1 is due to υ(N=N) aliphatic. Whereas in case of GNPs produced due to crude extract, 1079.93 represents υ(C-O-C) asym, 1195.87 cm−1 indicates υ(CC) alicyclic, aliphatic chain vibrations, υ(C=S), whereas 1308.64, 1435.69 cm−1 represents υ(N=N), 1570.13 cm−1 υ(C=C), and 1784.37 cm−1 indicates υ(C=N) and υ(C=C) respectively. Raman spectra of GNPs produced using *Termitomyces* pellets using chloroauric acid and crude extract is shown in **Fig 3.61 (a-b).**

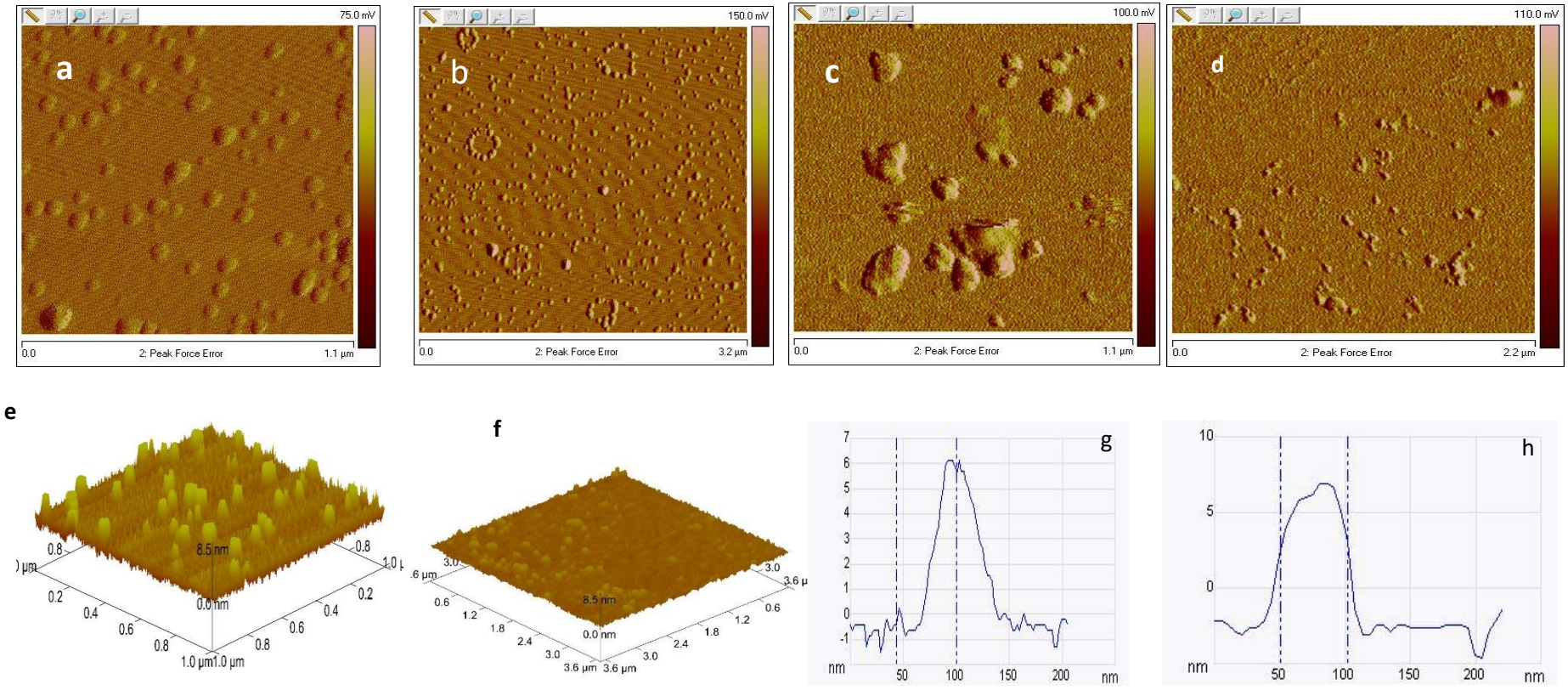

Figure 3.60 (a-h): a, b-AFM images of the GNPs produced using chloroauric acid; c, d-AFM images of the GNPs produced using crude; b, f- extracts; e, f: 3D-image of Gold nanoclusters at the mica surface; g, h-The histograms of the normalized number of Gold nanoparticles

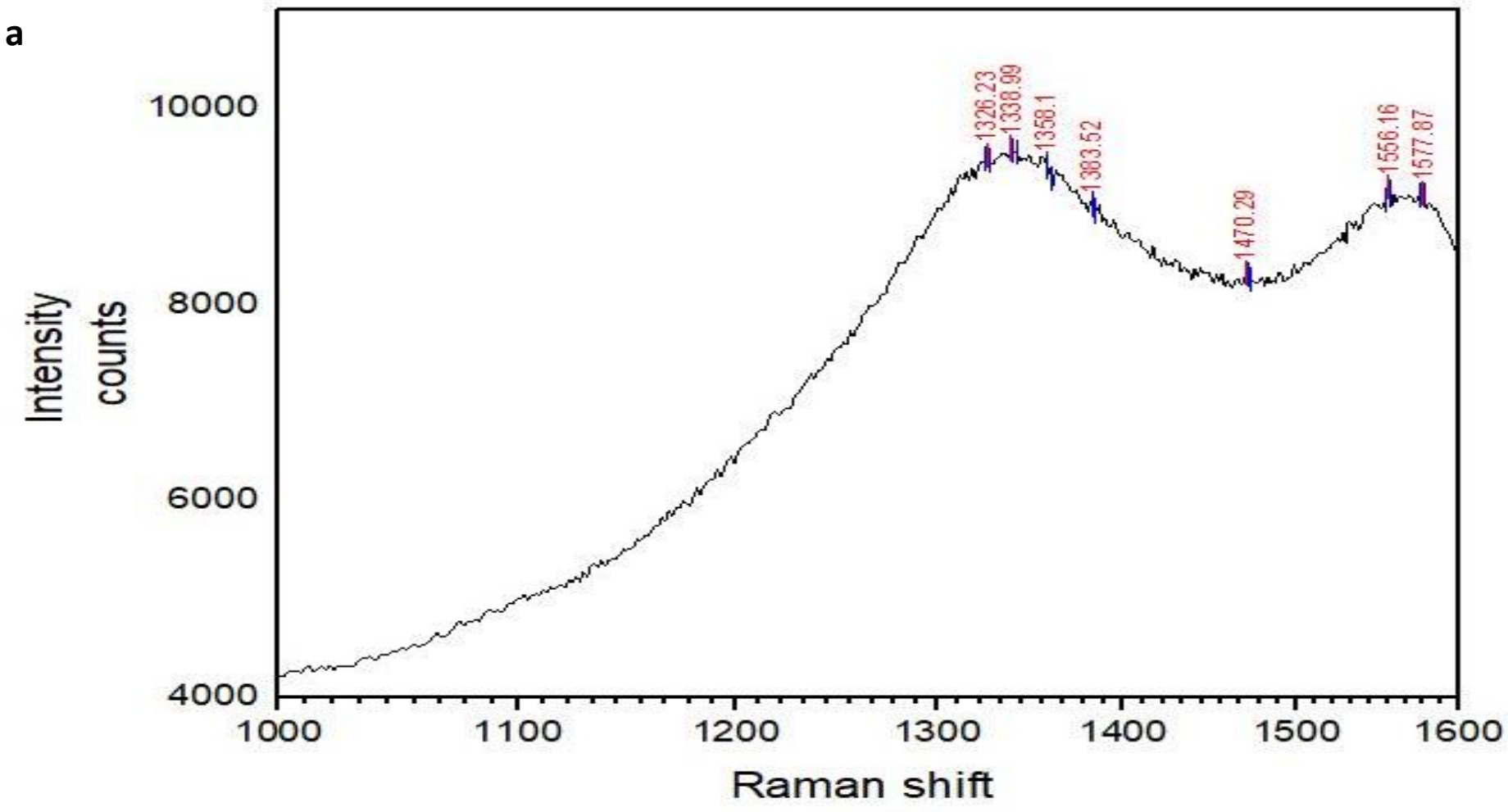

Figure 3.61a: Raman spectra of GNPs produced using *Termitomyces* pellets; results of chloroauric acid

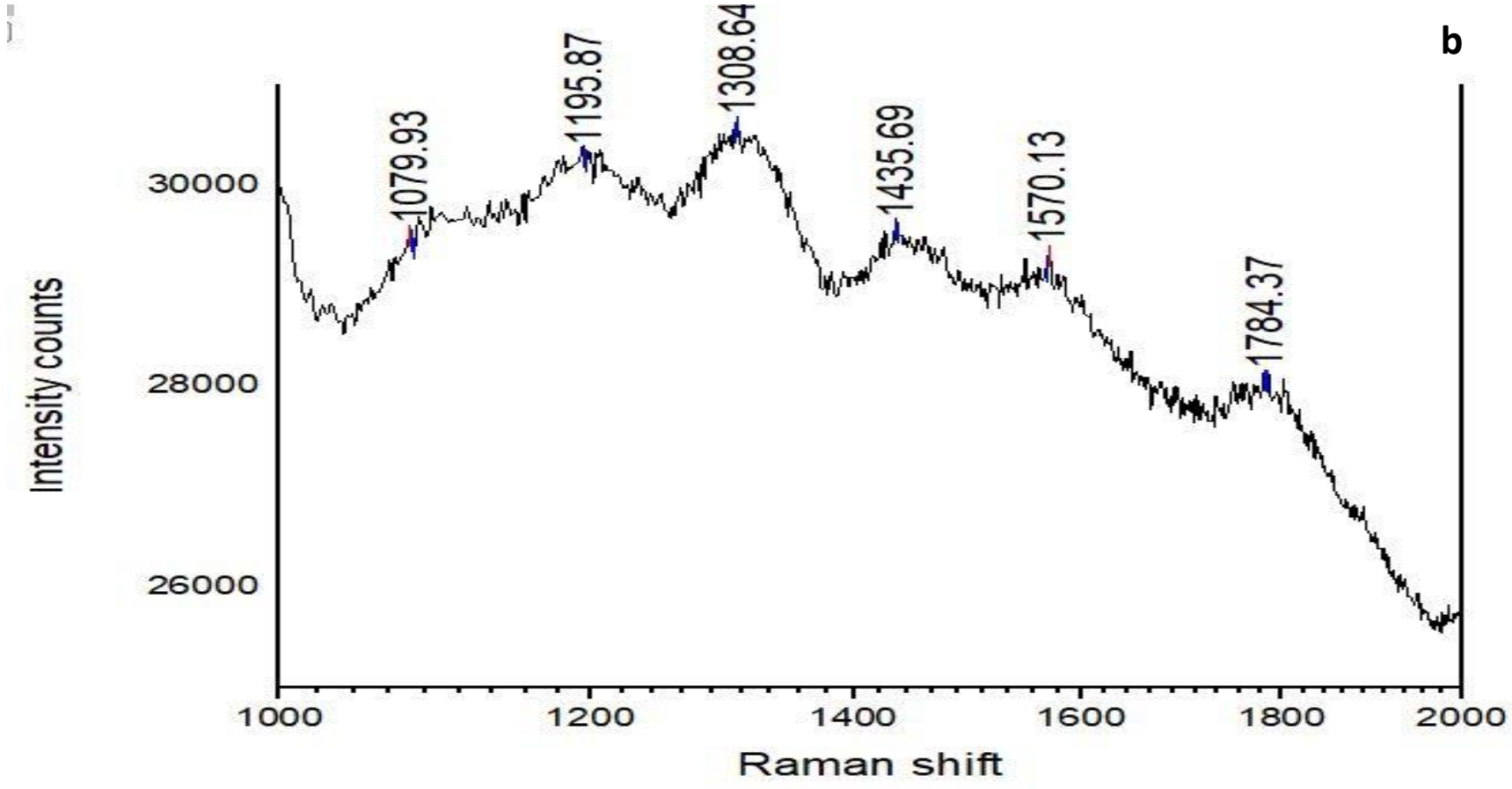

Figure 3.61b: Raman spectra of GNPs produced using *Termitomyces* pellets, results of crude extract

3.17. Detection of Gold sulphides in BHQ and Low-grade ore (mining reject)

3.17.1. Separation and detection of sulphide

We were successful in obtaining the powdered, dried sieved fractions of the samples. The fractions 150, 106, 53 µm showed high concentration of Gold and same fraction were thus used for the further studies. However, our studies have established that BHQ contains 12-13 ppm.

3.17.2. Optical microscopic studies

Microscopically 106 micron sieve fraction (**Fig 3.62a**) indicated the presence of the particles of secondary Gold, Gold sulphide, auriferous quartz, pyrite and other impurities. The morphological classification of Gold sulphide detected in this work is shown in **Fig 3.62 (b-c).**

3.17.3. Scanning Electron Microscopy (SEM-EDS)

Fig 3.63(a-b) shows the typological classification of Gold sulphide. **Fig 3.63a** and **Fig 3.63b** shows the irregular BFG with rough surface. These grains ranged from 0.1 to 1mm in diameter and varies from coarse, sub-angular to angular with no mechanical damage. The presence of the elemental Gold and sulphur is seen in the spectra presented in **Fig 3.63 c, d**.

3.17.4. CHNS/O Elemental Analysis

The sodium fusion test or Lassaigne's test is used to carry out the elemental analysis for the qualitative determination of the presence of foreign elements, sulphur in an organic compound. The appearance of violet colour indicates the presence of sulphur. Lead acetate test was also positive which was indicated by the formation of a brownish-black precipitate. Sulphur analysis showed the presence of 0.6% of sulphur corresponding to approximately 9% (w/w) Gold sulphide in heavy fraction of BMQ and that of BHQ showed the presence of 0.669 % (w/w) of sulphur corresponding to approximately 9.32 % (w/w) Gold sulphide in heavy fraction of BHQ.

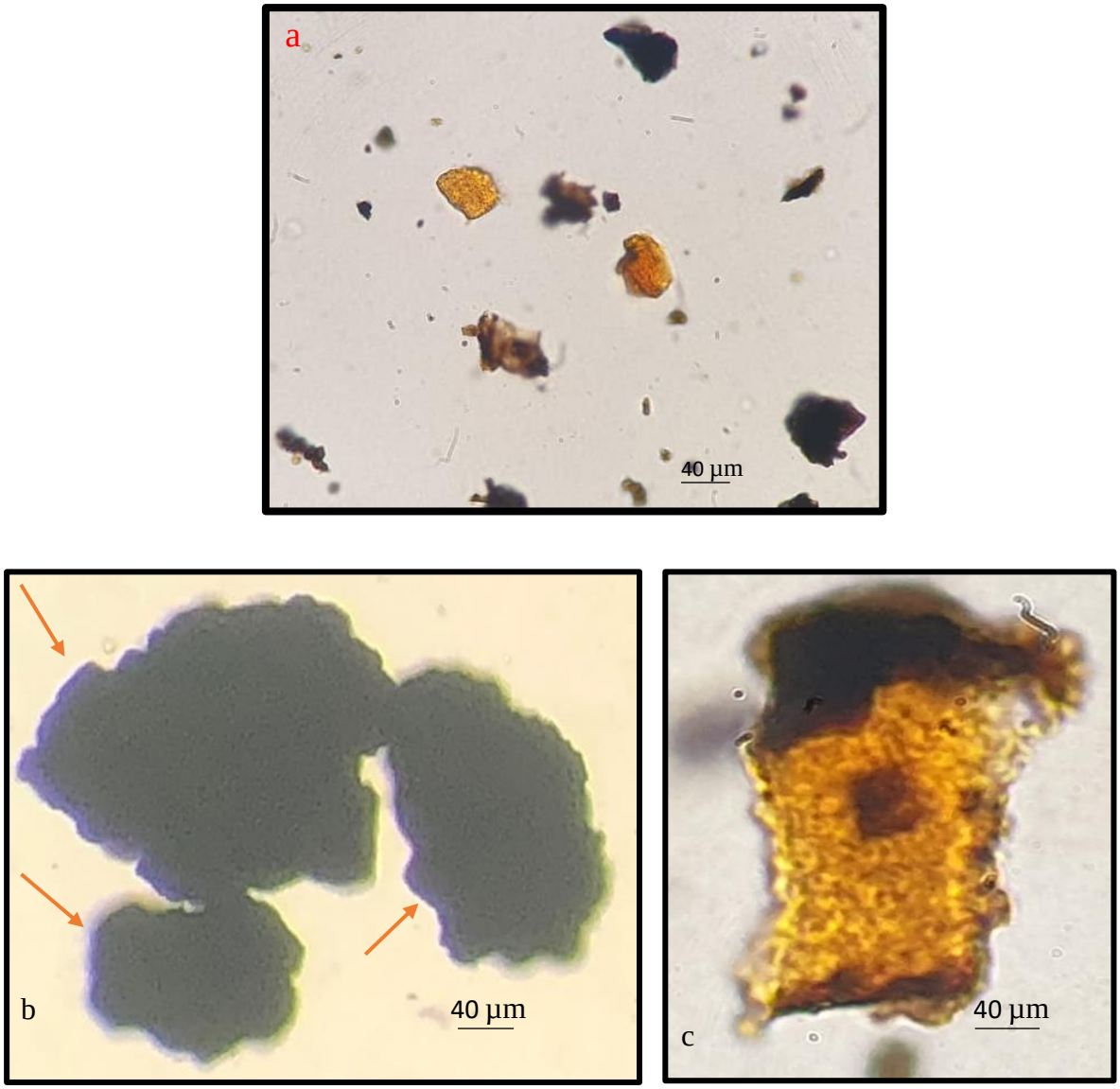

Figure 3.62 (a-c): a-Bright field microscopy of heavy fraction of BHQ (a) composite view of the heavy faction components; b-presumptive Gold sulphide particles showing the surface plasmon resonance (SPR); c-Gold sulphide particle attached to a Gold particle

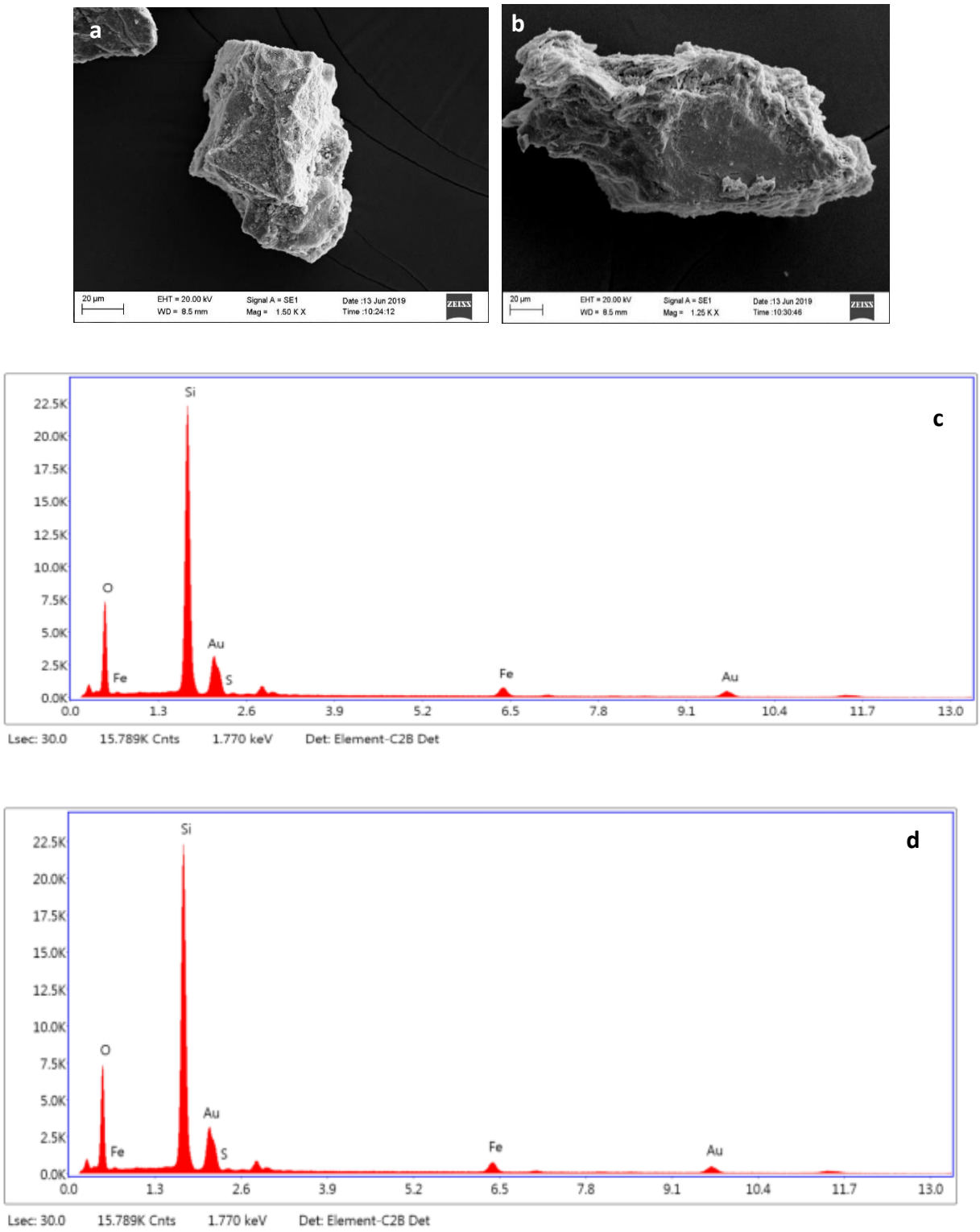

Figure 3.63 (a-d): SEM based typological classification of Gold sulphide grains; a, b- Irregular with rough surface. c and d: The presence of the elemental Gold can be seen in the spectra presented by the EDX analysis

3.18. Micro test plate assay for Biooxidation of Gold sulphides

Bio-oxidation process is based on chemolithotrophic microorganisms which uses iron and/or sulfur as their energy source. In highly aerated, operated at pH 1.6 and a temperature of 40ºC (Rawlings, 2002), the finely ground mineral is mixed with inorganic nutrients to promote microbial growth. The primary role of the microorganisms in this process is the oxidation of aqueous Fe^{2+} into Fe^{3+} and the production of sulfuric acid. Flux of solubilized liquid Gold in colloidal state released by action of hyperacidiphilic chemo lithotrophic iron bacteria viciously attacking the Gold sulphide (black amorphous masses) over a week, at the centre is fractal swarm of pure Gold nanoparticles sedimented as a product of microbial biooxidation as seen in **Fig 3.64 (a-b).** The annular flux of pure micro biogenic Gold indicates the intensity of bio solubilization in solution which has a highly acidic pH of 1.5. All three were showing biogenic reaction. Reaction was successful with both synthetic and crude Gold sulphide. There was formation of metallic Gold sulphide from amorphous Gold sulphide and also crude Gold sulphide therefore biooxidation assay was successful. It is a rapid assay. Results are positive and also cultures are active. Among all three, *Acidithiobacillus* was found to be more active followed by *leptospirillum* and *sulfobacillus* was the weakest. Fascinating fractal forms of pure Gold produced by bacterial culture as shown in **Fig 3.65 (a-h).**

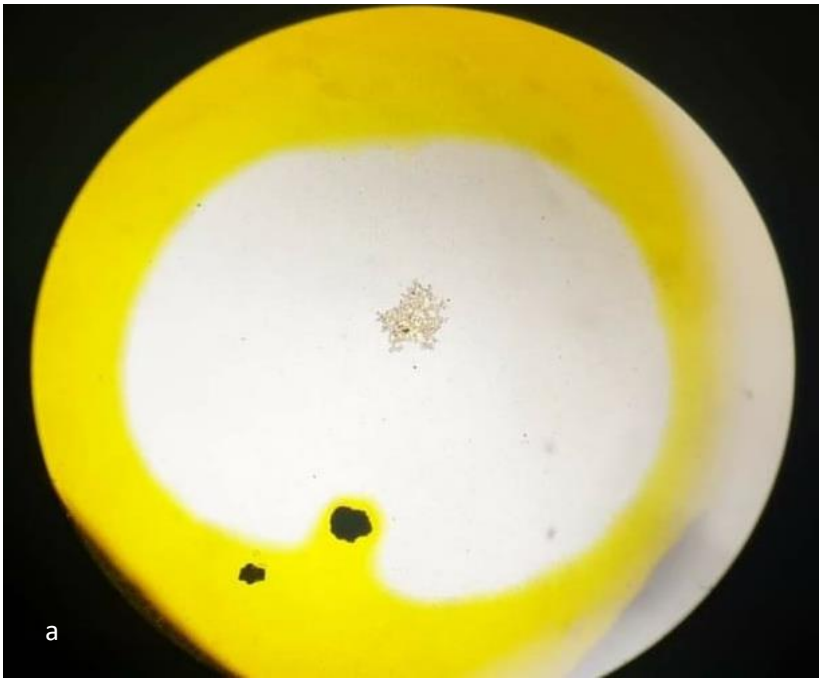

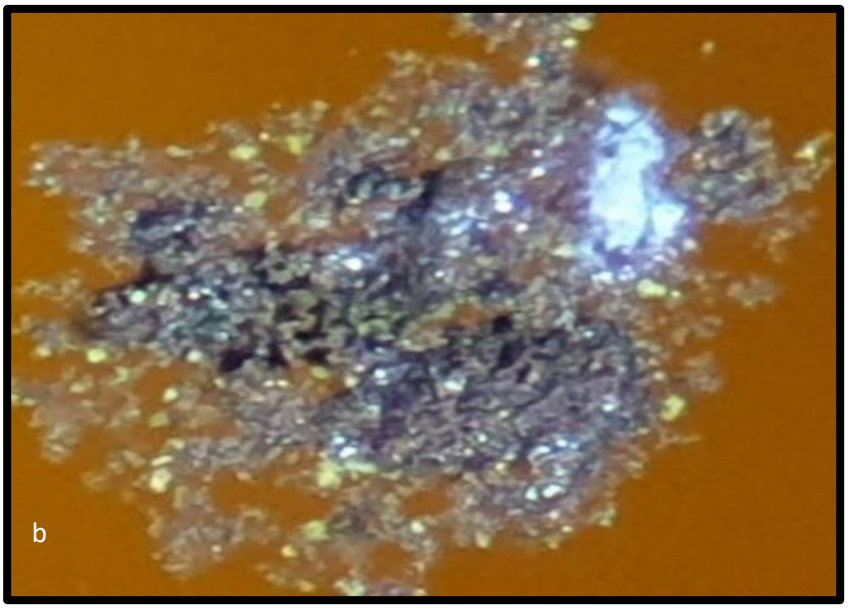

Figure 3.64 (a-b): Biooxidation of Gold sulphide and release of Gold

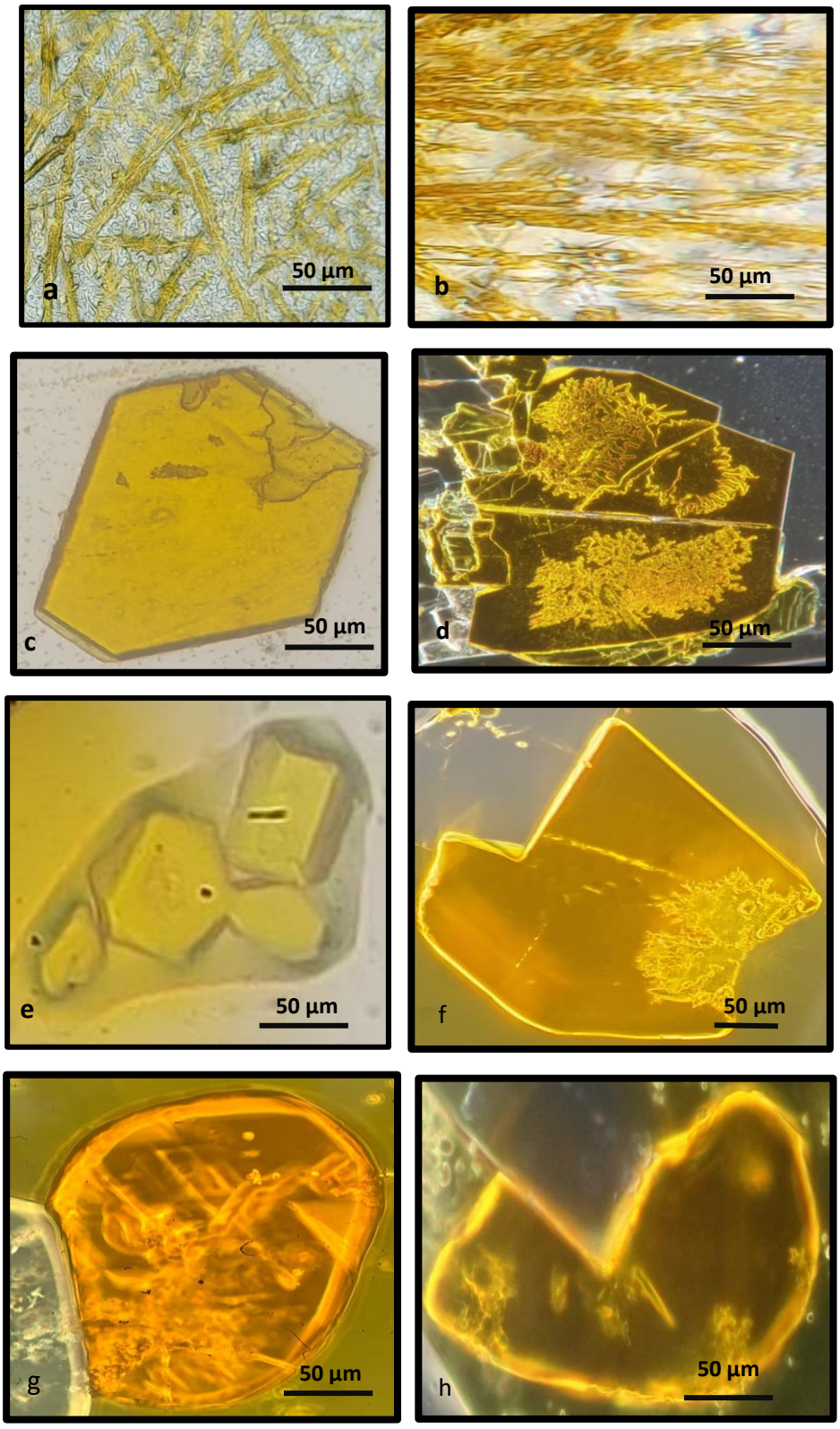

Figure 3.65 (a-h): Fascinating fractal forms of pure Gold produced by NOSOB culture

3.19. Immobilized reaction system

Successful biooxidation was carried out experiment in a 1000ml Borosil beaker with the help of slides-based coating technique. Successful Standardisation of the concentration of medium and culture was carried out so that the medium gets solidified and pH is maintained. Set up of immobilized system for biooxidation, placement of the slides inside the beaker and external aeration as seen from the top is shown in **Fig 3.66.**

3.19.1. Monitoring of the slides and formation of Gold

There was formation of colloidal Gold forms and detection of flux lines of colloidal Gold on the slides. There was evidence for formation of sulphuric acid as product of biooxidation. The formation of flux of sulphuric acid depolymerizes the agar and creates rough surface. In two dimensional slide coating it appears that the oxygen gradient is on five sides, the four edges and the surface. Therefore, Oxygen diffusion was found to be highest from the edges and decline towards the centre. Oxygen diffusion from surface was not uniform depending on thickness of the layer. Therefore, the reaction was rapid at the edges and showed clearance of sulphide, forming complex biofilms and flux of sulphuric acid which depolymerizes the agar and creates rough landscape. The Gold formed after oxidation was typically microbioform. After 14 days of process approximately 90% of Gold extraction were reached. It was found that the pH was dropping from 2 and reached to 1.8 by the end of weak and later 1.5 after 14 days. Film of Gold formed after dissolving in aquaregia indicated the formation of Gold which was formed at all the edges of the slide as can be seen in **Fig 3.67.** There was formation of colloidal Gold forms and the detection of flux lines of colloidal Gold on the slide. The concentration of Gold reported was 2133.5 mg/L, 2272.5 mg/L and 2100 mg/L.

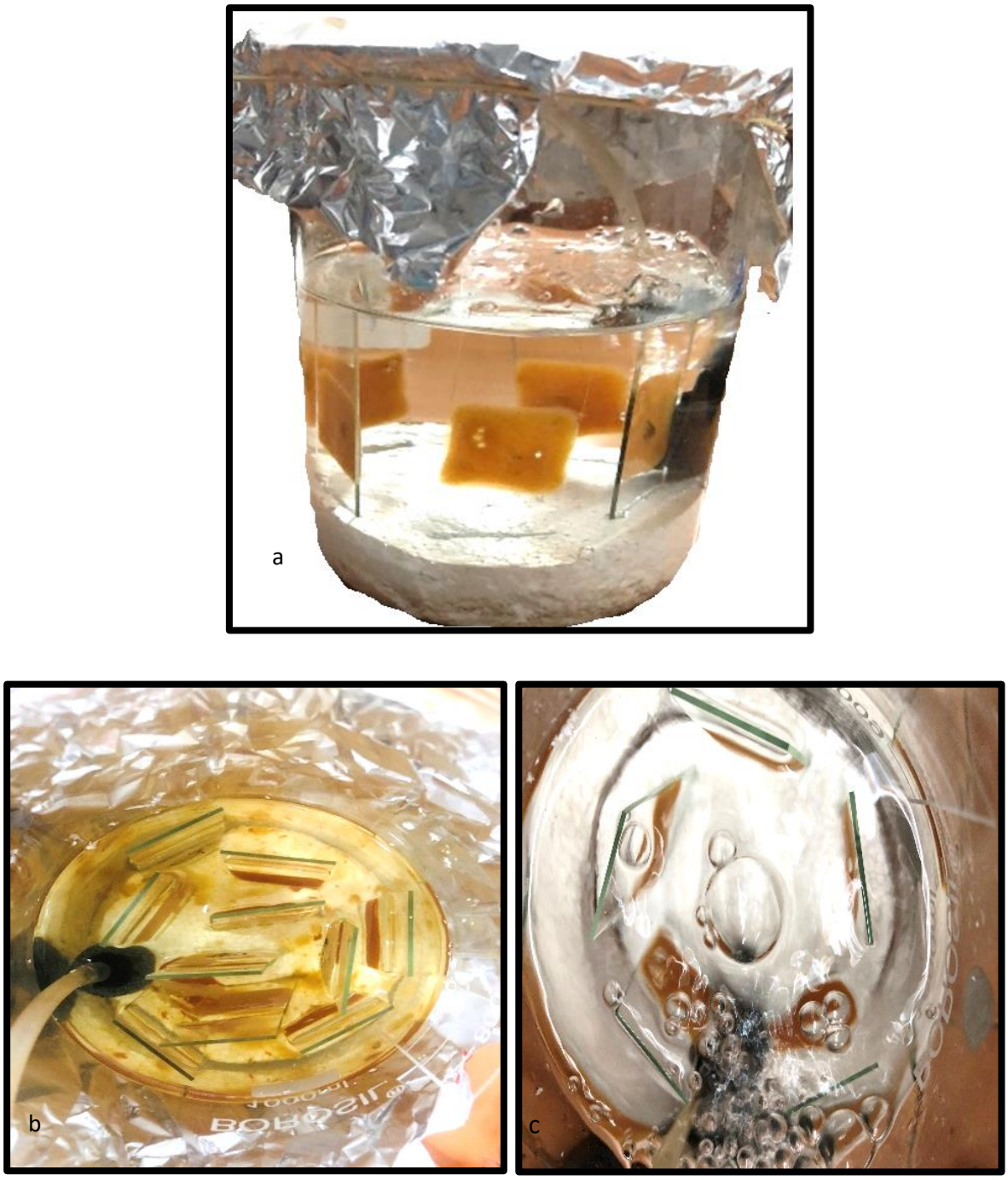

Figure 3.66 (a-c): Set up of immobilized system for biooxidation of Gold sulphide; b-Placement of the slides inside the beaker; c-external aeration as seen from the top

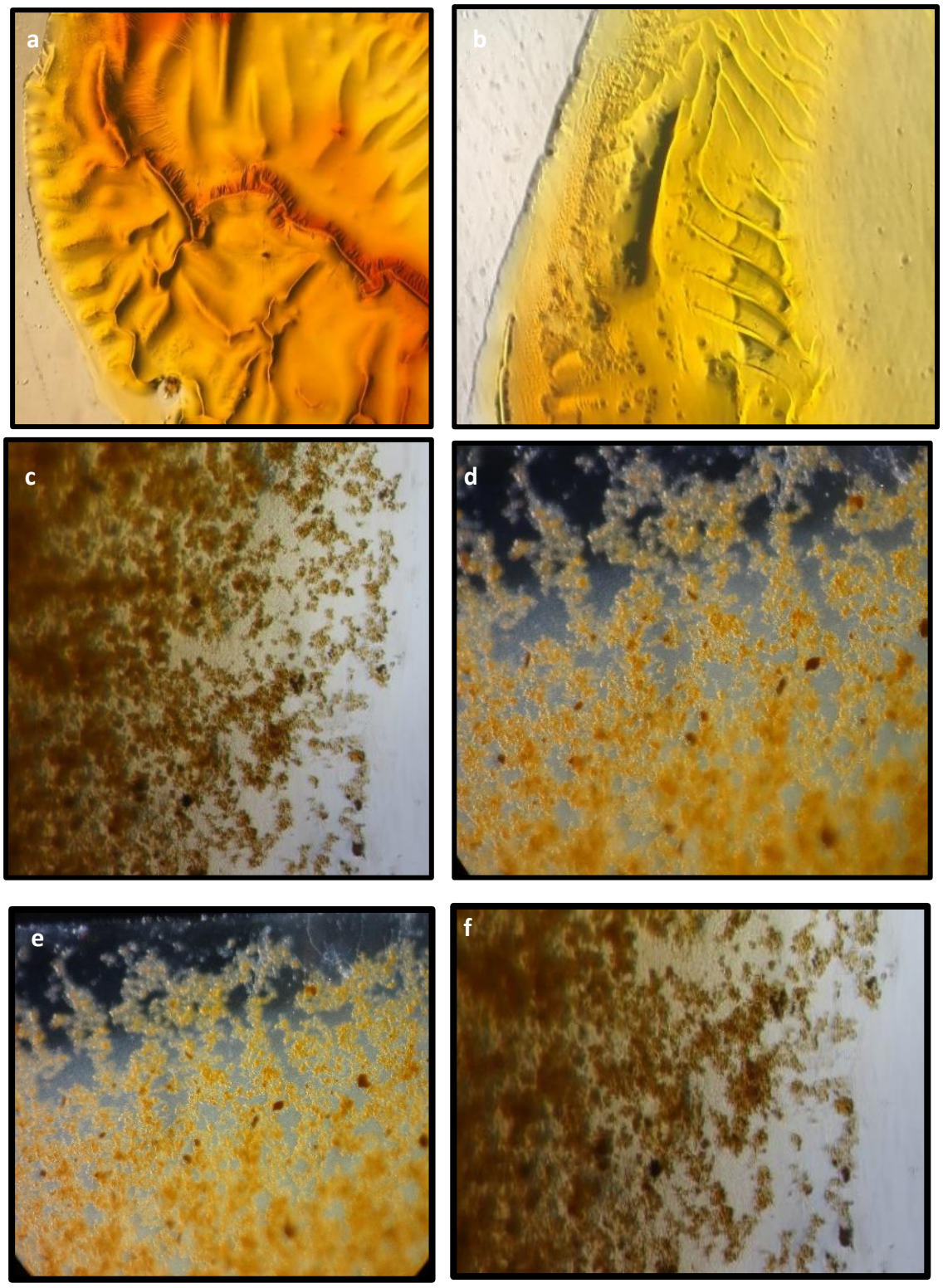

Figure 3.67(a-f): a,b-Film of Gold formed after dissolving in aquaregia indicating the formation of Gold; (c-f)- Gold formed at all the edges of the slide

CHAPTER IV

DISCUSSION

DISCUSSION

4.1. Selection of this topic

Goa forms the part of WDC which is India's major metallogenic province. The Iron ore occurs within the Ponda Group which has characteristics similar to Chitradurga Group of the Dharwad supergroup and with which it is correlated (Dessai, 2011). The former comprises predominantly greenstones (metabasalts) and rests on a basement of the 3300–3400 Ma Anmode Ghat trodhjemite gneiss with a crudely developed quartz-pebble conglomerate at the base, and shows lithological similarities with the lower part of the Bababudan Group. The conglomerate displays many similarities with conglomerate that occurs at the base of the Chitradurga Group (Dessai, 2011). There are reports that Goa forms the part of WDC and rocks found in Goa are similar to those found in Karnataka. These rocks are formed during Precambrian and shows the association of cyanobacteria in formation of rocks (Desai, 2018). Although a lot of work has been reported on detection and biomineralization of Gold (Sarkar & Nair, 2002; Biswas, 2021, Mohakul et al., 2021) in other parts of the WDC, there were no studies reported in Goa. Useful microorganisms associated with such samples can be isolated and studied further for their application in biotechnology and biomining.

4.2. Sample collection from mining and non-mining areas of Goa

The mining belt of Goa covers an area of approximately 700 sq. Kms, concentrated in four talukas namely Bicholim, Sattari, Sanguem and Quepem. Geochemical mapping has been carried out in Goa using soil/laterite and stream sediments (Ingale & Savoikar, 2022; Bhadke & Savoikar, 2021). Earlier studies have been reported on the geochemical maps for U, Th, Nb and Ta in the north western part of Goa around Usgaon area, east of Ponda, and this has indicated anomalous signature in the northern continuation of the Usgaon ultramafic complex (Purushothaman et al., 2009). Heavy mineral studies of beach sands of Vagator, North Goa,

India has been reported earlier (Sreenivasa et al., 2014). There are reports on mineralogy of beach and sand dunes of Morjim-Arambol beach of Goa (Kidwai & Wagle,1975). In this study we collected beach sands and beach placer samples from entire coastline of Goa starting from Keri in North and Pollem in South. The Goa group consist of green schist facies of metamorphic rocks and is divided into the Barcem formation, Sanvordem formation, Bicholim – Rivona formation. These formations comprises of basic and acid metavolcanics associated with Meta – tuffs of Meta sediments. The geochemical anomaly map has been prepared on the basis of 200 soil/laterite samples and 654 stream sediment samples (Purushothaman et al., 2009). The drilosphere of geophagous earthworms are involved in production of earthworm casts by dwelling inside soil and taking up of the organic and inorganic matters. Vermicasts were found to be mostly present under the tress and organically rich soils. The size, color of the vermicast varied depending on the size of earthworms and also type of soil. Stream sediments geochemistry and heavy mineral surveys are routinely used in the early stages of Gold exploration. Stream sediments were mainly explored from Madhai wild life sanctuary, Netravali wild life sanctuary, Bhagwan Mahaveer wildlife sanctuary and Mollem National parks. The forest is immense, luxuriant with a continuous canopy of leaves that shade the underneath from sunlight. Such vegetation is supported by daily high temperatures, rainfall and humidity all year as well as less seasonal and diurnal fluctuation. Laterite rock samples were studied for their geotechnical properties from boreholes at Dona Paula and Porvorim in North Goa (Ingale and Savoikar, 2022).

4.3. Detection of secondary Gold forms in auriferous samples

Gold occurs in India as lode Gold, in stratified sulphide deposits, in conglomerates, quartzites, in river placers, and in laterite /weathering profile (Radhakrishna and Curtis, 1991). The names such as suvarnarekha, Honnu hole, Suvarnavati, and Ponnu Puzza which means Golden stream indicated that Indian rivers are great source of alluvial Gold. There are reports on the occurrence of Gold as inclusion in amphiboles, in auriferous quartz and in the beach sands of Chavakkad-Ponnani, Kerala Coast (Nayak, 2011). In the Nilambur valley of Wynad Gold field in southern India, two types of Gold bearing gravels has been found, the older one which occurs at higher altitude and are rich in gold and other types which are the recent gravels (Santosh et al.,1992). Gold exploration in Niger using soils and termitaria has been reported (Gleeson & Poulin, 1989). The iron ore from BIF of Goa has not been subjected to multi-elemental analysis (such as Au, Ag, Pt including REE). In the present studies powdered, dried sieved fractions of the samples with the fraction size 150, 106, 53 µm showed high concentration of Gold and among this 106 µm was the most promising fraction and thus was used in further studies. **Table 4.1** gives the details of Gold reported in mining and non-mining regions of Goa showing the highest to lowest content. Present study have established that BHQ from Velguem, North Goa contains 12-13 ppm and BMQ from Sacorda was found to be 8.4 ppm whereas the Iron ore reject dumps from Shirgao contains 7.71 ppm which indicates that Gold values vary from 7-13 ppm in mining belts of Goa. The samples from non-mining areas also showed presence of Gold. The stream sediments from Bondla and Tambdi Surla showed Gold between range from 12.96-15.03 ppm. Sand sample showed very negligible Gold between 0.02-0.29 ppm. Earlier studies were on heavy mineral of beach sands of Vagator, North Goa (Sreenivasa et al., 2014). Studies on the placer deposits of Attappadi valley in southern India has shown the presence of both primary and secondary Gold grains, and both these forms are differentiated by marked contrast in micro textures and chemical corrosive cavities (Nakagawa et al., 2005). In this present study Gold in

placer deposits ranged from 0.76-1.08 ppm. In Moolart Well, Western Australia, Gold concentrations in termite nests contained high levels of Gold in higher concentrations in mound cores (2.4 ppb) and (mean 0.4 ppb) in soil 5 m from the nest (Stewart et al., 2012). Termite mounds have been reported as an effective geochemical tool in mineral exploration in Chromite mining area in Karnataka, India (Reddy, 2014). Occurrence of Gold in Guntipalli-Atkur area, Gadwal Schist Belt of Mahbubnagar district, in Andra Pradesh ranged from 0.025 to 0.07 ppm (Murthy & Bhattacharjee, 1997). In this study, the Gold in Termite mounds sample ranged from 0.66-6.85ppm. Earthworms play a major role in soil amendments, nutrient turnover and participate in the aeration as well as in mixing of various soil horizons. Earthworms are mentioned as one of the Uparasa in Indian Ayurvedic medicine due of its ability to uptake heavy metals. They are soil feeders and hyperaccumulators of heavy metals. There are studies on the bioavailability of Gold nanoparticles from soil and biodistribution within earthworms. All these results indicate that earthworms are involved in hyperaccumulation of heavy metals. Similar studies provided evidence for bioavailability of Gold nanoparticles from soil and biodistribution within earthworms (*Eisenia fetida*) and also trophic transfer of Au nanoparticles from soil along a simulated terrestrial food chain (Urine et al., 2012). Potentiality of earthworms as bioremediating agent for nanoparticles has been reported earlier (Yadav, 2017). Vermicast samples in Goa ranged from 0.66-6.85 ppm and this is the first report of Gold association in vermicast of Goa and India. In Nilambur region of south India, scientist have reported the occurrence of supergene Gold associated with laterites weathering upto 4.7 ppm (Nair et al., 1987), 0.05-2.9 ppm **(**Narayanaswamy & Ramkumar, 2004**)** where as in present study it was found that Gold in laterite ranged from 2-6.8 ppm. Laterite and powdery ore in Keri and Kalne, laterite and iron ores in Sindhudurg district showed the association of Gold values from 0.06 to 0.16 ppm and < 0.1 ppm Gold (Umathay, 1993). **Table 4.2** gives in details the Gold content reported in the present studies in India and other parts of the world.

Table 4.1: Detection of Gold in mining and non-mining areas in Goa

Designation	Samples	Au Ppm	Location
BS-01	**Beach Sand**	0.29	Keri
BS-02	**Beach Sand**	0.12	Mandrem
BS-03	**Beach Sand**	0.13	Morjim
BS-04	**Beach Sand**	0.02	Anjuna
BS-05	**Beach Sand**	0.1	Vagator
BS-06	**Beach Sand**	0.02	Miramar
BS-07	**Beach Sand**	0.28	Varca
BS-08	**Beach Sand**	0.03	Arossim
BS-09	**Beach Sand**	0.19	Cavellosim
BS-10	**Beach Sand**	0.17	Patnem
BS-11	**Beach Sand**	0.94	Pollem
PD-01	**River Sand**	0.88	Betki
PD-02	**River Sand**	6.28	Colvale
PD-03	**Monozitic Black Sand**	1.12	Chapora
TM-01	**Termite Mound**	1.13	Bondla
TM-02	**Termite Mound**	1.29	Tamdi Surla
SS-01	**Stream Sediment**	**12.96**	Bondla
SS-02	**Stream Sediment**	**15.03**	Tambdi Surla
VM-01	**Vermicast**	0.76	Taleigao
VM-02	**Vermicast**	0.87	Taleigao
VM-03	**Vermicast**	1.77	Shirgoa

VM-04	**Vermicast**	1.03	Usgoa
VM-05	**Vermicast**	0.76	Assnora
VM-06	**Vermicast**	0.66	Shiolim
LT-01	**Laterite**	**6.85**	Shirgao
LT-02	**Laterite**	3.78	Bambolim
RK-01	**Laterite**	2.83	Bondla
MR-01	**Mining Reject**	**7.71**	Shirgao
IO-01	**BHQ**	**10.35**	Shirgao
BH-01	**BHQ**	**12.93**	Velguem
BM-01	**BMQ**	**8.4**	Sacorda

Table 4.2: Detection of Gold in Goa, India and other regions of the world

State	Area and local geology	Gold reported	Reference
India Andra Pradesh	Gadwal Schist Belt	1. 0.035-4.25-Soil; 2. 0.025-0.07 ppm-Termite mound 3. 0.035-0.25 in ppm in meta basalt 4. 0.05-7.18 ppb-Termite soil	Murthy and Bhattacharjee,1997 Prasad et al., 1987
Maharashtra	1.1aterite and powdery ore, Keri and Kalne 2. laterite and iron ores, Sindhudurg	1. 0.06 to 0.16 ppm 2.< 0.1 ppm Gold	Umathay, 1993
Karnataka	Conglomerates, greywacke, (BIFs) and laterite Chitra Durga Schist Belt	3. Occurrence in sulphidic BIFs ranging from 0.7 to 3.2 g/t	Radhakrishna and Curtis 1999; Sawkar et al., 1995; Madusudan et al.,1994
Goa	1.Vermicast samples 2.Termite Mounds 3. Stream sediments 4. Beach Sand 5. BHQ 6. BMQ 7. Low grade iron ore (mining reject) 8. Laterite	**1. 0.66 to 1.77 ppm** **2. 2.83-3.78 ppm** **3. 12-15 ppm** **4. 0.02-0.87 ppm** **5. 12.93 ppm,** **6. 8.4 ppm** **7. 7.71 ppm** **8. 2-7 ppm**	Dabolkar and Kamat, 2019

Australia	1.Hillgrove Gold-antimony deposits 2. Ores	1. 255±1500 ppm Gold 2. 100 ppb to 1.1 ppm	Ashley et al., 2000
Canada	1. Magnetic sulphide 2. Sulfidic ores	1. <0.002 ppm 2. 0.11-10.9 ppm	Yang et al., 2006 McClenaghan et al.,2004
Africa	1.Birimian Gold depo sits, Ghana, West Africa 2. Quartz Vein	1. 2- > 30 ppm 2. 0.01-2.28 ppm	Dzigbodi-Adjimah, 1993 Mbenoun et al., 2021

4.4. Bacterioform Gold and Gold Geomicrobiology

Goldschmidt in the year 1954 suggested the dispersion and (re)concentration of metals in natural environments by biogeochemical processes. Microbial cell walls are identified as important structures separating intracellular and extracellular environments and also reported to play important role in mineral nucleation (Wang et al., 2021). Extracellular or intracellular formation of nanophase Au0 colloids or crystals occurs when microbes exposure to soluble Gold complexes often results in formation of secondary Gold structures. Cell envelopes of the bacteria function as kinetic factors that directly reduce soluble-Au complexes, forming elemental Gold in the form of nanophase colloids, as well as crystalline structures. Microbes capable of iron or sulfur oxidation/reduction are considered important contributors to Gold biomineralization, because the cycling of these elements is closely linked to the biogeochemical cycling of Gold. Some metal-resistant microbes, such as the *bacterium, Delftia acidovorans*, are known to contribute to Gold biomineralization by excreting secondary metabolites into the extracellular environment to bind and reduce soluble Gold (Reith et al., 2013). *Cupriavidus metallidurans* contributes to the bacterial diversity of biofilms living on the surface of Gold particles from numerous sites, worldwide (Fairbrother et al., 2013; Rea et al., 2016; Shuster & Reith, 2018). Additionally, secondary Gold structures can be physically altered during mechanical re-shaping, which suggests a balance between (bio) geochemical and mechanical weathering processes. Secondary Gold structures are physical evidence of past, biogeochemical processes that have transformed particle surfaces and have attributed to the activity of microbes (Shuster & Reith, 2018). Secondary Gold structures are nanometre–micrometre-scale features that occur on Gold particles. With increasing sophistication of electron microscopes, the characterization of these secondary Gold structures has greatly improved, thereby providing a better understanding of Gold particle transformation. Secondary Gold structures can be broadly categorized into two groups, based on the processes that contribute to their formation. The two

groups include Au/Ag dissolution and Au reprecipitation. Biogeochemical processes that drive the cycling of Gold and contributes to the transformation of Au particles depending on the balance between these two groups. The solubilization of Gold and Silver from Gold particles (for example, by dealloying or bacterially-catalysed solubilization) leads to the formation of dissolution features which include striations, porous structures, and bacteriomorphic Gold (Reith et al., 2013; Rea & Reith, 2016; Shuster & Reith, 2018; Wang et al., 2021). Dissolved Gold occurs as soluble-Au complexes that can be directly reduced by bacteria or other organic/inorganic reductants, to form pure, Gold nanoparticles. While these nanoparticles often appear quasi-spherical in shape, they are actually nanophase crystals. At micrometer-scales, euhedral crystals are more clearly-defined and variability in structures is apparent. Additionally, secondary Gold structures can be physically altered during mechanical re-shaping, which suggests a balance between (bio)geochemical and mechanical weathering processes. In a field-based approach, the morphology of secondary Gold grains that display 'bacterioform' structures has been used as evidence for microbial Gold precipitation and biomineralization in the environment (Watterson, 1992). The ability of *C. metallidurans* to actively accumulate Gold from solution was successfully tested suggesting that *C. metallidurans* may contribute to the formation of secondary Gold grains (Reith et al., 2006). *Cupriavidus metallidurans* and *D. acidovorans* were detected in biofilm communities on Au grains from moderate and tropical climates in Australia (Reith et al., 2006, 2010). The ability of sulphur-oxidizing and reducing (Lengke and Southam, 2006) bacteria to transform Gold complexes into octahedral Gold, suggests that bacteria contribute to the formation of Gold platelets in the supergene environment. Research in Gold (Au) geomicrobiology has developed extensively over the last ten years (Shuster & Reith, 2018) and plays role in a global Gold Biogeochemical cycle.

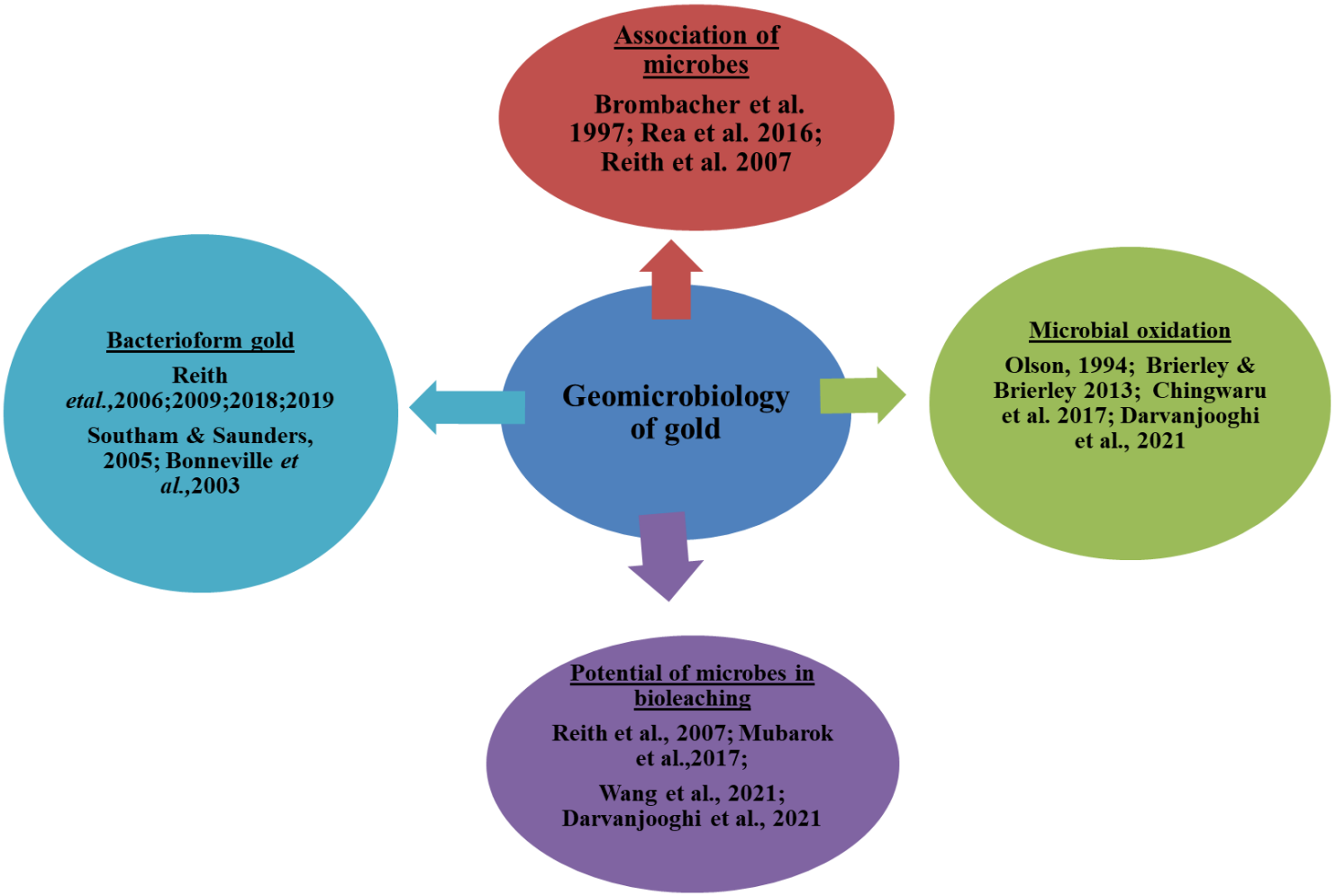

Fig 4.1. Geomicrobiology of Gold

4.5. Micromorphology and typological classification of BFG forms

Numerous specimens from different locations in Australia, South America and Canada have been studied, and many of the crevices in Gold grains were covered by Pedomicrobium-like pseudomorphs similar to those described from the Alaskan specimens (Bischoff et al., 1992; 1997; Reith, 2005; Reith et al., 2006). There were no reports on the morphological and typological classification of the auriferous samples from Goa. In this study the morphological and typological studies of BFG particles showed that the size varied ranging from 10 μm to 100 μm. BFG particles studied in each fraction per slide were between 5000 to 10,000. The color of the BFG particles ranged from yellow, lemon yellow, canary yellow, Golden yellow, and orange to red. Scanning Electron Microscopy (SEM) helped to reveal the size, shape and topography of the Gold particles. The shapes include rods, triangles, cubes, spherical, irregular shapes. The fraction size 150 μm showed less diversity in shape as compared to other fraction. Mostly irregular shapes were noticed on the surface of the BFG particles. The presence of bacterial fossils or Gold nanoparticles on BFG's and other Gold particles were observed on some of the samples. Triangular plate form Gold was found to be appearing on the surface of Gold, similar observations in Australian samples (Reith et al., 2013, 2018). The cylindrical rod shape BFG particles with a rough surface was found showing the influence of weathering. The auriferous fractions also showed the presence of xenomorphic single Gold grain with irregular and rough surface. Typological classification of microbioform secondary Gold shows the irregular BFG particles with smooth surface showing presence of bacterial fossils or Gold nanoparticles on the surface and irregular BFG with rough surface. Octahedral and 'triangular' shapes have been reported in these studies which matches with the earlier reports (Clough and Craw, 1989; Falconer et al., 2006). Morphology of the Gold particles reported in samples in other parts of the world is shown in **Table 4.3**.

Table 4.3: Morphology of the Gold particles showed in samples in other parts of the world

Shapes of Bacterioform Gold particles	**References**
Complex forms such as clusters, superclusters, clusters of stars, crowns	Townley et al.,2003
Triangular plate form Gold was found to be appearing on the surface of Gold	Reith et al., 2013
The cylindrical rod shape BFG particle with a rough surface. The auriferous fractions also showed the presence of xenomorphic single Gold grain with irregular and rough surface, similar presence of xenomorphic Gold grains	Suh et al., 2022
Morphologies include wire, dendritic, octahedral, porous and sponge Gold	Reith et al., 2007; Southam et al., 2009; Fairbrother, 2013
Gold-encrusted microfossils on placer Gold specimens from Lillian Creek in Alaska, and postulated a biological mechanism for the formation of Gold grains	Watterson,1992; Southam et al., 2009
Bud-like Gold growths are common on the surfaces of authigenic Gold which has been reported in New Zealand.	Falconer et al., 2006

4.6. Use of Metagenomic techniques to study the BHQ and BMQ samples

Metagenomic analysis served as a useful technique to study the microbes associated with the BIF samples of Goa. BHQ and BMQ which were tested for presence of microorganisms were showing the positive results. The number of sequences reads from the BHQ were 37,618. In case of BHQ, reads analyzed were 18,809, reads classified were 669 whereas the remaining reads were unclassified and were 18,140 in number. BHQ sample showed presence of 71% bacteria, 27% Eukaryota and 1% archaea. In case of BMQ, reads analyzed were 36,379, reads classified were 1,016 and reads unclassified were 35,363. Sample showed presence of 69% of Bacteria, 30% of Eukaryota, <1% of archaea and <1% viruses. This is the first study on the metagenomic analysis of BIF of Goa. In both the samples the bacterial association was high as compared to Eukaryotes, archaea and similar studies have been reported earlier (Rea et al., 2016). In the study we have reported useful microorganisms associated with the BHQ and BMQ samples as seen in **Fig.4.2a** and **Fig.4.2b**. There are reports on microorganisms involved in the development and effect of Au-cycling biofilm on Gold grain surfaces. *Staphylococcus, Corynebacterium* are involved in conditioning of surfaces to their attachment (Rea et al., 2016). Microorganisms such as *Pseudomonas, Burkholderia, Methylobacterium, Acinetobacter, Rhodobacter* the recruitment of phototrophic and heterotrophic Gram-negative bacteria are involved in EPS production and Au aggregation (Rea, 2018). The proliferation and growth of biofilm community including heterotrophic and metallophillic species such as *Rhodobacter* sp, *Rhizobium* sp, *Achromobacter* sp, *Methylobacterium, Achromobacter, Pseudomonas* sp. It was found that both the sample BHQ and BMQ showed the association of microorganisms. Overlapping of bacterial community in case of both BHQ and BMQ is shown in **Fig 4.2c.** Metagenomic analyses can provide extensive information on the structure, composition, and predicted gene functions of diverse environmental microbial assemblages. One strength of the metagenomic approach is in enabling researchers to investigate the phylogenetic and functional

diversity of microorganisms at the community level, independent from cultivation-associated biases (Schloss and Handelsman, 2003; Cowan et al., 2005). Metagenomics (16S amplicon sequencing) and DGGE analysis of bacterial diversity of acid mine drainage has been studied earlier (Yaman et al., 2020). For instance, *Bacillus cereus*, a common soil bacterium, has been shown to act as a biogeochemical indicator for concealed mineralization. Resident organotrophs are likely to metabolize a wide range of complex organic compounds commonly found in placer environments, e.g., low and high molecular weight organic acids especially, *Acinetobacter* spp., *Burkholderia* spp. (Xie and Yokota 2005). Microorganisms such as *Burkholderia, Methylobacterium, Acinetobacter, Rhodobacter* and heterotrophic Gram-negative bacteria are involved in EPS production. The proliferation and growth of biofilm community including heterotrophic and metallophillic species such as *Rhodobacter sp, Rhizobium sp, Achromobacter sp. Methylobacterium, Achromobacter,* play role in mobilization, detoxification and re-precipitation of secondary Au; and *Acinetobacte*r play role in seeding of dispersal cells with release of nano-particle and Au complexes (Rea et al., 2016). Association of *Chromobacterium* with samples can be useful source of natural cynide production which can be applied in Biomining (Campbell et al., 2001; Liang et al., 2014). Such microorganisms can help to know their role in formation of BIF. In this study we have reported archea *Haloferax* which are isolated from high saline environments. Earlier studies are reported from Dead Sea (Oren, 1993), solar salterns (Asker and Ohta, 2002; Xu et al., 2007), salt lake (Enache et al., 2008, Kumar et al., 2015) and Permian potassium salt deposits (Saralov et al., 2013). Equilibrium and Kinetics of Adsorption of Mn^{2+} by Haloarchaeon *Halobacterium* sp. GUSF (MTCC3265) has been reported from salt pans of Goa (Naik and Futardo, 2013). Isolation of a Halophilic, Bacteriorhodopsin-producing Archaeon, *Haloferax larsenii* RG3D.1 has been also reported from the Rocky Beach of Malvan, West Coast of India belonging to Bababudan group of the type area (Kanekar et al., 2017). There are reports that Goa forms part of WDC and rocks

found in Goa are similar to rocks found in Karnataka and are formed during precambrium and shows the association of cyanobacteria in formation of rocks in Goa (Desai, 2018). Acidophilic microorganisms capable of oxidizing iron and sulfur can be employed in industrial processes to recover metals from minerals. Biosensors can be developed on how microorganisms interact with Gold complexes which may further support exploration. This knowledge of bacterial diversity can be useful in Biomining, biogeochemistry, biohydrometallurgy of heavy metals (Pandey and Natarajan, 2015). Metagenomic studies could represent the endolithic communities associated with this samples. This study was done to get the idea of structure of microbial communities both being major iron ore exported in Goa and fill the major knowledge gap between these deposits. Samples were insulated from external environment and exposed during open cast mining. Metagenomic studies were carried out for the first time on auriferous samples.

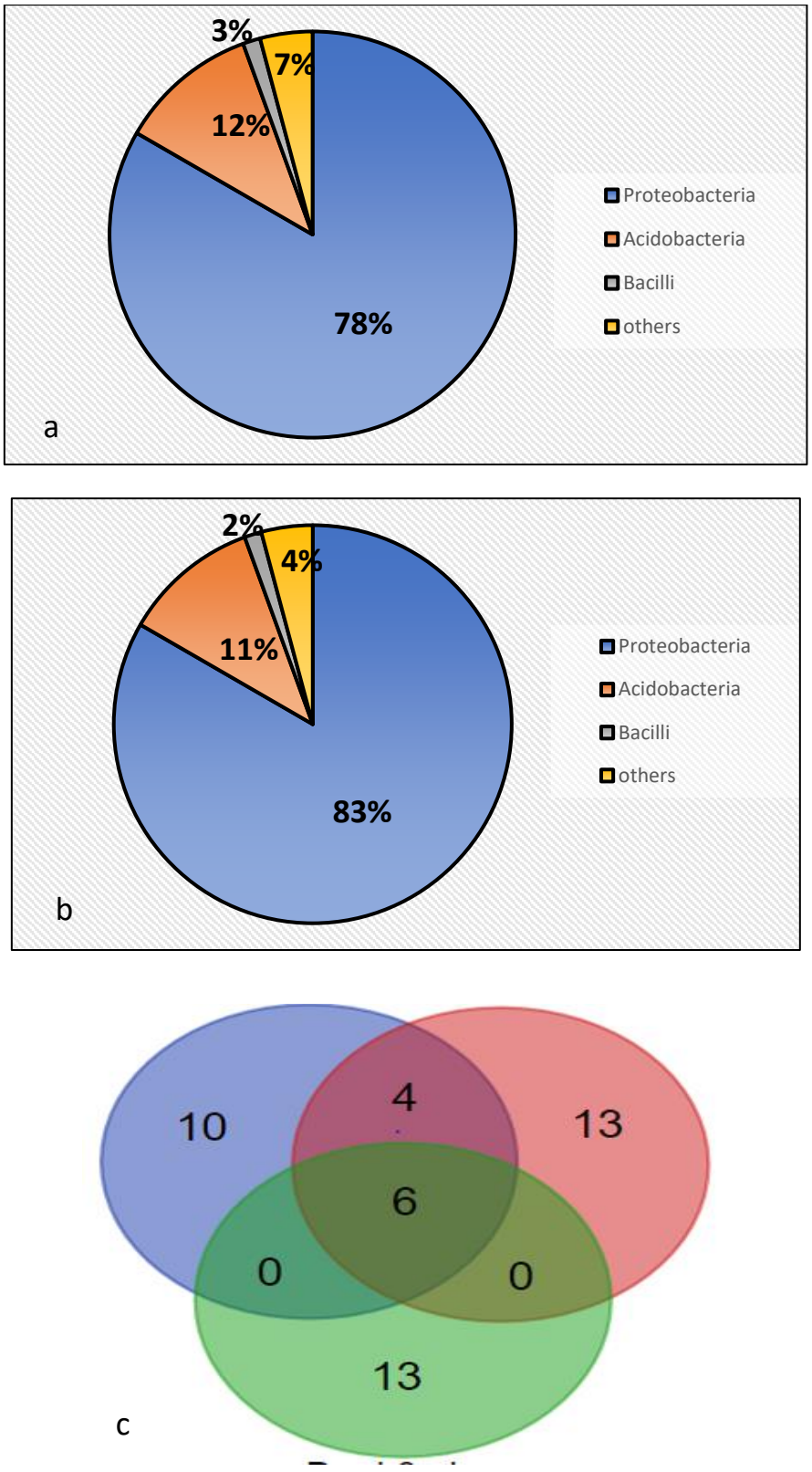

Figure 4.2 (a-c): a, b-Eubacterial members in the case of BHQ and BMQ; c- Number of overlapping Taxa in both samples

4.7. Use of Winogradsky Microcosm (WGMC)

We were successful in use of Winogradsky Microcosm (WGMC) by modification using simple, low-cost PET bottles. After prolong incubation in dark followed by exposure to light, interesting-coloured zones were identified in 24 columns from six samples indicating differential colonization of biofilms of Iron and Sulphur bacteria. The Winogradsky column is a miniature ecosystem in which microorganisms and nutrients interact over time. As oxygen diffuses downward from the surface, fermentation products from the breakdown of cellulose and hydrogen sulphide diffuse upward from the reduced lower zone (Prescott et al., 1996). After prolong incubation in dark followed by exposure to light, interesting-coloured zones were identified in 24 columns from six samples indicating differential colonization of biofilms of Iron and Sulphur bacteria. Biofilms are interface-associated colonies of microorganisms embedded in a matrix of extracellular polymeric substances (EPS) consisting of biopolymers like polysaccharides, proteins, lipids and nucleic acids (Costerton et al., 1995; Flemming and Wingender, 2010). Depending on the energy sources available, photosynthetic microbes, facultative chemo-organotrophs, or sulfate-reducing microorganisms may be present (Prescott et al. 1996). *Acidithiobacillus obtain* their energy through the oxidation of ferrous to ferric iron or through the reduction of inorganic sulphur compound to sulfate. Similar studies were carried out by Janet and Holmes in 1988. *Acidithiobacillus thiobacillus* is an autotrophic, acidophilic, mesophile occurring in single cells or occasionally in pairs or chains, depending on growth conditions (Bellenberg et al., 2012; Khan et al., 2012). Biofilms are interface-associated colonies of microorganisms embedded in a matrix of extracellular polymeric substances (EPS) consisting of biopolymers like polysaccharides, proteins, lipids and nucleic acids (Costerton et al., 1995; Flemming and Wingender, 2010). Rod shape cells of *Acidithiobacillus* (1000x) were obtained. Biofilms formed by chemolithotrophic leaching rowing on the *lepstopirillum* microorganisms on metal sulphides surfaces have an important influence on dissolution of the

substratum and consequently for bioleaching efficiency (Rohwerder et al., 2003). We were successful in use of Winogradsky in research experiments (Hairston, 1999; Loss et al., 2013; Parks, 2015). Successful in enrichment of microbial biofilms of Iron and Sulphur bacteria from different local mineral samples. Similar studies were carried out previously (Rawlings et al., 2013; Olson et al., 2003). Interesting coloured zones were identified in 24 columns from six samples indicating differential colonization of biofilms of Iron and Sulphur bacteria. we were successful to isolate useful cultures of particularly *Acidithiobacillus, Leptospirillum* and *Sulfobacillus* spp. which were identified tentatively. These cultures have excellent potential in bioleaching of Gold sulphides and green synthesis of pure Gold (Johnson, 2014; Hedrich et al.,2020). The abilities of acidophilic chemolithotrophic bacteria and archaea to accelerate the oxidative dissolution of sulphide minerals have been harnessed in the development and application of a biotechnology for extracting metals from sulfidic ores and concentrates. Biomining is currently used primarily to leach an oxidative pretreatment for refractory Gold ores. Recent developments have included using acidophiles to process electronic wastes, to extract metals from oxidized ores, and to selectively recover metals from process waters and waste streams (Johnson, 2013; Ehrlich, 2001; Van Aswegen et al., 2007; Rawlings and Johnson, 2007). Our technique is claimed to be potentially helpful to Indian researchers to build an indigenous collection of industrially useful, diverse and chemically creative strains of Iron and Sulphur bacteria. **Fig 4.3** shows how national culture collection of chemolithotrophs can be built up using Winogradsky column.

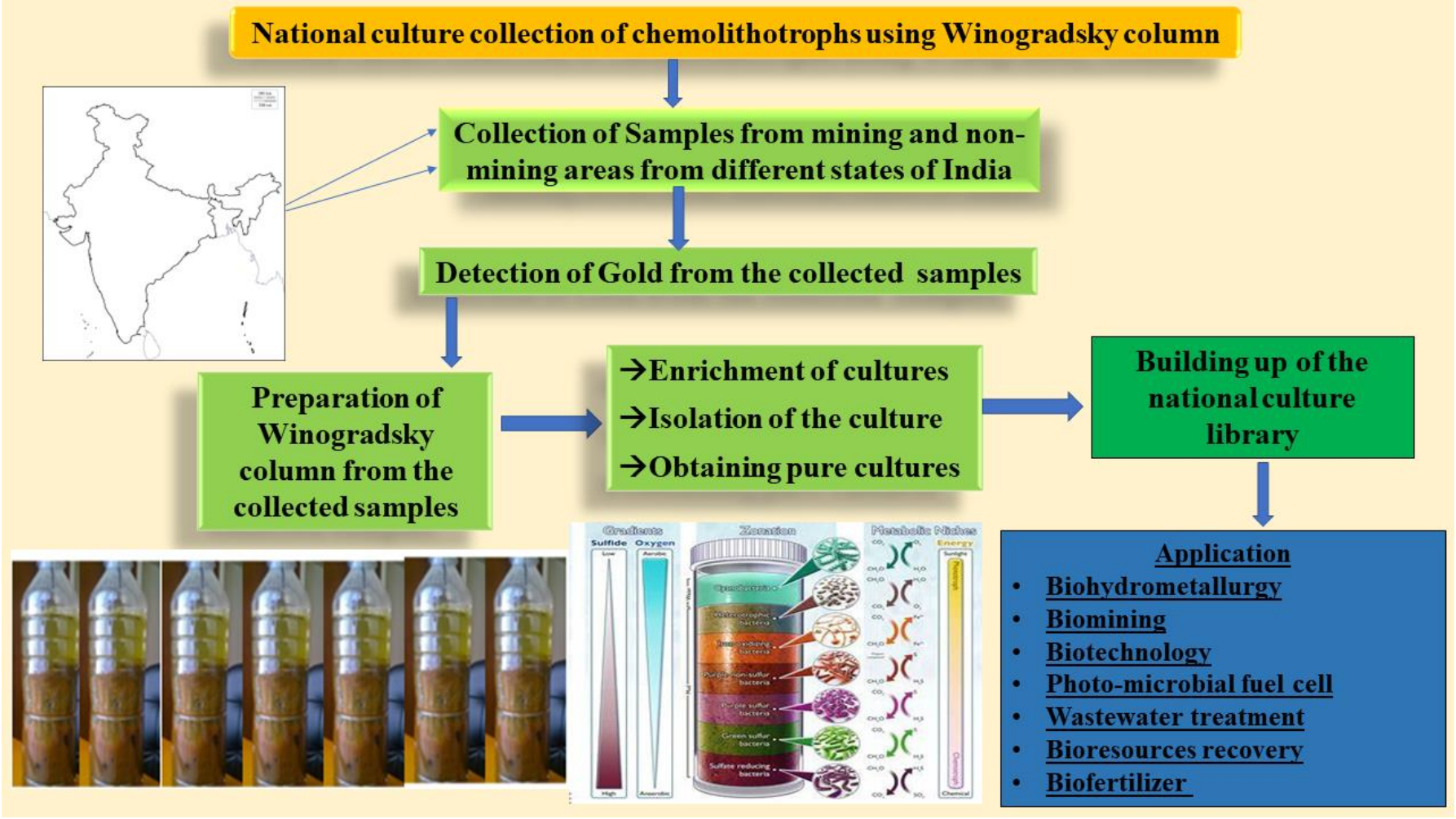

Figure 4.3: A postulated scheme for National culture collection of chemolithotrophs using Winogradsky column

4.8. Isolation of actinobacterial cultures from auriferous samples

Isolation of actinobacteria was carried out and total 30 isolates were obtained. The isolated strains were classified into various genera based on the spore morphology and mycelium. The colonies grown on oat meal agar showed a flat and hard texture. The aerial mycelial showed abundant growth after 10 days of incubation which were cream in colour. The microscopic character showed the presence of vegetative hyphae and spiral spore chains. Out of the 30 actinobacterial isolates, 12 isolates were tentatively identified as genus *Streptomyces* (spore chain with coiling, spiral and looped), 10 isolates as *Nocardia* and 10 were unidentified actinobacterial strains. Among the genera recorded in the present study, *Streptomyces* was the most predominant as compared to others in all the samples. The dominance of *Streptomyces* among the actinobacteria especially in soils has also been reported earlier (Velho-Pereira and Kamat, 2011; Hazarika & Thakur, 2020). Earlier studies have been reported on digital image analysis of actinomycetes colonies as a potential aid for rapid taxonomic identification (Velho-pereira and Kamat 2010) and biosurfactant, heavy metal resistance activity of *Streptomyces* spp. isolated from saltpan soil (Deepika et al., 2010; Ballav et al., 2015). Such fertile samples can be thus used for the isolation of micro-organisms, which can be further used in nanoparticle synthesis and biotechnology.

4.9. AuNPs synthesis using Actinobacteria

Actinobacterial biosynthesis of nanoparticles is a reliable, eco-friendly, and important aspect of green chemistry approach that interconnects microbial biotechnology and nanobiotechnology (Manivasagan et al., 2016). Actinobacteria are efficient producers of nanoparticles that show a range of biological properties such as antibacterial, antifungal, anticancer, anti-biofouling, anti-malarial, anti-parasitic, antioxidant, etc. It was found that the extracts of the actinobacterial cultures were found to be biosynthesizing nanoparticles on slide-

based assay. Among the actinobacteria, *streptomycetes* group is considered economically important because, out of the approximately more than 10000 known antibiotics, 50–55% is produced by *Streptomyces* (Chater, 1993; Manivasagan et al., 2016). Recently, actinobacteria isolated from different ecosystems have been recognized as the potential synthesizers of metal nanoparticles and biosynthesis of nanoparticles has been reported in *Thermomonospora* sp. (Ahmad et al., 2003a), *Streptomyces avidinii* (Park et al., 2006), *Streptomyces hygroscopicus* (Sadhasivam et al., 2012), *Rhodococcus* sp. (Ahmad et al., 2003b), *Streptomyces viridogens* (HM10) (Balagurunathan et al., 2011), *Nocardia farcinica* (Oza et al., 2012), *Streptomyces* sp. (Karthik et al., 2014), *Nocardiopsis* sp. MBRC-1 (Manivasagan et al., 2013a). As the time interval and thermal treatment increased the production of the AuNPs increased and thermal treatment led to the production of a complexed assemblages of GNPs. Thus, cultures exo polysaccharides can be used as Gold biosensors for detection of small amount of Gold in a sample. Polysaccharides have hydroxyl groups, a hemiacetal reducing end, and other functionalities that can play important roles in both the reduction and the stabilization of metallic nanoparticles (Park et al., 2011). Both monodispersed and polydispersed type of nanoparticles were produced. 45 sec thermal treatment showed most promising results. Cell Free Extract (CFE) showed good results compared to cell cultures. The results shows that a simple, glass slide based technique can be successfully used for rapid production, microscopic visualization, morphological analysis, study of swarming behavior and monitoring of effect of heat on Au NPs and Au MPs forms and assemblages using cell free microbial system.

4.10. AuNPs synthesis using *Termitomyces* spp by Bioinspired Microfluidics assay

Synthesis of nanoparticles using edible and medicinal mushrooms has emerged as an interesting field of research as these macrofungi act as eco-friendly biofactories that secrete enzymes essential for reduction of metal ions into their zerovalent or nano-form. Apart from being an

environmentally friendly, the nanoparticles synthesized using mushrooms exhibit higher stability, longer shelf life and enhanced biological activities. While the mechanism of synthesis is still not fully understood, reports suggest that fungal reductases and flavins have a major role to play. Microwell test plate was used to produce nanoparticles using fungal tissues. It was found that all body parts of the mushrooms were producing GNPs. Swarms were produced. Umbonal tissue produced autonomous swarms, self-recognition, identical, monodispersed GNPs. They were found to be producing islands and were rotating to get stable state. Other body parts of the mushrooms also successfully produced GNPs. The purple colour change indicates the production of nanoparticles. CIE chromaticity values ranged from L (16-75), a (3-33) and b (1-46) thus indicating the lightness from black to white, green to red and blue to yellow similar results were noticed in case of color difference amplification between GNPs in colorimetric analysis with actively controlled multiband illumination (Cheng et al.,2014). Choma values ranged from 4 to 47 and hue values from 40 to 199 indicating the strength or dominance of the hue, the quality of a color's purity, intensity or saturation (http://www.huevaluechroma.com/018.php). In the novel microfluidics-based assay system performed during the present investigations to detect Gold bioreduction capacity of different tissues from mature fruitbodies of *Termitomyces heimii*, viz. umbonal tissue, pileus context, lamellae, stipe context, stipe epicutis, pseudorrhiza context, pseudorrhiza epicutis (Kalia and Kaur, 2018; DeSouza and Kamat, 2017; 2018; 2019) in tissue based and cell free environment resulted in the production of GNPs for the first time. Success was also achieved in producing membrane filtered SWSE from the same tissues and GNPs from the same extracts. This assay is quite useful in working out large number of replicates under sterile forms. Microtest plates can be directly visualized due to their transparency and swarms can be directly characterized under stereomicroscope. Small amounts of Gold solutions and SWSE can be tested using this microfluidic assay. This assay is also useful in rapid screening of large number of biological or

microbiological Gold bioreduction systems. Preliminary characterization of GNP swarms, as has been melanin from edible mushroom *Termitomyces* attempted during the present investigations while working with *T. heimii*, is quite important. In comparison, high throughput screening systems are wasteful and time consuming but preliminary characterization can also help in standardization of the procedure and also there is no waste resources.

4.11. Selection of *Termitomyces heimii* as promising bioreducing culture

It was found that as compared to Actinobacteria, *Termitomyces heimii* was showing better results. *Termitomyces heimii* being the most dominant species in Goa and state mushroom of Goa was used for the present investigations. It can be grown on large scale in form of pellets and can be useful at large scale production of GNPs. Whereas for isolation of actinobacteria expensive AVA media, antifungals and antibiotics is required. Isolation of actinobacteria is also time consuming. The fungal GNP synthesis system has several advantages when compared to other microbial systems as the fungal mycelial mesh can withstand higher flow pressure and agitation in bioreactors or other chambers. As compared to bacteria, the use of fungus is more advantageous since they provide good biomass and easy recovery and have fewer requirements of additional steps to extract the filtrate (Srivastava & Bhargava, 2021). The fungal mycelium has proven to be quite sturdy in withstanding adverse conditions compared to other prokaryotic entities and even plants specially during culturing in bioreactors during the nanofabrication process (Srivastava & Bhargava, 2021).

4.12. Characterisation of GNPs based on spectroscopic techniques

UV–visible spectroscopy is most commonly used technique for characterization of noble nanoparticles which confirm the formation of nanoparticles and their stability. UV–vis spectroscopy is usually the first technique which is used in characterization of metallic nanoparticles because of surface plasmon resonance (SPR) phenomenon (Smitha et al., 2009).

Surface plasmon resonance is a collective excitation of the electrons in the conduction band around the nanoparticle surface. Therefore, metallic nanoparticles display characteristic optical absorption spectra in the UV–vis region (Fayaz et al., 2009, 2011). The wavelength ranging from 200–800 nm is usually used for characterization of nanoparticles in size range of 2–100 nm. The strong surface plasma absorption band in the range of 500–550 nm is used in characterization of Gold nanoparticles (Song et al., 2009; Srivastava et al., 2013). UV-VIS spectroscopy involves the absorption of light by molecules in the UV-Vis region and can be used to determine the color changes and concentration of the formed NPs solution based on the absorbance. Generally, AuNPs are absorbed in the visible region of the electromagnetic spectrum at 510–570 nm because of SPR transition. Metal NPs have free electrons, which cause an SPR absorption band because of their combined vibration in resonance with the light wave. An SPR spectrum for AuNPs was obtained at 552 nm. The results were similar in case of Gold nanoparticles produced using chloroauric acid and crude extract of chloroauric acid indicating that *Termitomyces heimii* can act as good bioreducing agent for both. The mixture color of the aqueous extract of (1 mM) changed from yellow to purple after 25 min. This change serves as evidence for the synthesis of AuNPs from the mushroom due to the behaviour of these NPs in the absorption of the UV-Visible (Sriram et al., 2014). This agrees with the results of mycosynthesized AuNPs from the oyster mushroom *Pleurotus cornucopiae* (Owaid et al., 2017). X-ray Diffraction spectroscopy is the important to know the exact crystal structure of the Gold particles formed and this can be achieved by measuring the XRD spectrum of the samples. XRD peaks at 38.2°, 44.5°, 64.7° and 77.7°can be indexed to the (111), (200), (220) and (311) reflections of FCC (face centered cubic) structure of metallic Gold respectively (JCPDS no. 04-0784) which reveals that the synthesized Gold nanoparticles are composed of pure crystalline Gold. The presence of intense peaks corresponding to the (111), (200), (220) and (311) Bragg reflections of Gold (identified in the diffraction pattern) agree with those

reported for Gold nanocrystals. An estimate of the mean size of the Gold nanoparticles formed in the cells was made by using the Debye–Scherrer equation by determining the width of the (111) Bragg reflection (Ahmad et al., 2003). The XRD spectrum shows two predominant peaks that agree with Bragg's reflection of AuNPs reported in a previous study. Diffraction peaks, which appeared at 31.6°C and 45.4°C corresponded to the (111) and (200) planes. No extra peak was observed in the diffraction peaks, which indicates that the as-prepared AuNPs were highly purified without any contamination in case of Gold nanoparticles produced using pure chloroauric acid but there were impurities seen in case of nanoparticles produced using crude extracts. Four different intense peaks at 2θ angle: 38.22, 44.42, 64.71, and 77.62 with Bragg reflections corresponding to (111), (200), (220), and (311) in biomass-associated AuNPs. Alternatively, only a single prominent peak was observed at 2θ angle: 38.22 with a Bragg reflection corresponding to (111) in extracellular AuNPs. Similar results were shown by the Gold nanoparticles produced by the crude chloroauric acid. Our present findings are consistent with earlier studies that used biological methods to synthesize AuNPs using plant extracts (Chelly et al., 2021), yeast (Krishnan et al., 2021), and bacteria (Kalimuthu et al., 2020; Sathiyaraj et al., 2021). Characterization using Zeta Potential and Dynamic light scattering reflects the potential difference between the EDL (electric double layer) of electrophoretically mobile particles and the layer of dispersant around them at the slipping plane. The stability of Au-NPs was performed using zeta potential. A zeta value of ±30 mV is needed for a suspension to be physically stable while ±20 mV is necessary for a combined electrostatic and steric condition. The reading of Au-NPs formed reduced to −21.07mV. Thus, Au-NPs formed show an acceptable stability with reading not less than the required stable expression (https://nanocomposix.com/pages/Gold-nanoparticles-physical-properties). In case of nanoparticles produced using crude extracts the zeta potential was found to be −13.48 mV

which indicates that these nanoparticles were less stable as compare to nanoparticles synthesized using pure chloroauric acid.

4.12.1. Characterization of GNPs based on FTIR

Mushrooms are rich in proteins and have high availability of the amino acid's lysine, tryptophan, glutamic acid and aspartic acid (Manzi et al., 2002; Ribeiro et al., 2008; Tagkouli et al., 2020). The major volatile constituents (Cateni et al., 2021; Selli et al., 2021) of mushroom extract are octanones, octanols and benzaldehyde. Polysaccharide/oligosaccharide complex has been reported in certain mushroom extract (Leong et al., 2021; Liu et al.,2021). In addition to these, mushrooms contain minerals like P, K, Cu, Se and Mg and nutrients like thiamine, riboflavin, niacin, folate, pantothenic acid and biotin. FTIR measurements were carried out to identify the possible biomolecules responsible for capping and efficient stabilization of the metal nanoparticles synthesized using mushroom extract. Chemically significant regions of FTIR called spectral windows were identified which included fatty acid region dominated by C–H (3450 –2850 cm^{-1}); amide region dominated by C=O amide I and N–H amide II bands of proteins and peptides (1800–1500 cm^{-1}); Mixed region (1500–1200 cm^{-1}); polysaccharides region (1200–900 cm^{-1}); true finger printing region (900 to 700 cm-1) (Das et al., 2007; Dziuba et al, 2007). As clearly observed in the spectrum, several absorption peaks were centered at 607, 1073, 1299, 1392, 1547, 1632, 2925, 3271 cm^{-1}.The AuNPs synthesized by pellets of *Termitomyces* mushroom and chloroauric acid were subjected to FTIR analysis to identify the biomolecules involved in stabilizing the nanoparticles in solution and the absorption peak centered at 1070 cm−1 referred to the C-O stretch vibration, which could be related to the Ester linkages, β (1→3) glucan, cell wall polysaccharide, 1315 cm−1 was corresponded to the O-H bending polysaccharide, Amide III, 1424 cm−1 was corresponded to the O-H bending polysaccharide. The intense peak at 1547 cm−1 was related to N-H bending -Amide II, chitosan.

The peak at 1652 cm−1 was related to amide I, which was created because of the vibrations of carbonyl stretch bonded to the protein. It seems that the proteins have binding ability with Au ions, which in turn creates a surrounded layer on the AuNPs and acts as a capping agent to decrease AuNP agglomeration and increases their stability in the medium (Carnovale et al.,2016; Lee et al., 2020; Sarfraz & Khan, 2021). The AuNPs synthesized 2916 cm−1 represents CH3, CH2 stretching and peak at 3271 cm−1 represents O-H stretching vibration of hydroxyl groups, Amine N-H stretching. Additionally, the bands at 3400 cm−1 can be assigned to the O-H stretching vibration of hydroxyl groups, and Amine N-H stretching. These bands correspond to the amide I, II, and III bands of polypeptides/proteins, and are consistent with previous reports. The polypeptides found in the mushroom extracts served as capping agents in AuNPs (Dumur et al., 2011; Gurunathan et al., 2014; Sardar & Mazumder, 2019). The AuNPs synthesized by pellets of *Termitomyces* mushroom and crude extract were subjected to FTIR analysis to identify the biomolecules involved in stabilizing the nanoparticles in solution. The absorption peak centered at 1070 cm−1 referred to the C-O stretch vibration, which could be related to the Ester linkages, β (1→3) glucan, cell wall polysaccharide. Wave number 1388 cm−1 was corresponded to the O-H bending polysaccharide, Amide III. The wave number of 1425 cm−1 was corresponded to the O-H bending polysaccharide. The intense peak at 1547 cm−1 was related to N-H bending -Amide II, chitosan. The peak at 1650 cm−1 was related to amide I, which was created because of the vibrations of carbonyl stretch bonded to the protein. It seems that the proteins have binding ability with Au ions, which in turn creates a surrounded layer on the AuNPs and acts as a capping agent to decrease AuNP agglomeration and increases their stability in the medium. The AuNPs synthesized 2916 cm−1 represents CH3, CH2 stretching and peak at 3271 cm−1 represents O-H stretching vibration of hydroxyl groups, Amine N-H stretching. Additionally, the bands at 3400 cm−1 can be assigned to the O-H

stretching vibration of hydroxyl groups, and Amine N-H stretching these bands correspond to the amide I, II, and III bands of polypeptides/proteins, and are consistent with previous reports.

4.12.2. SEM-EDX based characterization of GNPs

SEM micrographs of AuNPs in the form of different shapes such as spheres, hexagons, triangles, rhomboids and rectangular were reported in present study. SEM demonstrated a polymorphic distribution in size and shapes of AuNPs. Maximum nanoparticles were in the range of 20–50 nm. Few nanoparticles were in the range of 50–150 and 150–500 nm. Energy-dispersive X-ray spectroscopy (EDX) is an analytical technique that is used for the elemental analysis or chemical characterization. In this study, for verification of AuNPs, EDX spectroscopy analysis was carried out to confirm that the presence of elemental Au was confirmed by Gold signals. The synthesis of Gold nanoparticles was characterized by EDX analysis, which gives the additional evidence for the reduction of chloroauric acid to elemental Gold. The spectrum shows strong Gold signal along with weak signals could have been arisen from X-ray emission from macromolecules like proteins/enzymes bound to the NPs or in the vicinity of the particles The energy dispersive spectroscopic analysis is done to get an indication of the amount of Gold nanoparticles present in the biomass. EDS analysis of thin film of fungal biomass shows strong signals for Gold atoms along with weak signals from oxygen and potassium. These weak signals could have arisen from macromolecules like proteins/enzymes and salts of fungal biomass.

Table 4.4: Comparative FTIR spectroscopic characteristics of GNPs

Fungus	Bands (cm-1)	Assignments	References
Volvariella volvacea	1070 cm−1	C-O stretch vibration, which could be related to the Ester linkages, β (1→3) glucan, cell wall polysaccharide	Philip, 2009
Pleurotus florida	1315 cm−1	O-H bending polysaccharide, Amide III	Sen et al., 2013
Pleurotus cornucopiae var. citrinopileatus	1424 cm−1	corresponded to the O-H bending polysaccharide	Owaid et al., 2017
Agaricus bisporus	1547 cm−1	N-H bending -Amide II,	Eskandari-Nojedehi et al., 2018
Lentinula edodes	1652 cm−1	amide I, which was created because of the vibrations of carbonyl stretch bonded to the protein	Owaid et al., 2019
Agaricus bisporus	2916 cm−1	CH3, CH2 stretching	Dheyab et al., 2020
Volvariella volvacea	3271 cm−1	O-H stretching vibration of hydroxyl groups, and Amine N-H stretching	Philip, 2009

4.12.3. Transmission electron microscopy (TEM)

TEM analysis was conducted to evaluate the shape and microstructure of the synthesized AuNPs. As clearly observed, the synthesized NPs were well dispersed with spherical structures. In fact, spherical NPs were more abundant than NPs of other shapes. This spherical shape indicated that the synthesized NPs had minimum surface energy and high thermodynamic stability, which confirmed the high value of the zeta potential of the synthesized AuNPs. The obtained results were in agreement with the finding of Bhat et al., 2021. They indicated that the edible mushroom *Termitomyces* pellets can be used to biosynthesize spherical AuNPs with the particle size ranging from 10 to 50 nm. The TEM images showed a successful synthesis of triangular nano prisms to nearly spherical and hexagonal with different sizes between 20 and 150 nm. The produced NPs were 23.2 nm in size and were mostly spherical in shape. Similar results were shown by the GNPs produced by the crude chloroauric acid. TEM analysis was conducted to evaluate the shape and microstructure of the synthesized AuNPs. This spherical shape indicated that the synthesized NPs had minimum surface energy and high thermodynamic stability (Ahmad, 2003; Bhat et al., 2021). The size of the GNPs ranged from 5nm to 50nm in size. A large density of spherical Gold nanoparticles can be seen and the nanoparticles are quite ranged in size from 3–20 nm (Mishra et al., 2010). In Edible mushroom *V. volvacea* used for AuNP synthesis, showed a successful synthesis of triangular nano prisms to nearly spherical and hexagonal with different sizes between 20 and 150 nm (Philip 2009). They found that the particle size of AuNPs was 13 ± 5 nm and the shape of them was spherical.

Table 4.5: Classification of Gold nanoparticle morphology

Morphology	Morphometry	Percentage (%)
Spheres	320	80%
Hexagons	50	13%
Prisms	22	6%
Pentagons	5	1%
Total	397	100%

4.12.4.DLS VS TEM

TEM and DLS methods yield different but comparable data on the disparities of colloids. TEM images represent random samples applied to a grid; therefore, two problems always occur which include the changes that take place in a sample during its preparation and the second problem is associated with the need to provide undistorting statistics of display accesses. In TEM analysis, a sample must be prepared according to conventional protocols (washed, resuspended, etc.) to avoid the appearance of any artifacts relevant to the preparation when drying a sample on a TEM grid. The indisputable advantage of the DLS method, as well as the majority of other optical methods, is the feasibility to investigate the dispersity in situ with data averaging over a large ensemble of particles contained in an examined volume. TEM is a number-based technique making them fundamentally different whereas the samples for DLS are solvated (Kim et al., 2015). TEM works on dry samples under UHV (ultrahigh vacuum) conditions (Zhou et al., 2004). DLS measures the RH of the dispersed particles whereas TEM provides the projected surface which are based on how much the area of the incident electrons were

transmitted through the sample thus the size obtained by DLS is usually bigger than TEM. An advantage with DLS is its capability to measure bigger number of particles (in millions) compared to TEM (few hundreds). Therefore, DLS provides more robust data on size distribution and PDI. Second, the DLS method is also applicable to studying slow kinetic processes with characteristic times shorter than the time of the photocurrent auto correlation function accumulation (5–30 min). Moreover, compared to the majority of other optical methods, DLS makes it possible to determine particle size distribution functions with no prior information on the optical properties of the particles.

4.12.5. Atomic force microscopy (AFM) and Raman Spectroscopy

AFM has emerged as an effective tool to image NPs especially due to its ability to work on biological samples rich in water (Zhao et al., 2015). AFM provides precise information on particle size and shape while also able to recognize particles of different sizes in a mixture. However, the number of particles analysed by AFM is much smaller and thus DLS provides better size distribution and PDI. The small nanoclusters (nanoparticles with sizes smaller than 5 nm) and a 3D- image of Gold nanoclusters were easily distinguishable at the mica surface. It is well known that surface enhanced Raman signal is proportional to the Raman cross section of the adsorbed molecule, the excitation laser intensity, and the number of molecules that are involved in the SERS process (Moskovits, 2005). SERS effect occurs because of the very strong electromagnetic fields and field gradients available in the so-called “hot spots” of the colloidal cluster. Therefore, the molecules involved in the SERS effect are pre-dominantly those adsorbed on aggregates that have favourable surface plasmon resonances. Aggregated nanoparticles have additional plasmon resonances, associated with inter-particle plasmon coupling (Philip, 2008). They showed that longer wavelength, inter particle plasmon resonances of nanoparticle aggregates provide an even better excitation frequency for SERS. In case of

nanoparticles produced using chloroauric acid the peaks were obtained were at 1326.23, 1338.99, 1356, and 1363.52 cm−1 which are due to δCH2(wag), δCH2(twist) and νC single bond N modes, respectively and 1556.16 which are due to υ(C-(NO2)), 1577.87 cm−1 due to υ(N=N) aliphatic. In case of GNPs produced due to crude extract 1079.93 represents υ(C-O-C) asym, 1195.87 cm−1 indicates υ(CC) alicyclic, aliphatic chain vibrations, υ(C=S), whereas 1308.64, 1435.69 cm−1 represents υ(N=N), 1570.13 cm−1 υ(C=C), and 1784.37 cm−1 indicates υ(C=N) and υ(C=C) respectively. Similar studies are reported earlier (Gearheart et al., 2001; Roy et al., 2018).

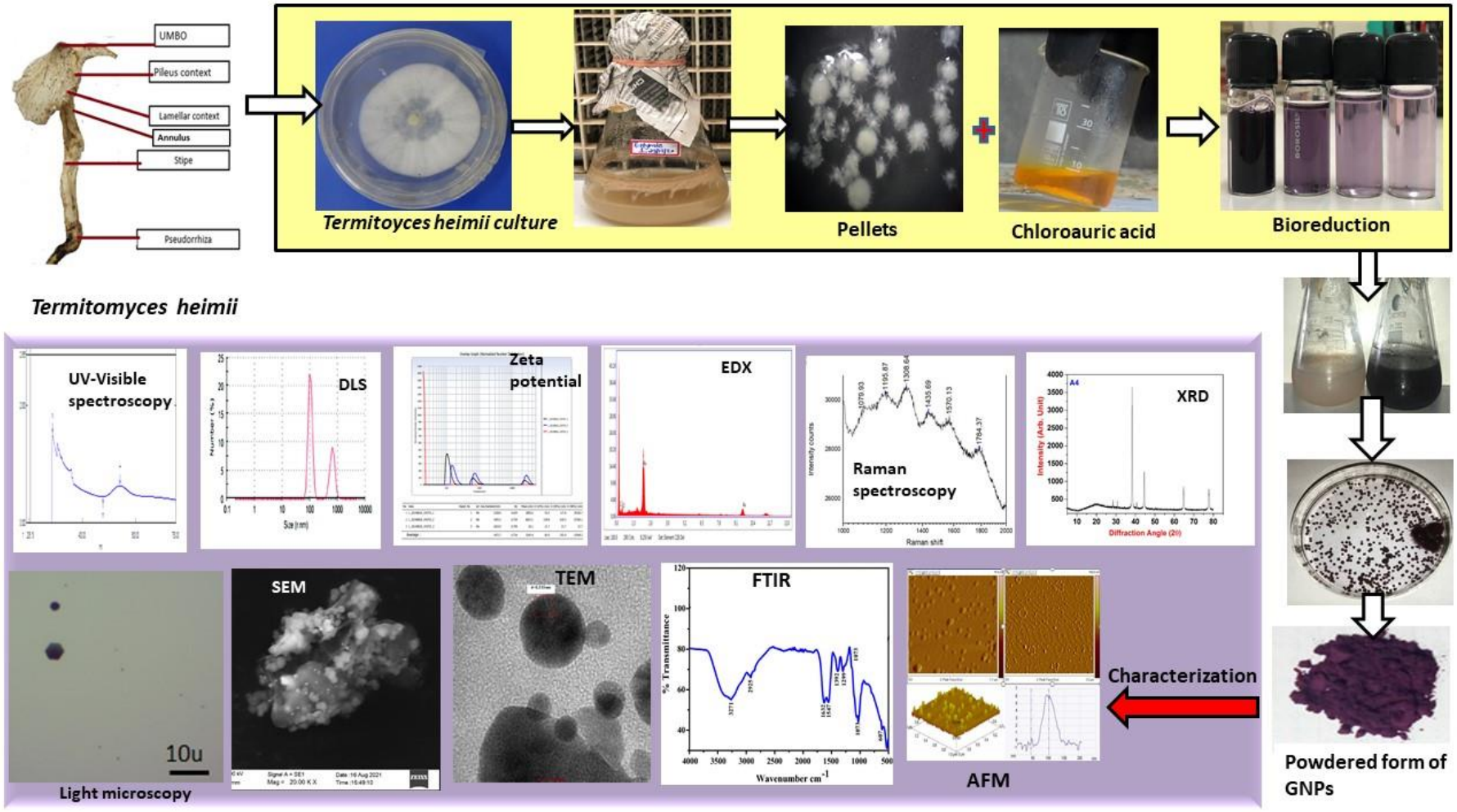

Figure 4.4: Biosynthesis of GNPs using *Termitomyces heimi*

Table 4.6: Global diversity of *Termitomyces* taxa which can be tested for GNPs

Sr.No	*Termitomyces* species
1	*Termitomyces albiceps* S.C. He 1985
2	*Termitomyces albidolaevis* Dhanch., J.C. Bhatt & S.K. Pant 1991
3	*Termitomyces epipolius* * (Singer) L.D. Gómez 1995
4	*Termitomyces albuminosus* (Berk.) R. Heim 1941
5	*Termitomyces badius* Otieno 1969
6	*Termitomyces heimii* ¥ Natarajan 1979
7	*Termitomyces entolomoides* R. Heim 1977
8	*Termitomyces clypeatus* R. Heim 1951
9	*Termitomyces citriophyllus* R. Heim 1942
10	*Termitomyces eurrhizus* (Berk.) R. Heim 1942
11	*Termitomyces aurantiacus* § (R. Heim) R. Heim 1977
12	*Termitomyces intermedius* Har. Takah & Taneyama 2016
13	*Termitomyces lanatus* R. Heim 1977
14	Termitomyces fuliginosus R. Heim 1942
15	*Termitomyces congolensis* (Beeli) Singer 1948
16	*Termitomyces infundibuliformis* Mossebo 2012
17	*Termitomyces cartilagineus* (Berk.) R. Heim 1941
18	*Termitomyces bulborhizus* T.Z. Wei, Y.J. Yao
19	*Termitomyces brunneopileatus* D.C. Mossebo & E.P.F. Essouman 2017
20	*Termitomyces indicus* € Natarajan 1976
21	*Termitomyces biyi* Otieno 1966
22	*Termitomyces griseiumbo* Mossebo 2003

23	*Termitomyces globulus* R. Heim & Gooss 1951
24	*Termitomyces albuminosus* (Berk.) R. Heim 1941
25	*Termitomyces mammiformis* ξ R. Heim 1942
26	*Termitomyces mboudaeinus* Mossebo 2003
27	*Termitomyces radicatus* Natarajan 1977
28	*Termitomyces sagittiformis* (Kalchbr. & Cooke) Reid 1975
29	*Termitomyces schimperi* (Pat.) R. Heim 1942
30	*Termitomyces perforans* R. Heim 1977

4.13. Detection of Gold sulphides in BHQ and mining rejects

Gold(I) sulphide is the inorganic compound with the formula Au_2S and principal sulphide of Gold. Gold occurs usually in its native form or hosts in sulphides (especially pyrite, arsenopyrite, and chalcopyrite), silicate, carbonate, and oxide minerals. It decomposes to Gold metal and elemental sulfur, illustrating the nobility of Gold. Recovering Gold from sulphide refractory Gold ores has been an important promise for the sustainable development of Gold industry, while there are many challenges in the treatment of sulphide refractory Gold ore, such as environmental pollution and low Gold recovery. The incorporation of Gold into sulphide minerals has long been inferred by several investigators We were successful in obtaining the powdered, dried sieved fractions of the samples. The fractions 150, 106, 53 µm showed high concentration of Gold and same fraction were thus used for the further studies. Similar finding has been reported in Brazilian mines (Oliveira and Larizzatti, 2005), Australian mines (Reith, 2002). The iron ore from the BIF of Goa has not been subjected to multi-elemental analysis (such as Au, Ag, Pt including REE). However, our studies have established that BHQ contains 12-13 ppm. Values of Gold (0.98–4.72 ppm) has been reported from Gadag greenstone belt, Western Dharwar Craton, Peninsular India (Ugarkar et al., 2016). Determination of Gold (0.5 to 50 ppm) in low grade ores and concentrates by anion exchange separation followed by neutron activation has been reported (Iyer and Krishnamoorthy, 2017). Invisible Gold recovery from sulphide minerals to liberate invisible Gold from refractory ores, most commonly, chemical or biological oxidation techniques that alter or destruct the mineral lattice of the sulphides are used. Gold sulphide show the irregular particles with the irregular BFG with rough surface. These grains ranged from 0.1 to 1 mm in diameter coarse, sub-angular to angular with no mechanical damage. The presence of the elemental Gold and sulphur is seen in the spectra of EDX. There were no earlier studies carried out on separation of Gold sulphide from iron ores of Goa. Sulphur analysis was carried out using CHNS/O Elemental analyzer

which showed the presence of 0.669% of sulphur in case of BHQ, 0.70% in BMQ and 0.678% Mining reject. This is claimed to be the first report on detection and separation of Gold sulphide in the heavy fraction of BHQ sourced from BIF in Goa. Similar finding has been reported in Brazilian and Australian mines (de Oliveira, and Larizzatti, 2005; Reith et al., 2006). Since there are huge deposits of BHQ in Goa which are exported without rational multi elemental analysis or detection or quantification of Gold sulphide this shows the potential for more advanced research in this area for systematic geochemical prospecting of auriferous ore bodies for Gold sulphides. This work is in progress with encouraging results. Sulphides can be used in biooxidation of Gold by using hyperacidophilic microbes (Reith et al., 2005; 2007). We recommend the simple technique used in present studies for detection of Gold sulphide in any ore with large ferromagnetic overload. This would help in undertaking more comprehensive and advanced analytical studies on auriferous ores in India and rest of the world. The deposits of refractory sulphide ores could be the main potential source of Gold production in the future.

4.14. Detection of Gold sulphide and its use in studying Gold sulphide of sea-floor massive sulphide deposits

Land-based massive sulphide deposits are of major importance to world mining and also to the world of commerce. Major products are base metals (Cu, Zn, Pb, Sn), precious metals (Au, Ag), and a number of special metals (In, Ga, Ge) (Hannington et al.,2010). More than 100 modern analogues of massive sulphide deposits and hydrothermal systems are presently known at the modern sea-floor, including some very large accumulations of metals such as in the Atlantis, deep in the Red Sea. Currently, mining of hydrothermal deposits at the sea-floor appears to be most attractive for sites with high Gold and base metal grades, site location close to land, shallow water depth not significantly exceeding 2000 m, although the technology exists for mining in deeper water (Scott, 1987; Hoagland et al., 2010). Some of the most prospective

Gold-rich deposits have been found in the territorial waters of Papua New Guinea. If drilling proves that mineralization extends to depth, these deposits may become the first marine mine sites for Gold and base metals. The main geological characteristics of Gold-rich VMS deposits have been extensively reviewed (Hannington et al., 2010).

4.15. Micro test plate assay for Biooxidation of Gold sulphide

Bio-oxidation is based on chemolithotrophic microorganisms using iron and/or sulfur as their energy source. In highly aerated, operated at pH 1.6 and a temperature of 40ºC (Rawlings, 2002), the finely ground mineral is mixed with inorganic nutrients to promote microbial growth. The primary role of the microorganisms in this process is the oxidation of aqueous Fe2+ into Fe3+ and the production of sulfuric acid. Microorganisms that play an essential role under mesophilic conditions are the acidophilic bacteria such as *Acidithiobacillus ferrooxidans* and *Leptospirillum ferrooxidans. Acidithiobacillus ferrooxidans* is able to oxidize both ferrous iron and reduced sulfur compounds (Schippers and Sand, 1999). Flux of solubilized liquid Gold in colloidal state released by action of chemolithotrophic iron bacteria vicipusly attacking the Gold sulphide (black amorphous masses) over a week, at the centre is fractal swarm of pure Gold nanoparticles sedimented as a product of microbial biooxidation as seen in **Fig 4.45 a.** The annular flux of pure micro biogenic Gold indicates the intensity of bio solubilization in solution which has a highly acidic pH of 1.5. Reaction was successful with both synthetic and crude Gold sulphide. There was formation of metallic Gold sulphide from amorphous Gold sulphide and also crude Gold sulphide therefore biooxidation assay was successful. It is a rapid assay. Results are positive and also cultures are active. Among all three tentatively identified *Acidithiobacillus* was found to be more active and promising bio-oxidizer followed by *leptospirillum* and *sulfobacillus* was found to the weakest among three. Fascinating fractal forms of pure Gold produced by bacterial culture as shown in **Fig 4.45 (b-c).** This work reports

the microfluidics-based assay system to detect promising Gold bio-oxidising capacity of different chemolithotrophc bacteria. This assay can serve as a quick, efficient method for testing large numbers of Gold sulphides for biooxidation. A robotic high throughput screening system for selecting hyper oxidizer can be developed to expedite the process. In this the robotic optical sensors will replace humans in monitoring thousands of test wells and digital image processing will create array of positive results followed by test for Gold films.

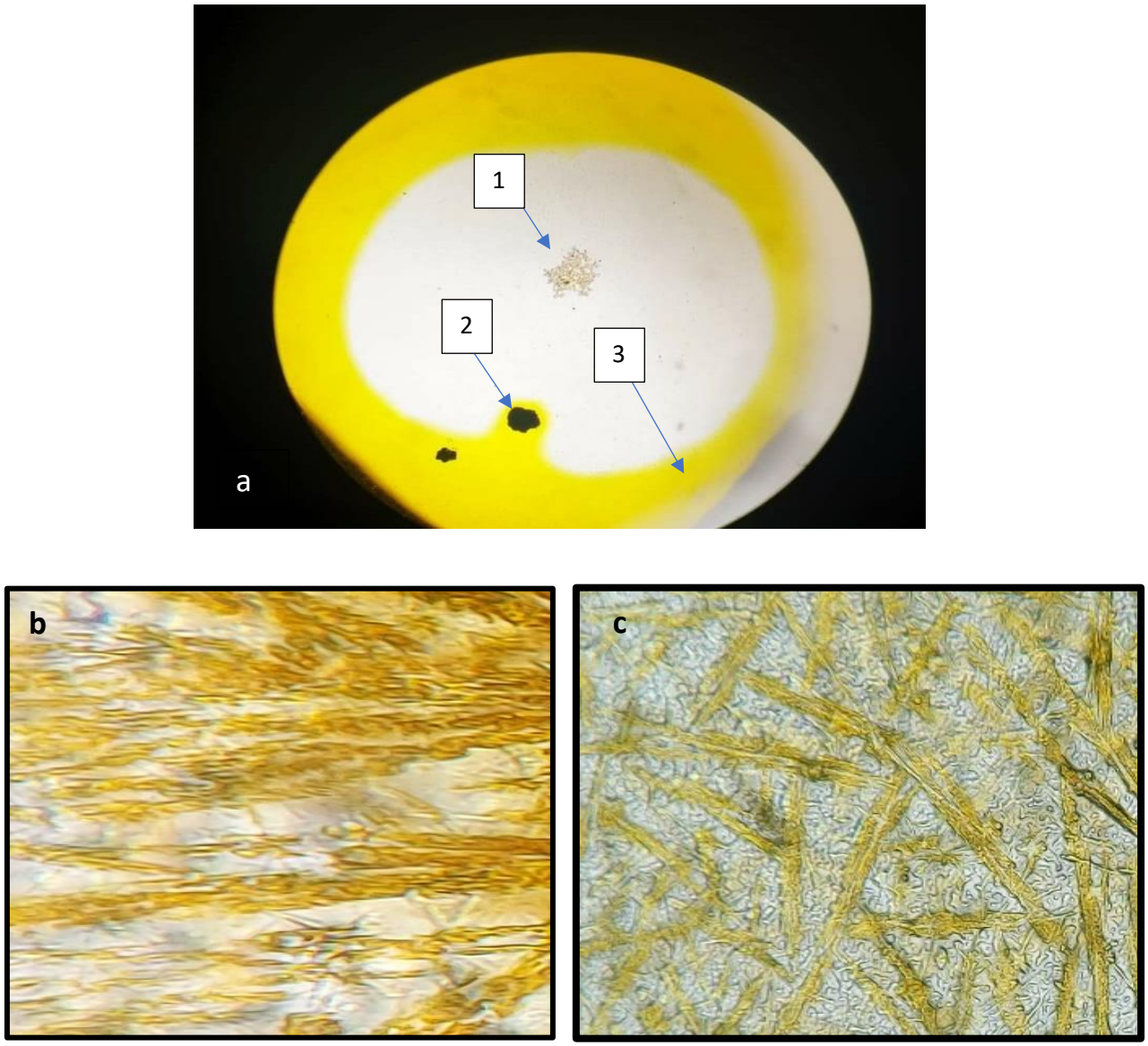

Figure 4.5 (a-c): Biooxidation and release of Gold; 1-Swarms of GNPs; 2-Gold sulphide, 3-Colloidal particles.

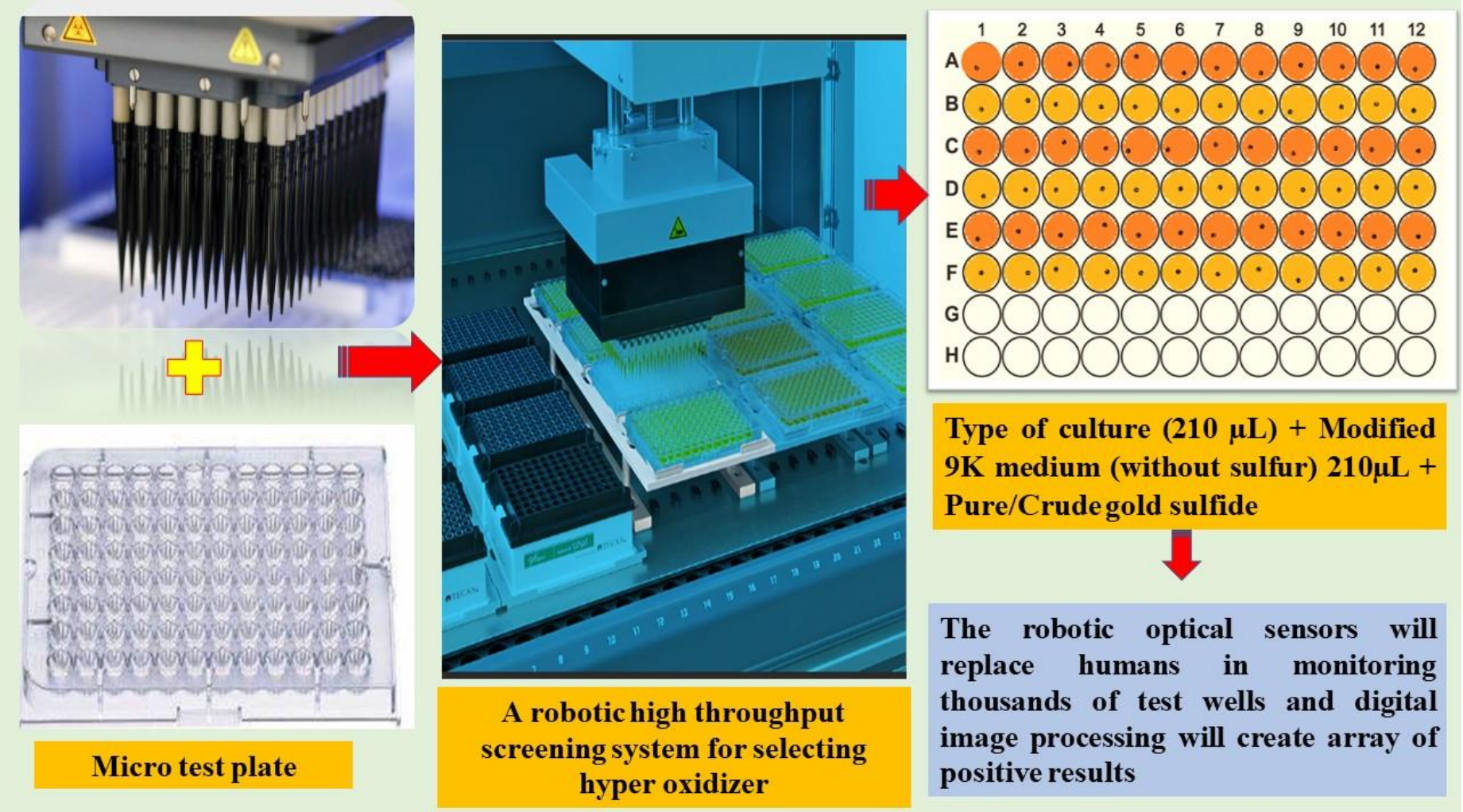

Figure 4.6: A robotic high throughput screening for selecting hyper oxidizer

4.16. Molecular identification of the promising bio-oxidizing culture

The culture which was tentatively identified as *Acidithiobacillus* and was showing promising bioxidation property was sent for molecular identification. The colony was cream in color, with fractal margin, raised elevation, opacity opaque. The morphological characters showed it was gram negative, motile, rods (0.5x1.0 µm) growing at the pH of 1.5 to 2. Thus, further we tried to carry out the genome sequencing studies. We name this culture as NOSOB (Novel Sulphur oxidizing bacteria) gram negative, rod shaped, highly aerobic, motile, powerful sulphide oxidizer, growing at the pH of 1.8. The phylogenetic tree of this culture is shown in **Fig 4.7**. NOSOB culture and its role in biogeochemistry of Goan mines is shown in the **Fig 4.8.**

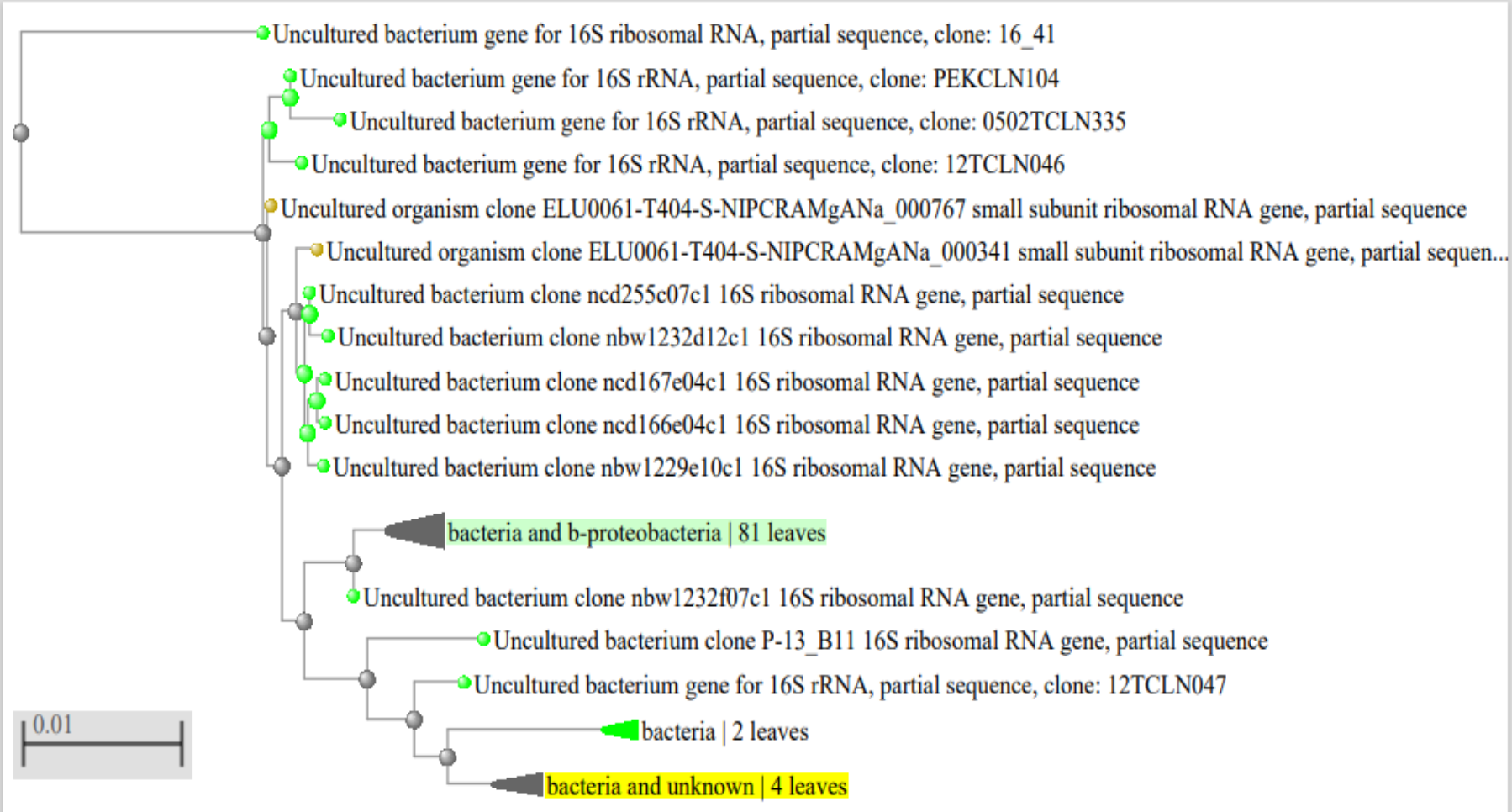

Figure 4.7: Phylogenetic tree of NOSOB

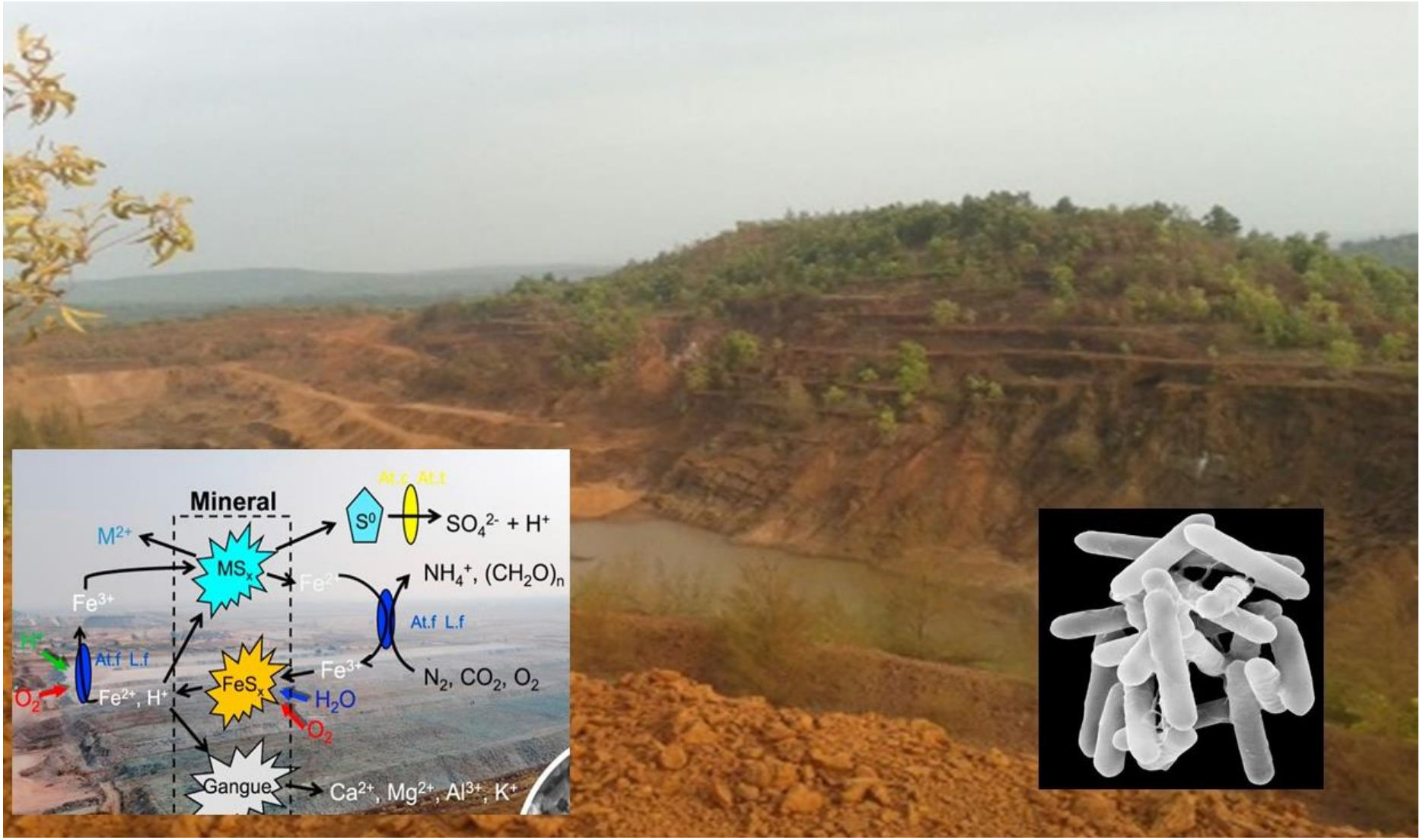

Figure 4.8: NOSOB culture and its possible role in biogeochemistry of Gold

4.17. Genome sequencing and problems

Microbial whole-genome sequencing is an important tool for mapping genomes of novel organisms, finishing genomes of known organisms, or comparing genomes across multiple samples (Donkor, 2013). Sequencing entire bacterial, viral, and other microbial genomes is important for generating accurate reference genomes, for microbial identification, and for other comparative genomic studies. With the advent of single-cell sequencing, genomes of uncultivated species are rapidly filling in unsequenced branches of the microbial phylogenetic tree. The wealth of new insights gained from these previously inaccessible groups is providing a deeper understanding of their basic biology, taxonomy and evolution, as well as their diverse roles in environmental ecosystems and human health (Lasken & McLean, 2014). However, the sequencing technologies require that the DNA is extracted in a form that meets particular quantity and quality requirements. A protocol for extraction and purification of high-quality and quantity bacterial DNA applicable for genome sequencing was followed (Salvà-Serra et al., 2018). It was repeated for three times but it was difficult to break the cell wall indicating that the cell wall of the bacteria was very strong. Low amounts of DNA were obtained that are highly-resistant to enzymatic and detergent lysis (e.g. *Mycobacterium* spp.). Therefore, mechanical lysis (e.g., bead beating) was also necessary.

4.18. Immobilized reaction system for Gold sulphide biooxidation

We were successful in setting up of small bench top booming experiment for extracting of Gold from local Iron ore sample and mining rejects. Oxygen was supplied using external aerator. Chemolithotrophic microorganisms such as *Acidithiobacillus ferrooxidans*, gram-negative bacterium obtains energy by the oxidation of ferrous ions to ferric ions and uses molecular oxygen as the terminal electron acceptor in aerobic conditions. Therefore, the dissolved oxygen (DO) plays an important role in the biooxidation process of refractory Gold gram-negative

bacterium which obtains energy by the oxidation of ferrous ions to ferric ions and uses molecular oxygen as the terminal electron acceptor in aerobic conditions. Therefore, the dissolved oxygen (DO) plays an important role in the biooxidation process of refractory Gold ore (Sun et al., 2012). There was formation of colloidal Gold forms and detection of flux lines of colloidal Gold on slide. Evidence for formation of Sulphuric acid as product of biooxidation. The formation of flux of sulphuric acid depolymerizes the agar and creates rough surface. There was drop in pH from 2 to 1.4 indicating formation of sulphuric acid. In two-dimensional slide coating it appears that the oxygen gradient is on five sides, the four edges and the surface. Therefore, Oxygen diffusion was found to be highest from the edges and decline towards the centre. Oxygen diffusion from surface will not be uniform depending on thickness of the layer. Therefore, the reaction is rapid the edges and shows clearance of sulphide, formation of complex biofilms and flux of Sulphuric acid which depolymerizes the agar and creates rough landscape. The Gold formed after oxidation is typically microbioform. After 14 days of process 90%, approximately, of Gold extraction were reached. It was found the pH was dropping from 2 it reached 1.8 by a weak and later 1.5 by 14 days. Elemental analysis had shown 9.35 % of Au_2S in sample based on total sulfur content and assuming other forms of Sulphides negligible so Corresponding Au_2S concentration in each slide is 9.35 % w/w or about 18 mg per slide (Stoichiometrically Maximum Gold obtainable from this amount of by biooxidation from each slide is 80 % of Au2S w/w or 14.4 mg per slide from 18 mg). Extrapolating this to Gold containing edges sampled there would be 143 mg X 9.35 = 13.4 mg of Au_2S. Since sampled only Gold was sampled from Au_2S available in edges in this marginal area it will be 80% of 13.4 mg or 10.72 mg. Now concentration of total Gold reported by ICP OES is 2.32 mg per litre. There was the formation of colloidal Gold forms and the detection of flux lines of colloidal Gold on the slide. The Gold formed after oxidation was found to be typically microbioform. After 14 days of the process, 90%, approximately, of Gold extraction was reached. The

concentration of Gold reported was ICP AES results Showed 2133.5 mg/L, 2272.5 mg/L and 2100 mg/L.

4.19. Phylogenetic fingerprinting

Phylogenetic fingerprinting involves identification of the microorganisms present in an environment. Research into the phylogenetic fingerprinting of heavy metal containing soils is ongoing, and strong correlative link has been established between the phylogenetic fingerprint of a give microbial community and the presence of metal contaminants (Hinojosa et al., 2010). DGGE method was used to demonstrate the phylogenetic fingerprint of bacterial communities at the Tom akin Park Gold mine in New South Wales, Australia which was influenced by the presence of Gold and its pathfinder elements (Reith & Rogers, 2008). Studies have been reported on soils overlying a volcanogenic massive sulphide (VMS) deposit in the northeast of Western Australia where investigation of the microbial community structure was coupled with soil geochemistry and biogeochemical analysis of plants (Wakelin et al., 2012). This demonstrates that the microbial community profiles can be used to identify mineralised zones. Similarly in our studies we used metagenomic nanopore sequencing technology which helped to know microorganisms associated with the BHQ and BMQ samples. Different microorganisms which are involved in the development and effect of Au-cycling biofilm on Au grain surfaces have been reported example *Staphylococcus, Corynebacterium* are involved in conditioning of surfaces to their attachment. Microorganisms such as *Pseudomonas, Burkholderia, Methylobacterium, Acinetobacter, Rhodobacter* the recruitment of phototrophic and heterotrophic Gram-negative bacteria are involved in EPS production and Au aggregation. The proliferation and growth of biofilm community including heterotrophic and metallophillic species such as *Rhodobacter* sp, *Rhizobium* sp, *Achromobacter* sp; *Methylobacterium*,

Achromobacter, *Pseudomonas* sp. It was found that both the sample BHQ and BMQ showed the association of microorganisms.

4.20. Bioindicators for Gold exploration

Bioindicators rely on organisms that are resident in the mineralised zone and/or that are sensitive to metal. Hence, the presence of these organisms can indicate the occurrence of a specific metal contents derived from a buried ore body. The use of microorganisms as bioindicators for mineral exploration has remained an underexplored avenue. The increasing sensitivity and decreasing cost of molecular methods make it possible to envisage the use of bioindicators as a new standard method in mineral exploration. The use of microorganisms as bioindicators holds many advantages as exhibit greater genetic diversity than macroorganisms. Modern molecular techniques have facilitated the generation of detailed phylogenetic profiles of environments that can be coupled with geochemical information to give a complete biological and geochemical picture of the system. Techniques such as terminal-restriction fragment length polymorphism (T-RFLP), denaturing gradient gel electrophoresis (DGGE), thermal gradient gel electrophoresis (TGGE), single strand conformation polymorphism (SSCP), microarrays and third generation DNA sequencing technologies, allow for the high-throughput analysis of microbial communities (Sharma et al., 2022) and can be adapted to aid in the detection of metal contaminants present in low concentrations (Reith and Rogers, 2007). The major advantages of using bioindicators as mineral exploration tools includes the possibility that a multitude of different metals will be detectable simultaneously; microorganisms have the ability to respond to very low concentrations of metals. Technically there are two possible avenues for the application of microbial bioindicators one is the comparison of microbial community profiles, known as ‘phylogenetic fingerprinting’ and second is the detection of specific genes, proteins and/or metabolites which will ultimately help

to help determine the geochemical composition of a site.

4.21. A novel bioinspired microfluidics assay for rapid screening of Gold bioreduction systems in *Termitomyces* mushrooms for designing Gold biosensor

Biosensors can be developed into inexpensive devices that are simple to operate, e.g., the electrochemical blood glucose biosensor (Wang, 2008). Specifically, the use of biosensing technologies over traditional techniques for mineral exploration holds value in the speed, portability and high selectivity of these devices. The development of biosensors for Gold exploration means that exploration teams will be able to obtain Gold concentrations from an environmental sample immediately, rather than weeks later, which is the current turn around time. In addition, biosensing devices may also aid in mineral processing where real-time in-line analysis of specific mineral components of ores could be determined, enabling real-time fine-tuning of the process to improve recovery and costs. Previous studies have reported the studies on the development of a Gold biosensor that is the bacterium *Cupriavidus (Ralstonia) metallidurans* (Van Houdt et al., 2009; Mergeay et al.,2015;). A major consideration for the implementation of a Gold biosensor is the solubilisation of Gold from an exploration or processing sample. Hence for any biosensor to work, a suitable method for the extraction of Gold from the sampling medium, e.g., the soil, has to be developed. Gold, unlike other metals, does not form free ions in aqueous solution at surface conditions, but occurs as aurous (+I) and auric (+III) complexes and metallic Gold nano-particles (Reith et al., 2007; Usher et al., 2009). We are reporting the novel microfluidics-based assay system to detect Gold bioreduction capacity of different tissues in Termitophilic mushrooms (Kalia & Kaur, 2018; DeSouza & Kamat, 2017; de Souza & Kamat, 2018, 2019) in tissue based and cell free environment. It was found that stipe was showing most promising results showing peaks at 455, 510,642 nm. Absorbance reading tells the composition and size of NPs (Sigma aldrich.com). The new apps such as digital colorimeter from laboratory tools make it possible to rapidly detect GNP

formation and perform quick and simple analysis. Different tissues such as umbo, pileus, lamellae, stipe context, stipe epicutis, pseudorhiza context, pseudorhiza epicutis of *Termitomyces heimii* mature fruit bodies successfully produced AuNps for the first time. Membrane filtered water soluble extracts from same tissues produced GNPs. Having seen the chemical creativity of termitophilic mushrooms in our laboratory we aim to use microfluidic assay for rapid screening of Gold bioreduction system in this species. However, it was not easy to rapidly to detect and characterize swarms of Gold micro and nanoparticles. It was at this point that we came across a mobile based digital colorimeter which was found useful in analysis of color of the GNPs swarms and help in colorimetric absorption characterization in the visible range. We aim to use both tissue based and cell free systems. In poor and under developed countries like India and poor universities researchers find it difficult to have easy excess to expensive instrumentation for characterization of GNP's. However now the new apps such as digital colorimeter from laboratory tools make it possible to rapidly detect GNP formation and perform quick and simple analysis. The results manifested by mono and polydisperse Gold nano and microparticles of mixed size groups demonstrated that cell free system can be potentially useful for fabrication of efficient Gold biosensors. The results in terms of production of distinct micro and nanoparticles were directly visualized microscopically and using mobile based digital colorimeter. This is useful in rapid screening of large number of biological or microbiological Gold bioreduction systems. In high throughput screening system, we recommend development of more such mobile based apps. Our approach has led us to a step closer to a very sensitive Gold biosensor. **Fig 4.9** gives the novel bioinspired microfluidics assay for rapid screening of Gold bioreduction systems in termitophilic mushrooms for designing Gold biosensor.

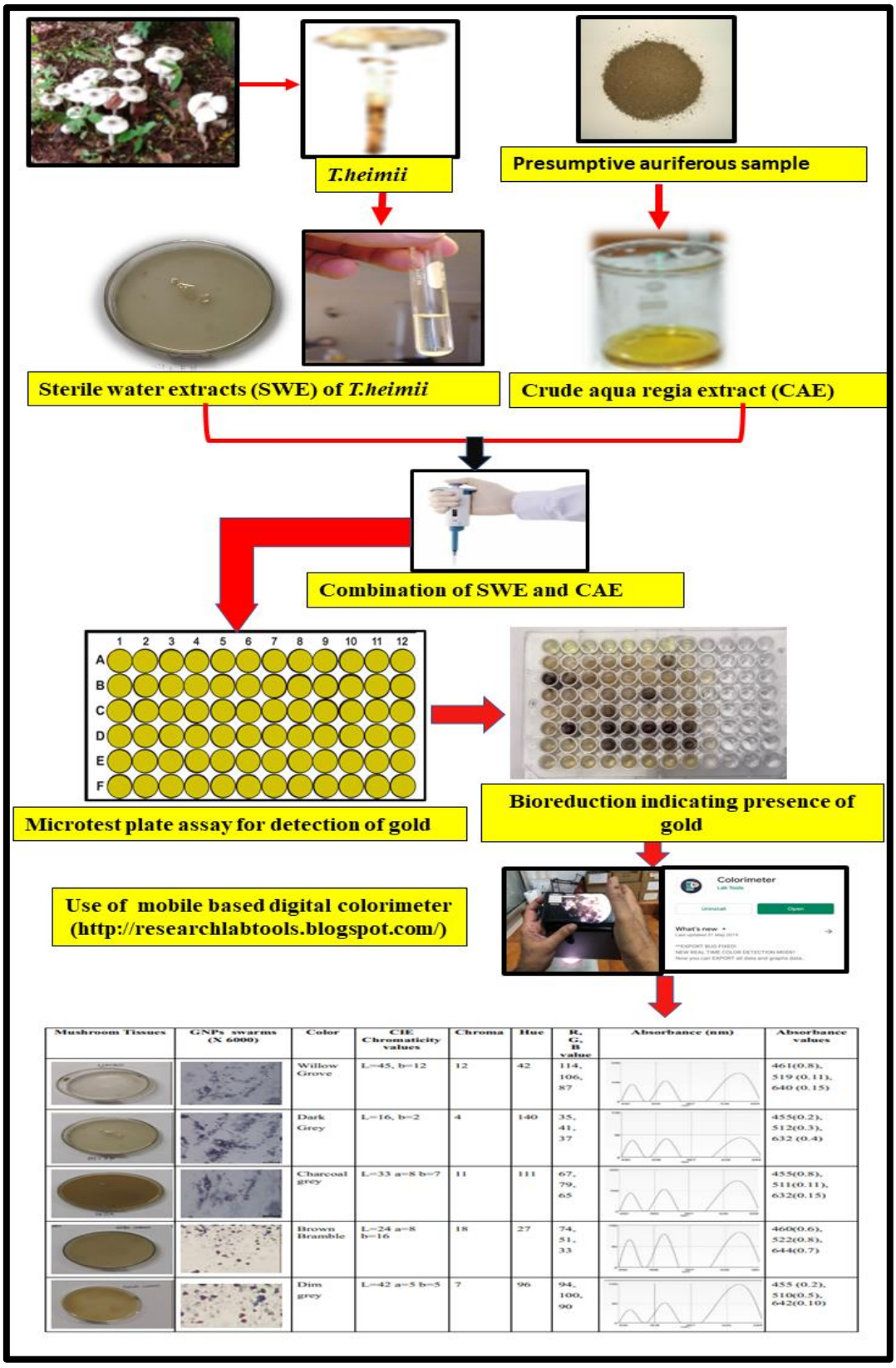

Figure 4.9: Novel bioinspired microfluidics assay for rapid screening of Gold bioreduction systems in termitophilic mushrooms for designing Gold biosensor.

4.22. A novel bioinspired slide-based biosensor for rapid detection of Gold sulphide in sample using NOSOB culture

A biosensor is an analytical device which is used for the detection of a chemical substance. It combines a biological component with a physicochemical detector. The sensitive biological element such as tissue, microorganisms, organelles, cell receptors, enzymes, antibodies, nucleic acids, etc., is a biologically derived material or biomimetic component that interacts with the analyte under study. The development of biosensing technologies for mineral exploration holds value in the speed, portability and potentially high selectivity and sensitivity of the assay (Coker 2010; Luong et al., 2008). To date, research into biosensors has focused around the detection and monitoring of heavy metal contamination, blood glucose levels, pathogens, food toxins, and illicit drugs (Luong et al., 2008). Biosensing devices may aid in mineral processing and help in analysis of ores by assisting in the tailoring of the processing method to maximize Au extraction and minimize chemical consumption. For the development of Au biosensor, biological elements that respond to Au are required. Biosensors are analytical devices that are based on biological components and are developed to detect specific compounds (Luong et al., 2008). We developed a novel bioinspired slide-based biosensor for rapid detection of Gold sulphide in sample using NOSOB culture. NOSOB was used as a biosensor. It is slide base system where culture and medium in placed on slide in a coverslip size area and the sample to be tested is incorporated at the centre. The slide is placed inside the acidic condition and pH is maintained to 2. whole system is provided with aerator to provide the dissolved oxygen. If the bio-oxidation occurs and Gold is released than it indicates the presence of Gold sulphide. Using this biosensor any sample can be checked for the presence of Gold sulphide thus providing a biosensing technology which can be used for mineral exploration.

4.23. Potential of Biomining in India

Gold occurs in multiple geological environments in India, thus there is a huge potential for exploration of Gold and biomining in India. Gold occurs in India as lode Gold, in stratified sulphide deposits, in conglomerates, quartzites, in river placers, in laterite /weathering profile (Radhakrishna and Curtis 1991). All these available auriferous samples opens a huge window to environmental friendly and economical technologies such as Biomining. The potential of biomining in India is explained in **Fig 10.** Rational sampling and collection of auriferous samples can be carried out from mining such as Banded Iron Formation (BIF), Banded Magnetite Quartzite (BMQ) mining rejects and non-mining such as beach sand, placer deposits, laterite, termite mounds areas of India. Such samples can be further crushed and grounded, sieved (Ramesh et al., 2009). Heavy metals can be separated by using floatation technique (Santosh et al., 1992). The samples can be further analysed by ICP-OES, ICP-IES, Fire assay techniques for detection of Au (Anand et al., 2016; Falconer et al., 2006; Szaloki et al., 1999). Morphological studies and biofilm association can be studied using microscopic techniques such as light microscopy, Phase contrast microscopy, SEM-EDX, TEM (Fairbrother et al., 2012; Reith et al., 2007). Association of microbial biofilms with such auriferous samples (Reith et al., 2016) shows that there is a huge potential for exploration and study of useful unexplored microbiological aspects from such auriferous samples. Microorganisms such as acidophiles, *Acidithiobacillus ferroxidans* and cyanide producing microbes such as *C.Violeceum* (Reith et al. 2007) are being used in biomining. Microorganisms are able to mobilize metals through the processes such as formation of organic and inorganic acids, excretion of complexing agents, oxidation and reduction reactions. Generally, sulfuric acid is the main inorganic acid formed in the leaching environment. It is formed by sulfur oxidizing microorganisms such as *thiobacilli.* Such microorganisms can be isolated from such environment and can be further used in bio-oxidation and bio-reduction at laboratory scale and further at pilot and commercial scale

(Brombacher et al. 1997). Biomining is commercially applied using three different engineered methods which includes dump bioleaching, heap bioleaching/biooxidation, and stirred tank bioleaching/ minerals biooxidation. Molecular identification of the most promising cultures can be carried out by PCR, Phylogenetic finger printing, Transcriptomics, proteomics (Zammit et al., 2012), and DGGE (Reith et al. 2006). Once culture is identified laboratory scale bioleaching (Brombacher et al. 1997) in stationary/ shake flasks conditions can be carried out followed by pilot scale Leaching in a columns/ agitated tanks or reactors (Lazar et al. 1993; Corral et al., 1993) and further can be applied at commercial scale by various techniques such as Dump leaching (Brierley 2001; Olson et al. 2003), Heap leaching (Kleid et al., 1991; Kohr, 1995), Chemostate leaching (Brombacher et al., 1997) and Vat leaching (Devasia and Natarajan 2004; Brombacher et al., 1997).

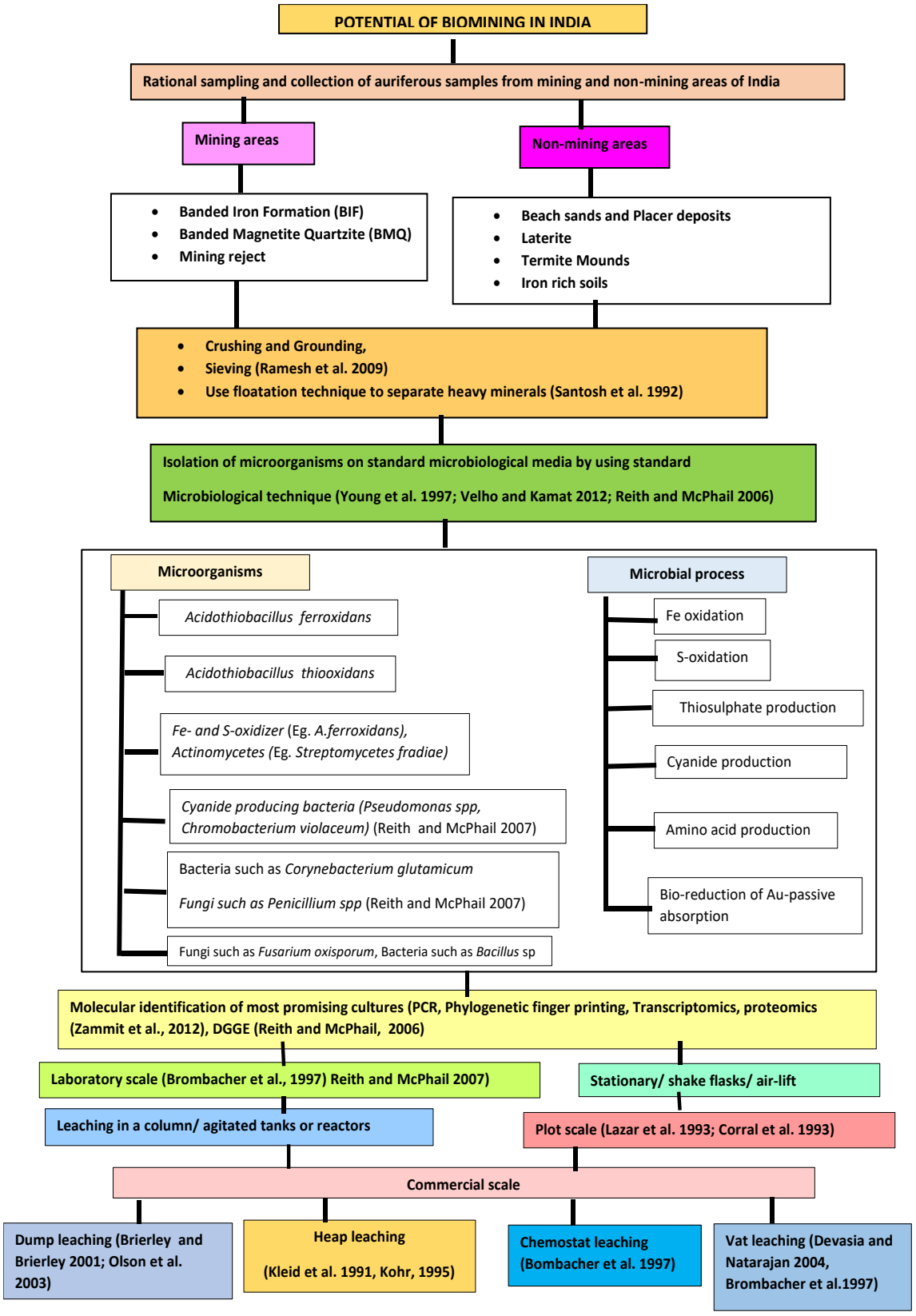

Figure 4.10: Potential of Biomining in India (Dabolkar and Kamat., 2021)

4.24. Prospects of Biomining of Gallium

Gallium, atomic number 31 is a strategic metal at present and would remain so in future. It does not occur in free form in nature, but as the Gallium (III) compounds that are in trace amounts in zinc ores and in bauxite and laterite. The average content of Gallium in bauxite is 50 parts per million (ppm). Bauxite deposits in the country contain Gallium and it is recovered during its processing. Gallium is used in optoelectronic and defence applications due to its property to expand by 3.1%. Gallium based compounds, such as Gallium arsenide (GaAs) and Gallium nitride (GaN), are semiconductors used in the electronic industry as well as in the manufacture of memory cells. However, the United States Geological Survey has estimated total world primary Gallium production to be about 78 tonnes, 182 tonnes, 292 and 273 tonnes in 2009, 2010, 2011 and 2012, respectively. There is no large-scale Gallium production in India. It is recovered as a by-product while producing alumina. As per working group report of 12th five Year Plan (2012-17), India produced around 55 kg Gallium in recent past. In Goa laterites occur in four physiographic divisions ie high level (600- >700 m), intermediate level (150-300m), low-level (>10-100m), near-sea level. The systematic collection of the lateritic samples was carried out successfully. The presence of Ga was detected by SEM-EDX. Microorganisms such as fungi, actinobacteria, chemolithotrophs were successfully isolated from the lateritic waste of Goa. It is possible to carry out bioleaching process using the microbes isolated from the laterite samples, similar studies have been reported (Lundgren et al., 1980). Average Ga content of Indian bauxites range 5-122 ppm (mean 60 ppm) and shows a close correlation with the titanium content concentrated by laterization. Conceptualization of a Gallium based supply chain is shown in **Fig 4.11.** We estimate that behind every metric tone of lateritic waste or aluminous lateritic waste Goa loses a recoverable quantity of 60 grams of Ga valued at Rs. 1200. To stop such phenomenal economic losses we propose an ecofriendly biohydrometallurgical approach by using crushed laterite of 20 to 400 mesh, treated with chemolithotrophic bacteria such as

Acidithiobacillus at 1-2.5 pH and temperature 25 to 85 °C under oxygenated, stirred conditions. The leached Ga can be recovered by Ion exchange, absorption or bioaccumulation process. It would be feasible to extract pure Gallium worth Rs. 19-21000 per metric tone of powdered laterite.

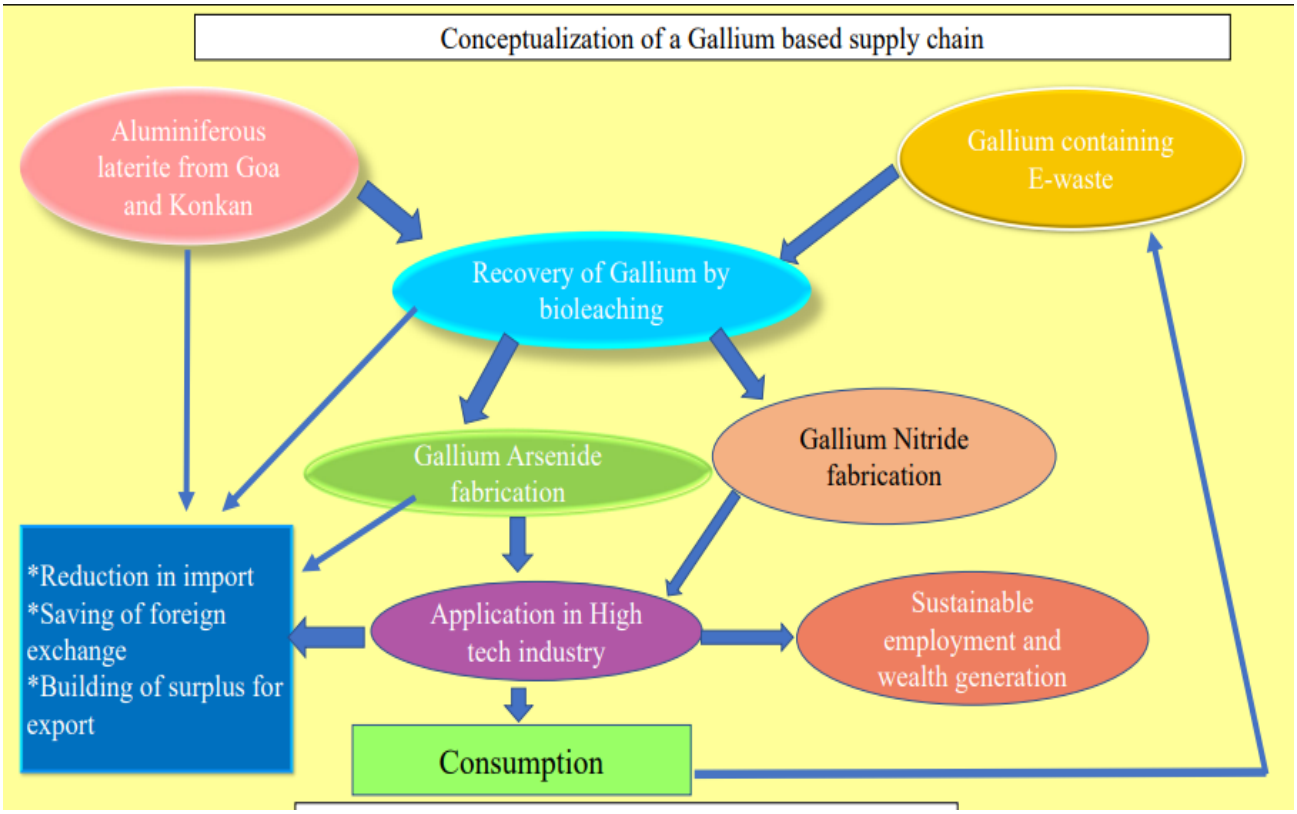

Figure 4.11: Conceptualization of a Gallium based supply chain (Dabolkar and Kamat., 2019).

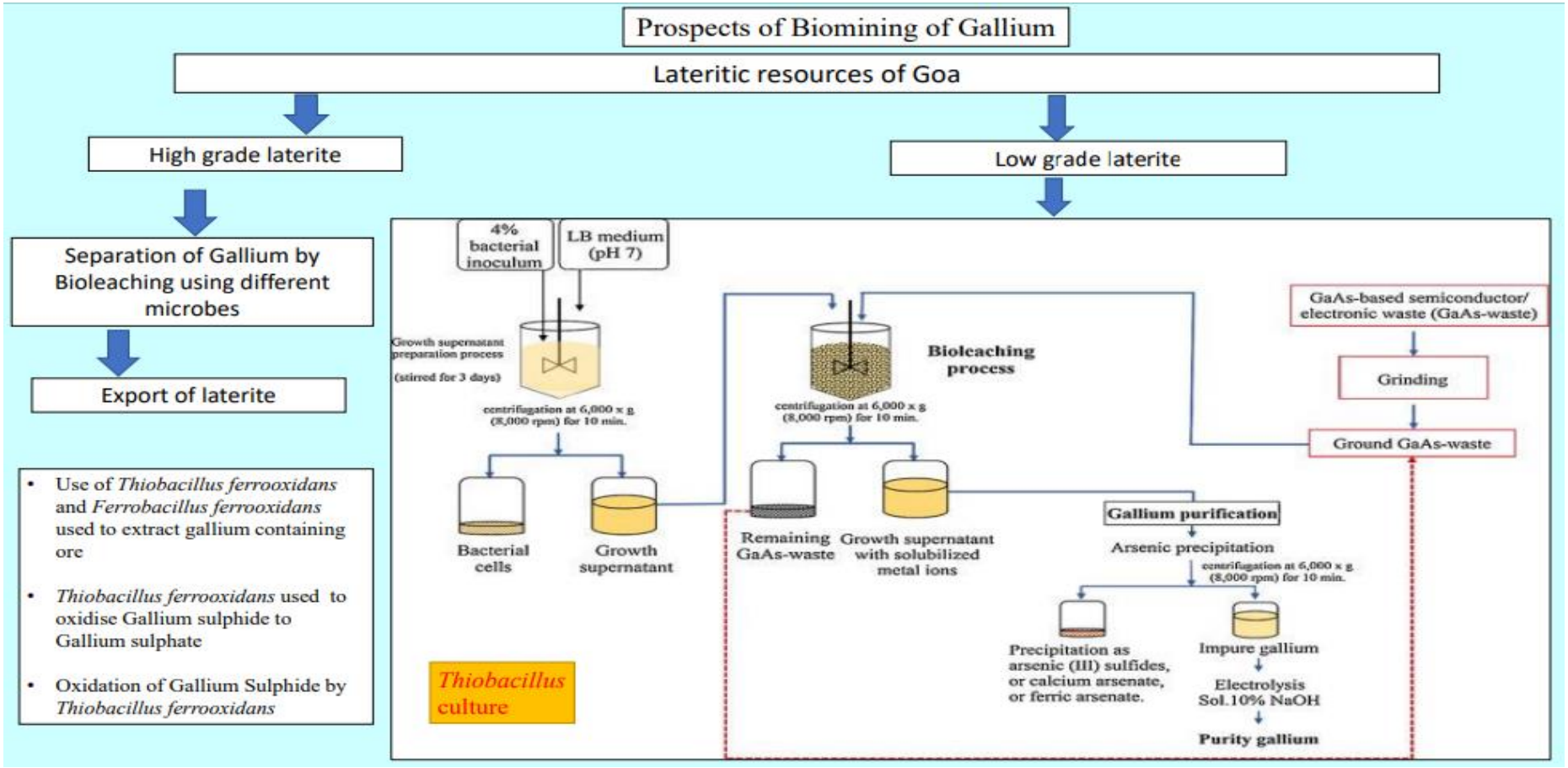

Figure 4.12: Prospects of Bioming of Gallium (Dabolkar and Kamat., 2019)

4.25. The eco-friendly and sustainable biomining of vermiform Gold from auriferous soils

The drilosphere of geophagous earthworms involved in production of earthworms casts by dwelling inside soil and taking up of the organic and inorganic matters. Present study report the presence of Gold particles in vermicasts in Goa for the first time on basis of our field collection and laboratory analysis. Potentiality of earthworms as bioremediating agent for nanoparticles has been reported earlier (Yadav, 2017). Goa forms the part of Western Dharwad Craton (WDC) which is Asia's major metallogenic province. There are various reports on presence of Gold in WDC (Radhakrishna & Curtis, 1991). There is possibility of artisanal extraction of metallic secondary Gold by intelligent, systematic and ecofriendly use of vermicasts by rearing local geophagous earthworms with a feedstock blend of organic matter and auriferous soil. This is like reinventing India's lost alchemic heritage because anyone with some patience can rear earthworms and extract small quantities of metallic Gold easily**.** **Fig 4.13** gives the future roadmap of ecofriendly and sustainable biomining of vermiform Gold from auriferous soils. The first step is establishing facility of rearing of earthworms which can feed on auriferous soils which acts as the raw material. Further in the next step mixture of the auriferous soil (which has been analysed for Gold) and the feeding materials (such as dry plant litter, humic rich materials, cowdung) need to be prepared. To this mixture, earthworms are to be added, to feed on the mixture and move through the soil and build a organo mineral structure (vermicasts) with specific physical, chemical and microbiological properties (Stage I). For the enrichment of Gold, the vermicasts formed during stage I are mixed with the litter feeding material and to this fresh earthworm are added. Further the vermicasts can be treated by powdering, sieving, magnetic separation, gravity separation/ floatation techniques and finally auriferous material is recovered and purified.

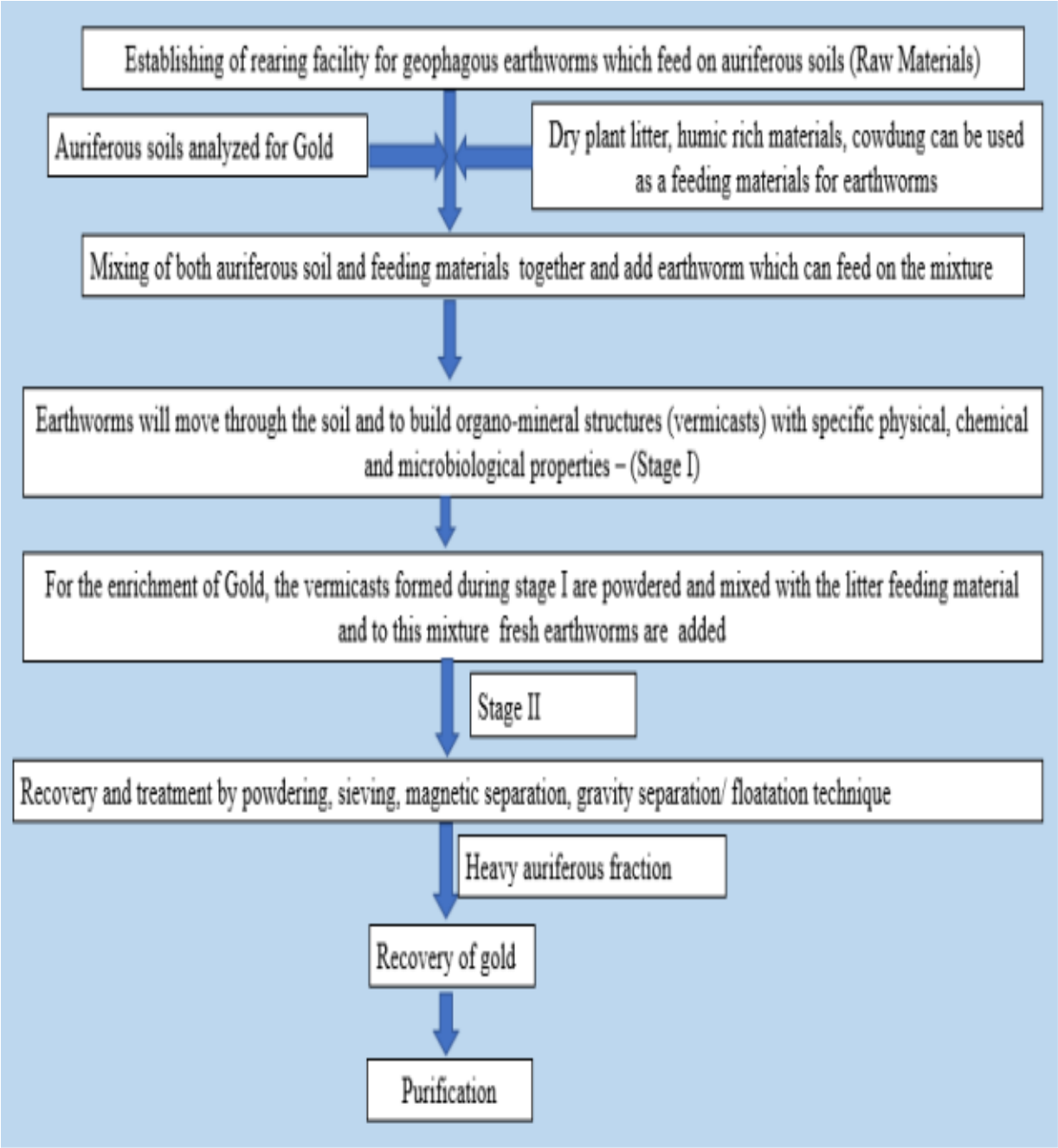

Figure 4.13: The eco-friendly and sustainable biomining of vermiform Gold from auriferous soils

4.26. Phytomining

Phytomining is based on the tendency of some plant species to bioaccumulate excessive amounts of metals from their host rock. The first report of induced hyperaccumulation of Gold was made for a greenhouse study (Anderson et al., 1998) in plants *Brassica juncea* (L.) Czern. (Indian mustard) and this plant was induced to accumulate Gold in leaf tissues to a concentration as high as 57 mg/ kg of dry matter from silica sand containing finely disseminated Gold at a concentration of 5 mg/kg of substrate. Laboratory tests using the crop plants *Raphanus sativus* L. (radish), *Allium cepa* L. (onion), *Beta vulgaris* L. (beet) and *Daucus carota* L. (carrot) cultivated in a silica sand containing 3.8 mg/kg Gold showed that Gold concentrations greater than 200 mg/kg of plant tissue in *R. sativus* could be achieved (Msuya et al., 2000). The list of hyperaccumulating plant is given in the **Table 4.7**, which shows that plant species such as *Chilopsis linearis* yielded high Gold content of 296 mg kg^{-1} and 197mg kg-1 (Rodriguez et al.,2006), which was followed by *B.coddii* and *Daucus carota* (Msuya et al., 2000). Earlier studies in our laboratory have also reported for the first time in Goa the ability of some plants species to take up and accumulate Gold. The work was based on analysis of pure Ash samples of dry aboveground litter of *Acacia auriculiformis, Alstonia scholaris, Anacardium occidentale, Artocarpus heterophyllus*, *Ficus benghalensis, Syzygium cumini* growing in North Goa Mining Banded Iron Formation Belt which comes under Western Dharwad Craton known to be rich in various metals including Gold (Naik and Kamat, 2012). Thus, indicating that Specific plant species can serve as biogeochemical indicators of local Gold deposits. Besides aurophilic tree species can be used in mining dump revegetation program and phytoextraction methods can be used to recover phytoformic Gold. This work could open a new chapter in geobotanical studies of Gold in Goa. The **Fig 4.14** shows how Phyto mining can be carried out in Goa.

Table 4.7: List of Gold hyperaccumulating plants

List of plants species	Chelating agent	Yield of Gold in mg kg−1	References
Daucus carota	$(NH_4)_2S_2O_3$	89	Msuya et al., 2000
B. coddii	NH_4SCN	97	Lamb et al.,2001
Zea mays	NaCN	20	Anderson et al., 2005
Chilopsis linearis	CH_4N_2S, NH_4SCN	296, 197	Rodriguez et al.,2006
Bothriochloa macra, Trifolium repens	NaCN	24, 27	Piccinin et al., 2007

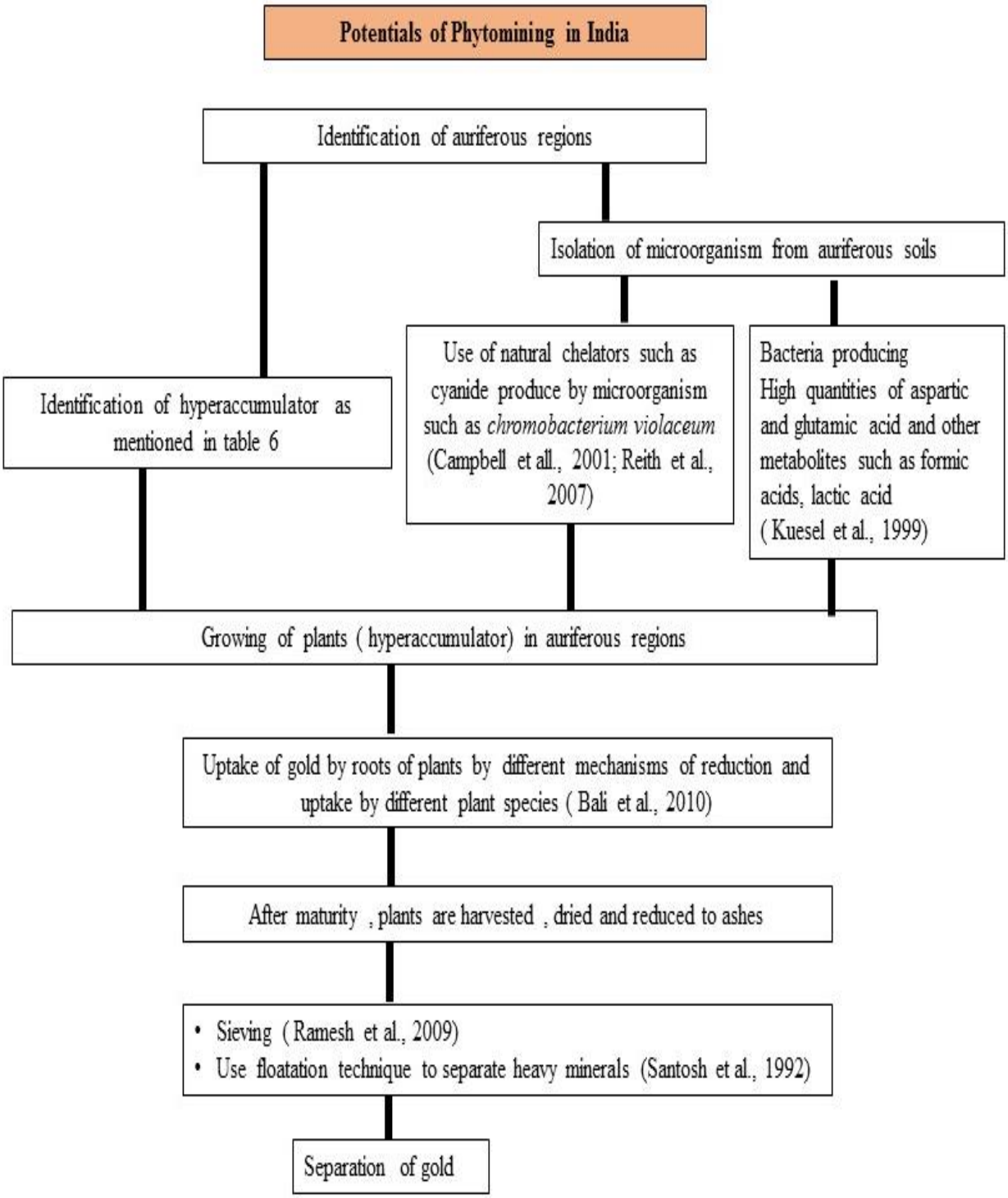

Figure 4.14: Potential of Gold Phytomining in India

4.27. How Indian state of Goa could attain its potential in sustainable biomining with new focus on neglected auriferous resources

In view of the closure of the 62 years old Iron ore industry in Indian state of Goa due to complex techno-legal and environmental issues, lack of systematic geochemical evaluation of the mineral wealth leading to waste of precious auriferous resources and potential of using novel approaches like biomining for Gold extraction this paper advocates a basic paradigm shift in the mining strategy of the state. Goa falling under Western Dharwar Craton (WDC), is one of Asia's major metallogenic provinces having Banded Iron Formation (BIF) of late Archean and Paleoproterozoic periods which provided the backbone of the local Iron ore industry since 1946 with Japan, People's Republic of China (PRC), South Korea and Eastern European Countries as major importers. Lacking in knowledge of systematic geochemical evaluation, Goa's Iron ore centred mining and export strategy had completely overlooked Gold mineralization of economic importance mainly restricted to Archean greenstone terranes of WDC. Despite endowed with chemically the most diverse and creative Archean rocks in WDC, Goa still lacks an intensive knowledge based sustainable mining policy. We present a case for geochemical knowledge based biomining to exploit auriferous samples with 10-12 ppm Gold content. We also hypothesize that in absence of public disclosure of official data on domestic Gold mining, Goa's major Iron ore importer nation, the PRC could have been richly benefitted specifically from 2006 due to extractable Gold content in Goan ore. To clear the global ambiguity over auriferous nature of Goa's Iron ore, we analysed samples from Goa's BIF belt using Optical Microscopy, SEM-EDX and quantified the Gold using ICP-OES. A diversity of presumptive bacterioform Gold (BFG) particles were detected. This is first report on extractable Gold in Goa's Iron ore and low-grade reject. With an estimated one billion MT low grade Iron ore in dumps, we project substantial Gold mining potential and suggest a novel approach involving separation of auriferous fraction from ferromagnetic fraction and use of sustainable biomining

techniques involving microbial bio reduction and bio-oxidation processes. Present study presents the details of our findings and discusses the future roadmap to provide a knowledge-based orientation to Goa's mining industry for attaining its full economic potential as a metallogenic province in Asia as shown in **Table 4.8.**

Table 4.8: Recoverable Gold content

Type of Auriferous sample	**Gold Content g/Metric Tonne (MT)**	**Total quantity of Resources in million MT (MMT)**	**Total content of recoverable secondary Gold in MT**
BIF a) BHQ b) BMQ c) Goethite d) Limonite	 a) 12.93 b) 8 c) N.D d) N.D	800 N.A N. A	 a) 10,344 b) 6400 N.A N. A
Low grade ore in dumbs	7.71	1000	7710
Laterite	3.78	1000	3780
River Alluvial sands	1.77	1 per year	1.77
Vermicasts	1.7	Not known	-
Coastal beaches	0.1-0.29	Not known	-
Stream sediments	12-15	Not known	-

N.D-Not done, N.A-Not Available

4.27.1. Iron ore mining and export without geochemical analysis

Present day mining resumed in 1947 which marks the beginning of modern-day mining and export of iron ore. The exports of iron ore have steadily increased from 4,36,400 tonnes (1951) to 35 MT (2008-09) and has exported 800 MT of Iron ore (1951-2011). The Goan iron ore is exported to Peoples Republic of China, Japan, Taiwan, South Korea and Eastern European Countries (Directorate of Mines and Geology-Goa). Though Goa is restricted to Archean greenstone terranes of WDC, Gold mineralization of economic importance has been neglected by Iron ore centric mining and export strategy. Total exports of Iron ore till closure of mining is 800 million metric tons and average extractable Gold content 10 ppm or 10 grams per dry Metric ton so total extractable Gold lost 8000 million grams equals to 8000 Metric ton. Using a time series of Gold prices since beginning of Iron ore mining in Goa we can use this simple equation. Total value of Gold lost from Goa to foreign countries is equal to summation of (Quantity of auriferous or Gold containing Iron ore in metric tons exported in a particular year for 67 mining years 1946 to 2012) multiplied by (average Gold content in exported ore ,10 grams per metric ton) multiplied by (price of 24 carat Gold that year per gram). So over 52 years from 1950 to 2022 we can see those 24 carats Gold prices for 10 grams in India increased from just Rs. 99 TO 53285 or by a whopping 538 times. Compare high Gold prices with prices of high-grade Iron ore in same period. In 1950 a metric ton of Iron ore exported from Goa fetched US $55. The exchange rate of dollar was Rs. 4.76 in 1950. So, our exporters then got Rs 262 per metric ton. The same Iron ore gets US$ 105 metric ton today in China so Iron ore exporters can get Rs 8400 per metric ton today. Less price for lower grades obviously. That's is less than 62% Iron Oxide content. That means the prices of Iron ore increased from Rs 262 PMT to Rs 8400 PMT or by 32 times from 1950 to 2022. Now that can't be compared to phenomenal rise in the price of Gold. The rising Gold prices since 1950-2022 decade wise is given in **Table 4.9** and US Million per MT and Gold price of Gold in dollars is given in **Table**

4.10. Where price increase was 538 times. That means the Iron ore exporters in Goa were exporting (538/32) extractable secondary Gold, 17 times more valuable than Iron Oxide in ore. The estimated recovery of Gold is given in **Table 4.11.**

Table 4.9: The rising Gold Prices since 1950-2022 decade wise

Year	Price of Gold per 10 grams (Rs.)
1950	99
1960	112
1970	184.50
1980	1,330
1990	3,200
2000	4,400
2010	18,500
2020	48,651
2021	49000
2022	53285

Table 4.10: US Million dollar per MT price of Gold

Fiscal year	US Million per MT	Price of Gold in $
2002-2003	11	342.75
2003-04	13	417.25
2004-05	14	435.60
2005-06	16	513.00
2006-07	20	635.70
2007-08	28	836.50
2008-09	35	869.75
2009-10	46	1087.00
2010-11	49	1420.25
2011-12	54	1531.00

Table 4.11: Estimated recovery of Gold

Year	Exported Iron ore quantity in million metric tons (MMT)	Estimated total recoverable Gold in MT @10 ppm or 10 g /MT	US $ Million per MT price of Gold	Estimated total value as per price (₹) in million Indian rupees	Price of Gold in $ (10 ounce)
2002-2003	19	12.68	11	1904.95	342.75
2003-2004	22	13.82	13	2402.92	417.25
2004-2005	23	16.39	14	2979.94	435.60
2005-2006	26	28.11	16	5778.08	513.00
2006-2007	31	33.45	20	8196.81	635.70
2007-2008	33	36.63	28	9485.22	836.50
2008-2009	38	60.80	35	18259.05	869.75
2009-2010	46	72.51	46	26361.01	1087.00
2010-2011	47	125.91	49	46777.94	1420.25
2011-2012	38	179.63	54	53955.09	1531.00

SUMMARY

SUMMARY

1. Detection of gold in the natural samples from mining and non-mining areas of Goa was carried out. Our studies have established that BHQ contains 12-13 ppm and BMQ 8.4 ppm, whereas the Iron ore reject dumps contain 7.71ppm.
2. The stream sediments from Bondla and Tambdi Surla showed between range from 12.96-15.03 ppm ppm; sand samples showed very negligible between 0.02-0.29 ppm, placer deposits ranged from 0.76-1.08 ppm, and vermicast samples ranged from 0.66 - 6.85 ppm, Termite mounds sample ranged from 0.66-6.85ppm, and laterite and other rock samples ranged from 0.87-3.78ppm. BFG particles studied were 5000 to 10,000. The morphological studies of BFG particles showed that the size varied, ranging from 10 µm to 100 µm. BFG particles studied in each fraction per slide were between 100-400.
3. The BHQ and BMQ samples exhibited morphodiversity such as bird shape, tortoise shape, kite shape, rod shape, and star shape. The colour of the BFG particles ranged from yellow, lemon yellow, canary yellow, golden yellow, and orange to red. Stream sediment samples showed varying shapes such as rod shape, harpoon, star shape, and irregular shape.
4. Metagenomic results revealed that in the BMQ sample, the total number of sequence reads was 72,758. In the case of BMQ, reads analyzed were 36,379, reads classified were 1,016 and reads unclassified was 35,363. The sample showed the presence of 69% of Bacteria, 30% of Eukaryota, <1% of archaea and <1% viruses. In the case of BHQ, the reads analyzed were 18,809, and the reads classified were 669, whereas the remaining reads were unclassified and were 18,140. BHQ sample showed the presence of 71% Bacteria, 27% Eukaryota and 1% archaea.

5. Use of Winogradsky Microcosm (WGMC) by modification using simple, low-cost PET bottles helped in enrichment of microbial biofilms of Iron and Sulphur oxidizing bacteria from different local mineral samples tentatively identified cultures such as *Acidithiobacillus, Leptospirillum* and *Sulphobacillus*.
6. Total of 30 isolates of Actinobacteria were obtained. The isolated strains were classified into various genera based on the spore morphology and mycelium. Out of the 30 actinobacterial isolates, 12 isolates were tentatively identified as genus *Streptomyces* (spore chain with coiling, spiral and looped), 10 isolates as *Nocardia* and 10 were unidentified actinobacterial strains.
7. 400-500 specimens of *Termitomyces* mushrooms were collected. These comprised approx. 300 from field sampling locations and approx. 200 from five market locations.
8. In all, from 10 explants, about 1-2 explants per species yielded healthy colonies leading to the isolation of 10 cultures. From these, 5 cultures were growing rapidly, and 5 showed slow growth. *Termitomyces* cultures exhibited strictly filamentous colonies indicating typical hyphal morphology and branching patterns.
9. *Termitomyces heimii* was found to be promising bioreducing strains, and its assessment of their efficacy for green synthesis of GNPs was checked, which showed that it synthesized GNPs using both pure and crude chloroauric acid.
10. Novel sulphide oxidizing bacteria (NOSOB), which was aerobic, short rods, gram-negative, motile, hyperacidophilic, mesophilic, deposits sulphur globules in plates, oxidizes gold sulphide at room temperature showed promising Gold biooxidation.

BIBLIOGRAPHY

Abbasian, F., Lockington, R., Mallavarapu, M., & Naidu, R. (2015). A pyrosequencing-based analysis of microbial diversity governed by ecological conditions in the Winogradsky column. World Journal of Microbiology and Biotechnology, 31(7), 1115-1126.

Abdul-Hadi, S. Y., Owaid, M. N., Rabeea, M. A., Aziz, A. A., and Jameel, M. S. Rapid mycosynthesis and characterization of phenols-capped crystal gold nanoparticles from *Ganoderma applanatum*, Ganodermataceae. Biocatalysis and Agricultural Biotechnology. 2020; 27: 101683.

Acay, H. Utilization of *Morchella esculenta*-mediated green synthesis golden nanoparticles in biomedicine applications. Preparative Biochemistry & Biotechnology. 2021; 51(2):127-136.

Acharya C, Kar RN, Sukla LB, Misra VN. 2003. Fungal leaching of manganese ore. Vibhuti N. Mishra. 57:501-508.

Adegboye, M. F., Ojuederie, O. B., Talia, P. M., & Babalola, O. O. (2021). Bioprospecting of microbial strains for biofuel production: metabolic engineering, applications, and challenges. *Biotechnology for biofuels*, *14*(1), 1-21.

Agasnalli, C., Basavanna, M., & Lakkundi, T. K. (2015). Geochemistry of banded iron formations and associated gold mineralization of Nagavi, Gadag Schist Belt, Karnataka.

Ahmad, A., Senapati, S., Khan, M. I., Kumar, R., & Sastry, M. (2003). Extracellular biosynthesis of monodisperse gold nanoparticles by a novel extremophilic actinomycete, *Thermomonospora* sp. *Langmuir*, *19*(8), 3550-3553.

Ahmad, A., Senapati, S., Khan, M. I., Kumar, R., and Sastry, M. Extracellular biosynthesis of monodisperse gold nanoparticles by a novel extremophilic actinomycete, *Thermomonospora* sp. *Langmuir*. 2003; 19(8): 3550-3553.

Ahmad, A., Senapati, S., Khan, M. I., Kumar, R., and Sastry, M. (2005). Extra-/intracellular biosynthesis of gold nanoparticles by an alkalotolerant fungus, *Trichothecium* sp. Journal of Biomedical Nanotechnology, 1(1): 47-53.

Ahmad, A., Senapati, S., Khan, M. I., Kumar, R., Ramani, R., Srinivas, V., & Sastry, M. (2003). Intracellular synthesis of gold nanoparticles by a novel alkalotolerant actinomycete, *Rhodococcus* species. Nanotechnology, 14(7), 824.

Ahmad, R., Sellathoroe, S., Ngadi, E., Saharuddin, T. S. T., Zakaria, I. I., Selvakumaran, S., and Wan, W. A. A. Q. I. (2021).Isolation, identification, cultivation and determination of antimicrobial β-glucan from a wild-termite mushroom *Termitomyces heimii* RFES 230662. Biocatalysis and Agricultural Biotechnology, 37-102187.

Ahmed, H. A., & El-Midany, A. A. (2012). Gold recovery from sulphide minerals: a bioprocessing approach. *AfinidAd*, *69*(557).

Ajnai, G., Chiu, A., Kan, T., Cheng, C. C., Tsai, T. H., & Chang, J. (2014). Trends of gold nanoparticle-based drug delivery system in cancer therapy. *Journal of Experimental & Clinical Medicine*, *6*(6), 172-178.

Albrecht, M. A., Evans, C. W., & Raston, C. L. (2006). Green chemistry and the health implications of nanoparticles. *Green chemistry*, *8*(5), 417-432.

Anand R, Lintern M, Hough R, Noble R, Verrall M, Salama W, Radford N. 2017. The dynamics of gold in regolith change with differing environmental conditions over time. Geology. 45(2):127-130.

Anand, R. R., Hough, R. M., Salama, W., Aspandiar, M. F., Butt, C. R. M., González-Álvarez, I., & Metelka, V. (2019). Gold and pathfinder elements in ferricrete gold deposits of the Yilgarn Craton of Western Australia: A review with new concepts. *Ore Geology Reviews*, *104*, 294-355.

Ananda Murthy S, Bhattacharjee S.1997. Occurrences of Gold in Guntipalli-Atkur Area, Gadwal Schist Belt, Mahbubnagar District AP. Journal-Geological Society of India. 49:721-2.

Anderson, C., Moreno, F., & Meech, J. (2005). A field demonstration of gold phytoextraction technology. *Minerals Engineering*, *18*(4), 385-392.

Andreo, J., Ettlinger, R., Zaremba, O., Peña, Q., Lächelt, U., de Luis, R. F., ... & Wuttke, S. (2022). Reticular Nanoscience: Bottom-Up Assembly Nanotechnology. *Journal of the American Chemical Society*, *144*(17), 7531-7550.

Angerer, T., Duuring, P., Hagemann, S. G., Thorne, W., & McCuaig, T. C. (2015). A mineral system approach to iron ore in Archaean and Palaeoproterozoic BIF of Western Australia. *Geological Society, London, Special Publications*, *393*(1), 81-115.

Angerer, T., Hagemann, S. G., & Danyushevsky, L. V. (2012). Geochemical evolution of the banded iron formation-hosted high-grade iron ore system in the Koolyanobbing Greenstone Belt, Western Australia. *Economic Geology*, *107*(4), 599-644.

Angerer, T., Kerrich, R., & Hagemann, S. G. (2013). Geochemistry of a komatiitic, boninitic, and tholeiitic basalt association in the Mesoarchean Koolyanobbing greenstone belt, Southern Cross Domain, Yilgarn craton: Implications for mantle sources and geodynamic setting of banded iron formation. *Precambrian Research*, *224*, 110-128.

Anjum, F., Shahid, M., & Akcil, A. (2012). Biohydrometallurgy techniques of low grade ores: A review on black shale. *Hydrometallurgy*, *117*, 1-12.

Arhin, E., & Nude, P. M. (2010). Use of termitaria in surficial geochemical surveys: evidence for> 125-μm size fractions as the appropriate media for gold exploration in northern Ghana. *Geochemistry: Exploration, Environment, Analysis*, *10*(4), 401-406.

Arhin, E., Boadi, S., & Esoah, M. C. (2015). Identifying pathfinder elements from termite mound samples for gold exploration in regolith complex terrain of the Lawra belt, NW Ghana. *Journal of African Earth Sciences*, *109*, 143-153.

Arhin, E., Captain-Esoah, M., & Berdie, B. S. (2018). Economic Importance of Termites and Termitaria in Mineral Exploration. In *Termites and Sustainable Management* (pp. 241-258). Springer, Cham.

Arshi, N., Ahmed, F., Kumar, S., Anwar, M. S., Lu, J., Koo, B. H., & Lee, C. G. (2011). Microwave assisted synthesis of gold nanoparticles and their antibacterial activity against Escherichia coli (E. coli). *Current Applied Physics*, *11*(1), S360-S363.

Ashley, P. M., Creagh, C. J., & Ryan, C. G. (2000). Invisible gold in ore and mineral concentrates from the Hillgrove gold-antimony deposits, NSW, Australia. *Mineralium Deposita*, *35*(4), 285-301.

Asker D, Ohta Y. 2002. *Haloferax alexandrinus* sp. nov., an extremely halophilic canthaxanthin-producing archaeon from a solar saltern in Alexandria (Egypt). Int J Syst Evol Microbiol. 52:729–738.

Aswegen, P. C. V., Niekerk, J. V., & Olivier, W. (2007). The BIOX™ process for the treatment of refractory gold concentrates. In *Biomining* (pp. 1-33). Springer, Berlin, Heidelberg.

Atherton, R. J., Baird, A. J., & Wiggs, G. F. (2001). Inter-tidal dynamics of surface moisture content on a meso-tidal beach. *Journal of Coastal Research*, 482-489.

Atlas, R. M., & Bartha, R. (1993). Microbial ecology: fundamentals and applications. Redwood City.

Babu, S. B., Patel, S. K., Singh, R. B., & Balakrishna, B. (2019, November). Reconnaissance Geophysical Surveys for Gold: Karimpuzha-Thalipuzha Sector of Nilambur, Mallappuram Dist, Kerala, India. In *1st Indian Near Surface Geophysics Conference*

& Exhibition (Vol. 2019, No. 1, pp. 1-6). European Association of Geoscientists & Engineers.

Bae, A. H., Numata, M., Yamada, S., and Shinkai, S. New approach to preparing one-dimensional Au nanowires utilizing a helical structure constructed by schizophyllan. New Journal of Chemistry. 2007; 31(5): 618-622.

Balagurunathan, R., Radhakrishnan, M., Rajendran, R. B., & Velmurugan, D. (2011). Biosynthesis of gold nanoparticles by actinomycete *Streptomyces viridogens* strain HM10.

Bali, R., & Harris, A. T. (2010). Biogenic synthesis of Au nanoparticles using vascular plants. *Industrial & engineering chemistry research*, *49*(24), 12762-12772.

Ballav, S., Kerkar, S., Thomas, S., & Augustine, N. (2015). Halophilic and halotolerant actinomycetes from a marine saltern of Goa, India producing anti-bacterial metabolites. *Journal of bioscience and bioengineering*, *119*(3), 323-330.

Banerjee, and Rai. A Review on Mycosynthesis, Mechanism, and Characterization of Silver and Gold Nanoparticles. In BioNanoScience 2018; 8(1): 17–31. Springer New York LLC. https://doi.org/10.1007/s12668-017-0437-8

Banerjee, K., and Ravishankar Rai, V. A review on mycosynthesis, mechanism, and characterization of silver and gold nanoparticles. *BioNanoScience*. 2018; *8*(1): 17-31.

Barabadi, H., Honary, S., Ebrahimi, P., Mohammadi, M. A., Alizadeh, A., and Naghibi, F. Microbial mediated preparation, characterization and optimization of gold nanoparticles. 2014. www.sbmicrobiologia.org.br

Barton, C. M., Ullah, I. I., & Bergin, S. (2010). Land use, water and Mediterranean landscapes: modelling long-term dynamics of complex socio-ecological systems. *Philosophical Transactions of the Royal Society A: Mathematical, Physical and Engineering Sciences*, *368*(1931), 5275-5297.

Basiev, T. T., Sobol, A. A., Zverev, P. G., Osiko, V. V., and Powell, R. C. Comparative spontaneous Raman spectroscopy of crystals for Raman lasers. Applied Optics. 1999; 38(3): 594-598.

Basta, F. F., Maurice, A. E., Fontboté, L., & Favarger, P. Y. (2011). Petrology and geochemistry of the banded iron formation (BIF) of Wadi Karim and Um Anab, Eastern Desert, Egypt: implications for the origin of Neoproterozoic BIF. *Precambrian Research*, *187*(3-4), 277-292.

Bellenberg, S., Leon-Morales, C.F., Sand, W. and Vera, M. 2012. Visualization of capsular polysaccharide introduction in *Acidithiobacillus ferrooxidans*. Hydrometallurgy. 129: 82-89.

Bennur, T., Javdekar, V., Tomar, G. B., & Zinjarde, S. (2020). Gold nanoparticles biosynthesized by *Nocardiopsis dassonvillei* NCIM 5124 enhance osteogenesis in gingival mesenchymal stem cells. *Applied microbiology and biotechnology*, *104*(9), 4081-4092.

Bennur, T., Ravi Kumar, A., Zinjarde, S. S., & Javdekar, V. (2016). Nocardiopsis species: a potential source of bioactive compounds. *Journal of applied microbiology*, *120*(1), 1-16.

Beukes, N. J. (1984). Sedimentology of the Kuruman and Griquatown iron-formations, transvaal supergro James, H. L. (1954). Sedimentary facies of iron-formation. *Economic Geology*, *49*(3), 235-293.up, Griqualand West, South Africa. *Precambrian Research*, *24*(1), 47-84.

Beukes, N. J., Gutzmer, J., & Mukhopadhyay, J. (2003). The geology and genesis of high-grade hematite iron ore deposits. *Applied Earth Science*, *112*(1), 18-25.

Bhadke, P., & Savoikar, P. P. (2021). A case study of geotechnical investigations for soft lateritic soil site in South Goa. In *Recent Developments in Sustainable Infrastructure* (pp. 69-77). Springer, Singapore.

Bhambure, R., Bule, M., Shaligram, N., Kamat, M., & Singhal, R. (2009). Extracellular biosynthesis of gold nanoparticles using *Aspergillus niger*–its characterization and stability. *Chemical Engineering & Technology: Industrial Chemistry-Plant Equipment-Process Engineering-Biotechnology*, *32*(7), 1036-1041.

Bhat, M., Chakraborty, B., Kumar, R. S., Almansour, A. I., Arumugam, N., Kotresha, D., ... & Nayaka, S. (2021). Biogenic synthesis, characterization and antimicrobial activity of Ixora brachypoda (DC) leaf extract mediated silver nanoparticles. *Journal of King Saud University-Science*, *33*(2), 101296.

Bhat, Ravishankar, V. G. Sharanabasava, Raghunandan Deshpande, Ullas Shetti, Ganesh Sanjeev, and A. Venkataraman. Photo-bio-synthesis of irregular shaped functionalized gold nanoparticles using edible mushroom *Pleurotus florida* and its anticancer evaluation. Journal of Photochemistry and Photobiology B: Biology. 2013;125: 63-69.

Bhattacharya, A., Krishnakumar, K. R., Raith, M., & Sen, S. K. (1991). An improved set of a—X parameters for Fe—Mg—Ca garnets and refinements of the orthopyroxene–garnet thermometer and the orthopyroxene—garnet—plagioclase—quartz barometer. *Journal of Petrology*, *32*(3), 629-656.

Bhattarai, B., Zaker, Y., & Bigioni. Green synthesis of gold and silver nanoparticles: Challenges and opportunities. Current Opinion in Green and Sustainable Chemistry. 2018; 12: 91-100.

Binupriya, A. R., Sathishkumar, M., & Yun, S. I. (2010). Myco-crystallization of silver ions to nanosized particles by live and dead cell filtrates of *Aspergillus oryzae* var. viridis

and its bactericidal activity toward Staphylococcus aureus KCCM 12256. *Industrial & Engineering Chemistry Research*, *49*(2), 852-858.

Bischoff, G. C. (1997). The biological origin of bacterioform gold from Australia. *Neues Jahrbuch für Geologie und Paläontologie-Monatshefte*, 329-338.

BISCHOFF, G. C., COENRAADS, R. R., & LUSK, J. (1992). Microbial accumulation of gold. an example from Venezuela. *Neues Jahrbuch für Geologie und Paläontologie. Abhandlungen*, *185*(2), 131-159.

Biswas, S. K. (2021, August). Geological Setup for Gold Prospects and Deposits in India. In *Conference GSI* (pp. 1-13).

Botha, W. J., & Eicker, A. Cultural studies on the genus *Termitomyces* in South Africa. I. Macro-and microscopic characters of basidiome context cultures. *Mycological Research*. 1991; 95(4): 435-443.

Brierley JA, Brierley CL. 2001. Present and future commercial applications of biohydrometallurgy. Hydrometallurgy.59(2-3):233-9.

Brierley, J. A. (1978). Thermophilic iron-oxidizing bacteria found in copper leaching dumps. *Applied and Environmental Microbiology*, *36*(3), 523-525.

Brombacher, C., Bachofen, R., & Brandl, H. (1997). Biohydrometallurgical processing of solids: a patent review. *Applied microbiology and biotechnology*, *48*(5), 577-587.

Bulaev, A. G., Kanaeva, Z. K., Kanaev, A. T., & Kondrat'eva, T. F. (2015). Biooxidation of a double-refractory gold-bearing sulfide ore concentrate. *Microbiology*, *84*(5), 636-643.

Bulaev, A. G., Pivovarova, T. A., Melamud, V. S., Bumazhkin, B. K., Patutina, E. O., Kolganova, T. V., ... & Kondrat'eva, T. F. (2011). Species composition of the association of acidophilic chemolithotrophic microorganisms participating in the oxidation of gold-arsenic ore concentrate. *Microbiology*, *80*(6), 842-849.

Campbell, S. C., Olson, G. J., Clark, T. R., & McFeters, G. (2001). Biogenic production of cyanide and its application to gold recovery. *Journal of Industrial Microbiology and Biotechnology*, *26*(3), 134-139.

Cao, B., Xu, H., & Mao, C. (2011). Transmission electron microscopy as a tool to image bioinorganic nanohybrids: The case of phage-gold nanocomposites. *Microscopy research and technique*, *74*(7), 627-635.

Carnovale, C., Bryant, G., Shukla, R., & Bansal, V. (2016). Size, shape and surface chemistry of nano-gold dictate its cellular interactions, uptake and toxicity. *Progress in Materials Science*, *83*, 152-190.

Castro-Longoria, E., Vilchis-Nestor, A. R., & Avalos-Borja, M. (2011). Biosynthesis of silver, gold and bimetallic nanoparticles using the filamentous fungus *Neurospora crassa*. *Colloids and surfaces B: Biointerfaces*, *83*(1), 42-48.

Cateni, F., Gargano, M. L., Procida, G., Venturella, G., Cirlincione, F., & Ferraro, V. (2021). Mycochemicals in wild and cultivated mushrooms: nutrition and health. *Phytochemistry Reviews*, 1-45.

Chandra, R., Sathya, V., Prusty, B. A. K., Azeez, P. A., & Mahimairaja, S. (2014, December). The Kolar Gold Mines, India: present status and prospects for phytomining. In *2014-Sustainable Industrial Processing Summit* (Vol. 1, pp. 273-282). Flogen Star Outreach.

Chater, K. F. (1993). Genetics of differentiation in Streptomyces. *Annual review of microbiology*, *47*, 685-714.

Chauhan, A., Zubair, S., Tufail, S., Sherwani, A., Sajid, M., Raman, S. C., ... & Owais, M. (2011). Fungus-mediated biological synthesis of gold nanoparticles: potential in detection of liver cancer. *International journal of nanomedicine*, *6*, 2305-2319.

Chavarie C, Karamanev D, Godard F, Garnier A, Andre G. 1993. Comparison of the kinetics of ferrous iron oxidation by three different strains of *Thiobacillus ferrooxidans*. Geomicrobiology Journal. 11(1):57-63.

Chelly, M., Chelly, S., Zribi, R., Bouaziz-Ketata, H., Gdoura, R., Lavanya, N., and Neri, G. Synthesis of Silver and Gold Nanoparticles from Rumex roseus Plant Extract and Their Application in Electrochemical Sensors. Nanomaterials. 2021; 11(3): 739.

Chelly, S., Chelly, M., Zribi, R., Gdoura, R., Bouaziz-Ketata, H., & Neri, G. (2021). Electrochemical detection of dopamine and riboflavine on a screen-printed carbon electrode modified by AuNPs derived from *rhanterium suaveolens* plant extract. *ACS omega*, *6*(37), 23666-23675.

Chen, H., Yang, B., & Chen, X. (2009). Identification and characterization of four strains of *Acidithiobacillus ferrooxidans* isolated from different sites in China. Microbiological Research, 164(6), 613-623.

Chingwaru W, Vidmar J, Chingwaru C. 2017. Potential of biotechnology for metals extraction in Zimbabwe: a review. Journal of the Southern African Institute of Mining and Metallurgy. 117(4):381-386.

Chithrani, B. D., Ghazani, A. A., & Chan, W. C. (2006). Determining the size and shape dependence of gold nanoparticle uptake into mammalian cells. *Nano letters*, *6*(4), 662-668.

Cloud, P. (1973). Paleoecological significance of the banded iron-formation. *Economic Geology*, *68*(7), 1135-1143.

Clough, D. M., & Craw, D. (1989). Authigenic gold-marcasite association; evidence for nugget growth by chemical accretion in fluvial gravels, Southland, New Zealand. *Economic geology*, *84*(4), 953-958.

Colin, F., Sanfo, Z., Brown, E., Bourlès, D., & Minko, A. E. (1997). Gold: a tracer of the dynamics of tropical laterites. *Geology*, *25*(1), 81-84.

Cope, I. L., Wilkinson, J. J., Boyce, A. J., & Herrington, R. J. (2009, August). Oxygen isotope composition of hematite: Pic de Fon Deposit, Republic of Guinea, West Africa. In *Proceedings of the 10th Biennial SGA Meeting, Townsville* (pp. 17-20).

Corral MT, Gonzalez F, Blazquez ML, Ballester A, Munoz J.1993. Continuous bioleaching of mineral sulphides. Biohydrometallurgical Technologies.1:65-75.

Costerton, J.W., Lewandowski, Z., Caldwell, D.E., Korber, D.R. and Lappin-Scott, H.M. 1995. Microbial biofilms. Annual Review of Microbiology. 49(1): 711- 745.

Cowan D, Meyer Q, Stafford W, Muyanga S, Cameron R, Wittwer P. 2005. Metagenomic gene discovery: past, present and future. TRENDS in Biotechnology. 23(6): 321-329.

Dabolkar, S., & Kamat, N. M. (2019). Potential of geophagous earthworms in ecofriendly and sustainable biomining of gold from auriferous soils.

Dabolkar, S., & Kamat, N. M. (2020). Application of Digital Colorimeter for Preliminary Characterization of Gold Nanoparticle Swarms Produced by *Termitomyces heimii* Using a novel Bioinspired Microfluidics Assay. *bioRxiv*.

Dabolkar, S., & Kamat, N. M. (2021). Pioneer studies on metagenomic analysis of samples from banded iron formation (BIF) from iron ore mining belt of Goa, India.

Dabolkar, S., & Kamat, N. M. (2022). Method for separation and detection of gold sulphide from Banded Magnetite Quartzite (BMQ) of Goa. Eco. Env. & Cons. 28 (August Suppl. Issue): 2022; pp. (S250-S253) Copyright@ EM International ISSN 0971–765X.

Dabolkar, S., and Kamat, N. M. Application of digital colorimeter for preliminary characterization of gold nanoparticle swarms produced by *Termitomyces heimii* using a novel bioinspired microfluidics assay. Kavaka. 2020; 55:50-57

Dabolkar. S & Kamat. N.M. (2022). Use of the Modified Winogradsky Microcosm Technique to Help in Building an Indigenous Culture Collection of Iron and Sulphur Bacteria Valuable in Green Synthesis of Gold Nanoparticles. Eco. Env. & Cons. 28 (January Suppl. Issue): 2022; pp. (S233-S238) Copyright@ EM International ISSN 0971–765X.

Danae Voormeij (2021). Gold in exploration in tropical landscape, Fifth Edition, 2021 Mynah Exploration Inc. ISBN 978-0-9920934-5.

Darvanjooghi, M. H. K., Magdouli, S., Brar, S. K., Abdollahi, H., & Zolfaghari, M. (2022). Bio-oxidation of Gold from Refractory Sulfide Ores: A Journey Ahead. *Geomicrobiology Journal*, *39*(3-5), 399-415.

Das AP, Sukla LB, Pradhan N, Nayak S. 2011. Manganese biomining: a review. Bioresource technology. 102(16):7381-7387.

Das, A. P., Ghosh, S., Mohanty, S., & Sukla, L. B. (2015). Advances in manganese pollution and its bioremediation. In *Environmental microbial biotechnology* (pp. 313-328). Springer, Cham.

Das, K., Goswami, M. L. N., Dhar, A., Mathur, B. K., & Ray, S. K. (2007). Growth of Ge islands and nanocrystals using RF magnetron sputtering and their characterization. *Nanotechnology*, *18*(17), 175301.

Das, R. K., Borthakur, B. B., & Bora, U. Green synthesis of gold nanoparticles using ethanolic leaf extract of *Centella asiatica*. Materials Letters. 2010; 64(13): 1445-1447.

Das, S. K., Das, A. R., and Guha, A. K. Microbial synthesis of multishaped gold nanostructures. Small, 2010; 6(9):1012–1021. https://doi.org/10.1002/smll.200902011

de Oliveira, S. M. B., & Larizzatti, J. H. (2005). Some Observations on gold in the weathering profile at Garimpo Porquinho, an artisanal mine in the Tapajós region, Brazilian Amazon. *Geologia USP. Série Científica*, *5*(2), 1-11.

De Souza, R. A., Kamat, N. M., & Nadkarni, V. S. (2018). Purification and characterisation of a sulphur rich melanin from edible mushroom *Termitomyces albuminosus* Heim. *Mycology*, *9*(4), 296-306.

De Souza, R.A. and Kamat, N.M. Evaluation and characterization of pellet morphology of genus *Termitomyces heimii* of a wild tropical edible mushroom. Journal of Pharmaceutical, Chemical and Biological Sciences. 2018a; 6(4): 320-328.

De Souza, R.A. and Kamat, N.M. *Termitomyces* holomorph benefits from anomalous Sulphur content in teleomorph. International Journal of Life scinces Research. 2019; 1: 186-192.

De Souza, R.A., Kamat, N.M. and Nadkarni, V.S. Purification and characterisation of a sulphur rich melanin from edible mushroom *Termitomyces albuminosus Heim*. Mycology. 2018b; 9 (4): 296-306.

Dec, W., Jaworska-Kik, M., Simka, W., & Michalska, J. (2018). Corrosion behaviour of 2205 duplex stainless steel in pure cultures of sulphate reducing bacteria: SEM studies, electrochemical characterisation and biochemical analyses. *Materials and Corrosion*, *69*(1), 53-62.

Dedysh, S. N. Winogradsky Institute of Microbiology. *Russian Academy of Sciences, Russia*.

Deepika, L., & Kannabiran, K. (2010). Biosurfactant and heavy metal resistance activity of *Streptomyces* spp. isolated from saltpan soil. *Br J Pharm Toxicol*, *1*, 33-39.

Dessai, A. G. (2011). The geology of Goa Group: revisited. *Journal of the Geological Society of India*, *78*(3), 233-242.

Dessai, A. G. (2018). Geology and Mineral Resources of Goa, New Delhi publishers, New Delhi, ISBN: 978-93-86453-105.

Dessai, A. G., Arolkar, D. B., French, D., Viegas, A., & Viswanath, T. A. (2009). Petrogenesis of the Bondla layered mafic-ultramafic complex, Usgaon, Goa. *Journal of the Geological Society of India*, *73*(5), 697-714.

Dessai, A. G., Arolkar, D. B., French, D., Viegas, A., & Viswanath, T. A. (2009). Petrogenesis of the Bondla layered mafic-ultramafic complex, Usgaon, Goa. *Journal of the Geological Society of India*, *73*(5), 697-714.

Devaraju, T. C., Sudhakara, T. L., Kaukonen, R. J., Viljoen, R. P., Alapieti, T. T., Ahmed, S. A., & Sivakumar, S. (2010). Petrology and geochemistry of greywackes from Goa-Dharwar sector, western Dharwar Craton: Implications for volcanoclastic origin. *Journal of the Geological Society of India*, *75*(3), 465-487.

Devaraju, T. C., Viljoen, R. P., Sawkar, R. H., & Sudhakara, T. L. (2009). Mafic and ultramafic magmatism and associated mineralization in the Dharwar craton, southern India. *Journal of the Geological Society of India*, *73*(1), 73-100.

Devasia P, Natarajan KA. 2004. Bacterial leaching. Resonance. 9(8):27-34.

Dheyab, M. A., Aziz, A. A., Jameel, M. S., Noqta, O. A., Khaniabadi, P. M., & Mehrdel, B. (2020). Simple rapid stabilization method through citric acid modification for magnetite nanoparticles. *Scientific reports*, *10*(1), 1-8.

Dheyab, M. A., Owaid, M. N., Rabeea, M. A., Aziz, A. A., & Jameel, M. S. (2020). Mycosynthesis of gold nanoparticles by the Portabello mushroom extract, Agaricaceae, and their efficacy for decolorization of Azo dye. *Environmental nanotechnology, monitoring & management*, *14*, 100312.

Dhillon, G. S., Brar, S. K., Kaur, S., & Verma, M. Green approach for nanoparticle biosynthesis by fungi: current trends and applications. Critical reviews in biotechnology. 2012; 32(1): 49-73.

Dhoundial, D. P., Paul, D. K., Sarkar, A., Trivedi, J. R., Gopalan, K., & Potts, P. J. (1987). Geochronology and geochemistry of Precambrian granitic rocks of Goa, SW India. *Precambrian Research*, *36*(3-4), 287-302.

Dodd, M. S., Papineau, D., Grenne, T., Slack, J. F., Rittner, M., Pirajno, F., ... & Little, C. T. (2017). Evidence for early life in Earth's oldest hydrothermal vent precipitates. *Nature*, *543*(7643), 60-64.

Donkor, E. S. (2013). Sequencing of bacterial genomes: principles and insights into pathogenesis and development of antibiotics. *Genes*, *4*(4), 556-572.

Dreher, C. L., Schad, M., Robbins, L. J., Konhauser, K. O., Kappler, A., & Joshi, P. (2021). Microbial processes during deposition and diagenesis of Banded Iron Formations. *PalZ*, *95*(4), 593-610.

D'Souza, R. A., & Kamat, N. M. (2017). Potential of FTIR spectroscopy in chemical characterization of *Termitomyces* Pellets. *Journal of Applied Biology & Biotechnology Vol*, *5*(04), 080-084.

Dumur, F., Guerlin, A., Dumas, E., Bertin, D., Gigmes, D., & Mayer, C. R. (2011). Controlled spontaneous generation of gold nanoparticles assisted by dual reducing and capping agents. *Gold bulletin*, *44*(2), 119-137.

Durán M, Faljoni-Alario A, Durán N. 2010. *Chromobacterium violaceum* and its important metabolites. Folia microbiologica. 55(6):535-547.

Dzigbodi-Adjimah, K. (1993). Geology and geochemical patterns of the Birimian gold deposits, Ghana, West Africa. *Journal of geochemical exploration*, *47*(1-3), 305-320.

Dziuba, B., Babuchowski, A., Nałęcz, D., & Niklewicz, M. (2007). Identification of lactic acid bacteria using FTIR spectroscopy and cluster analysis. *International dairy journal*, *17*(3), 183-189.

Ehrlich H L. 1996. How microbes influence mineral growth and dissolution. Chem Geol. 132:1-3

Ehrlich, H. L. (2001). Past, present and future of biohydrometallurgy. *Hydrometallurgy*, *59*(2-3), 127-134.

Ehrlich, H. L., Newman, D. K., & Kappler, A. (2002). Geomicrobiology (p. 768). M. Dekker.

Ehrlich, H., Bailey, E., Wysokowski, M., & Jesionowski, T.(2021). Forced biomineralization: a review. Biomimetics, 6(3), 46.

Eisler, R. 2003. Biorecovery of gold. Indian Journal of Experimental Biology, 41(9): 967-971.

Elahi, N., Kamali, M., & Baghersad, M. H. (2018). Recent biomedical applications of gold nanoparticles: A review. *Talanta*, *184*, 537-556.

El-Batal, A. I., ElKenawy, N. M., Yassin, A. S., and Amin, M. A. Laccase production by *Pleurotus ostreatus* and its application in synthesis of gold nanoparticles. Biotechnology Reports. 2015; 5:31-39.

Enache M, Itoh T, Kamekura M, Popescu G, Dumitru L. 2008. Halophilic archaea of *Haloferax* genus isolated from Anthopocentric Telega (Palada) salt lake. Proc Rom Acad Series B. 1–2:11–16.

Eppler, A. S., Rupprechter, G., Anderson, E. A., & Somorjai, G. A. (2000). Thermal and chemical stability and adhesion strength of Pt nanoparticle arrays supported on silica studied by transmission electron microscopy and atomic force microscopy. *The Journal of Physical Chemistry B*, *104*(31), 7286-7292.

Eskandari-Nojedehi, M., Jafarizadeh-Malmiri, H., & Rahbar-Shahrouzi, J. (2018). Hydrothermal green synthesis of gold nanoparticles using mushroom (*Agaricus bisporus*) extract: physico-chemical characteristics and antifungal activity studies. *Green Processing and Synthesis*, *7*(1), 38-47.

Eugene, W. W. L., & Mujumdar, A. S. (2009). Gold extraction and recovery processes. *Minerals, Metals, and Materials Technology Centre, National University of Singapore*.

Evans, K. A., McCuaig, T. C., Leach, D., Angerer, T., & Hagemann, S. G. (2013). Banded iron formation to iron ore: A record of the evolution of Earth environments?. *Geology*, *41*(2), 99-102.

Fairbrother L, Brugger J, Shapter J, Laird JS, Southam G, Reith F. (2012). Supergene gold transformation: Biogenic secondary and nano-particulate gold from arid Australia. Chemical Geology. 320:17-31.

Fairbrother, L. (2013). *Cupriavidus metallidurans* and the Biomineralization of Gold. *Chemical Geology*, *320*, 17-31.

Fairbrother, L., Etschmann, B., Brugger, J., Shapter, J., Southam, G., & Reith, F. (2013). Biomineralization of gold in biofilms of *Cupriavidus metallidurans*. Environmental Science & Technology, 47(6), 2628-2635.

Falconer, D. M., Craw, D., Youngson, J. H., & Faure, K. (2006). Gold and sulphide minerals in Tertiary quartz pebble conglomerate gold placers, Southland, New Zealand. *Ore Geology Reviews*, *28*(4), 525-545.

Falconer, D.M. and Craw, D. (2009). Supergene gold mobility: a textural and geochemical study from gold placers in southern New Zealand. Econ. Geol., Spec. Publ., v. 14, pp. 77-93.

Farwell, A. J., Vesely, S., Nero, V., Rodriguez, H., Shah, S., Dixon, D. G., & Glick, B. R. (2006). The use of transgenic canola (*Brassica napus*) and plant growth-promoting bacteria to enhance plant biomass at a nickel-contaminated field site. *Plant and Soil*, *288*(1), 309-318.

Fayaz, A. M., Balaji, K., Kalaichelvan, P. T., & Venkatesan, R. (2009). Fungal based synthesis of silver nanoparticles—an effect of temperature on the size of particles. *Colloids and Surfaces B: Biointerfaces*, *74*(1), 123-126.

Fayaz, A. M., Girilal, M., Mahdy, S. A., Somsundar, S. S., Venkatesan, R., & Kalaichelvan, P. T. (2011). Vancomycin bound biogenic gold nanoparticles: a different perspective for development of anti VRSA agents. *Process biochemistry*, *46*(3), 636-641.

Fayaz, A. M., Girilal, M., Rahman, M., Venkatesan, R., & Kalaichelvan, P. T. (2011). Biosynthesis of silver and gold nanoparticles using thermophilic bacterium Geobacillus stearothermophilus. *Process Biochemistry*, *46*(10), 1958-1962.

Fernandes, G. Q., Iyer, S. D., & Kotha, M. (2016). The Origin and Tectonic Setting of Precambrian Greywacke of Ribandar-Chimbel, Goa, India: Petrological and Geochemical Evidence. *Acta Geologica Sinica-English Edition*, *90*(6), 2036-2048.

Flemming, H.C. and Wingender, J. 2010. The biofilm matrix. Nature Reviews Microbiology. 8(9): 623-633.

Fomchenko, N. V., Kondrat'eva, T. F., & Muravyov, M. I. (2016). A new concept of the biohydrometallurgical technology for gold recovery from refractory sulfide concentrates. *Hydrometallurgy*, *164*, 78-82.

French, J. E., Heaman, L. M., Chacko, T., & Srivastava, R. K. (2008). 1891–1883 Ma Southern Bastar–Cuddapah mafic igneous events, India: A newly recognized large igneous province. *Precambrian research*, *160*(3-4), 308-322.

Friedrich CG, Bardischewsky F, Rother D, Quentmeier A, Fischer J. 2005. Prokaryotic sulfur oxidation. Current opinion in microbiology. 8(3): 253-259.

Gadd, G. M. (2010). Metals, minerals and microbes: geomicrobiology and bioremediation. *Microbiology*, *156*(3), 609-643.

Gadd, G. M. (2016). Geomycology. In *Fungal applications in sustainable environmental biotechnology* (pp. 371-401). Springer, Cham.

Gadd, G. M., Rhee, Y. J., Stephenson, K., & Wei, Z. (2012). Geomycology: metals, actinides and biominerals. *Environmental Microbiology Reports*, *4*(3), 270-296.

Gagen, E. J., Levett, A., Shuster, J., Fortin, D., Vasconcelos, P. M., & Southam, G. (2018). Microbial diversity in actively forming iron oxides from weathered banded iron formation systems. *Microbes and environments*, *33*(4), 385-393.

Gahan, C. S., Srichandan, H., Kim, A. A., & Akcil, A. (2012). Biohydrometallurgy and biomineral processing technology: a review on its past, present and future. *Res J Recent Sci*, *2277*, 2502.

Gallegos, M. V., Falco, L. R., Peluso, M. A., Sambeth, J. E., & Thomas, H. J. (2013). Recovery of manganese oxides from spent alkaline and zinc–carbon batteries. An application as catalysts for VOCs elimination. *Waste management*, *33*(6), 1483-1490.

Ganesan, K., Jothi, V. K., Natarajan, A., Rajaram, A., Ravichandran, S., & Ramalingam, S. Green synthesis of Copper oxide nanoparticles decorated with graphene oxide for anticancer activity and catalytic applications. Arabian Journal of Chemistry. 2020; 13(8): 6802-6814.

Ganguly, S., Manikyamba, C., Saha, A., Lingadevaru, M., Santosh, M., Rambabu, S., ... & Linga, D. (2016). Geochemical characteristics of gold bearing boninites and banded iron formations from Shimoga greenstone belt, India: Implications for gold genesis

and hydrothermal processes in diverse tectonic settings. *Ore Geology Reviews*, *73*, 59-82.

Garcia, C., Moreno, D. A., Ballester, A., Blazquez, M. L., & Gonzalez, F. (2001). Bioremediation of an industrial acid mine water by metal-tolerant sulphate-reducing bacteria. *Minerals engineering*, *14*(9), 997-1008.

Garcia-Davis, S., Reyes, C. P., Lagunes, I., Padron, J. M., Fraile-Nuez, E., Fernandez, J. J., & Diaz-Marrero, A. R. (2021). Bioprospecting Antiproliferative Marine Microbiota From Submarine Volcano Tagoro. *Frontiers in Marine Science*, *8*(7).

García-Meza, J. V., Lara, R. H., & Navarro-Contreras, H. R. (2012). Application of Raman spectroscopy to the biooxidation analysis of sulfide minerals. *International Journal of Spectroscopy*, *2012*.

Gearheart, L. A., Ploehn, H. J., & Murphy, C. J. (2001). Oligonucleotide adsorption to gold nanoparticles: a surface-enhanced Raman spectroscopy study of intrinsically bent DNA. *The Journal of Physical Chemistry B*, *105*(50), 12609-12615.

George TS. 1995. Occurrence of Gold in Bhima Basin, Gulbarga District, Karnataka. Geological Society of India. 45(2): 235-236.

GFMS research and forecasts. 2015. New York. Thomson Reuters; 1/02/2017. http://financial-risk-solutions.thomsonreuters.info/GFMS.

Gholipourmalekabadi, M., Mobaraki, M., Ghaffari, M., Zarebkohan, A., Omrani, V. F., Urbanska, A. M., & Seifalian, A. (2017). Targeted drug delivery based on gold nanoparticle derivatives. *Current Pharmaceutical Design*, *23*(20), 2918-2929.

Ghorbani, Y., Franzidis, J. P., & Petersen, J. (2016). Heap leaching technology—current state, innovations, and future directions: a review. *Mineral Processing and Extractive Metallurgy Review*, *37*(2), 73-119.

Girling, C. A., & Peterson, P. J. (1980). Gold in plants. *Gold bulletin*, *13*(4), 151-157.

Gleeson, C. F., & Poulin, R. (1989). Gold exploration in Niger using soils and termitaria. *Journal of Geochemical Exploration*, *31*(3), 253-283.

Golani PR, Pandit MK. 1999. Evidence of epithermal activity and gold mineralization in Newania Carbonatite, Udaipur district, Rajasthan. Journal of the Geological Society of India. 54(3):251-7.

Goldschmidt VM. 1954. Geochemistry. Oxford: Clarendon Press https://www.abebooks.com/book-search/title/geochemistry/author/goldschmidt-v-m/.

González, P. D., Sato, A. M., Llambías, E. J., & Petronilho, L. A. (2009). Petrology and geochemistry of the banded iron formation in the Eastern Sierras Pampeanas of San Luis (Argentina): Implications for the evolution of the Nogolí Metamorphic Complex. *Journal of South American Earth Sciences*, *28*(2), 89-112.

Gour, A., and Jain, N. K. Advances in green synthesis of nanoparticles. Artificial cells, nanomedicine, and biotechnology. 2019; 47(1): 844-851.

Grema, H. M., Ibrahim, H. A., Abdulkarim, M., Lawal, M., Mbitsa, K., & Hassan, H. (2021). Sources of some heavy minerals and their association with gold-bearing stream sediments in the Gagare Drainage Basin, Wonaka Schist belt northwestern Nigeria. *Bayero Journal of Pure and Applied Sciences*, *13*(1), 68-79

Grigor'eva, N. V., Tsaplina, I. A., Panyushkina, A. E., & Kondrat'eva, T. F. (2014). Optimization of bioleaching and oxidation of gold-bearing pyrite-arsnopyrite ore concentrate in batch mode. *Microbiology*, *83*(5), 550-557.

Grote, M. (2018). Petri dish versus Winogradsky column: a longue durée perspective on purity and diversity in microbiology, 1880s–1980s. *History and Philosophy of the Life Sciences*, *40*(1), 1-30.

Gurunathan, S., Han, J., Park, J. H., & Kim, J. H. (2014). A green chemistry approach for synthesizing biocompatible gold nanoparticles. *Nanoscale research letters*, *9*(1), 1-11.

Hagemann, S. G., Angerer, T., Duuring, P., Rosière, C. A., e Silva, R. F., Lobato, L., ... & Walde, D. H. G. (2016). BIF-hosted iron mineral system: a review. *Ore Geology Reviews*, *76*, 317-359.

Hairston, R. V. (1999). The Winogradsky column & biofilms: models for teaching nutrient cycling & succession in an ecosystem. *The American Biology Teacher*, *61*(6), 453-459.

Handelsman, J. (2004). Metagenomics: application of genomics to uncultured microorganisms. *Microbiology and molecular biology reviews*, *68*(4), 669-685.

Hannington, M., Jamieson, J. O. H. N., Monecke, T., & Petersen, S. (2010). Modern sea-floor massive sulfides and base metal resources: toward an estimate of global sea-floor massive sulfide potential.

Hao, X., Leung, K., Wang, R., Sun, W., & Li, Y. (2010). The geomicrobiology of bauxite deposits. *Geoscience Frontiers*, *1*(1), 81-89.

Haugaard, R., Frei, R., Stendal, H., & Konhauser, K. (2013). Petrology and geochemistry of the~ 2.9 Ga Itilliarsuk banded iron formation and associated supracrustal rocks, West Greenland: Source characteristics and depositional environment. *Precambrian research*, *229*, 150-176.

Hazarika, S. N., & Thakur, D. (2020). Actinobacteria. In *Beneficial Microbes in Agro-Ecology* (pp. 443-476). Academic Press.

Heim, R.Termites and fungi; termitophilic fungi from black Africa and southern Asia, Societe Nouvelle des Eds. Boubee. Paris. 1977. ISBN 2850040045.1-207

Heim, Roger., New Descriptive Studies on *Termitophilic Agarics* from Tropical Africa. Arch. Mus. Natl. Hist. Nat. Paris. 1942; 6: 1-133.

Hendra, P. J., and Stratton, P. M. Laser-raman spectroscopy. Chemical reviews, 1969; 69(3): 325-344.

Hendra, P. J., and Vear, C. J. Laser Raman spectroscopy. A review. Analyst. 1970; 95(1129): 321-342.

Herizchi, R., Abbasi, E., Milani, M., & Akbarzadeh, A. Current methods for synthesis of gold nanoparticles. Artificial cells, nanomedicine, and biotechnology. 2016; *44*(2):596-602.

Hill, D. L., Brierley, J. 1993. Biooxidation Process for Recovery of Metal Values From Sulfur-Containing Ore Materials. Patent NumberEP 0522978.

Hinojosa, J. A., Méndez-Bértolo, C., & Pozo, M. A. (2010). Looking at emotional words is not the same as reading emotional words: Behavioral and neural correlates. *Psychophysiology*, *47*(4), 748-757.

Hirsch P, Eckhardt FEW & Palmer R J. 1995. Methods for the study of rock-inhabiting microorganisms—a mini review. Journal of microbiological methods. 23(2): 143-167.

Hoagland, P., Beaulieu, S., Tivey, M. A., Eggert, R. G., German, C., Glowka, L., & Lin, J. (2010). Deep-sea mining of seafloor massive sulfides. *Marine Policy*, *34*(3), 728-732.

Hougaard, K. S., Fadeel, B., Gulumian, M., Kagan, V. E., & Savolainen, K. M. (2011). Developmental toxicity of engineered nanoparticles. In *Reproductive and developmental toxicology* (pp. 269-290).

Huang, W., Pan, K., Wang, B., & Gong, Y. (2022). Grain Size Effects on Mechanical Properties of Nanocrystalline Cu6Sn5 Investigated Using Molecular Dynamics Simulation. *Materials*, *15*(11), 3889.

Hughes, M. J., Carey, S. P., & Kotsonis, A. N. D. R. E. W. (1999). Lateritic weathering and secondary gold in the Victorian Gold Province. In *Regolith* (Vol. 98, pp. 155-172).

Hughes, M. J., Phillips, G. N., & Carey, S. P. (2004). Giant placers of the Victorian gold province. *SEG Discovery*, (56), 1-18.

Hunter RM, Stewart FM, Darsow T, Fogelsong ML.1996. Method and apparatus for extracting precious metals from their ores and the product thereof. PCT patent WO 96/00308.

Husseiny, M. I., Abd El-Aziz, M., Badr, Y., & Mahmoud, M. A. (2007). Biosynthesis of gold nanoparticles using Pseudomonas aeruginosa. *Spectrochimica Acta Part A: Molecular and Biomolecular Spectroscopy*, *67*(3-4), 1003-1006.

Indian Bureau of mines. Excessed on 2/2/2018. http://www.ibm.nic.in .

Ingale, M., & Savoikar, P. P. (2021). Geotechnical properties of Lateritic rocks in North Goa. In *Recent Developments in Sustainable Infrastructure* (pp. 79-87). Springer, Singapore.

Ingale, M., & Savoikar, P. P. (2022). Mapping of Lateritic Rocks in Goa. In *Recent Developments in Sustainable Infrastructure (ICRDSI-2020)—GEO-TRA-ENV-WRM* (pp. 299-307). Springer, Singapore.

Jain, N., & Sharma, D. K. (2004). Biohydrometallurgy for nonsulfidic minerals—a review. *Geomicrobiology Journal*, *21*(3), 135-144.

James, H. L. (1954). Sedimentary facies of iron-formation. *Economic Geology*, *49*(3), 235-293.

Janssen PJ, Van Houdt R, Moors H, Monsieurs P, Morin N, Michaux A, Monchy S. 2010. The complete genome sequence of *Cupriavidus metallidurans* strain CH34, a master survivalist in harsh and anthropogenic environments. *PLoS One*. *5*(5): e10433.

Javed, I., Peng, G., Xing, Y., Yu, T., Zhao, M., Kakinen, A. and Lin, S. Inhibition of amyloid beta toxicity in zebrafish with a chaperone-gold nanoparticle dual strategy. Nature communications. 2019; 10(1): 1-14.

Jayaseelan, C., Ramkumar, R., Rahuman, A. A., & Perumal, P. (2013). Green synthesis of gold nanoparticles using seed aqueous extract of Abelmoschus esculentus and its antifungal activity. *Industrial Crops and Products*, *45*, 423-429.

Jeong, E. H., Jung, G., Hong, C. A., & Lee, H. (2014). Gold nanoparticle (AuNP)-based drug delivery and molecular imaging for biomedical applications. *Archives of pharmacal research*, *37*(1), 53-59.

Ji, Y., Cao, Y., & Song, Y. Green synthesis of gold nanoparticles using a *Cordyceps militaris* extract and their antiproliferative effect in liver cancer cells (HepG2). Artificial cells, nanomedicine, and biotechnology. 2019; 47(1): 2737-2745.

Jiang, J., Oberdörster, G., & Biswas, P. (2009). Characterization of size, surface charge, and agglomeration state of nanoparticle dispersions for toxicological studies. *Journal of Nanoparticle Research*, *11*(1), 77-89.

Johnson, D. B. 2013. Development and application of biotechnologies in the metal mining industry. Environmental Science and Pollution Research. 20(11): 7768- 7776.

Johnson, D. B. 2014. Biomining—biotechnologies for extracting and recovering metals from ores and waste materials. Current Opinion in Biotechnology. 30: 24- 31.

Jorjani, E., & Sabzkoohi, H. A. (2021). Gold leaching from ores using biogenic lixiviants-A review. *Current Research in Biotechnology*.

Jung, H., Inaba, Y., & Banta, S. (2021). Genetic engineering of the acidophilic chemolithoautotroph *Acidithiobacillus ferrooxidans*. *Trends in Biotechnology*.

K. Natarajan, South Indian Agaricales V: *Termitomyces heimii*. Mycologia. 1979; 71: 853–855.

Kai, M., Yano, T., Fukumori, Y., & Yamanaka, T. (1989). Cytochrome oxidase of an acidophilic iron-oxidizing bacterium, *Thiobacillus ferrooxidans*, functions at pH 3.5. *Biochemical and biophysical research communications*, *160*(2), 839-843.

Kalabegishvili, T., Kirkesali, E., & Rcheulishvili, A. (2012). *Synthesis of gold nanoparticles by blue-green algae Spirulina platensis* (No. JINR-E--14-2012-31). Frank Lab. of Neutron Physics.

Kalia, A. and Kaur, G., 2018. Biosynthesis of Nanoparticles Using Mushrooms. In: Biology of Macrofungi, pp. 351-360. Springer, Cham.

Kalimuthu, K., Cha, B. S., Kim, S., & Park, K. S. (2020). Eco-friendly synthesis and biomedical applications of gold nanoparticles: A review. *Microchemical Journal*, *152*, 104296.

Kalishwaralal, K., Deepak, V., Pandian, S. R. K., and Gurunathan, S.Biological synthesis of gold nanocubes from Bacillus licheniformis. Bioresource technology. 2009; 100(21): 5356-5358.

Kalisz, H. M., Moore, D., & Wood, D. A. (1986). Protein utilization by basidiomycete fungi. *Transactions of the British Mycological Society*, *86*(4), 519-525.

Kalisz, H. M., Wood, D. A., & Moore, D. Regulation of extracellular laccase production of Agaricus bisporus by nitrogen sources in the medium. *FEMS microbiology letters*. 1986; 34(1): 65-68.

Kamat, N (2018). Using Auriferous Dumps For Gold Mining, The Navhind Times,12 March 2018

Kamat, M. M. (2016). Iron-ore Exports and Goa's Economy, 1962-2012: A Time-series and Cross-sectional Analysis. *Indian Journal of Economics and Development*, *4*, 7.

Kamat, N. (2012 b). Auriferous Sands of Taleigao, New Frontiers, Sunday Panorama, June 10, 2012

Kamat, N. (2012c). Using Geophagous Earthworms as Gold detectors,New frontiers, Sunday Panorama, Navhind Times, Sept. 16, 2012

Kamat, N. (2015 b). Mystery of Volcano sedimentary Gold in Goa, New frontiers, August 16, 2015

Kamat, N. (2015 e). Ancient Alluvial Gold Mining in Goa,New New frontiers, Panoroma, August 23, 2015

Kamat, N. (2015 f). Mining Gold from River Sands Of Goa,New Frontiers, Sunday Panorama, Navhind Times, September 20, 2015

Kamat, N. (2015c). Ancient Gold Metallurgy In Goa-I, New Frontiers for Navhind Times, Sunday Panorama, August 23, 2015

Kamat, N. (2015d). Ancient metallurgists of Samblur and Kundiwatak, Sunday Panorama, The NAVHIND Times, September, 6, 2015

Kamat, N. (2019 a). The Chinese humger for Gild, New Frontiers, January 20, 2019

Kamat, N. (2019 b). How Gold Connects Humans to Cosmos, New frontiers, MAY 19, 2019

Kamat, N. (2019 c). History of Gold in Goa, Goa Today, August ,2019

Kamat, N. M. (2012 a). "Sunapranta revisited: Political ecology and economy of gold deposits in Goa."

Kamat, N., & Velho-Pereira, S. 2012. Screening of actinobacteria for antimicrobial activities by a modified" Cross-Streak" method. Nature Precedings, 1-1.

Kamat, Nandkumar M. (2011b). "How I discovered Goa's Microbial Eldorado."Accessible from https:///dr-nandakumar-kamat-article-discovery-gold-ore-goa/

Kamat, Nandkumar. (2011a). Pioneer Discovery of secondary gold deposits-unique bacterioforms andplacers in north Goa from deep core metabiosphere." Nature Precedings (2011): 1-1. Accessible from https:///articles/npre.2011.5497.1

Kamat,N. (2015 a). Neglecting Volcanosedimentary Gold In Goa-I, August 9,2015.

Kanekar, P. P., Kulkarni, S. O., Dhakephalkar, P. K., Kulkarni, K. G., & Saxena, N. (2017). Isolation of a halophilic, bacteriorhodopsin-producing Archaeon, Haloferax larsenii

RG3D. 1 from the rocky beach of Malvan, West Coast of India. *Geomicrobiology Journal*, *34*(3), 242-248.

Kang SH. 1994. Metal recovery from mine tailings using bacteria. Waste Management. 14(8):687-691.

Karavaiko, G. I., Dubinina, G. A., & Kondrat'eva, T. F. (2006). Lithotrophic microorganisms of the oxidative cycles of sulfur and iron. *Microbiology*, *75*(5), 512-545.

Karthik, L., Kumar, G., Kirthi, A. V., Rahuman, A. A., & Bhaskara Rao, K. V. (2014). Streptomyces sp. LK3 mediated synthesis of silver nanoparticles and its biomedical application. *Bioprocess and biosystems engineering*, *37*(2), 261-267.

Karun, N. C., and Sridhar, K. R. Occurrence and distribution of *Termitomyces* (Basidiomycota, Agaricales) in the Western Ghats and on the west coast of India. Czech Mycology. 2013; 65(2): 233-254.

Kataria, D., Krishnamoorthy, K., & Iyer, S. S. K. (2017). Increasing light coupling in a photovoltaic film by tuning nanoparticle shape with substrate surface energy. *Materials Research Express*, *4*(8), 085022.

Katas, H., Lim, C. S., Azlan, A. Y. H. N., Buang, F., and Busra, M. F. M. Antibacterial activity of biosynthesized gold nanoparticles using biomolecules from *Lignosus rhinocerotis* and chitosan. Saudi Pharmaceutical Journal. 2019; 27(2): 283-292.

Kaur, S., Sharma, P., Kalia, N., Singh, J., & Kaur, S. (2018). Anti-biofilm properties of the fecal probiotic lactobacilli against Vibrio spp. *Frontiers in cellular and infection microbiology*, *8*, 120.

Kebede, F. (2004). Use of termite mounds in geochemical exploration in North Ethiopia. *Journal of African Earth Sciences*, *40*(1-2), 101-103.

Kendall, B., Anbar, A. D., Kappler, A., & Konhauser, K. O. (2012). The global iron cycle. *Fundamentals of geobiology*, 65-92.

Khadivi Derakhshan, F., Dehnad, A., & Salouti, M. (2012). Extracellular biosynthesis of gold nanoparticles by metal resistance bacteria: Streptomyces griseus. *Synthesis and Reactivity in Inorganic, Metal-Organic, and Nano-Metal Chemistry*, *42*(6), 868-871.

Khan, A. K., Rashid, R., Murtaza, G., & Zahra, A. J. T. R. (2014). Gold nanoparticles: synthesis and applications in drug delivery. *Tropical journal of pharmaceutical research*, *13*(7), 1169-1177.

Khan, S., Haq, F., Hasan, F., Saeed, K. and Ullah, R. 2012. Growth and biochemical activities of *Acidithiobacillus thiooxidans* collected from black shale. J Microbiol Res. 2(4): 78-83.

Kharashqah, N. Y. (2002). *A comparative study of microbial communities using a Winogradsky column prepared from water and sediment from Gee Lake in Commerce, Texas*. Texas A&M University-Commerce.

Kidwai, R. M., & Wagle, B. G. (1975). Mineralogy of beach and dune sands of Morgim-Arambol beach on Goa Coast.

Kim, J. H., Bryan, W. W., & Randall Lee, T. (2008). Preparation, characterization, and optical properties of gold, silver, and gold− silver alloy nanoshells having silica cores. *Langmuir*, *24*(19), 11147-11152.

Kim, K. H., Kabir, E., & Kabir, S. (2015). A review on the human health impact of airborne particulate matter. *Environment international*, *74*, 136-143.

Kiyasudeen, K., Ibrahim, M. H., Quaik, S., & Ismail, S. A. (2015). *Prospects of organic waste management and the significance of earthworms*. Springer.

Kleid DG, Kohr WJ, Thibodeau FR. 1991. Processes to recover and reconcentrate gold from its ores. European patent 0 432 935.

Klein, C. (2005). Some Precambrian banded iron-formations (BIFs) from around the world: Their age, geologic setting, mineralogy, metamorphism, geochemistry, and origins. *American Mineralogist*, *90*(10), 1473-1499.

Klein, C., & Ladeira, E. A. (2002). Petrography and geochemistry of the least altered banded iron-formation of the Archean Carajás Formation, northern Brazil. *Economic Geology*, *97*(3), 643-651.

Knoblauch, A. M., Farnham, A., Ouoba, J., Zanetti, J., Müller, S., Jean-Richard, V., ... & Winkler, M. S. (2020). Potential health effects of cyanide use in artisanal and small-scale gold mining in Burkina Faso. *Journal of cleaner production*, *252*, 119689.

Knowles CJ, Bunch AW. 1986. Microbial cyanide metabolism. Adv Microb Physiol. 27(27):73-111.

Kohr WJ, Johansson C, Shield J, Shrader V. 1996. Method for heap biooxidation of ores. PCT patent WO 96/12826.

Kohr WJ. 1995. Biooxidation of refractory sulfide ores. PCT pa-tent WO 95/15403.

Kolb, J., Rogers, A., & Meyer, F. M. (2005). Relative timing of deformation and two-stage gold mineralization at the Hutti Mine, Dharwar Craton, India. *Mineralium Deposita*, *40*(2), 156-174.

Kondrat'Eva, T. F., Pivovarova, T. A., Tsaplina, I. A., Fomchenko, N. V., Zhuravleva, A. E., Murav'Ev, M. I., ... & Bulayev, A. G. (2012). Diversity of the communities of acidophilic chemolithotrophic microorganisms in natural and technogenic ecosystems. *Microbiology*, *81*(1), 1-24.

Konhauser KO. 1997. Bacterial iron biomineralisation in nature. FEMS Microbiology Reviews. 20(3-4):315-326.

Konhauser, K. O. (1998). Diversity of bacterial iron mineralization. *Earth-Science Reviews*, *43*(3-4), 91-121.

Konhauser, K. O., Newman, D. K., & Kappler, A. (2005). The potential significance of microbial Fe (III) reduction during deposition of Precambrian banded iron formations. *Geobiology*, *3*(3), 167-177.

Korobushkina, E. D., Karavaiko, G. I., & Korobushkin, I. M. (1983). Biochemistry of gold. *Ecological Bulletins*, 325-333.

Kothari, V., Sharma, S., & Padia, D. (2017). Recent research advances on *Chromobacterium violaceum*. *Asian Pacific journal of tropical medicine*, *10*(8), 744-752.

Kotlar, H. K., Lewin, A., Johansen, J., Throne-Holst, M., Haverkamp, T., Markussen, S., ... & Valla, S. (2011). High coverage sequencing of DNA from microorganisms living in an oil reservoir 2.5 kilometres subsurface. *Environmental microbiology reports*, *3*(6), 674-681.

KRISHNAKUMAR, N. (1991). Concentration of gold in insitu laterites at Maruda, Nilambur Valley, Kerala, Indian. In *Symposium Brazil Gold'91* (pp. 743-750).

Krishnamurthi, R. (2012). Current understanding on the genesis of lode gold mineralization in the Southern granulite Terrain, Peninsular India. *Journal of Applied Geochemistry*, *14*(4), 370-382.

Krishnan, S., & Chadha, A. Microbial Synthesis of Gold Nanoparticles and Their Applications as Catalysts. Handbook of Nanomaterials and Nanocomposites for Energy and Environmental Applications. 2021; 1081-1108.

Krishnan, S., Patel, P. N., Balasubramanian, K. K., & Chadha, A. (2021). Yeast supported gold nanoparticles: an efficient catalyst for the synthesis of commercially important aryl amines. *New Journal of Chemistry*, *45*(4), 1915-1923.

Kumar V, Saxena J, Tiwari SK. 2015. Description of a halocin-producing *Haloferax larsenii* HA1 isolated from Pachpadra Salt Lake in Rajasthan. Arch Microbiol. 198: 181-192. DOI: 10.1007/s00203-015-1175-3.

Kumar, S. A., Peter, Y. A., & Nadeau, J. L. (2008). Facile biosynthesis, separation and conjugation of gold nanoparticles to doxorubicin. *Nanotechnology*, *19*(49), 495101.

Kumar, V. A., Uchida, T., Mizuki, T., Nakajima, Y., Katsube, Y., Hanajiri, T., & Maekawa, T. (2016). Synthesis of nanoparticles composed of silver and silver chloride for a plasmonic photocatalyst using an extract from a weed Solidago altissima (goldenrod). *Advances in Natural Sciences: Nanoscience and Nanotechnology*, *7*(1), 015002.

Lamb, A. E., Anderson, C. W. N., & Haverkamp, R. G. (2001). The induced accumulation of gold in the plants Brassica juncea, Berkheya coddii and chicory.

Lasken, R. S., & McLean, J. S. (2014). Recent advances in genomic DNA sequencing of microbial species from single cells. *Nature Reviews Genetics*, *15*(9), 577-584.

Lazar I, Toniuc M, Popea FV, Velea I.1993. Investigations using large size percolators for microbial leaching of low-grade ores. Biohydrometallurgical Technologies.1:57-64.

Lee, C. S., Kim, T. W., Oh, D. E., Bae, S. O., Ryu, J., Kong, H., ... & Kim, T. H. (2020). In Vivo and In Vitro anticancer activity of doxorubicin-loaded DNA-AuNP nanocarrier for the ovarian cancer treatment. *Cancers*, *12*(3), 634.

Lee, K. D., Nagajyothi, P. C., Sreekanth, T. V. M., & Park, S. (2015). Eco-friendly synthesis of gold nanoparticles (AuNPs) using Inonotus obliquus and their antibacterial, antioxidant and cytotoxic activities. *Journal of Industrial and Engineering Chemistry*, *26*, 67-72.

Lee, S. O., Kim, M. J., Kim, D. G., & Choi, H. J. Antioxidative activities of temperature-stepwise water extracts from Inonotus obliquus. Journal of the Korean Society of Food Science and Nutrition. 2005; 34(2): 139-147.

Lengke, M., & Southam, G. (2006). Bioaccumulation of gold by sulfate-reducing bacteria cultured in the presence of gold (I)-thiosulfate complex. Geochimica et Cosmochimica Acta, 70(14), 3646-3661.

Leong, Y. K., Yang, F. C., & Chang, J. S. (2021). Extraction of polysaccharides from edible mushrooms: Emerging technologies and recent advances. *Carbohydrate Polymers*, *251*, 117006.

Li, L., Wei, S., Lollar, B. S., Wing, B., Bui, T. H., Ono, S., ... & van Heerden, E. (2022). In situ oxidation of sulfide minerals supports widespread sulfate reducing bacteria in the deep subsurface of the Witwatersrand Basin (South Africa): Insights from multiple sulfur and oxygen isotopes. *Earth and Planetary Science Letters*, *577*, 117247.

Liang CJ, Li JY, Ma CJ. 2014. Review on cyanogenic bacteria for gold recovery from E-waste. In Advanced Materials Research. Trans Tech Publications. 878: 355-367.

Liang-Cheng, Z. H. A. O., Jing-Gong, W. A. N. G., Xing, L. I., ZHANG, S., ZHANG, Z. F., Ming-Yue, H. U., ... & Hua-Jie, L. I. U. (2018). Application of inductively coupled plasma-atomic emission spectrometry/mass spectrometry to phase analysis of gold in gold ores. *Chinese Journal of Analytical Chemistry*, *46*(2), e1801-e1809.

Little BJ, Wagner PA, Lewandowski Z. 1997. Spatial relationships between bacteria and mineral surfaces. Reviews in Mineralogy and Geochemistry. 35(1):123-159.

Liu R, Li J, Ge Z. 2016. Review on *Chromobacterium violaceum* for Gold Bioleaching from E-Waste. Procedia Environmental Sciences.31:947-953.

Liu, Q., Cui, X., Song, Z., Kong, W., Kang, Y., Kong, W., & Ng, T. B. (2021). Coating shiitake mushrooms (Lentinus edodes) with a polysaccharide from Oudemansiella radicata improves product quality and flavor during postharvest storage. *Food Chemistry*, *352*, 129357.

Locci, R. (1989). Streptomyces and related genera. Bergey's manual of systematic bacteriology, 4, 2451-2508.

Logsdon, M. J., Hagelstein, K., & Mudder, T. (1999). *The management of cyanide in gold extraction* (p. 10). Ottawa: International Council on Metals and the Environment.

Long, D. A. 1977. Raman spectroscopy. *New York*, *1*.

Loss, R. A., Fontes, M. L., Reginatto, V. and Antônio, R. V. 2013. Biohydrogen production by a mixed photoheterotrophic culture obtained from a Winogradsky column prepared from the sediment of a southern Brazilian lagoon. Renewable Energy. 50: 648-654.

Lowe, D. R. (1980). Stromatolites 3,400-myr old from the Archean of Western Australia. *Nature*, *284*(5755), 441-443.

Madigan, M. T., Jung, D. O., Woese, C. R., & Achenbach, L. A. (2000). *Rhodoferax antarcticus* sp. nov., a moderately psychrophilic purple nonsulfur bacterium isolated from an Antarctic microbial mat. *Archives of microbiology*, *173*(4), 269-277.

Madusudan R, Venkatasubramanian M, Murthy TSS. 1994. A Note on Gold Mineralisation in Banded Iron Formation, Chinmulgund, Shimoga Schist Belt, Karnataka. Geological Society of India.44(5):593-594.

Malarkodi, C., Rajeshkumar, S., Paulkumar, K., Vanaja, M., Jobitha, G. D. G., & Annadurai, G. (2013). Bactericidal activity of bio mediated silver nanoparticles synthesized by Serratia nematodiphila. *Drug invention today*, *5*(2), 119-125.

Maluckov, B. S. (2017). The catalytic role of *Acidithiobacillus Ferrooxidans* for metals extraction from mining-metallurgical resource. *Biodiversity International Journal*, *1*(3), 1-12.

Mandal, M., Shareef, M., Gopalakrishna, G., & Kumar, B. (2021, August). Evidences of Partial Melting of Sulphides from Ajjanahalli Gold Deposit, Dharwar Supergroup, Karnataka. In *Conference GSI* (pp. 46-51).

Manivasagan, P., Venkatesan, J., Senthilkumar, K., Sivakumar, K., & Kim, S. K. (2013). Biosynthesis, antimicrobial and cytotoxic effect of silver nanoparticles using a novel Nocardiopsis sp. MBRC-1. *BioMed research international*, *2013*.

Manivasagan, P., Venkatesan, J., Sivakumar, K., & Kim, S. K. (2016). Actinobacteria mediated synthesis of nanoparticles and their biological properties: A review. *Critical reviews in microbiology*, *42*(2), 209-221.

Manivasagan, P., Venkatesan, J., Sivakumar, K., & Kim, S. K. (2014). Pharmaceutically active secondary metabolites of marine actinobacteria. *Microbiological research*, *169*(4), 262-278.

Manojkumar, P. 2013. A review of bhunag satw. International Ayurvedic medical journal, 1(4).

Manzi, P., Aguzzi, A., & Pizzoferrato, L. (2001). Nutritional value of mushrooms widely consumed in Italy. *Food chemistry*, *73*(3), 321-325.

Matsvayi T. 2016. The potential use microorganisms in the biooxidation of gold ore from a mine in Bulawayo [Doctoral dissertation]: National university of science and technology. Accessed from https://www.researchgate.net/profile/Tsungayi_Matsvayi2/publication/316789986_The_potential_use_microorganisms_in_the_biooxidation_of_gold_ore_from_a_mine_in_Bulawayo/links/5911d8c4a6fdcc963e6f3c3d

Mbenoun, A. M., Ngon, G. F. N., Mbog, M. B., Fouateu, R. Y., & Bilong, P. (2021). Study of the Behavior of Gold and Accompanying Chemical Elements in Weathering Profile on a Quartz Vein in Mintom (South Cameroon, Central Africa). *Earth Science Research*, *10*(2), 1-54.

McClenaghan, S. H., Lentz, D. R., & Cabri, L. J. (2004). Abundance and speciation of gold in massive sulfides of the Bathurst Mining Camp, New Brunswick, Canada. *The Canadian Mineralogist*, *42*(3), 851-871.

McNamara, K. J., & Awramik, S. M. (1992). Stromatolites: a key to understanding the early evolution of life. *Science Progress (1933-)*, 345-364.

Meissner, M. P., Xu, Z., Jones, G. C., Minnaar, S. H., & Harrison, S. T. (2014). A novel microwell-based analytical technique for studying ferrous iron biooxidation activity. *Minerals Engineering*, *60*, 8-13.

Menon, J. U., Kuriakose, A., Iyer, R., Hernandez, E., Gandee, L., Zhang, S., ... & Nguyen, K. T. (2017). Dual-drug containing core-shell nanoparticles for lung cancer therapy. *Scientific reports*, *7*(1), 1-13.

Mergeay, M. (2015). The history of Cupriavidus metallidurans strains isolated from anthropogenic environments. In *Metal response in Cupriavidus metallidurans* (pp. 1-19). Springer, Cham.

Merroun, M. L., & Selenska-Pobell, S. (2008). Bacterial interactions with uranium: an environmental perspective. *Journal of Contaminant Hydrology*, *102*(3-4), 285-295.

Meruga, J. M., Baride, A., Cross, W., Kellar, J. J., & May, P. S. (2014). Red-green-blue printing using luminescence-upconversion inks. *Journal of Materials Chemistry C*, *2*(12), 2221-2227.

Mewada, A., Oza, G., Pandey, S., & Sharon, M. (2012). Extracellular synthesis of gold nanoparticles using Pseudomonas denitrificans and comprehending its stability. *J Microbiol Biotechnol*, *2*(4), 493-499.

Meyers, M. A., Mishra, A., & Benson, D. J. (2006). Mechanical properties of nanocrystalline materials. *Progress in materials science*, *51*(4), 427-556.

Mimba, M. E., Nforba, M. T., & Suh, C. E. (2014). Geochemical dispersion of gold in stream sediments in the Paleoproterozoic Nyong Series, southern Cameroon. *Sci Res*, *2*(6), 155-165.

Mishra, A., Tripathy, S. K., Wahab, R., Jeong, S. H., Hwang, I., Yang, Y. B., ... & Yun, S. I. (2011). Microbial synthesis of gold nanoparticles using the fungus and their cytotoxic effects against mouse mayo blast cancer C2C12 cells. *Applied microbiology and biotechnology*, *92*(3), 617-630.

Mishra, D., Kim, D. J., Ahn, J. G., & Rhee, Y. H. (2005). Bioleaching: a microbial process of metal recovery; a review. *Metals and Materials International*, *11*(3), 249-256.

Mishra, S., Lalumière, M. L., & Williams, R. J. (2010). Gambling as a form of risk-taking: Individual differences in personality, risk-accepting attitudes, and behavioral preferences for risk. *Personality and Individual Differences*, *49*(6), 616-621.

Mishra, S., Panda, S., Akcil, A., & Dembele, S. (2022). Biotechnological Avenues in Mineral Processing: Fundamentals, Applications and Advances in Bioleaching and Bio-beneficiation. *Mineral Processing and Extractive Metallurgy Review*, 1-30.

Mishra, S.K. Tripathy, S. Il Yun, Fungus mediated synthesis of gold nanoparticles and their conjugation with genomic DNA isolated from *Escherichia coli* and *Staphylococcus aureus*, Process Biochem. 47 (2012),701–711.

Mohakul, J. P., Babu, P. H., Madusudanan, R., Khan, S. A., & Balakrishnan, S. (2021, August). Regional and Deposit Scale Controls of Gold Mineralization in Chitradurga Schist Belt, Dharwar Craton, India. In *Conference GSI* (pp. 23-33).

Morris, b. Notes on the genus *Termitomyces heim* in Malaŵi. The Society of Malawi Journal. 1986; 39(1):40-49.

Moskovits, M. (2005). Surface-enhanced Raman spectroscopy: a brief retrospective. *Journal of Raman Spectroscopy: An International Journal for Original Work in all Aspects of*

Raman Spectroscopy, Including Higher Order Processes, and also Brillouin and Rayleigh Scattering, *36*(6-7), 485-496.

Mossebo, D. C., Njouonkou, A. L., Piatek, M., Kengni Ayissi, B., & Djamndo Djasbe, M. *Termitomyces striatus f. pileatus* f. nov. and f. brunneus f. nov. from Cameroon with a key to central African species. Mycotaxon.2009; 107(1): 315-329.

Mossman, D., Reimer, T., & Durstling, H. (1999). Microbial processes in gold migration and deposition: modern analogues to ancient deposits. *Geoscience Canada*.

Msuya, F. A. M. (2000). Environmental implications of phytoextraction for mercury and gold: a thesis presented in partial fulfilment of the requirements for the degree of Master of Science in Earth Science (Doctoral dissertation, Massey University).

Msuya, F. A., Brooks, R. R., & Anderson, C. W. (2000). Chemically-induced uptake of gold by root crops: its significance for phytomining. *Gold Bulletin*, *33*(4), 134-137.

Mubarok MZ, Winarko R, Chaerun SK, Rizki IN, Ichlas ZT. 2017. Improving gold recovery from refractory gold ores through biooxidation using iron-sulfur-oxidizing/sulfur-oxidizing mixotrophic bacteria. Hydrometallurgy.168:69-75.

Mukherjee, P., Senapati, S., Mandal, D., Ahmad, A., Khan, M. I., Kumar, R., & Sastry, M. (2002). Extracellular synthesis of gold nanoparticles by the fungus *Fusarium oxysporum*. ChemBioChem, *3*(5), 461-463.

Murthy, S. A., & Bhattacharjee, S. (1997). Occurrence of gold in Guntipalli-Atkur area, Gadwal schist belt, Mahbubnagar district, AP. *Journal of the Geological Society of India*, 49(6), 721-722.

Nadeem, M., Abbasi, B. H., Younas, M., Ahmad, W., & Khan, T. A review of the green syntheses and anti-microbial applications of gold nanoparticles. *Green* Chemistry Letters and Reviews. 2017; 10(4): 216-227.

NAEEM, G. A., JALOOT, A. S., OWAID, M. N., & MUSLIM, R. F. Green synthesis of gold nanoparticles from *coprinus comatus*, agaricaceae, and the effect of ultraviolet irradiation on their characteristics. Walailak Journal of Science and Technology (WJST). 2021; 18(8): 9396-12.

Nagar, N., Garg, H., & Gahan, C. S. (2019). Integrated bio-pyro-hydro-metallurgical approach to recover metal values from petroleum refinery spent catalyst. *Biocatalysis and Agricultural Biotechnology*, *20*, 101252.

Naik S, Furtado, I. 2014. Equilibrium and kinetics of adsorption of Mn2+ by haloarchaeon Halobacterium sp. GUSF (MTCC3265). Geomicrobiology Journal. 31(8): 708-715.

Naik-Samant S, Furtado, I. 2019. Formation of Rhodochrosite by *Haloferax alexandrinus* GUSF-1. Journal of Cluster Science. 30(6): 1435-1441.

Nair NGK, Santosh M, Mahadevan R. 1987. Lateritisation as a possible contributor to gold placers in Nilambur Valley, Southwest India. Chemical geology. 60(1-4):309-315.

Nair, N. G. K., Santosh, M., & Mahadevan, R. (1987). Lateritisation as a possible contributor to gold placers in Nilambur Valley, Southwest India. *Chemical geology*, *60*(1-4), 309-315.

Nair, R. V. G. 1993. Primary Gold Mineralisation in Attapadi Valley, Palakkad District, Kerala. Journal of Geological Society of India (Online archive from Vol 1 to Vol 78), 41(4): 387-387.

Nakagawa, M., Santosh, M., Nambiar, C. G., & Matsubara, C. (2005). Morphology and chemistry of placer gold from Attappadi Valley, Southern India. *Gondwana Research*, *8*(2), 213-222.

Nakajima, A., & Sakaguchi, T. (1993). Uptake and recovery of gold by immobilized persimmon tannin. *Journal of Chemical Technology & Biotechnology*, *57*(4), 321-326.

Nandan KR, Chander S, Sisodia CP. 2003. Gold Mineralisation in the Palaeoproterozoic Rocks of Sanjela-Manpur-Dugocha Belt, Salumber Area, Udaipur District, Rajasthan. Journal of Geological Society of India. 62(1):123-124.

Nangia, Y., Wangoo, N., Goyal, N., Shekhawat, G., & Suri, C. (2009). A novel bacterial isolate Stenotrophomonas maltophilia as living factory for synthesis of gold nanoparticles. *Microbial Cell Factories*, *8*(1), 1-7.

Narayanan, K. B., & Sakthivel, N. (2011). Synthesis and characterization of nano-gold composite using *Cylindrocladium floridanum* and its heterogeneous catalysis in the degradation of 4-nitrophenol. *Journal of hazardous materials*, *189*(1-2), 519-525.

Narayanan, K. B., Park, H. H., and Han, S. S. Synthesis and characterization of biomatrixed-gold nanoparticles by the mushroom *Flammulina velutipes* and its heterogeneous catalytic potential. Chemosphere. 2015; 141: 169-175.

NARAYANASWAMY, N. K., & RAMKUMAR, N. KERALA, INDIA. (2004). Journal of economic geology.1 (39-44).

Natarajan, K. A. (2018). *Biotechnology of metals: principles, recovery methods and environmental concerns*. Elsevier.

Natarajan, K., 1979. South Indian Agaricales V: *Termitomyces heimii*. Mycologia.1979; 71(4): 853-855.

Nayak B. 2011. Gold in the beach placer sands of Chavakkad-Ponnani, Kerala coast, India. Journal of the Geological Society of India.78(4): 345-348.

Neale, J. (2006). Bioleaching technology in minerals processing. *Randburg, South Africa: Mintek.*

Nestor, D., Valdivia, U., & Chaves, A. P. (2001). Mechanisms of bioleaching of a refractory mineral of gold with *Thiobacillus ferrooxidans*. *International Journal of Mineral Processing*, *62*(1-4), 187-198.

New frontiers Navhind Times, Sunday Panorama, August 23, 2015

Nonomura H and Hayakawa M. (1988). New methods for the selective isolation of soil actinomycetes. In Biology of Actinomycetes' Eds. Y Okami, T Beppu and H Oegawara. pp 288-293. Japan Sci. Soc. Press, Tokyo, Japan

Nunoura, T., Hirayama, H., Takami, H., Oida, H., Nishi, S., Shimamura, S., ... & Horikoshi, K. (2005). Genetic and functional properties of uncultivated thermophilic crenarchaeotes from a subsurface gold mine as revealed by analysis of genome fragments. *Environmental microbiology*, *7*(12), 1967-1984.

Olson GJ, Brierley JA, Brierley CL. 2003. Bioleaching review part B. Applied microbiology and biotechnology. *63*(3):249-257.

Olson, G. J. (1994). Microbial oxidation of gold ores and gold bioleaching. *FEMS Microbiology Letters*, *119*(1-2), 1-6.

Oren A 1993. Ecology of extremely halophilic microorganisms. In: Vreeland RH, Hochstein LI, (eds) The biology of halophilic bacteria. Boca Raton. CRC Press. 25–54.

Owaid, M. N., Al-Saeedi, S. S. S., & Abed, I. A. Biosynthesis of gold nanoparticles using yellow oyster mushroom *Pleurotus cornucopiae* var. *citrinopileatus*. Environmental nanotechnology, monitoring & management. 2017; 8:157-162.

Owaid, M. N., Rabeea, M. A., Aziz, A. A., Jameel, M. S., & Dheyab, M. A. (2019). Mushroom-assisted synthesis of triangle gold nanoparticles using the aqueous extract of fresh *Lentinula edodes* (shiitake), Omphalotaceae. *Environmental Nanotechnology, Monitoring & Management*, *12*, 100270.

Oza, G., Pandey, S., Gupta, A., Kesarkar, R., & Sharon, M. (2012). Biosynthetic reduction of gold ions to gold nanoparticles by *Nocardia farcinica*. *J Microbiol Biotechnol Res*, *2*(4), 511-515.

P Singh, Y Kim and D Yang. A strategic approach for rapid synthesis of gold and silver nanoparticles by Panax ginseng leaves. Artif. Cell Nanomed. 2016; 44, 1949-57.

Pal, S., Tak, Y. K., & Song, J. M. (2007). Does the antibacterial activity of silver nanoparticles depend on the shape of the nanoparticle? A study of the gram-negative bacterium Escherichia coli. *Applied and environmental microbiology*, *73*(6), 1712-1720.

Palyanova, G., & Savva, N. (2009). Genesis of gold and silver sulphides at Yuny and Ulakhan deposits (north-east of Russia). *Journal of Geochemical Exploration*, *101*(1), 80.

Panda, L., Das, B., Rao, D.S. and Mishra, B.K. (2011). Selective flocculation of banded hematite quartzite (BHQ) ores. Open Miner. Process. Jour., v. 4, pp. 45-51.

Panda, T., & Deepa, K. (2011). Biosynthesis of gold nanoparticles. *Journal of nanoscience and nanotechnology*, *11*(12), 10279-10294.

Pandey, A., Srivastava, A., & Pandey, A. (2011). *Acidithiobacillus ferrooxidans*: A bioleaching bacteria for better iron (II) oxidation ability. *International Journal of Innovations in Biological and Chemical Sciences*, *1*(32), 32-37.

Pandey, B. D., & Natarajan, K. A. (Eds.). (2015). *Microbiology for minerals, metals, materials and the environment*. CRC Press.

Panyushkina, A. E., Tsaplina, I. A., Grigor'eva, N. V., & Kondrat'eva, T. F. (2014). Thermoacidophilic microbial community oxidizing the gold-bearing flotation concentrate of a pyrite-arsenopyrite ore. *Microbiology*, *83*(5), 539-549.

Panyushkina, A. E., Tsaplina, I. A., Kondrat'Eva, T. F., Belyi, A. V., & Bulaev, A. G. (2018). Physiological and morphological characteristics of acidophilic bacteria *Leptospirillum ferriphilum* and *Acidithiobacillus thiooxidans*, members of a chemolithotrophic microbial consortium. *Microbiology*, *87*(3), 326-338.

Paponetti B, 1989. Manganese leaching from MnO_2 ores by *Aspergillus niger*. Role of Metabolic Ontermediate. Biotechnology in minerals and metal processing. pp. 33-37.

Park, T. J., Lee, S. Y., Lee, S. J., Park, J. P., Yang, K. S., Lee, K. B., ... & Choi, I. S. (2006). Protein nanopatterns and biosensors using gold binding polypeptide as a fusion partner. *Analytical chemistry*, *78*(20), 7197-7205.

Park, Y., Hong, Y. N., Weyers, A., Kim, Y. S., & Linhardt, R. J. (2011). Polysaccharides and phytochemicals: a natural reservoir for the green synthesis of gold and silver nanoparticles. *IET nanobiotechnology*, *5*(3), 69-78.

Parks, S. T. (2015). Microbial life in a Winogradsky column: from lab course to diverse research experience. *Journal of microbiology & biology education*, *16*(1), 82-84.

Parks, S. T. 2015. Microbial life in a Winogradsky column: from lab course to diverse research experience. Journal of Microbiology & Biology Education. 16(1): 82.

Patel, M.K. and Parhate, S., 2018. A Pharmaceutico-Analytical Study of Bhunaga Satva. Journal of Ayurveda and Integrated Medical Sciences (ISSN 2456-3110), 3(3),79-85.

Pegler, D. N., and Vanhaecke, M. *Termitomyces* of southeast Asia. Kew Bulletin. 1994; 717-736.

Pharoe, B. K., Evdokimov, A. N., Gembitskaya, I. M., & Bushuyev, Y. Y. (2020). Mineralogy, geochemistry and genesis of the post-Gondwana supergene manganese deposit of the Carletonville-Ventersdorp area, North West Province, South Africa. *Ore Geology Reviews*, *120*, 103372.

Philip, D. (2008). Synthesis and spectroscopic characterization of gold nanoparticles. *Spectrochimica Acta Part A: Molecular and Biomolecular Spectroscopy*, *71*(1), 80-85.

Philip, D. (2009). Biosynthesis of Au, Ag and Au–Ag nanoparticles using edible mushroom extract. *Spectrochimica Acta Part A: Molecular and Biomolecular Spectroscopy*, *73*(2), 374-381.

Phillips, G. N., & Hughes, M. J. (1996). The geology and gold deposits of the Victorian gold province. *Ore Geology Reviews*, *11*(5), 255-302.

Piccinin, R. C., Ebbs, S. D., Reichman, S. M., Kolev, S. D., Woodrow, I. E., & Baker, A. J. (2007). A screen of some native Australian flora and exotic agricultural species for their potential application in cyanide-induced phytoextraction of gold. *Minerals Engineering*, *20*(14), 1327-1330.

Pimprikar, P. S., Joshi, S. S., Kumar, A. R., Zinjarde, S. S., & Kulkarni, S. K. (2009). Influence of biomass and gold salt concentration on nanoparticle synthesis by the tropical marine yeast *Yarrowia lipolytica* NCIM 3589. *Colloids and Surfaces B: Biointerfaces*, *74*(1), 309-316.

Portier RJ. 1991. U.S. Patent No. 5,021,088. Washington, DC: U.S. Patent and Trademark Office.

Posth, N. R., Konhauser, K. O., & Kappler, A. (2013). Microbiological processes in banded iron formation deposition. *Sedimentology*, *60*(7), 1733-1754.

Prasad, E. A. V., Gupta, M. J., & Dunn, C. E. (1987). Significance of termite mounds in gold exploration. Current Science, 1219-1222.

Prasad, K. S. S., Sankar, D. B., & Reddy, Y. V. (2012). Geochemistry and Origin of Banded Iron-Formation from the Granulitic Terrain of North Arcot District, Tamil Nadu, South India. *Chemical Science Transactions*, *1*(3), 482493.

Prescott, L.M., Harley, J.P. and Klein, D.A. 1996. Microbiology, 3rd ed. Dubuque, IA: Wm C. Brown Publisher.

Pring, A., Brugger, J., & Shuster, J. (2021). FRANK REITH (11 June 1972–14 October 2019) The man with the gold bug.

Purushothaman, D., Mohakul, J. P., Saha, A., Vidyadharan, K. T., & Rajendran, N. (2009). Soil and stream sediment based geochemical mapping: A case study in Goa. *Journal of the Geological Society of India*, *73*(6), 744-746.

Pyrzyńska, K. (2005). Recent developments in the determination of gold by atomic spectrometry techniques. *Spectrochimica Acta Part B: Atomic Spectroscopy*, *60*(9-10), 1316-1322.

Qiu, M., Tang, Y., Chen, J., Muriph, R., Ye, Z., Huang, C., ... & Xu, Q. (2022). Lung-selective mRNA delivery of synthetic lipid nanoparticles for the treatment of pulmonary lymphangioleiomyomatosis. *Proceedings of the National Academy of Sciences*, *119*(8), e2116271119.

Quach, N. T., Pham-Ngoc, C., Bui, T. L., Tran, T. H., Tran, T. A., Chu, H. H., & Phi, Q. T. (2022). Bioleaching Potential of Indigenous Bacterial Consortia from Gold-Bearing Sulfide Ore of Ta Nang Mine in Vietnam. *Polish Journal of Environmental Studies*, *31*(1), 803-813.

Quach, N. T., Pham-Ngoc, C., Bui, T. L., Tran, T. H., Tran, T. A., Chu, H. H., & Phi, Q. T. (2022). Bioleaching Potential of Indigenous Bacterial Consortia from Gold-Bearing Sulfide Ore of Ta Nang Mine in Vietnam. *Polish Journal of Environmental Studies*, *31*(1), 803-813.

Rabeea, M. A., Owaid, M. N., Aziz, A. A., Jameel, M. S., & Dheyab, M. A. (2020). Mycosynthesis of gold nanoparticles using the extract of *Flammulina velutipes*, Physalacriaceae, and their efficacy for decolorization of methylene blue. *Journal of Environmental Chemical Engineering*, *8*(3), 103841.

Rabeea, M. A., Owaid, M. N., Aziz, A. A., Jameel, M. S., and Dheyab, M. A. Mycosynthesis of gold nanoparticles using the extract of *Flammulina velutipes*, Physalacriaceae, and their efficacy for decolorization of methylene blue. Journal of Environmental Chemical Engineering. 2020; 8(3):103841.

Radhakrishna BP, Curtis LC. 1991. Gold: The Indian Scene. Mineral resources of India. Geological Society of India. pp. 19-41.

Radhakrishna BP, Naqvi SM. 1986. Precambrian continental crust of India and its evolution. The Journal of Geology. 94(2):145-166.

Radhakrishna BP. 2002. Gold in Bihar and Gujarat. Journal of Geological Society of India. 59(1):5-8.

Radhakrishna, B. P., & Curtis, L. C. (1991). Gold-The Indian Scene. *GSI Publications*, *3*(1).

Rajamanickam, M., Balakrishnan, S., & Bhutani, R. (2014). Rb–Sr and Sm–Nd isotope systematics and geochemical studies on metavolcanic rocks from Peddavura greenstone belt: Evidence for presence of Mesoarchean continental crust in easternmost part of Dharwar Craton, India. *Journal of Earth System Science*, *123*(5), 989-1011.

Raman, J., Hariprasath Lakshmanan, P. A. J., Zhijian, C., Periasamy, V., David, P., Naidu, M., and Sabaratnam, V. Neurite outgrowth stimulatory effects of myco synthesized auNPs from *Hericium erinaceus* (Bull.: Fr.) Pers. on pheochromocytoma (Pc-12) cells. International Journal of Nanomedicine. 2015; 10: 5853.

Ramesh SL, Raju PS, Anjaiah KV, Mathur R, Rao TG, Dasaram B, Balaram V. 2001. Determination of gold in rocks, ores, and other geological materials by atomic absorption techniques. Atomic Spectroscopy-norwalk Connecticut.22(1):263-268.

Rana, S., Mishra, P., Ab Wahid, Z., Thakur, S., Pant, D., & Singh, L. (2020). Microbe-mediated sustainable bio-recovery of gold from low-grade precious solid waste: A microbiological overview. *Journal of Environmental Sciences*, *89*, 47-64.

Rao NC, Ram M, Sutaone AT, Gundewar CS. 2006. Gold in Chrornite Ore of South Kaliapani Mines, Sukinda Ultramafic Belt, Jajpur District, Orissa. Geological Society of India.68(2):171-175.

Rao, P. P., Raju, A. V., & Nair, M. M. (1985). Geomorphology of Goa. *Earth resources for Goa's development*, 583-588.

Ravindranath, R., Periasamy, A. P., Roy, P., Chen, Y. W., & Chang, H. T. (2018). Smart app-based on-field colorimetric quantification of mercury via analyte-induced enhancement of the photocatalytic activity of TiO2–Au nanospheres. *Analytical and bioanalytical chemistry*, *410*(18), 4555-4564.

Rawlings, D. E. (2002). Heavy metal mining using microbes. *Annual Reviews in Microbiology*, *56*(1), 65-91.

Rawlings, D. E. (2007). *Biomining* (pp. 177-198). D. B. Johnson (Ed.). Berlin: Springer.

Rawlings, D. E., & Johnson, D. B. (2007). The microbiology of biomining: development and optimization of mineral-oxidizing microbial consortia. *Microbiology*, *153*(2), 315-324.

Rawlings, D. E., Dew, D. and du Plessis, C. 2003. Biomineralization of metal-containing ores and concentrates. TRENDS in Biotechnology. 21(1): 38-44.

Rea, M. A. (2018). *Biogeochemical cycling of gold: Exploring the links between gold transformation, microbial communities, biogeochemical processes and mineralisation style* (Doctoral dissertation).

Rea, M. A., Zammit, C. M., & Reith, F. (2016). Bacterial biofilms on gold grains—implications for geomicrobial transformations of gold. FEMS microbiology ecology, 92(6).

Reddy, L. C. S. (2014). Termite mound as an effective geochemical tool in mineral exploration: A study from chromite mining area, Karnataka, India. *Research Journal of Chemical Scienc. ISSN*, *2231*, 606X.

Reith F, Brugger J, Zammit CM, Nies DH, Southam G. 2013. Geobiological cycling of gold: from fundamental process understanding to exploration solutions. Minerals.3(4): 367-394.

Reith F, McPhail DC, Christy AG. 2005. *Bacillus cereus*, gold and associated elements in soil and regolith samples from Tomakin Park Gold Mine in south-eastern New South Wales, J Geochem Explor. 85:81-89

Reith F, McPhail DC. 2006. Effect of resident microbiota on the solubilization of gold in soils from the Tomakin Park Gold Mine, New South Wales, Australia, Geochim Cosmochim Acta.70: 1421-1438.

Reith F, McPhail DC. 2007. Microbial influences on solubilization and mobility of gold and arsenic in regolith samples from two gold mines in semi-arid and tropical Australia, Geochim Cosmochim Acta. 71:1183-1196.

Reith, F. (2002). Interactions of microorganisms with gold in regolith materials from a gold mine near Mogo in south eastern New South Wales. *Regolith and landscapes in Eastern Australia*, 107-110.

Reith, F. (2003). Evidence for a microbially mediated biogeochemical cycle of gold—a literature review. *Advances in Regolith*, 336-341.

Reith, F., & McPhail, D. C. (2006). Effect of resident microbiota on the solubilization of gold in soil from the Tomakin Park Gold Mine, New South Wales, Australia. *Geochimica et Cosmochimica Acta*, *70*(6), 1421-1438.

Reith, F., & Rogers, S. L. (2008). Assessment of bacterial communities in auriferous and non-auriferous soils using genetic and functional fingerprinting. *Geomicrobiology Journal*, *25*(3-4), 203-215.

Reith, F., Brugger, J., Zammit, C. M., Nies, D. H., & Southam, G. (2013). Geobiological cycling of gold: from fundamental process understanding to exploration solutions. *Minerals*, *3*(4), 367-394.

Reith, F., Etschmann, B., Grosse, C., Moors, H., Benotmane, M. A., Monsieurs, P., ... & Brugger, J. (2009). Mechanisms of gold biomineralization in the bacterium *Cupriavidus metallidurans*. Proceedings of the National Academy of Sciences, 106(42), 17757-17762.

Reith, F., Fairbrother, L., Nolze, G., Wilhelmi, O., Clode, P. L., Gregg, A., ... & Brugger, J. (2010). Nanoparticle factories: Biofilms hold the key to gold dispersion and nugget formation. Geology, 38(9), 843-846.

Reith, F., Lengke, M. F., Falconer, D., Craw, D., & Southam, G. (2007). The geomicrobiology of gold. The ISME Journal, 1(7), 567-584.

Reith, F., McPhail, D. C. 2006. Effect of resident microbiota on the solubilization of gold in soil from the Tomakin Park Gold Mine, New South Wales, Australia. Geochimica et Cosmochimica Acta, 70(6):1421-1438.

Reith, F., McPhail, D. C. 2006. Effect of resident microbiota on the solubilization of gold in soil from the Tomakin Park Gold Mine, New South Wales, Australia. Geochimica et Cosmochimica Acta, 70(6): 1421-1438.

Reith, F., McPhail, D. C. 2007. Mobility and microbially mediated mobilization of gold and arsenic in soils from two gold mines in semi-arid and tropical Australia. Geochimica et Cosmochimica Acta, 71(5): 1183-1196.

Reith, F., Mcphail, D. C., & Christy, A. G. (2005). *Bacillus cereus*, gold and associated elements in soil and other regolith samples from Tomakin Park Gold Mine in southeastern New South Wales, Australia. *Journal of Geochemical Exploration*, *85*(2), 81-98.

Reith, F., Nolze, G., Saliwan-Neumann, R., Etschmann, B., Kilburn, M. R., & Brugger, J. (2019). Unravelling the formation histories of placer gold and platinum-group mineral particles from Corrego Bom Successo, Brazil: A window into noble metal cycling. *Gondwana research*, *76*, 246-259.

Reith, F., Rea, M. A. D., Sawley, P., Zammit, C. M., Nolze, G., Reith, T., ... & Bissett, A. (2018). Biogeochemical cycling of gold: Transforming gold particles from arctic Finland. Chemical Geology, 483, 511-529.

Reith, F., Rogers, S. L., McPhail, D. C., & Brugger, J. (2007, October). Potential for the utilisation of micro-organisms in gold processing. In *World Gold* (pp. 1-8).

Reith, F., Rogers, S. L., McPhail, D. C., & Webb, D. (2006). Biomineralization of gold: biofilms on bacterioform gold. science, 313(5784), 233-236.

Reith, F., Stewart, L., & Wakelin, S. A. (2012). Supergene gold transformation: Secondary and nano-particulate gold from southern New Zealand. *Chemical Geology*, *320*, 32-45.

Reith, F., Zammit, C. M., Shar, S. S., Etschmann, B., Bottrill, R., Southam, G., Brugger, J. 2016. Biological role in the transformation of platinum-group mineral grains. Nature Geoscience, 9(4): 294-298.

Reshawn, M. I., Rajeshkumar, S., & Roy, A. (2022). Synthesis and Characterisation of Zinc Oxide Nanoparticles from Stevia and Ficus Benghalensis and Evaluation of Its Anticariogenic Activity. *International Journal of Early Childhood*, *14*(03), 2022.

Ribeiro, B., Lopes, R., Andrade, P. B., Seabra, R. M., Gonçalves, R. F., Baptista, P., & Quelhas, I. (2008). Comparative study of phytochemicals and antioxidant potential of wild edible mushroom caps and stipes. *Food chemistry*, *110*(1), 47-56.

Robinson, B. H., Brooks, R. R., Howes, A. W., Kirkman, J. H., & Gregg, P. E. H. (1997). The potential of the high-biomass nickel hyperaccumulator *Berkheya coddii* for phytoremediation and phytomining. *Journal of Geochemical Exploration*, *60*(2), 115-126.

Rogan, B., Lemke, M., Levandowsky, M., & Gorrell, T. (2005). Exploring the sulfur nutrient cycle using the Winogradsky column. *The American Biology Teacher*, *67*(6), 348-356.

Rogers JJ. 1986. The Dharwar craton and the assembly of peninsular India. The Journal of Geology. 94(2):129-143.

Rohwerder, T., Gehrke, T., Kinzler, K. and Sand, W. 2003. Bioleaching review part A. Applied Microbiology and Biotechnology. 63(3): 239-248.

Rónavári, A., Igaz, N., Adamecz, D. I., Szerencsés, B., Molnar, C., Kónya, Z., ... & Kiricsi, M. (2021). Green silver and gold nanoparticles: Biological synthesis approaches and potentials for biomedical applications. *Molecules*, *26*(4), 844.

Rosière, C. A., Heimann, A., Oyhantçabal, P., & Santos, J. O. S. (2018). The iron formations of the South American Platform. In *Geology of southwest Gondwana* (pp. 493-526). Springer, Cham.

Rossi, G. 2001. The design of bioreactors. Hydrometallurgy, 59(2-3): 217-231.

Roy, S. K., Shekhar, V., Lassar, W. M., & Chen, T. (2018). Customer engagement behaviors: The role of service convenience, fairness and quality. *Journal of Retailing and Consumer Services*, *44*, 293-304.

Rzhepishevska, O. (2008). *Physiology and Genetics of Acidithiobacillus species: Applications for Biomining* (Doctoral dissertation, Molekylärbiologi (Teknisk-naturvetenskaplig fakultet)).

Sachithanandam, V., Saravanane, N., Chandrasekar, K., Karthick, P., Lalitha, P., Elangovan, S. S., & Sudhakar, M. (2020). Microbial diversity from the continental shelf regions of the Eastern Arabian Sea: A metagenomic approach. *Saudi journal of biological sciences*, *27*(8), 2065-2075.

Sadhasivam, S., Shanmugam, P., Veerapandian, M., Subbiah, R., & Yun, K. (2012). Biogenic synthesis of multidimensional gold nanoparticles assisted by *Streptomyces hygroscopicus* and its electrochemical and antibacterial properties. *Biometals*, *25*(2), 351-360.

Sadler, P. J. (1976). The biological chemistry of gold: a metallo-drug and heavy-atom label with variable valency. In *Biochemistry* (pp. 171-214). Springer, Berlin, Heidelberg.

Sahoo, A. K., Krishnamurthi, R., Vadlamani, R., Pruseth, K. L., Narayanan, M., Varghese, S., & Pradeepkumar, T. (2016). Genetic aspects of gold mineralization in the Southern Granulite Terrain, India. *Ore Geology Reviews*, *72*, 1243-1262.

Salvà-Serra, F., Gomila, M., Svensson-Stadler, L., Busquets, A., Jaén-Luchoro, D., Karlsson, R., & Moore, E. R. (2018). A protocol for extraction and purification of high-quality and quantity bacterial DNA applicable for genome sequencing: a modified version of the Marmur procedure.

Samuels, T., Bryce, C., Landenmark, H., Marie-Loudon, C., Nicholson, N., Stevens, A. H., & Cockell, C. (2020). Microbial weathering of minerals and rocks in natural

environments. *Biogeochemical cycles: Ecological drivers and environmental impact*, 59-79.

Sanghi, R., and Verma, P. Biomimetic synthesis and characterisation of protein capped silver nanoparticles. Bioresource technology. 2009; 100(1)-501-504.

Sangurmath, P. (2014). An overview of primary, supergene and placer gold occurrences of Wayanad–Nilambur granulitic terrain, south India. *MINERAL RESOURCES OF KERALA*, 34.

Santosh, M., Omana, P. K., & YOSHIDA, M. (1990). Gold grains in laterite weathering profiles of Nilambur, South India and a model for the genesis of supergene gold deposits. *JOURNAL OF MINERALOGY, PETROLOGY AND ECONOMIC GEOLOGY*, *85*(9), 416-423.

Santosh, M., Philip, R., Jacob, M. K., & Omana, P. K. (1992). Highly pure placer gold formation in the Nilambur Valley, Wynad Gold Field, southern India. *Mineralium Deposita*, *27*(4), 336-339.

Saralov A, Baslerov R, Kuznetsov B. 2013. *Haloferax chudinovi* sp. nov., a halophilic archaeon from Permian potassium salt deposits. Extremophiles. 17:499–504.

Sardar, M., & Mazumder, J. A. (2019). Biomolecules assisted synthesis of metal nanoparticles. In *Environmental Nanotechnology* (pp. 1-23). Springer, Cham.

Sarfraz, R., Aqeel, M., Lactao, J., & Khan, S. (2021). Coping strategies, pain severity, pain anxiety, depression, positive and negative affect in osteoarthritis patients; a mediating and moderating model. *Nature-Nurture Journal of Psychology*, *1*(1).

Sarkar, B. C., & Nair, A. M. (2002). A geostatistical modelling approach to gold mineralisation at Hutti mine, Raichur District, Karnataka. *JOURNAL-GEOLOGICAL SOCIETY OF INDIA*, *60*(6), 639-648.

Sarkar, J., Roy, S. K., Laskar, A., Chattopadhyay, D., and Acharya, K. Bioreduction of chloroaurate ions to gold nanoparticles by culture filtrate of *Pleurotus sapidus* Quel. Materials letters. 2013; 92:313-316.

Sarma, D. S., Fletcher, I. R., Rasmussen, B., McNaughton, N. J., Mohan, M. R., & Groves, D. I. (2011). Archaean gold mineralization synchronous with late cratonization of the Western Dharwar Craton, India: 2.52 Ga U–Pb ages of hydrothermal monazite and xenotime in gold deposits. *Mineralium Deposita*, *46*(3), 273-288.

Sathiyaraj, S., Suriyakala, G., Gandhi, A. D., Babujanarthanam, R., Almaary, K. S., Chen, T. W., & Kaviyarasu, K. (2021). Biosynthesis, characterization, and antibacterial activity of gold nanoparticles. *Journal of Infection and Public Health*, *14*(12), 1842-1847.

Savitzky A, Golay MJ. Smoothing and differentiation of data by simplified least squares procedures. Analytical Chemistry. 1964; 36(8):1627-1639

Sawkar RH, Hussain SM, Naqvi SM. 1995. Gold Mineralization in the Sulphidic Bifs of Chitradurga Schist Belt, Karnataka-Possibility of New Workable Gold Deposits. Journal of Geological Society of India.46(1):91-93.

Sawle, B. D., Salimath, B., Deshpande, R., Bedre, M. D., Prabhakar, B. K., & Venkataraman, A. (2008). Biosynthesis and stabilization of Au and Au–Ag alloy nanoparticles by fungus, *Fusarium semitectum*. *Science and technology of advanced materials*.

Schippers, A., & Sand, W. (1999). Bacterial leaching of metal sulfides proceeds by two indirect mechanisms via thiosulfate or via polysulfides and sulfur. *Applied and environmental microbiology*, *65*(1), 319-321.

Schippers, A., Hedrich, S., Vasters, J., Drobe, M., Sand, W., & Willscher, S. (2014). Biomining: metal recovery from ores with microorganisms. *Geobiotechnology I: Metal-Related Issues*, 1-47.

Schloss PD, Handelsman J. 2003. Biotechnological prospects from metagenomics. Current opinion in biotechnology. 14(3): 303-310.

Schnell Henry A. 1997 Bioleaching of copper. Biomining. Springer Berlin Heidelberg. pp. 21-43.

Schopf, J. W. (2021). Precambrian Paleobiology: Precedents, Progress, and Prospects. *Frontiers in Ecology and Evolution*, *9*, 707072.

Schopf, J. W., & Packer, B. M. (1987). Early Archean (3.3-billion to 3.5-billion-year-old) microfossils from Warrawoona Group, Australia. *Science*, *237*(4810), 70-73.

Scott, J. D. (1987). Process mineralogy of silver and gold at Kidd Creek, from ore to anode slime. In *Proceedings of the Metallurgical Society of the Canadian Institute of Mining and Metallurgy* (pp. 125-132). Pergamon.

Selli, S., Guclu, G., Sevindik, O., & Kelebek, H. (2021). Variations in the key aroma and phenolic compounds of champignon (*Agaricus bisporus*) and oyster (*Pleurotus ostreatus*) mushrooms after two cooking treatments as elucidated by GC–MS-O and LC-DAD-ESI-MS/MS. *Food Chemistry*, *354*, 129576.

Sen, I. K., Maity, K., & Islam, S. S. (2013). Green synthesis of gold nanoparticles using a glucan of an edible mushroom and study of catalytic activity. *Carbohydrate polymers*, *91*(2), 518-528.

Shafiee, S., Topal, E. 2010. An overview of global gold market and gold price forecasting. Resources policy, 35(3):178-189.

Shahverdi, A. R., Yazdi, M. T., OULIAZADEH, M., & Darebidi, M. H. (2001). Biooxidation of mouteh refractory gold-bearing concentrate by an adapted *Thiobacillus ferrooxidans*.209-212.

Shanker R, Nag S, Shome S. 2002. Incidence of Gold in Subgreenschist to Greenschist Facies Metabasalt of Bhowali, Nainital District, Uttaranchal. Journal of the Geological Society of India. 59(4):379-383.

Sharma, P., Bano, A., Singh, S. P., Dubey, N. K., Chandra, R., & Iqbal, H. M. (2022). Microbial fingerprinting techniques and their role in the remediation of environmental pollution. *Cleaner Chemical Engineering*, 100026.

Sheikhloo, Z., Salouti, M., & Katiraee, F. (2011). Biological synthesis of gold nanoparticles by fungus *Epicoccum nigrum*. *Journal of Cluster Science*, *22*(4), 661-665.

Shokralla, S., Spall, J. L., Gibson, J. F., & Hajibabaei, M. (2012). Next-generation sequencing technologies for environmental DNA research. *Molecular ecology*, *21*(8), 1794-1805.

Shuster, J. P. (2013). The biogeochemical cycling of gold under surface and near-surface environmental conditions.

Shuster, J., & Reith, F. (2018). Reflecting on gold geomicrobiology research: thoughts and considerations for future endeavors. *Minerals*, *8*(9), 401.

Siddiqui MH, Kumar A, Kesari KK, Arif, JM. 2009. Biomining–a useful approach toward metal extraction. American-Eurasian Journal of Agronomy.2(2):84-88.

Singh, J., Sangode, S. J., Bagwan, M. F., Meshram, D. C., & Dhobale, A. (2020). Episodic ferricretization of the Deccan Laterites (India): Inferences from ore microscopy, mineral magnetic and XRD spectroscopic studies. *Journal of Earth System Science*, *129*(1), 1-18.

Singh, P., Kim, Y. J., Zhang, D., & Yang, D. C. (2016). Biological synthesis of nanoparticles from plants and microorganisms. *Trends in biotechnology*, *34*(7), 588-599.

Smitha, S. L., Philip, D., & Gopchandran, K. G. (2009). Green synthesis of gold nanoparticles using Cinnamomum zeylanicum leaf broth. *Spectrochimica Acta Part A: Molecular and Biomolecular Spectroscopy*, *74*(3), 735-739.

Solomon, C., & Breckon, T. (2011). Fundamentals of Digital Image Processing: A practical approach with examples *in Matlab*. John Wiley & Sons.

SOLTANI, N. M., SHAHIDI, B. G., & KHALEGHI, N. (2015). Biosynthesis of gold nanoparticles using Streptomyces fulvissimus isolate.

Song, X., Wang, Z., Liu, Y., Wang, C., & Li, L. (2009). A highly sensitive ethanol sensor based on mesoporous ZnO–SnO2 nanofibers. *Nanotechnology*, *20*(7), 075501.

South India and a model for the genesis of supergene gold deposits. *JOURNAL OF MINERALOGY, PETROLOGY AND ECONOMIC GEOLOGY*, *85*(9), 416-423.

Southam, G., & Saunders, J. A. (2005). The geomicrobiology of ore deposits. *Economic Geology*, *100*(6), 1067-1084.

Southam, G., Lengke, M.F. and Fairbrother, L.S.F. (2009). The biogeochemistry of gold. Elements, v. 5(5), pp. 303-307

Spencer PA, Budden JR, Barrett J, Hughes MN, Poole RK 1992. Oxidation of metal sulfides using thermotolerant bacteria. PCT patent WO 92/16667.

Sreenivasa, A., Jayasheela, H. M., Bejugam, P., & Gujar, A. R. (2014). Heavy mineral studies of beach sands of Vagathor, North Goa, India. *Int J Mod Eng Res (IJMER)*, *4*(70-78).

Sridharan, R., Krishnaswamy, V. G., & Kumar, P. S. (2021). Analysis and microbial degradation of Low-Density Polyethylene (LDPE) in Winogradsky column. *Environmental Research*, *201*, 111646.

Srinath, B. S., & Rai, V. R. (2015). Rapid biosynthesis of gold nanoparticles by Staphylococcus epidermidis: Its characterisation and catalytic activity. *Materials Letters*, *146*, 23-25.

Sriram, T., & Pandidurai, V. (2014). Synthesis of silver nanoparticles from leaf extract of Psidium guajava and its antibacterial activity against pathogens. *Int. J. Curr. Microbiol. App. Sci*, *3*(3), 146-152.

Srivastava, S. K., Yamada, R., Ogino, C., & Kondo, A. (2013). Biogenic synthesis and characterization of gold nanoparticles by Escherichia coli K12 and its heterogeneous catalysis in degradation of 4-nitrophenol. *Nanoscale research letters*, *8*(1), 1-9.

Srivastava, S., Usmani, Z., Atanasov, A. G., Singh, V. K., Singh, N. P., Abdel-Azeem, A. M., ... & Bhargava, A. (2021). Biological nanofactories: Using living forms for metal nanoparticle synthesis. *Mini Reviews in Medicinal Chemistry*, *21*(2), 245-265.

Stamets, P., & Chilton, J. S. (1983). The mushroom cultivator. *First Washington*.

Starkey, R. L. (1935). Isolation of some bacteria which oxidize thiosulfate. *Soil Science*, *39*(3), 197-220.

Stewart, A. D., Anand, R. R., & Balkau, J. (2012). Source of anomalous gold concentrations in termite nests, Moolart Well, Western Australia: implications for exploration. *Geochemistry: Exploration, Environment, Analysis*, *12*(4), 327-337.

Suh, C. E., Lehmann, B., & Mafany, G. T. (2022). Geology and geochemical aspects of lode gold mineralization at Dimako–Mboscorro, SE Cameroon. *Geology*.

Sun, L. X., Zhang, X., Tan, W. S., & Zhu, M. L. (2012). Effect of agitation intensity on the biooxidation process of refractory gold ores by *Acidithiobacillus ferrooxidans*. *Hydrometallurgy*, *127*, 99-103.

Sun, X., Gutierrez, A., Yacaman, M. J., Dong, X., & Jin, S. (2000). Investigations on magnetic properties and structure for carbon encapsulated nanoparticles of Fe, Co, Ni. *Materials Science and Engineering: A*, *286*(1), 157-160.

Syed, A., Al Saedi, M. H., Bahkali, A. H., Elgorgan, A. M., Kharat, M., Pai, K.,and Ahmad, A. αAu2S nanoparticles: Fungal-mediated synthesis, structural characterization and bioassay. Green Chemistry Letters and Reviews. 2020; 15(1): 59-68.

Sylvestre, G., Timoleon, N., Djibril, K. N. G., Paul, N. J., & Marianne, N. F. (2015). Petrology and geochemistry of the banded iron-formations from Ntem complex greenstones belt, Elom area, Southern Cameroon: implications for the origin and depositional environment. *Geochemistry*, *75*(3), 375-387.

Szaloki I, Somogyi A, Braun M, Tóth A.1999. Investigation of geochemical composition of lake sediments using ED-XRF and ICP-AES techniques. X-Ray Spectrometry. 28(5): 399-405.

Tagkouli, D., Kaliora, A., Bekiaris, G., Koutrotsios, G., Christea, M., Zervakis, G. I., & Kalogeropoulos, N. (2020). Free amino acids in three *Pleurotus* species cultivated on agricultural and agro-industrial by-products. *Molecules*, *25*(17), 4015.

Tang, X., Li, B., Lu, J., Liu, H. and Zhao, Y. (2020). Gold determination in soil by ICP-MS: comparison of sample pretreatment methods. Jour. Analyt. Sci. Technol., v. 11(1), pp. 1-8.

Tapia, J., Dueñas, A., Cheje, N., Soclle, G., Patiño, N., Ancalla, W., ... & Lazarte, A. (2022). Bioleaching of Heavy Metals from Printed Circuit Boards with an Acidophilic Iron-Oxidizing Microbial Consortium in Stirred Tank Reactors. *Bioengineering*, *9*(2), 79.

Tavakoli, H. Z., Bahrami-Bavani, M., Miyanmahaleh, Y., & Tajer-Mohammad-Ghazvini, P. (2021). Identification and characterization of a metal-resistant *Acidithiobacillus*

ferrooxidans as important potential application for bioleaching. *Biologia*, *76*(4), 1327-1337.

Teimuri-Mofrad, R., Hadi, R., Tahmasebi, B., Farhoudian, S., Mehravar, M., & Nasiri, R. Green synthesis of gold nanoparticles using plant extract: Mini-review. Nanochemistry Research. 2017; 2(1):8-19.

Tepale, N., Fernández-Escamilla, V. V., Carreon-Alvarez, C., González-Coronel, V. J., Luna-Flores, A., Carreon-Alvarez, A., and Aguilar. Nanoengineering of gold nanoparticles: Green synthesis, characterization, and applications. Crystals. 2019; 9(12): 612.

Tibuhwa, D. D. *Termitomyces* species from Tanzania, their cultural properties and unequalled basidiospores. Journal of Biology and Life Science. 2012; 3(1): 140-159.

Tibuhwa, D. D., Kivaisi, A. K., and Magingo, F. S. S. Utility of the macro-micromorphological characteristics used in classifying the species of *Termitomyces*. Tanzania Journal of Science. 2010: 36.

Townley, B. K., Hérail, G., Maksaev, V., Palacios, C., Parseval, P. D., Sepulveda, F., ... & Ulloa, C. (2003). Gold grain morphology and composition as an exploration tool: application to gold exploration in covered areas. *Geochemistry: Exploration, Environment, Analysis*, *3*(1), 29-38.

Trendall, A. F. (2002). The significance of iron-formation in the Precambrian stratigraphic record. *Precambrian sedimentary environments: A modern approach to ancient depositional systems*, 33-66.

Tsaplina, I. A., Zhuravleva, A. E., Grigor'eva, N. V., Belyi, A. V., Pivovarova, T. A., Bulaev, A. G., ... & Kondrat'eva, T. F. (2012). Biooxidation of a gold-containing sulfide concentrate in relation to changes in physical and chemical conditions. *Microbiology*, *81*(3), 288-298.

Tsutsui, Y., Hayakawa, T., Kawamura, G., and Nogami, M. Tuned longitudinal surface plasmon resonance and third-order nonlinear optical properties of gold nanorods. Nanotechnology. 2011; 22(27): 275203.

Tudu, S. C., Zubko, M., Kusz, J., and Bhattacharjee, A. CdS nanoparticles (< 5 nm): green synthesized using *Termitomyces heimii* mushroom–structural, optical and morphological studies. Applied Physics A. 2021; 127(2): 1-9.

Tupikina, O. V., Rassulov, V. A., & Kondrat'eva, T. F. (2009). Patterns of pyrite oxidation by different microorganisms. *Microbiology*, *78*(2), 165-169.

Tupikina, O. V., Samorukova, V. D., & Kondrat'eva, T. F. (2009). Patterns of growth and oxidation of natural pyrites by the representatives of acidophilic chemolithotrophic microorganisms. *Microbiology*, *78*(2), 170-179.

Ugarkar, A. G., Malapur, M. A., & Kumar, B. C. (2016). Archean turbidite hosted orogenic gold mineralization in the Gadag greenstone belt, Western Dharwar Craton, Peninsular India. *Ore Geology Reviews*, *72*, 1224-1242.

Umathay RM. 1993. Occurrence of Gold in the Iron Ores of Konkan Area, Maharashtra. Journal of Geological Society of India. 41(3):277-279.

Unrine, J. M., Shoults-Wilson, W. A., Zhurbich, O., Bertsch, P. M., and Tsyusko, O. V. 2012. Trophic transfer of Au nanoparticles from soil along a simulated terrestrial food chain. Environmental science & technology, 46(17), 9753-9760.

Unrine, J. M., Tsyusko, O. V., Hunyadi, S. E., Judy, J. D., & Bertsch, P. M. (2010). Effects of particle size on chemical speciation and bioavailability of copper to earthworms (Eisenia fetida) exposed to copper nanoparticles. *Journal of Environmental Quality*, *39*(6), 1942-1953.

Usher, E. L., & Pajares, F. (2009). Sources of self-efficacy in mathematics: A validation study. *Contemporary educational psychology*, *34*(1), 89-101.

Usman, A. I., Aziz, A. A., and Noqta, O. A. Application of green synthesis of gold nanoparticles: A review. Jurnal Teknologi. 2019: 81(1).

Vala, A. K. (2015). Exploration on green synthesis of gold nanoparticles by a marine-derived fungus *Aspergillus sydowii*. *Environmental Progress & Sustainable Energy*, *34*(1), 194-197.

Van Houdt, R., Monchy, S., Leys, N., & Mergeay, M. (2009). New mobile genetic elements in Cupriavidus metallidurans CH34, their possible roles and occurrence in other bacteria. *Antonie Van Leeuwenhoek*, *96*(2), 205-226.

Vandamme P, Coenye T. 2004. Taxonomy of the genus *Cupriavidus*: a tale of lost and found. International journal of systematic and evolutionary microbiology. 54(6):2285-2289.

Velho-Pereira, S., & Kamat, N. (2010). Digital image analysis of actinomycetes colonies as a potential aid for rapid taxonomic identification. *Nature Precedings*, 1-1.

Velho-Pereira, S., & Kamat, N. M. (2011). Antimicrobial screening of actinobacteria using a modified cross-streak method. Indian journal of pharmaceutical sciences, 73(2), 223.

Verma, V. C., Singh, S. K., Solanki, R., & Prakash, S. (2011). Biofabrication of anisotropic gold nanotriangles using extract of endophytic *Aspergillus clavatus* as a dual functional reductant and stabilizer. *Nanoscale Res Lett*, *6*(1), 1-7.

Vetchinkina, E. P., Loshchinina, E. A., Burov, A. M., and Nikitina, V. E. Bioreduction of gold (iii) ions from hydrogen tetrachloaurate to the elementary state by edible cultivated medicinal xylotrophic Basidiomycetes belonging to various systematic groups and molecular mechanisms of gold nanoparticles biological synthesis. Sci Pract J Heal Life Sci. 2013; 4:51-56.

Vetchinkina, E. P., Loshchinina, E. A., Vodolazov, I. R., Kursky, V. F., Dykman, L. A., & Nikitina, V. E. Biosynthesis of nanoparticles of metals and metalloids by

basidiomycetes. Preparation of gold nanoparticles by using purified fungal phenol oxidases. Applied microbiology and biotechnology. 2017; 101(3):1047-1062.

Vrinda, K. B., and Pradeep, C. K. *Termitomyces sagittiformis*-a lesser known edible mushroom from the Western Ghats. Mushroom Research. 2009; 18(1): 33-36.

Vuleta, S., LeGras, M., E Smith, R., Laukamp, C., Schoneveld, L., & Anand, R. (2019). Characterising lithium host minerals within the lateritic duricrust, Greenbushes, Western Australia. *ASEG Extended Abstracts*, *2019*(1), 1-2.

Wakelin, S. A., Anand, R. R., Reith, F., Gregg, A. L., Noble, R. R., Goldfarb, K. C., ... & Brodie, E. L. (2012). Bacterial communities associated with a mineral weathering profile at a sulphidic mine tailings dump in arid Western Australia. *FEMS Microbiology Ecology*, *79*(2), 298-311.

Wakelin, S., Mander, C., Gerard, E., Jansa, J., Erb, A., Young, S., ... & O'Callaghan, M. (2012). Response of soil microbial communities to contrasted histories of phosphorus fertilisation in pastures. *Applied soil ecology*, *61*, 40-48.

Wang, J. (2008). Electrochemical glucose biosensors. *Chemical reviews*, *108*(2), 814-825.

Wang, J., Faraji, F., Ramsay, J., & Ghahreman, A. (2021). A review of biocyanidation as a sustainable route for gold recovery from primary and secondary low-grade resources. *Journal of Cleaner Production*, *296*, 126457.

Wang, N., Wang, Z., Aust, K. T., & Erb, U. (1995). Effect of grain size on mechanical properties of nanocrystalline materials. *Acta Metallurgica et Materialia*, *43*(2), 519-528.

Wang, Z., Su, J., Ali, A., Zhang, R., Yang, W., Xu, L., & Zhao, T. (2021). Microbially induced calcium precipitation based simultaneous removal of fluoride, nitrate, and calcium by Pseudomonas sp. WZ39: Mechanisms and nucleation pathways. *Journal of Hazardous Materials*, *416*, 125914.

Watterson, J. R. (1992). Preliminary evidence for the involvement of budding bacteria in the origin of Alaskan placer gold. *Geology*, *20*(4), 315-318.

Weerasingha, P. D. S., & Gunawardane, M. M. (2015). Isolation and characterization of *Rhodomicrobium vannielii* from Winogradsky column.

Wei, T. Z., Tang, B. H., & Yao, Y. J. Revision of *Termitomyces* in China. *Mycotaxon*. 2009; 108(1): 257-285.

Widdowson, M. (2009). Evolution of laterite in Goa. *Proceedings of natural resources of Goa: a geological perspective. Geological Society of Goa, Miramar Goa*, 35-68.

World Gold Council. 2015. 1/02/2017. www.gold.org

Xie CH, Yokota A. 2005. Reclassification of Alcaligenes latus strains IAM 12599T and IAM 12664 and *Pseudomonas saccharophila* as *Azohydromonas lata* gen. nov., comb. nov., *Azohydromonas australica* sp. nov. and *Pelomonas saccharophila* gen. nov., comb. nov., respectively. International journal of systematic and evolutionary microbiology. 55(6): 2419-2425.

Xu, X. W., Wu, Y. H., Wang, C. S., Oren, A., Zhou, P. J., & Wu, M. (2007). *Haloferax larsenii* sp. nov., an extremely halophilic archaeon from a solar saltern. *International journal of systematic and evolutionary microbiology*, *57*(4), 717-720.

Yadav, S. (2017). Potentiality of earthworms as bioremediating agent for nanoparticles. In *Nanoscience and Plant–Soil Systems* (pp. 259-278). Springer, Cham.

Yaman, B. N., Mutlu, M. B., Çelik, P. A., & Çabuk, A. (2020). Metagenomics (16S amplicon sequencing) and DGGE analysis of bacterial diversity of acid mine drainage. *Journal of microbiology, biotechnology and food sciences*, *9*(5), 932-936.

Yang, G., Nanda, J., Wang, B., Chen, G., and Hallinan Jr, D. T. Self-assembly of large gold nanoparticles for surface-enhanced Raman spectroscopy. ACS applied materials & interfaces. 2017; 9(15): 13457-13470.

Yang, Q., Wang, L., Gao, J., Liu, X., Feng, Y., Wu, Q., ... & Xia, X. (2016). Tannin-rich fraction from pomegranate rind inhibits quorum sensing in *Chromobacterium violaceum* and biofilm formation in Escherichia coli. *Foodborne pathogens and disease*, *13*(1), 28-35.

Yang, X. Q., Zhang, Z. H., Duan, S. G., & Zhao, X. M. (2015). Petrological and geochemical features of the Jingtieshan banded iron formation (BIF): A unique type of BIF from the Northern Qilian Orogenic Belt, NW China. *Journal of Asian Earth Sciences*, *113*, 1218-1234.

Young, T., Evans, L., Finn, L., Palta, M. 1997. Estimation of the clinically diagnosed proportion of sleep apnea syndrome in middle-aged men and women. Sleep, 20(9): 705-706.

Zhao, P., Feng, X., Huang, D., Yang, G., & Astruc, D. (2015). Basic concepts and recent advances in nitrophenol reduction by gold-and other transition metal nanoparticles. *Coordination Chemistry Reviews*, *287*, 114-136.

Zhao, Y., Zhao, W., Lim, Y. C., & Liu, T. Salinomycin-loaded gold nanoparticles for treating cancer stem cells by ferroptosis-induced cell death. Molecular pharmaceutics. 2019; 16(6): 2532-2539.

Zhou, G., & Yang, J. C. (2005). Initial oxidation kinetics of Cu (100), (110), and (111) thin films investigated by in situ ultra-high-vacuum transmission electron microscopy. *Journal of Materials Research*, *20*(7), 1684-1694.

Zhou, Q. G., Bo, F., Hong Bo, Z., Xi, L., Jian, G., Fei Fei, L., & Xin Hua, C. (2007). Isolation of a strain of Acidithiobacillus caldus and its role in bioleaching of chalcopyrite. *World Journal of Microbiology and Biotechnology*, *23*(9), 1217-1225.

Zotchev, S. B. (2012). Marine actinomycetes as an emerging resource for the drug development pipelines. *Journal of biotechnology*, *158*(4), 168-175.

APPENDICES

Antibiotics solutions

0.01 mg/ml nalidixic acid Dissolve 0.1 g of nalidixic acid (HiMedia) in 25 ml ethanol and filter sterilize using 0.22-micron syringe driven filters (HiMedia). Pipette out 1100 µL for 250 ml medium.

0.01 mg/ml neomycin b sulphate

Dissolve 0.02 g of neomycin b sulphate (HiMedia) in 10 ml sterile distilled water and filter sterilize using 0.22-micron syringe driven filters (HiMedia). Pipette out 1250 µL for 250 ml medium.

Reagents

0.1 N sodium hydroxide

Dissolve 4 g NaOH and make the volume to 1000 ml in volumetric flask.

2 M sodium hydroxide

Dissolve 8 g NaOH and make the volume to 100 ml in volumetric flask.

0.1 N hydrochloric acid

Prepare 0.1 N HCl by mixing 10.43 ml of conc. 35% HCl (Merck) carefully with distilled water and make the volume to 1000 ml.

7 M hydrochloric acid

Prepare 7 N HCl by mixing 73 ml of conc. 35% HCl carefully with distilled water and make the volume to 100 ml.

10% (v/v) sterile glycerol

Take 10 ml of glycerol (Hi Media) and make the total volume to 100 ml using distilled water. Sterilize by autoclaving at 15 lbs pressure at 121°C for 15 min.

Preparation of alcohol series for SEM studies: 30%, 50%, 70%, 90% Ethanol

Take 30 ml of absolute ethanol and make the volume to 100 ml with milli Q water. Similarly, other concentrations of ethanol were prepared.

0.1 M phosphate buffer pH (7.2)

Stock solutions preparations:

1) 0.2 M di-sodium hydrogen phosphate, anhydrous (solution A) Take 1.42 g of Na HPO (HiMedia) in 100 ml distilled water 2 4

2) 0.2 M sodium di-hydrogen orthophosphate, dihydrate (solution B)

Take 1.56 g of NaH_2 PO_4 $2H_2$ O (HiMedia) in 100 ml distilled water. To prepare 0.1 M phosphate buffer add 36 ml of solution A to 14 solution B (0.2 M phosphate buffer) + 50 ml distilled water. To this more 100 ml of distilled water was added.

Stains

Lactophenol Cotton Blue (Commercial stain obtained from HiMedia)

Ammoniacal Congo Red (ACR)

Dissolve 0.1 g of congo red powder (HiMedia) in 100 ml strong ammonia solution.

Iodine potassium iodide solution

Iodine Crystals	0.6 % (w/v)
Potassium iodide	6 % (w/v)
Distilled water	100 ml

Congo red solution

Congo red	0.5 % (w/v)
Ethanol	5 % (w/v)
Distilled water	100 ml

Crystal violet

Crystal violet	2 g
Ethyl alcohol	20 ml
95% Ammonium citrate monohydrate	0.8 g
Deionized water	80 ml

Dissolve 2 g crystal violet in 20 ml of 95% ethyl alcohol. Dissolve 0.8 g ammonium oxalate monohydrate in 80 ml deionized water. Mix the crystal violet and ammonium 294 oxalate monohydrate solutions to make the crystal violet stain. Filter the stain if necessary.

Research papers published/accepted

1. Dabolkar, S., Furtado, I. J., & Kamat, N. M. (2023). Pioneer Studies on Metagenomic Evaluation of Diversity of Microbial Community in Banded Iron Formation (BIF) from Iron Ore Mining Belt of Goa, India. Geomicrobiology Journal, 40(5),427-433.Journal, DOI: 10.1080/01490451.2023.2184883. **(Appendix I)**
2. Sujata Dabolkar & Nandkumar Kamat (2022). Successful separation and detection of gold sulphide in ore samples from the banded iron formation of Goa, India. CURRENT SCIENCE, VOL. 123, NO. 11, 10 DECEMBER 2022. DOI: 10.18520/cs/v123/i11/1387-1390. **(Appendix II)**
3. Dabolkar, S., & Kamat, N. M. (2022). Method for Separation and Detection of Gold Sulphide from low grade (mining reject) of Goa Eco. Env. & Cons. 28 (January Suppl. Issue) pp. S233-S238.ISSN 0971–765X. **(Appendix III)**
4. Dabolkar, S., & Kamat, N. M. (2022). 21st century Prospects of Gold Biomining in India-A Review. Journal of applied Geochemistry-accepted (17/05/2022). **(Appendix IV)**
5. Dabolkar, S., & Kamat, N. M. (2022). Use of the Modified Winogradsky Microcosm Technique to Help in Building an Indigenous Culture Collection of Iron and Sulphur Bacteria Valuable in Green Synthesis of Gold Nanoparticles. Eco. Env. & Cons. 28 (January Suppl. Issue) pp. S233-S238.ISSN 0971–765X. **(Appendix V)**
6. Dabolkar, S., & Kamat, N. M. (2022). Gold from Auriferous Iron Ore of Goa, India. Journal of Geoscience research. 81-8 (10). ISSN 2455-1953**. (Appendix VI).**

7. Dabolkar, S., & Kamat, N. M. (2022). Pioneer studies on metagenomic analysis of samples from Banded Iron Formation (BIF) from iron ore mining belt of goa, India, 7th International Mardin Artuklu Scientific Researches Conference. The book of full text on applied sciences. Issued: 25.12.2021 ISBN: 978-625-8423-02-0. **(Appendix VII)**
8. Dabolkar, S., & Kamat, N. M. (2020). Application of digital colorimeter for preliminary characterization of gold nanoparticle swarms produced by *Termitomyces heimii* using a novel bioinspired microfluidics assay. KAVAKA 55: 50-57 (2020). **(Appendix VIII)**
9. Dabolkar, S., & Kamat, N. M. (2019). Potential of geophagous earthworms in ecofriendly and sustainable biomining of gold from auriferous soils, IJRAR. Volume 06, Issue 1. **(Appendix IX)**
10. Dabolkar, S., & Kamat, N. M. (2019). Fractal dimension analysis of swarms of gold nano/micro particles produced by wild *Rhizobium* cultures using a novel slide-based system. International Journal of Interdisciplinary Research and Innovations ISSN 2348-1226 (online) Vol. 7, Issue 1, pp: (416-425) **(Appendix X)**

Papers communicated

- Dabolkar, S., & Kamat, N. M. (2022). Biosynthesis and Characterization of AuNps produced using *Termitomyces heimii* pellets-Mycology journal Taylor and Francis.

Papers presented at conferences

Poster

- **Dabolkar** and Kamat. **"How Indian state of Goa could attain its potential in Asia as major Metallogenic province through knowledge based sustainable Biomining with New focus on neglected auriferous resources"** at the International Nature conference organised by Geological survey of Norway, NTNU, SINTEF and Nature materials on the topic on 13-15th September 2018. **(Appendix VII)**

- **Dabolkar** and Kamat. **"Comparative studies on swarms and morphology of AuNPs and micro particles produced by bacterial and fungal cellular and cell free extracts"** at international symposium on Fungal Biology: Advance, Application and conservation (INSFB 2018) & 45th Annual Meeting of Mycological Society of India organised by National Fungal Culture collection of India (DST National Facility) MACS' Agharkar Research institute, Pune 411004 presented poster paper entitled on 19-21th November 2018. **(Appendix VIII)**

- **Dabolkar** and Kamat. **"Generating sustainable wealth from lateritic waste-prospects of Biomining of Gallium"** at National conference on "Microbial Bioremediation: Novel Approaches and Trends "organised by Department of Microbiology in collaboration with Department of science, Technology and Environment Government of Goa on 27th and 28th February 2019. **Best poster award. (Appendix IX)**

- **Dabolkar** and Kamat. **"The Modified Winogradsky Microcosm Technique Can Help in Building An Indigenous Culture Collection Of Iron And Sulphur Bacteria Valuable In Green Synthesis Of Gold Nanoparticles"** at 1st International Conference on Evolving Materials and Nanotechnology for Sustainable Development (EMNSD-2020) Organized by Department of Physics, Central Institute of Technology Kokrajhar (Deemed to be University under MoE, Govt. of India), Kokrajhar, Assam, India, on 15-16th December 2020, online mode. **(Appendix X)**

- **Dabolkar** and Kamat**. "Subsurface Zircons with presumptive biogenic inclusions, biosphere in Goa** at National seminar on topic Advances in life sciences at St. Xavier's college. **(Appendix XI)**

- **Dabolkar** and Kamat. "**Implications for climate change: Role of sea shell infecting calcimycocavites in efficient biogeochemical cycling of calcium and carbon** at National conference of changing environment -challenges, solution and strategies organised by Dempe college of Arts and science, Miramar Goa on 8th and 9th March 2018. **(Appendix XII)**

Oral

- **Dabolkar** and Kamat. **"Design of Biosinspired microporous fungal biomass based nanoporous Agar hydrogel Beads as efficient Gold biosensors"** at International Conference on Porous Materials for Energy and Environment (PMEE 2021) organized by Cluster Research centre, PG & UG Department of Chemistry in association with IQAD, GCASCK, Khandola, Marcela-Goa on 12-13 March 2021, Online mode. **(Appendix XIII)**

- **Dabolkar** and Kamat. **"History of gold mining in Goa through the ages"** at XXth History seminar 2019, organised by Department of History of Goa University and amp; Directorate of Archives & amp, on topic on 10th January 2019. **(Appendix XIV)**

- **Dabolkar** and Kamat. **"Reinventing the Indian Alchemic heritage of Bhunagas- How Geophagous Earthworms can help in Eco-friendly and sustainable Biomining of Gold from Auriferous soils"** at one day seminar on appropriate technology for rural sectors organised by IIT Goa and presented on topic on October 27th, 2018. **(Appendix XV)**

- **Dabolkar** and Kamat. "**Recovery of Chemolithotrophs microbial forms from BIF of Goa"** at National conference of changing environment -challenges, solution

and strategies organised by Dempe college of Arts and science, Miramar Goa on 8th and 9th March 2018. **(Appendix XVI)**

Workshops attended

- Role on three-dimensional structures in biological function, Organized by Department of Biotechnology, Goa University from 13- 15th December, 2017.
- Chemical analysis of biomolecules and computation organized by Department of Biotechnology, Goa University on 23- 24th November, 2017.
- Training on Urkund Plagiarism checking software held at Goa University Library on 21st September, 2017.
- State level workshop for Biology Teachers from HSS, organized by Department of Botany, Goa University in association with Goa Board of secondary and Higher secondary education on 23rd February 2018
- Two days capacity building programme on Intellectual property rights (IPRs) organized by Goa state council for science & Technology, Saligao, Bardez Goa association with Technology information forecasting & assessment council, DST, GoI, New Delhi & IP Cell, Goa University, 26-27th September, 2019

Other presentations made

- Presented to the Chairman of MPT, Vasco Goa on **how indian state of goa could attain its potential in asia as major metallogenic province through knowledge based sustainable biomining with new focus on neglected auriferous resources** on 2nd February 2019
- Presented to the Honorable Chief Minister of Goa **on Discovery of Bacterioform secondary gold and Sustainable Biomining** policy on 26th June 2019.

- Presented to the Honorable Chief Minister of Goa on **Discovery of Bacterioform secondary gold, Gold Sulfide and Sustainable Biomining policy** on 29th June 2022

Other Courses and Conferences attended

- Attended course on What's this thing called science taught by Dr. Milan Desai under the Board of Extra Mural studies & Extension studies, Goa University from 16 July to 27 Oct 2017.
- World Gold Conference (WGC): Unlocking sustainable value from Gold deposits organized by the Australasian Institute of mining and Metallurgy (AuSIMM), the Southern African Institute of Mining and Metallurgy (SAIMM) and the Canadian Institute of mining, Metallurgy and Petroleum (CIM), Perth, Australia on 11-13 September 2019.
- Volunteered for successful organization of Nobel Exhibition as a part of the Nobel Media Prize series, India 2018 events Organized by Nobel Media AB, Department of Biotechnology, Govt. of India and Department of Science and Technology, Govt. of Goa at Kala Academy, Panaji, Goa, during 01-28 February, 2018.
- Member of Outreach committee- National Conference of Young Researchers 2017 'New Frontiers in Life science & Environment, Organized by Faculty of Life Sciences and Environment, Goa University on 16-17 March, 2017.
- EU INDIA STI COOPERATION DAYS 2016 at CSIR National Institute of Oceanography, Goa, on 21-22 September, 2016.
- National seminar on New Frontiers in Plant Sciences and Biotechnology, organized by Department of Botany at Goa University on 29- 30 January, 2015.

- Attended talk on “Participatory Democracy and Economic Development Debating Cooperative Mining in Goa”-Goa University.
- Attended talk on the topic “Bio-inorganic chemistry approach to nanozymes and eukaryotic viruses and their biomedical applications”- By Dr Amit A. Vernekar.
- Attended one day seminar on the topic ‘Novel Vistas in plant sciences’ organized by the Department of Botany, Goa University on 25th January 2019.
- •Attended Intellectual Property Right (IPR) awareness Programme organized by ASSOCHAM, and IP office at Goa University, 11th December 2018.
- Webinar series on ‘Advances in Biological Science’; The fourth lecture is on ‘Enzymes for bio-refineries: Addressing technical challenges and limitations’ by Dr. Rajeev Sukumaran, Principal Scientist and Head, Microbial Processes and Technology Division, CSIR- NIIST, Thiruvananthapuram, Kerala.
- National webinar on Elemental Analysis by CHNS/O analyser organized by Sophisticated Instrumentation centre for applied Research and testing (SICART) Vallabh Vidyanagar on 8/10/2021.